

Design and synthesis of potent bioactive scaffolds *via* [3+2] cycloaddition, Glaser and Cadiot-Chodkiewicz coupling reactions; Cu catalyzed C–C bond forming reactions employing donor-accepter cyclopropanes and bioactives from *Aspergillus terreus*

by

Lakshmi Goswami
10CC17A26013

A thesis submitted to the
Academy of Scientific & Innovative Research
for the award of the degree of
DOCTOR OF PHILOSOPHY
in
SCIENCE

Under the supervision of
Dr. Asish K. Bhattacharya



CSIR- National Chemical Laboratory, Pune



Academy of Scientific and Innovative Research
AcSIR Headquarters, CSIR-HRDC campus
Sector 19, Kamla Nehru Nagar,
Ghaziabad, U.P. – 201 002, India

May, 2023

Certificate

This is to certify that the work incorporated in this Ph.D. thesis entitled, “Design and synthesis of potent bioactive scaffolds via [3+2] cycloaddition, Glaser and Cadiot-Chodkiewicz coupling reactions; Cu catalyzed C–C bond forming reactions employing donor-accepter cyclopropanes and bioactives from *Aspergillus terreus*”, submitted by Lakshmi Goswami to the Academy of Scientific and Innovative Research (AcSIR) in partial fulfillment of the requirements for the award of the Degree of Doctor of Philosophy in Science, embodies original research work carried-out by the student. We, further certify that this work has not been submitted to any other University or Institution in part or full for the award of any degree or diploma. Research material(s) obtained from other source(s) and used in this research work has/have been duly acknowledged in the thesis. Image(s), illustration(s), figure(s), table(s) etc., used in the thesis from other source(s), have also been duly cited and acknowledged.



Ms. Lakshmi Goswami

Research Scholar

Date: 25/05/2023



Dr. Asish K. Bhattacharya

Research Supervisor

Date: 25/05/2023

STATEMENTS OF ACADEMIC INTEGRITY

I Lakshmi Goswami, a Ph.D. student of the Academy of Scientific and Innovative Research (AcSIR) with Registration No. 10CC17A26013 hereby undertake that, the thesis entitled “Design and synthesis of potent bioactive scaffolds *via* [3+2] cycloaddition, Glaser and Cadiot-Chodkiewicz coupling reactions; Cu catalyzed C–C bond forming reactions employing donor-accepter cyclopropanes and bioactives from *Aspergillus terreus*” has been prepared by me and that the document reports original work carried out by me and is free of any plagiarism in compliance with the UGC Regulations on “*Promotion of Academic Integrity and Prevention of Plagiarism in Higher Educational Institutions (2018)*” and the CSIR Guidelines for “*Ethics in Research and in Governance (2020)*”.




Signature of the Student

Date : 25/05/2023

Place : P u n e

It is hereby certified that the work done by the student, under my supervision, is plagiarism-free in accordance with the UGC Regulations on “*Promotion of Academic Integrity and Prevention of Plagiarism in Higher Educational Institutions (2018)*” and the CSIR Guidelines for “*Ethics in Research and in Governance (2020)*”.



Signature of the Supervisor

Name : Dr. Asish K Bhattacharya

Date : 25/05/2023

Place : P u n e



In memory of...

My dear mamaji Shri Sunder Giri

And

My beloved brother Kailash Goswami

Contents

	Page No.
Acknowledgment	i
Abbreviations	iii
General remarks	xi
Synopsis Report	Xiii

Chapter 1

Design and synthesis of potent bioactive scaffolds *via* [3+2] cycloaddition, Glaser and Cadiot-Chodkiewicz coupling reactions

1.1 Section A: Design and synthesis of potent anticancer artemisinin glycoconjugates

1.1.1	Introduction	1
1.1.1.1	Glycoconjugates of natural products as new potent drugs	3
1.1.2	Present work	4
1.1.3	Conclusions	8
1.1.4	Experimental procedures	9
1.1.5	References	17
1.1.6	Copies of NMR spectra	19

1.2 Section B: Design and synthesis of eugenol/isoegenol glycoconjugates and other azole derivatives as potent antifungal

1.2.1	Introduction	30
1.2.1.1	Development of resistance toward known antifungals	30
1.2.1.2	Secondary metabolites as potent antifungals	31
1.2.2	Present work	32
1.2.2.1	Chemical modifications of eugenol 1a and isoeugenol 1b	32
1.2.2.2	Biological evaluations of synthesized compounds	37
1.2.3	Conclusions	40
1.2.4	Experimental procedures	42
1.2.5	References	60
1.2.6	Copies of NMR spectra	63

Contents

1.3 Section C: Design and synthesis of eugenol/isoegenol based homo/hetero coupled products *via* Glaser and Cadiot-Chodkiewicz coupling reactions

1.3.1	Introduction	86
1.3.1.1	Introduction to Glaser-Hay or Cadiot-Chodkiewicz coupling reactions	87
1.3.1.2	Eugenol 1a and isoeugenol 1b as potent antifungals	88
1.3.2	Present work	89
1.3.2.1	Chemical modifications of phenolics (1c-e)	89
1.3.2.2	Structure-Activity-Relationship analysis	91
1.3.3	Conclusions	94
1.3.4	Experimental procedures	95
1.3.5	References	106
1.3.6	Copies of NMR spectra	109

Chapter 2

Cu-catalyzed C–C bond-forming reactions employing donor-accepter cyclopropanes

2.1	Introduction	124
2.1.1	Donor–Acceptor cyclopropane reactivity	125
2.1.2	Donor–Acceptor cyclopropane ring opening <i>via</i> heteroatom-centered nucleophiles	126
2.1.3	Donor–Acceptor cyclopropane ring opening <i>via</i> carbon-centered nucleophiles	127
2.1.4	Conclusions	129
2.2.	Present work	130
2.2.1	Preliminary studies towards the enantioselective Friedel-Crafts adducts	136
2.3	Conclusions	137
2.4	Experimental procedures	139
2.5	References	158
2.6	Copies of NMR spectra	160

Chapter 3

Bioactives from *Aspergillus terreus*

Contents

3.1	Introduction	195
3.2	Present work	205
3.3	Conclusions	209
3.4	Experimental procedures	210
3.5	References	212
3.6	Copies of NMR spectra	214

Abstract for Indexing	222
Details of publications and Patents	223
List of Poster, oral presentations and Conferences attended	224
Erratum	225

Acknowledgement

During the long period of my research work, I have been acquainted, accompanied and supported by many people. It is a pleasant aspect that I have now the opportunity to express my gratitude for all of them.

I am highly grateful to my deity lord Shiva for blessing me and giving me strength, energy and patience to surpass all the difficulties and reach to this ambition.

*It is my great privilege to express my deepest sense of gratitude to my guide **Dr. Asish. K. Bhattacharya** for his excellent guidance, constant encouragement, and constructive criticism during my doctoral research. I consider extremely fortunate to have an advisor who not only educated me in chemistry but also taught me discipline and shown unique ways to achieve my goals. I sincerely acknowledge the freedom rendered by him in the laboratory for the independent thinking, planning, and execution of the research. I believe the better way of thanking him would be through my future contribution to the scientific community.*

I owe to thank my Doctoral Advisory Committee members, Dr. K. Krishnamoorthy, Dr. Moneesha Fernandes and Dr. Santosh B. Mhaske for their continued support, guidance, and suggestions. I am grateful to Dr. Ashish Lele (Director, CSIR- National Chemical Laboratory and Dr. Ashwini K. Nangia (Former Director, CSIR- National Chemical Laboratory), Dr. Chepuri V. Ramana, (Chair, Division of Organic Chemistry), Dr. N. P. Argade, Dr. S. P. Chavan and Dr. Pradeep Kumar (Former HOD's, Division of Organic Chemistry) for providing all necessary infrastructure and facilities.

I owe to thank Dr. V. Koteshwara Rao (Senior Scientist, Biochemical Sciences Division, CSIR-NCL, Pune) for providing crude microbial extract for natural product isolations. I am grateful towards Dr. Pooja Vijayaraghavan (Associate Professor, Amity University) and her student, Lovely Gupta (PhD) for conducting biological assays.

It is my pleasure to thank all my past and present lab mates Dr. Hemender, Dr. Tharun, Dr. Eswar, Dr. Tushar, Pratiksha, Balaji, Ajay, Sanjay and Rushabh for devoting their precious time and made many valuable suggestions, which indeed helped me during this research work. I express my hearty thanks to Dr. Sayantan for his support and valuable advices in my work.

Acknowledgement

No words are sufficient to acknowledge my prized friends (Suman, Priyanka Kataria, Gitanjali, Aman, Nilanjana, Vikas, Tanuja, Sadhna, Priyanka Haldar, Amrita, Balu, Subhranshu and Krishna) who have helped me during my tenure in NCL. I am very much thankful to Manjeet who untiringly supported me, helped me, understood me and encouraged me in all situations.

Personally, I am immensely thankful to my teachers in college and University for their valuable teachings in my Bachelor's and Master's degree. I express my special thanks to my school teacher Mrs. Bhavani Rawat for her immense support to me and my family throughout this journey.

Without the funding I received, this Ph.D. would not have been possible, and I would like to express my sincere appreciation to University Grants Commission New Delhi for awarding JRF and SRF.

*My family is always a source of inspiration and great moral support for me in perceiving my education. This acknowledgment would not be complete without mentioning the painstaking efforts and patience of my uncle (mama ji) **Late Shri Sunder Giri** and my aunt (bua ji) Smt. Shankari Devi. I sincerely express my deep sense of gratitude to them for nurturing me with their unconditional love, sacrifice and support. I wholeheartedly express my gratitude to my grandparents Shri Ghananand Goswami (dada ji) and Smt. Kunti Devi (dadi ji), my parents Shri Shankar Prasad Goswami (papa ji) and Pramila Devi (maa) for their selfless love, blessings, and encouragement. I am also blessed with the love and encouragement from my uncle (tau ji) Shri Shiv Prasad Goswami and my aunt (tai ji) Smt. Surji Devi throughout my studies. I owe this thesis to my family members who always stood by me and provided strength in pursuing this work.*

I am grateful towards my adorable sibling Himanshu shekhar, Poonam Goswami and Kailash Goswami for encouraging me and bringing lots of joy. I am forever indebted to my family

I wish to thank the great scientific community whose achievements are a constant source of inspiration for me.

With regards

Lakshmi Goswami

AcOH	Acetic acid
ABCG2	ATP-binding cassette transporter G2
ACN	Acetonitrile
ACHN	Human renal adenocarcinoma cell line
AChE	Acetylcholinesterase
AD	Asymmetric dihydroxylation
<i>A. fumigatus</i>	<i>Aspergillus fumigatus</i>
AgNO ₃	Silver nitrate
Amp B	Amphotericin B
Ar	Aryl
ASPC-1	Pancreatic cancer cell line
A549	Lung adenocarcinoma cell line
<i>A. terreus</i>	<i>Aspergillus terreus</i>
Atm	Unit for measurement of atmospheric pressure
A498	Renal cancer cell line
BGC- 823	Gastric carcinoma cells
Br	Bromo
BF ₃ .OEt ₂	boron trifluoride diethyl etherate
Bu ₄ NHSO ₄	Tetrabutylammonium hydrogen sulfate
BnBr	Benzyl bromide
Bu ₄ NI	Tetra-n-butyl ammonium iodide
Bi(OTf) ₃ .	Bismuth(III) triflate
Bi(NO ₃) ₃ ·5H ₂ O	Bismuth(III) nitrate pentahydrate
°C	Degree Celsius
cat.	Catalytic

CCl ₃ CN	Trichloroacetonitrile
CC ₅₀	Cytotoxic concentration
CDCl ₃	Deuterated chloroform
CDK	Cyclin-dependent kinase
CF ₃	Trifluoromethyl
CH ₃ CN	Acetonitrile
CHO	Aldehyde
CK	Creatine kinase
Cl	Chloro
CLSI	Clinical and Laboratory Standards Institute
CLSM	Confocal laser scanning microscopy
COOEt	Ethoxycarbonyl
Con.	Concentrate
Conc.	Concentration
COX	Cyclooxygenase
CSIR	Council of Scientific & Industrial Research
Cs ₂ CO ₃	Cesium carbonate
CTMS	Trimethylsilyl chloride
Cu	Copper
CuI	Copper (I) Iodide
Cu(OAc) ₂	Copper (II) acetate
Cu(OTf) ₂	Copper(II) trifluoromethanesulfonate
CzB	Czapek Dox Broth
D-A	Donar-Acceptor
DCM	Dichloromethane

DHN-Melanin	Dihydroxynaphthalene melanin
DIPEA	<i>N, N</i> -Diisopropylethylamine
DMAP	4-Dimethylaminopyridine
DMSO	Dimethyl sulfoxide
DMEM	Dulbecco's modified Eagle's medium
DMF	<i>N, N'</i> -Dimethylformamide
D ₂ O	Deuterium oxide; heavy water
<i>ee</i>	Enantiomeric excess
EDA	Electron donor-acceptor
equiv.	Equivalent
EtOAc	Ethyl acetate
EWG	Electron withdrawing group
EDG	Electron donating group
ECM	Extracellular matrix
ESI	Electrospray ionization
FBS	Foetal bovine serum
FDA	Food and Drug Administration
g	Gram
GSK	Glycogen synthase kinase
h	Hour
H ⁺	Acid
HBr	Hydrobromic acid
HCl	Hydrochloric acid
HL-60	Human leukemia cell line
HeLa	Cervical cancer cells

HepG2	Human liver cancer cell line
HFIP	Hexafluoroisopropanol
HMBC	Heteronuclear Multiple Bond Coherence
HPLC	High-pressure liquid chromatography
HRMS	High Resolution Mass Spectrometry
HSQC	Heteronuclear Single Quantum Coherence
H1N1	Human swine flu virus
H3N2	Influenza A virus subtype
H ₂ O	Dihydrogen monoxide; Water
H ₂ SO ₄	Sulfuric acid
H ₂	Hydrogen
I	Iodo
IR	Infrared
IC ₅₀	Half-maximal inhibitory concentration
<i>J</i>	Coupling constant (in NMR)
K	Potassium
K ₂ CO ₃	Potassium carbonate
KOH	Potassium hydroxide
KPF ₆	Potassium hexafluorophosphate
KB	Human epithelial carcinoma cells
K562	Erythroid leukemic cell line
L	Ligand
l	Litre
LCMS	Liquid chromatography-mass spectrometry
L-132	Human lung epithelial cancer cell line

M	Molar (unit for molarity)
MBEC	Minimal biofilm-eradicating concentration
MCF-7	human breast cancer cell line
<i>m</i> -CPBA	<i>m</i> -Chloroperbezoic acid
Me	Methyl
MeCN	Acetonitrile
MeI	Methyl iodide
MeOH	Methanol
MeSO ₃ H	Methane sulfonic acid
mg	Milligram
MHz	Megahertz
mins	Minutes
mL	Millilitre
mm	millimeter
mmol	Millimoles
Mn(OAc) ₂	Manganese (II) acetate
MOLT-4	Acute lymphoblastic leukemia cells
m.p.	Melting point
MTT	3-(4,5-dimethylthiazol-2-yl)-2,5-diphenyl-2H-tetrazolium bromide
<i>m/z</i>	Mass to charge ratio
Na	Sodium
NaBH ₄	Sodium borohydride
NaH	Sodium hydride
NaHCO ₃	Sodium bicarbonate
NaN ₃	Sodium azide

NaOH	Sodium hydroxide
Na ₂ MoO ₄ .2H ₂ O	Sodium molybdate dehydrate
NBS	<i>N</i> -Bromosuccinimide
NCCS	National Centre for Cell Science, Pune
NCI-H187	Human lung cancer cell line
NCI-H460	Human lung cancer cell line
NCL	National Chemical Laboratory
NEt ₃	Triethyl amine
NEt ₂ H	Diethyl amine
Ni(ClO ₄) ₂ .6H ₂ O	Nickel(II) Perchlorate Hexahydrate
NMR	Nuclear Magnetic Resonance
NOESY	Nuclear Overhauser Effect Spectroscopy
NOE	Nuclear Overhauser Effect
NRPS	Nonribosomal peptide synthetase
N ₃	Azide
O	Oxygen
OH	Hydroxyl
OMe	Methoxy
OS-RC-2	Renal Cancer Cell Line
OVCAR-3	Human Ovarian Cancer Cell Line
PANC-1	Human pancreatic cancer cell line
PBS	Phosphate buffered saline
PDA	Potato dextrose agar
Pd	Palladium
PKS	polyketide synthases


ppm	parts per million
<i>p</i> TSA	<i>para</i> -Toluenesulfonic acid
R_f	Retention factor
RPMI	Roswell Park Memorial Institute
rt	Room temperature
S	Sulfur
Sc(OTf) ₃	Scandium (III) trifluoromethanesulfonate
SEM	Scanning electron microscope
-SH	Thiol
SI	Selectivity index
SiO ₂	Silicon dioxide; silica gel
SMMC-7721	Human hepatoma cell line
SW1990	Human pancreatic cancer cell line
TBDMSCl	<i>Tert</i> -Butyldimethylsilyl chloride
TEM	Transmission electron microscope
TEMPO	(2,2,6,6-Tetramethylpiperidin-1-yl)oxyl
<i>Tert</i>	Tertiary
TfOH	Triflic acid or trifluoromethanesulfonic acid
THF	Tetrahydrofuran
TLC	Thin layer chromatography
TMEDA	Tetramethylethylenediamine
TMSCl	Trimethylsilyl chloride
TOF mass analyzer	Time-of-flight mass analyzer
TPSA	Topological Polar Surface Area
TsCl	4-Toluenesulfonyl chloride

UV	Ultraviolet
U937	Human leukemic monocyte lymphoma cells
VIS	Visible light region
Yb(OTf) ₃	ytterbium (III) triflate
μL	Microlitre
μM	Micromolar
μm	Micrometer or micron
786-O	Hypotriploid renal cancer cell line

- Independent compound and reference numbering have been used for each chapter as well as for sections of the chapters.
- All the reagents and solvents were purchased from commercial suppliers and used as such without further purification.
- Solvents were distilled and dried following standard procedures prior to use. Petroleum ether used for column chromatography was of 60-80 °C boiling range.
- Flash chromatography was carried out by **CombiFlash®Rf 200i** Isco Teledyne Inc., USA instrument equipped with UV detector and Evaporative light scattering detector (ELSD), 230-400 mesh silica gel Redisep® column and appropriate solvent system.
- All reactions were monitored by TLC with 0.25 mm pre-coated E-Merck silica gel plates (60 F254) and TLC spots were made visible by exposing to UV light, Iodine adsorbed on silica gel or by immersion into a solution of phosphomolybdic acid (PMA), *p*-anisaldehyde or KMnO₄ followed by heating with a heat gun for ~15sec.
- NMR spectra were recorded on Bruker AV200 (200.13 MHz for ¹H NMR and 50.03 MHz for ¹³C NMR), AV 400 (400.13 MHz for ¹H NMR and 100.61 MHz for ¹³C NMR), Jeol-400 (399.78 MHz for ¹H NMR and 100.53 MHz for ¹³C NMR) and DRX 500 (500.13 MHz for ¹H NMR and 125.0376 MHz for ¹³C NMR) spectrometers. In experimental section for the sake of clarity ¹H NMR were mentioned as recorded in 200, 400 or 500 MHz and ¹³C NMR were mentioned as recorded in 50, 101, 126 MHz.
- Chemical shifts (δ) have been expressed in ppm units relative to tetramethylsilane (TMS) as an internal standard and coupling constants (*J*) were measured in Hertz.
- The following abbreviations were used for ¹H NMR: s = singlet, d = doublet, t = triplet, q = quartet, m = multiplet, brs = broad singlet, dd = doublet of doublet, dt = doublet of triplet, td = triplet of doublet and ddd = doublet of doublet of doublet.
- All the reported melting points are uncorrected and were recorded using Buchi melting point apparatus (Buchi B-540).
- Optical rotations were recorded on a JASCO P-1020 polarimeter at 589 nm (sodium D-line). Specific rotations $[\alpha]_D$ are reported in deg/dm, and the concentration (c) is given in g/100 mL in the specific solvent.

- Structures and IUPAC nomenclature were generated using ChemBioDraw Ultra 15.1 software.
- Mass spectra were recorded on LC-MS/MS-TOF API QSTAR PULSAR spectrometer, samples introduced by fusion method using Electrospray Ionization Technique.
- High-resolution mass spectra (HRMS) (ESI) were recorded on an Orbitrap (quadrupole plus ion trap) and TOF mass analyzer.
- FTIR was recorded in a Bruker ALPHA-E FT-IR spectrometer. IR spectrum was recorded as a thin film by dissolving the samples in in chloroform.
- Chiral HPLC was performed using Agilent 1260 Infinity normal phase HPLC unit (with 254 nm wavelength and 1 mL/min flow rate), HPLC Chemstation software, CHIRALART AMYLOSE SA column (250 x 4.6 mm, 5 μ m) and 10% isopropanol in hexane as mobile phase.

Synopsis

	Synopsis of the thesis to be submitted to the Academy of Scientific and Innovative Research for award of the degree of Doctor of philosophy in Chemical Science
Name of the Candidate	Lakshmi Goswami
Enrollment No. and Date	Ph. D. in Chemical Sciences (10CC17A26013); August 2017
Title of the Thesis	"Design and synthesis of potent bioactive scaffolds <i>via</i> [3+2] cycloaddition, Glaser and Cadiot-Chodkiewicz coupling reactions; Cu catalyzed C–C bond forming reactions employing donor-accepter cyclopropanes and bioactives from <i>Aspergillus terreus</i> "
Research Supervisor	Dr. Asish K. Bhattacharya

1. Introduction:

The present thesis is divided into three main chapters. Chapter **1** deals with the design and synthesis of glycoconjugates of natural products of medicinal importance. The glycoconjugates were synthesised *via* coupling of propargylated natural products and azido sugars employing [3+2] cycloaddition reaction. Other potent bioactive scaffolds were also synthesised *via* Glaser and Cadiot-Chodkiewicz coupling reactions. All of these synthesised analogues were tested for their biological activities. Chapter **2** presents C–alkylation of phenols employing Donor–Acceptor cyclopropanes as alkylating agents *via* transition-metal free conditions. Chapter **3** describes the isolation of secondary metabolites from microbial culture of *Aspergillus terreus*, a pathogenic fungus and also a prolific source of medicinally important secondary metabolites. Hence, we have undertaken the chemical examination of *Aspergillus terreus* for the isolation of bioactive secondary metabolites.

2. Statement of the problem:

Various processes such as solubility, stability and bioavailability of drugs in biological systems are quiet demanding now a days. Extensive use of marketed drugs rendered pathogens immune to host cell defense mechanism and helped the strain to slowly develop the resistance against certain drugs. Hence it is necessary to develop potent drugs with better efficacy and least toxicity *via* synthetic modifications of the parent drug molecules. Apart from this the isolation of new bioactives from natural sources can also provide us with new chemical motifs with unique biochemistry and structural framework.

3. Objectives:

According to literature reports, various biological processes such as solubility, stability and bioavailability are resolved by the fusion of a carbohydrate scaffold to a natural product. Synthetic modification of parent drugs or new motifs isolated from natural sources is the key to reduce drug resistance of different pathogens. Development of new synthetic methodologies devoid of any transition-metal is of great importance. Discovery of new structural motifs or having diverse biological activity from different natural sources is of utmost important. Hence we have undertaken the isolation and structural elucidation of natural products from microbial culture.

4. Methodology and Result:

Chapter 1: Design and synthesis of potent bioactive scaffolds via [3+2] cycloaddition, Glaser and Cadiot-Chodkiewicz coupling reactions

Artemisinin (a sesquiterpene lactone endoperoxide obtained from the plant, *Artemisia annua*) is being clinically used as anti-malarial drug worldwide (**Figure 1**). It was discovered by Prof. Tu You You (Nobel prize, 2015, medicine).¹⁻³ Artemisinin and its semi-synthetic derivatives, which are commonly used in malaria therapy have also shown potent anticancer activity. Artemisinin itself has displayed moderate anticancer activity against various cancer cell lines but some of its semi-synthetic derivatives including artemisinin hybrids have exhibited promising anticancer activities (**Figure 1**).⁴⁻⁶ Due to the extensive utility of the glycoconjugates in medicinal chemistry, we envisioned that synthesis of artemisinin based glycoconjugates may serve as potent anti-cancer molecules.

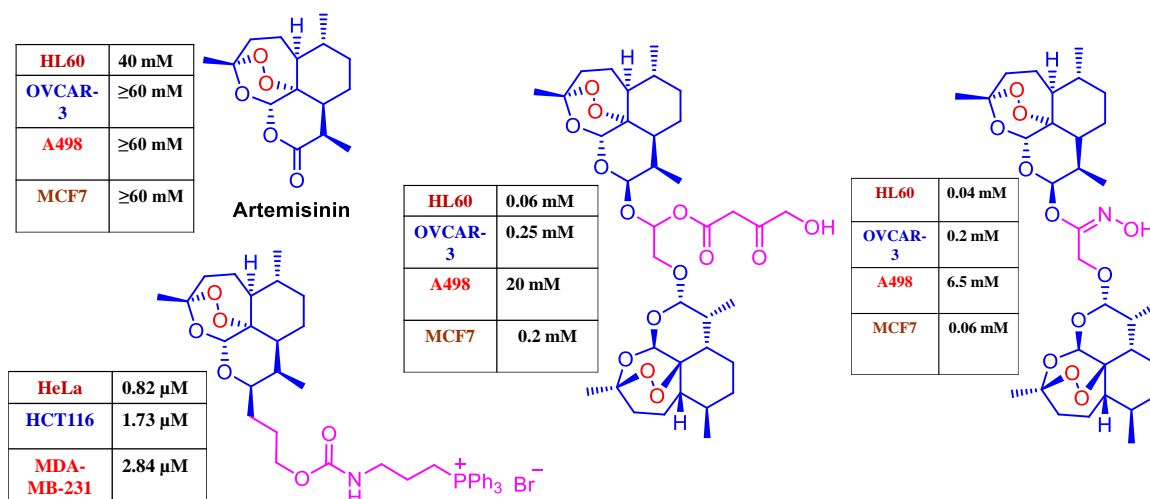
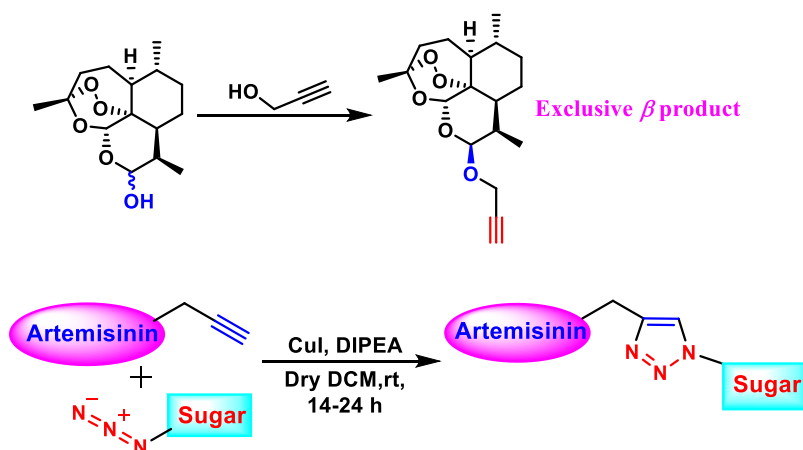


Figure 1. Artemisinin and artemisinin based molecules as potent anti-cancer agents.

In our present work we coupled propargylated dihydroartemisinin and azido sugar to furnish glycoconjugates of artemisinin by employing Cu(I) catalyzed click reaction as the bridging tool (Scheme 1).^{7, 10} In order to synthesise exclusive β -propargylated dihydroartemisinin (Scheme 1) we utilized the method developed by our group and β -sugar azides were prepared the following literature methods.^{8, 9} At present all the synthesised glycoconjugates of artemisinin are being assayed for their anticancer activity.



Scheme 1. Synthesis artemisinin based glycoconjugates

Synopsis Report

Eugenol and isoeugenol being isolated from *Eugenia caryophyllata*, *Myristica fragrans*, *Syzygium aromaticum*, *Ocimum basilicum* etc. and have shown antifungal activities against *Aspergillus fumigatus* with IC₅₀ value of 1.9 mM (**Figure 2**).¹¹

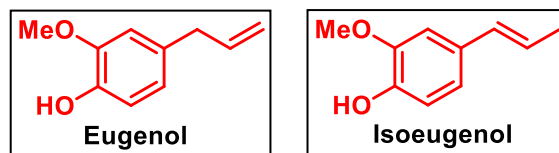
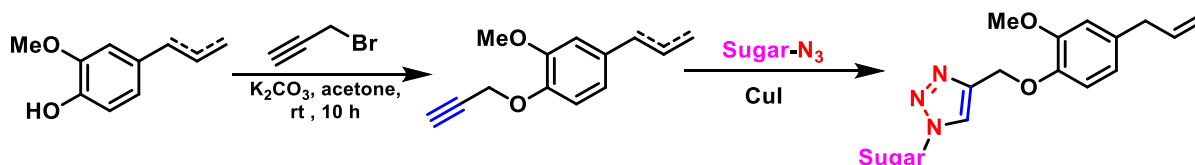


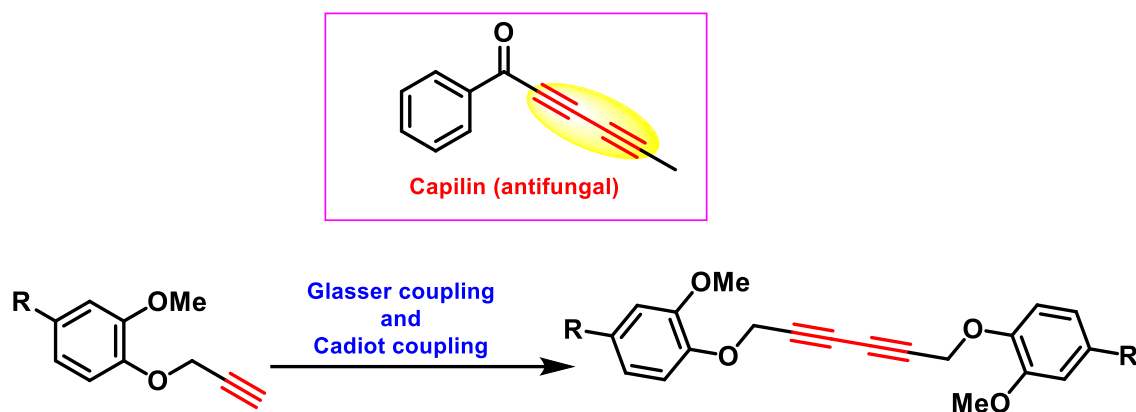
Figure 2. Structure of eugenol and isoeugenol

Therefore, design and synthesis of novel glycoconjugates was achieved by reacting propargylated eugenol and isoeugenol with sugar azides under click reaction condition (**Scheme 2**). All the synthesised compounds have shown promising antifungal activity IC₅₀ values ranging from **5.42-15.18 μM** against *Aspergillus fumigatus* compared to the parent molecules.¹²



Scheme 2. Synthesis of eugenol/isoeugenol based glycoconjugates

Acetylene based drugs such as capelin motivated us to design new antifungal compounds. Henceforth, we synthesised homo/hetero coupled eugenol/isoeugenol based acetylenic compounds employing Glasser and Cadiot-Chodkiewicz coupling reactions (**Scheme 3**). All synthesised compounds have shown good to moderate antifungal activity against *Aspergillus fumigatus*.¹³⁻¹⁵

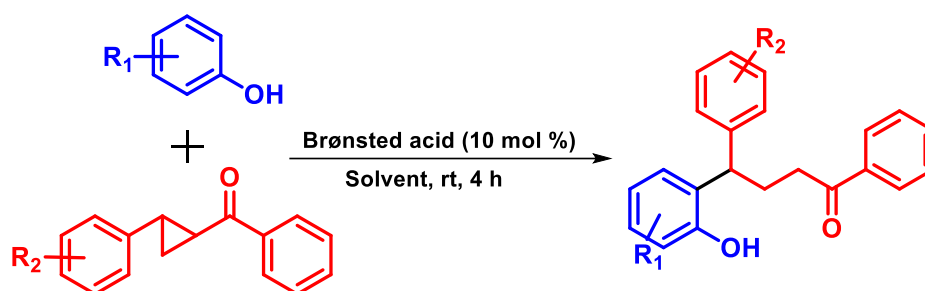


Scheme 3. Synthesis of eugenol/isoegenol based polyacetylene type compounds

Chapter 2: Cu catalyzed C–C bond forming reactions employing donor-accepter cyclopropanes

Donor–Acceptor cyclopropanes have been extensively used in past few years to explore new entities for the synthesis of complex organic molecules. D–A cyclopropanes are reactive species due to the formation of dipolar ion or 1, 3-zwitterion intermediate in presence of Lewis/Brønsted acids. These dipolar ions are trapped by electrophiles, nucleophiles and dipolarophiles to furnish versatile products. D–A cyclopropanes have been used at different stages of total synthesis and semi-synthesis of natural and unnatural products. In general D–A cyclopropanes rendered cyclized product through ring opening annulation reaction, which plays a prominent role in the development of new reactive molecular entities.^{16, 17} However there are few reports in literature regarding Donor–Acceptor cyclopropanes ring opening reactions leading to C–alkylation.¹⁸

Therefore, we envisioned a transition-metal free C–alkylation of phenols with Donor–Acceptor cyclopropanes to furnish functionalized 1, 4-diphenylbutan-1-one derivatives, which are biologically important core of many plant based chalcones and synthetically available compounds (**Scheme 4**).



Scheme 4. Synthesis of functionalized 1, 4-diphenylbutan-1-one derivatives

We optimised our reaction conditions with methane sulphonate as Brønsted acid at rt in dichloromethane employing *p*-cresol as phenol partner and EDG inserted D–A cyclopropanes with the product yield of 86%.

After optimised reaction conditions in hand we explored substrate scope by reacting various phenols with D–A cyclopropanes surrogated with EDG, weak EWG and strong EWG. We also elaborated our substrate scope with thiols and observed very good yields in all the cases.

Chapter 3: Bioactives from *Aspergillus terreus*

The discovery of penicillin by Alexander Fleming and streptomycin by Selman Waksman, has kindled the exploration of newer secondary metabolites from microbial cultures. Microorganisms are known as diverse source of natural products, many of which are medicinally important.^{19, 20}

We have undertaken isolation and structure elucidation of secondary metabolites from *Aspergillus terreus*. This particular species of genus *Aspergillus* has been a source of natural products with new motifs and biologically active compounds (**Figure 3**).²¹⁻²⁶

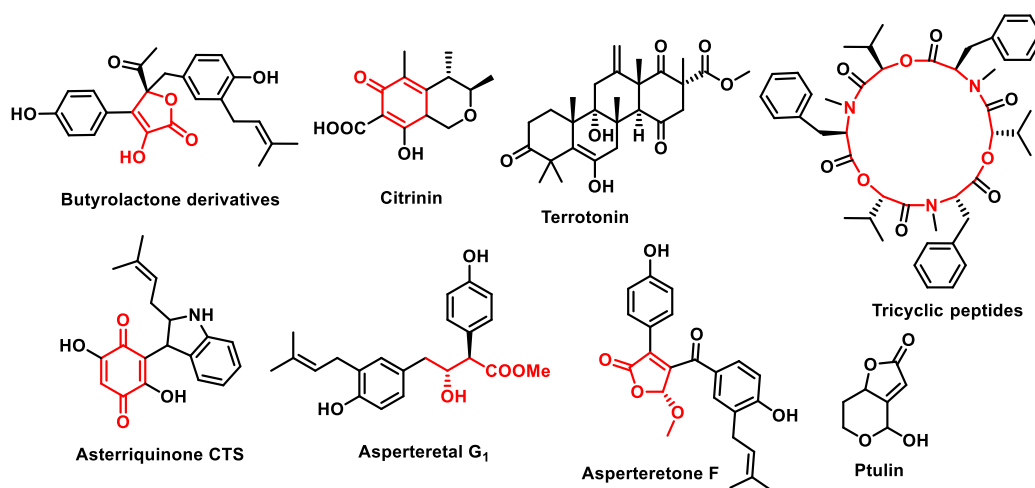


Figure 3. Compounds isolated from *Aspergillus terreus*

The strain was initially grown on PDA medium in a petri dish for 7 days and then it was directly inoculated into 500 mL in a Erlenmeyer flasks each containing 100 mL of the seed medium (agar-agar, dextrose). The crude lyophilized material obtained was extracted with EtOAc which on evaporation yielded 1.3 g of crude extract. This extract was chromatographed on flash chromatography using ethyl acetate-pet. ether as eluent to furnish three products (10 mg, 38 mg and 14 mg) which have been characterized by spectral data.

5. Summary:

- 1) Synthesis of artemisinin, eugenol and isoeugenol based glycoconjugates along with homo/hetero coupled eugenol and isoeugenol based acetylenic compound were achieved. All the eugenol based semi-synthetic derivatives were tested against *Aspergillus fumigatus* and anticancer activity of artemisinin glycoconjugates are presently being pursued.
- 2) Transition-metal free C-alkylation of phenols by employing D-A cyclopropanes as alkylating agents was achieved using Brønsted acid.
- 3) Secondary metabolites were isolated from *Aspergillus terreus* (microbial culture) and their structure elucidation is under process.

6. Future directions:

Synopsis Report

1. We would like to extend out transition-metal free alkylation strategy to different scaffolds and along with the development of enantioselective reaction condition for ring opening of D–A cyclopropanes.
2. We would like to isolate secondary metabolites in large scale for their synthetic modifications and study of anticancer activities.

7. Publications:

List of Publications and Patents:

1. Synthesis of artemisinin derived glycoconjugates inspired by click chemistry.
L. Goswami,[†] S. Paul,[†] T. K. Kotamagari and A. K. Bhattacharya, *New J Chem.* **2019**, *43*, 4017-4021.
2. Design and synthesis of eugenol/isoegenol glycoconjugates and other analogues as antifungal agents against *Aspergillus fumigatus*.
L. Goswami, L. Gupta, S. Paul, M. Vermani, P. Vijayaraghavan, A. K. Bhattacharya, *RSC Med. Chem.* **2022**, *13*, 955-962.
3. **L. Goswami**, L. Gupta, S. Paul, P. Vijayaraghavan, A. K. Bhattacharya, *ChemMedChem*, **2023**, e202300013. (doi.org/10.1002/cmdc.202300013)

8. References:

1. <https://www.nobelprize.org/prizes/medicine/2015/tu/facts/> Youyou Tu, *Nature Medicine*, **2011**, *17*, 1217-1220.
2. A. Brossi *et al.* *J. Med. Chem.* **1988**, *31*, 645.
3. A. J. Lin *et al.* *J. Med. Chem.* **1989**, *32*, 1249; *J. Med.Chem.***1987**, *30*, 2147.
4. C. Xu, H. Zhang, L. Mu, X, Yang, *Front. Pharmacol*, **2020**.
5. F. Gao, Z. Sun, F. Kong, J. Xiao, *Eur J Med Chem*, **2020**, *15*, 188.
6. *Essentials of Glycobiology* (2nd Edition), Editors A. Varki, Cummings, Esko, Freeze, Stanley, Bertozzi, Hart and Etzler, Cold Spring Harbor Laboratory Press; **2009**.
7. V. V. Rostovtsev, L. G. Green, V. V. Fokin and K. B. Sharpless, *Angew. Chem., Int. Ed.*, **2002**, *41*, 2596-2599.
8. H. R. Chand, A. K. Bhattacharya, *Asian J. Org. Chem.*, **2016**, *5*, 201 – 206.
9. R. M. Cicchillo, P. Norris, *Carbohydr. Res.*, **2000**, *328*, 431–434.
10. L. Goswami, S. Paul, T. K. Kotamagari and A. K. Bhattacharya, *New J. Chem.*, **2019**, *43*, 4017-4021.
11. Koeduka *et al.*, *Proc.Natl. Acad. Sci. U. S. A.*, **2006**, *103*, 10128–10133.

Synopsis Report

12. L. Goswami, L. Gupta, S. Paul, M. Vermani, P. Vijayaraghavan, A. K. Bhattacharya, *RSC Med. Chem.*, **2022**, *13*, 955-962.
13. L.C. Whelan, M.F. Ryan, *Anticancer Research.*, **2004**, *24*, 2281-2286.
14. C. Glaser, *Annalen der Chemie und Pharmacie.*, **1870**, *2*, 137–171.
15. Chodkiewicz, *W. Ann. Chim. Paris*, **1957**, *2*, 819–69.
16. H. K. Grover, M. R. Emmett, M. A. Kerr, *Org. Biomol. Chem.*, **2015**, *13*, 655-671.
17. O. Lifchits, A. B. Charette, *Org. Lett.* **2008**, *10*, 2809.
18. P. Harrington, M. A. Kerr, *Tetrahedron Lett.* **1997**, *38*, 5949.
19. D. Malcolm, K. B. Richardson, W. Hope, *Clinical Mycology (SECOND EDITION)*, **2009**, 271-296.
20. Li et al, *Curr Med Chem.* **2020**, *27*, 6244-6273.
21. Cox et al, *J. Org. Chem.* **1979**, *26*, 4852- 4854.
22. Zain et al, *Phytother. Res.*, **2012**, *26*, 1872–1877.
23. Wang et al, *Org. Lett.*, **2013**, *14*, 3562–3565.
24. Zhang et al, *Fitoterapia*, **2020**, 104685.
25. Qiu et al, *Mar. Drugs*, **2018**, *16*, 428.
26. Lin et al, *Mar. Drugs*, **2013**, *11*, 2616-2624.

Chapter 1

*Design and synthesis of
potent bioactive scaffolds via
[3+2] cycloaddition, Glaser
and Cadiot-Chodkiewicz
coupling reactions*

1.1. Design and synthesis of potent anticancer artemisinin glycoconjugates

1.1.1 Introduction

The plant *Artemisia annua* L. is used as a remedy by Chinese people to treat malarial fever for years.^{1-3a,b} Prof. Tu Youyou (Nobel Prize 2015, medicine) in 1972 first isolated and identified artemisinin (**1**) as the chemical constituent from this Chinese herb responsible to cure malaria.⁴ Artemisinin (**1**) is principally a sesquiterpene lactone endoperoxide, which is being clinically used as an anti-malarial drug. 1,2,4-Trioxane motif present in artemisinin (**1**) is the necessary core for its antimalarial activity. Artemisinin (**1**) and its semi-synthetic derivatives (**2-8**) depicted in (Figure 1) are commonly used in malaria therapy in combination with other antimalarial drugs.^{1-3a,b}

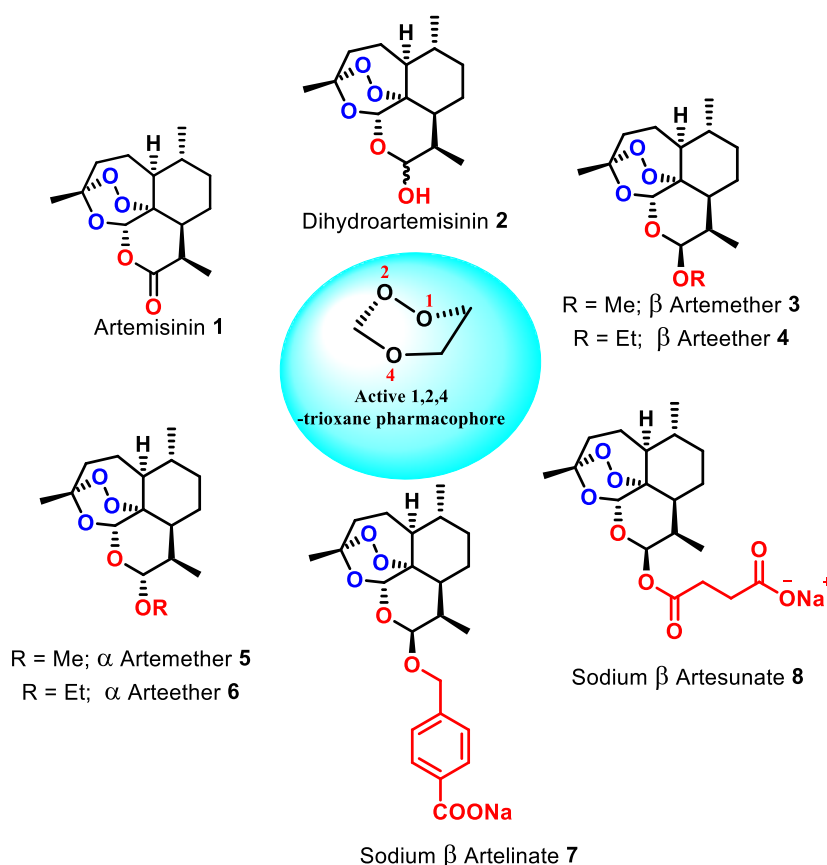


Figure 1: Artemisinin (**1**) and its semi-synthetic derivatives (**2-8**)

Artemisinin (**1**), dihydroartemisinin (**2**) along with its semi-synthetic derivatives arteethers (**4** and **6**) and artemethers (**3** and **5**) are oil-soluble and taken intramuscularly while water-based sodium artelinate (**7**) and artesunate (**8**) are taken orally to treat malaria.¹⁻⁴ Artemisinin (**1**) and its semi-synthetic derivatives as well as some of the artemisinin-based hybrids (**9-11**) have also been reported to exhibit potent anticancer activities (**Figure 2**).^{5a-c}

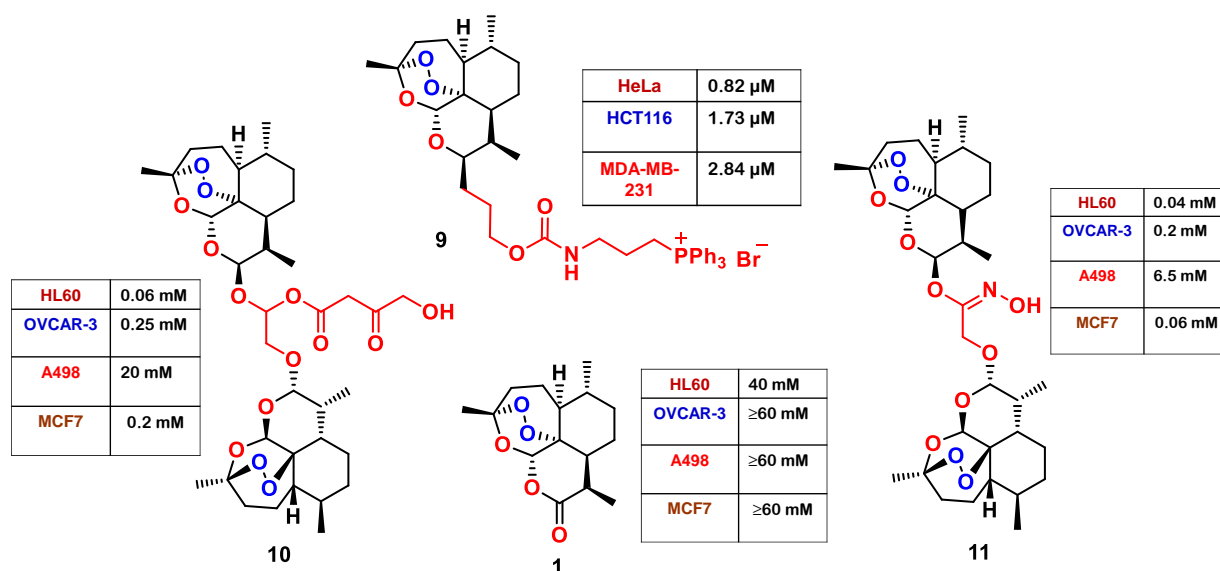


Figure 2: Artemisinin and artemisinin-based molecules as potent anti-cancer agents

The cytotoxicity of artemisinin **1** and its semi synthetic derivatives were first studied against Ehrlich ascites cancer cell line and till date these pharmacophore have been assayed against many other tumor cell lines. Among all the tumor cell lines studied, highest activities were found against leukemia cell lines whereas lower cytotoxicities were observed against lung cancer cells. In the case of deoxyartemisinin (**13**) where the endoperoxide linkage is replaced by an ether bond, anticancer activity was very mild thus underlying the peroxide assisted mechanism for cancer cells destruction. Deoxydihydroartemisinin derivative (**16**) where endoperoxide linkage was absent displayed 50 times less cytotoxicity than dihydroartemisinin (**2**) and its semi-synthetic derivatives (**14** and **15**) against HL-60 cell line (where doxorubicin was used as a positive control) consequently indicating the role of endoperoxide linkage in cytotoxicity (**Figure 3**).^{5a-c} Literature reports^{5a-c} demonstrated that iron-activated artemisinin destroys cancer cells *via* forming highly alkylating carbon-centered radicals and reactive oxygen species (ROS) (**Figure 3**). It is proposed in the literature that endoperoxide bond is activated by ferrous ion which in turn generates carbon-centered radicals to destroy tumor

cells *via* apoptosis or necrosis pathway. Studies showed that activation of endoperoxide motifs in artemisinin (**1**) is due to free or protein confined ferrous ion (heme) (**Figure 3**). However, the involvement of endoperoxide linkage in cytotoxicity is still unclear unlike in malaria therapy where it is well defined with proper justification.^{5a-c}

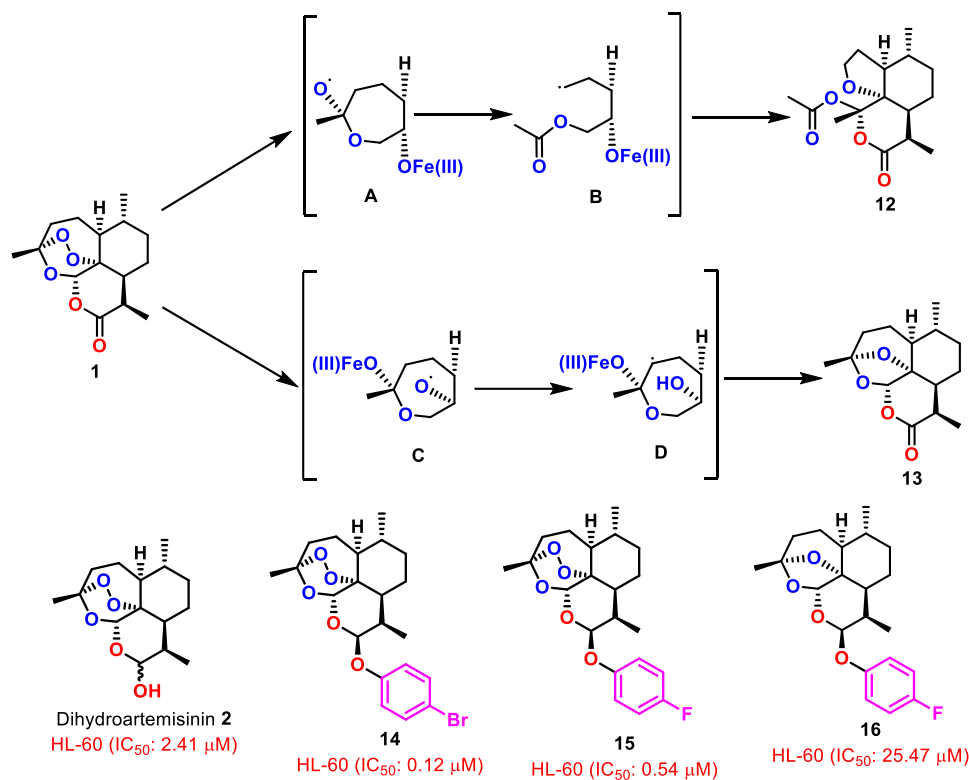


Figure 3: The proposed endoperoxide bridge assisted mechanism of the artemisinin **1** and dihydroartemisinin (**2**) and its synthetic derivatives (**14** and **15**) along with deoxydihydroartemisinin derivative (**16**) for cancer cells destruction

1.1.1.1 Glycoconjugates of natural products as new potent drugs

Glycoconjugates are biologically significant molecules as they gravitate towards intra and extra cellular processes, *i.e.* cell-cell interaction and cell-matrix interaction. It has been significantly demonstrated in literature that coupling of carbohydrate scaffold with natural products accelerates their biological process like solubility, stability and bioactivity consequently improving bioactivities profusely as compared to parent compound. All these properties of glycoconjugates are attributed to hypervalent nature of sugar scaffolds which aids in drug delivery to the desired destination.⁶ The glycoconjugates of natural products are well documented in literature with their bioassays (**Figure 4**).⁶⁻¹¹ Glycoconjugates of

isosteviol (**I**) (diterpenoid), with hexose and pentose sugars have shown cytotoxicity ranging from IC_{50} 1.7–1.9 μ M using anticancer drug doxorubicin with IC_{50} of 3.0 μ M as positive control.⁷ Artemisinic acid based glycoconjugates (**II**) displayed mild cytotoxicity when assayed against MCF7 tumor cells.⁸ Glycoconjugates of 8-hydroxy quinoline (**III**) were assayed for their cytotoxicity against HCT 116 and MCF-7 cell lines displaying the IC_{50} values in the range of 9 μ M to 0.02 μ M. These synthesised glycoconjugates of 8-hydroxy quinoline (**III**) have shown up to 72 % inhibition of β -1,4-galactosyltransferase exertion.⁹ Noscapine, an alkaloid isolated from *Papaver somniferum* was conjugated with different carbohydrate scaffolds to furnish noscapine derived glycoconjugates (**IV**).¹⁰ Glycosides and glycoconjugates of isoflavones (**V**) synthesised by various literature methods represent a new set of biologically important motifs.¹¹ These reports from various authors inspired us to synthesise artemisinin based glycoconjugates.⁶⁻¹¹

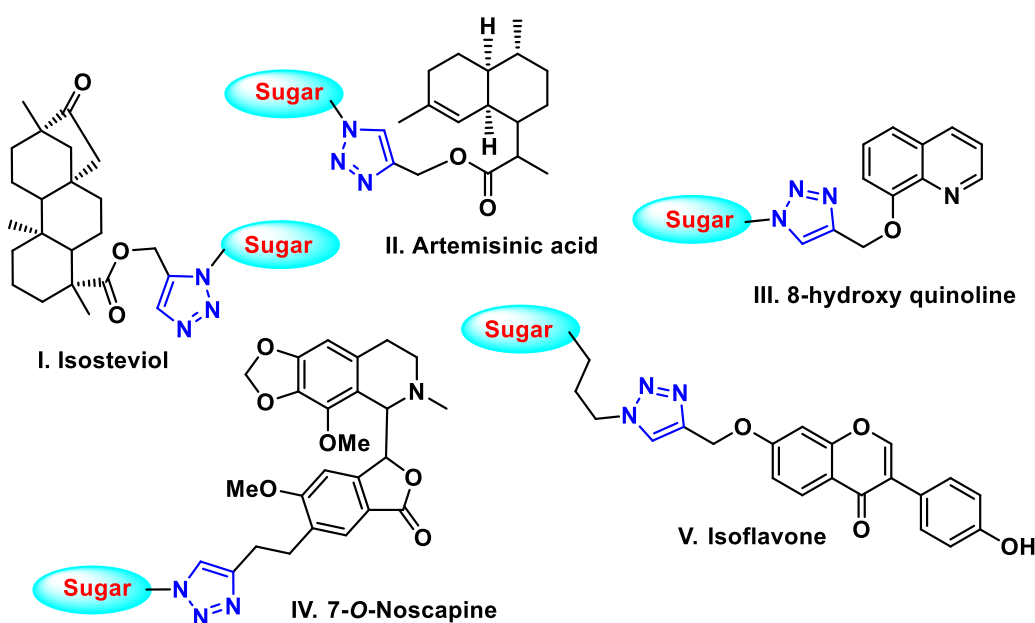


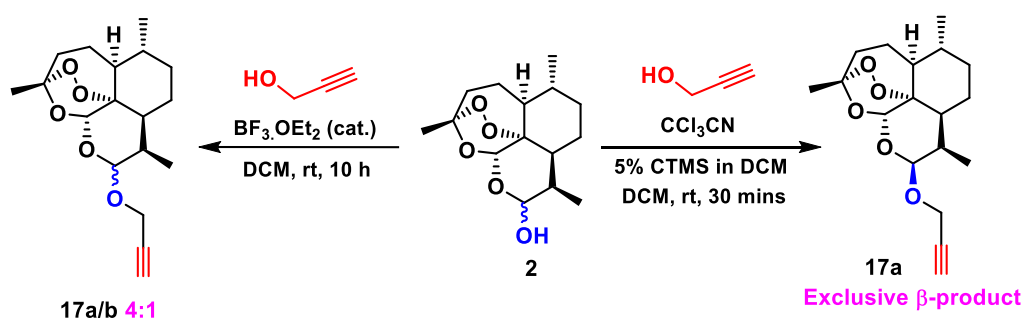
Figure 4: Reported glycoconjugates of natural products

1.1.2 Present work

In view of the emerging importance of the glycoconjugates and artemisinin derivatives we opined that artemisinin based glycoconjugates could prove to be significant class of biologically active molecules. In our present work, we have coupled propargylated dihydroartemisinin **17a** and azido sugars (**S1-9**) to furnish artemisinin derived

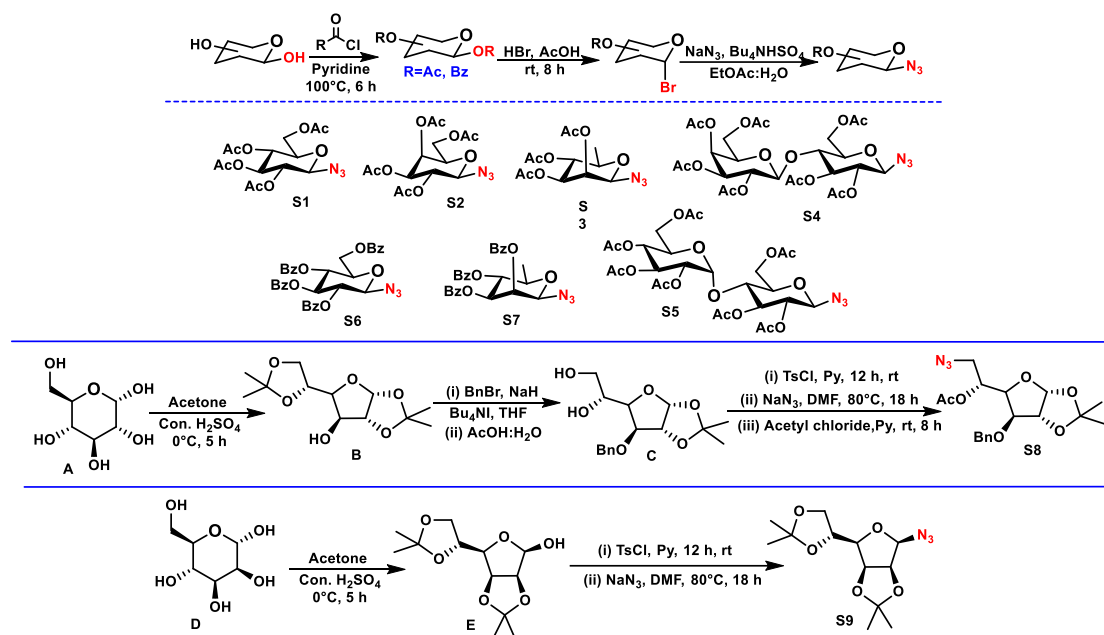
glycoconjugates employing Cu(I)-catalyzed click reaction as the coupling tool between artemisinin moiety and the carbohydrate scaffolds.^{12a,b,13a-d}

Initially, propargylation of dihydroartemisinin (**2**)^{14a,b} was carried out by reacting it with propargyl alcohol in DCM as solvent. $\text{BF}_3 \cdot \text{Et}_2\text{O}$ ¹⁵ was added as a catalyst at 0 °C to this reaction mixture and then it was stirred continuously at room temperature which resulted in the formation of diastereomeric mixture of β - and α -propargylated dihydroartemisinin (**17**) in the ratio of 4:1 (as evident from ^1H NMR spectra). To accomplish stereoselective synthesis of β -propargylated dihydroartemisinin (**17a**) we employed the method previously developed in our group.¹⁶ According to the previous reports, there is role of nitrile to achieve this β -stereoselectivity.^{17a,b} In this regard, dihydroartemisinin (**2**) was dissolved in DCM followed by addition of propargyl alcohol, trichloroacetonitrile and 5% of TMSCl in DCM (catalytic amount) at ambient temperature to furnish the exclusive β -propargylated dihydroartemisinin (**17a**) in good yield (Scheme 1).



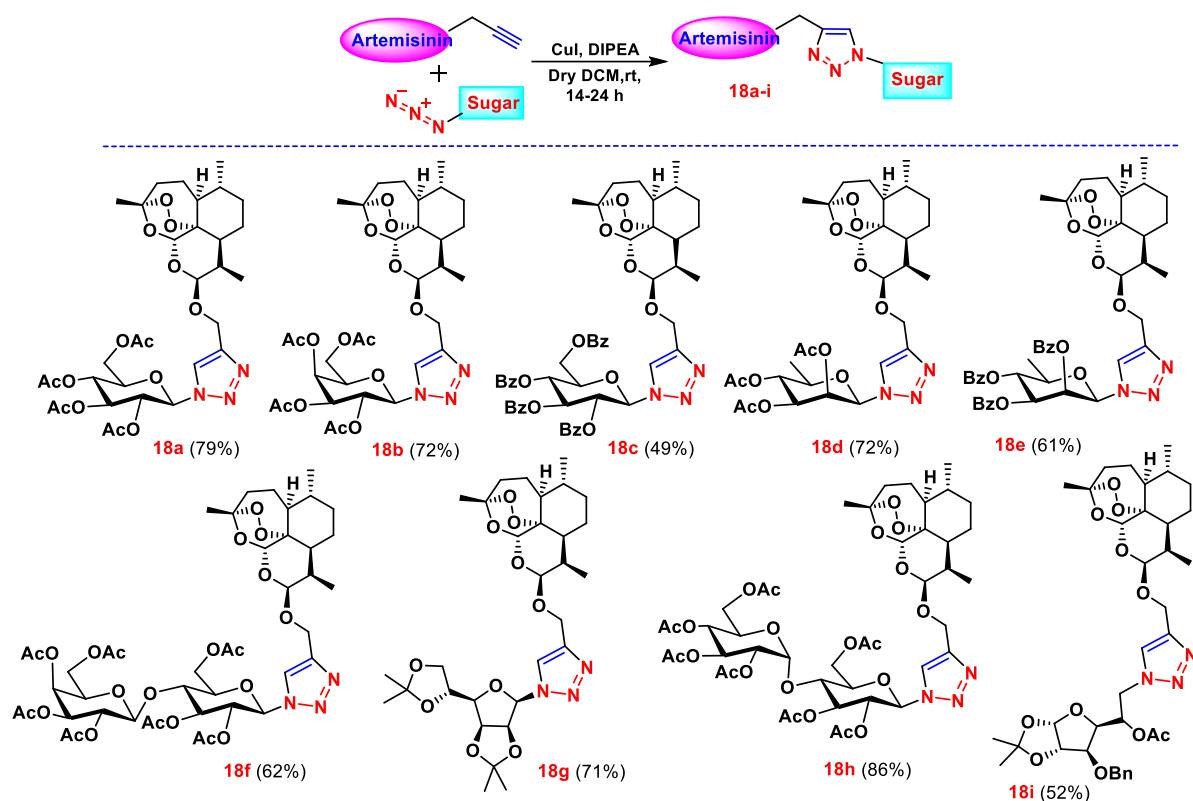
Scheme 1: Synthesis of 12-*O*-propargylated dihydroartemisinin (**17**)

Preparation of azido sugars were accomplished by following the literature methods and the data of all the synthesised azido sugars were in agreement with the published literature data.^{18a-d} We have synthesised tetra-*O*-acetyl azido glucose (**S1**), tetra-*O*-acetyl azido galactose (**S2**), triacetyl azido rhamnose (**S3**), hepta-*O*-acetyl azido lactose (**S4**), hepta-*O*-acetyl azido maltose (**S5**), tetra-*O*-benzoyl azido glucose (**S6**), tribenzoyl azido rhamnose (**S7**), 3-benzy 4,5 acetonide, acetyl azido furanose (**S8**) and 2,3,5,6-diacetonide azido furanose (**S9**) (Scheme 2). The stereochemistires of azido group were found to be β especially in case of hexose sugar azides as described in previous reports.^{6-11,18a-d}



Scheme 2: Synthesis of sugar azides (**S1-S9**)

The β -configurations of the sugar azides were also confirmed on the basis of their coupling constant in the ^1H NMR spectra as their anomeric proton showed a doublet in the range of 4.61–4.98 ppm with the value of coupling constant ranging from 8.5 Hz to 8.8 Hz. After the synthesis of starting materials, β -propargylated dihydroartemisinin (**17a**) and azido sugars (**S1-9**) were coupled *via* Click chemistry. We treated β -propargylated dihydroartemisinin (**17a**) with tetra-*O*-acetyl glucose azide (**S1**) in DCM using DIPEA as base and copper iodide (CuI) as catalyst to furnish desired glycoconjugate (**18a**) in good yield. Further, this reaction was extended to other synthesized azido sugars to obtain artemisinin derived glycoconjugates (**18b-18i**) in moderate to very good yields (**Table 1**).

Table 1: Substrate scope^{a,b}

^a Reaction conditions: propargylated β -dihydroartemisinin (**17a**) (30 mg, 0.0929 mmol, 1 equiv.), azido sugars (**S1-9**) (0.1115 mmol, 1.2 equiv.), DCM (3 mL), CuI (8.9 mg, 0.0465 mmol, 0.5 equiv.), and DIPEA (16 mL, 0.0929 mmol, 1.0 equiv.). ^b Isolated yield.

The formation of triazoles was confirmed by the only proton present on triazole ring which appeared as a singlet in the range of 7.5-8.5 ppm, thus confirming the product formation. The characteristic peaks of artemisinin were also well marked in the aliphatic region of ¹H NMR spectra. The triazoles were also found to be having β -orientations which was evident from the coupling constant of the anomeric proton in the ¹H NMR spectra of the glycoconjugates (**18a-18i**). It is pertinent to mention here that the highest yield was observed in case of hepta-*O*-acetyl maltose glycoconjugate (**18h**) (86%), whereas in the case of hepta-*O*-acetyl lactose glycoconjugate (**18f**) (62%) yield was moderate. It was also noticed that the yields of benzoate protected sugars derived artemisinin glycoconjugates (**18c** and **18i**) were low as compared to the acetyl protected sugars derived artemisinin glycoconjugates (**18a**, **18b**, **18d**, **18f** and **18h**). Reaction proceeded slowly in case of pentose sugars (**18g** and **18i**) *i.e.* 24 hours as compared to the hexose sugars (**18a-18f** and **18h**) which took 14 hours to complete the reaction. The diacetonide furanose artemisinin glycoconjugate (**18g**) gave better yield (71%) than mono acetonide furanose sugar based artemisinin glycoconjugate (**18i**) (52%). Apart

from this all the artemisinin glycoconjugates (**18-18i**) furnished single diastereomers which is evident from their ^1H NMR spectra. A postulated reaction mechanism for this coupling reaction is given below (**Figure 5**).^{12a,b,13a-d}

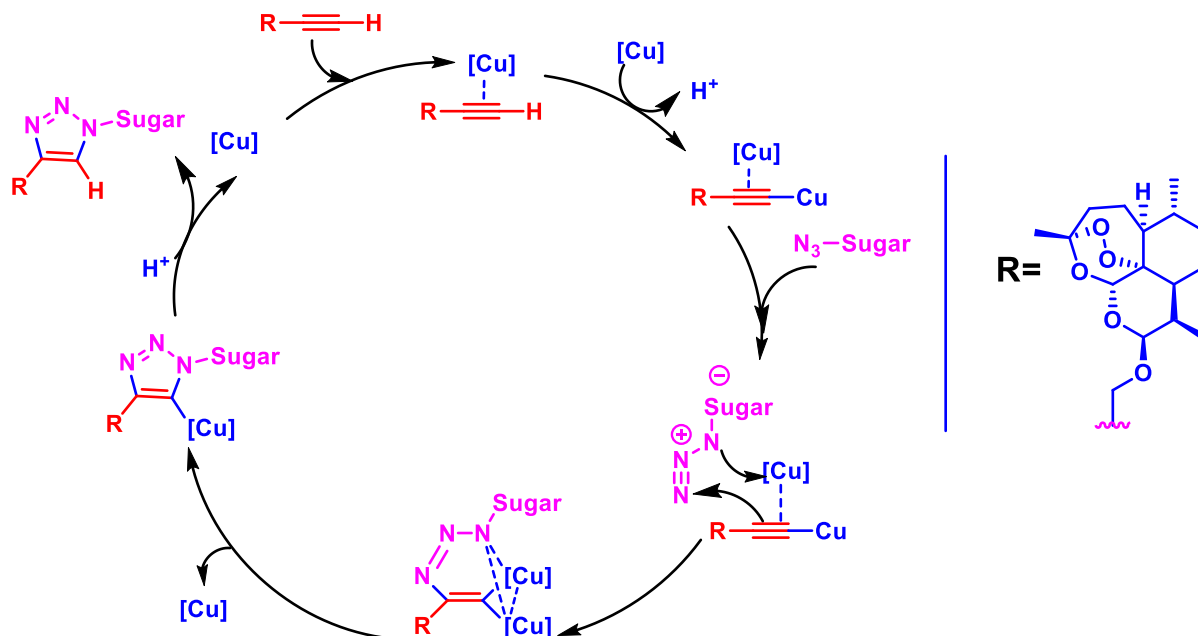


Figure 5: Plausible mechanism for formation of artemisinin glycoconjugates

1.1.3 Conclusions

In summary, we have accomplished synthesis of artemisinin based glycoconjugates in very good to moderate yields by employing Huisgen's 1,3-dipolar cycloaddition reactions between β -propargylated dihydroartemisinin and various sugar azides. We have synthesised exclusively β -propargylated dihydroartemisinin by utilizing method developed by our group. At present their anti-cancer activities are being pursued.

1.2.4 Experimental procedures

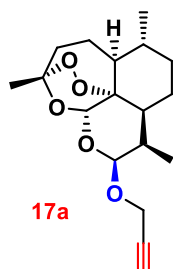
General procedure for the reduction of artemisinin (1) to dihydroartemisinin (2):

To a stirred solution of artemisinin (1) (3 g, 10.64 mmol) in methanol (30 mL), sodium borohydride (1.2 g, 31.92 mmol) was added at 0 °C over a period of 20 min in small quantities. After being stirred for an additional period of 1 h under the same reaction conditions, the mixture was neutralized with glacial acetic acid while the temperature was maintained at 0–5 °C with the pH adjusted to 6–7. Then the reaction mixture was concentrated under reduced pressure. The residue was poured into water (40 mL). The solid product formed was collected *via* filtration, washed with water and dried, furnishing compound 2 in 84% yield as a colourless solid whose spectral data was found to be identical to the reported data.⁸

General procedure for the propargylation of dihydroartemisinin (17a):

Compound 2 (100 mg, 0.35 mmol) was taken in a 50 mL round bottom flask and dissolved in dry DCM (3 mL) at room temperature. Then CCl₃CN (0.5 mL, 5 mmol, 14.2 equiv.), propargyl alcohol (0.5 mL) and TMSCl (5% in CH₂Cl₂, 1.0 mL, 0.039 mmol) were added to the stirred solution, and the reaction mixture was stirred at room temperature. The completion of the reaction was monitored via TLC, then the reaction mixture was filtered through Celite and the filtrate was evaporated in vacuo. The residue was purified via flash chromatography using a RediSep column (silica gel, 12 g) with 5–15% EtOAc in petroleum ether and the pure product was obtained in 75% yield as a colourless solid.

Artemisinin-12-β-O-propargyl (17a):



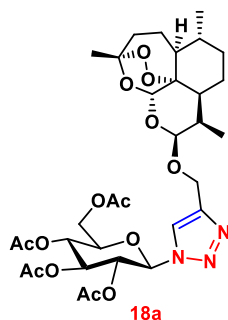
Colourless solid (85 mg, 75%); m.p.: 106–108 °C; R_f = 0.83 (40% ethyl acetate in petroleum ether); $[\alpha]_D^{25}$: +252.7 (c 2.5, CHCl₃); ¹H NMR (200 MHz, CDCl₃) δ_H 5.42 (s, 1H), 4.98 (d, J = 3.5 Hz, 1H), 4.31 (d, J = 2.4 Hz, 2H), 2.76–2.57 (m, 1H), 2.46–2.29 (m, 2H), 2.11–2.02 (m,

1H), 1.82–1.68 (m, 2H), 1.65–1.56 (m, 2H), 1.56–1.36 (m, 6H), 1.33–1.21 (m, 2H), 0.94 (d, $J = 2.7$ Hz, 3H), 0.94 (d, $J = 10.7$ Hz, 3H); ^{13}C NMR (50 MHz, CDCl_3) δ_{C} 104.2, 100.6, 88.1, 81.1, 79.8, 74.0, 55.0, 52.6, 44.4, 37.4, 36.4, 34.6, 30.6, 26.1, 24.7, 24.5, 20.3, 12.8; HRMS: m/z for $\text{C}_{18}\text{H}_{26}\text{O}_5\text{Na}$ ($\text{M} + \text{Na}$) $^+$, calcd: 345.1283, found: 345.1345.

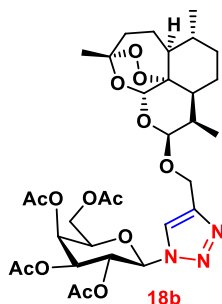
General procedure for the coupling of azido sugar (S1-S9) with propargylated dihydroartemisinin (17a)

To a stirred solution of **17a** (30 mg, 0.0929 mmol) in anhydrous DCM (3 mL), azido sugar (**S1-S9**, 0.1115 mmol, 1.2 equiv.), CuI (8.9 mg, 0.0465 mmol, 0.5 equiv.) and DIPEA (16 mL, 0.0929 mmol, 1.0 equiv.) were added, and the mixture was stirred at room temperature for 14–24 hours under an inert atmosphere. After the completion of the reaction (TLC), the reaction mixture was concentrated in vacuo to obtain the crude product, which was purified using silica gel (230–400) flash column chromatography (EtOAc/ pet. ether) to furnish the desired artemisinin glycoconjugate (**18a-i**).

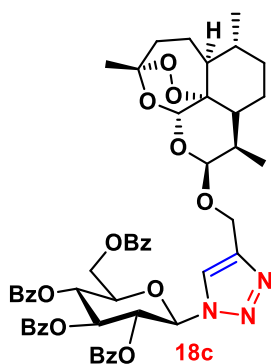
Compound 18a:



Colourless solid (51 mg, 79%); m.p.: 170–172 $^{\circ}\text{C}$; $[\alpha]_{\text{D}}^{25} +44.2$ (c 0.4, CHCl_3); $R_{\text{f}} = 0.19$ (40% ethyl acetate in petroleum ether); ^1H NMR (200 MHz, CDCl_3) δ_{H} 7.74 (s, 1H), 5.91–5.85 (m, 1H), 5.48 (s, 1H), 5.46–5.39 (m, 2H), 4.93–4.83 (m, 2H), 4.77–4.65 (m, 1H), 4.29 (d, $J = 4.8$ Hz, 1H), 4.19 (d, $J = 2.0$ Hz, 1H), 2.1–2.02 (m, 11H), 1.87 (s, 4H), 1.79–1.68 (m, 2H), 1.64–1.60 (m, 3H), 1.46 (s, 4H), 1.27 (dd, $J = 6.6, 10.2$ Hz, 2H), 0.92 (dd, $J = 6.8, 10.4$ Hz, 7H); ^{13}C NMR (50 MHz, CDCl_3) δ_{C} 170.5, 169.9, 169.4, 168.8, 153.2, 134.2, 120.7, 104.2, 101.4, 88.0, 85.8, 81.2, 75.2, 72.7, 70.3, 67.7, 61.6, 61.2, 52.6, 44.4, 37.3, 36.5, 34.6, 30.8, 26.2, 24.7, 24.4, 20.7, 20.5, 20.4, 20.1, 12.9, 4.5, 3.4; HRMS: m/z for $\text{C}_{32}\text{H}_{46}\text{O}_{14}\text{N}_3$ ($\text{M} + \text{H}$) $^+$, calcd: 696.2974, found: 696.2968; m/z for $\text{C}_{32}\text{H}_{45}\text{O}_{14}\text{N}_3\text{Na}$ ($\text{M} + \text{Na}$) $^+$, calcd: 718.2794, found: 718.2787.

Compound 18b:

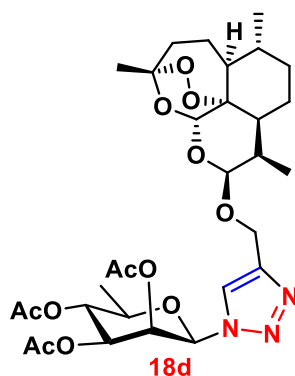
Colourless solid (47 mg, 72%); m.p: 143-145 1°C; $[\alpha]_{D^{25}} +44.7$ (*c* 0.4, CHCl₃); $R_f = 0.16$ (40% ethyl acetate in petroleum ether); ¹H NMR (500 MHz, CDCl₃) δ_H 7.79 (s, 1H), 5.84 (d, *J* = 9.2 Hz, 1H), 5.58–5.54 (m, 2H), 5.50 (s, 1H), 5.25 (dd, *J* = 3.4, 10.3 Hz, 1H), 4.93 (d, *J* = 12.6 Hz, 1H), 4.89 (d, *J* = 3.4 Hz, 1H), 4.70 (d, *J* = 12.6 Hz, 1H), 4.25–4.13 (m, 3H), 2.69–2.62 (m, 1H), 2.38 (dt, *J* = 4.0, 14.0 Hz, 1H), 2.23 (s, 3H), 2.05 (s, 3H), 2.02 (s, 3H), 1.88 (s, 3H), 1.80–1.71 (m, 2H), 1.64–1.59 (m, 4H), 1.46 (s, 3H), 1.25 (s, 4H), 0.95 (d, *J* = 6.5 Hz, 3H), 0.88 (d, *J* = 7.2 Hz, 3H); ¹³C NMR (126 MHz, CDCl₃) δ_C 169.8, 145.5, 121.0, 104.2, 100.8, 88.1, 86.2, 81.2, 74.1, 70.8, 67.7, 66.9, 61.2, 60.6, 52.6, 44.4, 37.3, 36.4, 34.7, 30.7, 29.7, 26.2, 24.7, 24.4, 20.7, 20.5, 20.4, 20.2, 12.9; HRMS: *m/z* for C₃₂H₄₆O₁₄N₃ (M + H)⁺, calcd: 696.2974, found: 696.2968; *m/z* for C₃₂H₄₅O₁₄N₃Na (M + Na)⁺, calcd: 718.2794, found: 718.2786.

Compound 18c:

Colourless solid (43 mg, 49%); m.p.: 156-158 1°C; $[\alpha]_{D^{25}} +43.4$ (*c* 0.5, CHCl₃); $R_f = 0.48$ (40% ethyl acetate in petroleum ether); ¹H NMR (400 MHz, CDCl₃) δ_H 8.03 (d, *J* = 7.9 Hz, 2H), 7.98–7.90 (m, 3H), 7.83 (d, *J* = 7.3 Hz, 2H), 7.78 (d, *J* = 7.9 Hz, 2H), 7.63–7.50 (m, 3H), 7.45 (d, *J* = 7.9 Hz, 2H), 7.43–7.28 (m, 7H), 6.29 (d, *J* = 9.8 Hz, 1H), 6.16–6.10 (m,

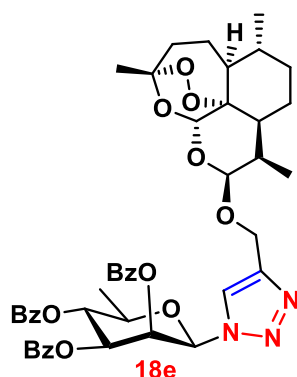
1H), 6.00–5.86 (m, 2H), 5.49 (s, 1H), 4.96–4.86 (m, 2H), 4.73–4.66 (m, 2H), 4.59–4.46 (m, 2H), 2.70–2.58 (m, 1H), 2.39 (dt, $J = 4.0, 13.9$ Hz, 1H), 2.07 (s, 1H), 1.92–1.83 (m, 1H), 1.73 (dd, $J = 4.0, 7.6$ Hz, 2H), 1.66–1.52 (m, 3H), 1.47 (s, 2H), 1.32–1.24 (m, 4H), 0.94 (d, $J = 6.1$ Hz, 3H), 0.84 (d, $J = 7.3$ Hz, 3H); ^{13}C NMR (101 MHz, CDCl_3) δ_{C} 166.0, 165.6, 165.1, 164.7, 146.0, 133.7, 133.5, 133.3, 129.9, 129.8, 129.7, 129.3, 128.5, 128.4, 128.4, 127.9, 120.8, 104.1, 101.6, 88.0, 86.1, 81.2, 75.5, 73.0, 71.0, 68.9, 62.7, 61.5, 60.4, 52.6, 44.4, 37.2, 36.5, 34.6, 31.9, 30.8, 29.7, 26.2, 24.6, 24.4, 21.1, 20.4, 14.2, 12.9; HRMS: m/z for $\text{C}_{52}\text{H}_{54}\text{O}_{14}\text{N}_3$ ($\text{M} + \text{H}$) $^+$, calcd: 944.3600, found: 944.3600; m/z for $\text{C}_{52}\text{H}_{53}\text{O}_{14}\text{N}_3\text{Na}$ ($\text{M} + \text{Na}$) $^+$, calcd: 966.3420, found: 966.3414.

Compound 18d.



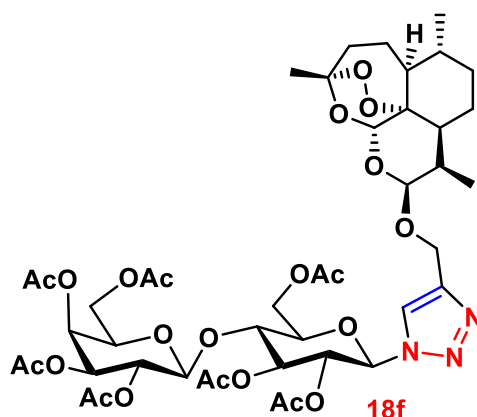
Colourless solid (43 mg, 72%); m.p.: 152–154 $^{\circ}\text{C}$; $[\alpha]_{\text{D}}^{25} +53.6$ (c 0.6, CHCl_3); $R_{\text{f}} = 0.32$ (40% ethyl acetate in petroleum ether); ^1H NMR (200 MHz, CDCl_3) δ_{H} 7.72 (s, 1H), 6.15–6.07 (m, 1H), 5.74–5.66 (m, 1H), 5.44 (s, 1H), 5.23–5.18 (m, 2H), 5.01–4.86 (m, 2H), 4.62 (d, $J = 12.5$ Hz, 1H), 3.83 (dd, $J = 6.3, 9.0$ Hz, 1H), 2.67 (dt, $J = 3.5, 7.2$ Hz, 1H), 2.45–2.29 (m, 1H), 2.09 (d, $J = 2.7$ Hz, 6H), 2.00 (s, 3H), 1.95–1.80 (m, 2H), 1.80–1.64 (m, 4H), 1.63–1.47 (m, 4H), 1.45 (s, 4H), 1.36 (d, $J = 6.1$ Hz, 3H), 1.26 (s, 3H), 0.91 (dd, $J = 6.6, 8.8$ Hz, 8H); ^{13}C NMR (50 MHz, CDCl_3) δ_{C} 208.0, 204.6, 165.6, 133.7, 133.4, 129.8, 128.9, 128.6, 128.3, 71.6, 70.6, 70.0, 69.6, 56.3, 52.4, 45.4, 41.1, 34.4, 31.9, 30.3, 29.7, 22.7, 20.6, 20.1, 17.9, 14.1, 11.0; HRMS: m/z for $\text{C}_{30}\text{H}_{44}\text{O}_{12}\text{N}_3$ ($\text{M} + \text{H}$) $^+$, calcd: 638.2920, found: 638.2913.

Compound 18e:



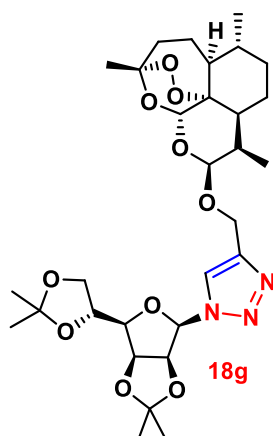
Colourless solid (47 mg, 61%); m.p.: 145-148 1°C; $[\alpha]_{\text{D}}^{25}$: -136.4 (c 0.17, CHCl_3); $R_f = 0.55$ (40% ethyl acetate in petroleum ether); $^1\text{H NMR}$ (500 MHz, CDCl_3) δ_{H} 8.06–7.94 (m, 4H), 7.83–7.74 (m, 3H), 7.68–7.63 (m, 1H), 7.57–7.49 (m, 3H), 7.45–7.38 (m, 4H), 7.24 (t, $J = 7.8$ Hz, 2H), 6.45 (brs, 1H), 6.20 (brs, 1H), 5.83–5.71 (m, 2H), 5.37–5.29 (m, 1H), 5.22–5.12 (m, 1H), 4.71 (brs, 1H), 4.12 (q, $J = 7.2$ Hz, 4H), 2.50–2.42 (m, 1H), 2.37–2.29 (m, 1H), 2.19–2.14 (m, 2H), 2.07–2.03 (m, 7H), 1.99 (s, 1H), 1.53 (d, $J = 6.1$ Hz, 4H), 1.42 (s, 5H), 0.61 (d, $J = 7.2$ Hz, 3H); $^{13}\text{C NMR}$ (126 MHz, CDCl_3) δ_{C} 171.2, 165.6, 165.4, 164.4, 134.0, 133.6, 133.4, 129.8, 128.9, 128.8, 128.6, 128.3, 104.1, 101.4, 87.9, 87.5, 85.2, 81.0, 74.4, 71.7, 70.6, 70.5, 70.0, 69.5, 68.6, 68.3, 61.4, 60.4, 52.5, 44.3, 37.2, 36.4, 34.5, 30.6, 29.7, 26.1, 24.6, 24.1, 21.1, 20.3, 17.9, 14.2, 12.8; HRMS: m/z for $\text{C}_{45}\text{H}_{50}\text{O}_{12}\text{N}_3$ ($\text{M} + \text{H}$) $^+$, calcd: 824.3389, found: 824.3384; m/z for $\text{C}_{45}\text{H}_{49}\text{O}_{12}\text{N}_3\text{Na}$ ($\text{M} + \text{Na}$) $^+$, calcd: 846.3208, found: 846.3196.

Compound 18f:



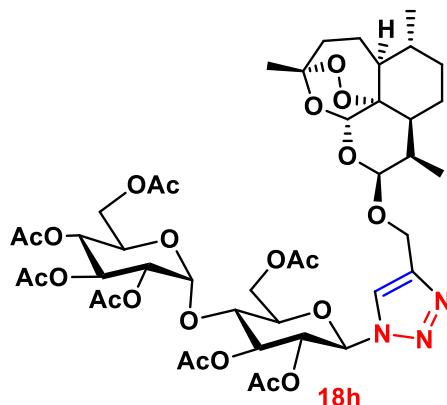
Colourless solid (57 mg, 62%); m.p.: 73-76 1°C; $[\alpha]_{\text{D}}^{25}$: -4.4 (c 0.66, CHCl_3); $R_f = 0.83$ (40% ethyl acetate in petroleum ether); $^1\text{H NMR}$ (500 MHz, CDCl_3) δ_{H} 7.67 (s, 1H), 5.85 (d,

$J = 8.8\text{Hz}$, 1H), 5.48 (s, 1H), 5.44–5.37 (m, 3H), 5.14 (dd, $J = 8.0, 10.3\text{ Hz}$, 1H), 4.98 (dd, $J = 3.4, 10.3\text{ Hz}$, 1H), 4.95–4.87 (m, 2H), 4.68 (d, $J = 12.6\text{ Hz}$, 1H), 4.56–4.47 (m, 2H), 4.19–4.08 (m, 6H), 4.00–3.86 (m, 4H), 2.65 (td, $J = 4.0, 7.2\text{Hz}$, 1H), 2.38 (dt, $J = 3.8, 14.1\text{ Hz}$, 1H), 2.17 (s, 3H), 2.12 (s, 3H), 2.08 (s, 3H), 2.07 (d, $J = 3.4\text{Hz}$, 6H), 2.04 (s, 3H), 1.98 (s, 3H), 1.86 (s, 4H), 1.45 (s, 3H), 1.26 (t, $J = 7.1\text{ Hz}$, 4H), 0.95 (d, $J = 6.5\text{ Hz}$, 3H), 0.88 (d, $J = 7.2\text{ Hz}$, 3H); ^{13}C NMR (126 MHz, CDCl_3) δ_{C} 171.1, 170.3, 170.2, 170.1, 170.0, 169.4, 169.1, 145.6, 120.7, 116.4, 111.0, 104.1, 101.1, 101.1, 88.0, 85.5, 81.1, 75.9, 75.6, 72.6, 70.9, 70.8, 70.5, 69.0, 66.6, 61.7, 61.0, 60.8, 60.4, 52.5, 44.3, 37.3, 36.4, 34.6, 30.7, 26.1, 24.6, 24.4, 21.0, 20.8, 20.7, 20.6, 20.5, 20.3, 20.2, 14.2, 12.9; HRMS: m/z for $\text{C}_{44}\text{H}_{62}\text{O}_{22}\text{N}_3$ ($\text{M} + \text{H}$) $^+$, calcd: 984.3819, found: 984.3806; m/z for $\text{C}_{44}\text{H}_{62}\text{O}_{22}\text{N}_3\text{Na}$ ($\text{M} + \text{Na}$) $^+$, calcd: 1006.3639, found: 1006.3624.

Compound 18g:

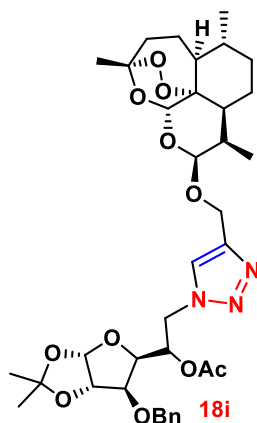
Colourless solid (40 mg, 71%); m.p.: 135–140 $^{\circ}\text{C}$; $[\alpha]_{\text{D}}^{25}$: +68.6 (c 0.4, CHCl_3); $R_{\text{f}} = 0.24$ (40% ethyl acetate in petroleum ether); ^1H NMR (200 MHz, CDCl_3) δ_{H} 7.82 (s, 1H), 6.09 (d, $J = 3.4\text{ Hz}$, 1H), 5.49 (s, 1H), 5.04–4.83 (m, 5H), 4.69 (d, $J = 12.6\text{ Hz}$, 1H), 4.56–4.44 (m, 1H), 4.19–4.03 (m, 2H), 3.77 (dd, $J = 3.5, 7.7\text{ Hz}$, 1H), 2.66 (dd, $J = 3.7, 7.8\text{ Hz}$, 1H), 2.47–2.30 (m, 1H), 2.16–1.96 (m, 2H), 1.82–1.66 (m, 4H), 1.55 (s, 3H), 1.46 (d, $J = 2.3\text{ Hz}$, 6H), 1.40 (s, 3H), 1.35 (s, 3H), 1.25 (s, 3H), 0.95 (d, $J = 5.9\text{Hz}$, 3H), 0.89 (s, 3H); ^{13}C NMR (50 MHz, CDCl_3) δ_{C} 113.8, 109.6, 104.2, 101.1, 88.8, 88.0, 81.1, 79.7, 79.2, 72.7, 66.9, 61.3, 52.6, 44.4, 37.4, 36.4, 34.6, 30.8, 29.7, 27.0, 26.2, 25.5, 25.2, 24.7, 24.5, 24.1, 20.3, 13.0; HRMS: m/z for $\text{C}_{30}\text{H}_{46}\text{O}_{10}\text{N}_3$ ($\text{M} + \text{H}$) $^+$, calcd: 608.3175, found: 608.3178; m/z for $\text{C}_{30}\text{H}_{45}\text{O}_{10}\text{N}_3\text{Na}$ ($\text{M} + \text{Na}$) $^+$, calcd: 630.2997, found: 630.2990.

Compound 18h.



Colourless solid (78 mg, 86%); m.p.: 160-165 °C; $[\alpha]_{\text{D}}^{25}$: +85.8 (*c* 1, CHCl₃); R_{f} = 0.54 (40% ethyl acetate in petroleum ether); ¹H NMR (200 MHz, CDCl₃) δ_{H} 7.65 (s, 1H), 5.90 (d, *J* = 9.2 Hz, 1H), 5.53–5.27 (m, 5H), 5.08 (t, *J* = 9.9 Hz, 1H), 4.98–4.84 (m, 3H), 4.76–4.60 (m, 1H), 4.58–4.43 (m, 1H), 4.33–4.08 (m, 4H), 4.06–3.91 (m, 2H), 2.65 (td, *J* = 3.8, 7.3 Hz, 1H), 2.45–2.29 (m, 1H), 2.13 (d, *J* = 5.1 Hz, 6H), 2.07 (s, 3H), 2.04 (d, *J* = 1.1 Hz, 6H), 2.02 (brs, 3H), 1.84 (s, 3H), 1.79–1.50 (m, 7H), 1.45 (s, 3H), 1.36–1.18 (m, 3H), 0.94 (d, *J* = 5.9 Hz, 3H), 0.87 (d, *J* = 7.3 Hz, 3H); ¹³C NMR (50 MHz, CDCl₃) δ_{C} 170.6, 170.3, 169.9, 169.4, 169.1, 104.2, 101.3, 100.6, 95.9, 88.0, 81.1, 75.4, 75.2, 74.0, 72.4, 70.9, 70.0, 69.2, 68.8, 68.0, 61.5, 55.0, 52.6, 44.4, 37.4, 37.3, 36.4, 34.6, 30.7, 29.7, 26.2, 24.7, 24.5, 20.8, 20.6, 20.4, 20.1, 12.9; HRMS: *m/z* for C₄₄H₆₁O₂₂N₃Na (M + Na)⁺, calcd: 1006.3639, found: 1006.3633.

Compound 18i:



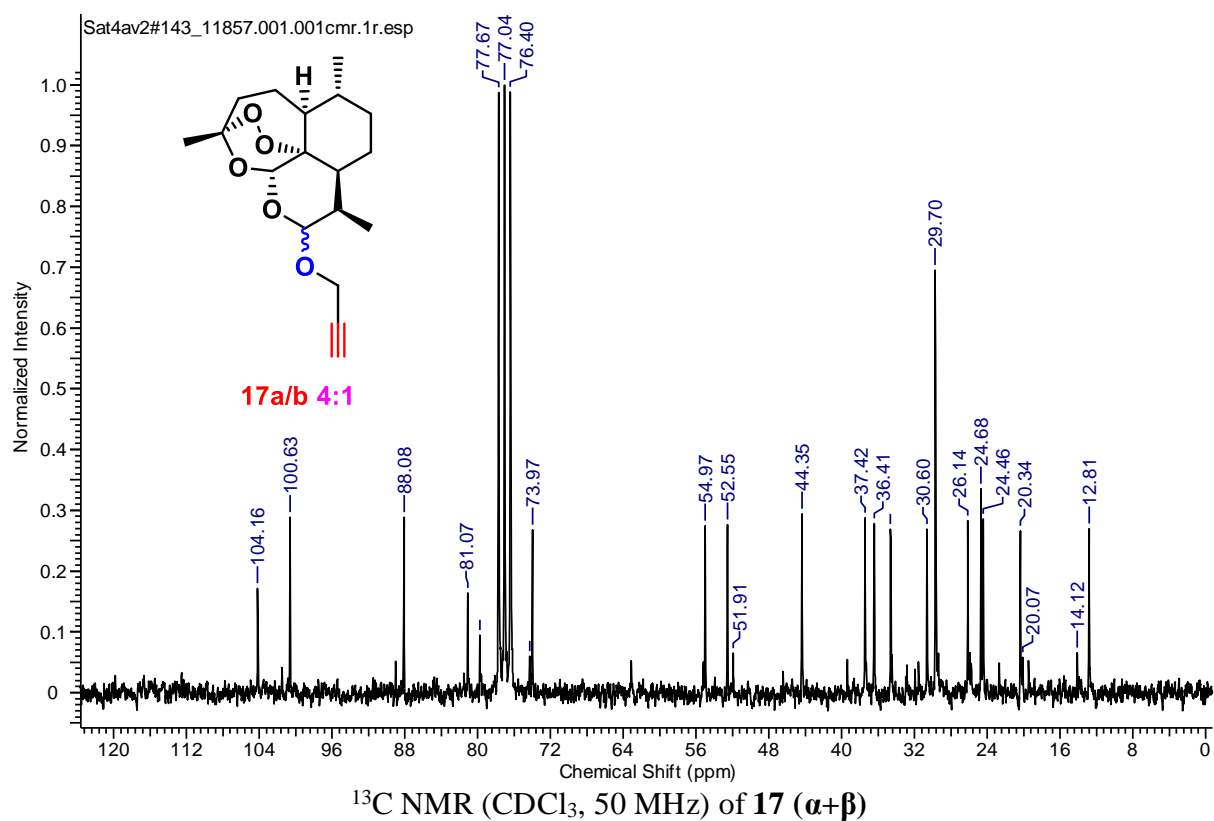
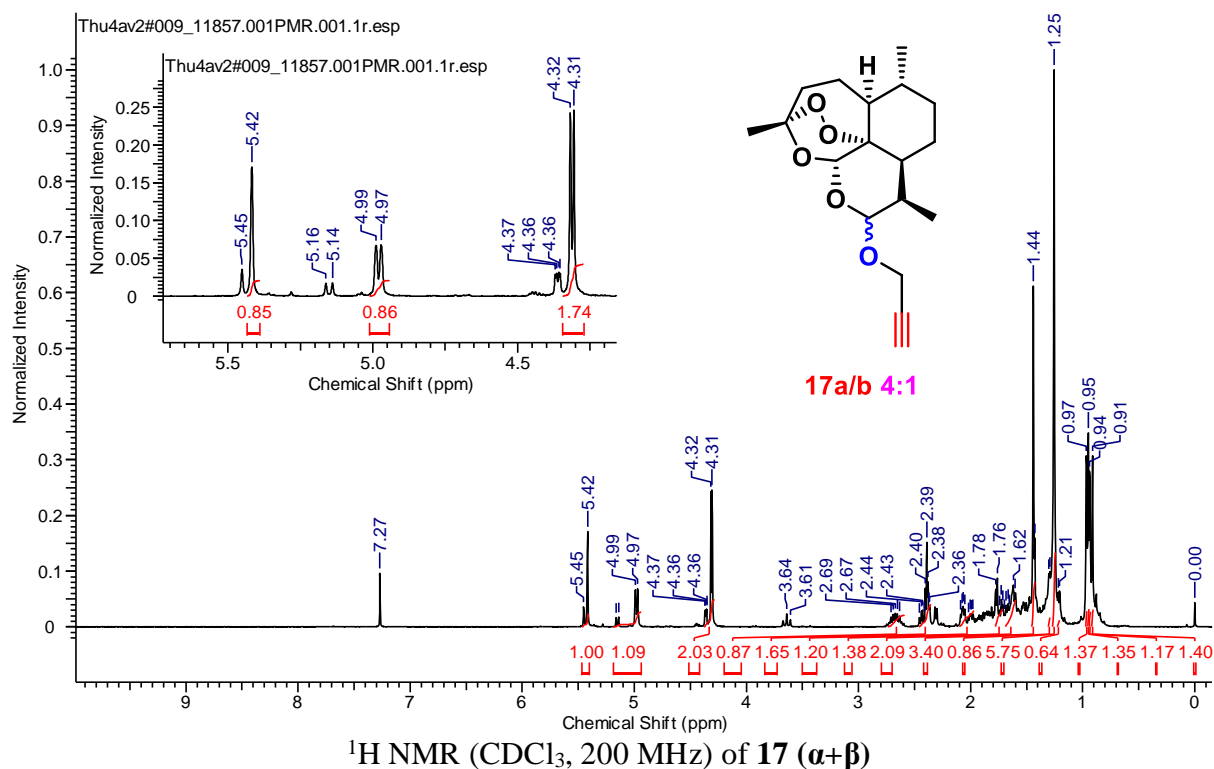
Yellow semi-solid (33 mg, 52%); $[\alpha]_{\text{D}}^{25}$: +79.2 (*c* 0.3, CHCl_3); R_f = 0.43 (40% ethyl acetate in petroleum ether); ^1H NMR (400 MHz, CDCl_3) δ_{H} 7.56 (s, 1H), 7.37–7.28 (m, 5H), 5.96 (d, J = 3.7 Hz, 1H), 5.46 (s, 1H), 5.43–5.37 (m, 1H), 4.98–4.89 (m, 3H), 4.68–4.63 (m, 2H), 4.61–4.55 (m, 2H), 4.43 (d, J = 11.6 Hz, 1H), 3.97 (dd, J = 2.7, 8.2 Hz, 1H), 3.91 (d, J = 3.1 Hz, 1H), 2.69–2.61 (m, 1H), 2.37 (dt, J = 3.7, 14.0 Hz, 1H), 2.07–1.99 (m, 2H), 1.80–1.68 (m, 3H), 1.59 (dd, J = 3.1, 12.8 Hz, 2H), 1.44 (s, 3H), 1.42 (s, 3H), 1.33 (s, 3H), 1.26 (brs, 3H), 0.93 (d, J = 6.1 Hz, 3H), 0.87 (d, J = 7.3 Hz, 3H); ^{13}C NMR (101 MHz, CDCl_3) δ_{C} 221.6, 220.7, 218.5, 180.8, 169.5, 167.1, 163.0, 160.9, 150.2, 144.8, 143.5, 136.6, 132.3, 128.7, 128.4, 128.3, 123.7, 123.3, 112.3, 105.1, 104.1, 101.4, 92.6, 88.0, 81.8, 81.1, 80.2, 78.5, 77.8, 77.0, 72.1, 68.2, 63.9, 61.4, 52.6, 50.0, 45.4, 44.4, 37.3, 36.4, 34.6, 30.8, 29.7, 26.7, 26.3, 26.2, 25.4, 24.7, 24.4, 20.8, 20.3, 13.0, 6.6; HRMS: m/z for $\text{C}_{36}\text{H}_{50}\text{O}_{11}\text{N}_3$ ($\text{M} + \text{H}$)⁺, calcd: 700.3440, found: 700.3432; m/z for $\text{C}_{36}\text{H}_{49}\text{O}_{11}\text{N}_3$ ($\text{M} + \text{Na}$)⁺, calcd: 722.3259, found: 722.3245. s

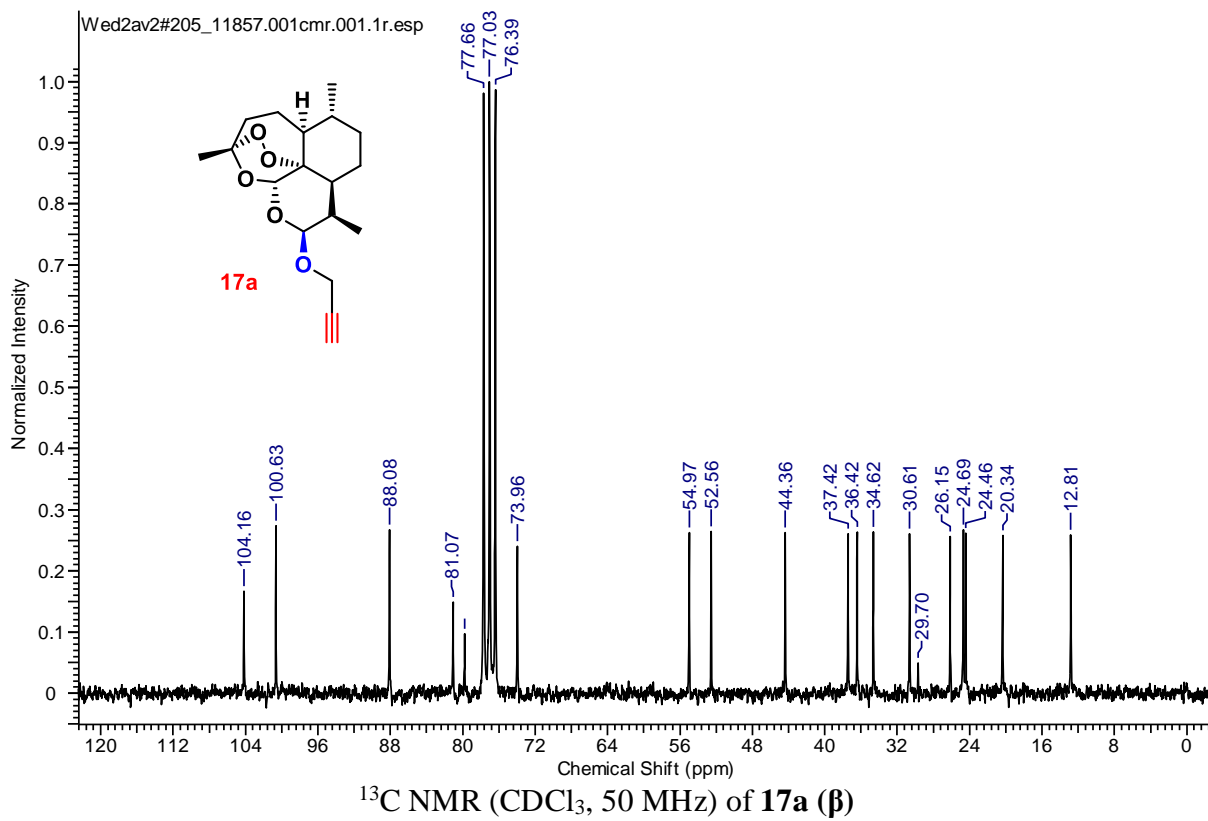
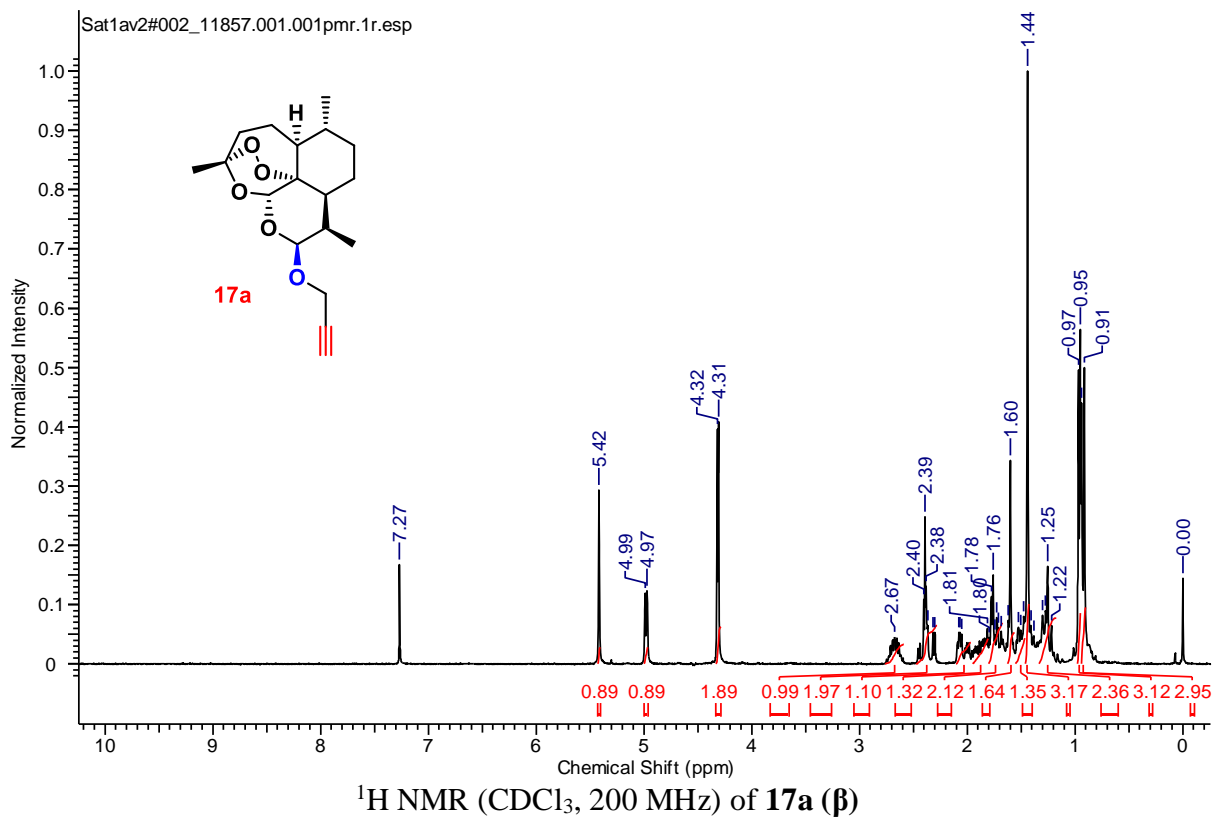
1.2.5 References:

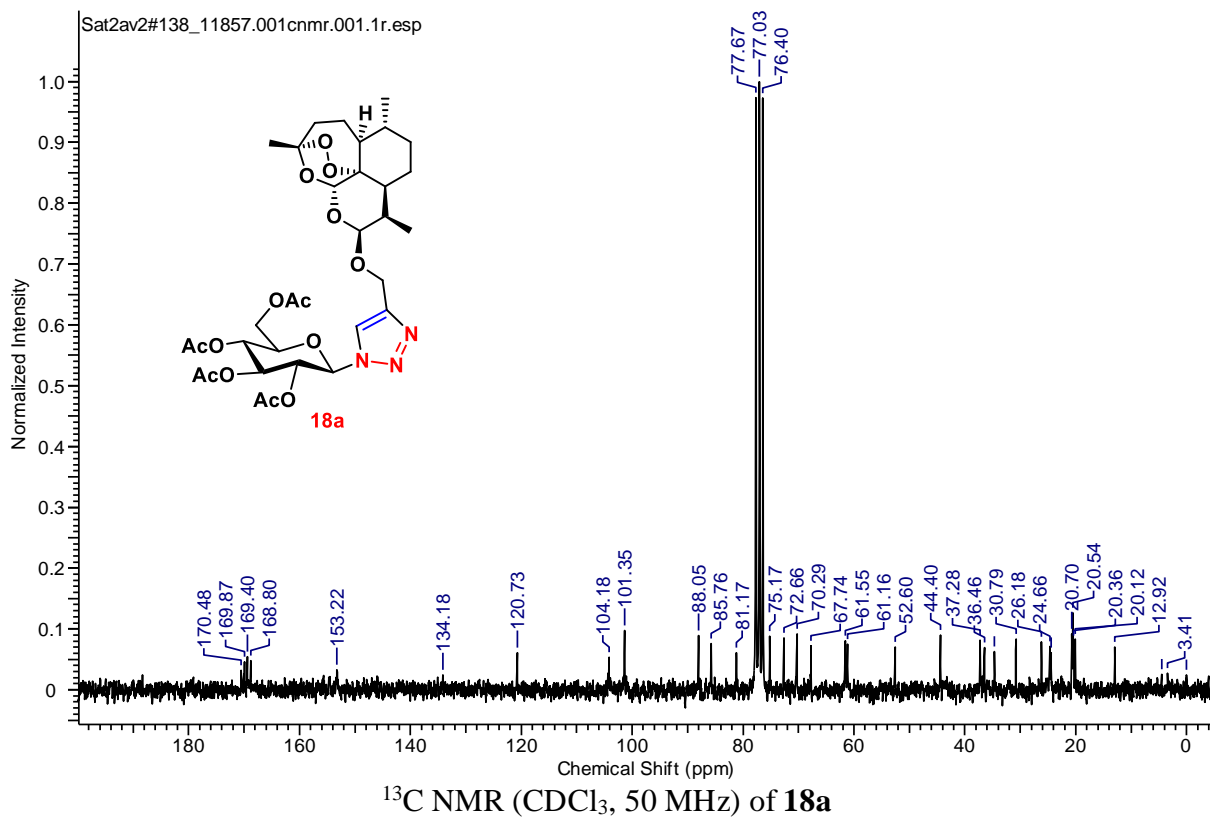
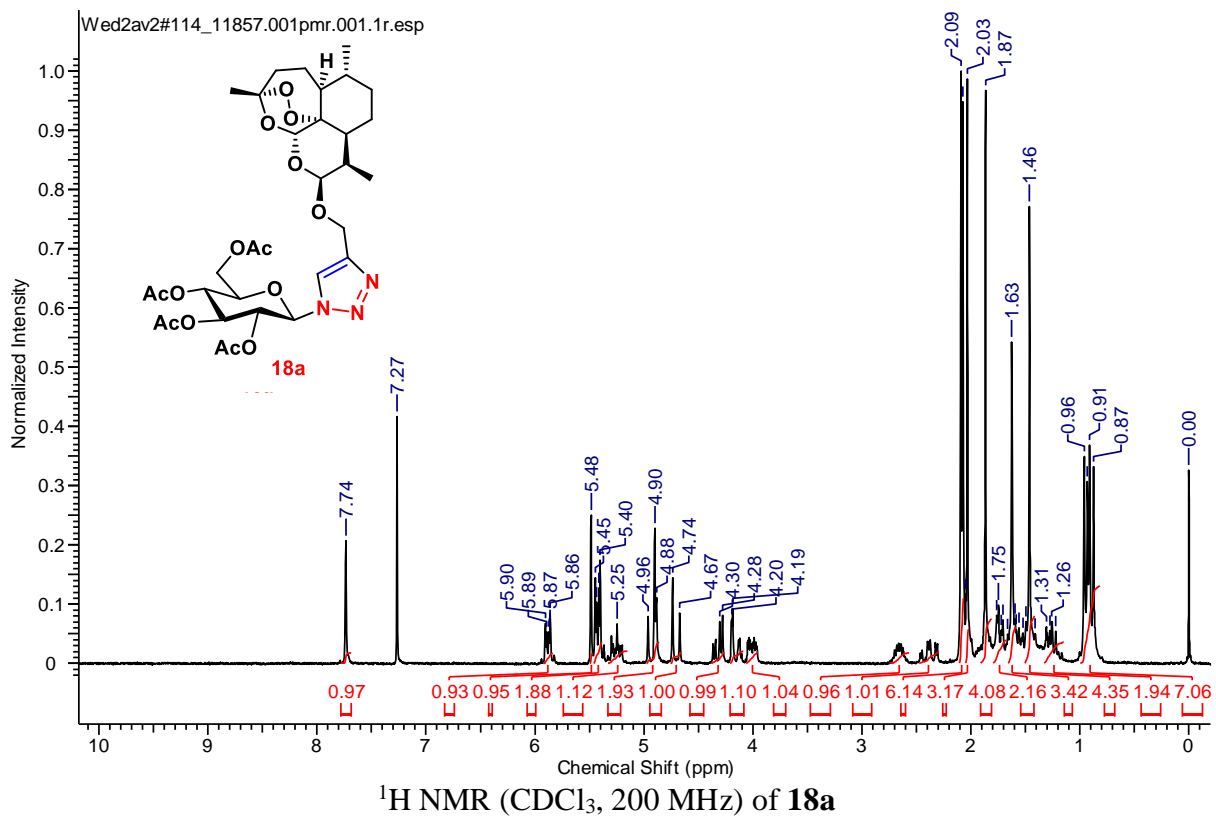
1. D. L. Klayman, *Science*, **1985**, 228, 1049–1055.
2. A. K. Bhattacharya and R. P. Sharma, *Heterocycles*, **1999**, 51, 1681–1745.
3. (a) S. R. Meshnick, T. E. Taylor and S. Kamchonwongpaisan, *Microbial Rev.*, **1996**, 60, 301–315. (b) Q. Li, P. Weina and W. Milhous, *Curr. Drug Ther.*, **2007**, 2, 210–223.
4. Youyou Tu, *Nature Medicine*, **2011**, 17, 1217–1220.
5. (a) H. J. Woerdenbag, T. A. Moskal, N. Pras, T. M. Malingre', F. S. El-Feraly, H. H. Kampinga and A. W. T. Konings, *J. Nat. Prod.*, **1993**, 56, 849–856. (b) A. E. Mercer, I. M. Copple, J. L. Maggs, P. M. O'Neill, and B. K. Park, *J Biol Chem.*, 286, 987–996. (c) A. E. Mercer, J. L. Maggs, X-M. Sun, G. M. Cohen, J. Chadwick, P. M. O'Neill and B. K. Park, *J Biol Chem.*, 282, 9372–9382.
6. *Essentials of Glycobiology*, ed. A. Varki, R. D. Cummings, J. D. Esko, H. H. Freeze, P. Stanley, C. R. Bertozzi, G. W. Hart and M. E. Etzler, Cold Spring Harbor Laboratory Press, 2nd edn, **2009**.
7. O. V. Andreeva, B. F. Garifullin, R. R. Sharipova, I. Yu. Strobykina, A. S. Sapunova, A. D. Voloshina, M. G. Belenok, A. B. Dobrynin, L. R. Khabibulina, and V. E. Kataev, *J. Nat. Prod.* **2020**, 83, 2367–2380.
8. T. K. Kotammagari, S. Paul, G. K. Barik, M. K. Santra, A. K. Bhattacharya, *Org. Biomol. Chem.*, **2020**, 18, 2252–2263.
9. M. Krawczyk, G. Pastuch-Gawolek, A. Pluta, K. Erfurt, A. Domi'nski and P. Kurcok, *Molecules*, **2019**, 24, 4181.
10. K. B. Mishra, R. C. Mishra and V. K. Tiwari, *RSC Adv.*, **2015**, 5, 51779–51789.
11. W. Szeja, G. Gryniewicz and A. Rusin, *Curr. Org. Chem.*, **2017**, 21, 218–235.
12. (a) R. Huisgen, *Angew. Chem., Int. Ed.*, **1963**, 2, 565–598. (b) R. Huisgen, *Angew. Chem., Int. Ed.*, **1963**, 2, 633–645.
13. (a) C. W. Meldal, C. Tornoe and M. Meldal, *J. Org. Chem.*, **2002**, 67, 3057–3064. (b) V. V. Rostovtsev, L. G. Green, V. V. Fokin and K. B. Sharpless, *Angew. Chem., Int. Ed.*, **2002**, 41, 2596–2599. (c) B. C. Boren, S. Narayan, L. K. Rasmussen, L. Zhang, H. Zhao, Z. Lin, G. Jia and V. V. Fokin, *J. Am. Chem. Soc.*, **2008**, 130, 8923–8930. (d) B. T. Worell, J. A. Malik and V. V. Fokin, *Science*, **2013**, 340, 457–460.

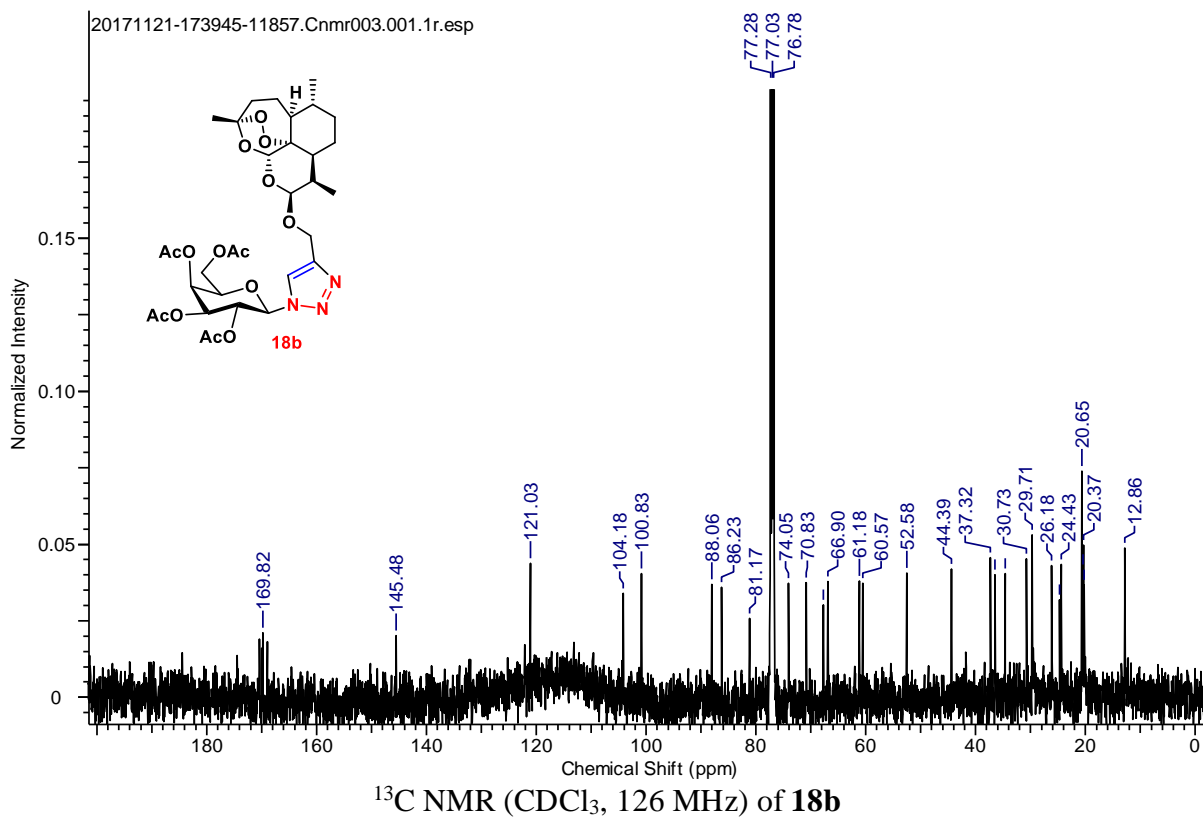
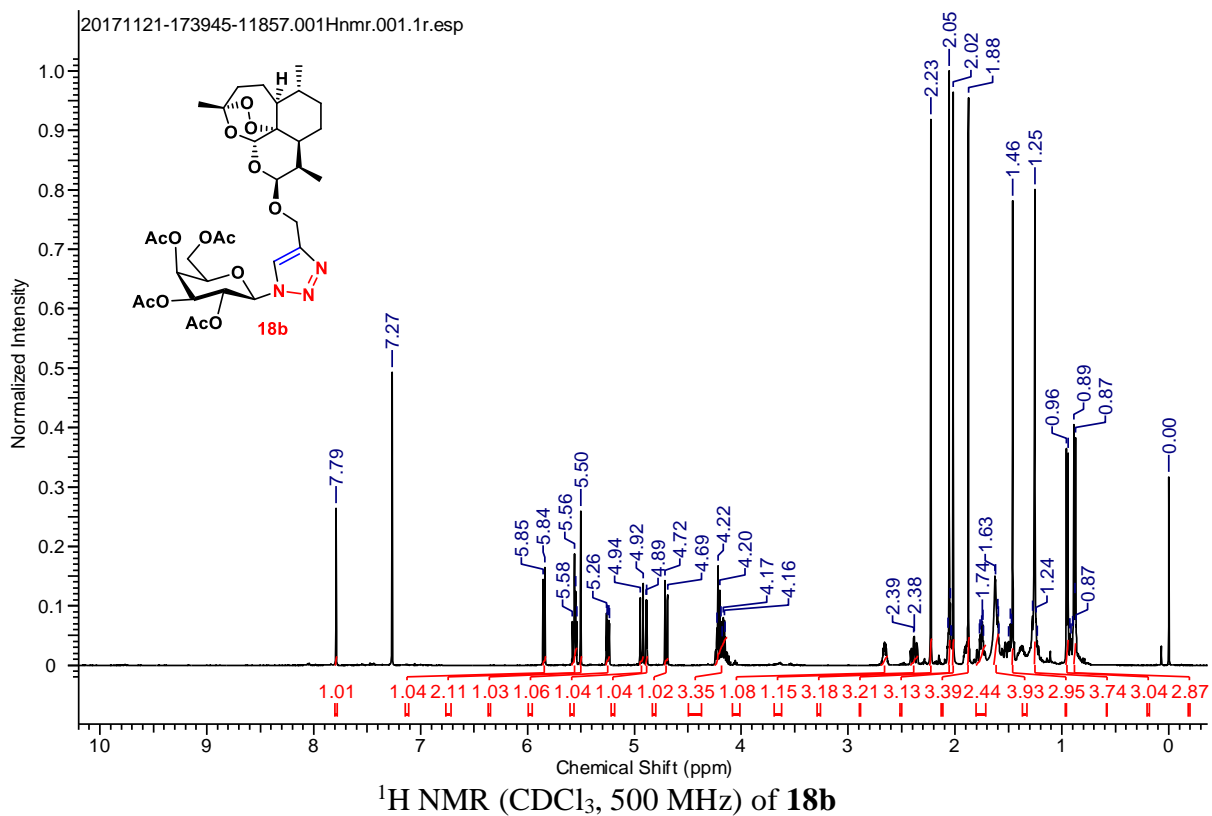
14. (a) A. Brossi, B. Venugopalan, L. D. Gerpe, H. J. C. Yeh, J. L. Flippen-Anderson, P. Buchs, X. D. Luo, W. Milhous and W. Peters, *J. Med. Chem.*, **1988**, *31*, 645–650. (b) A. J. Lin and R. E. Miller, *J. Med. Chem.*, **1995**, *38*, 764–770.
15. R. K. Haynes, *Curr. Top. Med. Chem.*, **2006**, *6*, 509–537.
16. H. R. Chand and A. K. Bhattacharya, *Asian J. Org. Chem.*, **2016**, *5*, 201–206.
17. (a) R. R. Schmidt, M. Behrendt and A. Toepfer, *Synlett*, **1990**, 694–696. (b) Y. D. Vankar, P. S. Vankar, M. Behrendt and R. R. Schmidt, *Tetrahedron*, **1991**, *47*, 9985–9992.
18. (a) B. H. M. Kuijpers, S. Groothuys, A. Keereweer, R. Bram, P. J. L. M. Quaedflieg, R. H. Blaauw, F. L. van Delft and F. P. J. T. Rutjes, *Org. Lett.*, **2004**, *6*, 3123–3126 and references cited therein. (b) S. Chittaboina, F. Xie and Q. Wang, *Tetrahedron Lett.*, **2005**, *46*, 2331–2336. (c) R. M. Cicchillo and P. Norris, *Carbohydr. Res.*, **2000**, *328*, 431–434. (d) M. A. Maier, C. G. Yannopoulos, N. Mohamed, A. Roland, H. Fritz, V. Mohan, G. Just and M. Manoharan, *Bioconjugate Chem.*, **2003**, *14*, 18–29.

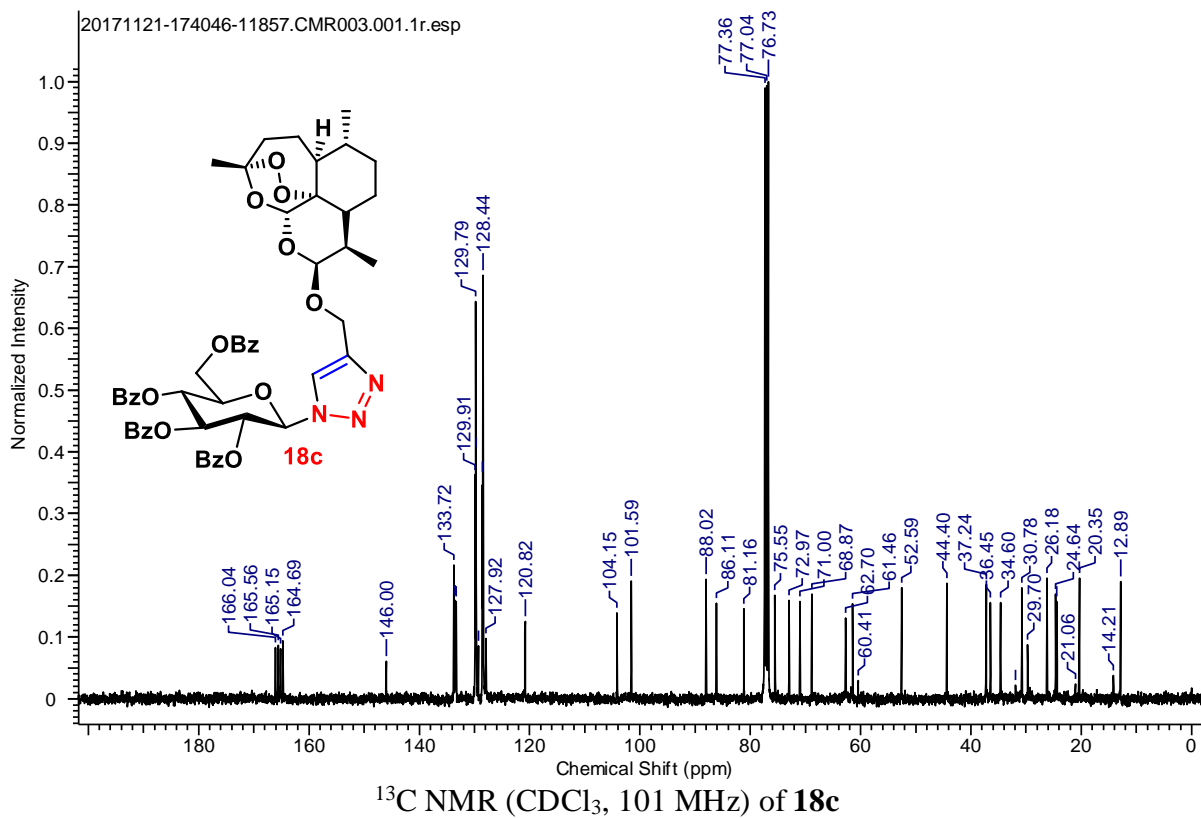
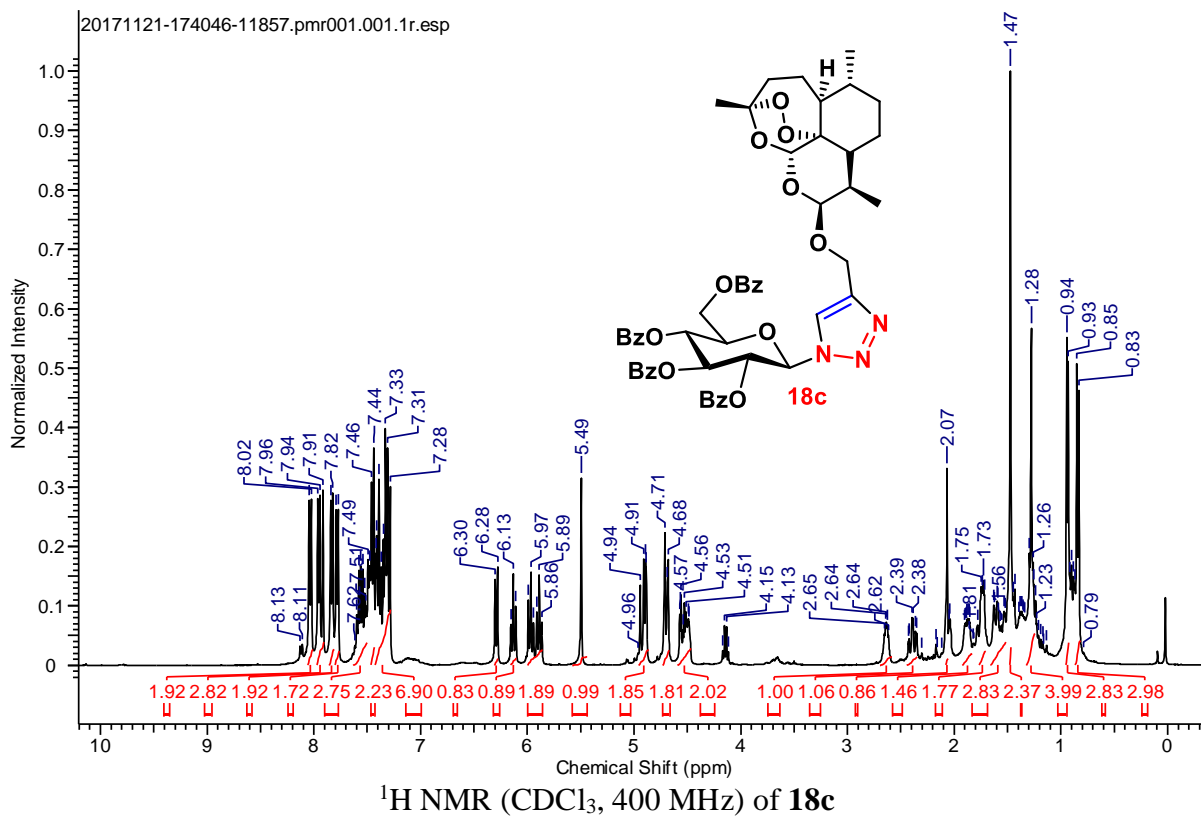
1.2.6 Copies of NMR spectra

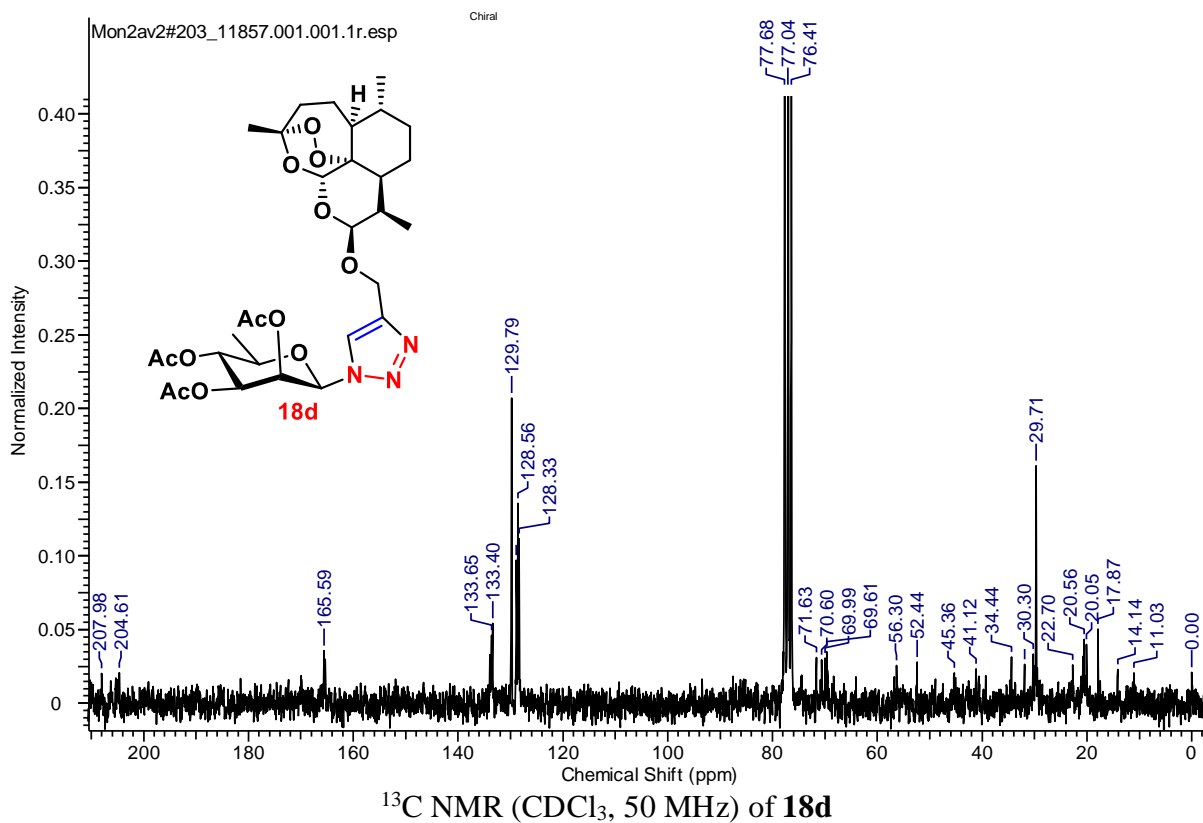
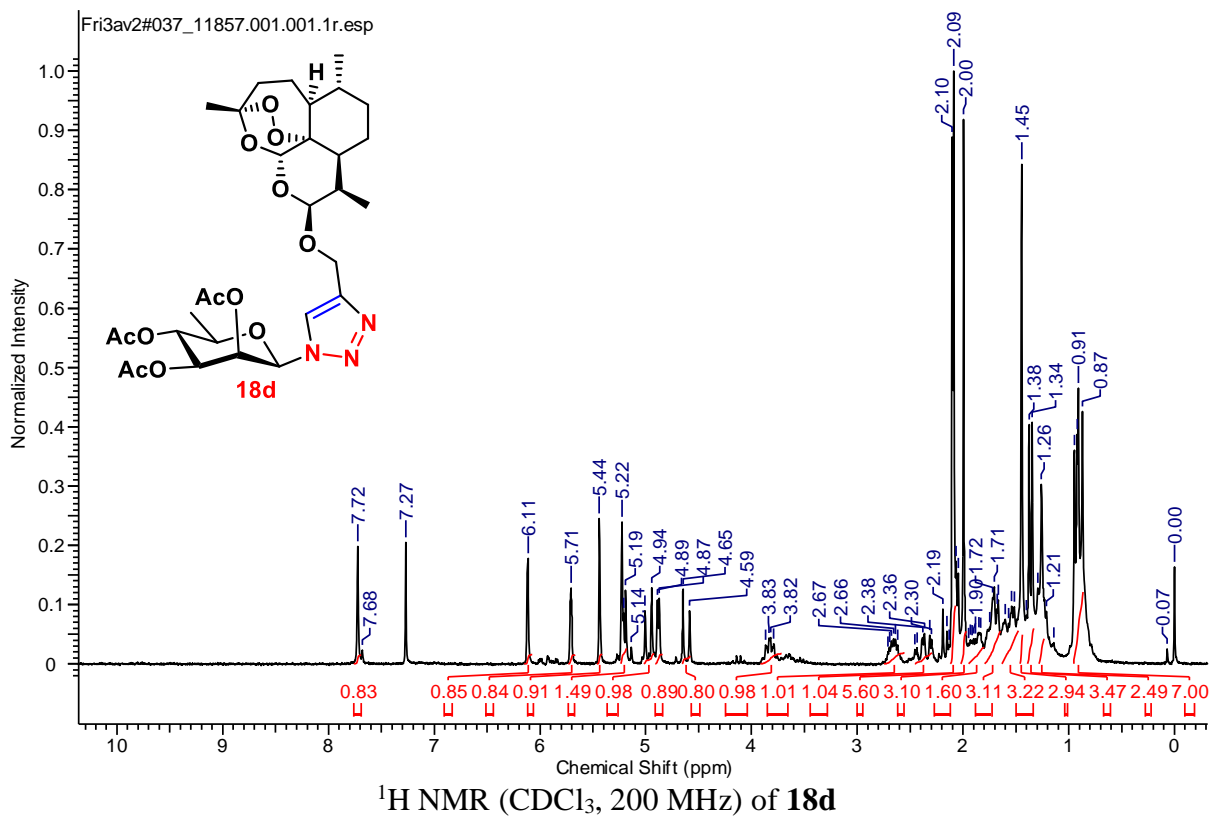


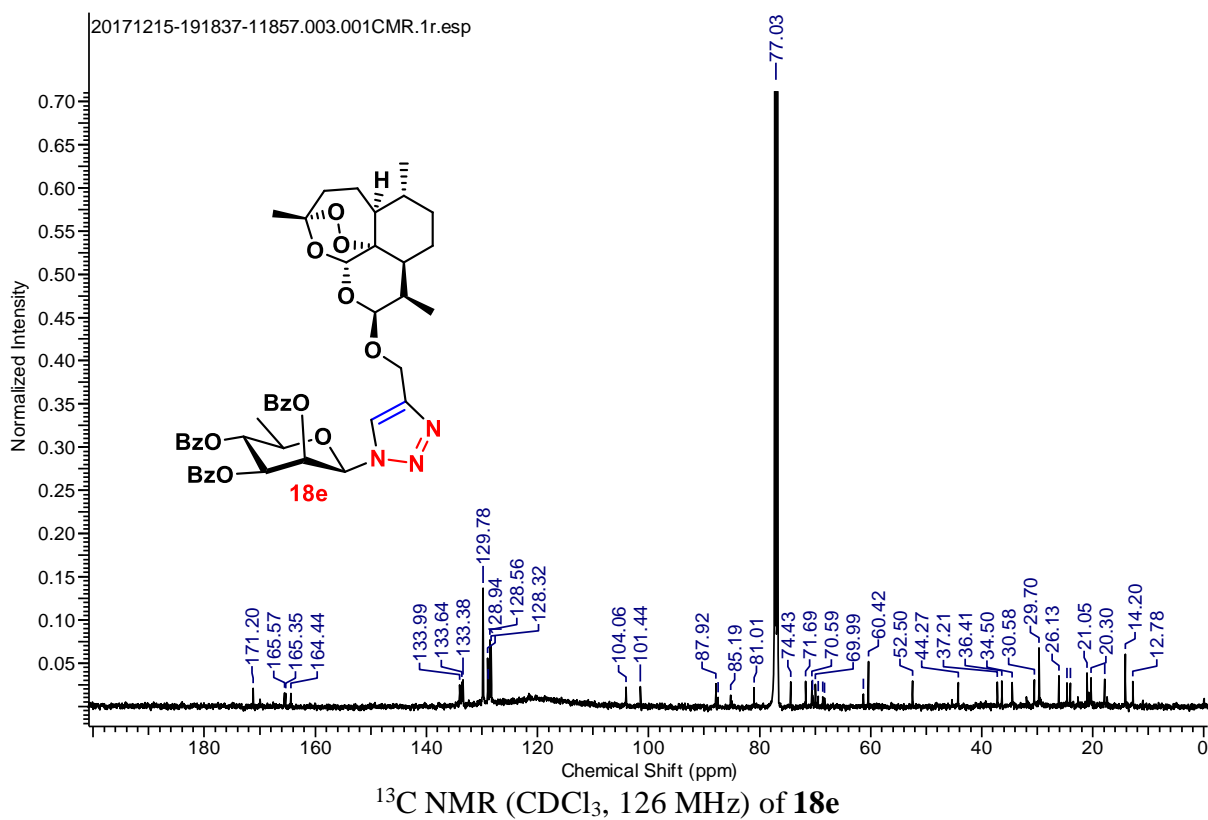
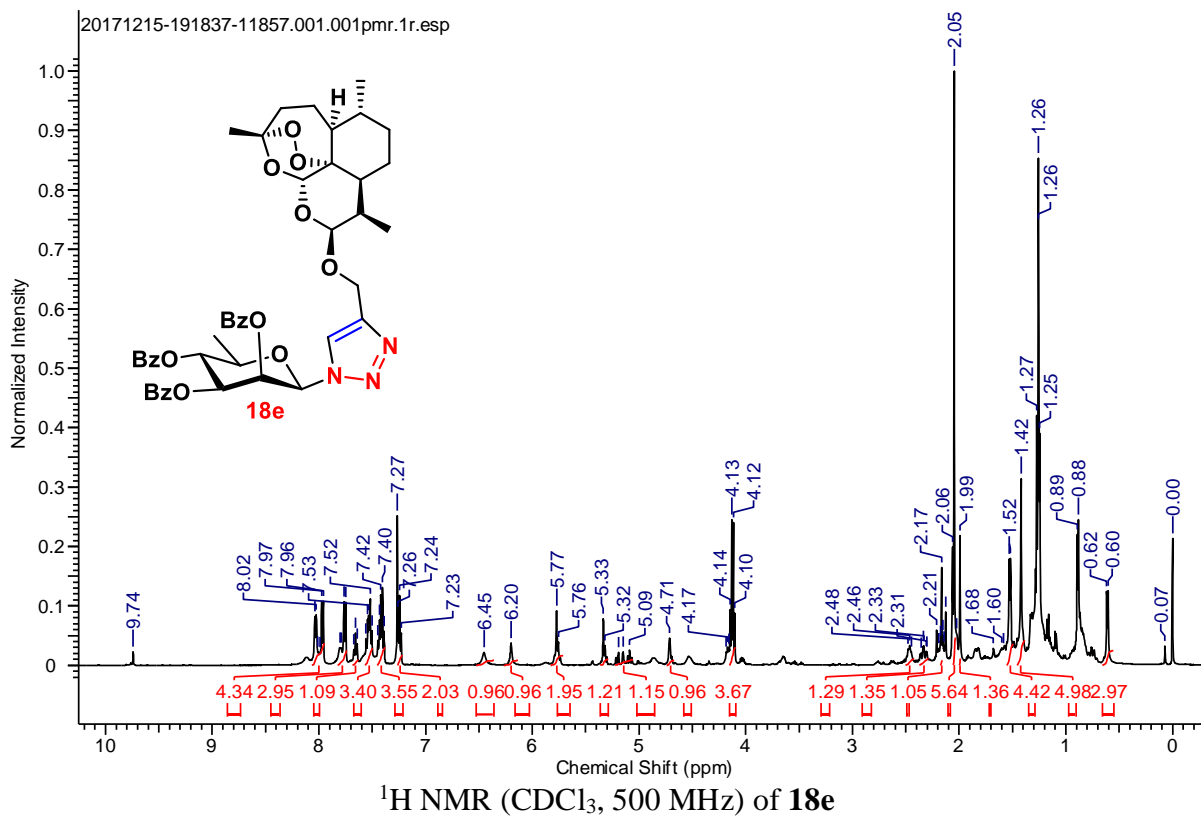


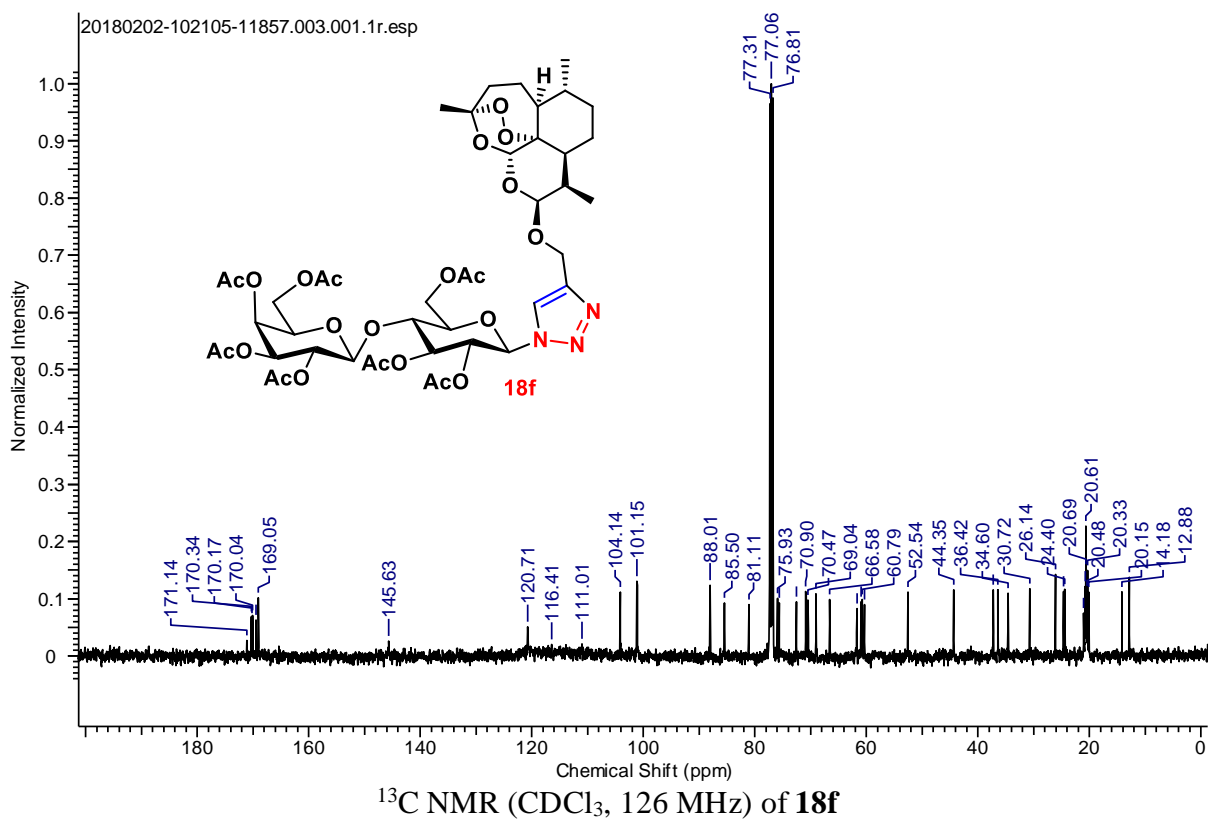
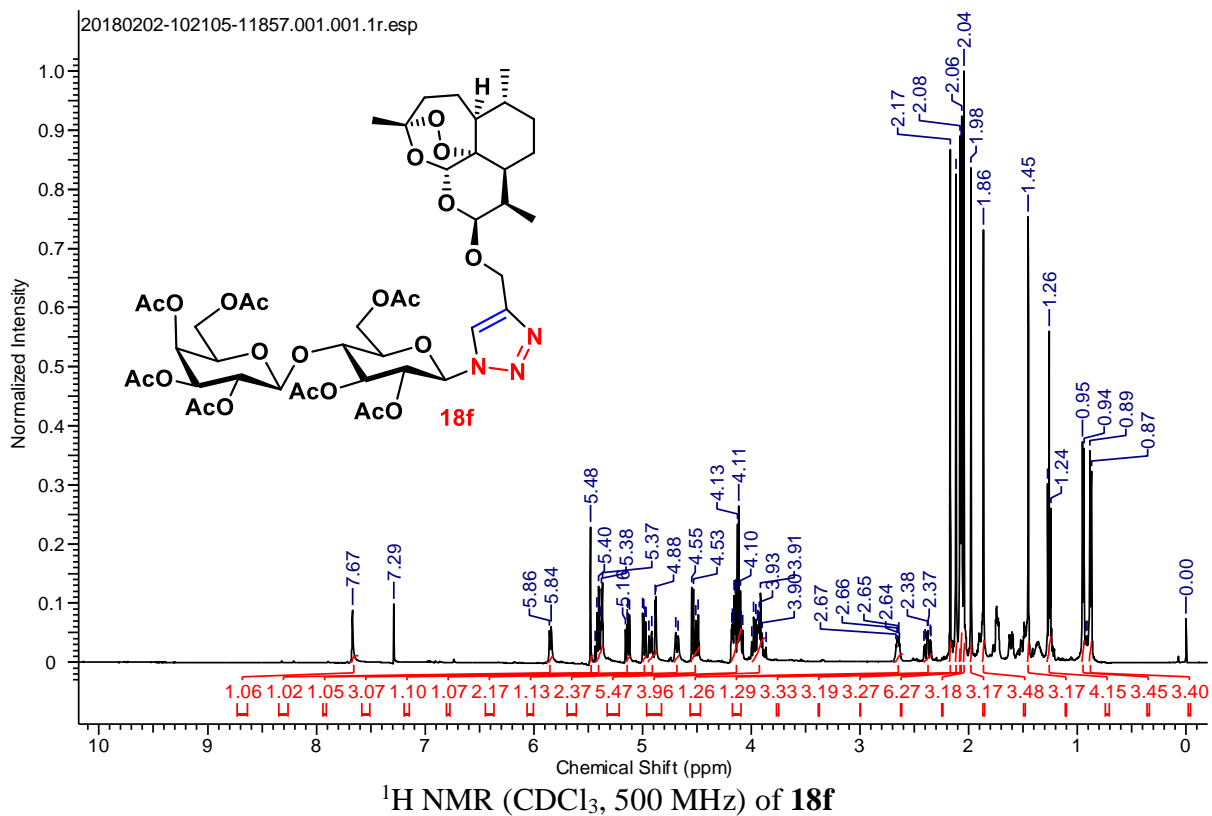


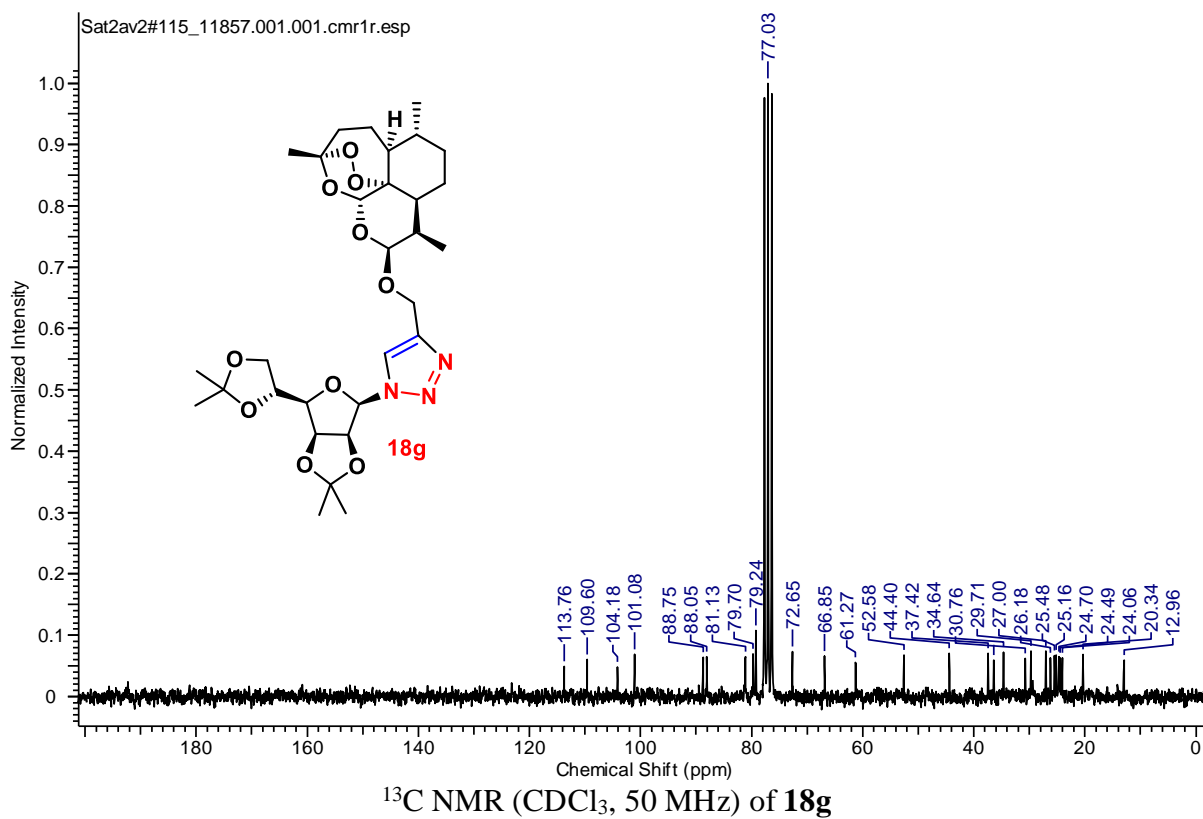
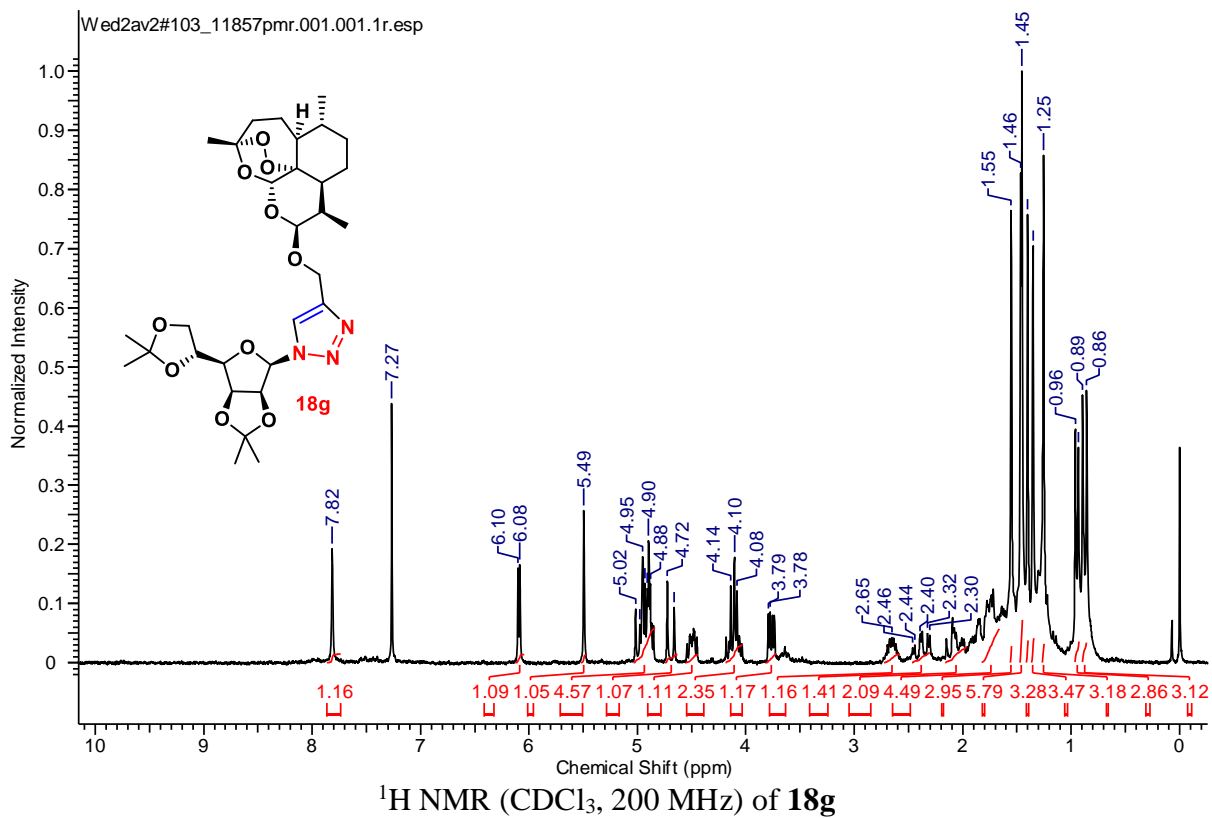


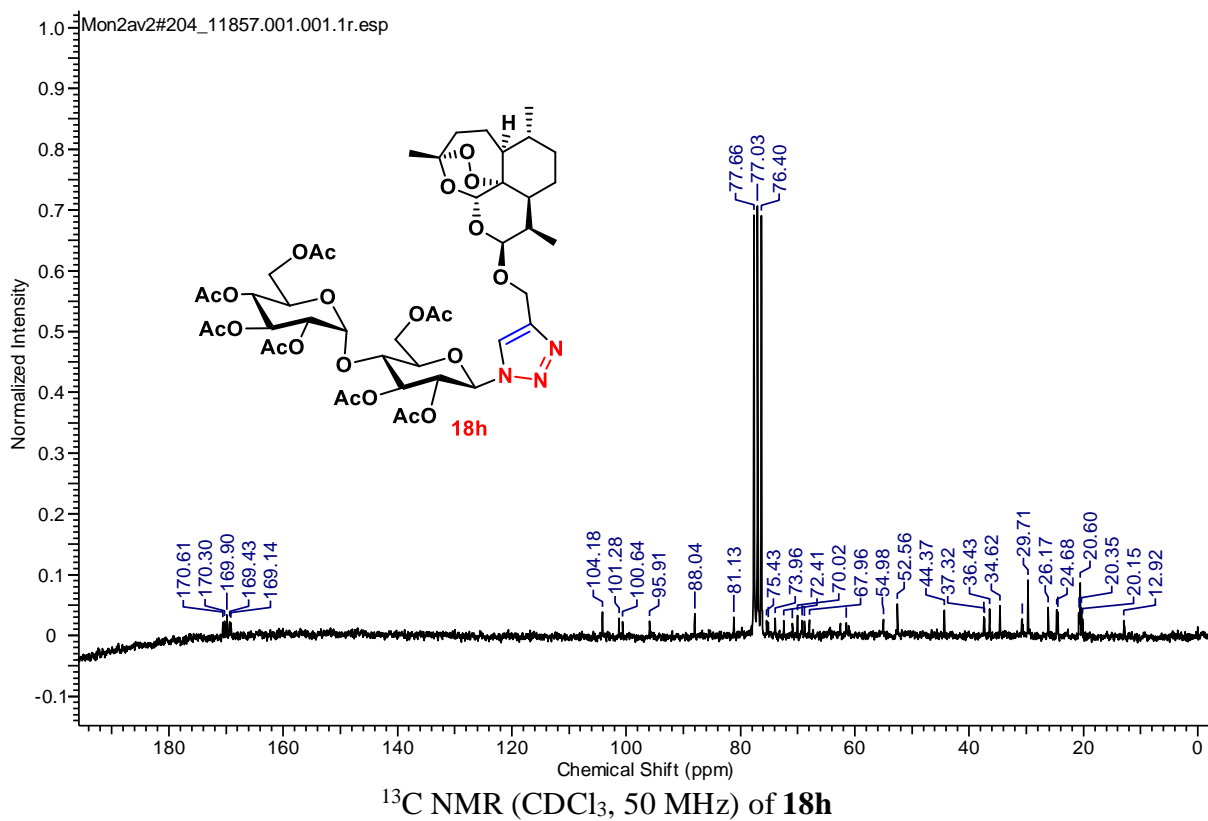
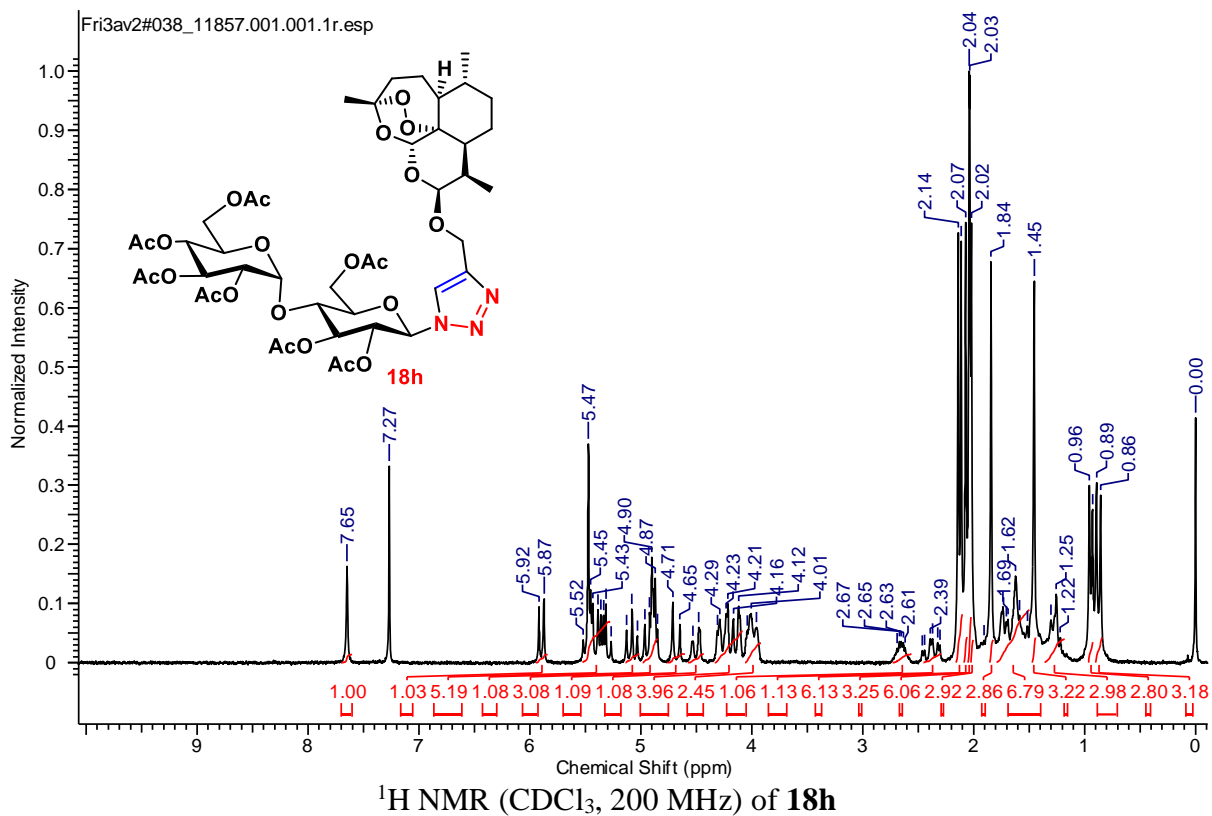


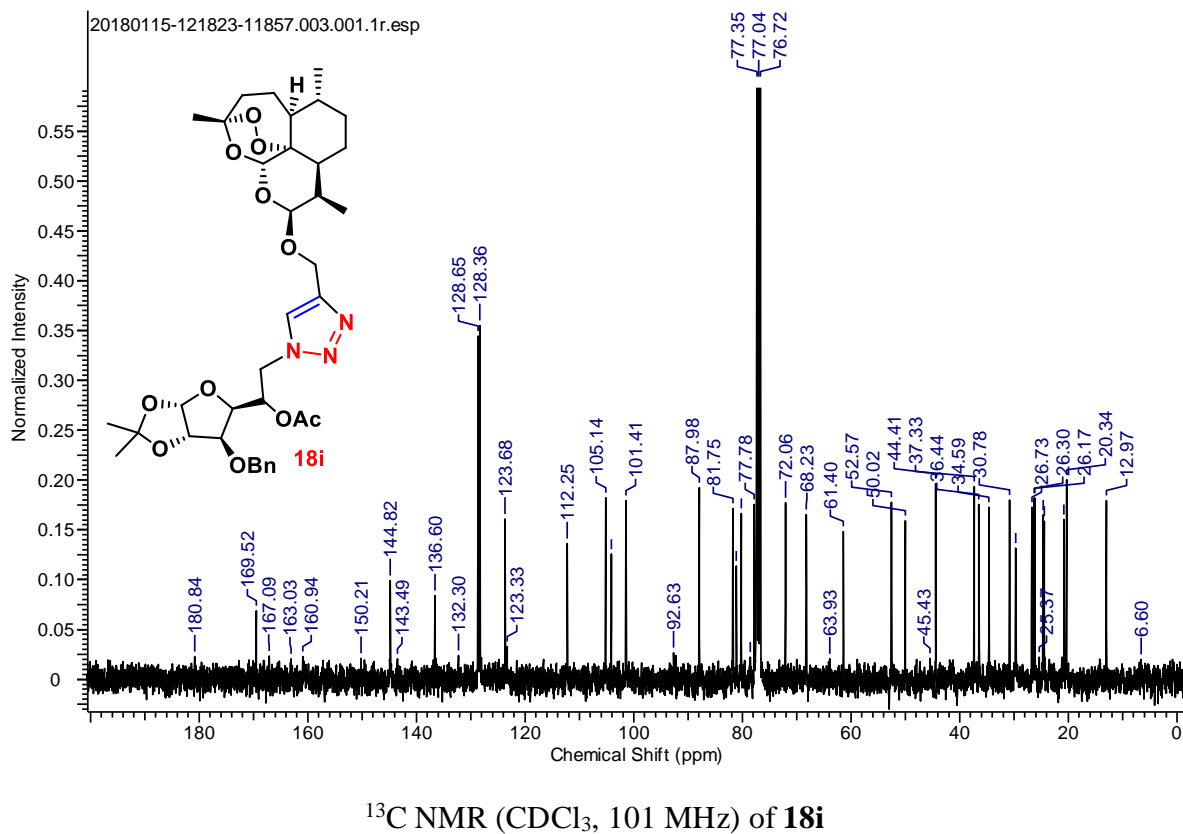
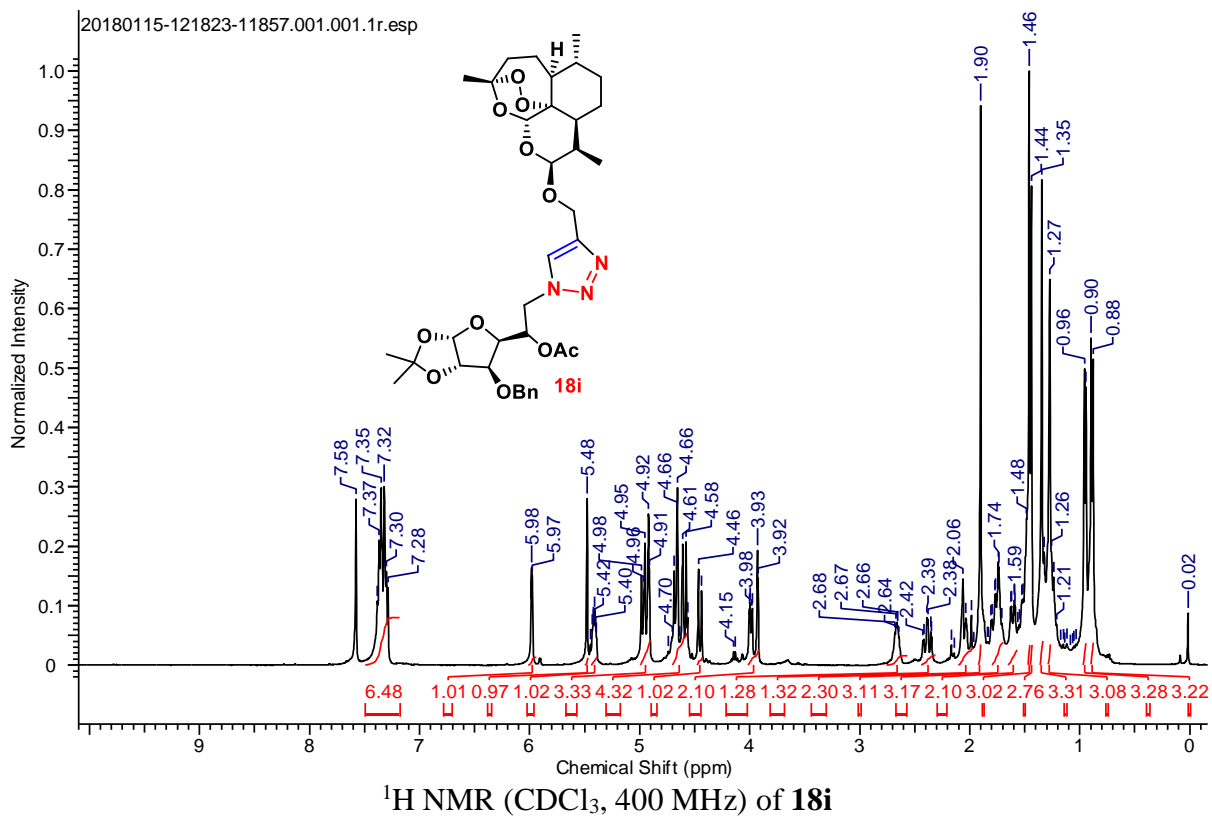












1.2. Design and synthesis of eugenol/isoeugenol glycoconjugates and other azole derivatives as potent antifungal

1.2.1 Introduction

Aspergillus fumigatus is a saprobic fungus that has harmonized itself with extreme climatic conditions, whilst this fungal strain also evolved its resistance against host cell defense mechanism and many marketed drugs. Over 1-4 million people are infected throughout the world from various forms of aspergillosis as per reported data.^{1a,b} Asexual spores of *Aspergillus* like arthrospores, chlamydospores, and sporangiospores are habitually inhaled by us in our daily life. These spores are hazardous for people with a debilitated immune system and lurking pulmonary diseases like tuberculosis, lung cancer, asthma, pneumonia and other respiratory intricacies. Smaller conidial size of *Aspergillus* spp and their proficient adhesion to the host cell surface for sustenance increases its propagation deep inside the respiratory tract which puts people with underlying lung diseases and delicate immunology at a higher stake of getting lethal fungal infections. The surface proteins on its conidia provide it with camouflage from the host cell defense mechanism thus making it unrecognizable.^{1c} Lately, studies have shown emergences of co-fungal infection cases of respiratory aspergillosis in 19.6–33.3% of people forbearing COVID-19.²

1.2.1.1 Development of resistance toward known antifungals

In the recent past, this genus has shown resistance toward marketed antifungal drugs as well as host cell defence mechanisms.³ Common used antifungal drugs are designated into four main classes, polyenes, azoles, allylamines and echinocandins according to their action of mechanism and structure. Amphotericin B (Amp B), miconazole, ketoconazole, fluconazole, voriconazole, itraconazole, etc. are some of the marketed drugs (**Figure 1**). Mostly these drugs make fungal cell walls porous by affecting the biosynthesis of the fungal cell wall at different stages which in turn inhibits the further proliferation of fungal cells though some other drugs which may affect fungal cell wall components, nucleic acids, and microtubule biosynthesis.^{1c,4} Due to excessive usage of these pharmacophores renders *A. fumigatus* unresponsive to these above-mentioned classes of antifungals to some extent. Hence, there is

a compelling need to design and synthesize new antifungals with enhanced bioavailability and least toxicity.³

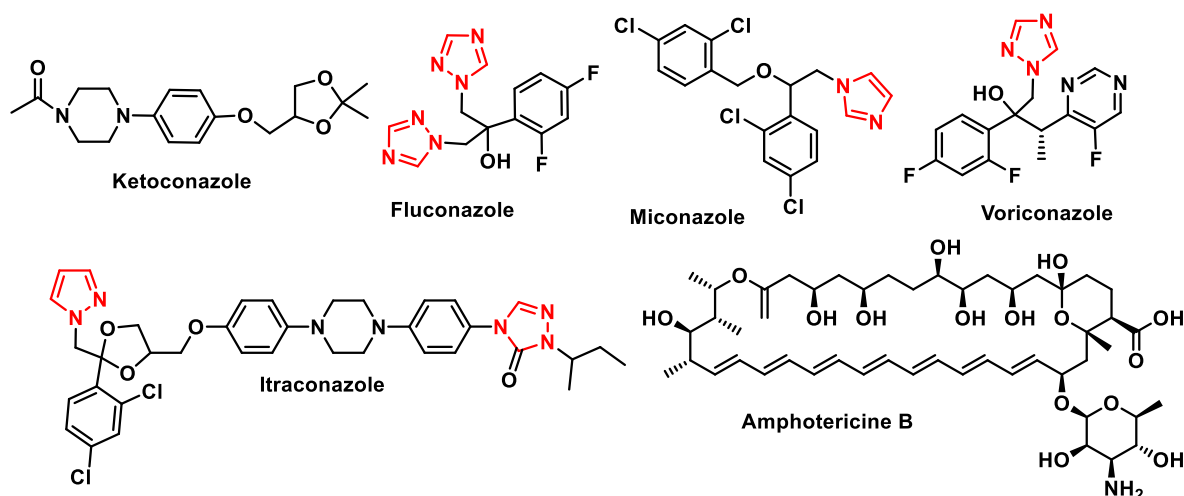


Figure 1: Common antifungal drugs

1.2.1.2 Secondary metabolites as potent antifungals

Natural phenylpropanoid, eugenol (**1a**) is isolated from the plants like *Myristica fragrans*, *Eugenia caryophyllata* and *Syzygium aromaticum* etc. and also it is one of the main components of clove oil.^{5a} Isoeugenol (**1b**) is isolated from *Clarkia breweri* and *Ocimum basilicum* etc.^{5b} Eugenol (**1a**) and isoeugenol (**1b**) (**Figure 2**) hold analgesic, anti-inflammatory, cardiovascular, anti-carcinogenic, antioxidant and antimutagenic properties. Eugenol (**1a**) itself exhibits local antiseptic and anaesthetic properties in dentistry.^{5c} Eugenol (**1a**) /isoeugenol (**1b**) has shown antifungal activity at IC₅₀ value of 1900 μ M against *A. fumigatus*, respectively.^{1c,4b,5}

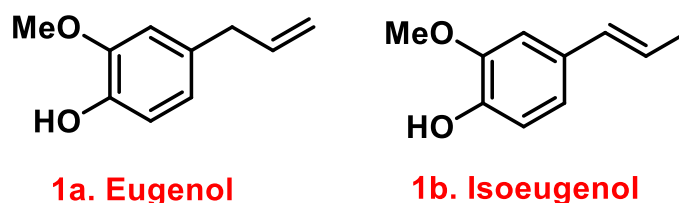


Figure 2: Structure of eugenol (**1a**) and isoeugenol (**1b**)

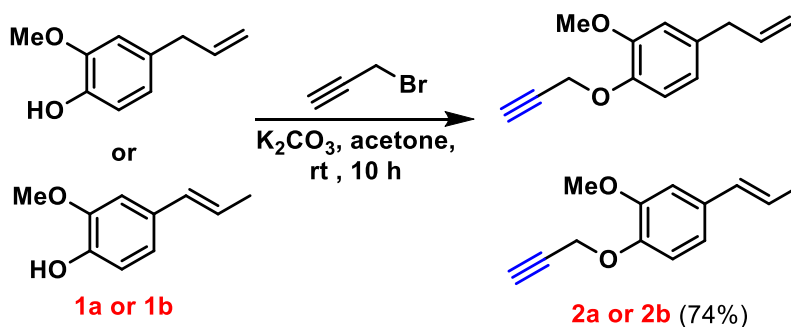
Due to all the above properties and their wide range of adaptable uses, eugenol and isoeugenol (**1a** and **1b**) have become potent candidates for the design and synthesis of potent

drugs. Structural alterations in potent drug motifs either isolated from natural products or synthesized can render existing drugs more efficient and less toxic.^{1c,6} It is well published⁷ in the literature that adjoining sugar scaffolds to naturally occurring potent drug motifs enhances its bioavailability by aiding in its solubility, stability and permeability in the biological system. It is all attributed to the hyper-valent nature of carbohydrate scaffolds that guides the prodrug to reach the targeted site. Hence glycoconjugates of natural products are considered as preferred pharmacophores in drug delivery.⁷ Moreover, the insertion of triazole rings within the therapeutic compound assists in enhancing the bioactivity of antifungals. Hence, we opined synthesis of eugenol and isoeugenol (**1a** and **1b**) based glycoconjugates and their structure modification to further improve their antifungal activities.⁸

1.2.2 Present work

1.2.2.1 Chemical modifications of eugenol **1a** and isoeugenol **1b**

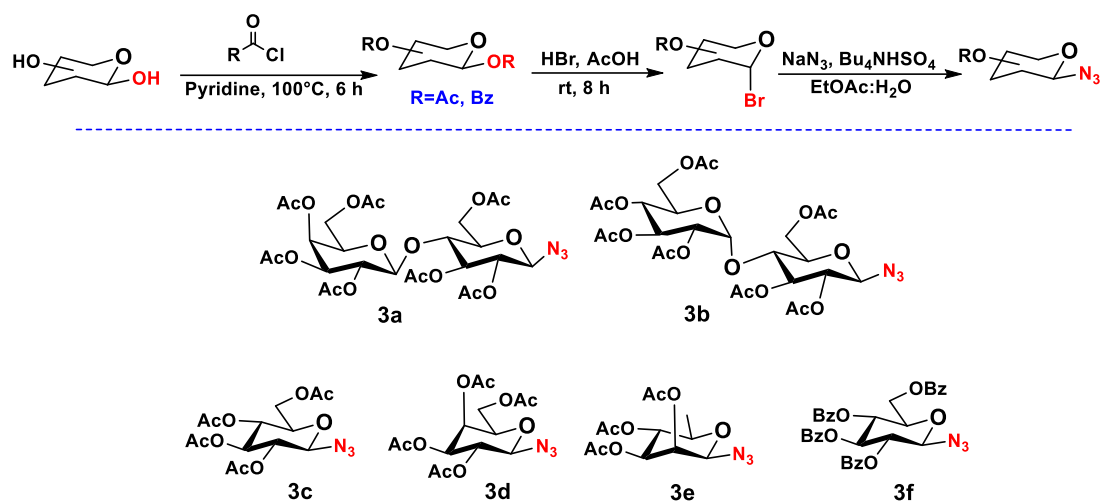
Herein, we report synthesis of eugenol (**1a**) /isoeugenol (**1b**) based glycoconjugates in addition to other structural modifications in order to study their antifungal properties. We treated eugenol (**1a**) and isoeugenol (**2a**) with propargyl bromide in acetone using potassium carbonate (K_2CO_3) as a base at ambient temperature which furnished eugenol/isoeugenol propargyls (**2a** and **2b**) in good yields (**Scheme 1**).



Scheme 1: Synthesis of propargylated eugenol/isoeugenol (**2a/2b**)

Sugar azides or azido sugars (**3a–f**) (**Scheme 2**) were prepared as per previously published approaches and spectral data was found in agreement with the reported literature data.^{4,7,9} The β -orientation of the azido groups at anomeric position was confirmed by the coupling

constant (ranges from 8.5–8.88 Hz) of anomeric protons which appeared at δ_{H} 4.61–4.98 ppm in ^1H NMR spectra and the data was compatible with the reported literature data.^{4b,7a,9}



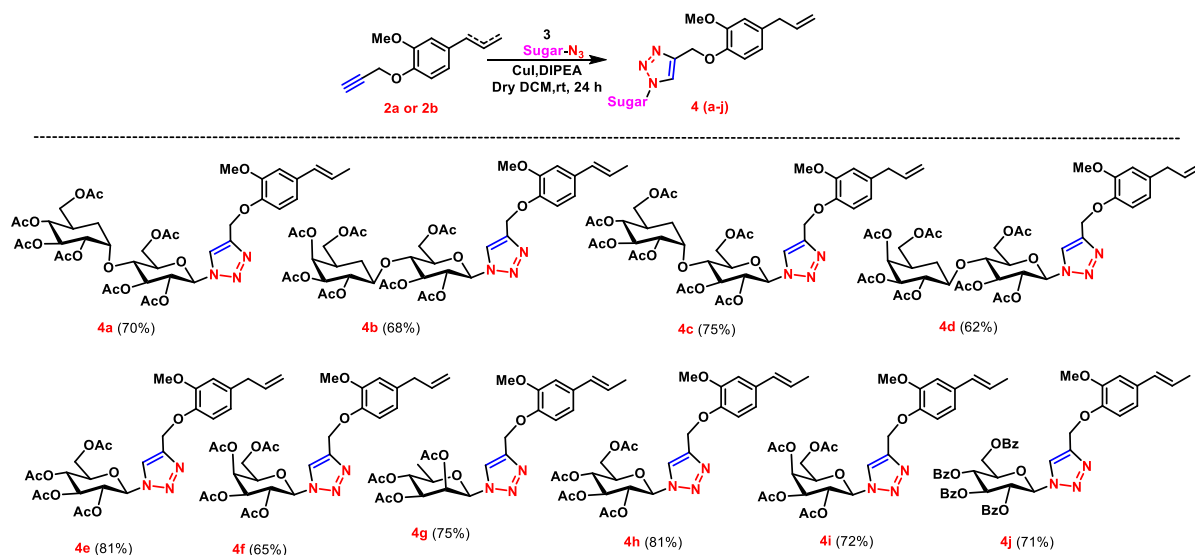
Scheme 2: Synthesis of azido sugars (**3a-f**)

Finally propargylated eugenol/isoegenol (**2a/2b**) and azido sugars (**3a-f**) were coupled employing click chemistry in presence of catalytic amount of copper iodide and *N,N*-diisopropylethylamine (DIPEA) as a base in dichloromethane (DCM) to furnish natural product based glycoconjugates (**4a-j**) (**Table 1**) in good to excellent yields (65–81%).¹⁰ Lactose azide showed better yields (**4a** and **4c**) of glycoconjugate products than maltose azide (**4b** and **4d**). Acetylated monosaccharides azides *i.e.* tetra-*O*-acetyl azido glucose, tetra-*O*-acetyl azido galactose and triacetyl azido rhamnose furnish good yields of glycoconjugates (**4e-4i**). Tetra-*O*-benzoyl azido glucose (**3f**) also furnished isoegenol glycoconjugate (**4j**) in good yield. All the eugenol/isoegenol derived glycoconjugates were assayed for their antifungal activity against *A. fumigatus*. Among all the synthesized glycoconjugates, compound (**4e**) has shown promising antifungal activity with the IC_{50} value of 5.42 μM against *A. fumigatus*. Although, all other glycoconjugates did not show promising activities but they were multiple folds active than their parent compounds.

We reduced the aliphatic double bond in eugenol (**1a**) to observe the role of this exo-methylene double bond of eugenol (**1a**) in antifungal assays against *A. fumigatus*. In order to achieve this, the exo-methylene double was reduced by utilizing Pd–C/ H_2 to furnish euganol (**5**) in very good yield¹¹ (**Scheme 3**). Upon reduction, the free–OH group of euganol was

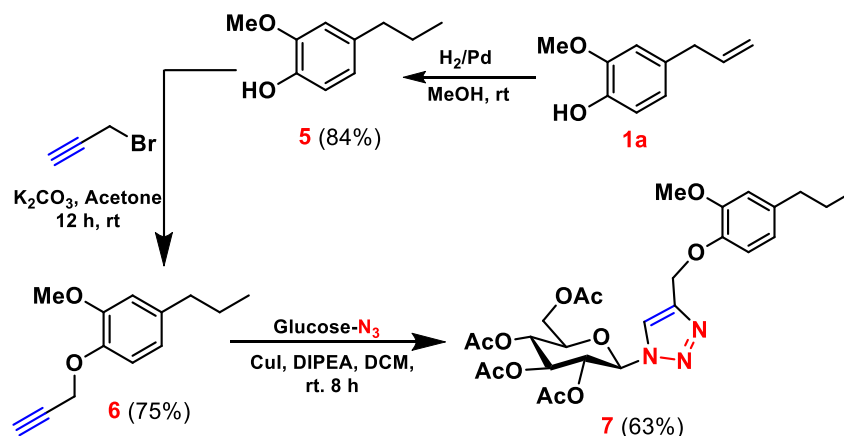
treated with propargyl bromide, K_2CO_3 as a base in acetone to furnish propargylated eugenol derivative (**6**).

Table 1: Substrate scope^{a,b}:



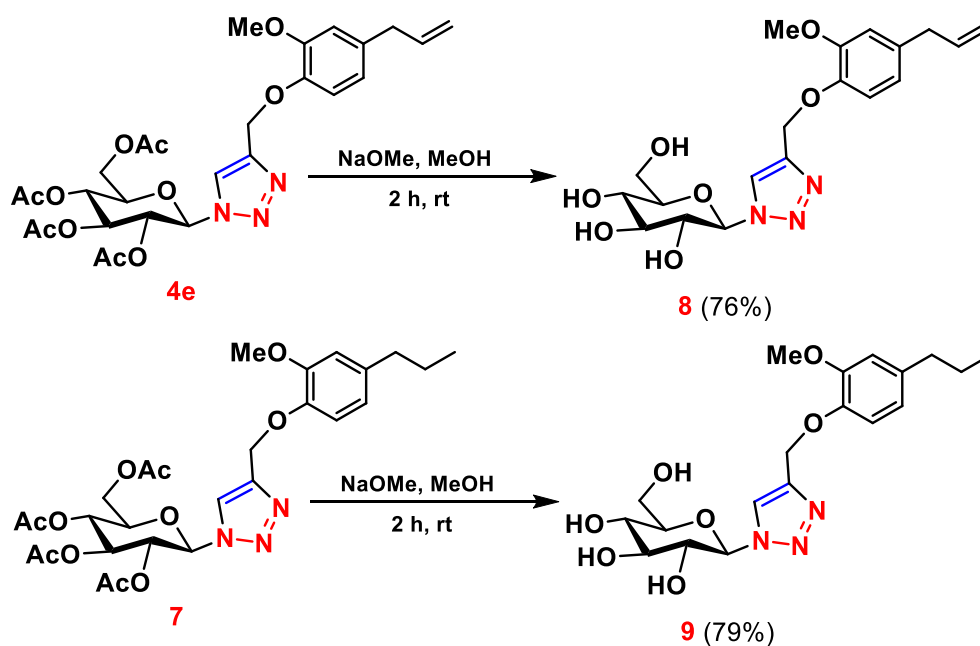
^a Reaction conditions: propargylated eugenol/isoegenol (**2a**) or (**2b**) (30 mg, 0.1485 mmol, 1 equiv.), azido sugars (**3a–f**) (0.1782 mmol, 1.2 equiv.), DCM (3 mL), CuI (15.55 mg, 0.0816 mmol, 0.55 equiv.), and DIPEA (26 μ L, 0.1485 mmol, 1.0 equiv.). ^b Isolated yield.

We finally coupled compound (**6**) with previously synthesized tetra-*O*-acetyl azido glucose (**3c**) to afford glycoconjugate (**7**) (**Scheme 3**). Amid all these synthesized compounds of eugenol (**1a**) derivatives, only compound (**5**) displayed encouraging antifungal activity with an IC_{50} value of 9.39 μ M.



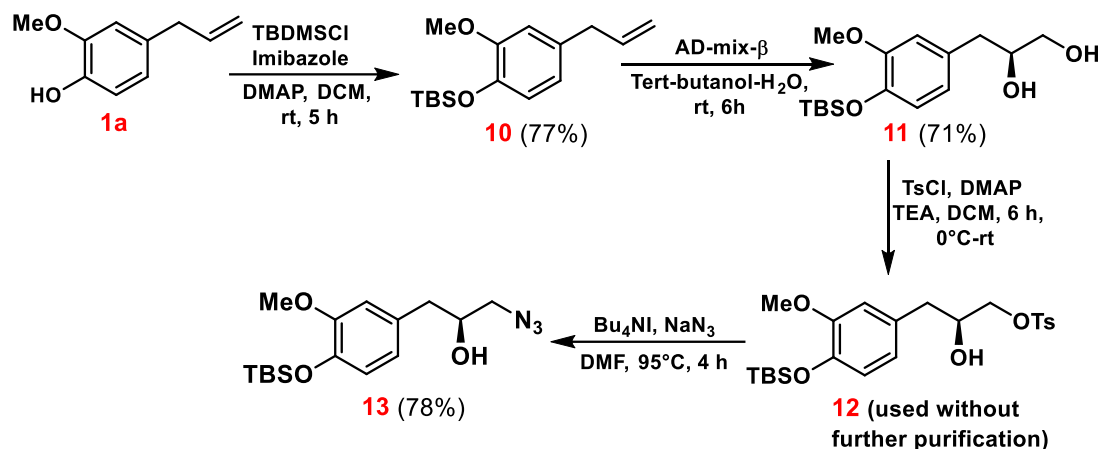
Scheme 3: Reduction of eugenol (**1a**) with subsequent glycoconjugation

Further deprotection of compounds (**4e** and **7**) was taken up to study the role of acetyl groups present on sugar scaffolds on the antifungal activities. The acetyl groups were deprotected in presence of sodium methoxide in methanol to afford deprotected compounds (**8** and **9**) (**Scheme 4**).¹² However, these deprotected motifs on antifungal assay against *A. fumigatus* displayed IC₅₀ values above 25 μ M.



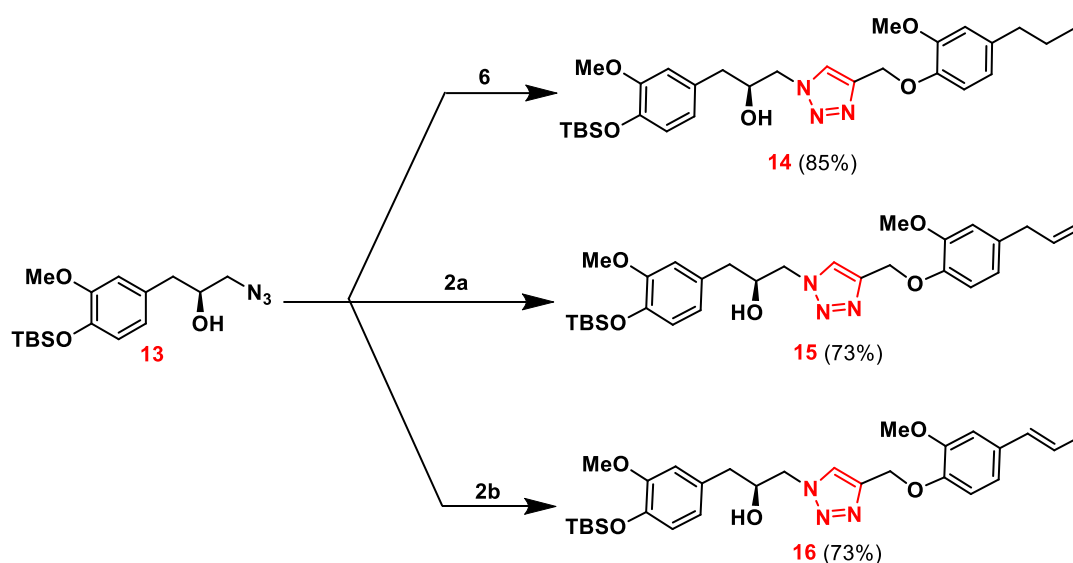
Scheme 4: Deprotection of compounds (**4e** and **7**)

We further utilized the free –OH group of eugenol (**1a**) to synthesize various derivatives apart from glycoconjugates. The free –OH group was protected using *tert*-butyldimethylsilyl chloride (TBDMS-Cl) in presence of imidazole and 4-dimethyl-aminopyridine (DMAP) as combined bases in DCM to yield compound (**10**) *i.e.* TBS protected eugenol (**10**). Compound (**10**) was then treated with AD-mix- β in a water–*tert* butanol solvent system to furnish dihydroxylated¹³ product (**11**) which was further subjected to tosylation. The tosylated compound (**12**) was used without any further purification to expedite azidation when treated with sodium azide (NaN₃) in dimethylformamide (DMF) in the presence of a catalytic amount of tetrabutylammonium iodide (TBAI) to obtain compound (**13**) (**Scheme 5**). All these synthesized compounds were further evaluated for their antifungal activities against *A. fumigatus* but all the compounds showed IC₅₀ values above 25 μ M.



Scheme 5: Dihydroxylation of eugenol (**1a**) followed by azidation

It is widely reported in the literature¹⁴ that dimers of therapeutic agents possess higher biological activities than their monomers. We were interested to synthesize some dimeric compounds and study their antifungal efficacies. In this regard, compound (**13**) was considered as the ideal candidate for the synthesis of dimeric analogues. Hence, we coupled azide compound (**13**) with propargylated analogue synthesized earlier employing click reaction to obtain compounds (**14**, **15** and **16**) (**Scheme 6**). Again all these compounds were tested against *A.fumigatus* for their antifungal efficacy. However, all the three dimeric compounds showed IC₅₀ values above the range of 25 μ M.



Scheme 6: Synthesis of dimeric analogs (**14-16**)

1.2.2.2 Biological evaluations of synthesized compounds

All the synthesized molecules along with their parent molecules were tested for their antifungal activities against *A. fumigatus* as per the Clinical and Laboratory Standards Institute (CLSI) protocol (**Table 2**).¹⁵ Eugenol (**1a**) and isoeugenol (**1b**) exhibited IC₅₀ value of 1900 μ M against *A. fumigatus*. All the synthesized glycoconjugates (**4a-4j**) had shown more than 100 folds better activities than the parent compounds. It could be attributed to the addition of sugar scaffolds to eugenol/isoeugenol along with a triazole bridge which might be increasing the antifungal potency.

Table 2: IC₅₀ values of compounds against *A.fumigatus*

Compound codes	IC ₅₀ values (μ M)	Compound codes	IC ₅₀ values (μ M)
1a/1b	1900	5	9.39
2a/2b	≥ 25	6	≥ 25
4a	14.47	7	≥ 25
4b	14.47	8	≥ 25
4c	14.47	9	≥ 25
4d	14.47	10	≥ 25
4e	5.42	11	≥ 25
4f	10.86	13	≥ 25
4g	12.08	14	≥ 25
4h	21.73	15	≥ 25
4i	10.86	16	≥ 25
4j	15.18	Amp B	1.08

Amidst all glucose conjugates of eugenol (**4e**), showed the IC₅₀ value of 5.42 μM. It is notable that other glycoconjugates did not show any promising activities. We observed that glycoconjugate of C-4 epimer of glucose *i.e.* galactose (**3d**) was not active as potent antifungal as compared to glucose conjugate of eugenol (**4e**). Hence, it may be presumed that equatorial position of the –OH group is vital for biological interactions. However, when we coupled glucose with isoeugenol (**4h**) we did not notice any significant activity. It could be accounted due to non-terminal positioning of the double bond whereas; in active compound **4e**, a terminal double bond is present.

To observe the role of terminal double bond, we reduced eugenol (**1a**) to euganol (**5**) and this reduced compound (**5**) exhibited an IC₅₀ value of 9.39 μM (**Table 2**). Hence, we envisioned to couple compound **5** with glucose azide (**3c**). However, no substantial activity was recorded in this case. Antifungal activity assay of dimeric compounds (**14-16**) revealed their least potency (IC₅₀ values above 25 μM). Among the entire range of compounds assayed, we only compounds **4e** and **5** were able to check the growth of *A. fumigatus* conidia and mycelium substantially with MIC values of 10.86 μM and 15.54 μM, respectively. MIC values for rest of the compounds were ranging above 20 μM therefore, they were not considered appropriate for further biological analysis. The MIC and IC₅₀ values of original molecules (eugenol **1a** and isoeugenol **1b**) were 3800 μM and 1900 μM, respectively. Amphotericin B (Amp B) was used as positive control drug for the biological studies. It is evident from the data of MIC (10–20 μM) and IC₅₀ values (5.42–21.73 μM) of synthesised compounds (**2-15**) that these possess higher antifungal potency as compared to the parent molecules (eugenol **1a** and isoeugenol **1b**, MIC values of 3800 μM).

The most critical condition for evolution of any drug molecule is its selective virulence for fungal cells without altering mammalian cells. Herein we used L-132 cells, an epithelial cell line from the lungs of human embryo for cytotoxicity studies of compound **4e** and **5** where FDA-approved antifungal agent Amp B was used as a standard drug.¹⁶ Both the compounds **4e** and **5** were found to be non-toxic on L-132 cells with IC₅₀ value of 43.46 μM and 150.05 μM, respectively. Whilst the cytotoxicity of the antifungal drug Amp B was in the range of 5.4–10.82 μM.¹⁷ The CC₅₀ (cytotoxic concentration-50) values for compounds **4e** and **5** were calculated as 43.46 μM and 150.5 μM, respectively. The reported sub-lethal cytotoxicity of the antifungal drug Amp B was in the range of 5.4–10.82 μM.¹⁷ The selectivity index values for **4e** and **5** were figured as 8.01 and 16.02, respectively,. Higher selectivity index

suppositionally indicates that drug will be more efficient and safer to apply as lower concentration of drug is needed to treat any kind of microbial infections. All the synthesised derivatives are theoretically safe to use in further studies due to their higher SI values as compared to the parent molecule eugenol (**1a**) for which SI values was 0.2 according to the reports.¹⁸ A study towards formation of the DHN-melanin, a factor imparting greenish-grey colour to the fungal conidia was also accomplished. Previous report suggests significant decrease in the formation of this protective coat in fungal conidia treated with isoeugenol (**1b**).¹⁹ Compound **4e** and **5** were able to reduce the production of this particular melanin efficiently when compared to eugenol (**1a**) and Amp B (positive control). This reduction in DHN-melanin is a loss in cell defence factors in fungal cell wall as it alters the colonisation properties of conidia as well as their morphologies.²⁰ This loss in melanin slackens down the glued conidia from each other. When fungal strain was treated with compound **4e** and **5** we observed a smooth outer surface and decrease in conidia count *via* scanning electron microscopy (SEM) unlike untreated conidia which possess spinous surface and higher conidia count (**Figure 3**).

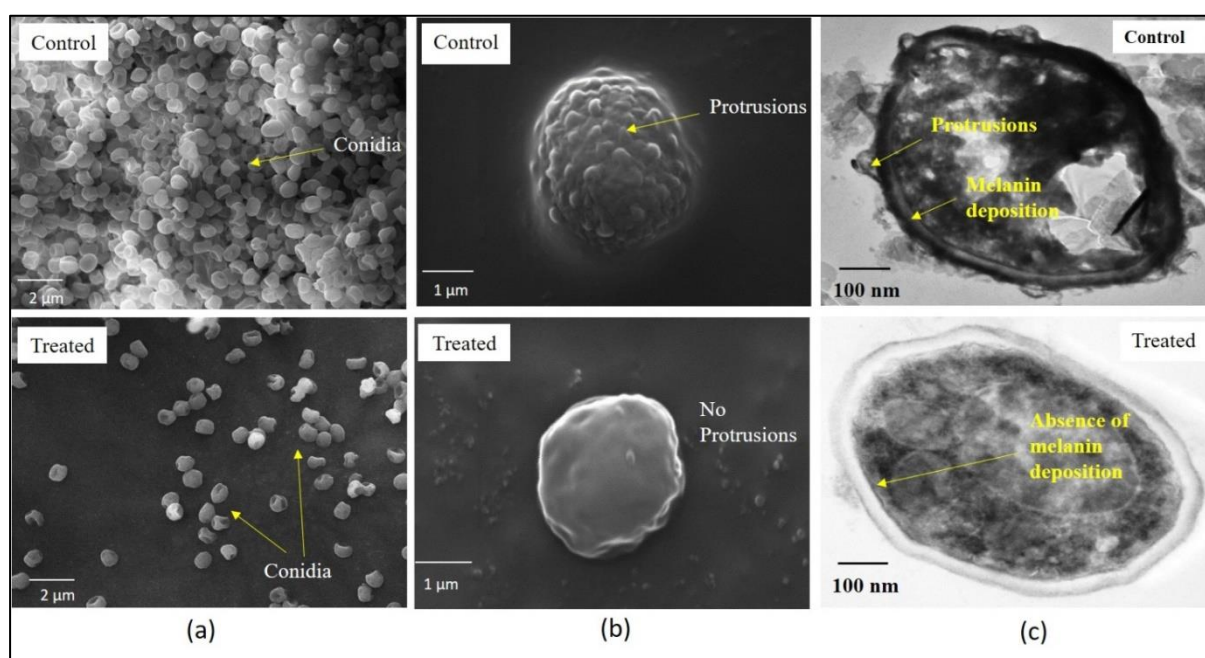


Figure 3: SEM and TEM images displaying the conidial surface of *A. fumigatus* (a) Decrease in conidia count in analogue treated sample as compare to control; (b) analogue treated single conidia with smooth surface as compared to spinous conidial surface in untreated control; and (c) analogue treated single conidia with reduced melanin content and softer surface compared to control conidia showing protrusion and melanin deposition

Fungal biofilm transmits an extracellular matrix (ECM) to stick all mycelia hyphae together post colonization which provides a protective covering to the pathogen to flourish in within the host.²¹ ECM consists of polysaccharide, hydrophobic proteins and melanin is a necessary component to glue mycelia threads.²² The eradication of fungal biofilms was adequate at concentration ranges of 69.53–86.92 μM and 243.60–304.5 μM for **4e** and **5**, respectively. Along with this, ECM generated by fungal biofilm was also absent on surface. Meanwhile SEM analysis shows dense ECM accumulation on fungal surface with well interconnected hyphal network, whereas compound treated strains lesser hyphal arrangements with no ECM accumulations (**Figure 4**).

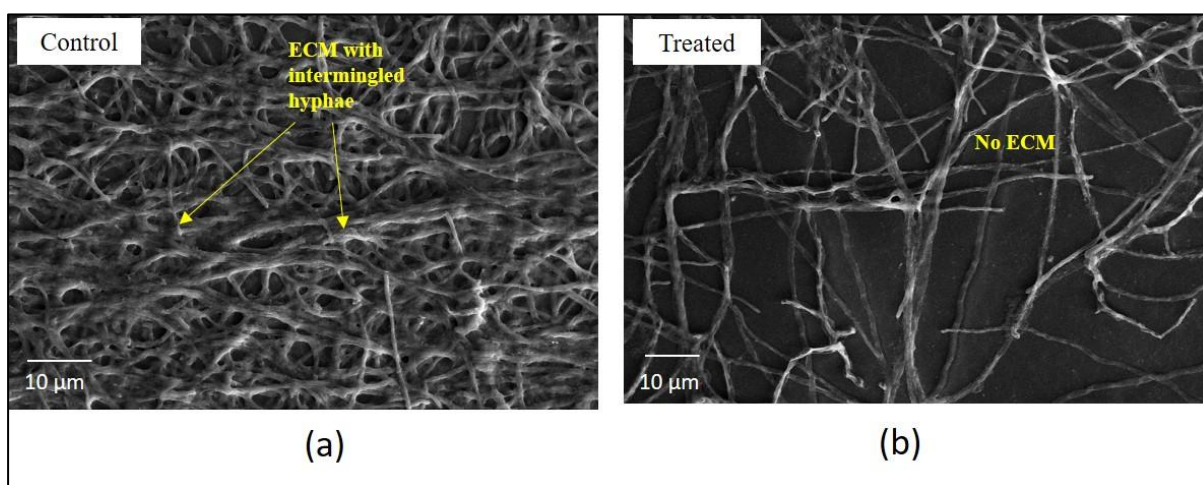


Figure 4: SEM of *A. fumigatus* biofilm surface. (a) *A. fumigatus* biofilm; Yellow arrow indicates ECM embedded in the hyphal network; (b) Analogue 8 treated *A. fumigatus* without ECM Magnification at 1K x; Scale- 10 μm

1.2.3 Conclusions

Concisely, we have synthesised eugenol and isoeugenol based glycoconjugates *via* click coupling reaction and assayed all the novel glycoconjugates for their antifungal activities against *A. fumigatus*. Further derivatisation of eugenol was achieved by the functionalization of olefinic double bond. Promising antifungal activity was observed in case of glucose glycoconjugate of eugenol and reduced eugenol *i.e.* euganol amongst all the synthesised derivatives. Other than antifungal studies we have also conducted experiments regarding eradication of cell wall virulence factor in *A. fumigatus* like DHN- melanin, biofilm with ECM production *via* utilizing SEM and TEM visualisations. Fungal strain treated with most

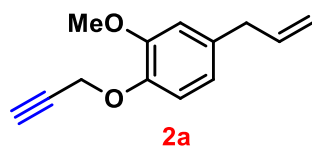
active compounds showed encouraging reduction in DHN- melanin production and decreased ECM production by fungal biofilms.

1.2.4 Experimental procedures

General Procedure for the propargylation of isoeugenol/eugenol:

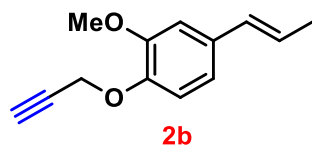
Compound **1a** or **1b** (5 g, 30.4506 mmol, 1 equiv.) was taken in a 250 mL round bottom flask and dissolved in acetone (20 mL) at room temperature under inert atmosphere. Then K_2CO_3 (6.3 g, 45.6759 mmol, 1.5 equiv.) and propargyl bromide (5.8 mL, 76.1266 mmol, 2.5 equiv.) were added to the above-mentioned solution at room temperature. After reaction was completed (monitored by TLC) the reaction mixture was filtered over Celite bed and the filtrate was evaporated *in vacuo* to furnish a residue which was purified by flash chromatography using a RediSep column (SiO_2 , 12g) with EtOAc-petroleum ether mixture as eluent.

4-Allyl-2-methoxy-1-(prop-2-yn-1-yloxy) benzene (**2a**):



Yellow liquid (4.5 g, 73%); R_f 0.34 (5% ethyl acetate in petroleum ether); 1H NMR (200 MHz, $CDCl_3$): δ_H 6.98–6.90 (m, 1H), 6.74–6.66 (m, 2H), 6.05–5.82 (m, 1H), 5.15–5.06 (m, 1H), 5.03 (s, 1H), 4.70 (d, $J = 2.4$ Hz, 2H), 3.82 (s, 3H), 3.32 (d, $J = 6.7$ Hz, 2H), 2.48 (t, $J = 2.4$ Hz, 1H); ^{13}C NMR (50 MHz, $CDCl_3$): δ_C 149.5, 145.0, 137.3, 134.1, 120.1, 115.6, 114.6, 112.2, 78.7, 75.4, 56.8, 55.6, 39.6; LCMS: m/z 203.1 for $C_{13}H_{15}O_2$ ($M+H$) $^+$.

(*E*)-2-Methoxy-4-(prop-1-en-1-yl)-1-(prop-2-yn-1-yloxy) benzene (**2b**):

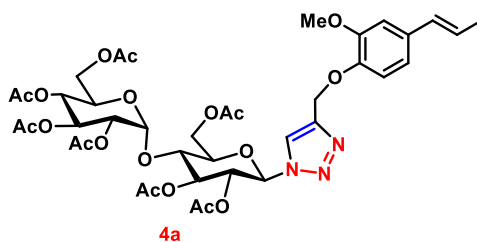


Colourless semisolid (4.6 g, 74%); R_f 0.34 (5% ethyl acetate in petroleum ether); 1H NMR (200 MHz, $CDCl_3$): δ_H 6.99–6.81 (m, 3H), 6.41–6.25 (m, 1H), 6.22–6.03 (m, 1H), 4.75 (d, $J = 2.4$ Hz, 2H), 3.88 (s, 3H), 2.50 (t, $J = 2.3$ Hz, 1H), 1.87 (dd, $J = 1.3, 6.4$ Hz, 3H); ^{13}C NMR (50 MHz, $CDCl_3$): δ_C 149.7, 145.8, 132.6, 130.5, 124.4, 118.4, 114.6, 109.1, 78.6, 75.6, 56.9, 55.8, 18.3; LCMS: m/z 203.1 for $C_{13}H_{15}O_2$ ($M+H$) $^+$.

General Procedure for the coupling of sugar azide with propargylated eugenol and isoeugenol:

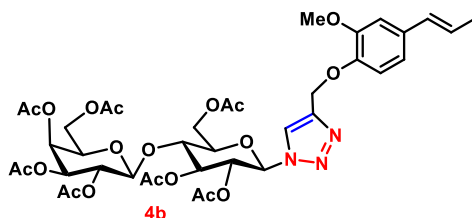
To a stirred solution of propargylated eugenol/isoeugenol (**2a** or **2b**) (30 mg, 0.1485 mmol, 1 equiv.) in DCM (3 mL) azido sugars (**3a-f**) (0.1782 mmol, 1.2 equiv.), CuI (15.55 mg, 0.0816 mmol, 0.55 equiv.) and DIPEA (26 μ L, 0.1485 mmol, 1.0 equiv.) were added and stirred for 14-24 hours under an inert atmosphere at 25 °C. After completion of reaction (monitored by TLC) the reaction mixture was concentrated *in vacuo* to obtain crude, which was purified by flash chromatography using a RediSep column (SiO₂, 12g) with EtOAc in petroleum ether to furnish desired eugenol/isoeugenol glycoconjugates (**4a-j**).

(2R,3S,4S,5R,6S)-2-(acetoxymethyl)-6-(((2R,3R,4S,5R,6R)-4,5-diacetoxy-2-(acetoxymethyl)-6-(4-((2-methoxy-4-((E)-prop-1-en-1-yl)phenoxy)methyl)-1H-1,2,3-triazol-1-yl)tetrahydro-2H-pyran-3-yl)oxy)tetrahydro-2H-pyran-3,4,5-triyl triacetate (4a**):**



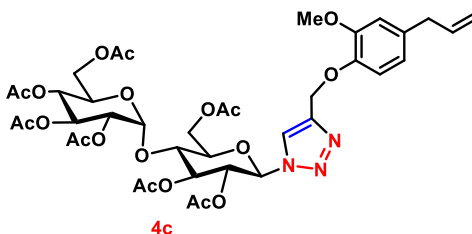
Colourless solid (89.7 mg, 70%); m.p.: 85-87 °C; R_f 0.13 (40% ethyl acetate in petroleum ether); ¹H NMR (400 MHz, CDCl₃): δ_H 7.78 (s, 1H), 6.91–6.86 (m, 2H), 6.84–6.76 (m, 1H), 6.30 (dd, $J = 1.5, 15.3$ Hz, 1H), 6.08 (dd, $J = 6.5, 15.6$ Hz, 1H), 5.83–5.76 (m, 1H), 5.39–5.33 (m, 3H), 5.23 (s, 2H), 5.10 (dd, $J = 8.0, 10.3$ Hz, 1H), 4.95 (dd, $J = 3.4, 10.3$ Hz, 1H), 4.50 (d, $J = 7.6$ Hz, 1H), 4.44 (d, $J = 13.0$ Hz, 1H), 4.15–4.04 (m, 3H), 3.93–3.86 (m, 3H), 3.85 (s, 3H), 2.14 (s, 3H), 2.08 (s, 3H), 2.05 (s, 3H), 2.03 (s, 6H), 1.95 (s, 3H), 1.83 (dd, $J = 1.5, 6.9$ Hz, 3H), 1.80 (s, 3H); ¹³C NMR (101 MHz, CDCl₃): δ_C 170.5, 170.3, 170.2, 170.2, 169.6, 169.2, 149.7, 146.6, 145.1, 132.4, 130.5, 124.5, 121.6, 118.7, 114.5, 109.1, 101.2, 85.6, 75.9, 75.7, 72.7, 71.0, 70.9, 70.5, 69.1, 66.7, 63.2, 61.8, 60.9, 55.9, 20.9, 20.8, 20.7, 20.7, 20.6, 20.2, 18.5; HRMS: m/z for C₃₉H₄₉O₁₉N₃Na (M+Na)⁺: calcd 886.2852, found 886.2847.

(2*R*,3*R*,4*S*,5*R*,6*R*)-2-(acetoxymethyl)-6-(((2*R*,3*R*,4*S*,5*R*,6*R*)-4,5-diacetoxy-2-(acetoxymethyl)-6-(4-((2-methoxy-4-((*E*)-prop-1-en-1-yl)phenoxy)methyl)-1*H*-1,2,3-triazol-1-yl)tetrahydro-2*H*-pyran-3-yl)oxy)tetrahydro-2*H*-pyran-3,4,5-triyl triacetate (4b):



Colourless solid (87.2 mg, 68%); m.p.: 171-173 °C; R_f 0.20 (40% ethyl acetate in petroleum ether); ^1H NMR (400 MHz, CDCl_3): δ_{H} 7.86–7.76 (m, 1H), 6.97–6.87 (m, 2H), 6.86–6.76 (m, 1H), 6.33 (dd, $J = 1.3, 15.7$ Hz, 1H), 6.22–6.02 (m, 1H), 5.90–5.77 (m, 1H), 5.47–5.34 (m, 3H), 5.26 (s, 2H), 5.13 (dd, $J = 7.7, 10.4$ Hz, 1H), 5.04–4.93 (m, 1H), 4.61–4.36 (m, 2H), 4.17–4.09 (m, 3H), 4.00–3.89 (m, 3H), 3.87 (s, 3H), 2.16 (s, 3H), 2.10 (s, 3H), 2.07 (s, 3H), 2.06–2.04 (m, 6H), 1.97 (s, 3H), 1.86 (dd, $J = 1.0, 6.4$ Hz, 3H), 1.82 (s, 3H); ^{13}C NMR (101 MHz, CDCl_3): δ_{C} 170.3, 170.2, 170.1, 170.0, 169.5, 169.1, 149.7, 146.5, 145.0, 132.4, 130.5, 124.3, 121.5, 118.6, 114.7, 109.3, 101.1, 85.5, 75.9, 75.6, 72.7, 70.9, 70.9, 70.5, 69.1, 66.7, 63.2, 61.8, 60.9, 60.4, 55.9, 21.0, 20.7, 20.6, 20.4, 20.1, 18.4; HRMS: m/z for $\text{C}_{39}\text{H}_{49}\text{O}_{19}\text{N}_3\text{Na}$ ($\text{M}+\text{Na}$) $^+$: 886.2852, found 886.2847.

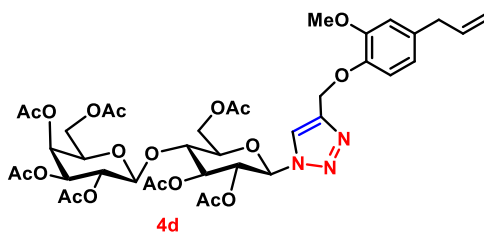
(2*R*,3*S*,4*S*,5*R*,6*S*)-2-(acetoxymethyl)-6-(((2*R*,3*R*,4*S*,5*R*,6*R*)-4,5-diacetoxy-2-(acetoxymethyl)-6-(4-((4-allyl-2-methoxyphenoxy)methyl)-1*H*-1,2,3-triazol-1-yl)tetrahydro-2*H*-pyran-3-yl)oxy)tetrahydro-2*H*-pyran-3,4,5-triyl triacetate (4c):



Yellow solid (96 mg, 75%); m.p.: 73-75 °C; R_f 0.22 (40% ethyl acetate in petroleum ether); ^1H NMR (200 MHz, CDCl_3): δ_{H} 7.85 (s, 1H), 6.92 (d, $J = 8.1$ Hz, 1H), 6.76–6.65 (m, 2H), 6.02–5.82 (m, 2H), 5.46–5.34 (m, 3H), 5.24 (s, 2H), 5.15–5.05 (m, 2H), 5.05–4.98 (m, 2H), 4.61–

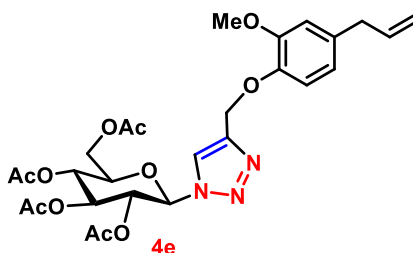
4.43 (m, 2H), 4.13 (td, $J = 3.5, 7.2$ Hz, 3H), 4.01–3.93 (m, 3H), 3.85 (s, 3H), 3.32 (d, $J = 6.6$ Hz, 2H), 2.16 (s, 3H), 2.10 (s, 3H), 2.08–2.02 (m, 10H), 1.97 (s, 3H), 1.82 (s, 3H); ^{13}C NMR (50 MHz, CDCl_3): δ_{C} 170.3, 170.2, 170.1, 170.0, 169.5, 169.1, 169.1, 149.6, 145.8, 145.0, 137.4, 134.0, 121.6, 120.5, 115.7, 114.7, 112.4, 101.0, 85.3, 75.7, 75.6, 72.6, 70.9, 70.8, 70.5, 69.0, 66.7, 63.2, 61.8, 60.9, 60.3, 55.8, 39.8, 21.0, 20.7, 20.6, 20.5, 20.1, 14.1; HRMS: m/z for $\text{C}_{39}\text{H}_{51}\text{O}_{19}\text{N}_3$ ($\text{M}+\text{H}$) $^+$: calcd 864.3033, found 864.3029; m/z for $\text{C}_{39}\text{H}_{49}\text{O}_{19}\text{N}_3\text{Na}$ ($\text{M}+\text{Na}$) $^+$: calcd 886.2852, found 886.2844.

(2*R*,3*R*,4*S*,5*R*,6*R*)-2-(acetoxymethyl)-6-(((2*R*,3*R*,4*S*,5*R*,6*R*)-4,5-diacetoxy-2-(acetoxymethyl)-6-(4-((4-allyl-2-methoxyphenoxy)methyl)-1*H*-1,2,3-triazol-1-yl)tetrahydro-2*H*-pyran-3-yl)oxy)tetrahydro-2*H*-pyran-3,4,5-triyl triacetate (4d):



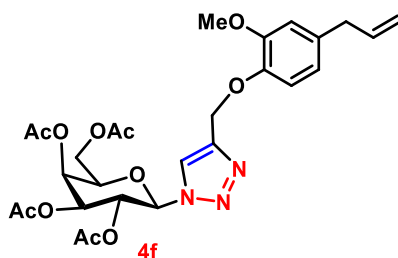
Colourless solid (79 mg, 62%); m.p.: 136–138 °C; R_f 0.26 (40% ethyl acetate in petroleum ether); ^1H NMR (200MHz, CDCl_3): δ_{H} 7.82 (s, 1H), 6.92 (d, $J = 8.0$ Hz, 1H), 6.77–6.64 (m, 2H), 6.02–5.83 (m, 2H), 5.49–5.30 (m, 4H), 5.25 (s, 2H), 5.16–5.00 (m, 4H), 4.89 (dd, $J = 3.9, 10.5$ Hz, 1H), 4.54–4.42 (m, 1H), 4.31–4.19 (m, 2H), 4.18–4.05 (m, 2H), 4.04–3.93 (m, 2H), 3.85 (s, 3H), 3.33 (d, $J = 6.7$ Hz, 2H), 2.12 (d, $J = 3.8$ Hz, 6H), 2.07 (s, 3H), 2.05–2.01 (m, 9H), 1.81 (s, 3H); ^{13}C NMR (50MHz, CDCl_3): δ_{C} 170.5, 170.5, 170.3, 169.9, 169.9, 169.4, 169.1, 149.6, 145.8, 145.1, 137.5, 134.0, 121.5, 120.5, 115.7, 114.7, 112.4, 95.9, 85.2, 75.2, 75.2, 72.4, 70.8, 70.0, 69.2, 68.7, 67.9, 63.3, 62.5, 61.5, 55.8, 39.8, 20.8, 20.7, 20.7, 20.6, 20.1; HRMS: m/z for $\text{C}_{39}\text{H}_{50}\text{O}_{19}\text{N}_3$ ($\text{M}+\text{H}$) $^+$: calcd 864.3033, found 864.3033; m/z for $\text{C}_{39}\text{H}_{49}\text{O}_{19}\text{N}_3\text{Na}$ ($\text{M}+\text{Na}$) $^+$: calcd 886.2852; found 886.2847.

(2*R*,3*R*,4*S*,5*R*,6*R*)-2-(acetoxymethyl)-6-(4-((4-allyl-2-methoxyphenoxy)methyl)-1*H*-1,2,3-triazol-1-yl)tetrahydro-2*H*-pyran-3,4,5-triyl triacetate (4e):



Colourless solid (69.1 mg, 81%); m.p.: 151-153 °C; R_f 0.21 (40% ethyl acetate in petroleum ether); ^1H NMR (200 MHz, CDCl_3): δ_{H} 7.88 (s, 1H), 6.93 (d, $J = 8.0$ Hz, 1H), 6.76–6.65 (m, 2H), 6.03–5.84 (m, 2H), 5.52–5.35 (m, 2H), 5.30–5.18 (m, 3H), 5.13–5.07 (m, 1H), 5.03 (s, 1H), 4.36–4.24 (m, 1H), 4.13 (dd, $J = 1.9, 12.5$ Hz, 1H), 4.06–3.94 (m, 1H), 3.86 (s, 3H), 3.33 (d, $J = 6.7$ Hz, 2H), 2.08 (d, $J = 3.3$ Hz, 6H), 2.03 (s, 3H), 1.84 (s, 3H); ^{13}C NMR (50 MHz, CDCl_3): δ_{C} 170.5, 169.9, 169.3, 168.8, 149.7, 145.9, 145.3, 137.5, 134.1, 121.4, 120.5, 115.8, 114.8, 112.5, 85.7, 75.1, 72.7, 70.3, 67.7, 63.3, 61.6, 55.9, 39.8, 20.7, 20.5, 20.1; HRMS: m/z for $\text{C}_{27}\text{H}_{33}\text{O}_{11}\text{N}_3\text{Na}$ ($\text{M}+\text{Na}$) $^+$: calcd 598.2007, found 598.2008.

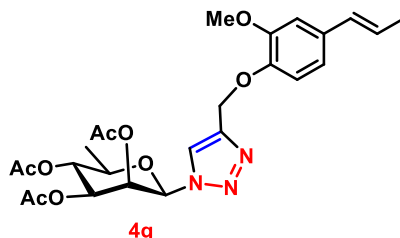
(2*R*,3*S*,4*S*,5*R*,6*R*)-2-(acetoxymethyl)-6-(4-((4-allyl-2-methoxyphenoxy)methyl)-1*H*-1,2,3-triazol-1-yl)tetrahydro-2*H*-pyran-3,4,5-triyl triacetate (4f):



Colourless solid (55.4 mg, 65%); m.p.: 105-107 °C; R_f 0.18 (40% ethyl acetate in petroleum ether); ^1H NMR (200MHz, CDCl_3): δ_{H} 7.95 (s, 1H), 6.94 (d, $J = 7.8$ Hz, 1H), 6.76–6.65 (m, 2H), 6.06–5.90 (m, 1H), 5.89–5.81 (m, 1H), 5.64–5.51 (m, 2H), 5.29–5.20 (m, 3H), 5.10 (d, $J = 6.6$ Hz, 1H), 5.04 (s, 1H), 4.28–4.09 (m, 3H), 3.87 (s, 3H), 3.33 (d, $J = 6.7$ Hz, 2H), 2.25–2.17 (m, 3H), 2.05 (s, 3H), 2.01 (s, 3H), 1.86 (s, 3H); ^{13}C NMR (50 MHz, CDCl_3): δ_{C} 170.4, 170.0, 169.8, 169.0, 149.7, 145.9, 145.2, 137.5, 134.1, 121.5, 120.5, 115.8, 114.9, 112.4, 86.2, 74.0, 70.9, 67.8, 66.9, 63.4, 61.3, 55.9, 39.8, 20.7, 20.5, 20.2; found 598.2007; m/z for

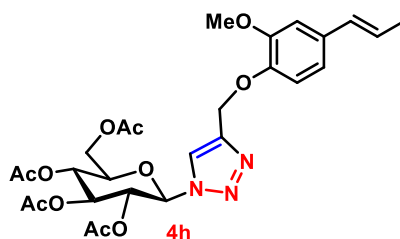
$C_{27}H_{33}O_{11}N_3Na$ ($M+Na$)⁺: calcd 598.2006., found 598.2006.

(3*R*,4*R*,5*S*,6*S*)-2-(4-((2-methoxy-4-((*E*)-prop-1-en-1-yl)phenoxy)methyl)-1*H*-1,2,3-triazol-1-yl)-6-methyltetrahydro-2*H*-pyran-3,4,5-triyl triacetate (4g):



Colourless solid (57.6 mg, 75%); m.p.: 112-114 °C; R_f 0.20 (40% ethyl acetate in petroleum ether); 1H NMR (200 MHz, $CDCl_3$): δ_H 7.86 (s, 1H), 6.98–6.77 (m, 3H), 6.40–6.24 (m, 1H), 6.23–6.03 (m, 2H), 5.74–5.62 (m, 1H), 5.28 (s, 2H), 5.24–5.13 (m, 2H), 3.94–3.74 (m, 4H), 2.09 (s, 3H), 1.98 (s, 3H), 1.92 (s, 3H), 1.85 (d, $J = 6.3$ Hz, 3H), 1.33 (d, $J = 6.1$ Hz, 3H); ^{13}C NMR (50 MHz, $CDCl_3$): δ_C 169.9, 169.2, 149.5, 146.5, 144.5, 132.2, 130.5, 124.3, 121.9, 118.6, 114.1, 109.1, 84.7, 73.9, 70.7, 69.6, 69.2, 63.1, 55.8, 20.7, 20.5, 20.2, 18.4, 17.5; HRMS: m/z for $C_{25}H_{32}O_9N_3$ ($M+H$)⁺: calcd 518.2133, found 518.2131.

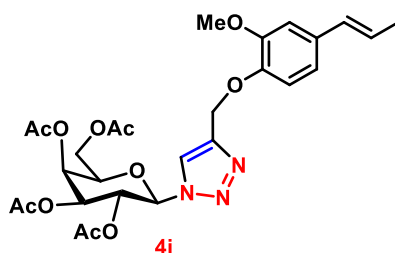
(2*R*,3*R*,4*S*,5*R*,6*R*)-2-(acetoxymethyl)-6-(4-((2-methoxy-4-((*E*)-prop-1-en-1-yl)phenoxy)methyl)-1*H*-1,2,3-triazol-1-yl)tetrahydro-2*H*-pyran-3,4,5-triyl triacetate (4h):



Colourless solid (69.2 mg, 81%); m.p.: 181-183 °C; R_f 0.25 (40% ethyl acetate in petroleum ether); 1H NMR (400 MHz, $CDCl_3$): δ_H 7.86 (s, 1H), 6.93–6.89 (m, 2H), 6.86–6.80 (m, 1H), 6.33 (dd, $J = 1.5, 15.8$ Hz, 1H), 6.11 (qd, $J = 6.6, 15.7$ Hz, 1H), 5.89–5.85 (m, 1H), 5.47–5.38 (m, 2H), 5.28–5.20 (m, 3H), 4.28 (dd, $J = 5.1, 12.6$ Hz, 1H), 4.14 (dd, $J = 2.0, 12.6$ Hz, 1H), 4.02–3.96 (m, 1H), 3.89–3.87 (m, 3H), 2.08 (s, 3H), 2.07 (s, 3H), 2.02 (s, 3H), 1.86 (dd, $J = 1.5, 6.6$ Hz, 3H), 1.84–1.82 (m, 3H); ^{13}C NMR (101 MHz, $CDCl_3$): δ_C 170.5, 169.9,

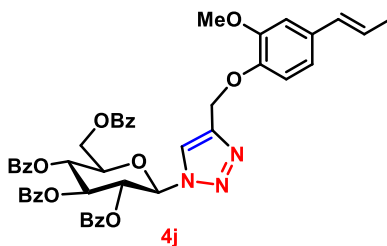
169.3, 168.8, 149.7, 146.5, 145.1, 132.4, 130.5, 124.4, 121.4, 118.6, 114.6, 109.1, 85.7, 75.1, 72.7, 70.2, 67.7, 63.1, 61.5, 55.9, 20.7, 20.5, 20.5, 20.1, 18.4; HRMS: m/z for $C_{27}H_{33}O_{11}N_3Na$ ($M+Na$)⁺: calcd 598.2007, found 598.2004.

(2*R*,3*S*,4*S*,5*R*,6*R*)-2-(acetoxymethyl)-6-(4-((2-methoxy-4-((*E*)-prop-1-en-1-yl)phenoxy)methyl)-1*H*-1,2,3-triazol-1-yl)tetrahydro-2*H*-pyran-3,4,5-triyl triacetate (4i):



Yellow solid (61.4 mg, 72%); m.p.: 105-107 °C; R_f 0.18 (40% ethyl acetate in petroleum ether); 1H NMR (400 MHz, $CDCl_3$): δ_H 7.92 (s, 1H), 6.93–6.88 (m, 2H), 6.85–6.78 (m, 1H), 6.31 (dd, $J = 1.5, 15.3$ Hz, 1H), 6.16–6.05 (m, 1H), 5.81 (d, $J = 9.2$ Hz, 1H), 5.58–5.51 (m, 2H), 5.27–5.19 (m, 3H), 4.21–4.18 (m, 1H), 4.13 (dd, $J = 6.5, 11.8$ Hz, 2H), 3.87 (s, 3H), 2.20 (s, 4H), 2.03 (s, 4H), 1.99 (s, 4H), 1.86–1.83 (m, 7H); ^{13}C NMR (101 MHz, $CDCl_3$): δ_C 170.5, 170.1, 169.9, 169.1, 149.7, 146.7, 145.1, 132.4, 130.5, 124.5, 121.6, 118.7, 114.7, 109.1, 86.3, 74.1, 70.9, 67.8, 66.9, 63.3, 61.3, 55.9, 20.8, 20.6, 20.3, 18.5; HRMS: m/z for $C_{27}H_{33}O_{11}N_3Na$ ($M+Na$)⁺: calcd 598.2007, found 598.2002.

(2*R*,3*S*,4*S*,5*R*,6*R*)-2-((benzoyloxy)methyl)-6-(4-((2-methoxy-4-((*E*)-prop-1-en-1-yl)phenoxy)methyl)-1*H*-1,2,3-triazol-1-yl)tetrahydro-2*H*-pyran-3,4,5-triyl tribenzoate (4j):



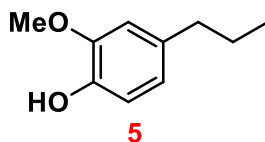
Colourless solid (86.7 mg, 71%); m.p.: 130-132 °C; R_f 0.20 (40% ethyl acetate in petroleum ether); 1H NMR (200 MHz, $CDCl_3$): δ_H 8.02 (d, $J = 8.5$ Hz, 3H), 7.92 (d, $J = 7.2$ Hz, 2H),

7.81 (d, $J = 7.2$ Hz, 2H), 7.73 (d, $J = 7.3$ Hz, 2H), 7.60–7.46 (m, 2H), 7.45–7.35 (m, 5H), 7.34–7.21 (m, 5H), 6.85 (d, $J = 8.1$ Hz, 2H), 6.80–6.69 (m, 1H), 6.38–6.24 (m, 2H), 6.20–5.97 (m, 3H), 5.96–5.81 (m, 1H), 5.24 (s, 2H), 4.75–4.59 (m, 1H), 4.57–4.42 (m, 2H), 3.83 (s, 3H), 1.85 (d, $J = 5.8$ Hz, 3H); ^{13}C NMR (50 MHz, CDCl_3): δ_{C} 166.1, 165.6, 165.1, 164.7, 149.8, 146.7, 145.2, 133.7, 133.6, 133.5, 133.3, 132.3, 130.6, 129.8, 129.8, 129.4, 128.5, 128.5, 128.4, 128.0, 124.2, 121.6, 118.7, 114.7, 109.3, 86.1, 75.5, 73.1, 71.0, 68.9, 63.3, 62.7, 55.9, 18.4; HRMS: m/z for $\text{C}_{47}\text{H}_{42}\text{O}_{11}\text{N}_3$ ($\text{M}+\text{H}$) $^+$: calcd 824.2814, found 824.2814.

Synthesis of 5:

Compound **1a** was dissolved in anhydrous methanol under argon at 0 °C. After dissolution of compound Pd/C was added in catalytic amount and reaction mixture was kept under H_2 atmosphere for 3 hours at 25 °C. After completion of reaction (monitored by TLC) the reaction mixture was filtered over celite bed and concentrated *in vacuo* to obtain crude, which was purified by flash chromatography using a RediSep column (silica gel, 12g) with EtOAc in petroleum ether to furnish desired compound **5**.

2-Methoxy-4-propylphenol (**5**):



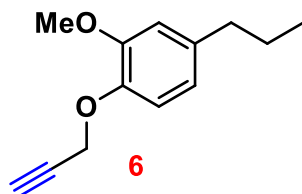
Brown oil (183 mg, 84%); R_f 0.40 (40% ethyl acetate in petroleum ether); ^1H NMR (200 MHz, CDCl_3): δ_{H} 6.89–6.76 (m, 1H), 6.72–6.58 (m, 2H), 5.65 (br. s., 1H), 3.90–3.79 (m, 3H), 2.50 (t, $J = 7.5$ Hz, 2H), 1.60 (qd, $J = 7.4, 14.9$ Hz, 2H), 0.99–0.86 (m, 3H); ^{13}C NMR (50 MHz, CDCl_3): δ_{C} 146.5, 143.6, 134.8, 121.1, 114.3, 111.2, 55.9, 37.8, 25.0, 13.9; HRMS: m/z for $\text{C}_{10}\text{H}_{13}\text{O}_2$ ($\text{M}+\text{H}$) $^+$: calcd 165.0910, found 165.0910.

Synthesis of 6:

Compound **5** (2 g, 12.0336 mmol, 1 equiv.) was dissolved in dry acetone (20 mL) at room temperature followed by addition of K_2CO_3 (2.5 g, 18.0504 mmol, 1.5 equiv.) and propargyl bromide (2.3 mL, 30.0842 mmol, 2.5 equiv.) at room temperature. After completion of reaction (monitored by TLC) reaction mixture was filtered through Celite bed and the filtrate was evaporated *in vacuo*. Residue was purified by flash chromatography using a

RediSep column (silica gel, 12g) with EtOAc in petroleum ether to furnish product (**6**).

2-Methoxy-1-(prop-2-yn-1-yloxy)-4-propylbenzene: (6):

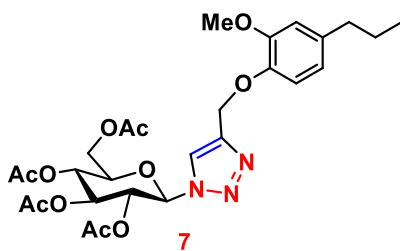


Brown oil (1.8 g, 75%); R_f 0.33 (2% ethyl acetate in petroleum ether); ^1H NMR (200 MHz, CDCl_3): δ_{H} 6.94 (d, $J = 8.7$ Hz, 1H), 6.74–6.65 (m, 2H), 4.72 (d, $J = 2.3$ Hz, 2H), 3.85 (s, 3H), 2.59–2.45 (m, 3H), 1.72–1.52 (m, 2H), 0.94 (t, $J = 7.3$ Hz, 3H); ^{13}C NMR (50 MHz, CDCl_3): δ_{C} 149.6, 146.4, 137.0, 121.0, 114.8, 112.4, 79.0, 75.5, 57.0, 55.8, 37.8, 24.7, 13.8; HRMS: m/z for $\text{C}_{13}\text{H}_{16}\text{O}_2\text{Na}$ ($\text{M}+\text{Na}$) $^+$: calcd 227.1043, found 227.1043.

Synthesis of compound 7:

Compound **7** was synthesized by treating compound **6** and **3c** according to the general procedure for synthesizing compounds (**4a-j**).

(2R,3R,4S,5R,6R)-2-(acetoxymethyl)-6-(4-((2-methoxy-4-propylphenoxy)methyl)-1H-1,2,3-triazol-1-yl)tetrahydro-2H-pyran-3,4,5-triyl triacetate (7):

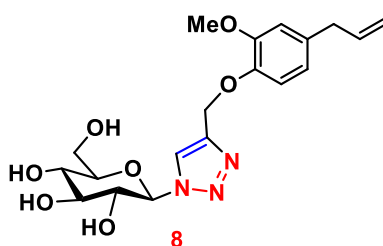


Yellowish liquid (80 mg, 63%); R_f 0.14 (40% ethyl acetate in petroleum ether); ^1H NMR (400 MHz, CDCl_3): δ_{H} 7.87 (s, 1H), 6.89 (d, $J = 8.1$ Hz, 1H), 6.71–6.69 (m, 1H), 6.66 (dd, $J = 1.6, 8.1$ Hz, 1H), 5.86 (d, $J = 8.9$ Hz, 1H), 5.47–5.36 (m, 2H), 5.27–5.19 (m, 3H), 4.25 (d, $J = 5.0$ Hz, 1H), 4.15–4.09 (m, 1H), 3.85 (s, 3H), 2.53–2.47 (m, 2H), 2.06 (s, 3H), 2.05 (s, 3H), 2.01 (s, 3H), 1.82 (s, 3H), 1.63–1.56 (m, 2H), 0.91 (t, $J = 7.3$ Hz, 3H); ^{13}C NMR (101 MHz, CDCl_3): δ_{C} 170.5, 169.9, 169.3, 168.8, 149.4, 145.4, 136.7, 120.3, 114.6, 112.3, 85.6, 75.0, 72.6, 70.1, 67.6, 63.2, 61.5, 55.8, 37.6, 24.6, 20.6, 20.5, 20.4, 20.1, 13.8; HRMS: m/z for $\text{C}_{27}\text{H}_{36}\text{O}_{11}\text{N}_3$ ($\text{M}+\text{H}$) $^+$: calcd 578.2350, found 578.2347.

Procedure for the synthesis of compound 8 and 9 via deprotection of 4e and 7:

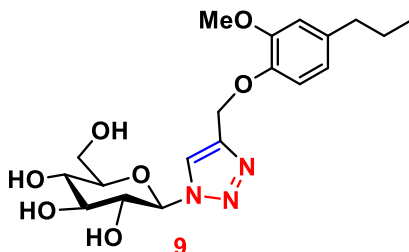
Compound (4e or 7) (1.0 equiv.) was dissolved in MeOH (10 mL) at room temperature followed by addition of NaOMe (0.5 equiv.). After 2 hours of stirring, the reaction mixture was quenched with 10% HCl with the pH attains 7. The solvent was removed *in vacuo* to afford crude mixture which was purified using silica gel (230-400) flash column chromatography (MeOH/DCM) to furnish deprotected compound (8 or 9).

(2R,3R,4S,5S,6R)-2-(4-((4-allyl-2-methoxyphenoxy) methyl)-1H-1,2,3-triazol-1-yl)-6-(hydroxymethyl)tetrahydro-2H-pyran-3,4,5-triol (8):



Colorless semisolid (76 %); R_f 0.06 (70% ethyl acetate in petroleum ether); ^1H NMR (400 MHz, Methanol- d_4): δ_{H} 8.27 (s, 1H), 7.00 (d, $J = 8.1$ Hz, 1H), 6.83–6.81 (m, 1H), 6.73 (dd, $J = 1.7, 8.2$ Hz, 1H), 5.65 (d, $J = 9.1$ Hz, 1H), 5.16 (s, 2H), 5.12–5.03 (m, 2H), 3.98–3.88 (m, 2H), 3.80 (s, 3H), 3.75 (s, 1H), 3.64–3.58 (m, 2H), 3.57–3.51 (m, 1H), 3.34 (d, $J = 6.5$ Hz, 2H); ^{13}C NMR (101 MHz, Methanol- d_4): δ_{C} 151.3, 147.5, 145.4, 139.2, 135.7, 125.0, 121.9, 116.4, 116.0, 114.1, 89.7, 81.2, 78.5, 74.1, 70.9, 63.9, 62.5, 56.5, 40.9; HRMS: m/z for $\text{C}_{19}\text{H}_{26}\text{O}_7\text{N}_3(\text{M}+\text{H})^+$: calcd 408.1766, found 408.1766.

(2R,3S,4S,5R,6R)-2-(hydroxymethyl)-6-(4-((2-methoxy-4-propylphenoxy)methyl)-1H-1,2,3-triazol-1-yl)tetrahydro-2H-pyran-3,4,5-triol (9):



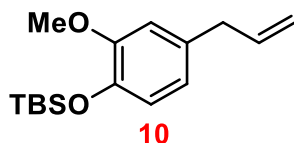
Colorless semisolid (79 %); m.p.: 128-130 °C; R_f 0.06 (70% ethyl acetate in petroleum ether); ^1H NMR (400 MHz, Methanol- d_4): δ_{H} 8.25 (s, 1H), 6.95 (d, $J = 8.1$ Hz, 1H), 6.79 (d, $J = 1.6$ Hz, 1H), 6.69 (dd, $J = 1.8, 8.1$ Hz, 1H), 5.62 (d, $J = 9.1$ Hz, 1H), 5.13 (s, 2H), 3.95–

3.85 (m, 2H), 3.79 (s, 3H), 3.73 (s, 1H), 3.62–3.55 (m, 2H), 3.55–3.48 (m, 1H), 2.52 (t, $J = 7.6$ Hz, 2H), 1.67–1.56 (m, 2H), 1.15 (d, $J = 6.1$ Hz, 1H), 0.93 (t, $J = 7.4$ Hz, 3H); ^{13}C NMR (101 MHz, Methanol- d_4): δ_{C} 151.2, 147.2, 138.3, 125.0, 121.8, 116.4, 114.0, 89.7, 81.2, 78.5, 74.1, 71.0, 64.0, 62.5, 56.5, 38.8, 26.0, 14.2; HRMS: m/z for $\text{C}_{19}\text{H}_{28}\text{O}_7\text{N}_3(\text{M}+\text{H})^+$: calcd 410.1922, found 410.1924.

Procedure for the OTBDMS protection (10):

Eugenol **1a** (10 g, 60.9756 mmol, 1 equiv.) was dissolved in DCM (30 mL) and to this solution imidazole (4.6 g, 67.0731 mmol, 1.1 equiv.) DMAP (1.1 g, 9.1463 mmol, 0.15 equiv.) and TBDMSCl (10 g, 67.0731 mmol, 1.1 equiv.) were added sequentially and stirred for 12 hours at 25 °C. After completion of reaction (monitored by TLC) the reaction mixture was concentrated *in vacuo* to obtain crude, which was purified using silica gel (230-400) flash column chromatography (EtOAc/pet. ether) to furnish the desired product **10**.

(4-allyl-2-methoxyphenoxy)(*tert*-butyl)dimethylsilane (10):

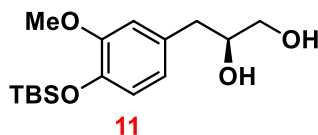


Yellow oil (12.8 g, 77%); R_f 0.77 (10% ethyl acetate in petroleum ether); ^1H NMR (200 MHz, CDCl_3): δ_{H} 6.68–6.57 (m, 1H), 6.55–6.43 (m, 2H), 5.92–5.70 (m, 1H), 4.93 (d, $J = 4.9$ Hz, 1H), 4.87 (s, 1H), 3.62 (s, 3H), 3.16 (d, $J = 6.6$ Hz, 2H), 0.85 (s, 9H), 0.00 (s, 6H); ^{13}C NMR (50 MHz, CDCl_3): δ_{C} 150.8, 143.3, 137.8, 133.5, 120.8, 115.6, 112.6, 55.5, 40.0, 25.8, 18.5, -4.6; HRMS: m/z for $\text{C}_{16}\text{H}_{25}\text{O}_2\text{Si}$ (M-H) $^+$: calcd 277.1618, found 277.1617.

Procedure for the dihydroxylation (11):

To a solution of *tert*-butanol and water (total 120 mL, 1:1 v/v ratio) AD-mix β (22.4 g, 28.7769 mmol, 1.0 equiv.) was added and resulting mixture was cooled to 0°C. Compound **10** (8 g, 28.7769 mmol, 1.0 equiv.) was added to this slurry and reaction mixture was stirred 8 h at 25°C. After completion of reaction (monitored by TLC) the reaction was quenched by addition of sodium sulphite (43 g). Then the reaction mixture was extracted with ethyl acetate (3X40 mL) and combined organic layers were washed with brine and dried over anhydrous sodium sulphate and concentrated *in vacuo*. Crude obtained was purified using silica gel (230-400) flash column chromatography (EtOAc/pet. ether) to furnish the desired product

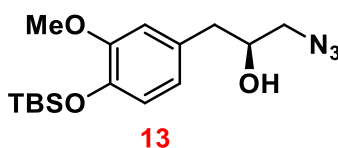
11.

(S)-3-(4-((tert-Butyldimethylsilyl)oxy)-3-methoxyphenyl)propane-1,2-diol (11):

Yellow oil (6.3 g, 71%); R_f 0.02 (50% ethyl acetate in petroleum ether); ^1H NMR (200 MHz, CDCl_3): δ_{H} 6.68–6.47 (m, 3H), 3.76 (d, $J = 5.3$ Hz, 1H), 3.64 (s, 3H), 3.52 (br. s., 1H), 3.38 (d, $J = 6.9$ Hz, 1H), 2.62–2.48 (m, 2H), 2.12 (br. s., 2H), 0.89–0.80 (m, 9H), 0.03–0.05 (m, 6H); ^{13}C NMR (50 MHz, CDCl_3): δ_{C} 151.0, 143.8, 131.0, 121.4, 121.0, 113.2, 73.0, 66.0, 55.5, 39.6, 25.7, 18.5, -4.6; HRMS: m/z for $\text{C}_{16}\text{H}_{28}\text{O}_4\text{SiNa}$ ($\text{M}+\text{Na}$) $^+$: calcd 335.1649, found 335.1647.

Synthesis of compound (13):

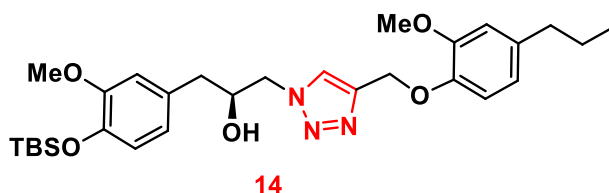
Compound **11** (1 g, 3.2051 mmol, 1 equiv.) was dissolved in DCM (15 mL) and resulting solution was cooled to 0 °C. To this reaction mixture triethyl amine (431.62 μL , 3.2051 mmol, 1 equiv.), DMAP (234 mg, 1.9230 mmol, 0.6 equiv.) and *p*-toluene sulfonyl chloride (730 mg, 3.8461 mmol, 1.2 equiv.) was added at 0°C. Reaction mixture was stirred for 10 h at 25 °C. After completion of reaction (monitored by TLC) the reaction mixture was diluted with DCM (20-30 mL) and washed with CuSO_4 , NaHSO_4 and NaCl solutions subsequently. Organic layer was dried over anhydrous sodium sulphate and concentrated *in vacuo* to furnish tosylated product (**12**) which was directly used for next without further purification. A solution of monotosylate, TBAI (59 mg, 0.1602 mmol, 0.05 equiv.) and NaN_3 (624.9 mg, 9.6153 mmol, 3 equiv.) in DMF (10 mL) was heated at 95°C for 3-4 h. After completion of reaction (monitored by TLC) the reaction mixture was cooled at 0 °C and was diluted with water (20 mL). The aqueous layer was extracted three times with ethyl acetate (30 mL). Combined organic layers were dried over sodium sulphate and concentrated *in vacuo* to obtain crude, which was purified using silica gel (230-400) flash column chromatography (EtOAc/pet.ether) to furnish the desired product.

(S)-1-Azido-3-(4-((tert-butyldimethylsilyl)oxy)-3-methoxyphenyl)propan-2-ol (13):

Yellow oil (845 mg, 78%); R_f 0.05 (50% ethyl acetate in petroleum ether); ^1H NMR (200 MHz, CDCl_3): δ_{H} 6.68–6.45 (m, 3H), 3.88–3.73 (m, 1H), 3.64 (s, 3H), 3.23–3.02 (m, 2H), 2.57 (d, $J = 6.7$ Hz, 2H), 0.84 (s, 9H), 0.00 (s, 6H); ^{13}C NMR (50 MHz, CDCl_3): δ_{C} 151.1, 144.0, 130.3, 121.5, 121.1, 113.2, 71.8, 55.9, 55.5, 40.6, 25.7, 18.5, -4.6; HRMS: m/z for $\text{C}_{16}\text{H}_{27}\text{O}_3\text{N}_3\text{NaSi}$ ($\text{M}+\text{Na}$) $^+$: calcd 360.1714, found 360.1712.

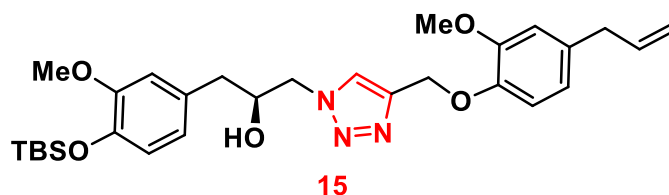
General procedure for the synthesis of compounds 14-16:

Compound **14-16** were synthesized by treating compound **12** with compound **6**, **2a** and **2b** respectively, according the general procedure for synthesizing compounds **4a-j**.

(S)-1-(4-((tert-Butyldimethylsilyl)oxy)-3-methoxyphenyl)-3-(4-((2-methoxy-4-propylphenoxy)-methyl)-1H-1,2,3-triazol-1-yl)propan-2-ol (14):

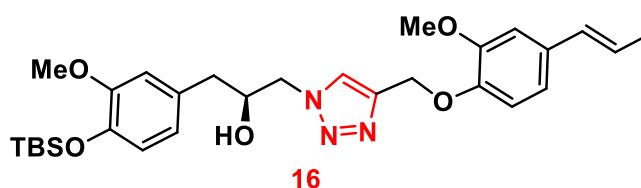
Colourless semisolid (112.8 mg, 85%); R_f 0.25 (40% ethyl acetate in petroleum ether); ^1H NMR (200 MHz, CDCl_3): δ_{H} 7.61 (s, 1H), 6.78 (d, $J = 7.8$ Hz, 1H), 6.66–6.60 (m, 1H), 6.59–6.53 (m, 3H), 6.52–6.46 (m, 1H), 5.07 (s, 2H), 4.32 (d, $J = 10.7$ Hz, 1H), 4.09 (d, $J = 9.3$ Hz, 2H), 3.65 (d, $J = 8.8$ Hz, 7H), 2.84 (br. s., 1H), 2.63–2.52 (m, 2H), 2.37 (t, $J = 7.6$ Hz, 2H), 1.541.38 (m, 2H), 0.85 (s, 9H), 0.82–0.74 (m, 4H), 0.00 (s, 6H); ^{13}C NMR (50 MHz, CDCl_3): δ_{C} 151.1, 149.4, 145.6, 144.2, 144.0, 136.6, 130.0, 124.6, 121.5, 121.0, 120.4, 114.4, 113.2, 112.3, 71.3, 63.3, 55.8, 55.5, 55.1, 40.6, 37.7, 25.7, 24.7, 18.4, 13.9, -4.6; HRMS: m/z for $\text{C}_{29}\text{H}_{44}\text{O}_5\text{N}_3\text{Si}$ ($\text{M}+\text{H}$) $^+$: calcd 542.3045, found 542.3044, m/z for $\text{C}_{29}\text{H}_{43}\text{O}_5\text{N}_3\text{NaSi}$ ($\text{M}+\text{Na}$) $^+$: calcd 564.2864, found 564.2859.

(S)-1-(4-((4-allyl-2-methoxyphenoxy)methyl)-1H-1,2,3-triazol-1-yl)-3-(4-((tert-butyl-dimethylsilyl)oxy)-3-methoxyphenyl)propan-2-ol (15):



Yellowish semisolid (115.6 mg, 73%); R_f 0.14 (40% ethyl acetate in petroleum ether); ^1H NMR (200 MHz, CDCl_3): δ_{H} 7.60 (s, 1H), 6.83–6.60 (m, 4H), 6.58–6.44 (m, 2H), 6.14 (s, 1H), 6.05–5.86 (m, 1H), 5.10 (s, 2H), 4.37–4.25 (m, 1H), 4.19–4.01 (m, 2H), 3.70 (s, 3H), 3.63 (s, 3H), 2.64–2.49 (m, 2H), 1.71 (d, $J = 6.4$ Hz, 3H), 0.85 (s, 9H), 0.00 (s, 6H); ^{13}C NMR (50 MHz, CDCl_3): δ_{C} 151.1, 149.6, 146.6, 144.0, 132.2, 130.5, 129.9, 124.6, 124.3, 121.5, 121.1, 118.6, 114.3, 113.2, 109.0, 71.3, 63.1, 55.8, 55.5, 55.1, 40.6, 25.7, 18.4, -4.6; HRMS: m/z for $\text{C}_{29}\text{H}_{42}\text{O}_5\text{N}_3\text{Si}$ ($\text{M}+\text{H}$) $^+$: calcd 540.2888, found 540.2888, m/z for $\text{C}_{29}\text{H}_{41}\text{O}_5\text{N}_3\text{NaSi}$ ($\text{M}+\text{Na}$) $^+$: calcd 562.2708, found 562.2703.

(S,E)-1-(4-((tert-butyl-dimethylsilyl)oxy)-3-methoxyphenyl)-3-(4-((2-methoxy-4-(prop-1-en-1-yl)phenoxy)methyl)-1H-1,2,3-triazol-1-yl)propan-2-ol (16):



Yellowish semisolid (97.2 mg, 73%); R_f 0.20 (40% ethyl acetate in petroleum ether); ^1H NMR (200 MHz, CDCl_3): δ_{H} 7.61 (s, 1H), 6.80 (d, $J = 8.2$ Hz, 1H), 6.67–6.45 (m, 5H), 5.79 (tdd, $J = 6.7, 10.2, 16.7$ Hz, 1H), 5.07 (s, 2H), 4.99–4.92 (m, 1H), 4.88 (s, 1H), 4.32 (d, $J = 10.9$ Hz, 1H), 4.16–4.04 (m, 2H), 3.63 (s, 3H), 3.68 (s, 3H), 3.17 (d, $J = 6.6$ Hz, 2H), 2.78 (brs, 1H), 2.69–2.47 (m, 2H), 0.84 (s, 9H), 0.00 (s, 6H); ^{13}C NMR (50 MHz, CDCl_3): δ_{C} 151.1, 149.5, 145.9, 144.1, 144.0, 137.5, 133.8, 130.0, 124.5, 121.5, 121.0, 120.5, 115.8, 114.5, 113.2, 112.3, 71.3, 63.3, 55.8, 55.5, 55.1, 40.6, 39.8, 25.7, 18.5, -4.6; HRMS: m/z for

$C_{29}H_{42}O_5N_3Si$ (M+H)⁺: calcd 540.2888, found 540.2887, *m/z* for $C_{29}H_{41}O_5N_3NaSi$ (M+Na)⁺: calcd 562.2708, found 562.2700.

Biological Evaluation

Fungal strain, culture maintenance and inoculum preparation.

Aspergillus fumigatus (ATCC-46645) strain was a gift from Prof. Axel Brakhage, Department of Molecular and Applied Microbiology, Leibnitz Institute for Natural Product Research, and Infection Biology- HKI, Germany. It was maintained by subculturing on Czapek Dox Agar (CzA), grown at $28 \pm 2^\circ C$ for 5 days. The *A. fumigatus* spores were harvested in sterile phosphate buffered saline (1xPBS) supplemented with 0.05% Tween 20. The conidial suspension was adjusted to 10^6 conidia/mL (0.1 OD) at 530 nm wavelength, further diluted in Czapek Dox Broth (CzB;1:50 ratio) to adjust the final suspension to 5×10^4 conidia/mL according to CLSI M38-A2 reference method (CLSI, 2008).

In-vitro antifungal activity of synthesized analogues of compounds 1a and 1b.

Minimum inhibitory concentration (MIC) and IC_{50} was calculated according to the CLSI M38-A2 microbroth dilution method for filamentous fungi (CLSI, 2008). The experiment was carried out in triplicates in a 96-well polystyrene plate (Tarsons, India). All the twenty three synthesized analogues of compound 1a and 1b (compound 2a, 2b, 4a-j, 5-16), amphotericin B (Amp B) were dissolved in DMSO. Two-fold dilutions of synthesized analogues and parent compounds were prepared in growth media CzB. Prepared conidial suspension (100 μ L) was added to each well except negative control. The plates were incubated statically for 5 days at $28 \pm 2^\circ C$. The MIC and IC_{50} were defined as the lowest concentration of the compound, which completely inhibit the microbial growth and 50% inhibition of microbial growth, respectively (CLSI, 2008). The results were expressed in micromolar value.

Assessment of cytotoxicity of synthetic analogues in normal lung epithelial cell line L-132.

Cytotoxicity analysis of selected analogues, which showed antifungal results at lowest concentrations against *A. fumigatus*, was performed. The selected analogues 4e and 5 were taken forward for all experiments.

The lung epithelial normal cell line L-132 was procured from National Centre for Cell Science (NCCS), Pune, India. Cells were grown in T-25 vented neck flask in Dulbecco's modified Eagle's medium (DMEM) supplemented with 10% foetal bovine serum (FBS), 1% penicillin/ streptomycin and 1% L-glutamine in a humidified atmosphere of 5% CO₂ and 95% air at 37°C. L-132 cells were seeded at density 1 x 10⁵ cells per well in 100 µl culture medium containing 10% FBS on 96 multi-well culture plates and incubated overnight for adherence. After that, the medium was removed, and cells were incubated in FBS free medium containing different concentrations of **4e** and **5** and drug amp B for another 24 h. The wells containing media plus cells as positive control and only media as negative control. After 24 h, the reaction medium was removed, and the adhering cells washed with PBS. 100 µl of MTT solution (0.5g/L in

medium) was added to each culture well and incubated for 4 h at 37°C. Next, MTT reaction medium was removed, and formazan blue was solubilised in 100 µl of DMSO. The formazan- blue formation absorbance was recorded at 570 nm using micro-plate reader (Cloud-Clone smart microplate reader, Model no. SMR-16.1). All experiments were performed in triplicates. The percentage relative cell viability was calculated as (A₅₇₀ of treated samples/A₅₇₀ of untreated samples) * 100 (Venkatraman et al. 2005).

The selectivity index (SI) was determined by CC₅₀/IC₅₀ ratio against *A. fumigatus*. The SI is an indirect measure of the therapeutic window, and it can serve as a predictor of safety during *in vivo* trials for a given pathogen infection (Insuasty et al. 2019). (CC₅₀ -cytotoxic concentration 50)

***In-silico* screening of analogues for therapeutic activity.**

In-silico study was conducted to determine drug-likeness and health effect prediction profile of synthetic analogues **4e** and **5**. The structures of compounds were drawn manually using ChemSketch (Advanced Chemistry Development, inc., ACD/Labs, freeware 12.0, Toronto, Canada). Molecular property and drug likeness were analysed using online software ACD/I-Lab version 4.5 and MolSoft LLC 3.5-0, San Diego, CA, respectively. The parameters deployed to predict the physicochemical properties of the compound and describe its disposition within the host organism are summarized in Table 3 (Lipinski et al., 2001).

Evaluating the effect of the analogues on cell wall associated virulence factors in *A. fumigatus*.

A) Conidiation- The effect of selected analogues at their respective IC₅₀ on fungal conidiation was estimated spectrophotometrically (CLSI 2008). One cubic centimeter of agar block containing treated and untreated fungal culture was excised from CzA media plate supplemented with IC₅₀ using a sterile surgical blade and transferred to a sterile test tube. Phosphate buffer supplemented with 0.25% Tween-20 (5 mL) was added to each tube, shaken vigorously and absorbance was observed. The absorbance of treated (**1b**, **4e**, **5**, amp B), and positive control (untreated) samples of *A. fumigatus* conidia were measured at 530nm using UV- Vis spectrophotometer.

B) Melanin pigment- The isolation and estimation of cell wall associated melanin was performed at the calculated IC₅₀ of analogues (**4e** and **5**) and compound **1b** treated conidia using the modified protocol of Kumar et al. (2011) and Gupta et al (2022). Briefly, in 12 well tissue culture plate, 1×10^4 conidia with IC₅₀ of analogues (**4e** and **5**), **1b** and AmpB was added and incubated at 28°C for 5 days. After incubation, conidia from treated as well as untreated culture were harvested using 1×PBS and centrifuged (5000 g) for 10 min, followed by washing twice with sterile distilled water. The conidia melanin was extracted with 1M NaOH (2 mL) and further autoclaved at 120°C for 20 mins. The autoclaved suspension was further centrifuged (5000 g) for 5 min to recover the supernatant containing the pigment. The alkaline pigmented supernatant was acidified to pH 2 with 7M HCl (2 mL) in a sealed glass vial and kept for 2 h at 100 °C. After cooling, precipitate was recovered by centrifugation (5000g; 10 min). Precipitate was suspended in 100 mM borate buffer and the extracted melanin was scanned by UV-Vis absorption spectrum between 250-800 nm on a UV-Vis spectrophotometer. 100 mM borate buffer was used as a blank.

C) Scanning electron microscopy (SEM) and Transmission electron microscopy (TEM) of the treated *A. fumigatus* conidial surface

Synthesized compounds (**4e** and **5**) and compound **1b** treated conidial surfaces of *A. fumigatus* were analysed by electron microscopy. For SEM, conidia were harvested, washed, and fixed in 4% glutaraldehyde in 1x PBS under vacuum for 24 hours. After washing, the cells were post-fixed with 1% osmium tetroxide for 60 min and dehydrated by passage through ethanol solutions of increasing concentration. The sample were then mounted on aluminium sheet and coated with gold-palladium alloy. The observations were made using a Zeiss SEM, MA EVO -18 Special Edition (Pihet, 2009). For TEM analysis, conidia were harvested, washed, and fixed overnight at room temperature with 2.5%

glutaraldehyde in 0.1 M sodium cacodylate buffer (pH 7.4). Conidia were incubated for 1.5 h at 20°C in a solution of 4% formaldehyde and 1% glutaraldehyde in 0.1% PBS and then incubated in 2% osmium tetroxides for 1.5 h. Dehydration was accomplished by serial washings in graded ethanol solutions of 50-95% for 10 min, followed by two final washes in 100% ethanol for 15 min. The cells were embedded in Spurr's resin, sectioned onto nickel grids, and examined on a JEOL 2100F transmission electron microscope to obtain micrographs (Graham, 2007).

The minimal biofilm-eradicating concentration (MBEC) of synthesized compounds (**4e** and **5**) on pre-formed *A. fumigatus* biofilm was calculated by performing MTT assay in a 96-well flat bottom microtiter plate with minor modifications (Sav et al., 2018). Briefly, conidia in RPMI + 2% glucose (100µL) were added to each well and incubated at 37 °C for 24 h without agitation for biofilm formation. After 24 h, non-adherent conidia were removed by washing with 1× PBS and treated with synthesized compounds (**4e** and **5**) and compound **1b**. Microtiter plate was further incubated at 37 °C statically for an additional 24 h. The wells with preformed biofilms (without any treatment) were considered as positive control. After 24 h, the reaction medium was removed, and the fungal biofilm washed with PBS. 100 µl of MTT solution (0.5g/L in medium) was added to each well and incubated for 4 h at 37°C. Subsequently, MTT was removed, and formazan blue was solubilized in 100 µl of DMSO. The formazan-blue formation absorbance was recorded at 570 nm using micro-plate reader (Cloud-Clone smart microplate reader, Model no. SMR-16.1).

Statistical analyses

For the statistical analyses, one-way ANOVA was used, comparing the results of conidiation for compounds and isoeugenol treated culture with wild type, antifungal drug treated strain. All experiments were conducted in biological triplicates. All the statistics was performed using GraphPad Prism software 8.0.2.263 version and Microsoft Excel. $p < 0.05$ was considered statistically significant.

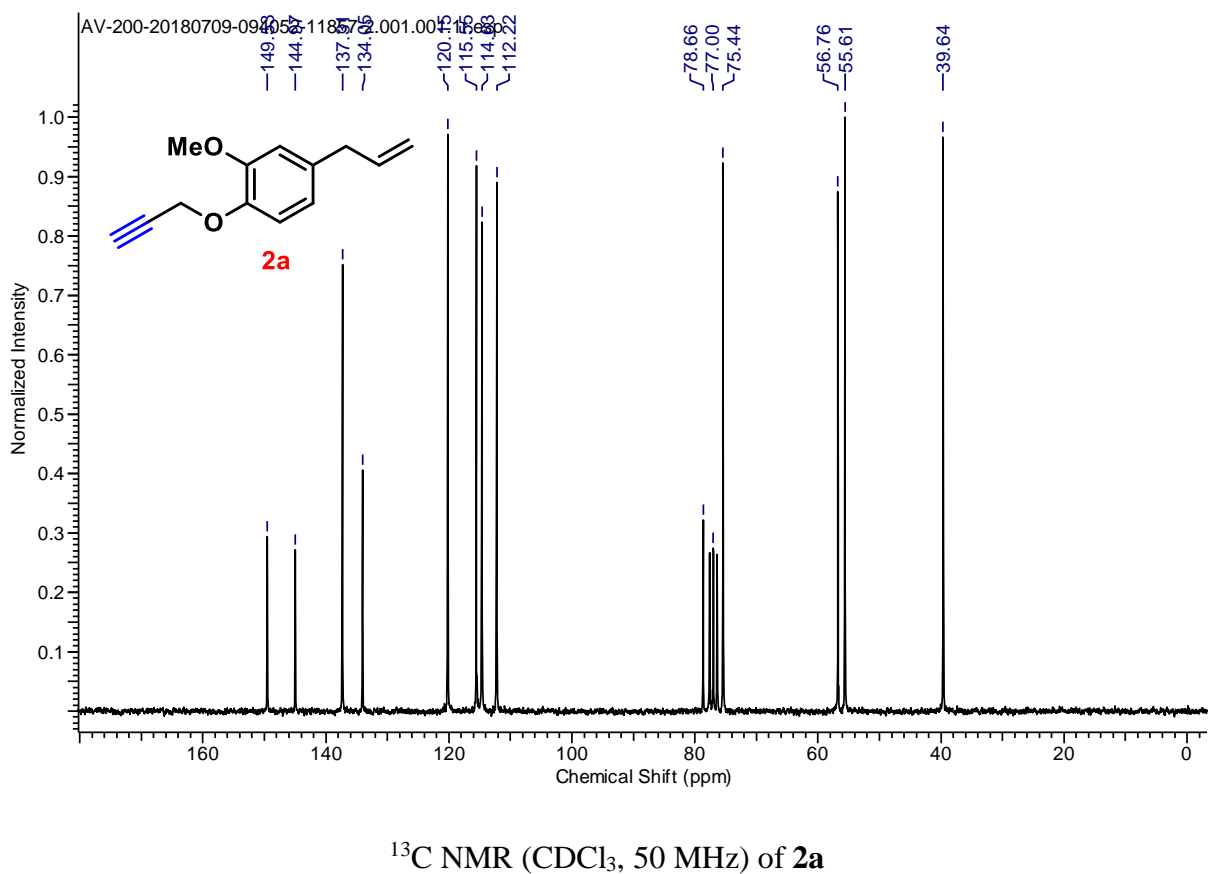
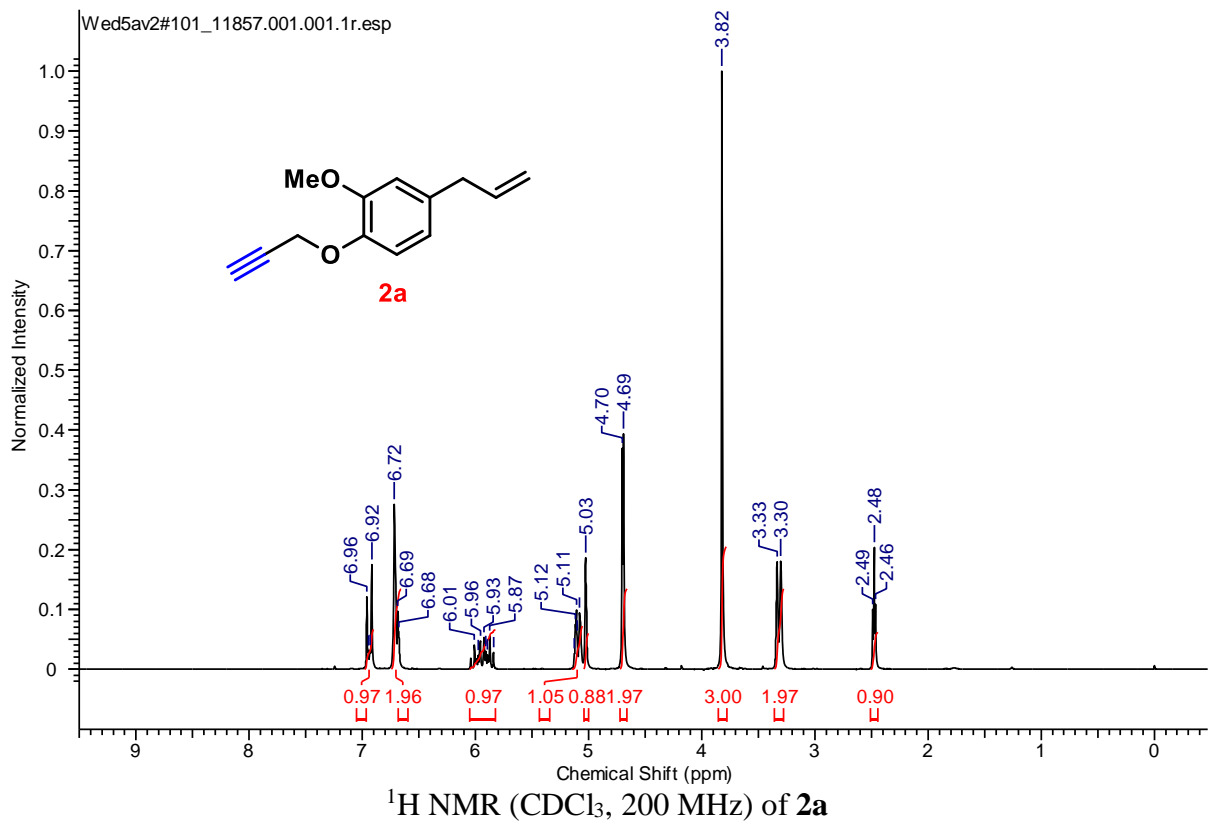
1.2.5 References:

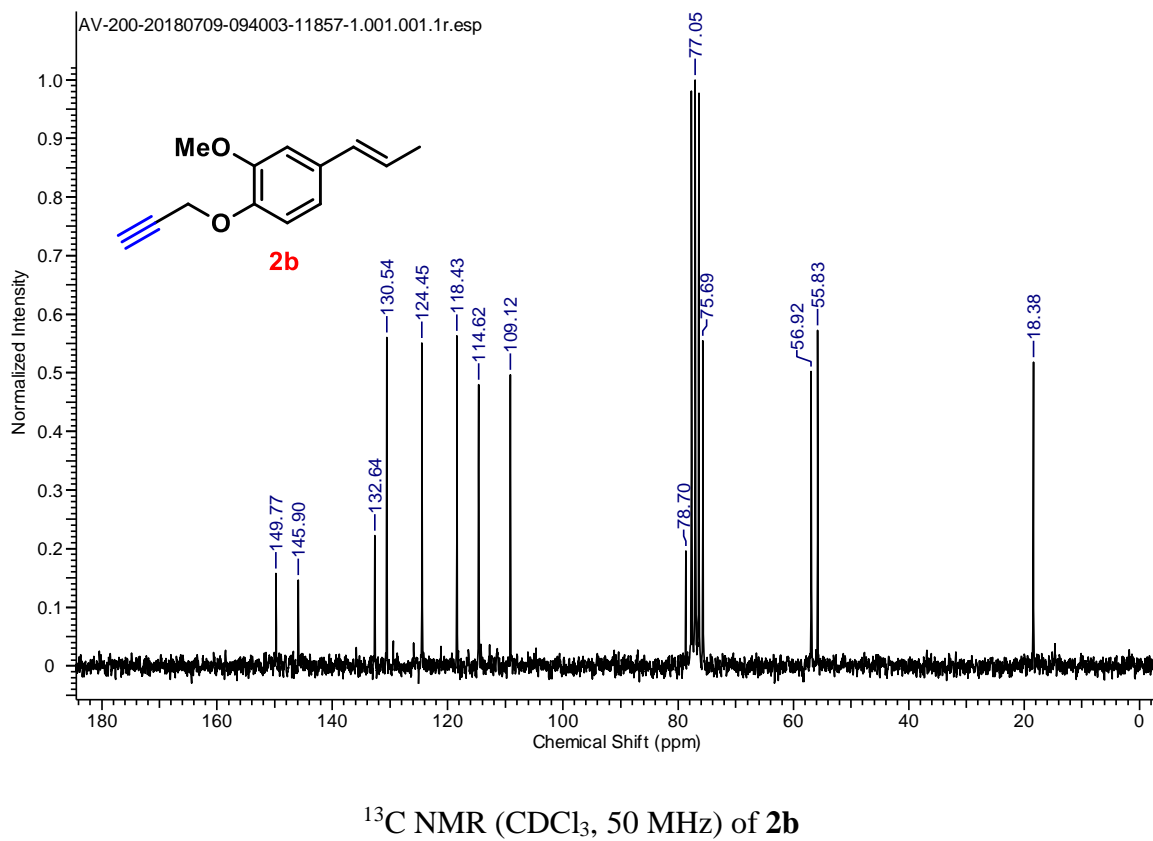
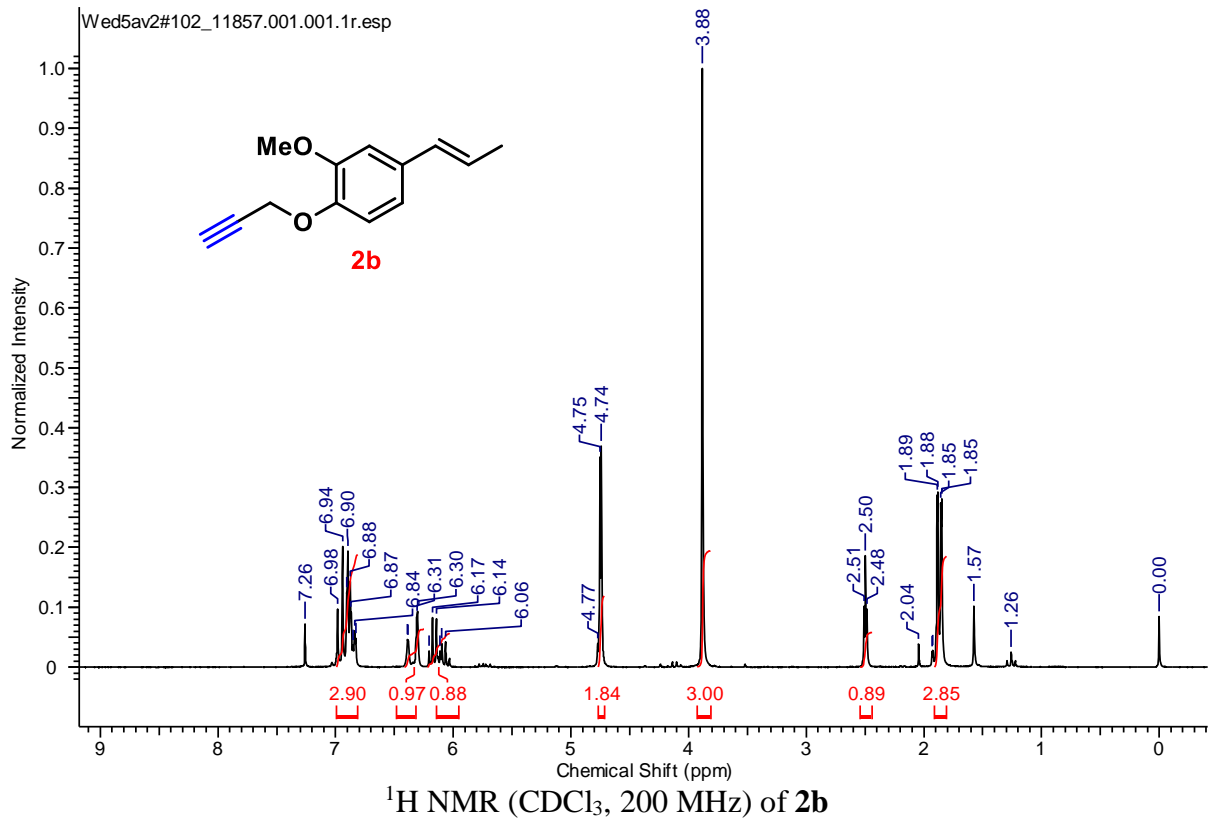
1. (a) C. Kosmidis and D. W. Denning, *Thorax*, **2015**, *70*, 270–277. (b) M. Richardson, P. Bowyer and R. Sabino, *Med. Mycol.*, **2019**, *57*(Supplement_2), S145–S154. (c) L. Goswami, L. Gupta, S. Paul, M. Vermani, P. Vijayaraghavan and A. K. Bhattacharya, *RSC Med. Chem.*, **2022**, *13*, 955–962.
2. (a) C.-C. Lai and W.-L. Yu, *J. Microbiol., Immunol. Infect.*, **2021**, *54*, 46–53. (b) A. M. Borman, M. D. Palmer, M. Fraser, Z. Patterson, C. Mann, D. Oliver, C. J. Linton, M. Gough, P. Brown, A. Dzietyczyk, M. Hedley, S. McLachlan, J. King and E. M. Johnson, *J. Clin. Microbiol.*, **2020**, *59*, e02136-20.
3. M. Richardson, P. Bowyer and R. Sabino, *Med. Mycol.*, **2019**, *57*(Supplement_2), S145–S154.
4. (a) L. Scorzoni, A. C. A. de Paula, E. Silva, C. M. Marcos, P. A. Assato, W. C. M. A. de Melo, H. C. de Oliveira, C. B. Costa-Orlandi, M. J. S. Mendes-Giannini and A. M. Fusco-Almeida, *Front. Microbiol.*, **2017**, *8*, 36. (b) L. Goswami, L. Gupta, S. Paul, P. Vijayaraghavan, A. K. Bhattacharya, *ChemMedChem*, **2023**, e202300013.
5. (a) T. Koeduka, E. Fridman, D. R. Gang, D. G. Vassão, B. L. Jackson, C. M. Kish, I. Orlova, S. M. Spassova, N. G. Lewis, J. P. Noel, T. J. Baiga, N. Dudareva and E. Pichersky, *Proc. Natl. Acad. Sci. U. S. A.*, **2006**, *103*, 10128–10133. (b) G. Chung, S. T. Im, Y. H. Kim, S. J. Jung, M.-R. Rhyu and S. B. Oh, *Neuroscience*, **2014**, *261*, 153–160. (c) E. Pinto, L. Vale-Silva, C. Cavaleiro and L. Salgueiro, *J. Med. Microbiol.*, **2009**, *58*, 1454–1462.
6. (a) S. K. Shrestha, A. Garzan and S. G. Tsodikova, *Eur. J. Med. Chem.*, **2017**, *133*, 309–318. (b) H. X. Ngo, S. K. Shrestha and S. G. Tsodikova, *ChemMedChem*, **2016**, *11*, 1507–1516.
7. (a) T. K. Kotammagari, S. Paul, G. K. Barik, M. K. Santra and A. K. Bhattacharya, *Org. Biomol. Chem.*, **2020**, *18*, 2252–2263, and references cited therein. (b) in *Essentials of Glycobiology*, ed. A. Varki, R. D. Cummings, J. D. Esko, H. H. Freeze, P. Stanley, C. R. Bertozzi, G. W. Hart and M. E. Etzler, Cold Spring Harbor Laboratory Press, 2nd edn, **2009**. (c) W. Szeja, G. Gryniewicz and A. Rusin, *Curr. Org. Chem.*, **2017**, *21*, 218–235.

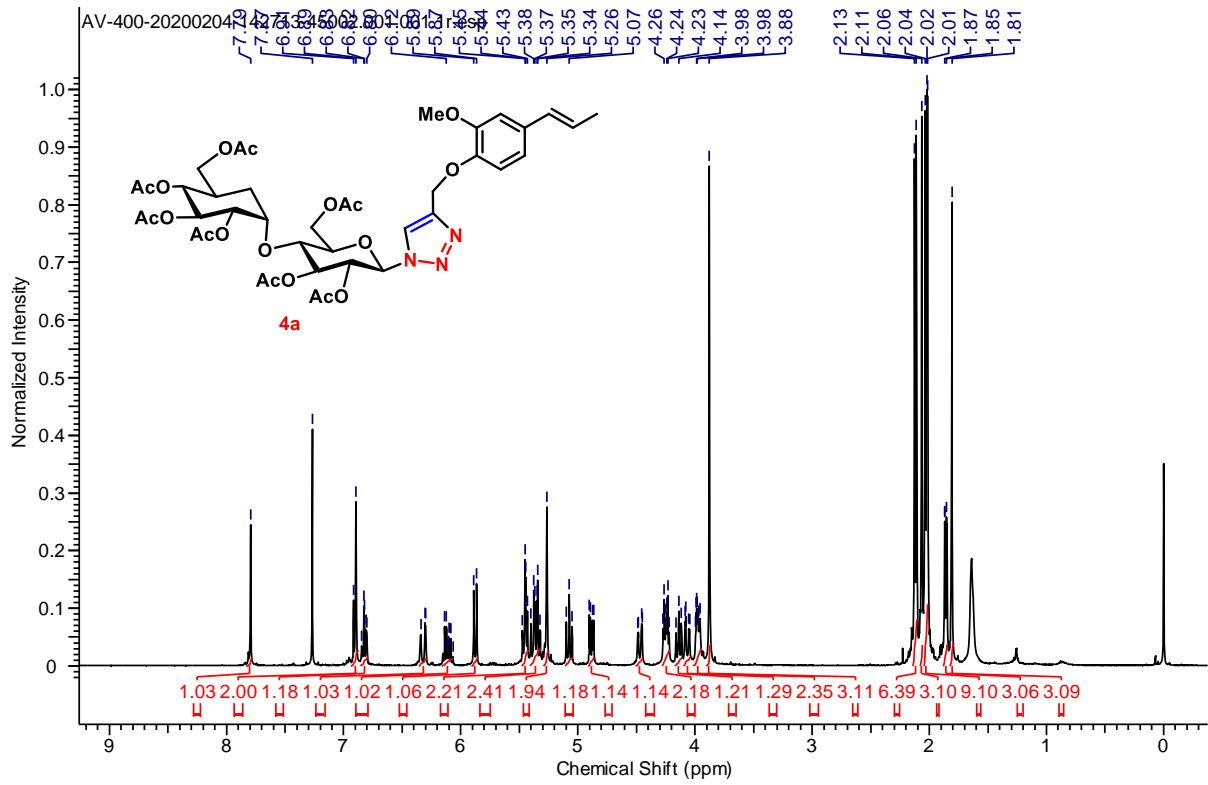
8. (a) D. Gupta and D. K. Jain, *J. Adv. Pharm. Technol. Res.*, **2015**, *6*, 141–146. (b) B. S. Holla, M. Mahalinga, M. S. Karthikeyan, B. Poojary, P. M. Akberali and N. S. Kumari, *Eur. J. Med. Chem.*, **2005**, *40*, 1173–1178.
9. B. H. M. Kuijpers, S. Groothuys, A. R. Keereweer, P. J. L. M. Quaedflieg, R. H. Blaauw, F. L. van Delft and F. P. J. T. Rutjes, *Org. Lett.*, **2004**, *6*, 3123–3126.
10. (a) B. H. M. Kuijpers, S. Groothuys, A. R. Keereweer, P. J. L. M. Quaedflieg, R. H. Blaauw, F. L. van Delft and F. P. J. T. Rutjes, *Org. Lett.*, **2004**, *6*, 3123–3126. (b) R. Huisgen, *Angew. Chem., Int. Ed. Engl.*, **1963**, *2*, 565–632. (c) R. Huisgen, *Angew. Chem., Int. Ed. Engl.*, **1963**, *2*, 633–696. (d) V. V. Rostovtsev, L. G. Green, V. V. Fokin and K. B. Sharpless, *Angew. Chem., Int. Ed.*, **2002**, *41*, 2596–2599.
11. J. Bomon, M. Bal, T. K. Achar, S. Sergeyeve, X. Wu, B. Wambacq, F. Lemièrre, B. F. Sels and B. U. W. Maes, *Green Chem.*, **2021**, *23*, 1995–2009.
12. M. Bednarski and S. Danishefsky, *J. Am. Chem. Soc.*, **1986**, *108*, 7060–7067.
13. E. K. Aratikatla, T. R. Valkute, S. K. Puri, K. Srivastava and A. K. Bhattacharya, *Eur. J. Med. Chem.*, **2017**, *138*, 1089–1105.
14. (a) A. Paquin, C. R. Moreno and G. Bérubé, *Molecules*, **2021**, *26*, 2340. (b) A. Çapcı, L. Herrmann, H. M. Sampath Kumar, T. Fröhlich and S. B. Tsogoeva, *Med. Res. Rev.*, **2021**, *41*, 2927–2970.
15. Clinical and Laboratory Standards Institute [CLSI], *Reference Method for Broth Dilution Antifungal Susceptibility Testing of Filamentous Fungi*, Clinical and Laboratory Standard Institute, Wayne, PA, 2nd edn, 2008.
16. M. Kasper, C. Roehlecke, M. Witt, H. Fehrenbach, A. Hofer, T. Miyata, C. Weigert, R. H. W. Funk and E. D. Schleicher, *Am. J. Respir. Cell Mol. Biol.*, **2000**, *23*, 485–491.
17. S. Harmsen, A. C. McLaren, C. Pauken and R. McLemore, *Clin. Orthop. Relat. Res.*, **2011**, *469*, 3016–3021.
18. L. I. S. de Carvalho, D. J. Alvarenga, L. C. F. do Carmo, L. G. de Oliveira, N. C. Silva, A. L. T. Dias, L. F. L. Coelho, T. B. de Souza, D. F. Dias and D. T. Carvalho, *J. Chem.*, **2017**, e5207439.
19. (a) L. Gupta, P. Sen, A. K. Bhattacharya and P. Vijayaraghavan, *Arch. Microbiol.*, **2022**, *204*, 214, DOI: 10.1007/s00203-022-02817-w. (b) C. G. Kumar, P. Mongolla, S. Pombala, A. Kamle and J. Joseph, *Lett. Appl. Microbiol.*, **2011**, *53*, 350–358.

20. (c) J. P. Latgé, A. Beauvais and G. Chamilos, *Annu. Rev. Microbiol.*, **2017**, *71*, 99–116. (b) V. Aimanianda, J. Bayry, S. Bozza, O. Kniemeyer, K. Perruccio, S. R. Elluru, C. Clavaud, S. Paris, A. A. Brakhage, S. V. Kaveri, L. Romani and J.-P. Latgé, *Nature*, **2009**, *460*, 1117–1121.
21. E. Melloul, S. Luiggi, L. Anaïs, P. Arné, J.-M. Costa, V. Fihman, B. Briard, E. Dannaoui, J. Guillot, J.-W. Decousser, A. Beauvais and F. Botterel, *PLoS One*, **2016**, *11*, e0166325.
22. N. A. R. Gow, J.-P. Latge and C. A. Munro, *Microbiol. Spectrum*, **2017**, *5*, DOI: 10.1128/microbiolspec.FUNK-0035-2016.

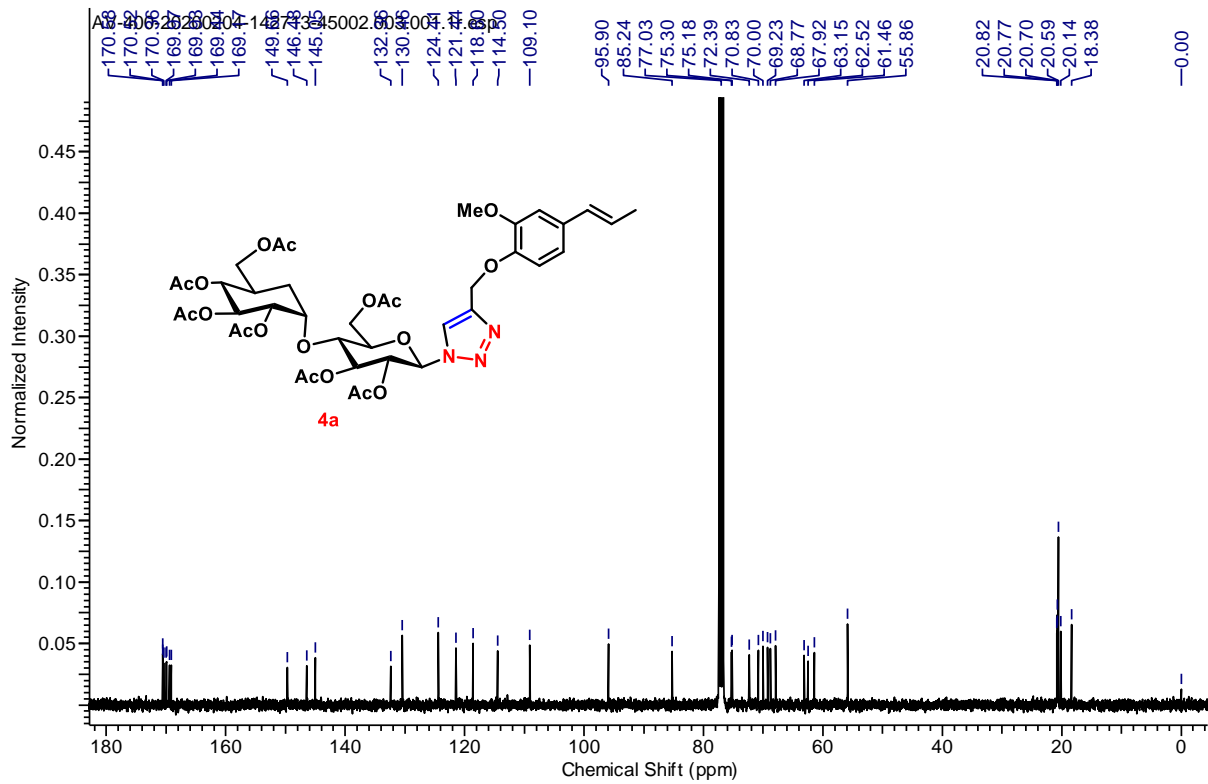
1.2.6 Copies of NMR spectra



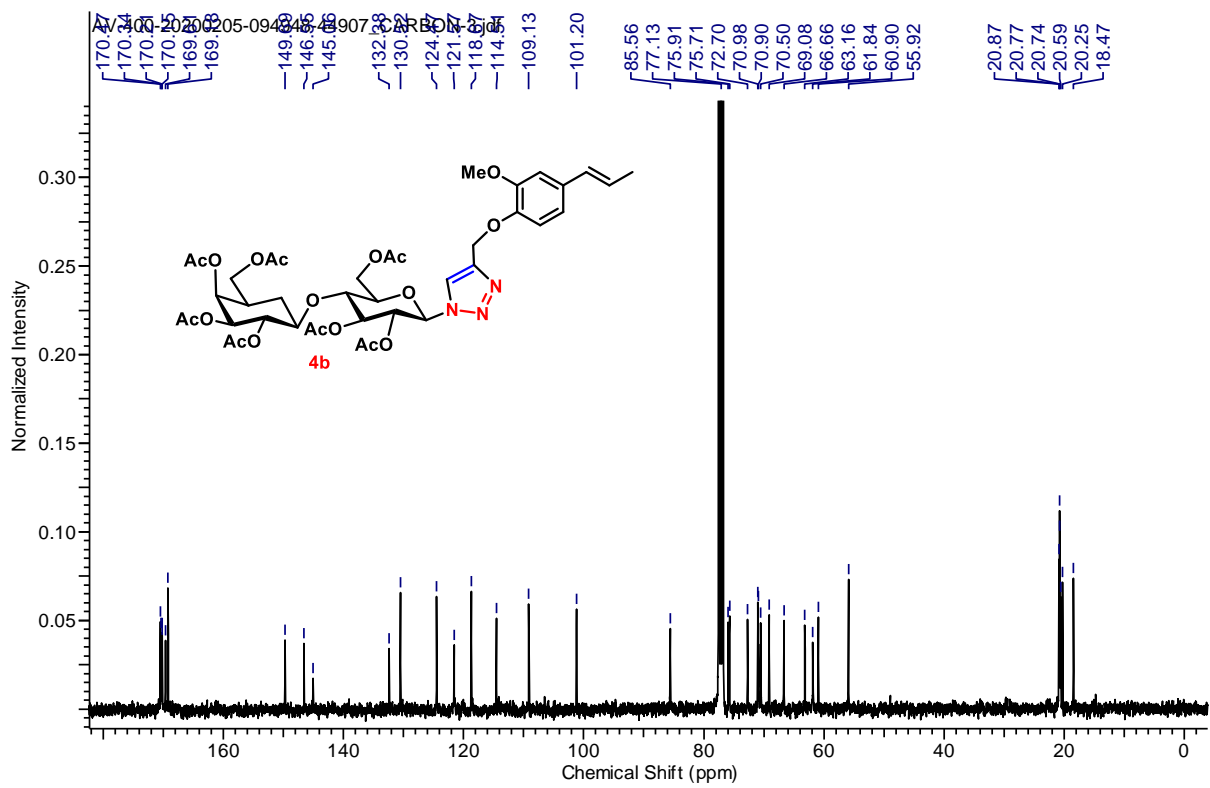
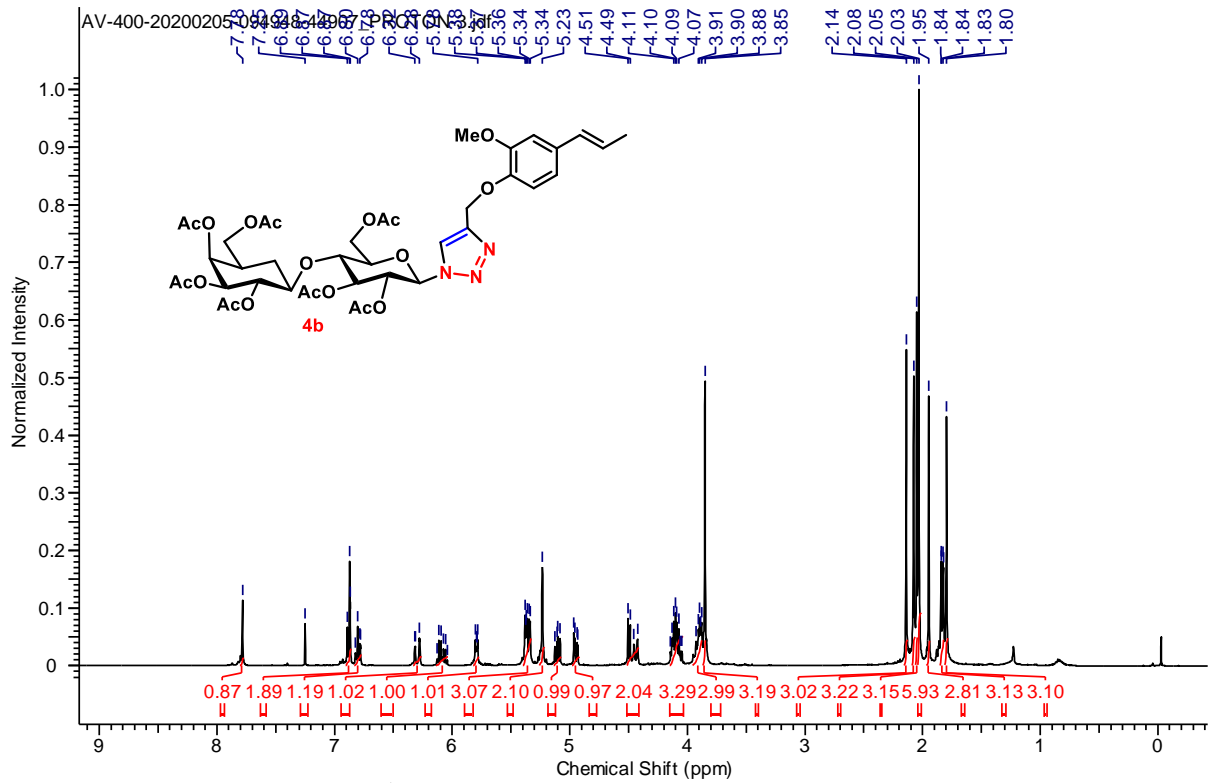


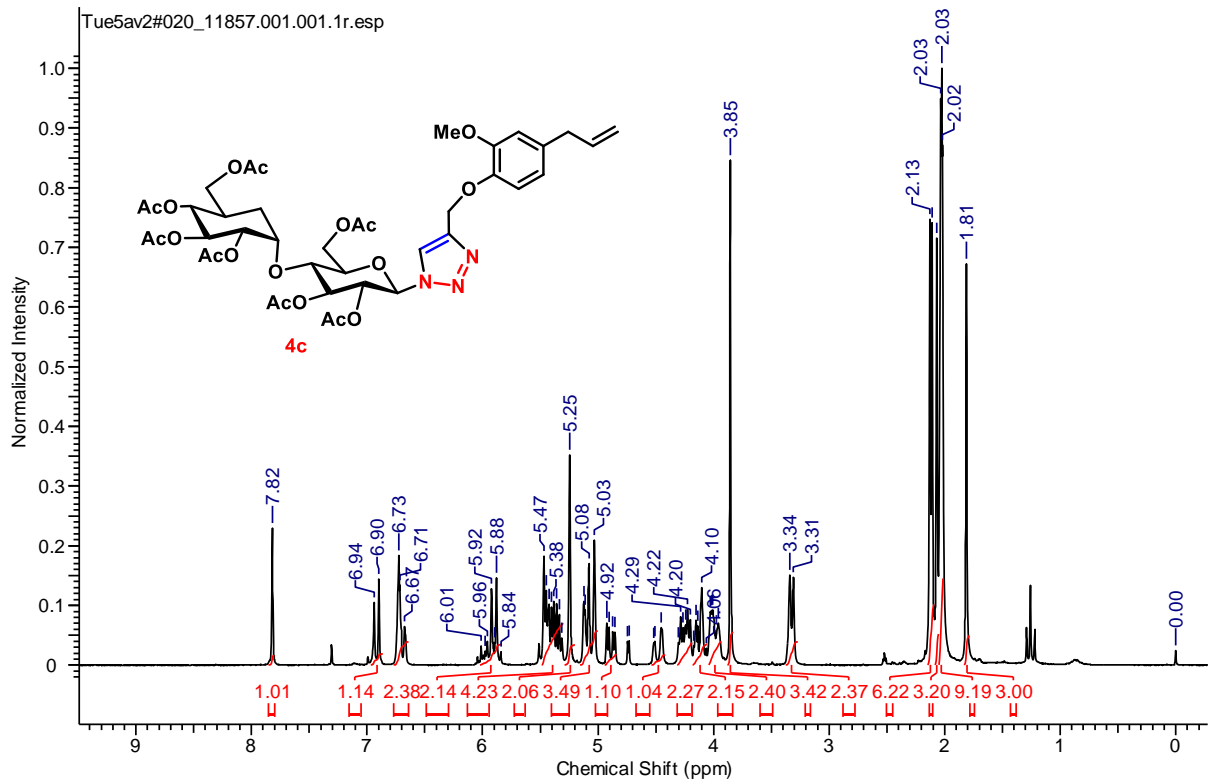
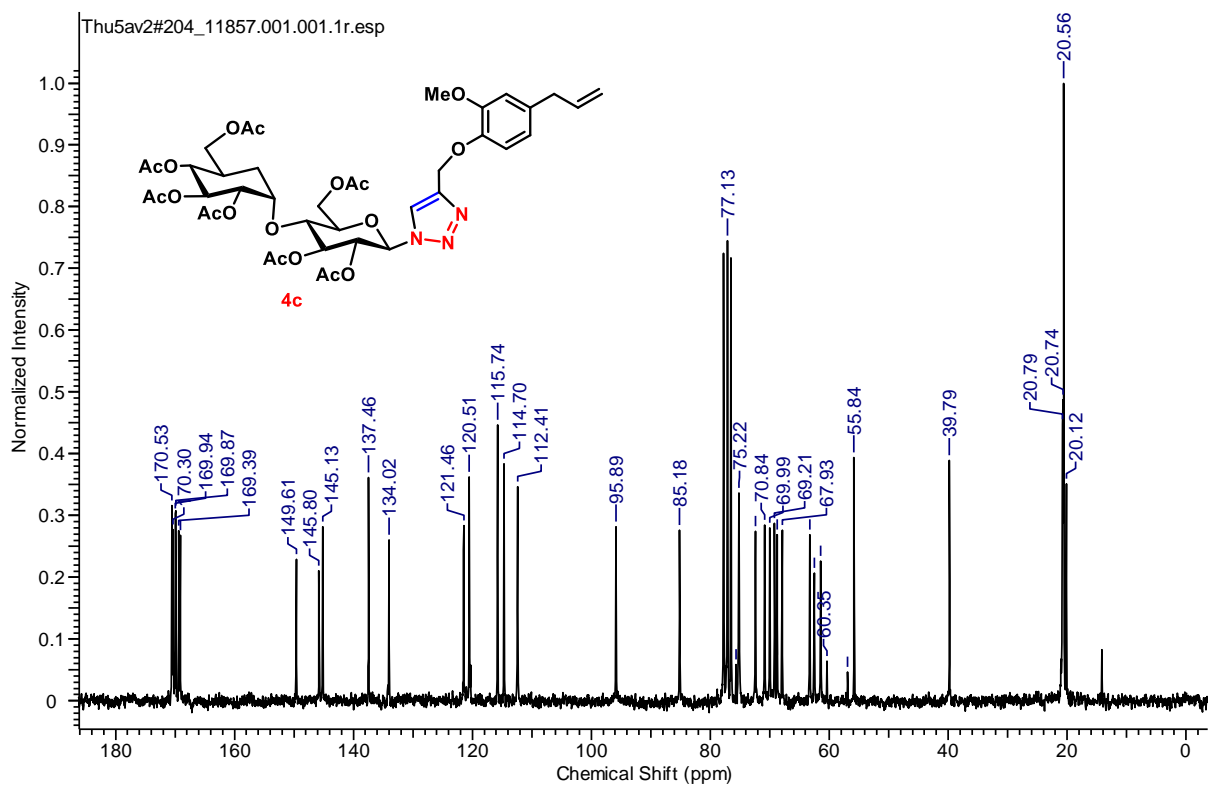


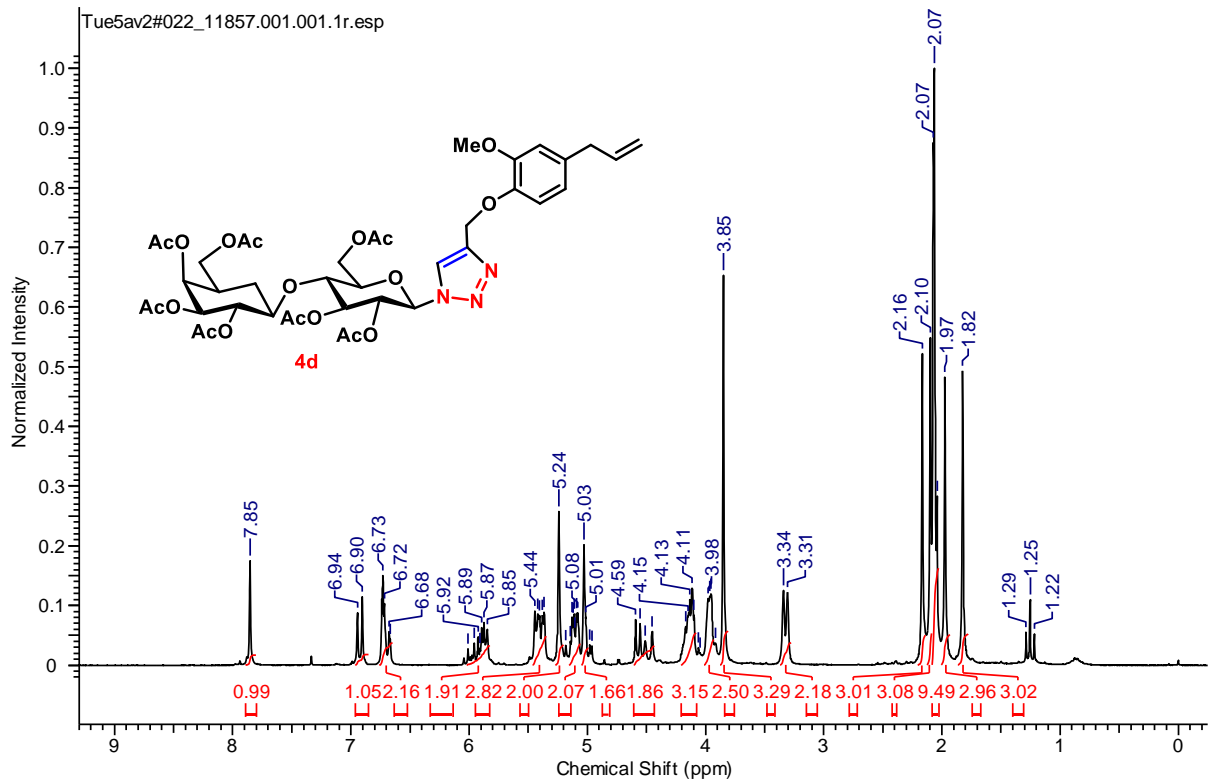
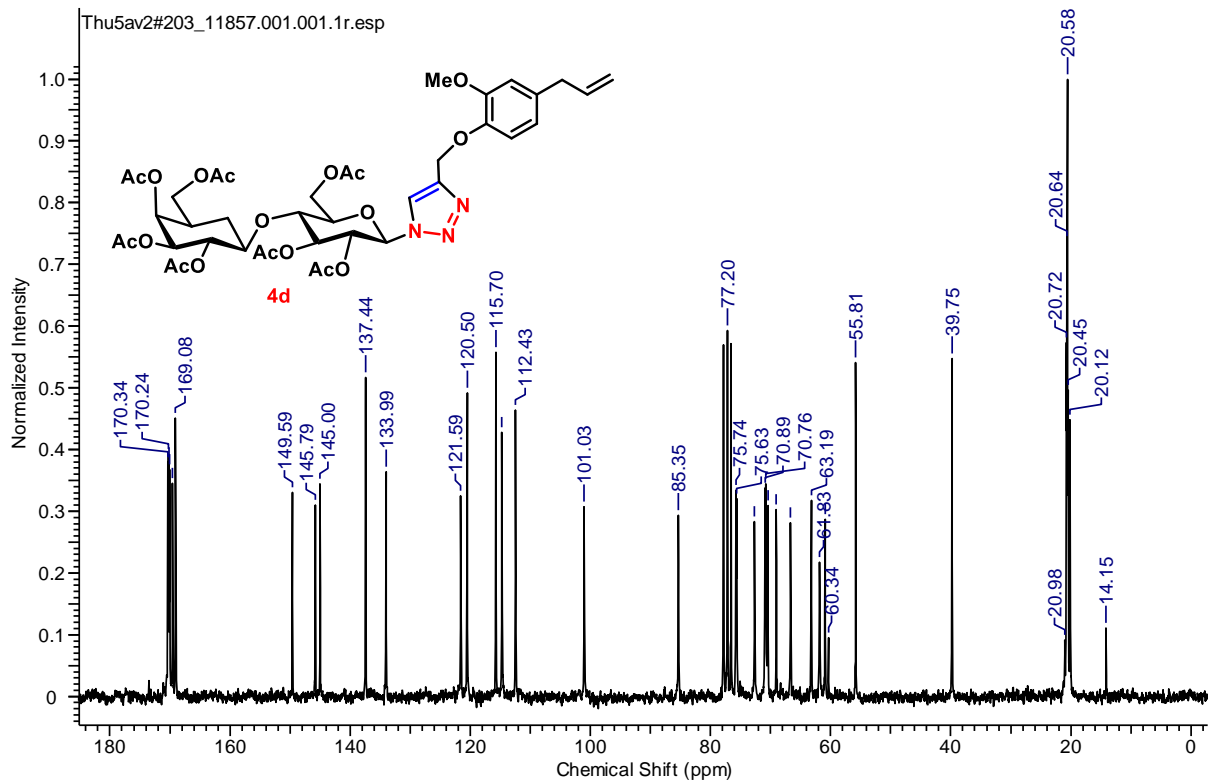
¹H NMR (CDCl₃, 400 MHz) of **4a**

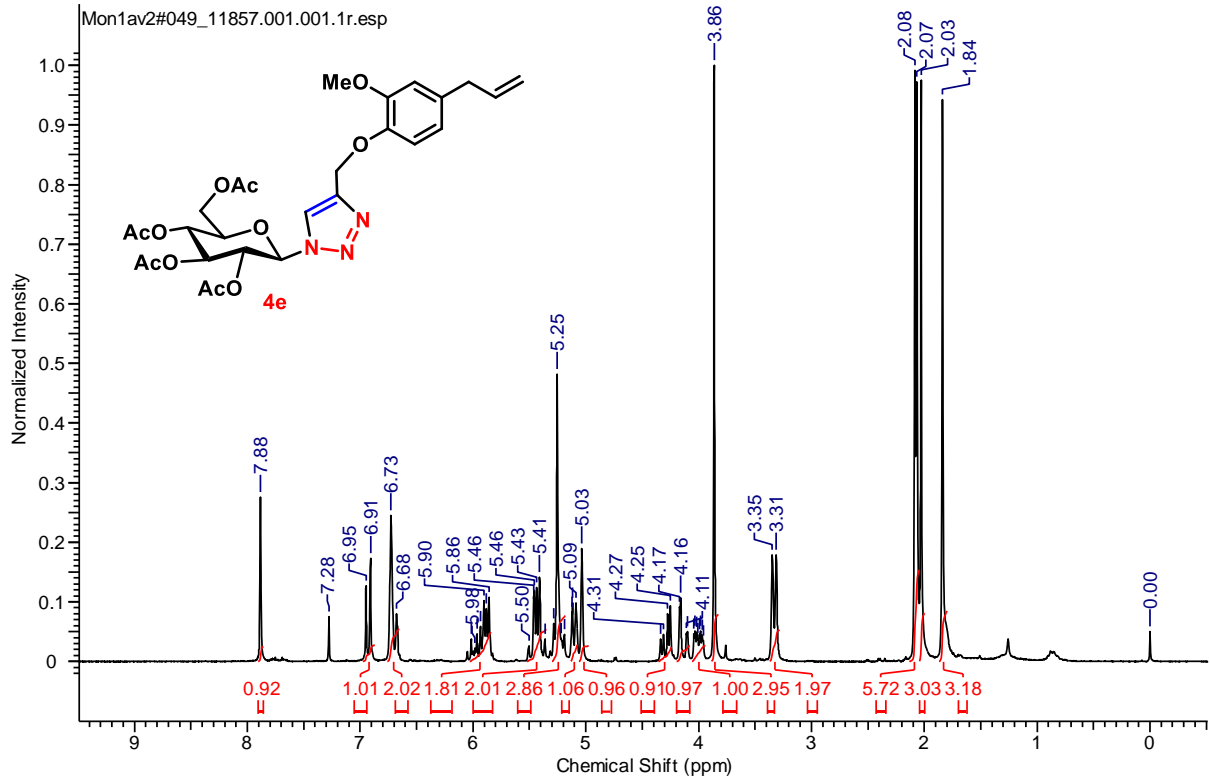
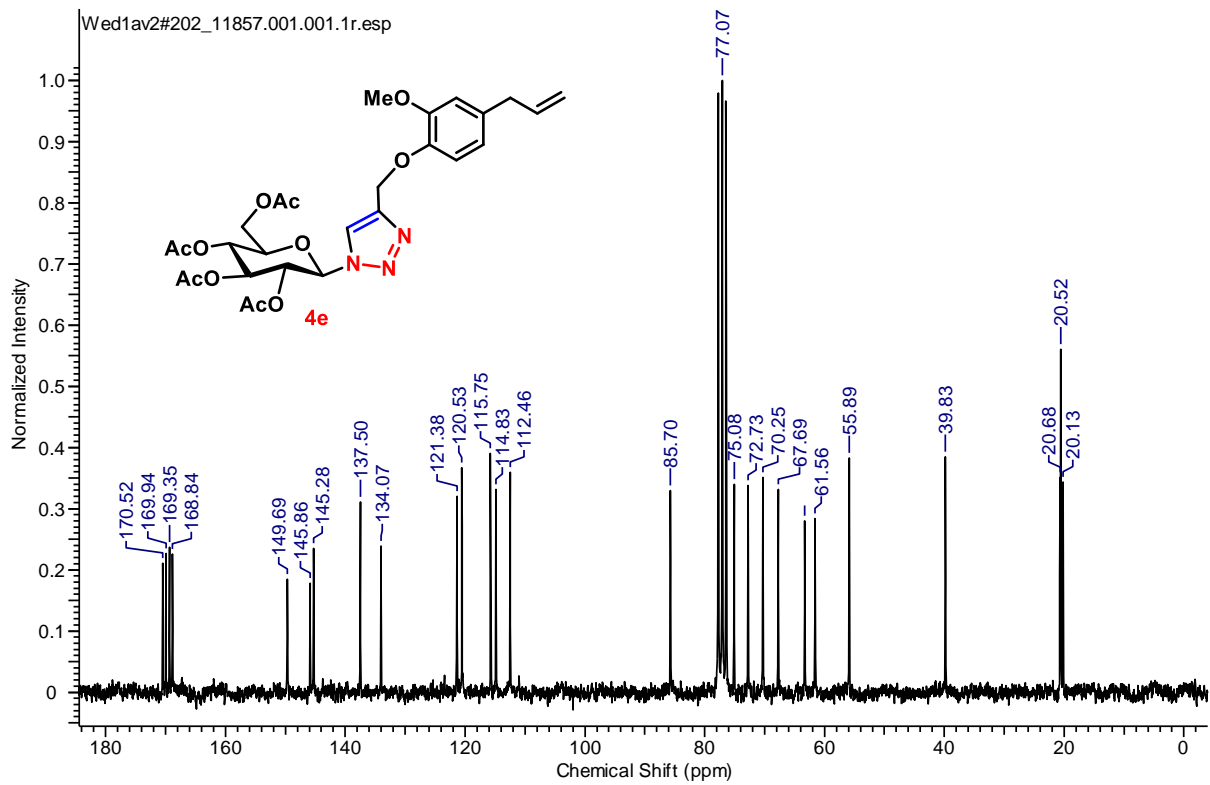


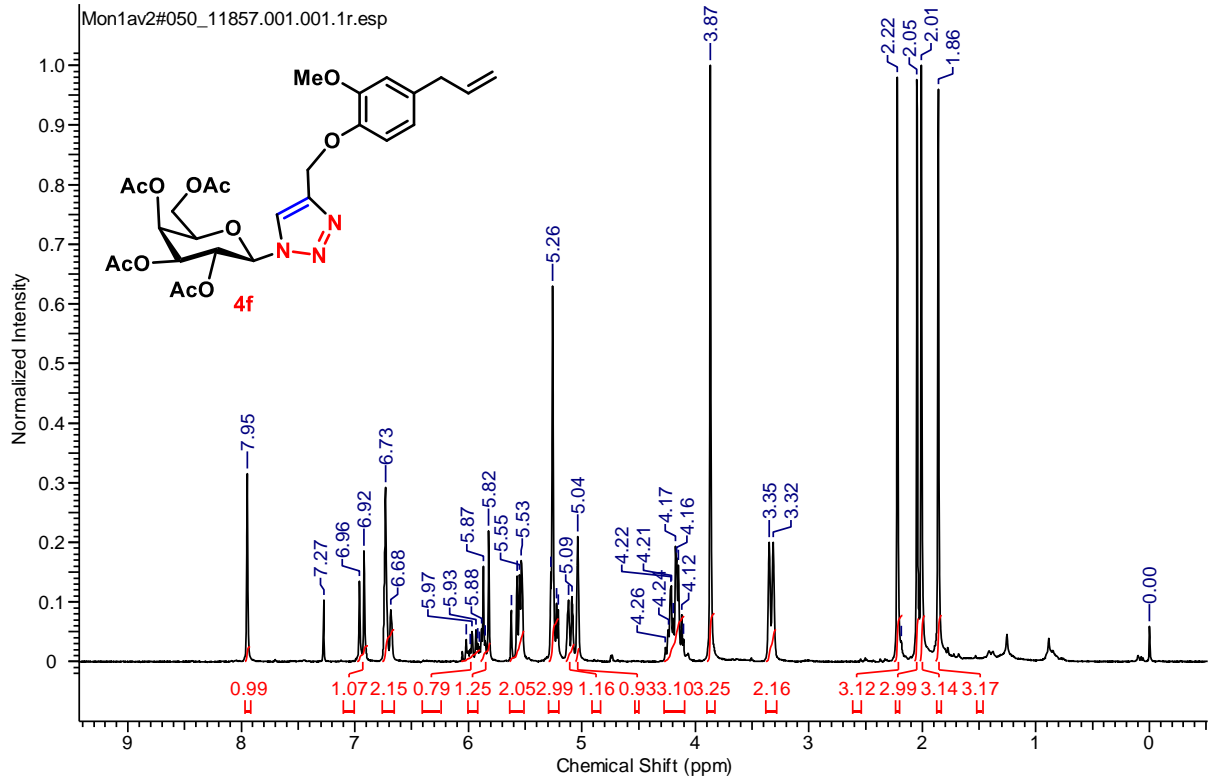
¹³C NMR (CDCl₃, 101 MHz) of **4a**



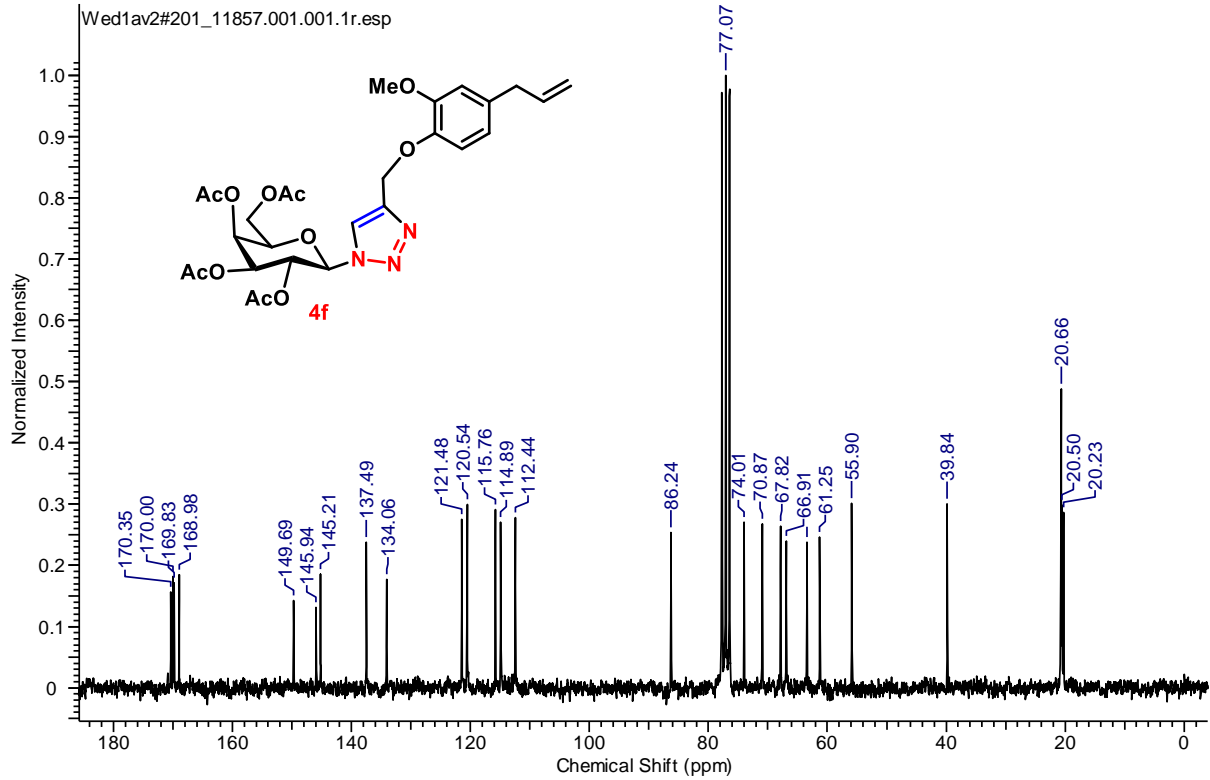
 ^1H NMR (CDCl_3 , 200 MHz) of **4c** ^{13}C NMR (CDCl_3 , 50 MHz) of **4c**

 ^1H NMR (CDCl_3 , 200 MHz) of **4d** ^{13}C NMR (CDCl_3 , 50 MHz) of **4d**

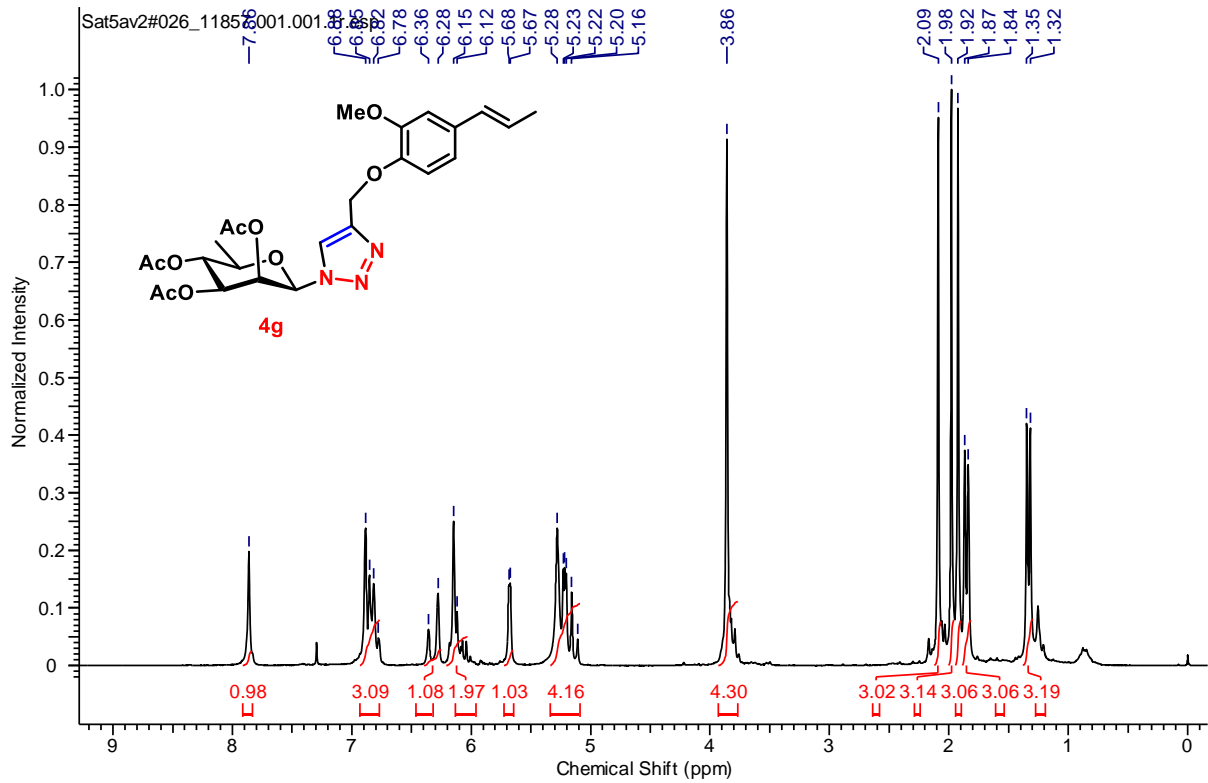
 ^1H NMR (CDCl_3 , 200 MHz) of **4e** ^{13}C NMR (CDCl_3 , 50 MHz) of **4e**



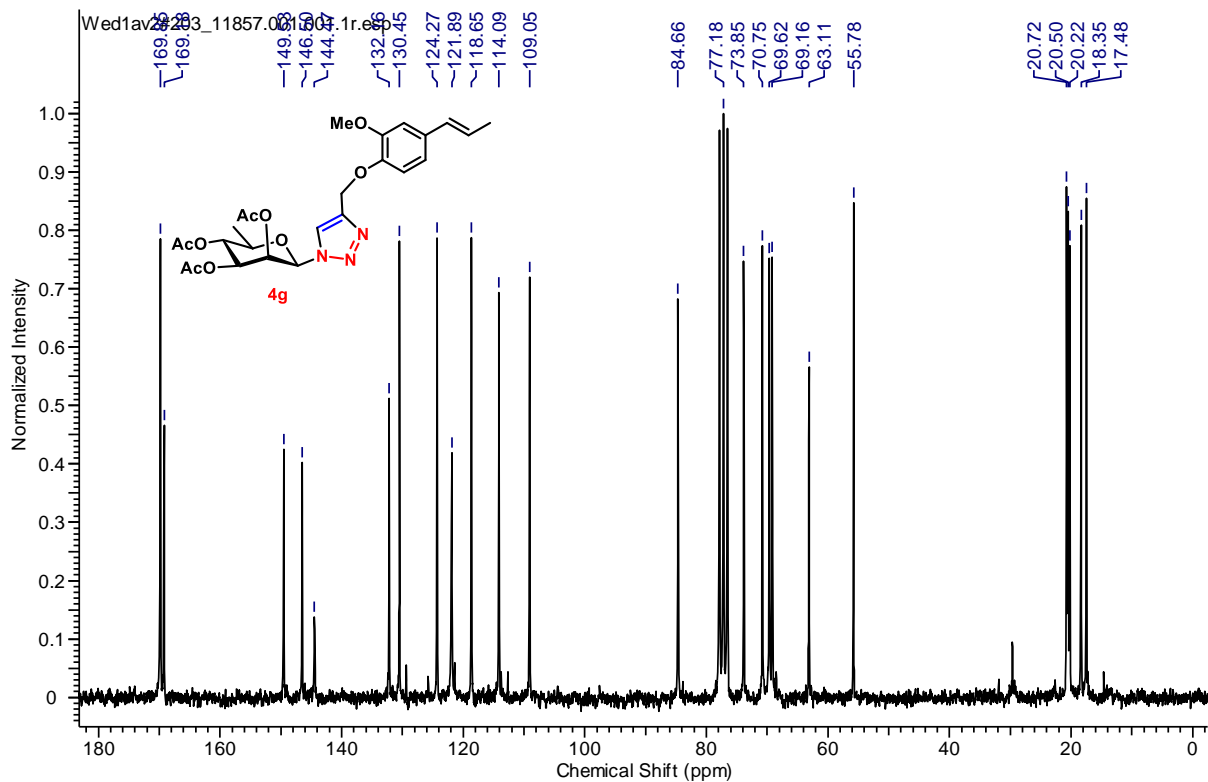
^1H NMR (CDCl_3 , 200 MHz) of **4f**



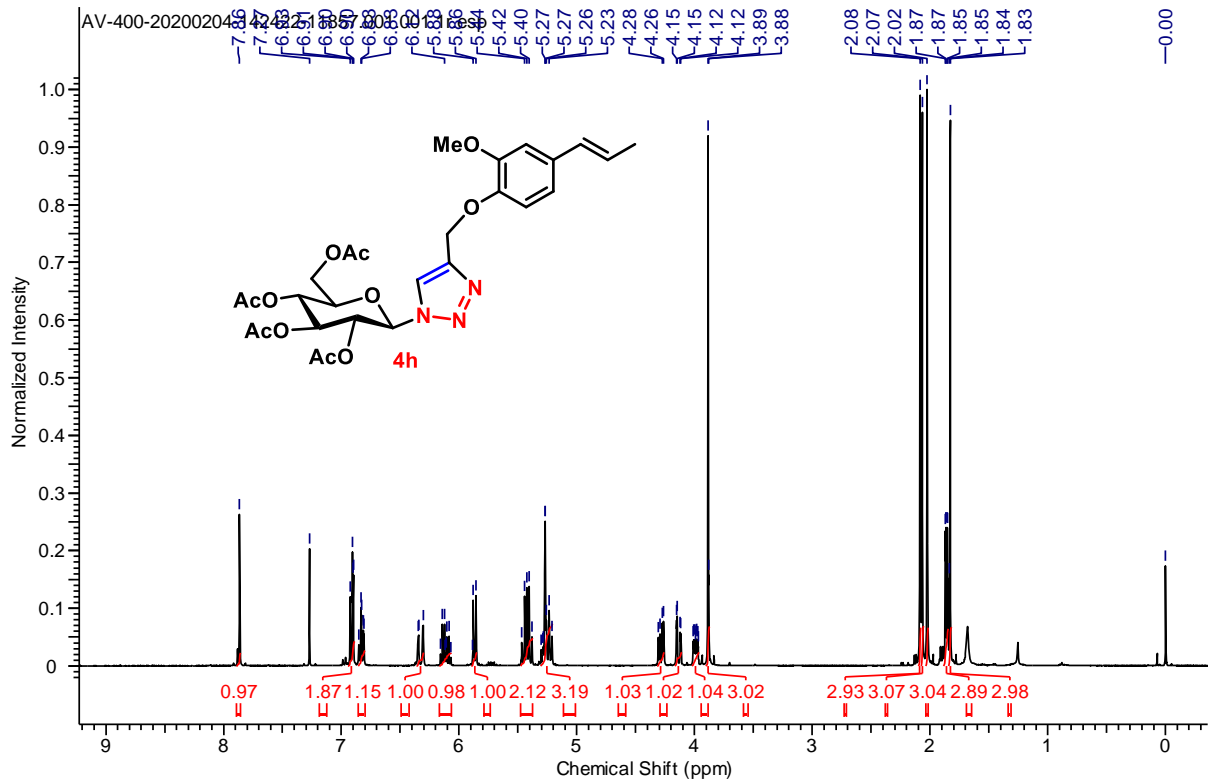
^{13}C NMR (CDCl_3 , 50 MHz) of **4f**



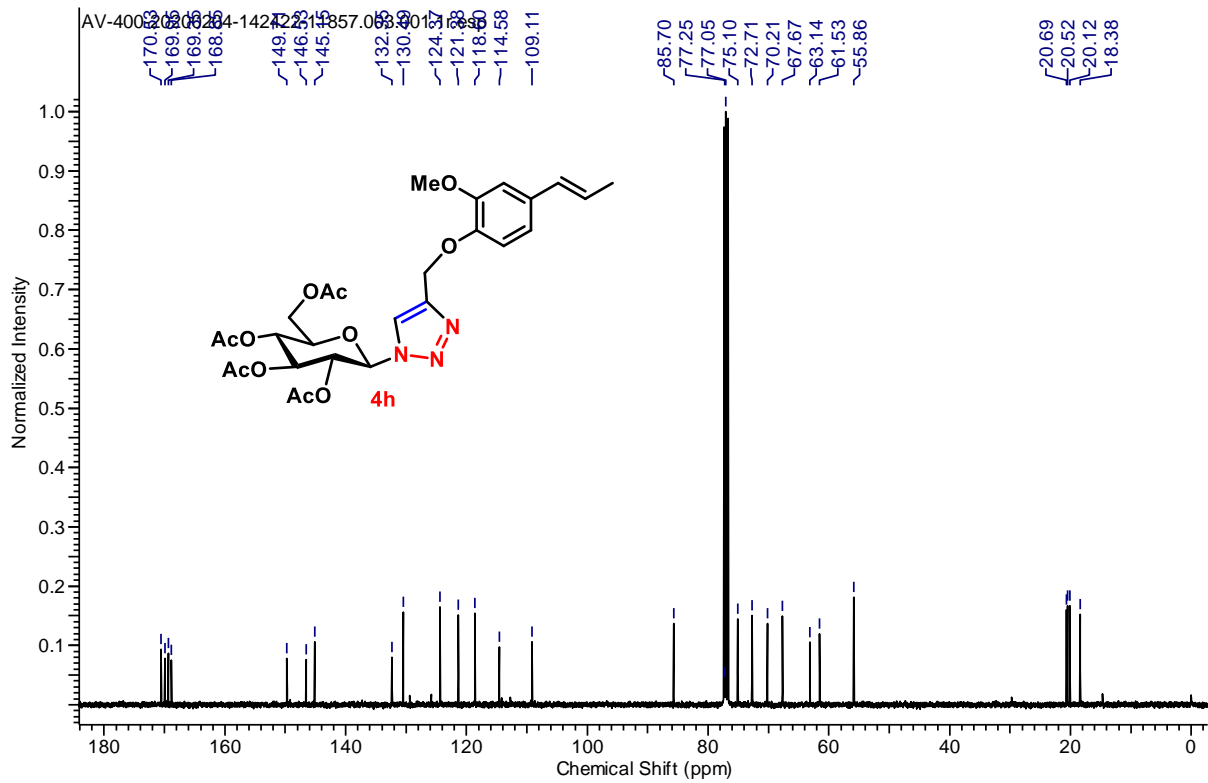
¹H NMR (CDCl₃, 200 MHz) of **4g**



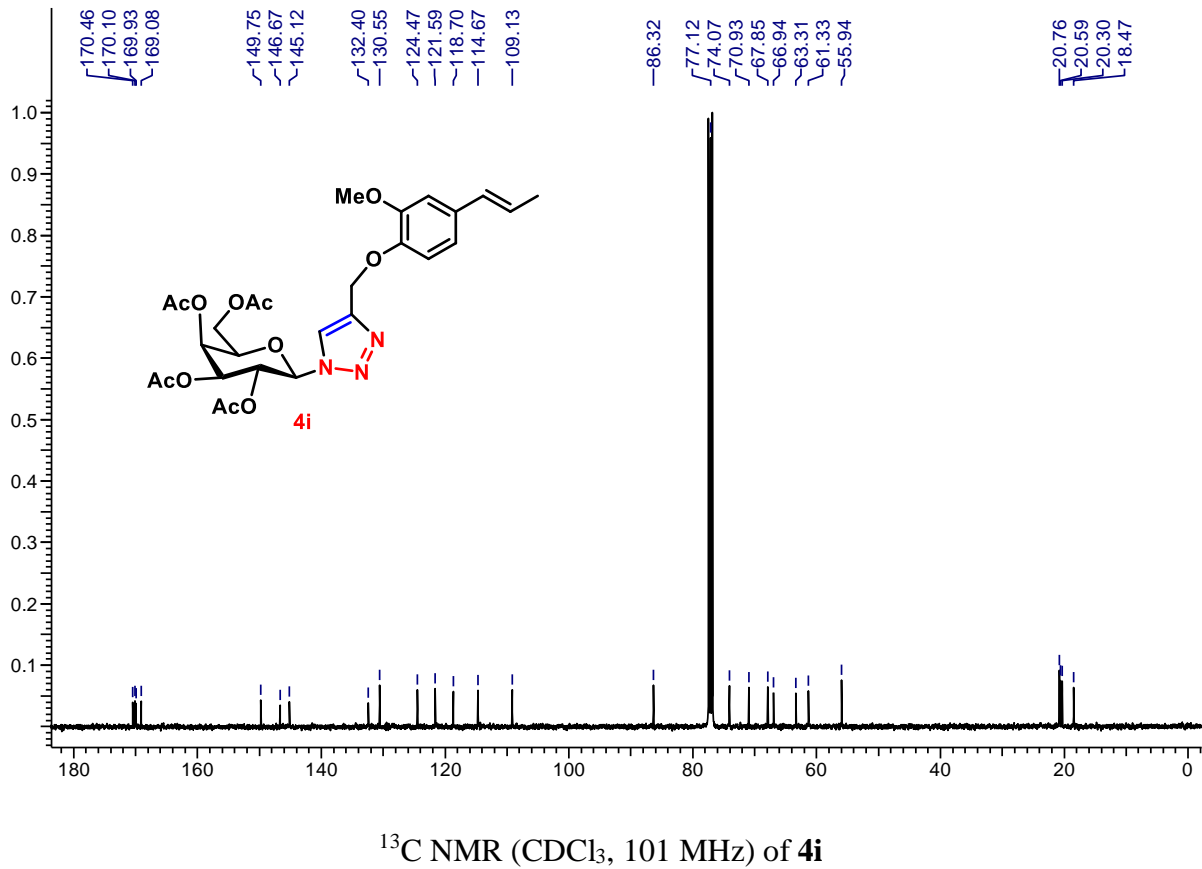
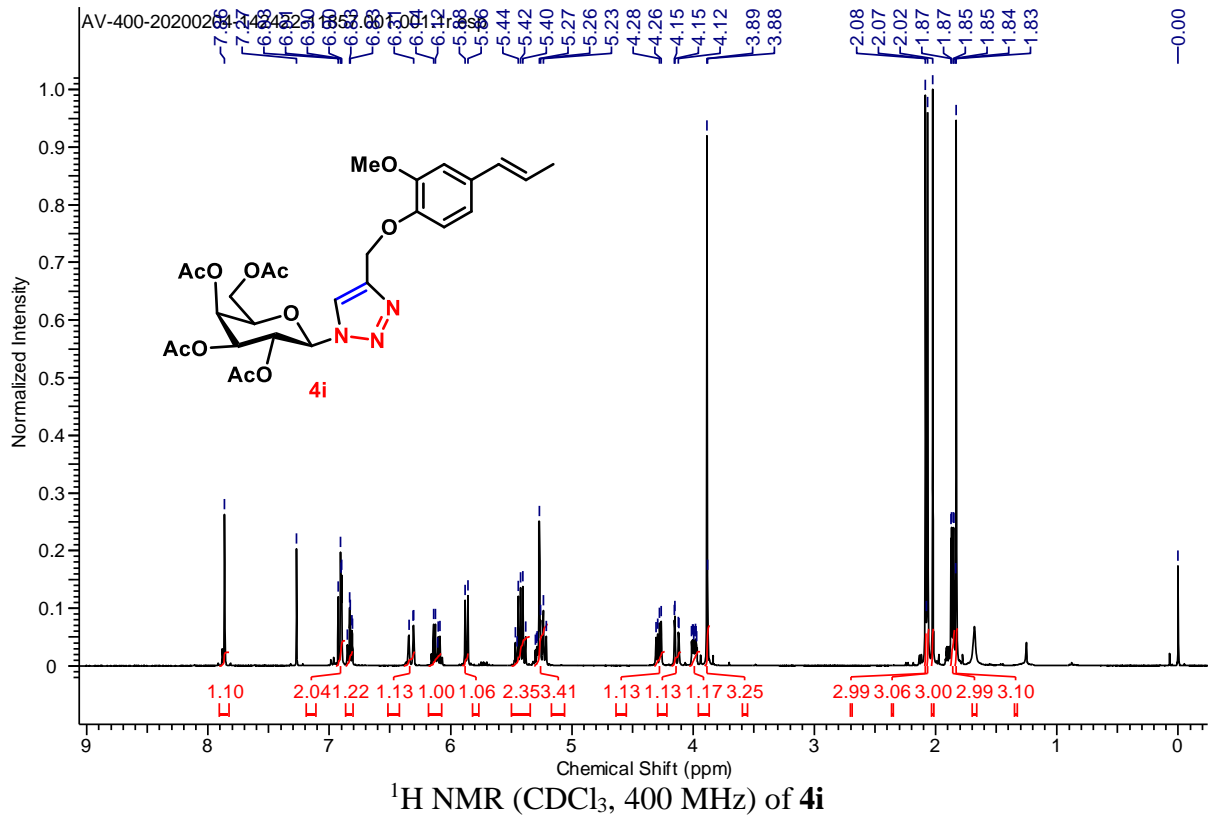
¹³C NMR (CDCl₃, 50 MHz) of **4g**

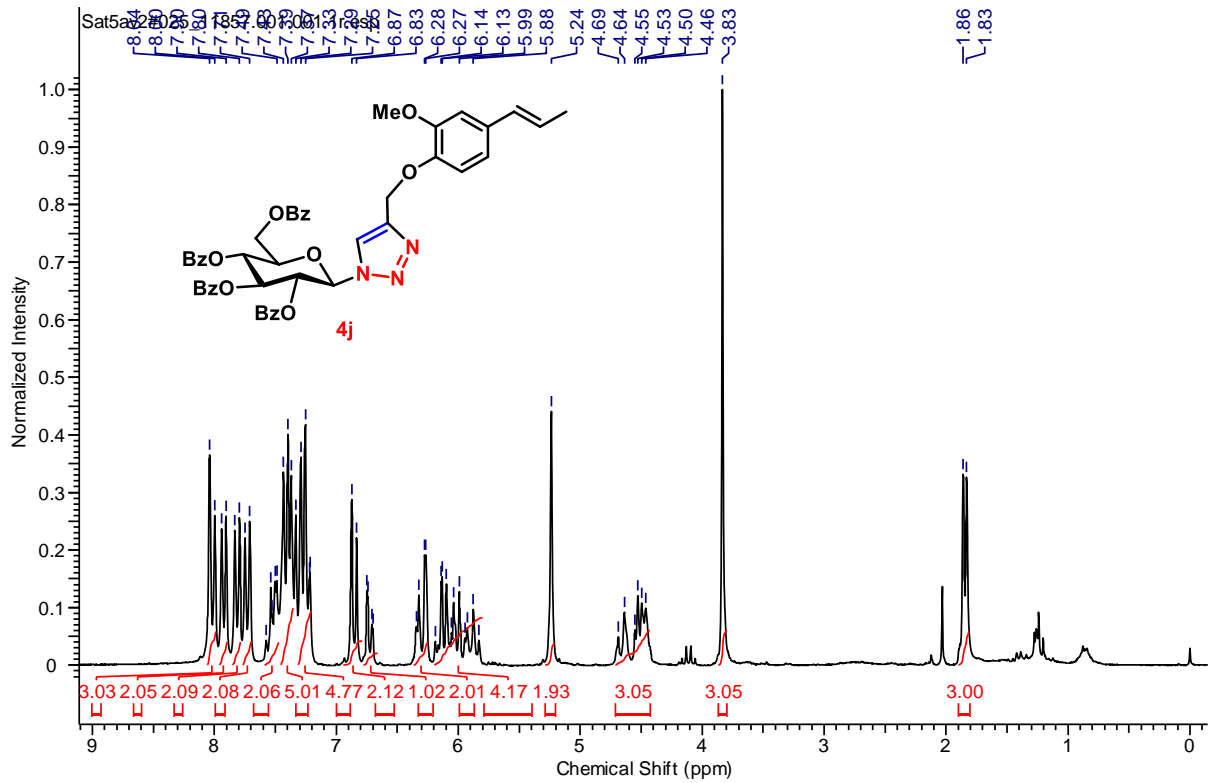


^1H NMR (CDCl_3 , 200 MHz) of **4h**

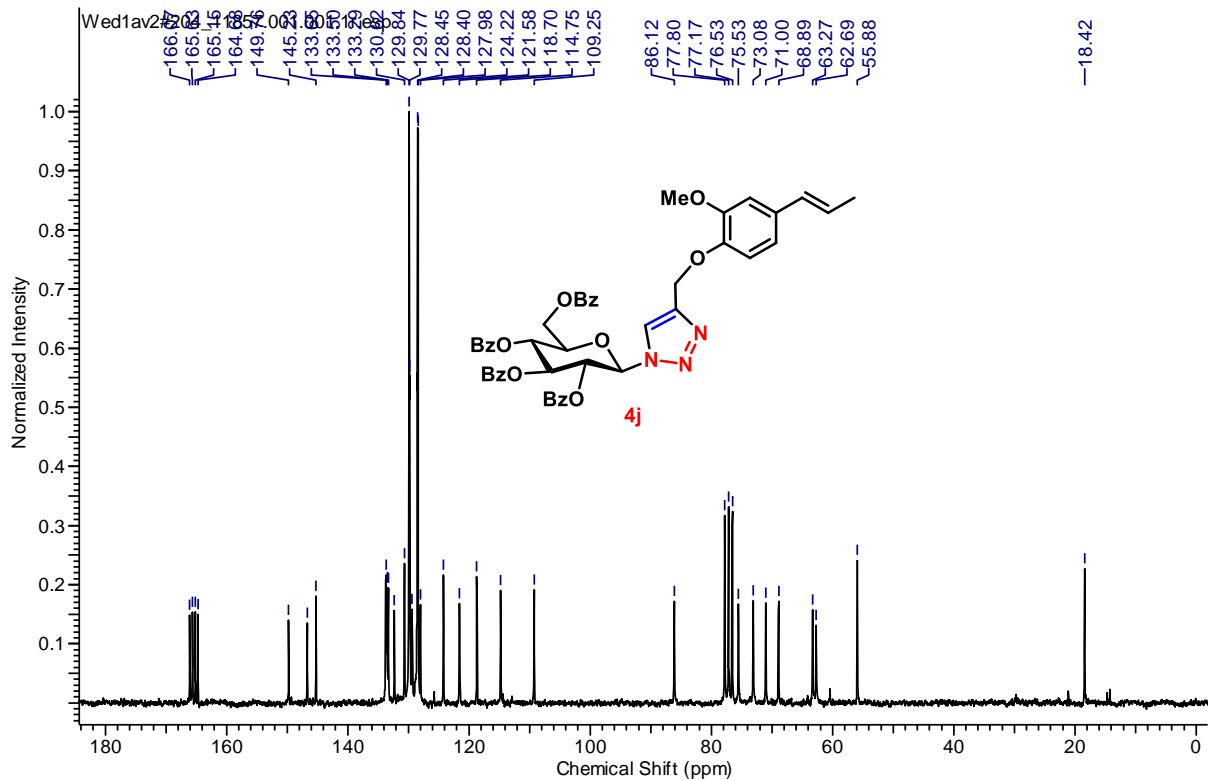


^{13}C NMR (CDCl_3 , 50 MHz) of **4h**

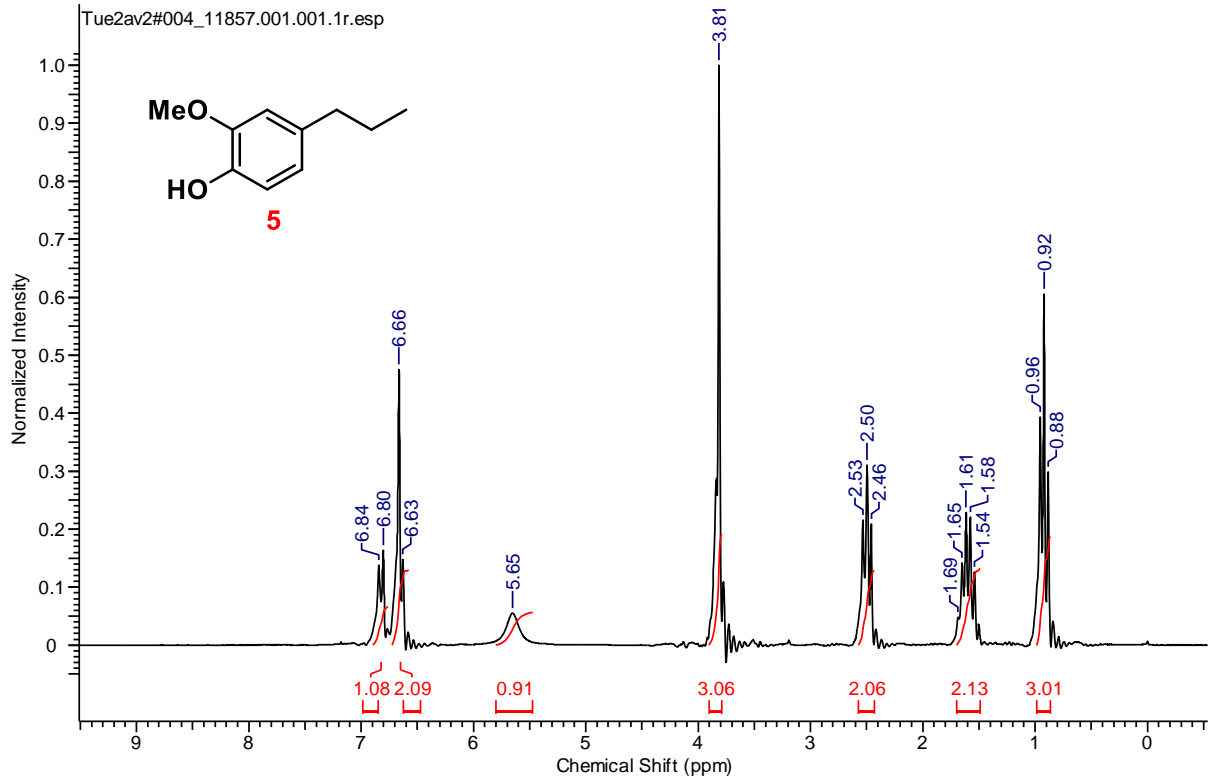
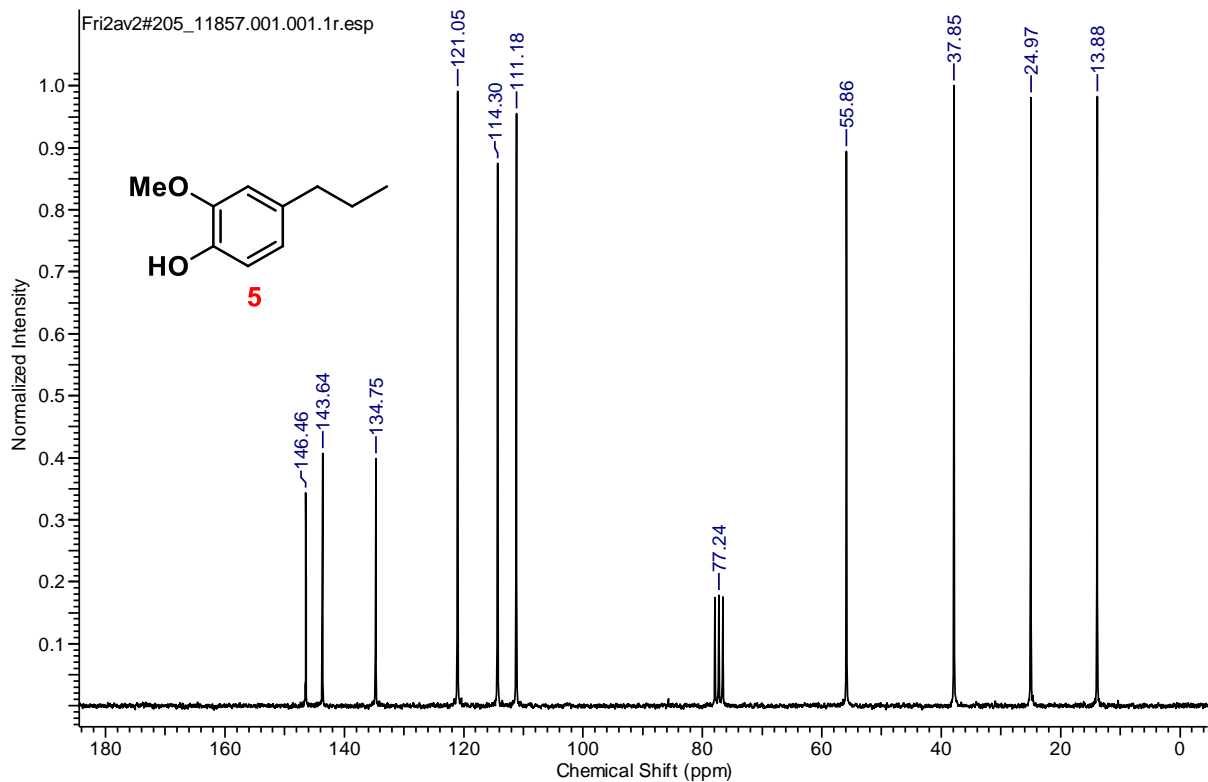


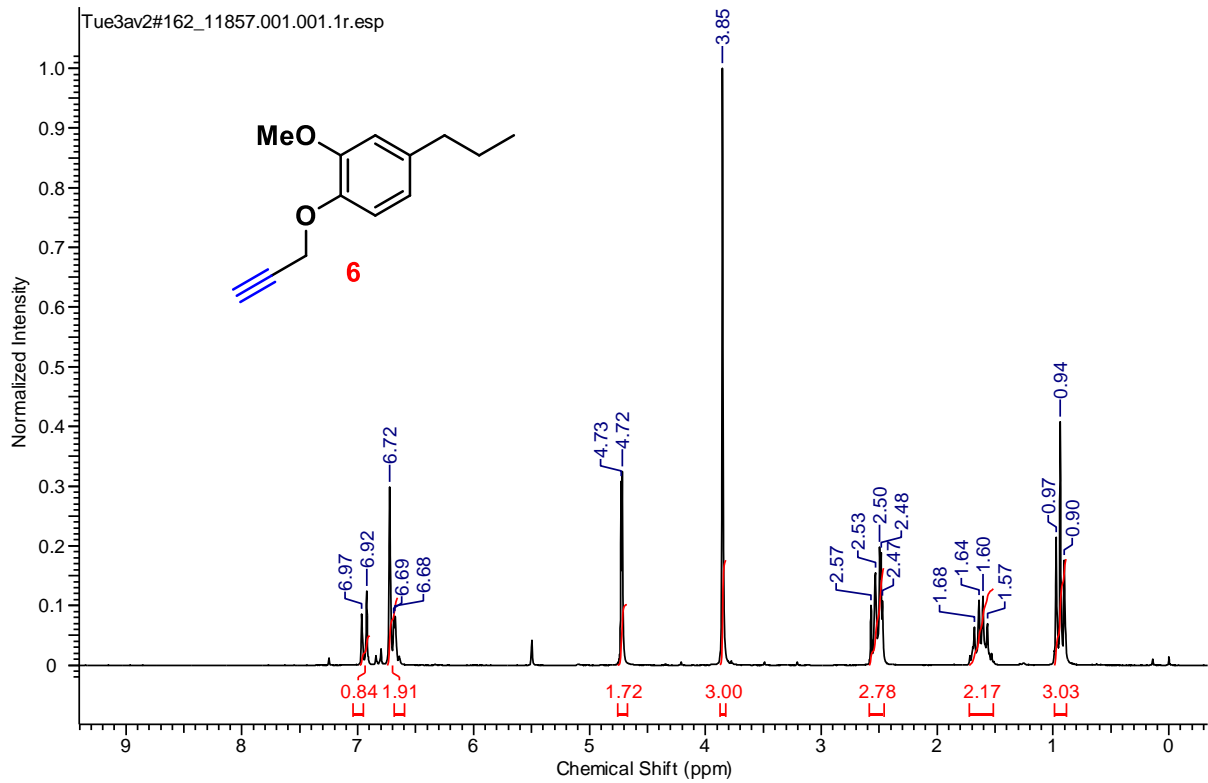
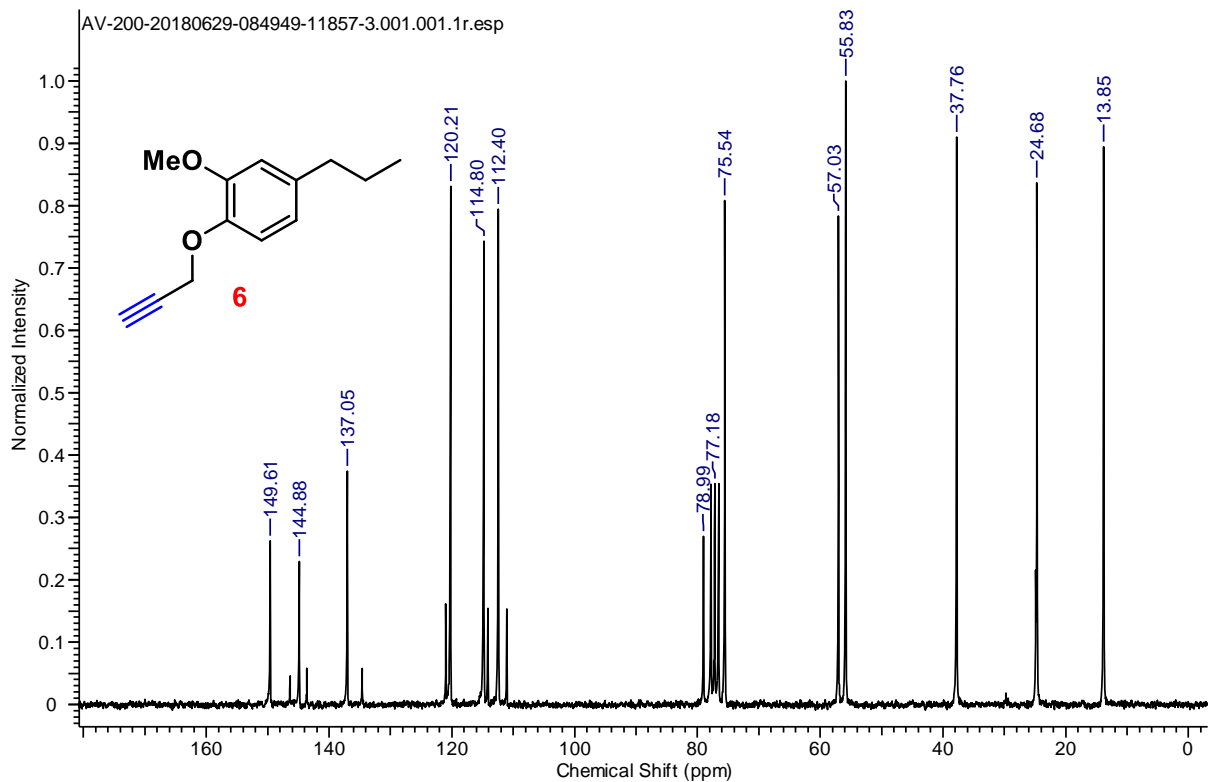


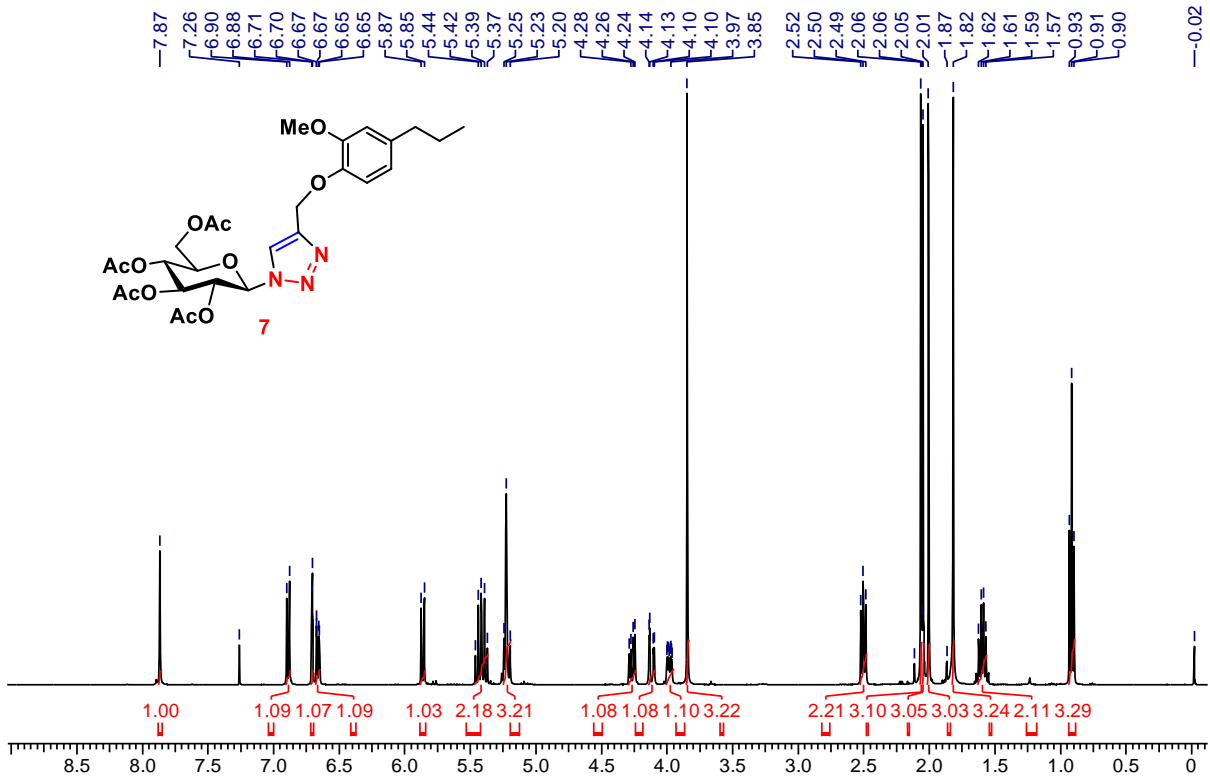
¹H NMR (CDCl₃, 200 MHz) of **4j**



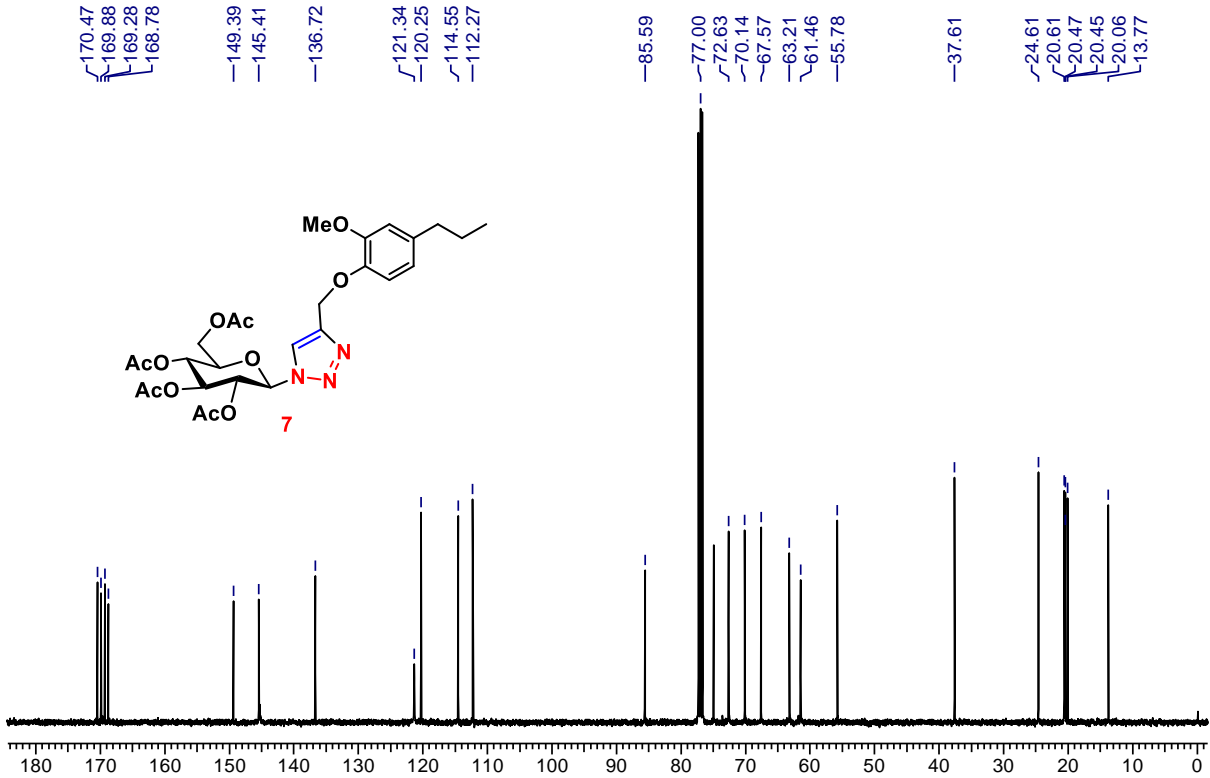
¹³C NMR (CDCl₃, 50 MHz) of **4j**

 ^1H NMR (CDCl_3 , 200 MHz) of **5** ^{13}C NMR (CDCl_3 , 50 MHz) of **5**

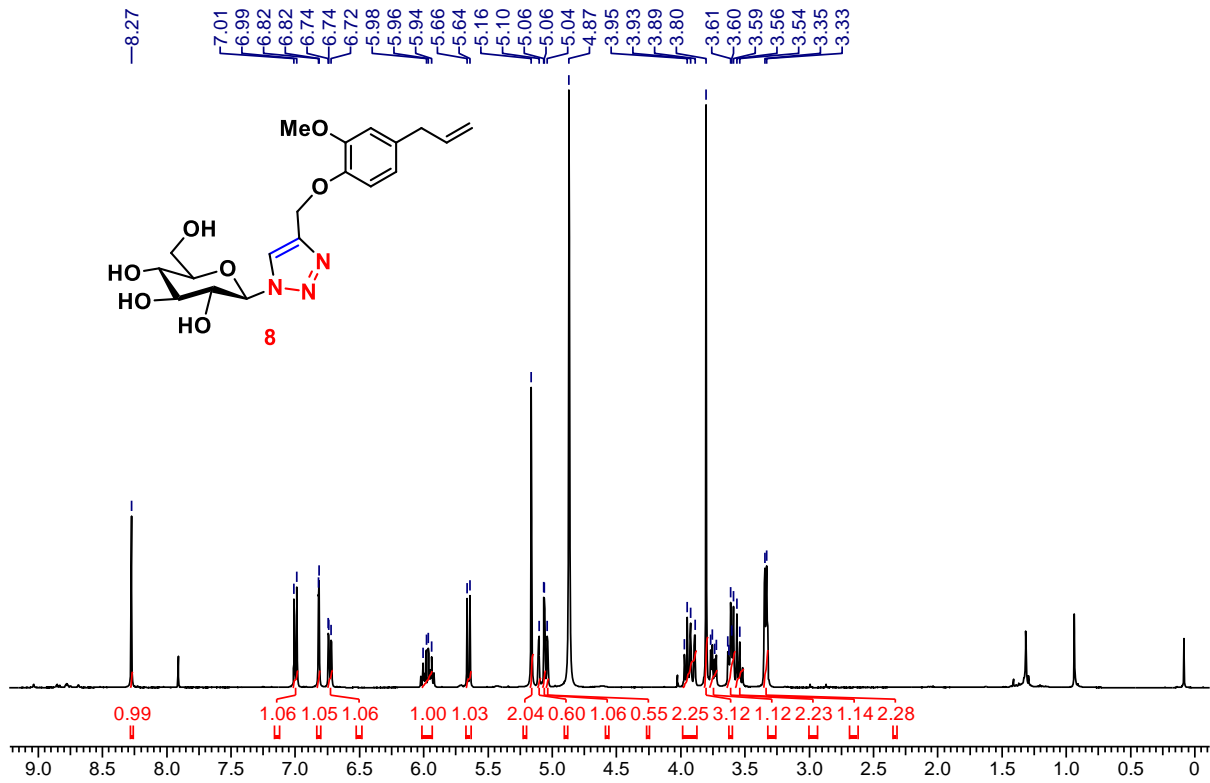
 ^1H NMR (CDCl_3 , 200 MHz) of **6** ^{13}C NMR (CDCl_3 , 50 MHz) of **6**



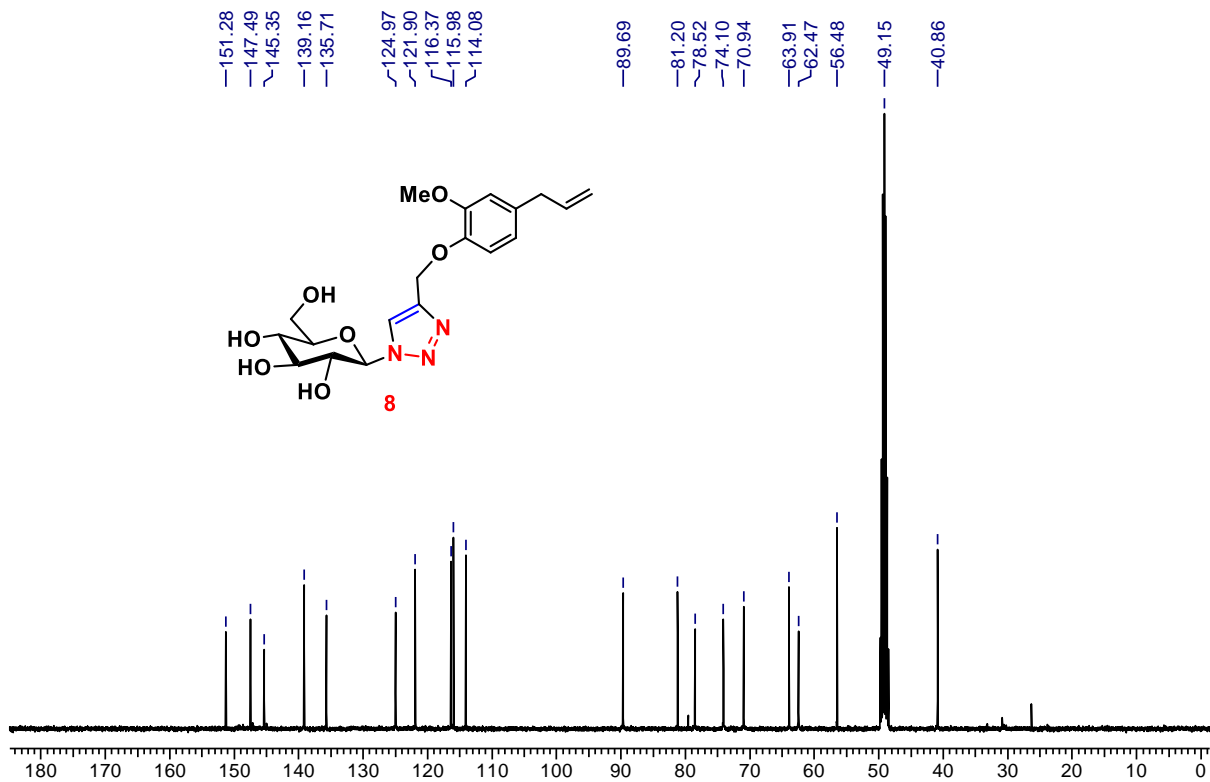
^1H NMR (CDCl_3 , 400 MHz) of 7



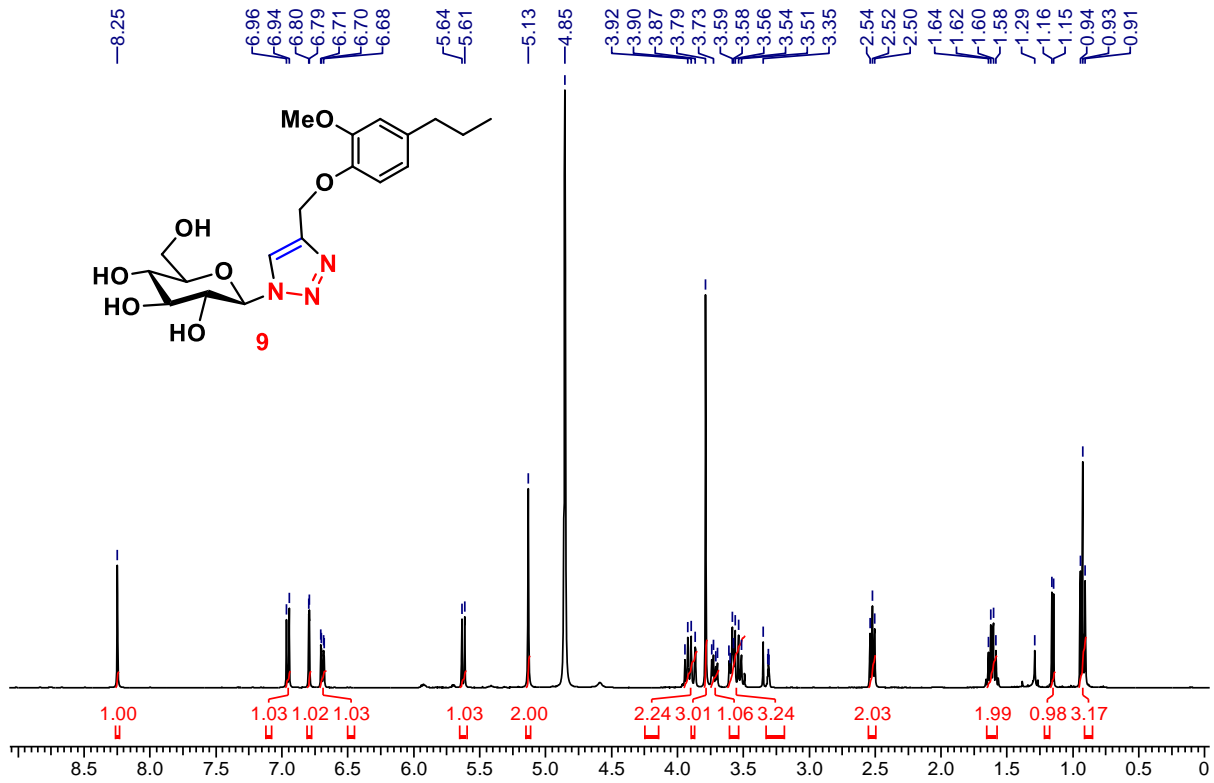
^{13}C NMR (CDCl_3 , 101 MHz) of 7



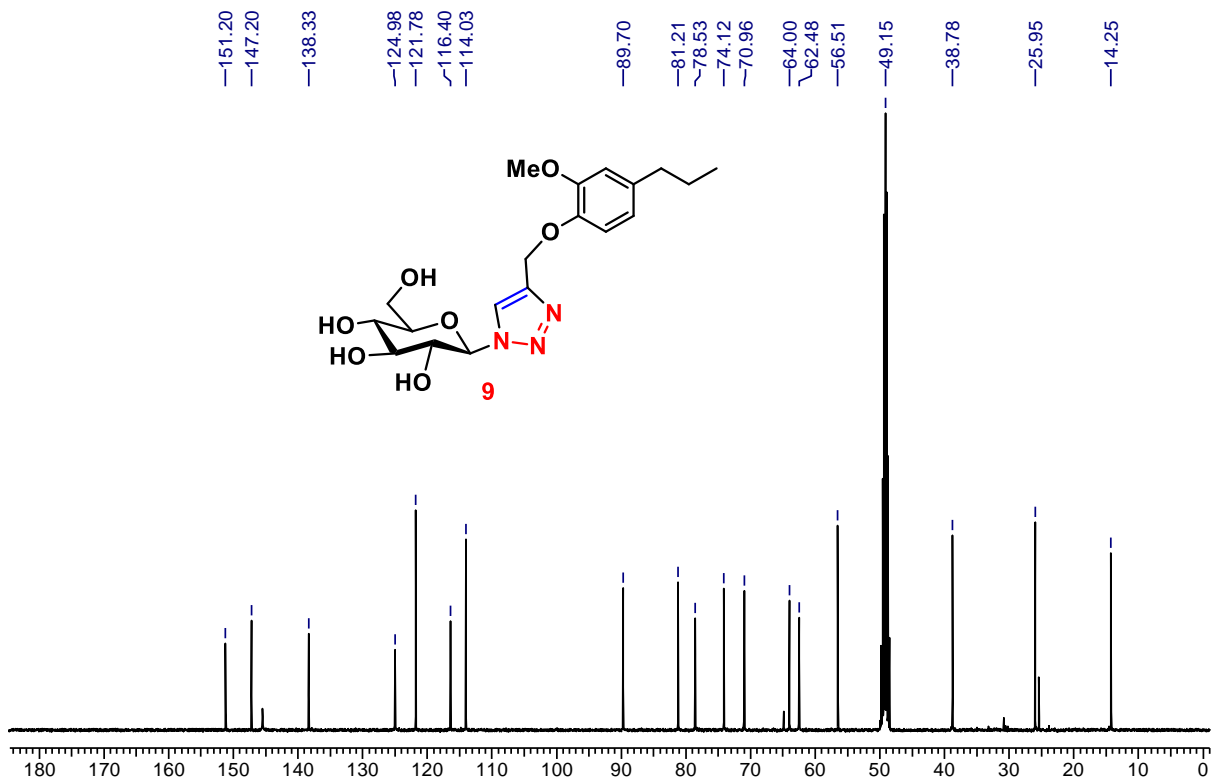
¹H NMR (CDCl₃, 400 MHz) of 8



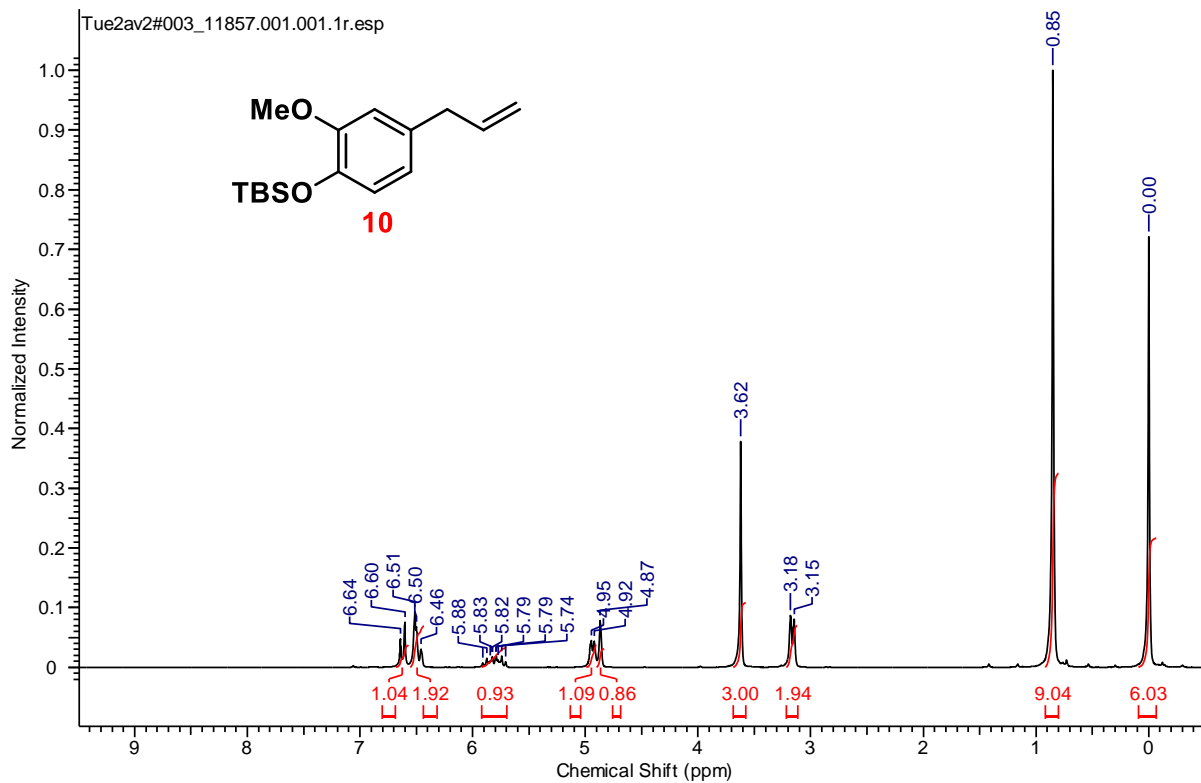
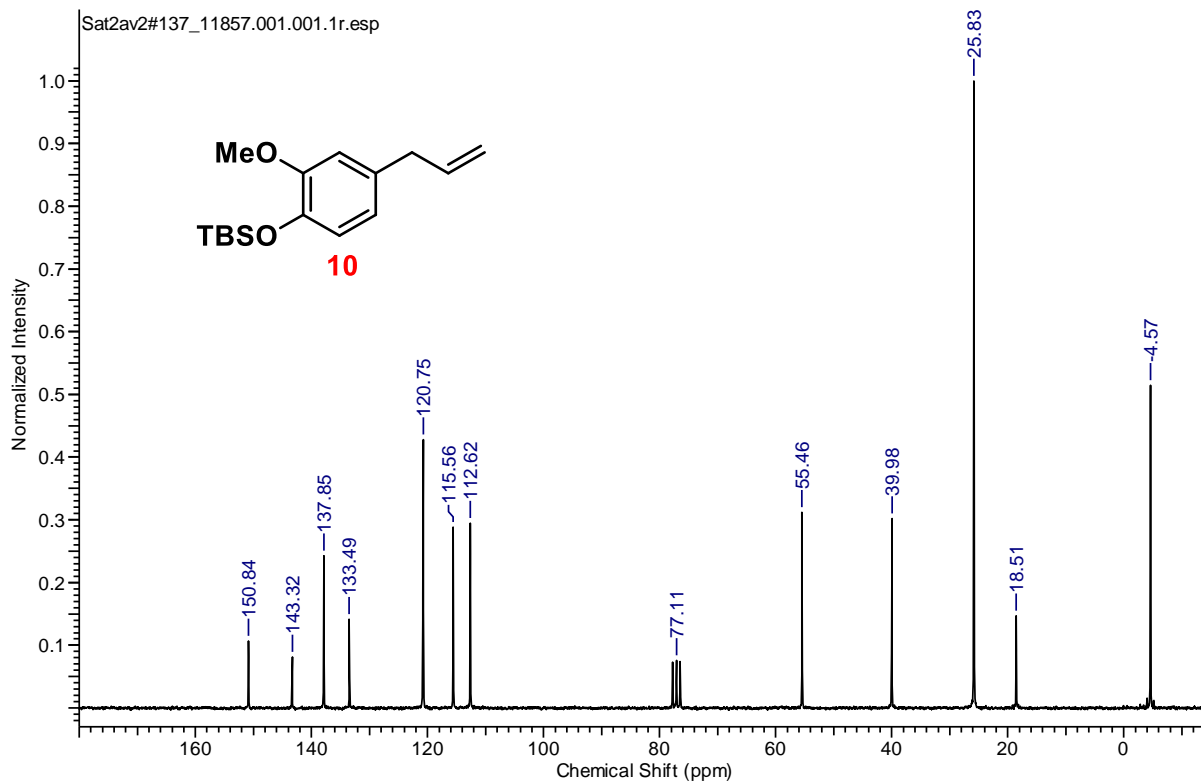
¹³C NMR ((MeOH-d₄, 101 MHz) of 8

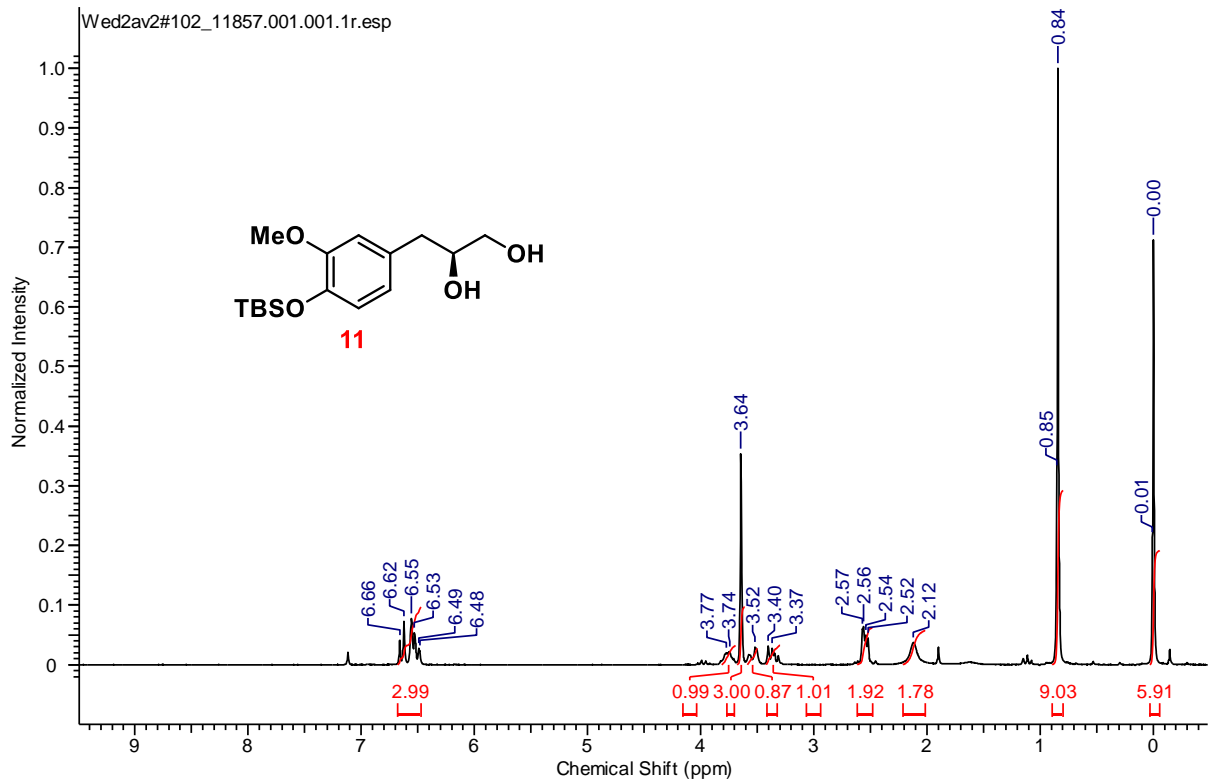
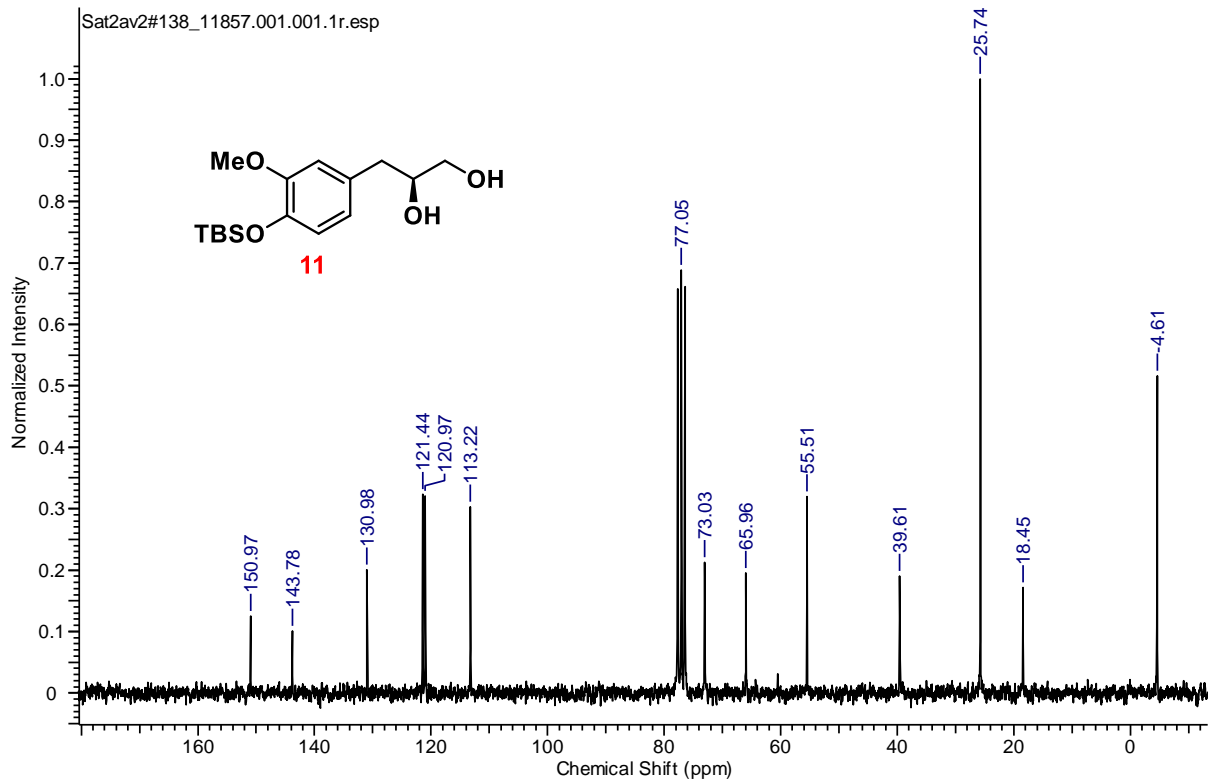


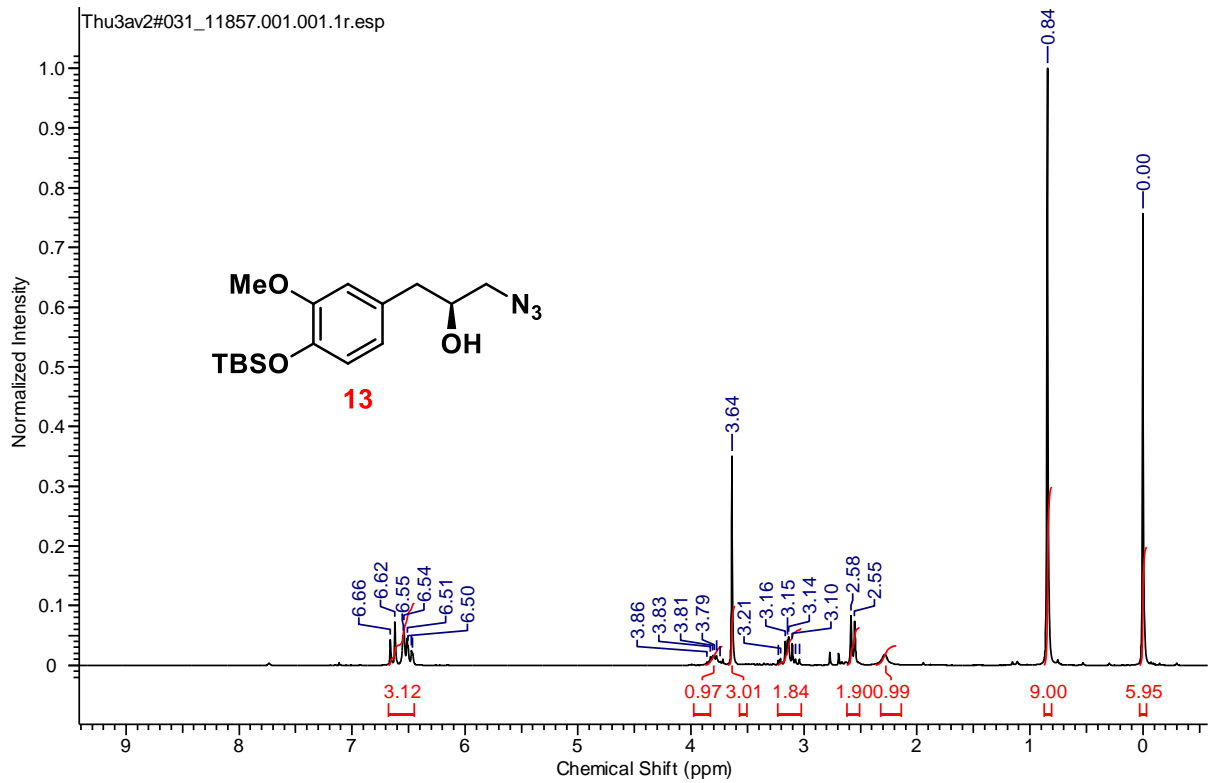
¹H NMR (MeOH-d₄, 400 MHz) of 9



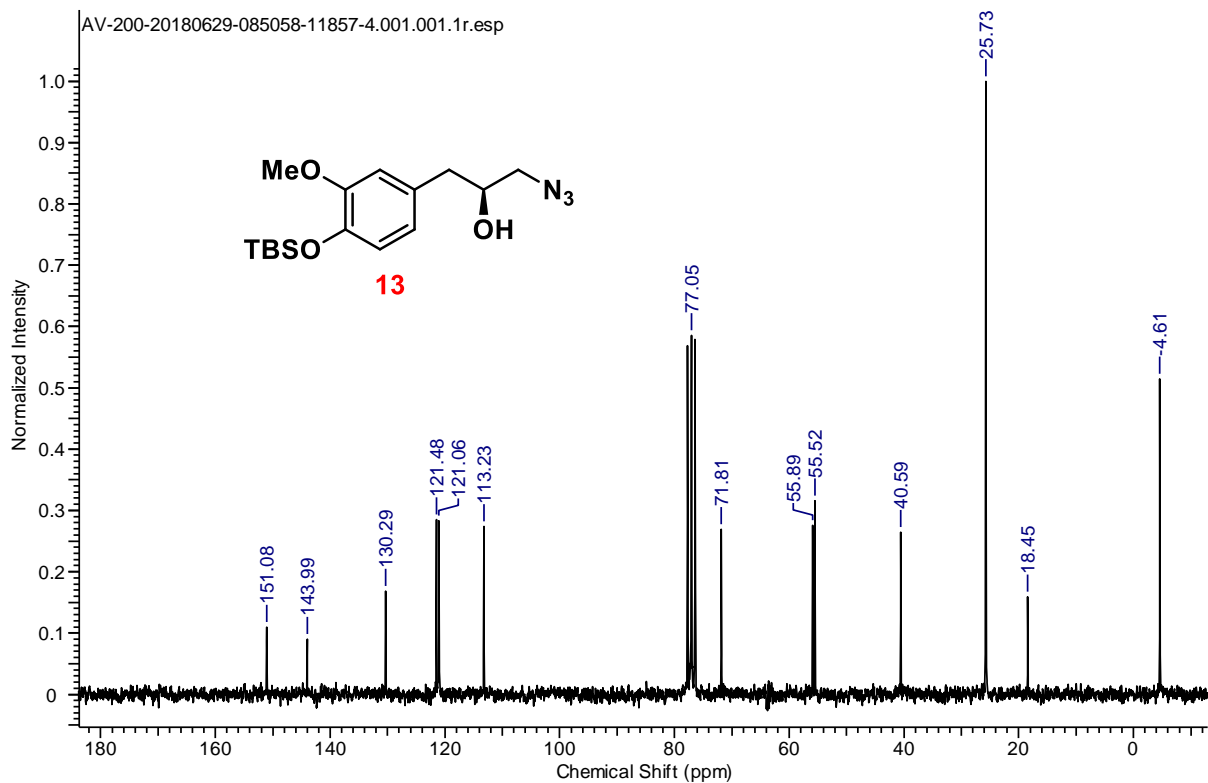
¹³C NMR ((MeOH-d₄, 101 MHz) of 9

 ^1H NMR (CDCl_3 , 200 MHz) of **10** ^{13}C NMR (CDCl_3 , 50 MHz) of **10**

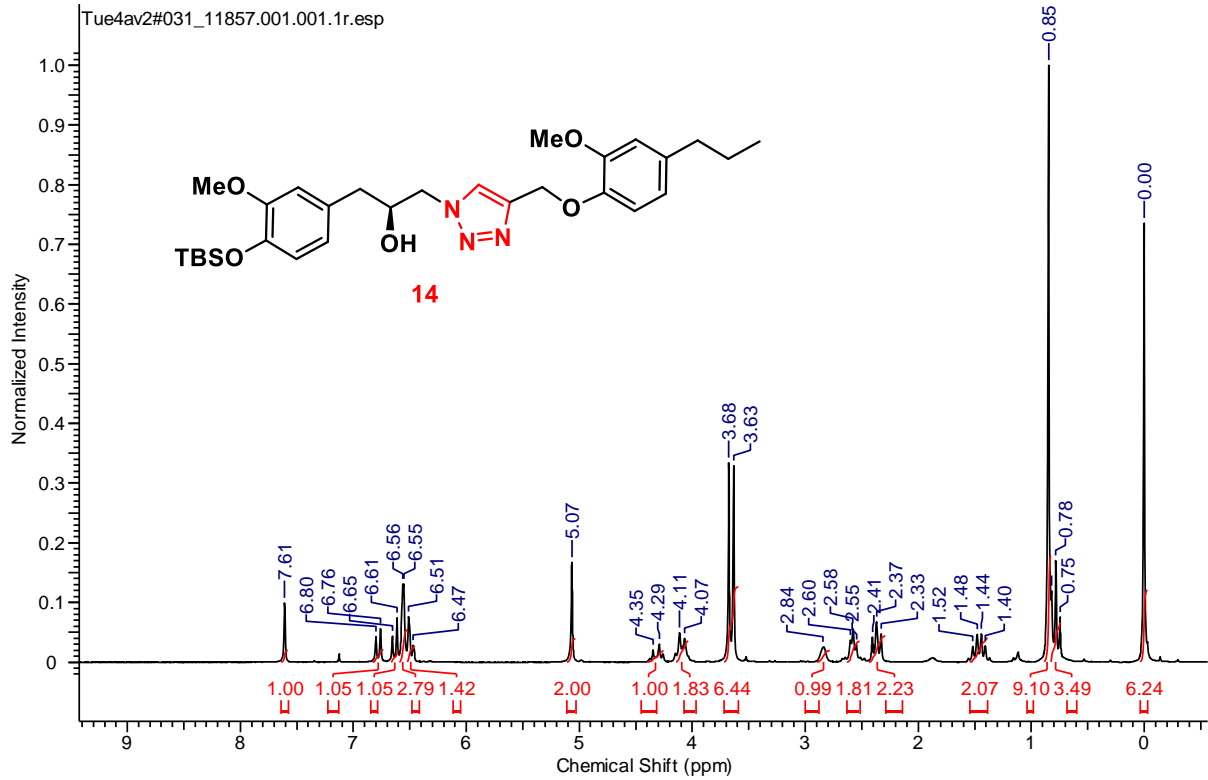
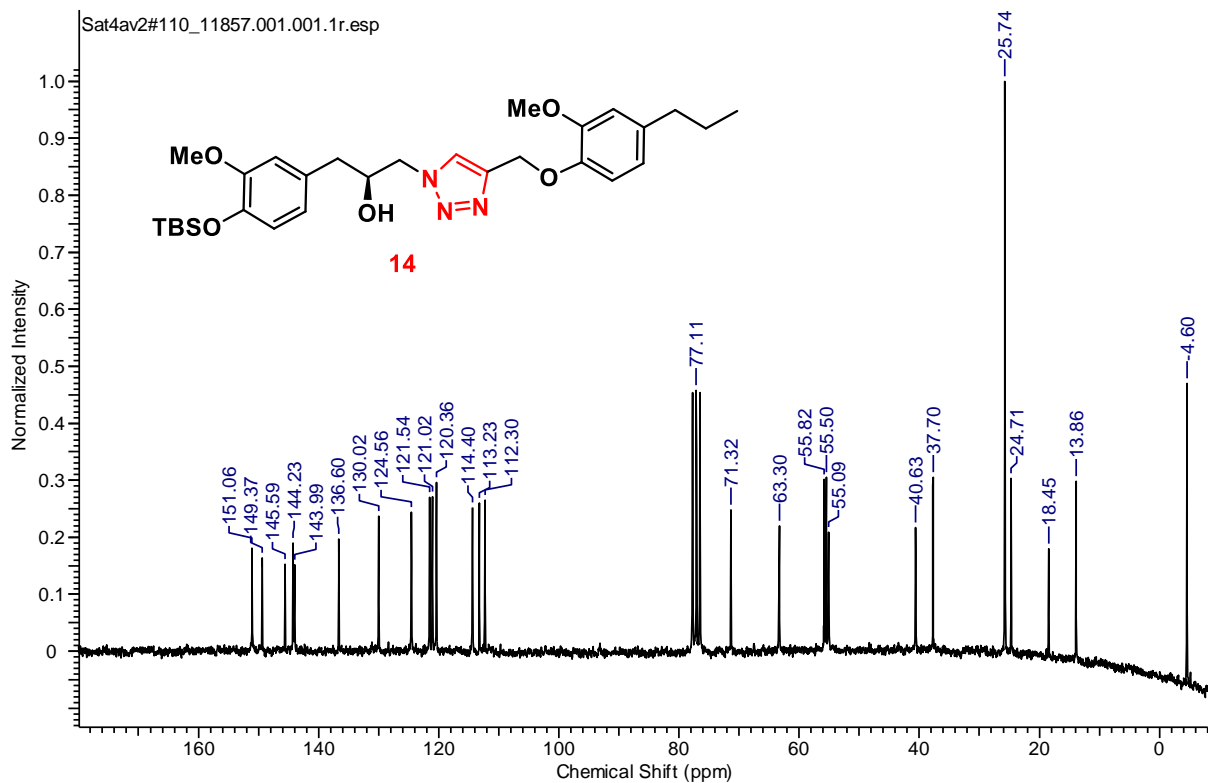
 ^1H NMR (CDCl_3 , 200 MHz) of **11** ^{13}C NMR (CDCl_3 , 50 MHz) of **11**

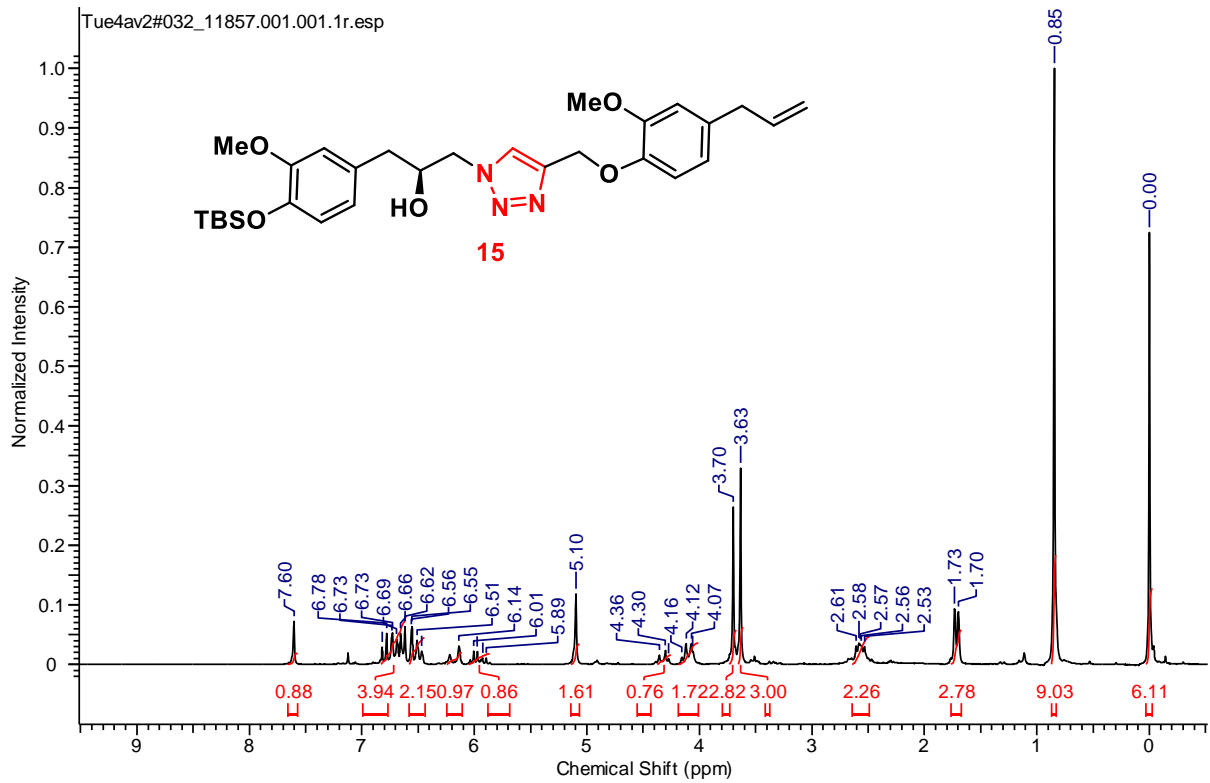
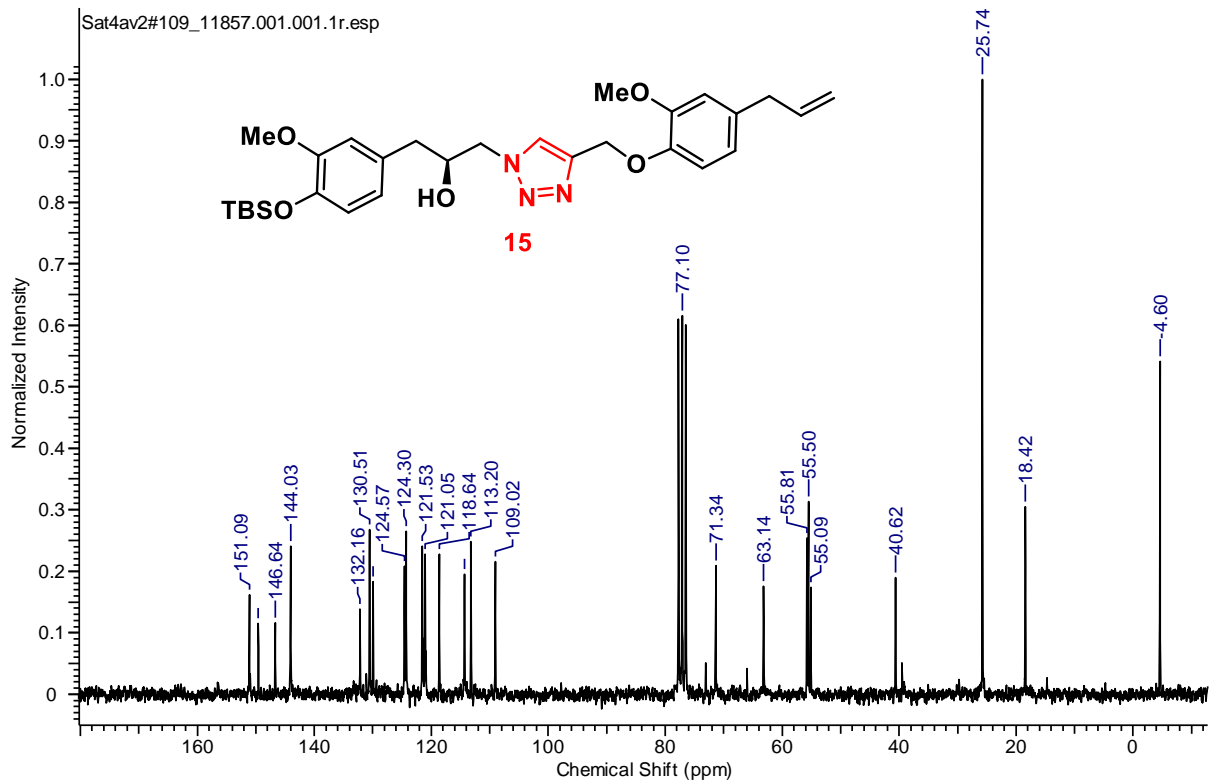


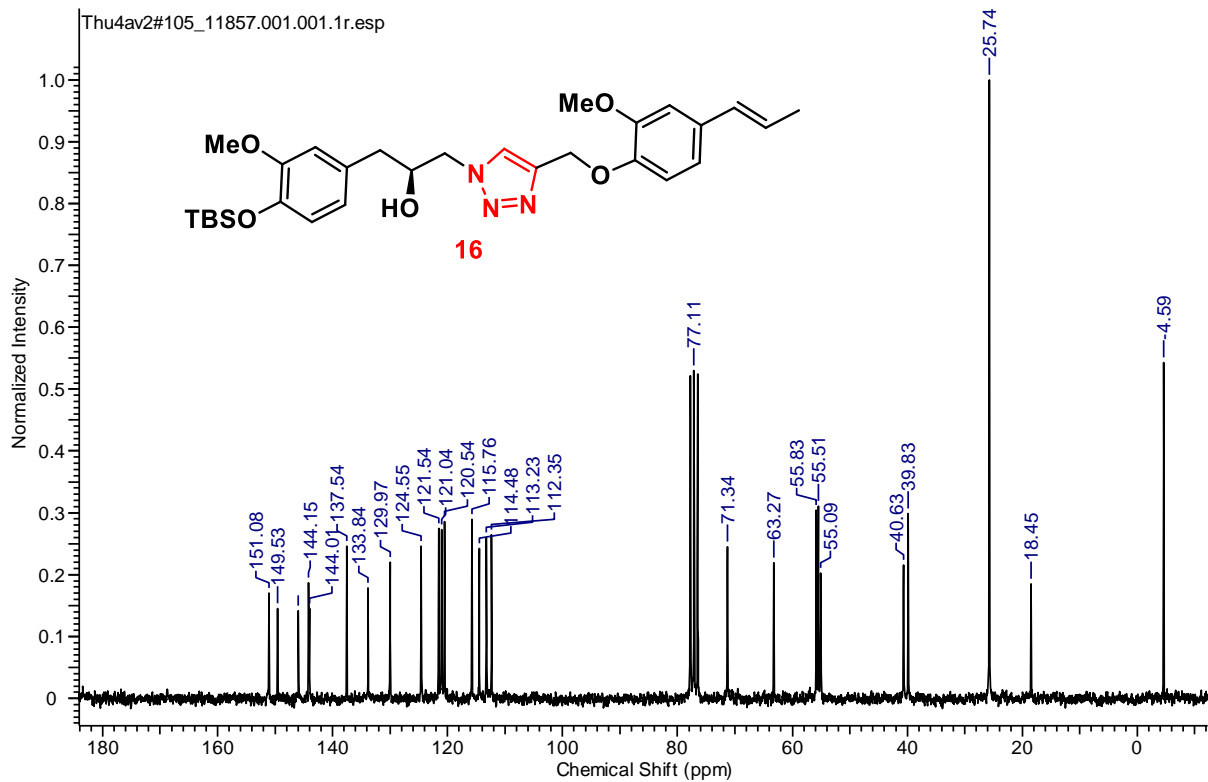
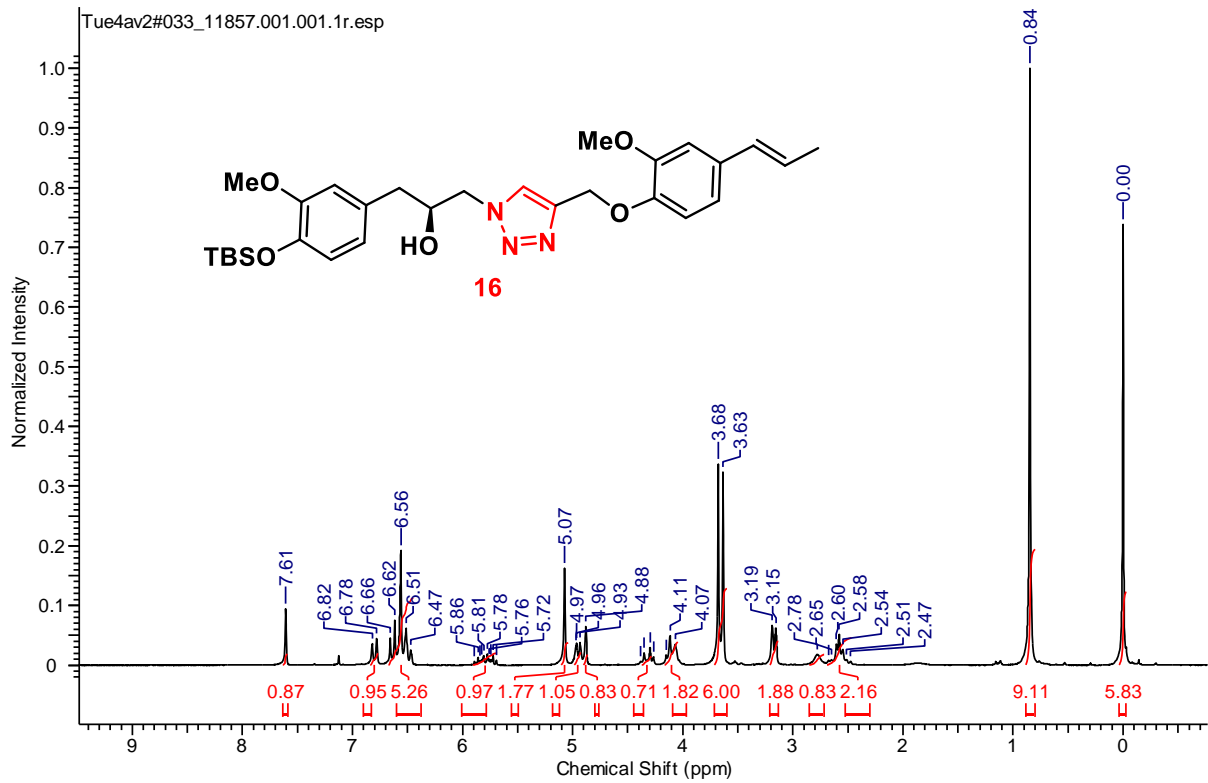
¹H NMR (CDCl₃, 200 MHz) of **13**



¹³C NMR (CDCl₃, 50 MHz) of **13**

 ^1H NMR (CDCl_3 , 200 MHz) of **14** ^{13}C NMR (CDCl_3 , 50 MHz) of **14**

 ^1H NMR (CDCl_3 , 200 MHz) of **15** ^{13}C NMR (CDCl_3 , 50 MHz) of **15**



1.3. Design and synthesis of eugenol/isoeugenol based homo/hetero coupled products via Glaser and Cadiot-Chodkiewicz coupling reactions

1.3.1 Introduction

Aspergillus fumigatus is an aerosol saprotrophic pathogen that has acclimatized itself to survive in adverse atmospheric conditions; hence it is capable of imposing serious health issues in humans.¹ We often inhale spores of *Aspergillus* in daily life, but patients with incompetent immunology and lurking pulmonary diseases like tuberculosis, lung cancer, asthma, pneumonia, and other respiratory complications are most vulnerable to this situation. The small conidial size helps it to invade deep into the respiratory system reaching the alveoli and causing fatal invasive infections in immunocompromised hosts.²⁻⁴ Adhesion of these inhaled conidia to the epithelial cells of the respiratory system of the host assists in their nourishment and cell multiplication.⁵ Proteins on the conidial surface mask its recognition by the host immune system.⁶ Commonly known marketed drugs are amphotericin B (Amp B), nystatin, miconazole, ketoconazole, fluconazole, voriconazole, terbinafine, itraconazole, etc. (Figure 1).⁷

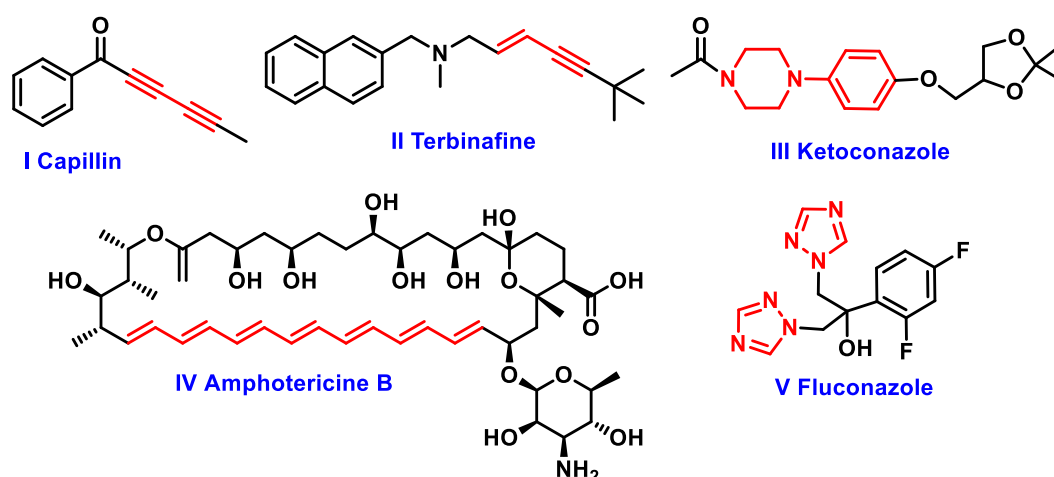


Figure 1: Commonly known antifungal drugs (I-V)

Polyenes and allylamines are one of the major classes of antifungal drugs. Capillin, amphotericin B, terbinafine etc. are some of the reported antifungals which make fungal cell walls porous by inhibiting the enzyme secretion by fungal cell walls hence resulting in the death of fungal cells.⁷

But over time this fungus strain has developed resistance against the cellular self-defense mechanism of host cells and extensively used marketed drugs. Hence, recognizing natural products as new antifungals is a crucial step in the development of potent antifungal agents with higher efficiency and lower cytotoxicity.^{8,9} Capillin, a conjugated ynone is one of the major components of the essential oil extracted from the capillaries of *Artemisia monosperma* and *Artemisia dracunculus*. It also possesses a 1,3-diyne motif and exhibited strong antifungal properties along with other biological potentials.¹⁰ To unfold new possibilities, we envisioned that symmetrical or unsymmetrical 1,3-diyne scaffolds could prove to be potent antifungals. Cu(I)-catalysed Glaser-Hay or Cadiot-Chodkiewicz coupling reactions can be utilized to synthesize 1,3-diynes derivatives.^{13,14}

1.3.1.1 Introduction to Glaser-Hay or Cadiot-Chodkiewicz coupling reactions

The Glaser coupling is one of the oldest acetylene coupling reaction which is primarily catalysed *via* Cu(I) salts like copper chloride or copper bromide and an additional oxidant like oxygen (**Figure 2**).¹³ This reaction was first reported by Carl Andreas Glaser in 1869 originally using ammonia as base and water and alcohol as solvent.¹³ Further modification of this reaction was shown in Elington reaction where two terminal alkynes of same kind were coupled by using stoichiometric amount Cu(OAc)₂ in presence of a base.¹³ The most recent variant of Glaser coupling was Hay coupling uses catalytic amount of Cu(I) salt in presence of Oxygen (present in open air) oxidized Cu(I) to Cu(II) and TMEDA complex of copper(I) chloride activates the terminal alkynes.¹³ The Cadiot–Chodkiewicz coupling is a coupling reaction between a terminal alkyne and a haloalkyne catalyzed by a Cu(I) salt and an amine base to couple two different kind of terminal alkynes in good yields (**Figure 2**).¹⁴

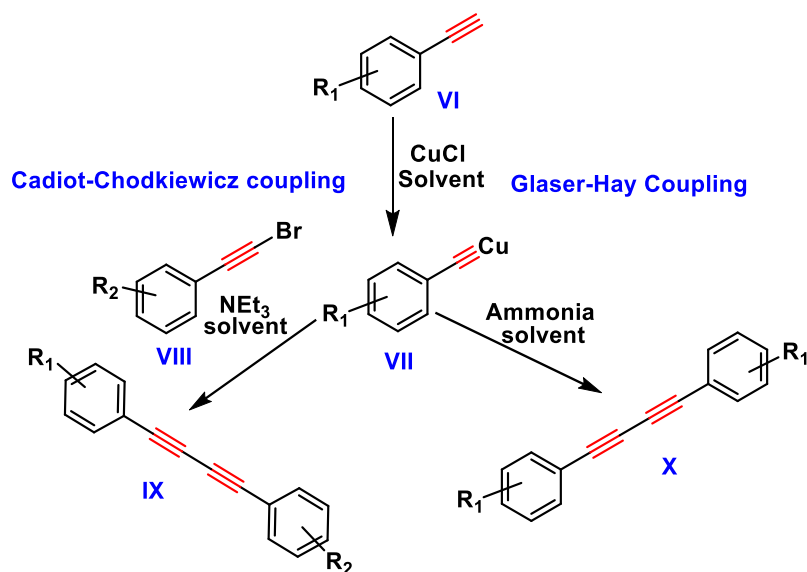


Figure 2: Cu(I)-catalysed Glaser-Hay or Cadiot-Chodkiewicz coupling reactions

1.3.1.2 Eugenol 1a and isoeugenol 1b as potent antifungals

Eugenol (**1a**) and isoeugenol (**1b**) are isolated from the essential oil of the plants *Syzygium aromaticum* and *Eugenia caryophyllata* and *Myristica fragrans* (**Figure 3**).^{11,12} Both compounds have shown antifungal activities against filamentous as well as non-filamentous *A.fumigatus* with an IC₅₀ value of 1900 μ M.^{11b} These compounds deform the morphological features of the conidia and hyphae leading to easy rupture of fungal cell walls.^{9b} The antifungal activity could be due to the aromatic nucleus or phenolic -OH group which may get involved in hydrogen bonding with the surface enzymes of the fungal cell wall. Here, we utilized propargylated of eugenol (**2a**), isoeugenol (**2b**), guaiacol (**2c**), vanillin (**2d**) and dihydrogenated eugenol or euganol (**2e**) (**Figure 3**) to synthesise corresponding symmetrical or unsymmetrical 1,3-diynes.

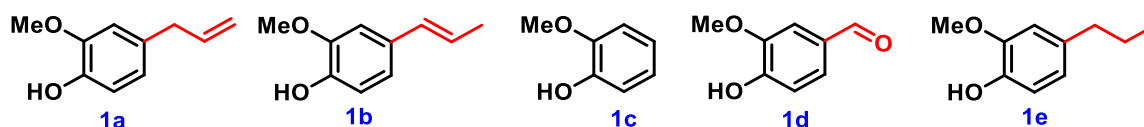
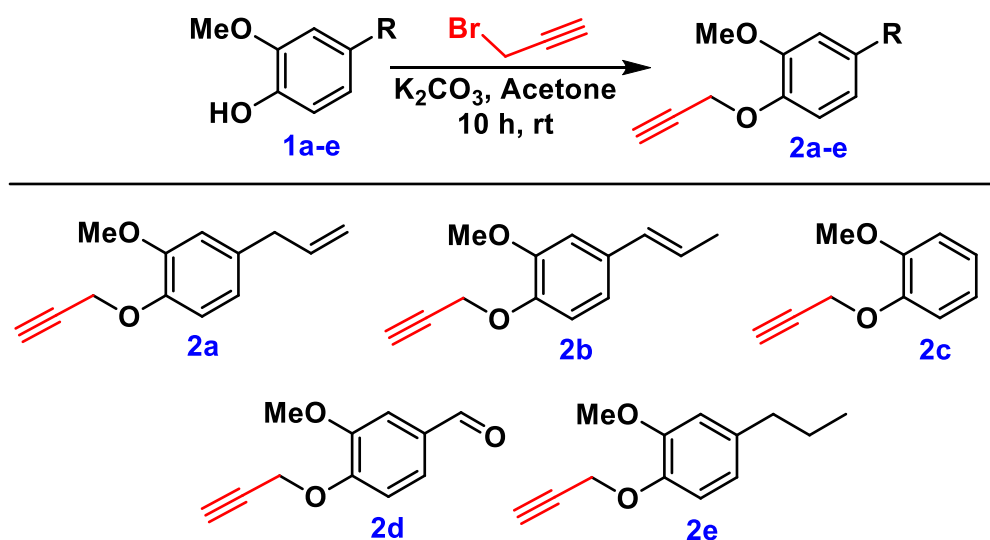


Figure 3: Eugenol (**1a**), isoeugenol (**1b**) and other phenolics (**1c-e**)

1.3.2 Present work

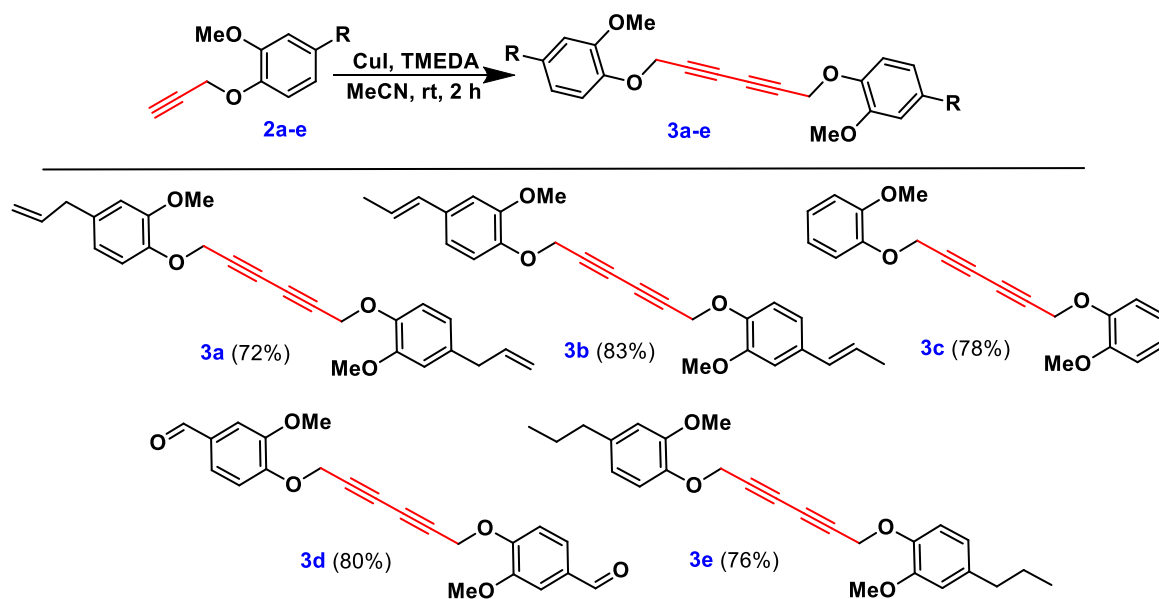
1.3.2.1 Chemical modifications of phenolics (1c-e)

In this regard, Glaser-Hay coupling reaction conditions met our need to synthesize symmetrical diynes.¹³ To synthesize homo diynes, we treated all phenolic compounds (**1a-e**) with propargyl bromide in presence of potassium carbonate (K_2CO_3) as a base in acetone as a solvent to afford propargylated phenolic derivatives (**2a-e**) (**Scheme 1**).



Scheme 1: Synthesis of propargylated phenols (**2a-e**)

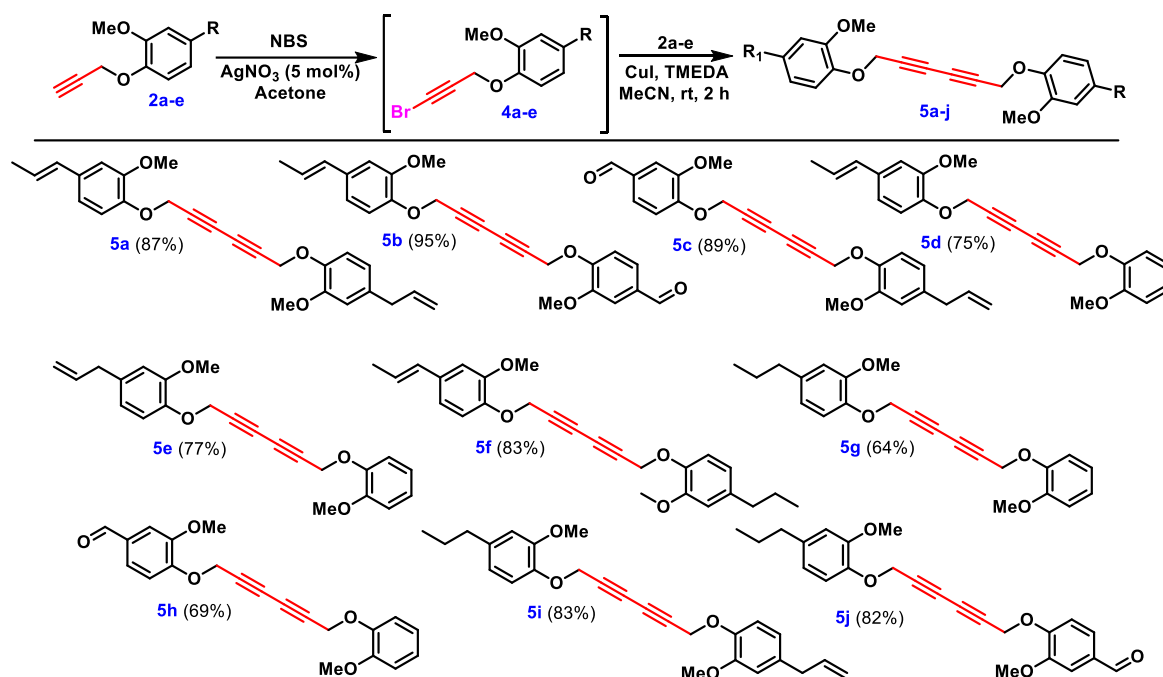
After this, we applied Glaser-Hay coupling conditions to intra coupled all the compounds (**2a-e**) by reacting them in presence of a catalytic amount of copper iodide (CuI) and tetramethylethylenediamine (TMEDA) in acetonitrile which in turn furnished homo coupled products (**3a-e**) in good to excellent yields (**Scheme 2**). All these homo diynes (**5a-j**) were well characterized by their NMR spectra. In all the cases, acetylenic proton which appears at δ_H 2.48 ppm (in compounds **2a-e**) was found absent in the 1H NMR spectra of Glaser-Hay product.^{11b} Further, for the synthesis of hetero-coupled products, we utilized Cadiot-Chodkiewicz coupling reaction as this predominantly furnishes hetero-coupled product.¹⁴



Scheme 2: Synthesis of homo coupled products (**3a-e**)

In order to synthesize hetero diynes, we brominated all the propargylated derivatives by applying *N*-bromosuccinamide (NBS) in presence of catalytic amount of silver nitrate (AgNO_3) in acetone at ambient temperature to furnish compounds (**4a-e**). These all brominated compounds were used without any prior purification for the Cadiot-Chodkiewicz coupling. All the previously propargylated compounds (**2a-e**) were coupled with brominated ones (**4a-e**) in presence of catalytic amount of CuI, TMEDA as a base in acetonitrile as solvent at room temperature to provide unsymmetrical diynes (**5a-j**) in good to excellent yields (**Scheme 3**). All the hetero-coupled diynes were found to be in agreement with their assigned structure as evident from their ^1H , ^{13}C NMR spectra and HRMS.

All the 1,3-diynes were assayed for their antifungal activities against *A. fumigatus* according to the Clinical and Laboratory Standards Institute (CLSI) protocol.¹⁵ Among all the compounds synthesized, only **3a** was able to show promising antifungal data with an IC_{50} value of 7.75 μM .



Scheme 2: Synthesis of hetero coupled products (**5a-j**)

1.3.2.2 Structure-Activity-Relationship analysis

It is apparent from the data presented in **Table 1** that all the diynes (**3a-e** and **5a-j**) have displayed many folds better antifungal activities against *A. fumigatus* than their monomeric units (**2a-e**).^{11b,20b} Also the homocoupled dyne (**3a**) possessed better antifungal activity than its parent molecule eugenol (**1a**) (1900 μM). It is evident from the IC_{50} values of diynes, that conjugation has an important role to play for enhanced antifungal activities against *A. fumigatus*. In all the cases except for compound **3b** and **3c**, IC_{50} values range from 7.75 to 17.85 μM for symmetrical and unsymmetrical diynes. Compounds containing an olefinic side chain were apparently more active than others.

The CC_{50} (cytotoxic concentration-50) value of compound (**3a**) was evaluated at 62.16 μM for normal lung epithelial cell line L-132 using the antifungal drug Amp B as a positive control. It indicates low cytotoxicity of compound (**3a**). The sub-lethal cytotoxicity of Amp B reported was in the range of 5.4-10.82 μM .¹⁶ Further, the selectivity index (SI)¹⁷ of compound (**3a**) was calculated as 8.01 which was higher than that of the reported SI of eugenol (**1a**) *i.e.* 0.2 against non-filamentous fungi.¹⁸

Table 1: IC₅₀ of synthesised compounds (**2a-e**, **3a-e**, **5a-j**) against *A. fumigatus*

Compound codes	IC ₅₀ values (μM)	Compound codes	IC ₅₀ values (μM)
1a	1900	3d	16.52
1b	1900	3e	15.38
1c	≥25	5a	15.54
1d	≥25	5b	16.01
1e	9.39	5c	16.01
2a	≥25	5d	17.25
2b	≥25	5e	17.25
2c	≥25	5f	15.46
2d	≥25	5g	17.16
2e	≥25	5h	17.85
3a	7.75	5i	15.46
3b	31.08	5j	15.93
3c	38.81	Amp B	1.08

Hence compound (**3a**) has a much better SI than the original compound. compound (**3a**) obeyed Lipinski's rule¹⁹ of five with no violation (molecular weight is 402.18 g/mol, 4 hydrogen bond acceptors, no hydrogen bond donor, LogP value 4.17, Topological Polar Surface Area (TPSA) is 36.92 Å.²⁻⁴ There was a considerable amount of reduction in the conidiation process when fungal strain was cultured in presence of compound (**3a**). It can be proved with reduced absorbance at 530 nm whereas, there was an acceleration in conidia formation in presence of eugenol (**1a**) and Amp B in comparison to the control.^{20b}

Ergosterol is a necessary content for maintaining fluidity, survival from outer impacts and development etc.^{20a} The percentage of ergosterol at IC₅₀ of eugenol (**1a**) and compound (**3a**) was not so prominent as compared to Amp B (drug control). But still, there was some amount of reduction in the ergosterol level in presence of compound (**3a**) (**Figure 4**).^{20b}

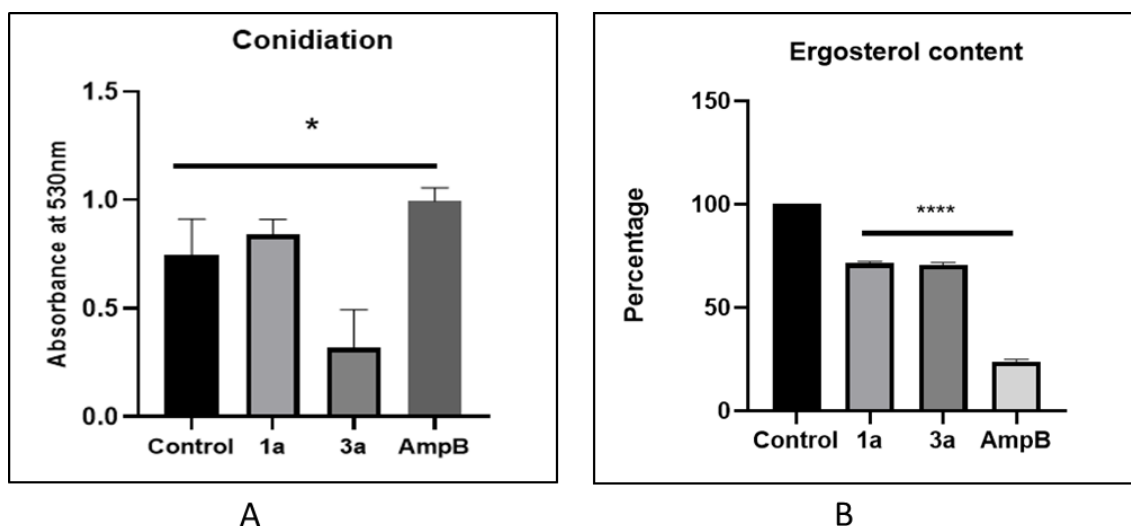


Figure 4: Effect of eugenol (**1a**), compound (**3a**) on the (A) production of *A. fumigatus* conidia and (B) ergosterol content in comparison to control, where control-untreated *A. fumigatus*; $p < 0.05$.

Originally, untreated conidia surface is echinulated with round to oval shapes in maximum cases.^{21,20b} The conidial surface of *A. fumigatus* was found with altered morphology *i.e.* smooth surface with the absence of spikes when treated with compound (**3a**) and these effects of compound (**3a**) on conidial surface elements (hydrophobin layer, dense melanin layer, polysaccharides, proteins and then plasma membrane) were reflected through SEM images (**Figure 5**).

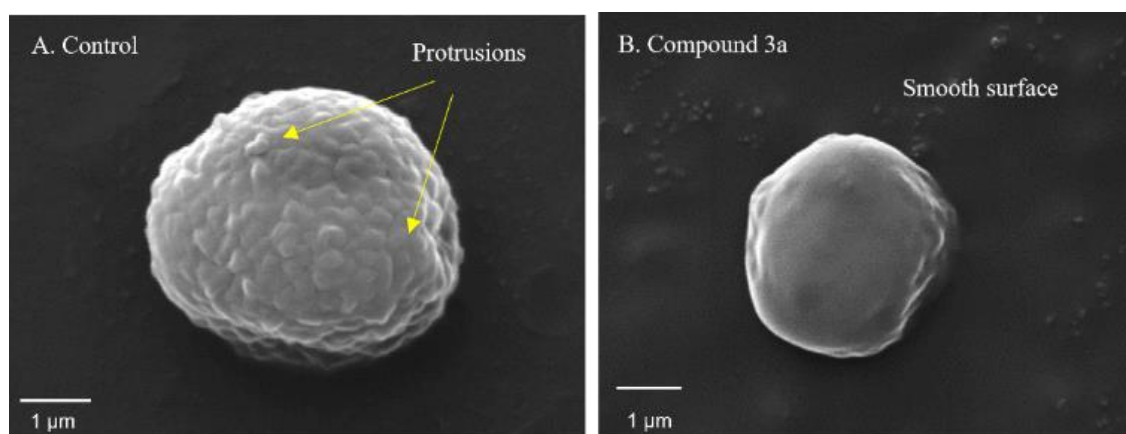


Figure 5: Scanning electron microscope images of resting conidia of *A. fumigatus* (A) control (B) compound (**3a**) treated. Scale bar- 1 μm .

Antibiofilm activity of compound **3a** was evaluated at IC₅₀ of 62.16 μ M and was visualized through confocal laser scanning microscopy (CLSM) (**Figure 6**). The fungal biofilm²² component was stained with a fluorescence dye (calcofluor white), which showed dis-coordinated fungal hyphae in presence of compound (**3a**).^{20b}

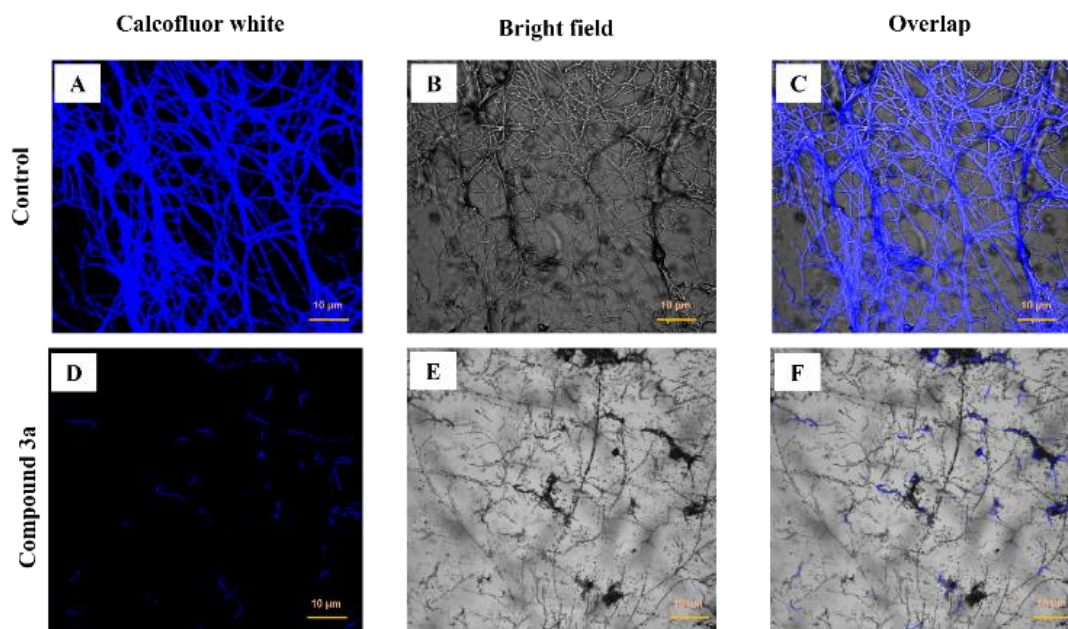


Figure 6: *Aspergillus fumigatus* biofilm eradication. Confocal laser scanning microscopy (CLSM) images of 48 h *A. fumigatus* biofilm on glass coverslips (A–C) control were stained with Calcofluor white dye depicting intense hyphal growth with ECM; (D–F) compound **3a** treated biofilm possess disintegrated hyphae at 40 \times magnification. Scale Bar- 10 μ m

1.2.3 Conclusions

In summary, we have synthesized symmetrical and unsymmetrical diynes by employing Glaser-Hay as well as Cadiot- Chodkiewicz coupling reactions, respectively. The homo diyne synthesized using propargylated eugenol (**3a**) has shown promising antifungal activity against *A. fumigatus*. Apart from the antifungal assays of synthesized compounds, we also carried out different studies like cytotoxicity, conidia formation, ergosterol biosynthesis and fungal biofilm formation. It considerably modified the surface of conidia along with significant decrease in the integrity of hyphae by eradicating biofilm upon treatment. It was also effective in case of ergosterol synthesis reduction.

1.2.4 Experimental procedures

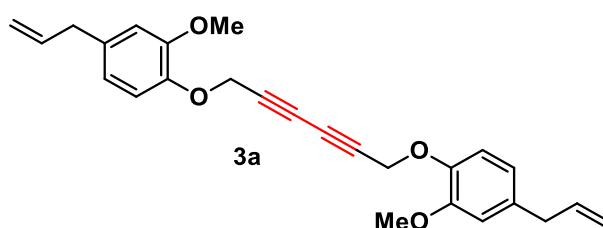
General Procedure for the propargylation of phenols:

Appropriate phenol (1 equiv.) was dissolved in acetone (20 mL) at 25°C under inert atmosphere. After that, potassium carbonate K_2CO_3 (1.5 equiv.) and propargyl bromide (2.5 equiv.) were added to the above-mentioned solution at 25°C. After completion of the reaction (TLC), the reaction mixture was evaporated *in vacuo* to obtain residue which was purified by flash chromatography using a RediSep column (SiO_2 , 12g) with EtOAc-petroleum ether mixture as eluent to furnish compound (2a-e). Spectral data of all the synthesized propargylated phenol were found to be consistent with the previous literature reports.^{11b,23}

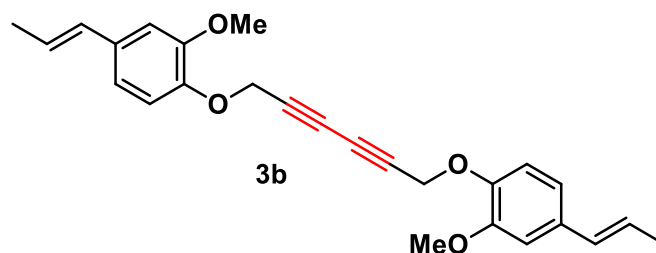
General procedure for the Glasser coupling of propargylated phenols:

Compounds (2a-e) (1 equiv.) were dissolved in acetonitrile (5 mL) and treated with catalytic amount (5 mol%) of copper iodide (CuI) and *N,N,N,N*-tetramethylethylenediamine (TMEDA) (1.2 equiv.). After completion of the reaction (TLC), the reaction mixture was evaporated to dryness to furnish a crude which was further purified *via* flash chromatography using a RediSep column (SiO_2 , 12g) with EtOAc-petroleum ether mixture as eluents to yield purified compounds (3a-e).

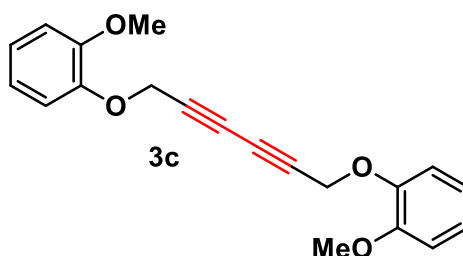
1,6-Bis(4-allyl-2-methoxyphenoxy)hexa-2,4-diyne (3a):



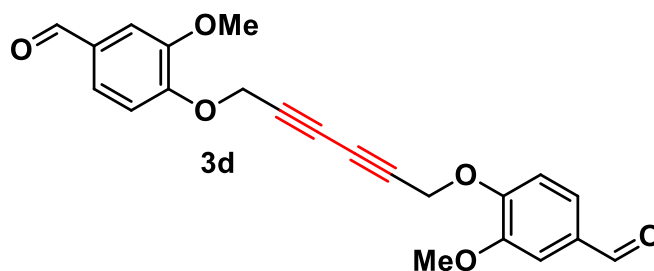
Brown liquid (722 mg, 72%); 1H NMR (200 MHz, $CDCl_3$) δ_H 6.96-6.84 (m, 2H), 6.79-6.66 (m, 4H), 6.07-5.85 (m, 2H), 5.17-5.07 (m, 2H), 5.04 (s, 2H), 4.83-4.71 (m, 4H), 3.85 (s, 6H), 3.34 (d, $J = 6.6$ Hz, 4H); ^{13}C NMR (50 MHz, $CDCl_3$) δ_C 149.7, 145.0, 137.5, 134.6, 134.0, 120.4, 115.9, 114.9, 112.4, 74.8, 71.3, 57.5, 56.9, 55.8, 39.9; HRMS: m/z for $C_{26}H_{27}O_4$ (M+H)⁺: calcd 403.1904, found 403.1899, m/z for $C_{26}H_{26}O_4Na$ (M+Na)⁺: calcd 425.1723, found 425.1719.

1,6-Bis (2-methoxy-4-((*E*)-prop-1-en-1-yl) phenoxy) hexa-2,4-diyne (3b):

Yellowish solid (830 mg, 83%); m.p.: 110-112 °C; R_f 0.3 (10% EtOAc in petroleum ether); ^1H NMR (400 MHz, CDCl_3): δ_{H} 6.92-6.86 (m, 4H), 6.86-6.81 (m, 2H), 6.31 (d, $J = 1.5$ Hz, 1H), 6.35 (d, $J = 1.6$ Hz, 1H), 6.18-6.06 (m, 2H), 4.82-4.73 (m, 4H), 3.86 (s, 6H), 1.86 (dd, $J = 1.6, 6.6$ Hz, 6H); ^{13}C NMR (101 MHz, CDCl_3): δ_{C} 164.8, 161.9, 148.4, 147.1, 133.4, 130.2, 128.5, 127.2, 126.8, 124.0, 116.4, 114.5, 113.8, 55.5, 18.4; HRMS: m/z for $\text{C}_{26}\text{H}_{27}\text{O}_4$ (M^+): calcd 403.1904, found 403.1902.

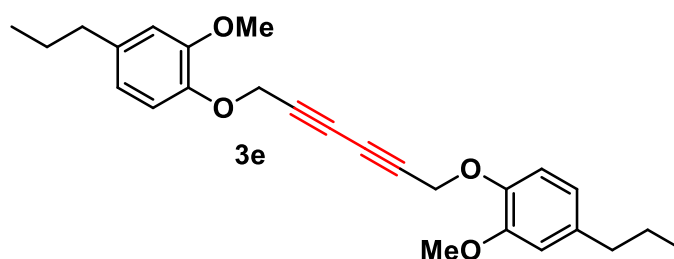
1,6-Bis (2-methoxyphenoxy) hexa-2,4-diyne (3c):

Brown solid (780 mg, 78%); m.p.: 64-66 °C; R_f 0.65 (40% EtOAc in petroleum ether); ^1H NMR (400 MHz, CDCl_3): δ_{H} 7.04-6.95 (m, 4H), 6.95-6.86 (m, 4H), 4.81 (s, 4H), 3.86 (s, 6H); ^{13}C NMR (101 MHz, CDCl_3): δ_{C} 149.7, 146.6, 122.6, 120.8, 114.7, 111.8, 74.7, 71.3, 57.3, 55.8; HRMS: m/z for $\text{C}_{20}\text{H}_{19}\text{O}_4$ (M^+): calcd 323.1278, found 323.1277.

4,4'-(Hexa-2,4-diyne-1,6-diylbis (oxy)) bis (3-methoxybenzaldehyde) (3d):

Off-white solid (800 mg, 80%); m.p.: 158-160 °C; R_f 0.31 (40% EtOAc in petroleum ether); ^1H NMR (400 MHz, CDCl_3): δ_{H} 9.88 (s, 2H), 7.50-7.39 (m, 4H), 7.07 (d, $J = 8.0$ Hz, 2H), 4.91 (s, 4H), 3.94 (s, 6H); ^{13}C NMR (101 MHz, CDCl_3): δ_{C} 190.9, 151.9, 150.0, 131.2, 126.2, 112.7, 109.6, 74.0, 71.8, 57.0, 56.1; HRMS: m/z for $\text{C}_{22}\text{H}_{19}\text{O}_6$ (M^+): calcd 379.1176, found 379.1170.

1,6-Bis (2-methoxy-4-propylphenoxy) hexa-2,4-diyne (3e):



Brown solid (760 mg, 76%); m.p.: 60-62 °C; R_f 0.2 (10% EtOAc in petroleum ether); ^1H NMR (400 MHz, CDCl_3): δ_{H} 6.89 (d, $J = 8.0$ Hz, 2H), 6.77-6.67 (m, 4H), 4.77 (s, 4H), 3.85 (s, 6H), 2.59-2.49 (m, 4H), 1.66-1.60 (m, 4H), 0.94 (t, $J = 7.3$ Hz, 6H); ^{13}C NMR (101 MHz, CDCl_3): δ_{C} 149.5, 144.6, 137.3, 120.3, 114.9, 112.3, 74.9, 71.3, 57.6, 55.8, 37.7, 24.7, 13.8; HRMS: m/z for $\text{C}_{26}\text{H}_{31}\text{O}_4$ (M^+): calcd 407.2217, found 407.2216.

General procedure for the bromination of propargylated phenols:

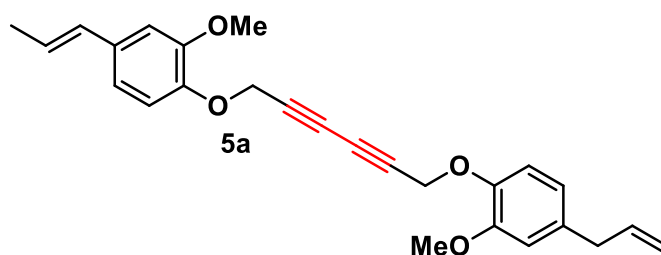
Terminal alkynes **2a-e** (1 equiv.) were dissolved in acetone (10-15 mL) and to this silver nitrate (5 mol%) and *N*-bromosuccinimide (1.2 equiv.) were added subsequently and stirred at room temperature for 3 h. After completion of the reaction, reaction mixture was diluted with dichloromethane (20 mL) and filtered through celite; the filtrate was concentrated to furnish compounds **4a-e** which were used without further purification in the next step.

General procedure for the Cadiot-Chodkiewicz coupling of propargylated phenols (2a-e) with brominated derivatives (4a-e):

Terminal alkynes (**2a-e**) (1 equiv.) and brominated propargyl (**4a-e**) (1.1 equiv.) in acetonitrile (10 mL) and afterwards TMEDA (1.5 equiv.) and copper iodide (5 mol %) were added in an inert atmosphere. The reaction mixture was stirred at room temperature for 3 h. After completion of the reaction (TLC), reaction mixture was evaporated *in vacuo* and

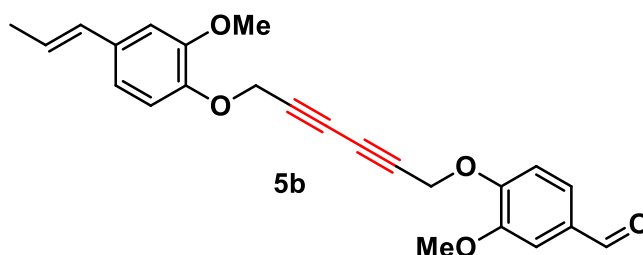
further purified *via* flash chromatography using a RediSep column (SiO₂, 12g) with EtOAc-petroleum ether mixture as eluent to yield purified compounds (**5a-j**).

(E)-4-allyl-2-methoxy-1-(((6-(2-methoxy-4-(prop-1-en-1-yl) phenoxy) hexa-2,4-diyn-1-yl) oxy) benzene (5a):



Brown solid (250 mg, 87%); m.p.: 103-105 °C; *R_f* 0.28 (10% EtOAc in petroleum ether); ¹H NMR (400 MHz, CDCl₃): δ_H 6.93-6.87 (m, 3H), 6.86-6.82 (m, 1H), 6.76-6.65 (m, 2H), 6.33 (dd, *J* = 1.4, 15.7 Hz, 1H), 6.12 (qd, *J* = 6.6, 15.7 Hz, 1H), 6.02-5.89 (m, 1H), 5.13-5.03 (m, 2H), 4.78 (d, *J* = 3.4 Hz, 4H), 3.84 (s, 3H), 3.86 (s, 3H), 3.34 (d, *J* = 6.8 Hz, 2H), 1.86 (dd, *J* = 1.5, 6.6 Hz, 3H); ¹³C NMR (101 MHz, CDCl₃): δ_C 149.8, 149.7, 145.7, 145.0, 137.5, 134.6, 132.9, 130.5, 129.4, 126.0, 124.6, 121.3, 120.4, 118.5, 115.8, 115.0, 114.9, 114.4, 112.7, 112.4, 109.1, 74.9, 74.8, 74.7, 74.7, 71.4, 71.4, 71.3, 71.3, 59.5, 58.9, 57.5, 57.5, 57.4, 56.1, 55.8, 55.8, 39.9, 29.0, 18.4, 17.8, 14.7; HRMS: *m/z* for C₂₆H₂₇O₄ (M⁺)⁺: calcd 403.1904, found 403.1898.

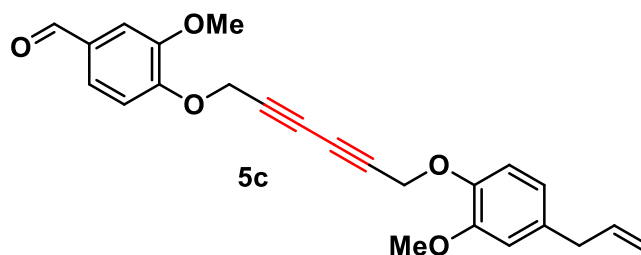
(E)-3-methoxy-4-(((6-(2-methoxy-4-(prop-1-en-1-yl) phenoxy) hexa-2,4-diyn-1-yl) oxy) benzaldehyde (5b):



Brown solid (138 mg, 95%); m.p.: 110-112 °C; *R_f* 0.37 (10% EtOAc in petroleum ether); ¹H NMR (400 MHz, CDCl₃): δ_H 9.87 (d, *J* = 1.1 Hz, 1H), 7.48-7.41 (m, 2H), 7.08 (d, *J* = 8.1 Hz, 1H), 6.91-6.81 (m, 3H), 6.33 (d, *J* = 15.6 Hz, 1H), 6.18-6.07 (m, 1H), 4.91 (s, 2H), 4.79 (s, 2H), 3.93 (s, 3H), 3.86 (s, 3H), 1.87 (d, *J* = 6.6 Hz, 3H); ¹³C NMR (101 MHz, CDCl₃): δ_C

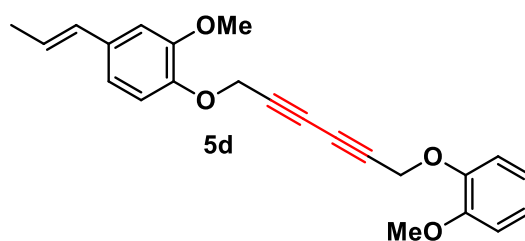
190.9, 151.9, 150.1, 149.8, 145.6, 133.0, 131.1, 130.4, 126.4, 124.7, 118.4, 114.8, 112.7, 109.5, 109.1, 75.5, 73.3, 72.2, 71.0, 57.4, 57.1, 56.1, 55.8, 18.4; HRMS: m/z for $C_{24}H_{22}O_3Na$ ($M+Na$)⁺: calcd 413.1364, found 413.1358.

4-((6-(4-Allyl-2-methoxyphenoxy) hexa-2,4-diyne-1-yl) oxy)-3-methoxybenzaldehyde (5c):

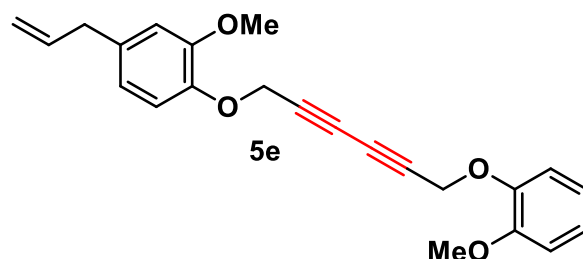


Yellowish solid (130 mg, 89%); m.p.: 106-108 °C; R_f 0.34 (10% EtOAc in petroleum ether); 1H NMR (400 MHz, $CDCl_3$): δ_H 9.88 (s, 1H), 7.48-7.42 (m, 2H), 7.08 (d, $J = 8.4$ Hz, 1H), 6.90 (d, $J = 8.4$ Hz, 1H), 6.74-6.69 (m, 2H), 6.01-5.89 (m, 1H), 5.12-5.05 (m, 2H), 4.91 (s, 2H), 4.78 (s, 2H), 3.94 (s, 3H), 3.85 (s, 3H), 3.34 (d, $J = 6.1$ Hz, 2H); ^{13}C NMR (101 MHz, $CDCl_3$): δ_C 190.9, 151.9, 150.0, 149.7, 144.9, 137.4, 134.7, 131.1, 126.4, 120.4, 115.9, 114.9, 112.7, 112.4, 109.5, 75.6, 73.2, 72.2, 70.9, 57.5, 57.1, 56.1, 55.8, 39.9; HRMS: m/z for $C_{24}H_{23}O_5$ (M)⁺: calcd 391.1540, found 391.1537.

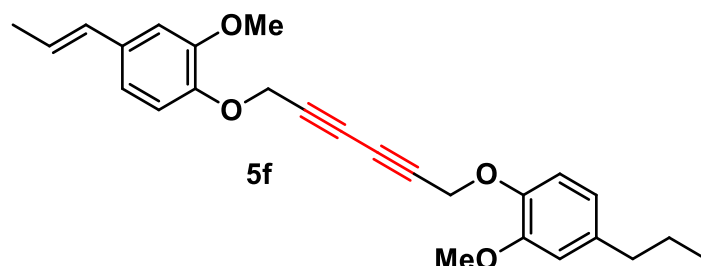
(E)-2-methoxy-1-((6-(2-methoxyphenoxy) hexa-2,4-diyne-1-yl) oxy)-4-(prop-1-en-1-yl) benzene (5d):



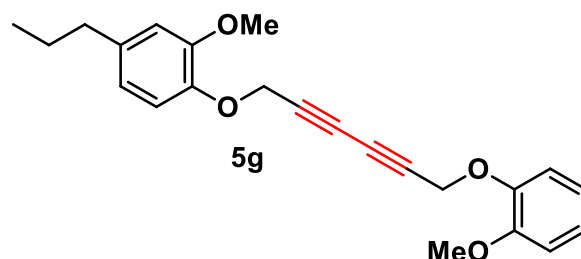
Brown solid (60 mg, 75%); m.p.: 68-70 °C; R_f 0.33 (10% EtOAc in petroleum ether); 1H NMR (400 MHz, $CDCl_3$): δ_H 7.01-6.97 (m, 1H), 6.94-6.86 (m, 4H), 6.86-6.83 (m, 1H), 6.34 (dd, $J = 1.6, 15.6$ Hz, 1H), 6.12 (dd, $J = 6.6, 15.7$ Hz, 1H), 4.80 (d, $J = 9.3$ Hz, 4H), 3.86 (d, $J = 1.9$ Hz, 6H), 1.87 (dd, $J = 1.6, 6.5$ Hz, 3H); ^{13}C NMR (101 MHz, $CDCl_3$): δ_C 149.7, 149.7, 146.6, 145.7, 132.8, 130.5, 124.6, 122.6, 120.8, 118.5, 114.8, 111.9, 109.1, 74.7, 71.3, 57.4, 57.3, 55.8, 55.8, 18.4; HRMS: m/z for $C_{23}H_{23}O_4$ (M)⁺: calcd 363.1591, found 363.1584.

4-Allyl-2-methoxy-1-((6-(2-methoxyphenoxy) hexa-2,4-diyn-1-yl) oxy) benzene (5e):

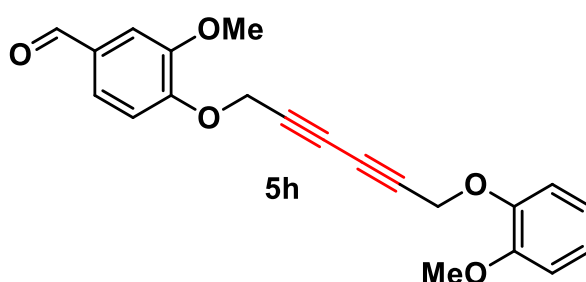
Brown semisolid (200 mg, 77%); R_f 0.33 (10% EtOAc in petroleum ether); ^1H NMR (400 MHz, CDCl_3): δ_{H} 7.02-6.95 (m, 2H), 6.93-6.86 (m, 3H), 6.73-6.69 (m, 2H), 5.95 (tdd, $J = 6.6, 10.3, 17.0$ Hz, 1H), 5.12-5.04 (m, 2H), 4.77 (d, $J = 11.4$ Hz, 4H), 3.83 (s, 3H), 3.84 (s, 3H), 3.33 (d, $J = 6.9$ Hz, 2H); ^{13}C NMR (101 MHz, CDCl_3): δ_{C} 149.8, 149.8, 146.7, 145.0, 137.5, 134.6, 122.7, 120.9, 120.5, 115.9, 115.0, 114.9, 112.5, 112.0, 75.0, 74.9, 74.8, 74.8, 71.4, 71.4, 71.4, 71.3, 57.6, 57.4, 55.9, 39.9; HRMS: m/z for $\text{C}_{23}\text{H}_{23}\text{O}_4\text{Na}$ ($\text{M}+\text{Na}$) $^+$: calcd 385.1415, found 385.1415.

(E)-2-methoxy-1-((6-(2-methoxy-4-(prop-1-en-1-yl) phenoxy) hexa-2,4-diyn-1-yl) oxy)-4-propylbenzene (5f):

Yellowish solid (120 mg, 83%); m.p.: 60-62 °C; R_f 0.28 (10% EtOAc in petroleum ether); ^1H NMR (400 MHz, CDCl_3): δ_{H} 6.91-6.85 (m, 3H), 6.85-6.82 (m, 1H), 6.72-6.67 (m, 2H), 6.33 (dd, $J = 1.5, 16.0$ Hz, 1H), 6.12 (dd, $J = 6.5, 15.6$ Hz, 1H), 4.77 (d, $J = 5.3$ Hz, 4H), 3.85 (s, 3H), 3.84 (s, 3H), 2.55-2.47 (m, 2H), 1.86 (dd, $J = 1.5, 6.1$ Hz, 3H), 1.67-1.55 (m, 2H), 0.93 (t, $J = 7.2$ Hz, 3H); ^{13}C NMR (101 MHz, CDCl_3): δ_{C} 149.8, 149.6, 145.8, 144.7, 137.4, 132.9, 130.6, 124.7, 120.3, 118.6, 114.9, 114.9, 112.4, 109.1, 75.1, 75.0, 74.8, 74.7, 71.5, 71.4, 71.3, 71.3, 57.6, 57.5, 55.9, 37.8, 24.8, 18.5, 13.9; HRMS: m/z for $\text{C}_{26}\text{H}_{29}\text{O}_4$ (M) $^+$: calcd 405.2060, found 405.2053.

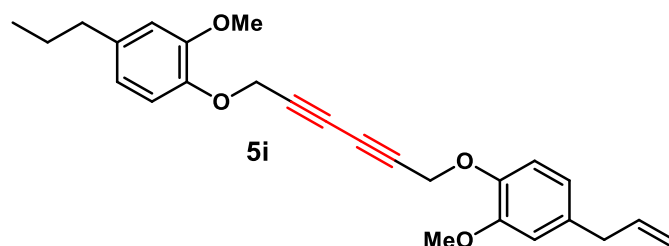
2-Methoxy-1-((6-(2-methoxyphenoxy) hexa-2,4-diyne-1-yl) oxy)-4-propylbenzene (5g):

Brown semisolid (50 mg, 64%); R_f 0.4 (10% EtOAc in petroleum ether); ^1H NMR (400 MHz, CDCl_3): δ_{H} 7.02-6.85 (m, 4H), 6.73-6.67 (m, 2H), 4.78 (d, $J = 13.7$ Hz, 4H), 3.84 (s, 4H), 3.85 (s, 2H), 2.58-2.48 (m, 2H), 1.66-1.58 (m, 3H), 0.94 (t, $J = 7.2$ Hz, 3H); ^{13}C NMR (101 MHz, CDCl_3): δ_{C} 149.8, 149.6, 146.7, 144.7, 137.4, 122.7, 120.9, 120.3, 115.0, 114.9, 112.4, 112.0, 75.1, 75.0, 74.8, 74.7, 71.5, 71.4, 71.3, 71.3, 57.6, 57.4, 55.9, 55.9, 37.8, 24.8, 13.9; HRMS: m/z for $\text{C}_{23}\text{H}_{25}\text{O}_4$ (M^+): calcd 365.1747, found 365.1746.

3-Methoxy-4-((6-(2-methoxyphenoxy) hexa-2,4-diyne-1-yl) oxy) benzaldehyde (5h):

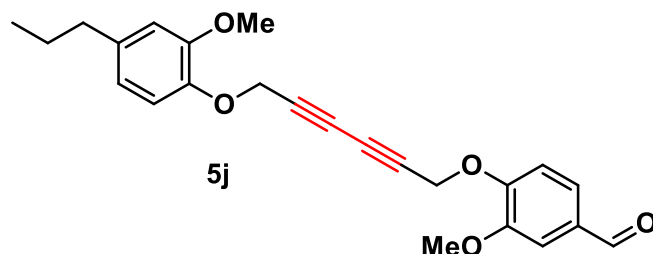
Yellowish solid (90 mg, 69%); m.p.: 85-87 °C; R_f 0.27 (10% EtOAc in petroleum ether); ^1H NMR (400 MHz, CDCl_3): δ_{H} 9.88 (s, 1H), 7.48-7.43 (m, 2H), 7.08 (d, $J = 8.1$ Hz, 1H), 7.02-6.96 (m, 2H), 6.94-6.88 (m, 2H), 4.91 (s, 2H), 4.81 (s, 2H), 3.94 (s, 3H), 3.87 (s, 3H); ^{13}C NMR (101 MHz, CDCl_3): δ_{C} 190.9, 151.9, 150.0, 149.8, 146.6, 131.1, 126.4, 122.7, 120.8, 114.8, 112.7, 111.9, 109.5, 75.4, 73.2, 72.2, 71.0, 57.3, 57.1, 56.1, 55.8; HRMS: m/z for $\text{C}_{21}\text{H}_{18}\text{O}_5$ (M^+): calcd 351.1227, found 351.1222, m/z for $\text{C}_{21}\text{H}_{18}\text{O}_5\text{Na}$ ($\text{M}+\text{Na}^+$): calcd 373.1046, found 373.1035.

4-Allyl-2-methoxy-1-((6-(2-methoxy-4-propylphenoxy) hexa-2,4-diyne-1-yl) oxy) benzene (5i):



Yellowish semisolid (120 mg, 83%); R_f 0.34 (10% EtOAc in petroleum ether); ^1H NMR (400 MHz, CDCl_3): δ_{H} 6.92-6.86 (m, 2H), 6.74-6.67 (m, 4H), 6.00-5.89 (m, 1H), 5.12-5.03 (m, 2H), 4.77-4.73 (m, 4H), 3.84 (s, 6H), 3.33 (d, $J = 6.9$ Hz, 2H), 2.57-2.48 (m, 2H), 1.62 (qd, $J = 7.5, 14.9$ Hz, 2H), 0.98-0.89 (m, 3H); ^{13}C NMR (101 MHz, CDCl_3): δ_{C} 149.8, 149.6, 145.0, 144.7, 137.5, 137.4, 134.6, 120.5, 120.3, 115.9, 115.0, 115.0, 112.4, 112.4, 75.0, 74.9, 71.4, 71.3, 57.6, 57.6, 55.9, 40.0, 37.8, 24.8, 14.0; HRMS: m/z for $\text{C}_{26}\text{H}_{28}\text{O}_4\text{Na}$ ($\text{M}+\text{Na}$) $^+$: calcd 427.2020, found 427.2012.

3-Methoxy-4-((6-(2-methoxy-4-propylphenoxy) hexa-2,4-diyne-1-yl) oxy) benzaldehyde (5j):



Yellowish solid (120 mg, 82%); m.p.: 58-60 °C; R_f 0.27 (10% EtOAc in petroleum ether); ^1H NMR (400 MHz, CDCl_3): δ_{H} 9.88 (s, 1H), 7.48-7.42 (m, 2H), 7.08 (d, $J = 8.4$ Hz, 1H), 6.88 (d, $J = 8.4$ Hz, 1H), 6.73-6.68 (m, 2H), 4.91 (s, 2H), 4.77 (s, 2H), 3.94 (s, 3H), 3.85 (s, 3H), 2.56-2.50 (m, 2H), 1.67-1.57 (m, 4H), 0.94 (t, $J = 7.2$ Hz, 3H); ^{13}C NMR (101 MHz, CDCl_3): δ_{C} 190.9, 151.9, 150.0, 149.5, 144.6, 137.5, 131.1, 126.4, 120.2, 114.8, 112.7, 112.3, 109.5, 75.8, 73.1, 72.3, 70.8, 57.5, 57.1, 56.1, 55.8, 37.7, 24.7, 13.8; HRMS: m/z for $\text{C}_{24}\text{H}_{24}\text{O}_5\text{Na}$ ($\text{M}+\text{Na}$) $^+$: calcd 415.1516, found 415.1497.

Biological Evaluation

***In-vitro* antifungal activity of synthesized compounds of 1a and 1b.** Antifungal activity of synthesized compounds **3a-e** and **5a-j** against *A. fumigatus* was performed according to the CLSI M38-A2 microbroth dilution method for filamentous fungi (CLSI, 2016). Briefly, *A. fumigatus* ATCC-46645 strain was cultured on Czapek Dox broth/agar (CzB/CzA) and incubated at $28 \pm 2^\circ\text{C}$ for 5 days for conidiation. The conidia were harvested, and conidia/mL concentration was adjusted as per our previous published paper.^{11b} Two-fold dilutions of synthesized compounds (**3a-e** and **5a-j**) and eugenol **1a** were carried out in triplicate using a 96-well polystyrene plate (Tarsons, India), having growth media CzB. 100 μL of conidial suspension was added to each well except negative control. The wells which contain only inoculated broth, was kept as positive control and amphotericin B (Amp B) was used as drug control. The plates were incubated statically for 5 days at $28 \pm 2^\circ\text{C}$. The MIC and IC₅₀ values were calculated and expressed in micro molar.

Cytotoxicity of compound 3a in normal lung epithelial cell line L-132 as well as *in-silico* screening for its therapeutic activity. Cytotoxicity analysis of compound **3a**, which showed antifungal activity at lowest concentration among all tested compounds against *A. fumigatus*, was performed. The selected compound **3a** was taken forward for all experiments. The lung epithelial normal cell line L-132 were grown, cultured as reported in the supplier's guide which was provided by National Centre for Cell Science (NCCS), Pune, India. The MTT assay was applied as described in our previous studies.^{11b} The CC₅₀ and IC₅₀ value of compound **3a** was calculated from the graph of percentage viability against concentrations by applying regression analysis on GraphPad prism software 8.0.2.263 version. All experiments were performed in triplicates.

The percentage relative cell viability (Venkatraman et al. 2005) was calculated as (where A570 = absorbance at wavelength 570)

$$([\text{A570 of treated sample}]) / ([\text{A570 of untreated sample}]) \times 100$$

The selectivity index (SI) was determined by CC₅₀/IC₅₀ ratio against *A. fumigatus*. The SI is an indirect measure of the therapeutic window and it can serve as a predictor of safety during *in vivo* trials for a given pathogen infection.²⁴ (CC₅₀ -cytotoxic concentration 50 where 50% cells were found to be dead)

In-silico study was conducted to determine drug-likeness and quantitative parameters of absorption, distribution, metabolism, excretion, and toxicity of compound **3a** which was predicted by Swiss ADME program (<http://www.swissadme.ch/index.php>). The parameters deployed to predict the physicochemical properties of the compound (molecular weight, hydrogen donor, hydrogen acceptor, LogP value and TPSA).²⁵

Effect of compound 3a on conidia production- One cubic centimeter of agar block containing treated and untreated fungal culture was excised from CzA media plate supplemented with IC₅₀ of compound **1a**, **3a** and AmpB using a sterile surgical blade and transferred to a sterile test tube. 5 mL of phosphate buffered saline with 0.05% Tween 20 (1× PBST) was added to each tube, shaken vigorously to remove conidia. The absorbance of treated and untreated *A. fumigatus* conidia was measured at 530nm using UV-vis spectrophotometer (CLSI 2008).

Biochemical estimation of ergosterol content- Fungal ergosterol content was isolated from compound **1a**, **3a**, Amp B treated *A. fumigatus* culture and compared with the control as described by.²⁶ Briefly, fungal mycelia were harvested, washed with autoclaved distilled water, dried, and weighed. Alcoholic potassium hydroxide solution (25%, 3 mL) was added to each pellet in a test tube and vortexed it for 1 min. Test tubes were incubated at 85 °C for 1 h in boiling water bath. After cooling to room temperature, sterols were extracted in the 1:3 ratio of water: n-octane mixture by a vigorous vortex for 3 min and then allowed to get separate in two phases. The octane layer was collected in screw capped test tube and stored at -20 °C. For analysis, 200 µl of extracted sterol was mixed with 800 µL absolute ethanol and was spectrophotometrically measured at 281.5 nm and 230 nm. The conversion from optical density to ergosterol was calculated as follows:

$$\text{Ergosterol\%} = [(A_{281.5}/290 \times F) \div \text{weight of pellet}] - [(A_{230}/518 \times F) \div \text{weight of pellet}]$$

F= ethanol dilution factor

Scanning electron microscopy (SEM) of *A. fumigatus* conidial surface - Synthesized compound **3a** treated and untreated conidia of *A. fumigatus* were harvested, washed, and fixed in 4% glutaraldehyde in 1x PBS under vacuum for 24 hours. After washing, the cells were post-fixed with 1% osmium tetroxide for 60 min and dehydrated by passage through

ethanol solutions of increasing concentration. The prepared sample were then mounted on aluminium sheet and coated with gold-palladium alloy. The observations were made using a Zeiss SEM, MA EVO -18 Special Edition.^{27,29}

Effect of compound 3a on *A. fumigatus* biofilm. The IC₅₀ of biofilm eradication concentration of compound **3a** on pre-formed *A. fumigatus* biofilm was calculated by performing MTT assay in a 96-well flat bottom microtiter plate. The MTT assay was applied according to our previous studies.^{11b} Biofilm eradication property of compound **3a** was analysed on fully grown *A. fumigatus* biofilm on 12-well polystyrene plate for 48 h. The biofilm was treated with IC₅₀ of compound **3a** for another 24 h.^{28,29} To visualise the effect of compound **3a** in comparison to positive control (untreated), confocal laser scanning microscopy (CLSM) was performed, and samples were processed as described by Vijayaraghavan et al²⁸ and viewed under Nikon Instruments A1 Confocal Laser Microscope Series with NIS elements C software, Japan.

Statistical analyses

For the statistical analyses, one-way ANOVA was used, comparing the results of conidiation, ergosterol for compound **3a** with wild type untreated and Amp B treated strain. All experiments were conducted in biological triplicates. GraphPad Prism software 8.0.2.263 version was used for all the statistics analysis and Microsoft Excel. $p < 0.05$ was considered statistically significant.

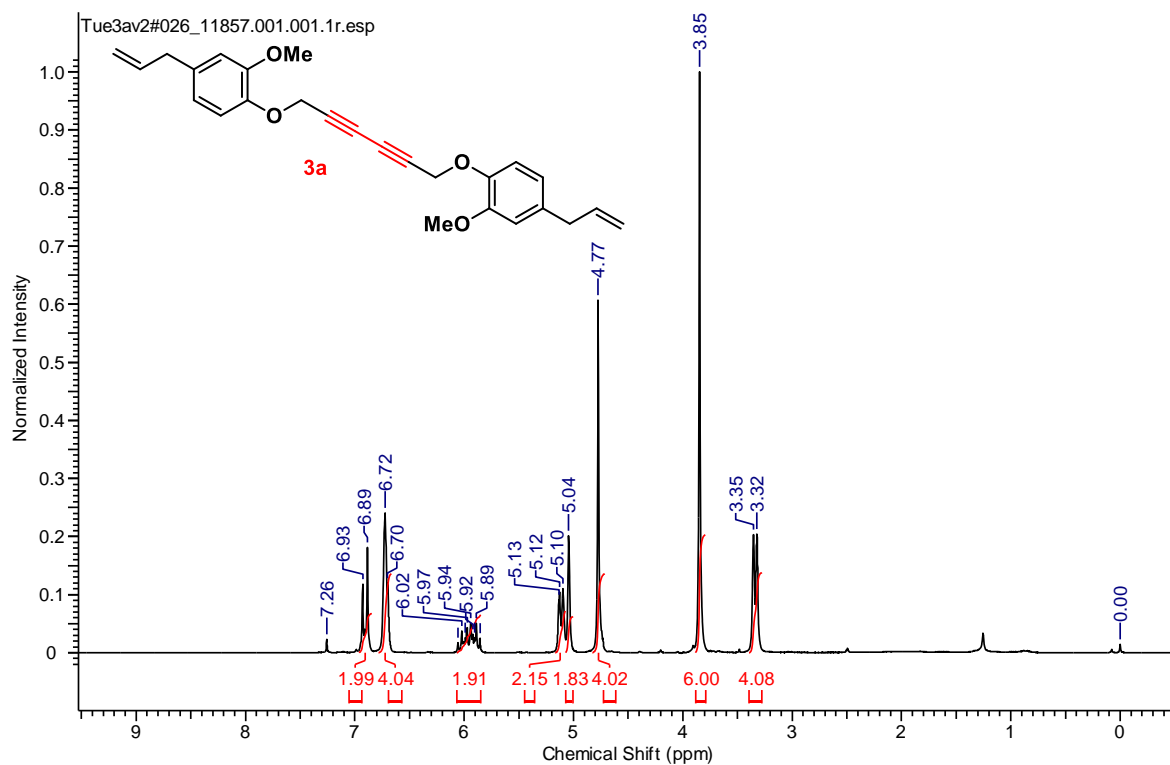
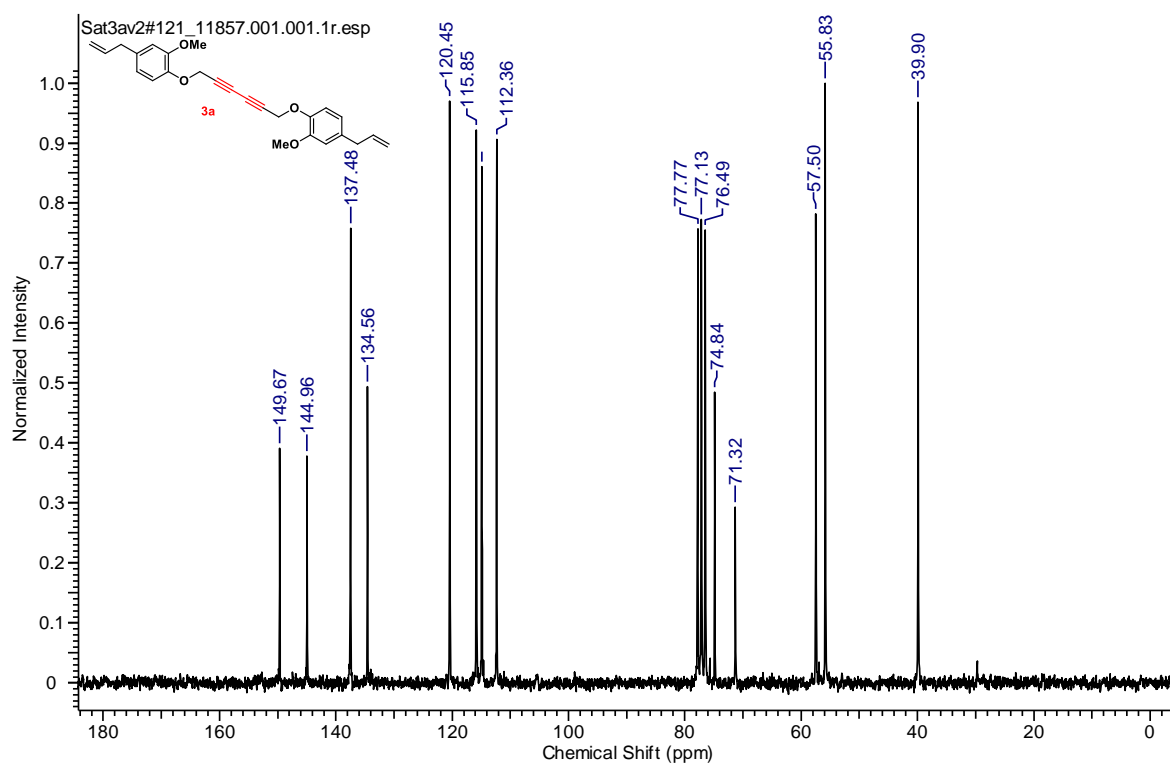
1.2.5 References:

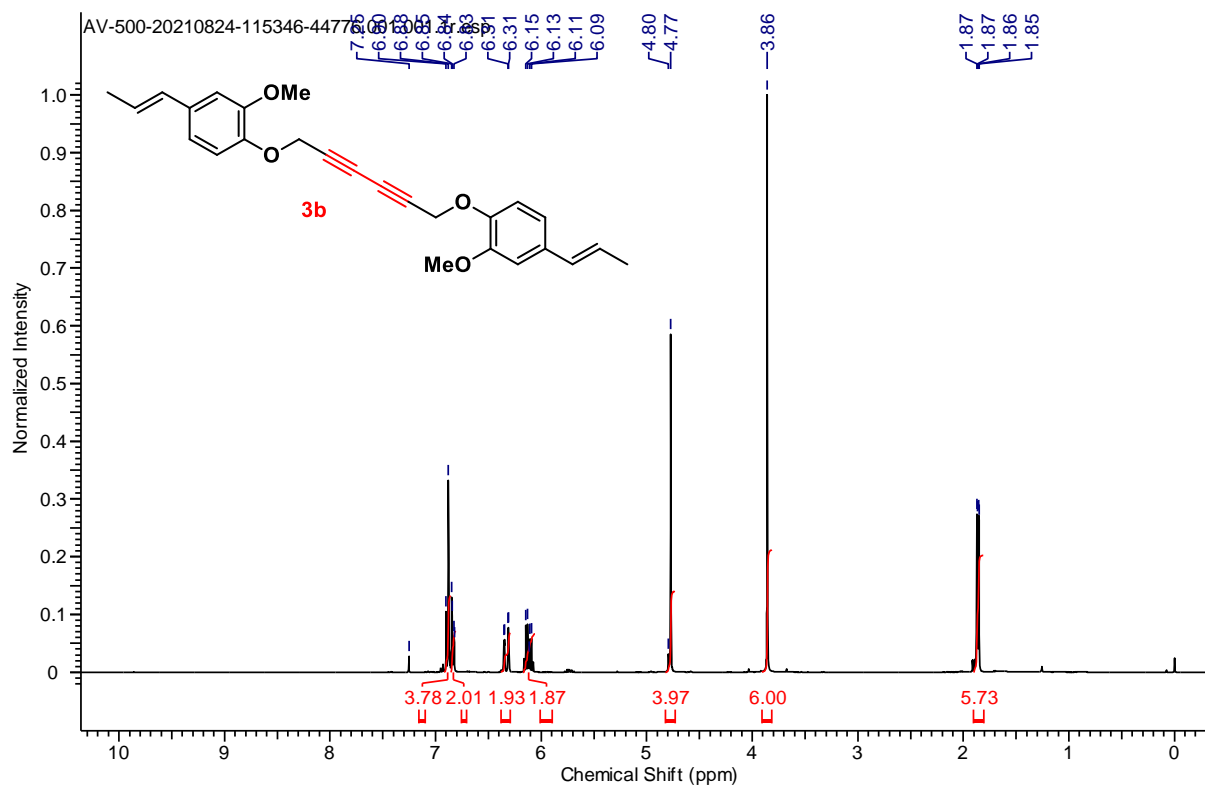
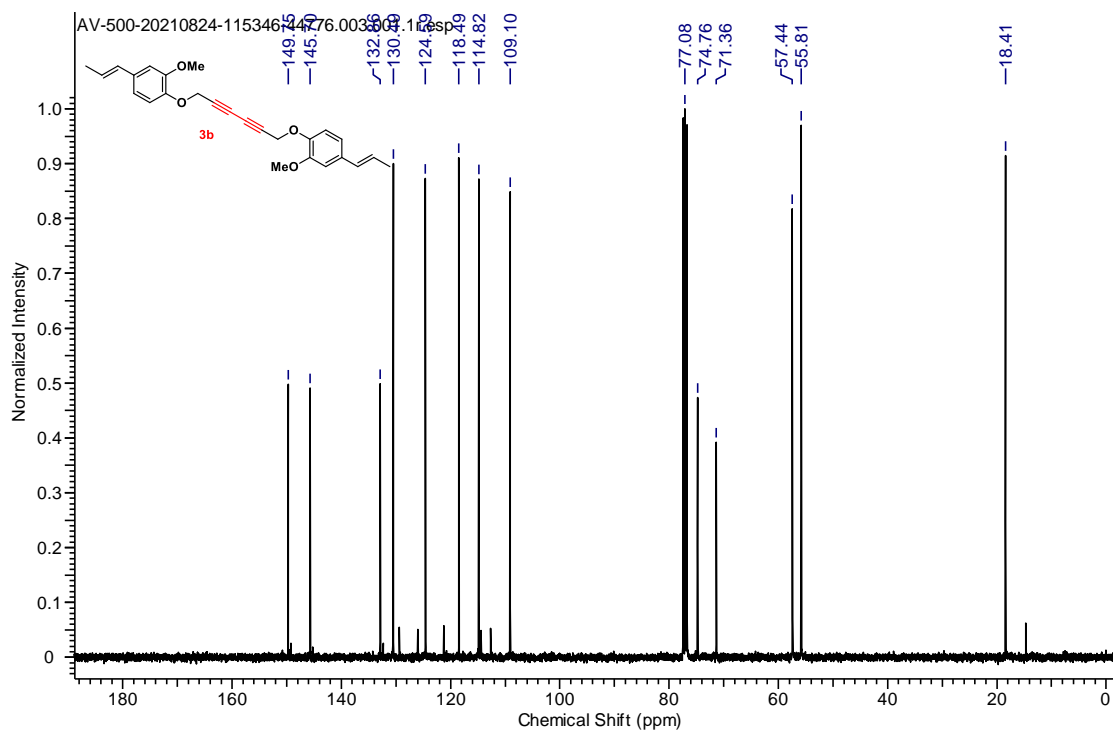
1. (a) A. Arastehfar, A. Carvalho, J. Houbraken, L. Lombardi, R. G. -Rubio, J. D. Jenks, O. R.-Menendez, R. Aljohani, I. D. Jacobsen, J. Berman, N. Osherov, M. T. Hedayati, M. Ilkit, D. A. -James, T. Gabaldón, J. Meletiadis, M. Kostrzewa, W. Pan, C. L.-Flörl, D.S. Perlin, M. Hoenigl, *Stud. Mycol.* **2021**, *100*, 100115. (b) J.-P. Latgé, *Clin. Microbiol. Rev.* **1999**, *12*, 310-350.
2. (a) D. W. Denning, *Clin. Infect. Dis.* **1998**, *26*, 781-803; b) K. A. Marr, R. A. Carter, M. Boeckh, P. Martin, L. Corey, *Blood* **2002**, *100*, 4358-4366;
3. L. Pagano, C. Girmenia, L. Mele, P. Ricci, M. E. Tosti, A. Nosari, M. Buelli, M. Picardi, B. Allione, L. Corvatta, D. D'Antonio, M. Montillo, L. Melillo, A. Chierichini, A. Cenacchi, A. Tonso, L. Cudillo, A. Candoni, C. Savignano, A. Bonini, P. Martino, A. D. Favero, *Haematologica* **2001**, *86*, 862-870;
4. (a) M. J. Post, C. Lass-Floerl, G. Gastl, D. Nachbaur, *Transpl. Infect. Dis.* **2007**, *9*, 189-195; (b) N. P. Wiederhold, R. E. Lewis, D. P. Kontoyiannis, *Pharmacother.* **2003**, *23*, 1592-1610.
5. C. A. Croft, L. Culibrk, M. M. MooreS, J. Tebbutt, *Front. Microbiol.* **2016**, *7*, 472.
6. V. Amanianda, J. Bayry, S. Bozza, O. Knemeyer, K. Perruccio, S. R. Elluru, C. Clavaud, S. Paris, A. A. Brakhage, S. V. Kaveri, L. Romani, J. -P. Latgé, *Nature*, **2009**, *460*, 1117–1121.
7. (a) S. C. A. Chen, T. C. Sorrell, *Med J Aust.* **2007**, *187*, 404-409; (b) M. A. Ghannoum, L. B. Rice, *Clin. Microbiol Rev.* **1999**, *12*, 501–517.
8. (a) V. S. Brauer, C. P. Rezende, A. M. Pessoni, R. G. De Paula, K. S. Rangappa, S. C. Nayaka, V. K. Gupta, F. Almeida, *Biomolecules* **2019**, *9*, 521; (b) G. Wall, J. L. L.-Ribot, *Antibiotics* **2020**, *9*, 445;
9. (a) Q. Lin, Y. Li, M. Sheng, J. Xu, X. Xu, J. Lee, Y. Tan, *LWT*, **2023**, *173*, 114237; (b) J. Prajapati, P. Rao, L. Poojara, D. Acharya, S. K. Patel, D. Goswami, R. M. Rawal, *Curr. Microbiol.* **2023**, *80*, 47.
10. B. W. Nash, D. A. Thomas, W. K. Warburton and T. D. Williams, *J Chem Soc.*, **1965**, *46*, 2983-2988.
11. (a) T. Koeduka, E. Fridman, D. R. Gang, D. G. Vassão, B. L. Jackson, C. M. Kish, I. Orlova, S. M. Spassova, N. G. Lewis, J. P. Noel, T. J. Baiga, N. Dudareva, E. Pichersky, *Proc. Natl. Acad. Sci.* **2006**, *103*, 10128-10133; (b) L. Goswami, L. Gupta,

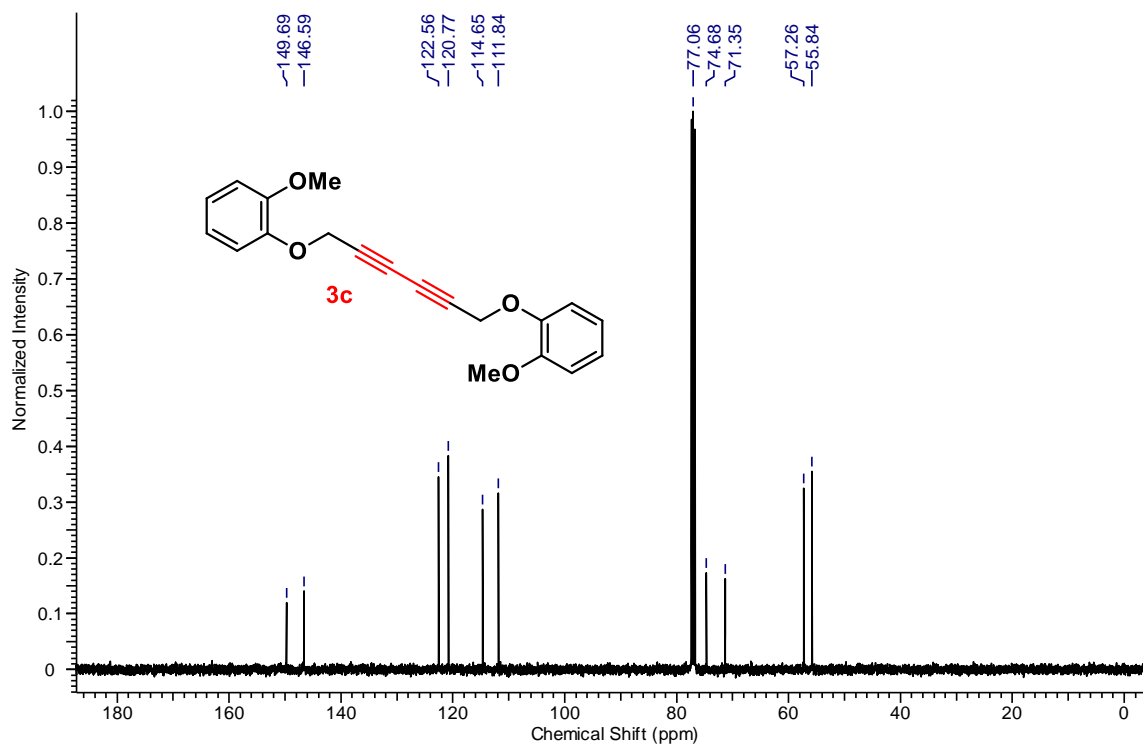
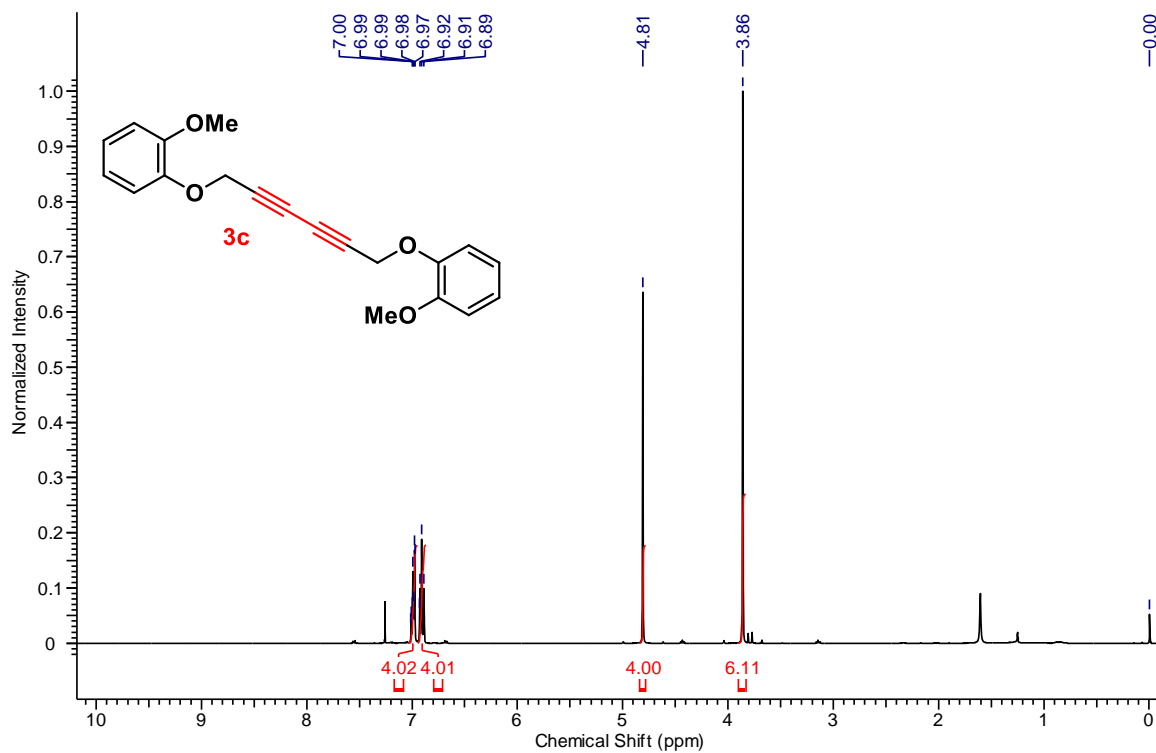
- S. Paul, M. Vermani, P. Vijayaraghavan, A. K. Bhattacharya, *RSC Med Chem.* **2022**, *13*, 955-965;
12. (a) H. A. Hassan, M. M. Geniady, S. F. Abdelwahab, M. I. Abd-Elghany, H. A. Sarhan, A. A., Abdelghany, M. S. Kamel, A. E. Rodriguez, J. L. Alio, *Ophthalmic Res.* **2018**, *60*, 69-79; (b) D. Campaniello, M. R. Corbo, M. Sinigaglia, *J. Food Prot.* **2010**, *73*, 1124-1128.
13. (a) C. Glaser, *Liebigs Annalen.* **1870**, *154*, 137-171; (b) C. Glaser, *Chem. Ber.* **1869**, *2*, 422-424; (c) A. S. Hay, *J. Org. Chem.* **1962**, *27*, 3320-3321. d) K. S. Sindhu, G. Anilkumar, *RSC Adv.* **2014**, *4*, 27867-27887.
14. (a) P. Cadiot, W. Chodkiewicz, in *Chemistry of Acetylenes*, (Eds: Marcel Dekker), Viehe, HG., New York, **1969**, 597-647. (b) W. Chodkiewicz, P. Cadiot, A. Willemart, *Compt. Rend.* **1957**, *245*, 2061. (c) W. Chodkiewicz, *Ann. Chim. Paris*, **1957**, *2*, 819. (d) K. S. Sindhu, A. P. Thankachan, P. S. Sajithaa, G. Anilkumar, *Org. Biomol. Chem.* **2015**, *13*, 6891-6905.
15. Clinical and Laboratory Standards Institute. (2016). Performance standards for antimicrobial susceptibility testing, 26th ed CLSI document M100-S. Clinical and Laboratory Standards Institute, Wayne, PA.
16. S. Harmsen, A. C. McLaren, C. Pauken, R. McLemore, *Clin. Orthop. Relat. Res.* **2011**, *469*, 3016-3021.
17. J. Krzywik, W. Mozga, M. Aminpour, J. Janczak, E. Maj, J. Wietrzyk, J. A. Tuszyński, A. Huczynski, *Molecules* **2020**, *25*, 1789.
18. L. I. S. de Carvalho, D. J. Alvarenga, L. C. F. do Carmo, L. G. de Oliveira, N. C. Silva, A. L. T. Dias, L. F. L. Coelho, T. B. de Souza, D. F. Dias, D. T. Carvalho, *J. Chem.* **2017**, e5207439.
19. L. Z. Benet, C. M. Hosey, O. Ursu, T. I. Oprea, *Adv Drug Deliv Rev.* **2016**, *101*, 89-98.
20. (a) L. Scorzoni, A. C. A. de Paula e Silva, C. M. Marcos, P. A. Assato, W. C. M. A. de Melo, H. C. de Oliveira, C. B. Costa-Orlandi, M. J. S. M. -Giannini and A. M. F.-Almeida *Front. Microbiol.* **2017**, *8*, 36. (b) L. Goswami, L. Gupta, S. Paul, P. Vijayaraghavan and A. K. Bhattacharya, (doi.org/10.1002/cmdc.202300013)
21. (a) V. Voltersen, M. G. Blango, S. Herrmann, F. Schmidt, T. Heinekamp, M. Strassburger, T. Krüger, P. Bacher, J. Lothar, E. Weiss, K. Hünninger, H. Liu, P. Hortschansky, A. Scheffold, J. Löffler, S. Krappmann, S. Nietzsche, O. Kurzai, H.

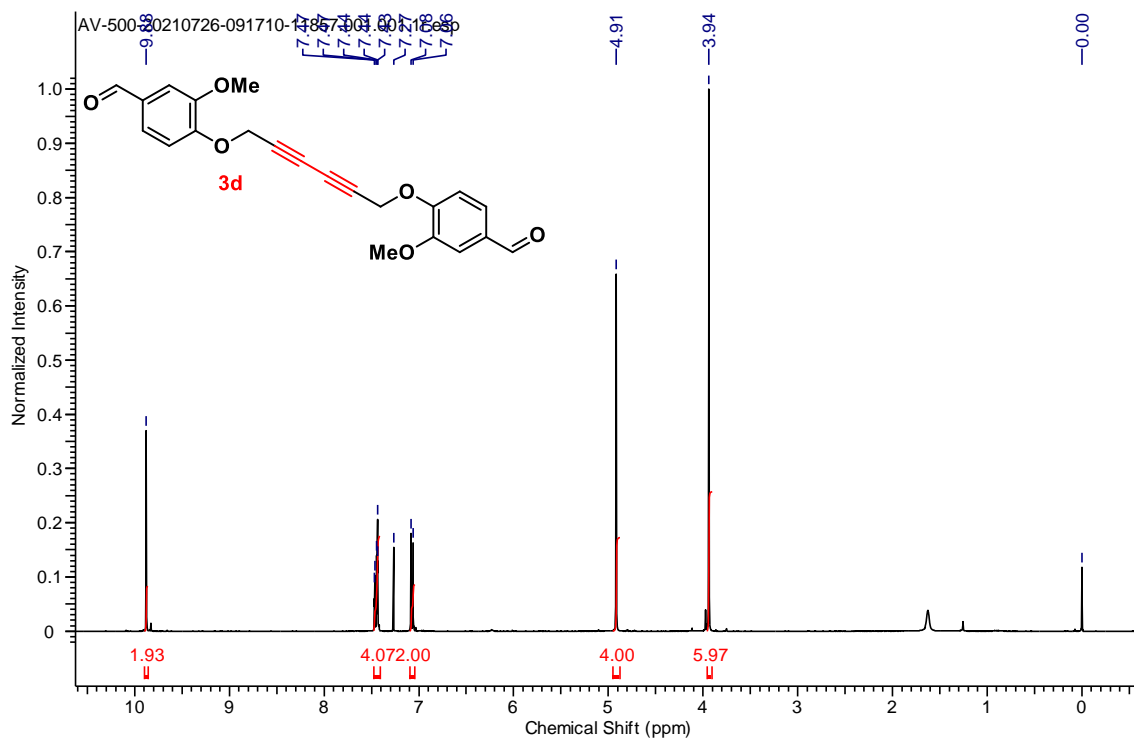
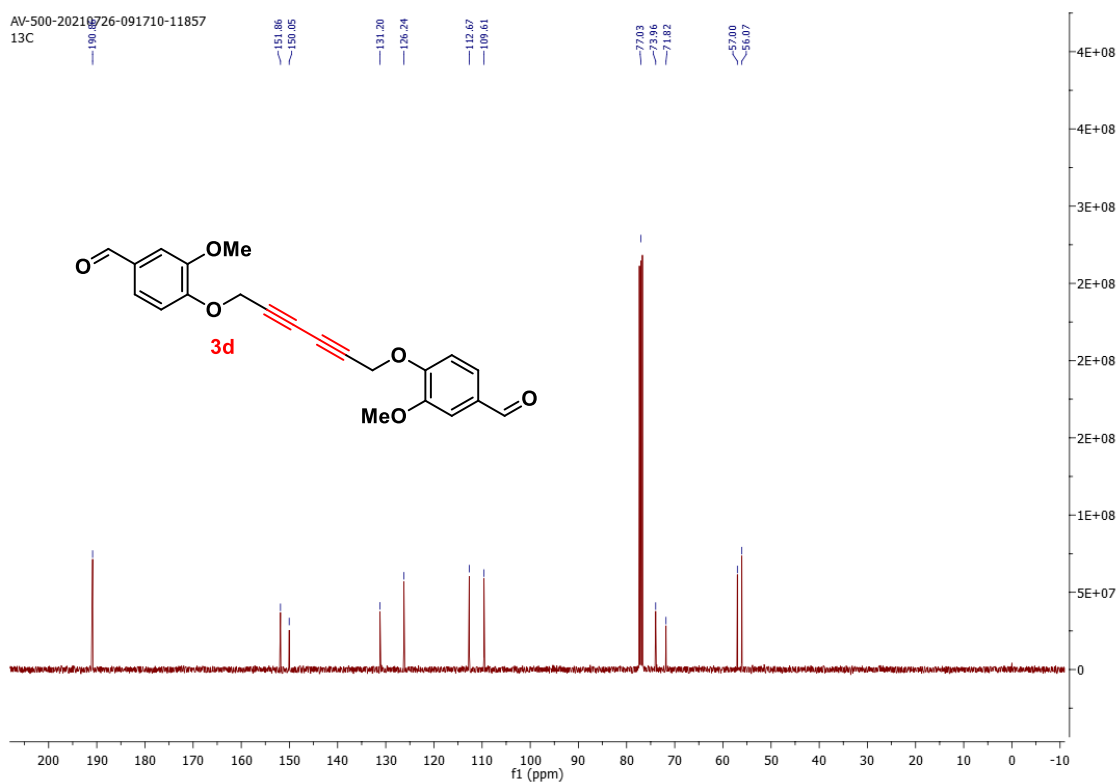
- Einsele, O. Kniemeyer, S. G. Filler, U. Reichard, A. A. Brakhage, *mBio* **2018**, *9*, e01557-18. (b) L. Gupta, S. Hoda, M. Vermani, P. Vijayaraghavan, *Mycol. Progress* **2021** *20*, 365–380.
22. F. -M. C. Müller, M. Seidler, A. Beauvais *Med. Mycol.* **2011**, *49*, S96–S100.
23. P. S. Hellwig, A. M. Barcellos, R. Cargnelutti, T. Barcellos, G. Perin, *J. Org. Chem.* **2022**, *87*, 15050–15060.
24. D. Insuasty, O. Vidal, A. Bernal, E. Marquez, J. Guzman, B. Insuasty, J. Quiroga, L. Svetaz, S. Zacchino, G. Puerto, R. Abonia, *Antibiotics* **2019**, *8*, 239.
25. C. A. Lipinski, F. Lombardo, B. W. Dominy, P. J. Feeney, *Adv. Drug Deliv. Rev.* **2001**, *46*, 3–26.
26. S. Hoda, M. Vermani, R. K. Joshi, J. Shankar, P. Vijayaraghavan, *BMC Complementary Med. Ther.* **2020**, *20*, 67.
27. M. Pihet, P. Vandeputte, G. Tronchin, G. Renier, P. Saulnier, S. Georgeault, R. Mallet, D. Chabasse, F. Symoens, J. -P. Bouchara, *BMC Microbiol.* **2009**, *9*, 177.
28. (a) S. Hoda, L. Gupta, H. Agarwal, G. Raj, M. Vermani, P. Vijayaraghavan, *J Pure Appl. Microbiol.* **2019**, *13*, 1207–1216; (b) H. Sav, H. Rafati, Y. Öz, B. D.-Cilo, B. Ener, F. Mohammadi, M. Ilkit, A. D. V. Diepeningen, S. Seyedmousavi, *J. Fungi.* **2018**, *4*, 16.
29. L. Gupta, P. Sen, A. K. Bhattacharya, P. Vijayaraghavan, *Archiv. Microbiol.*, **2022**, *204*, 214-227.

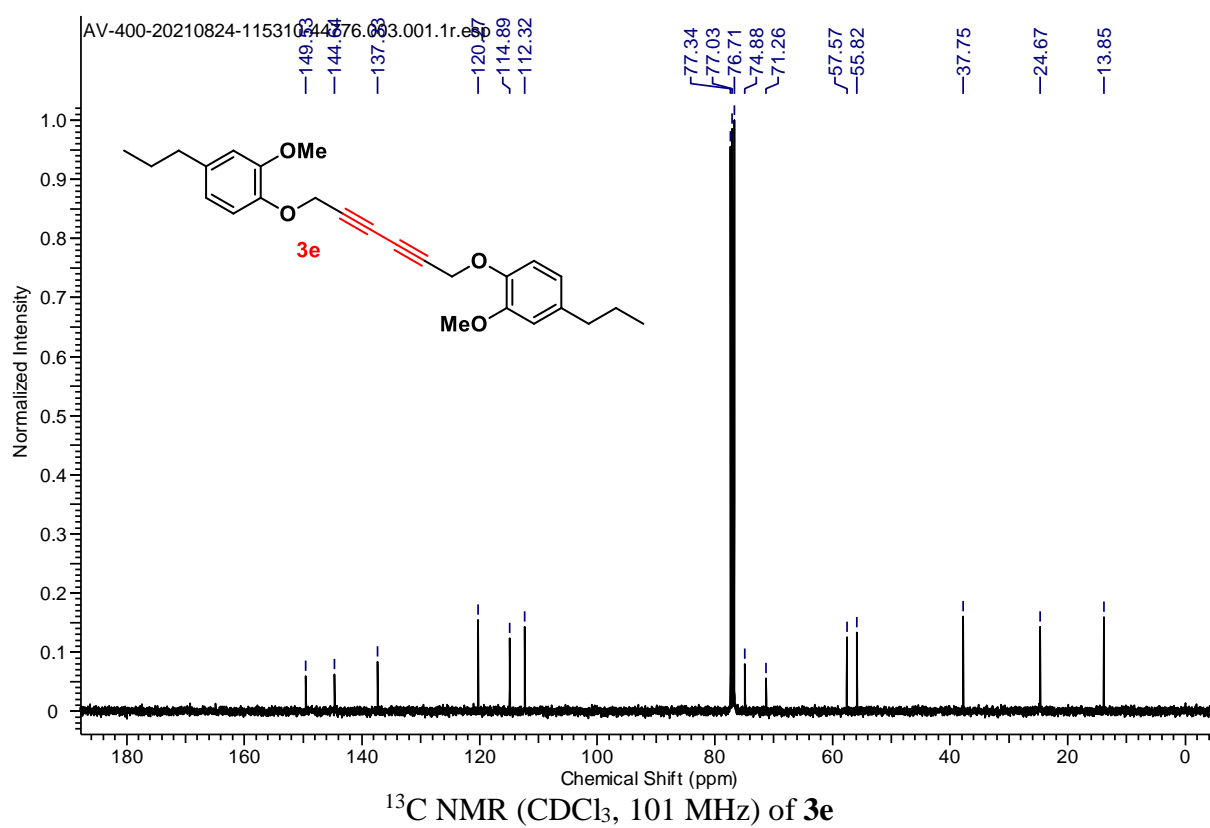
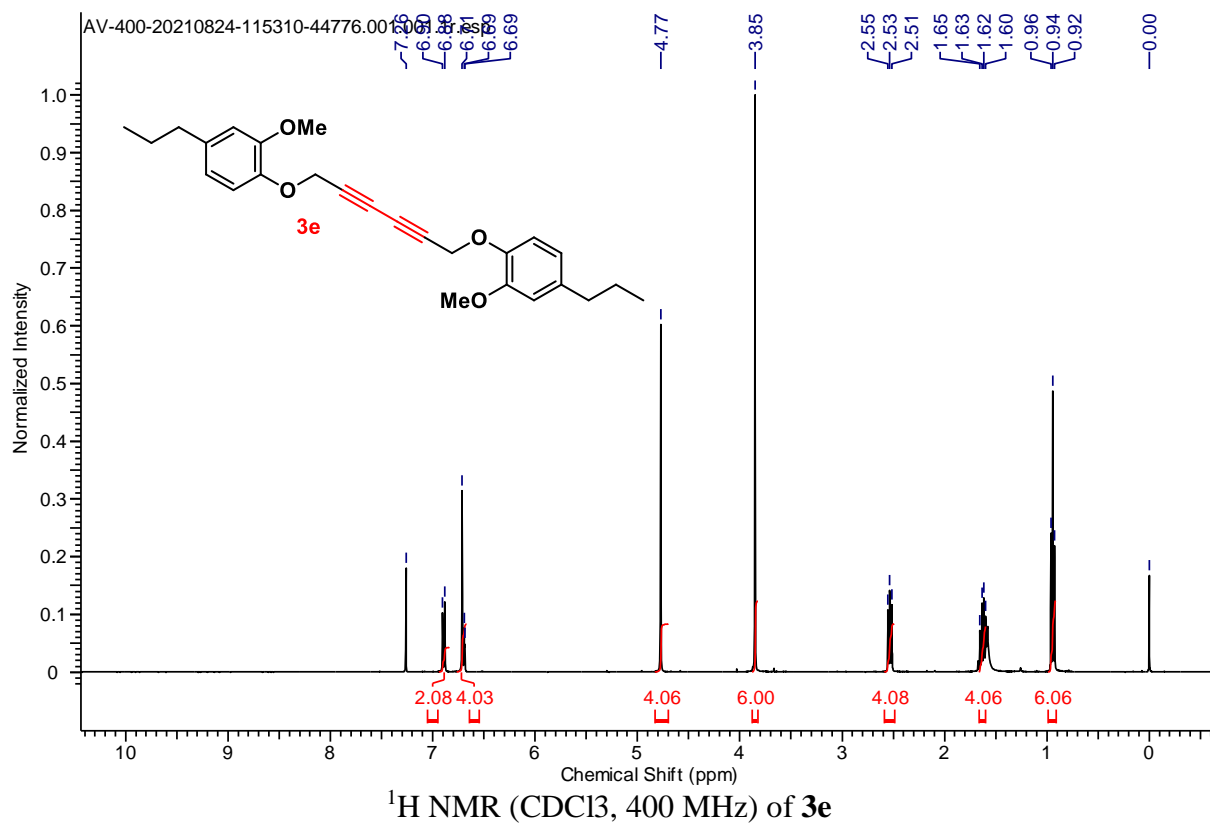
1.2.6 Copies of NMR Spectra:

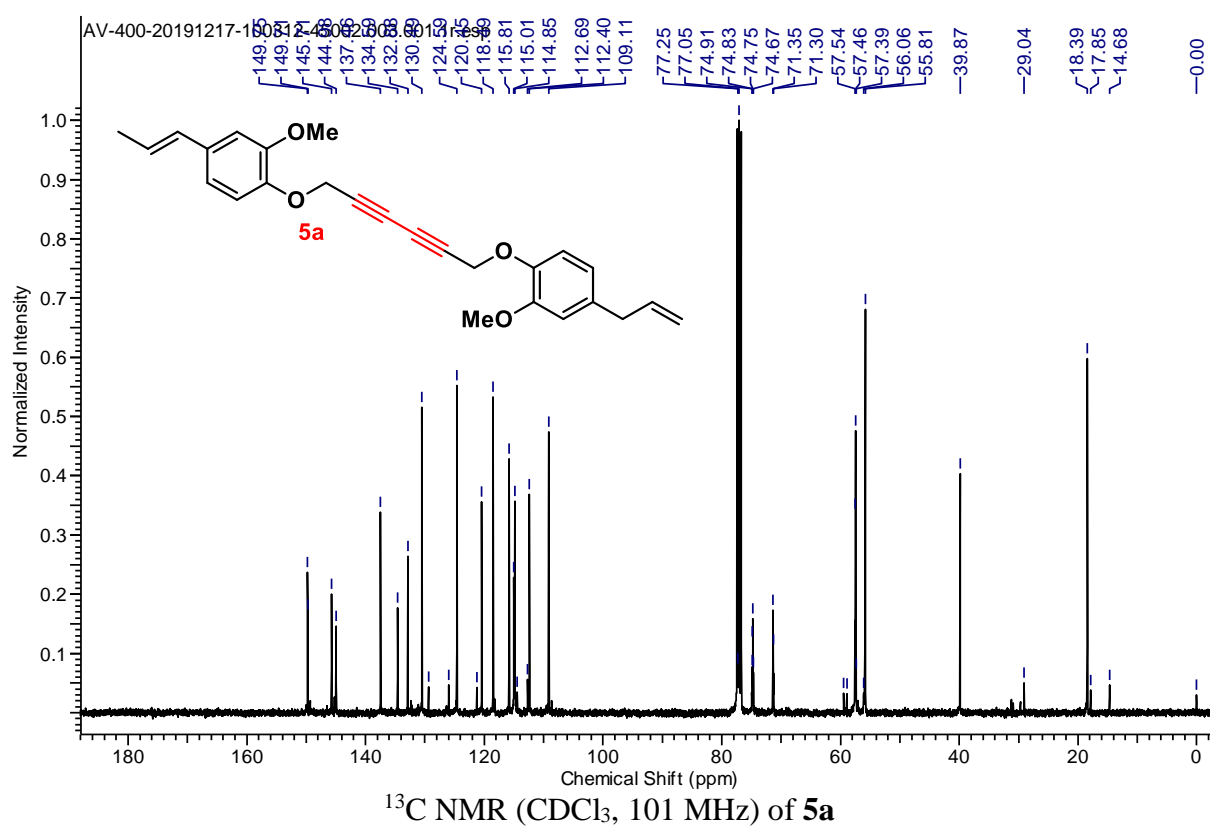
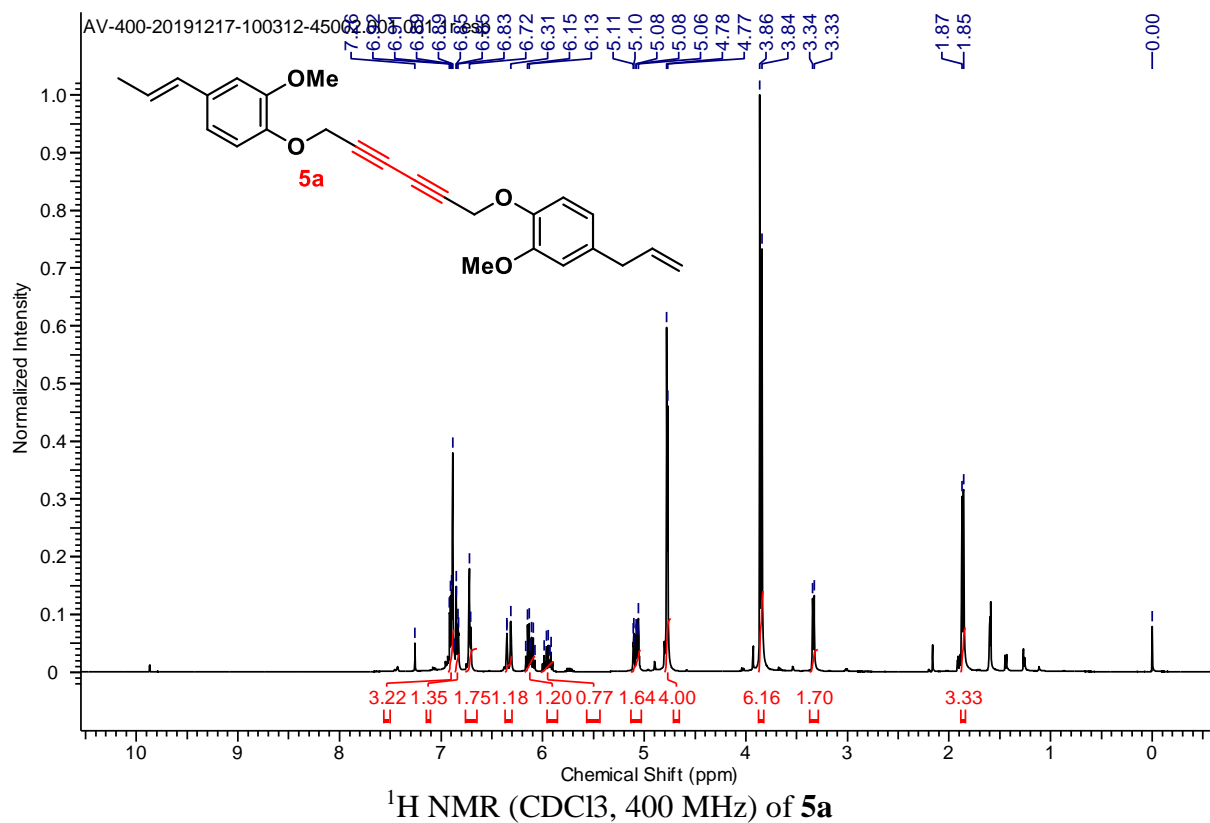
 ^1H NMR (CDCl_3 , 200 MHz) of **3a** ^{13}C NMR (CDCl_3 , 50 MHz) of **3a**

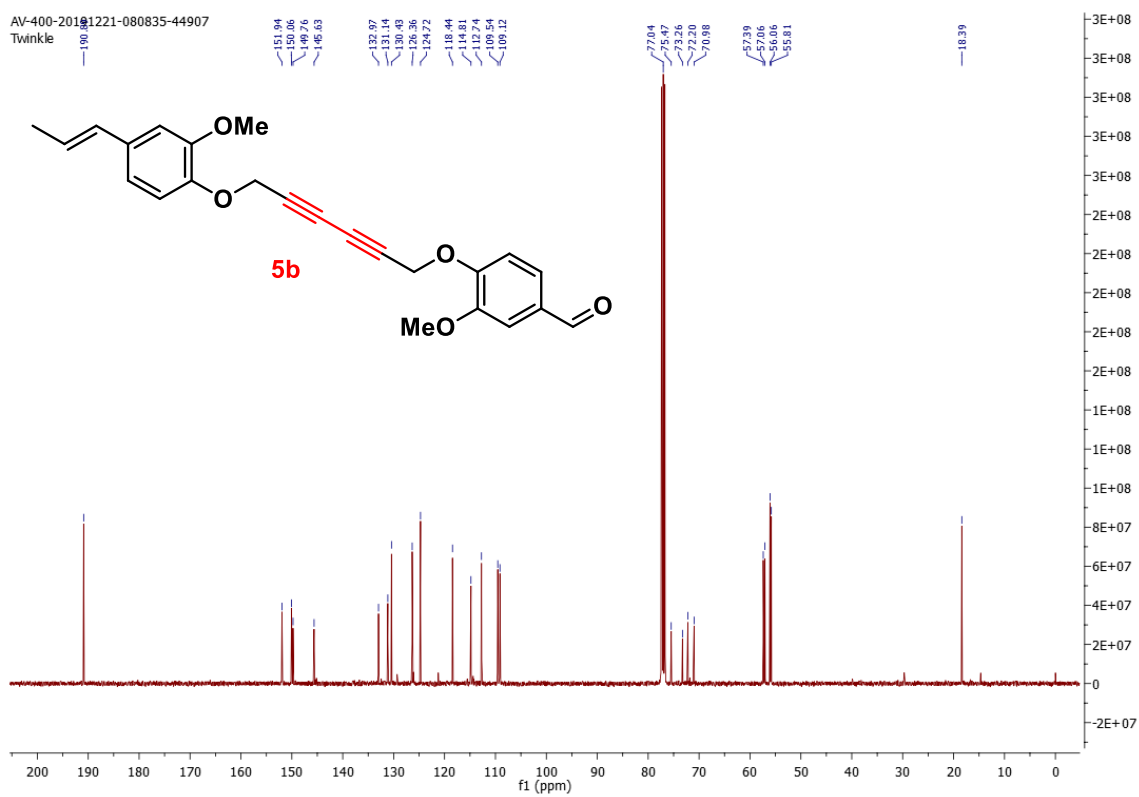
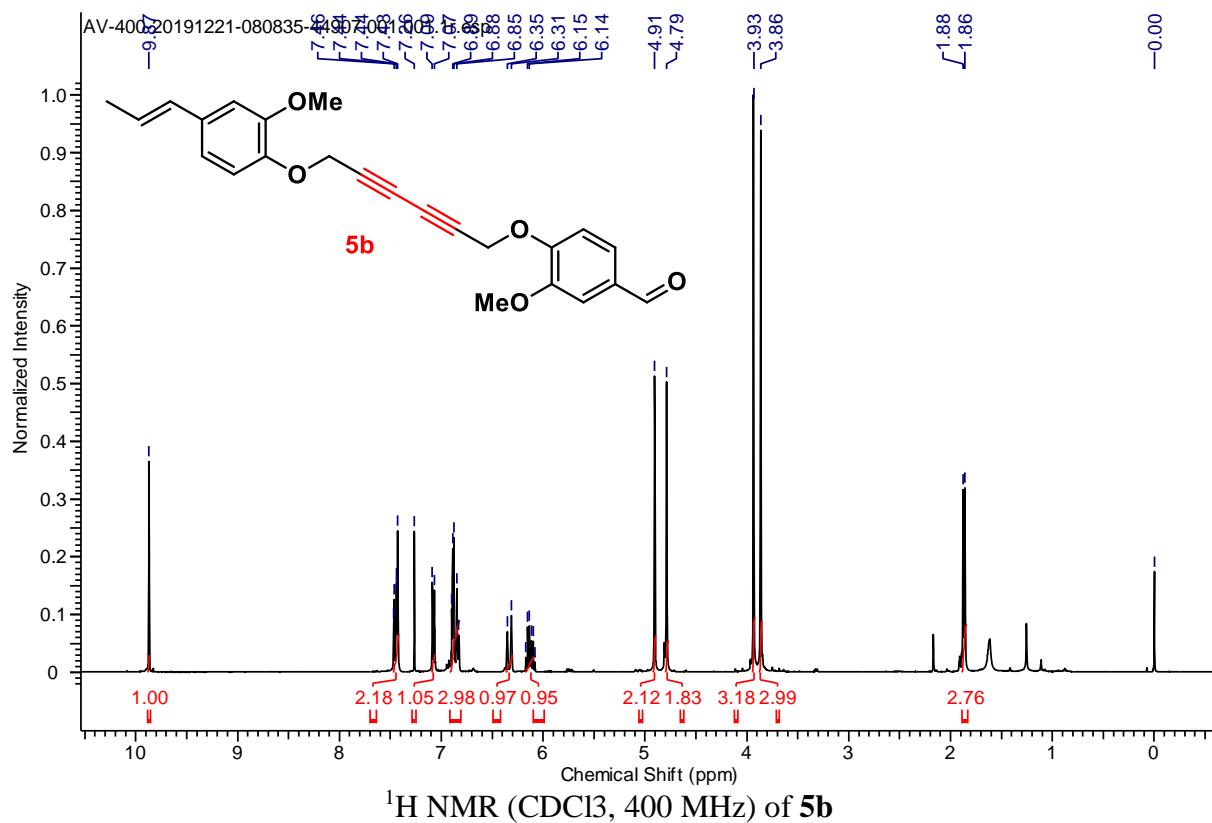
 ^1H NMR (CDCl₃, 500 MHz) of **3b** ^{13}C NMR (CDCl₃, 126 MHz) of **3b**

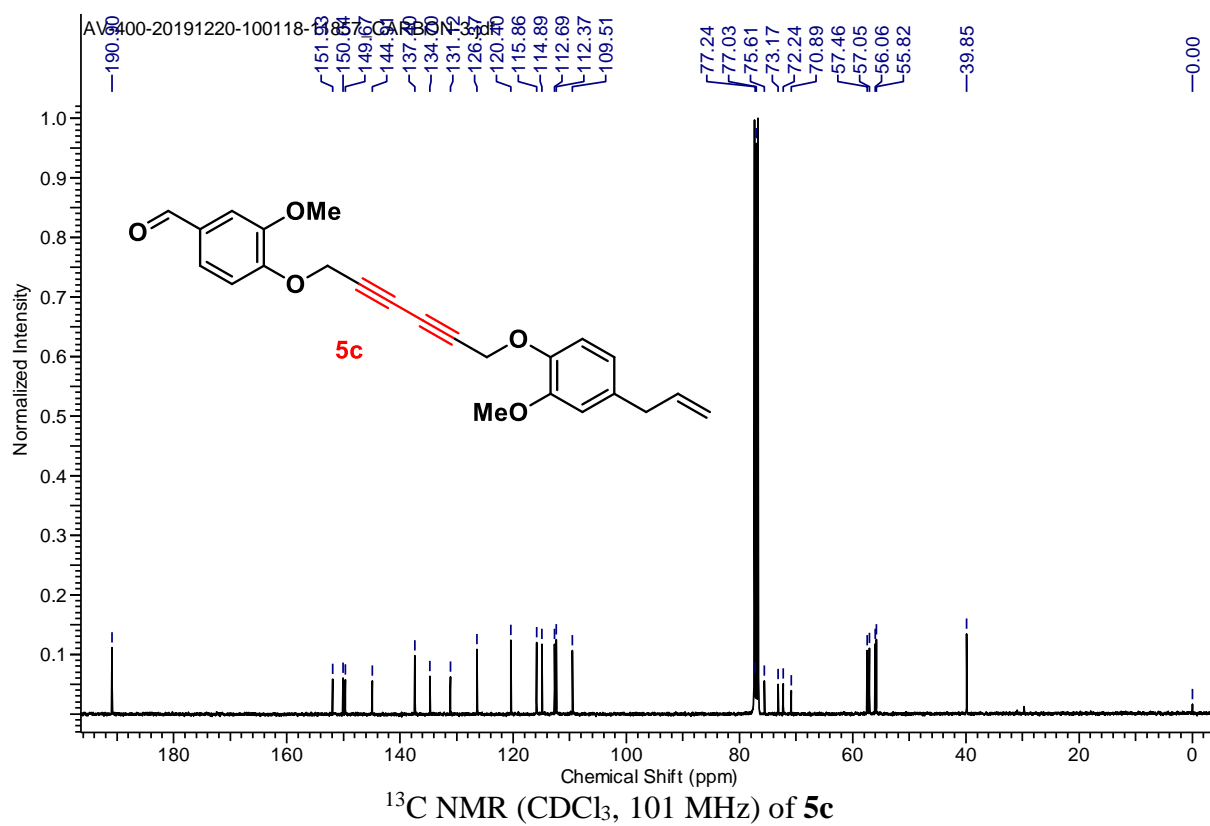
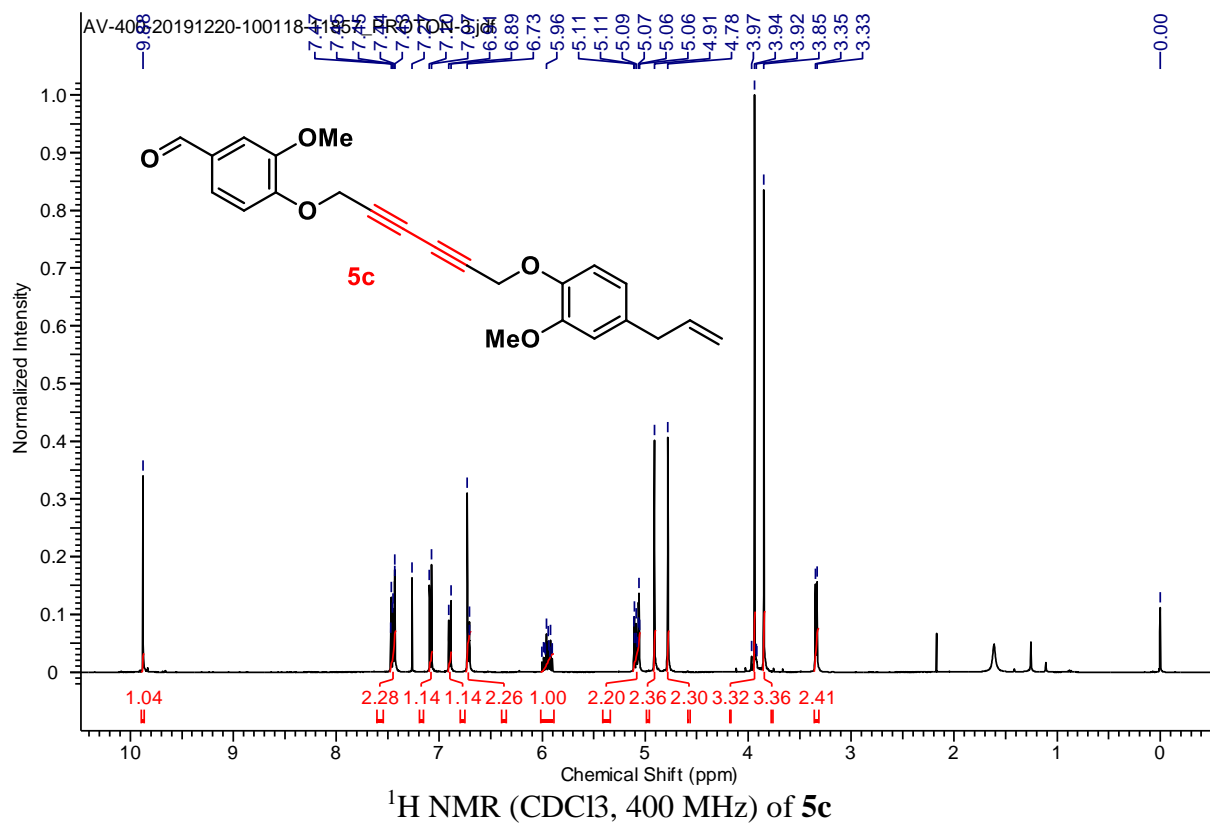


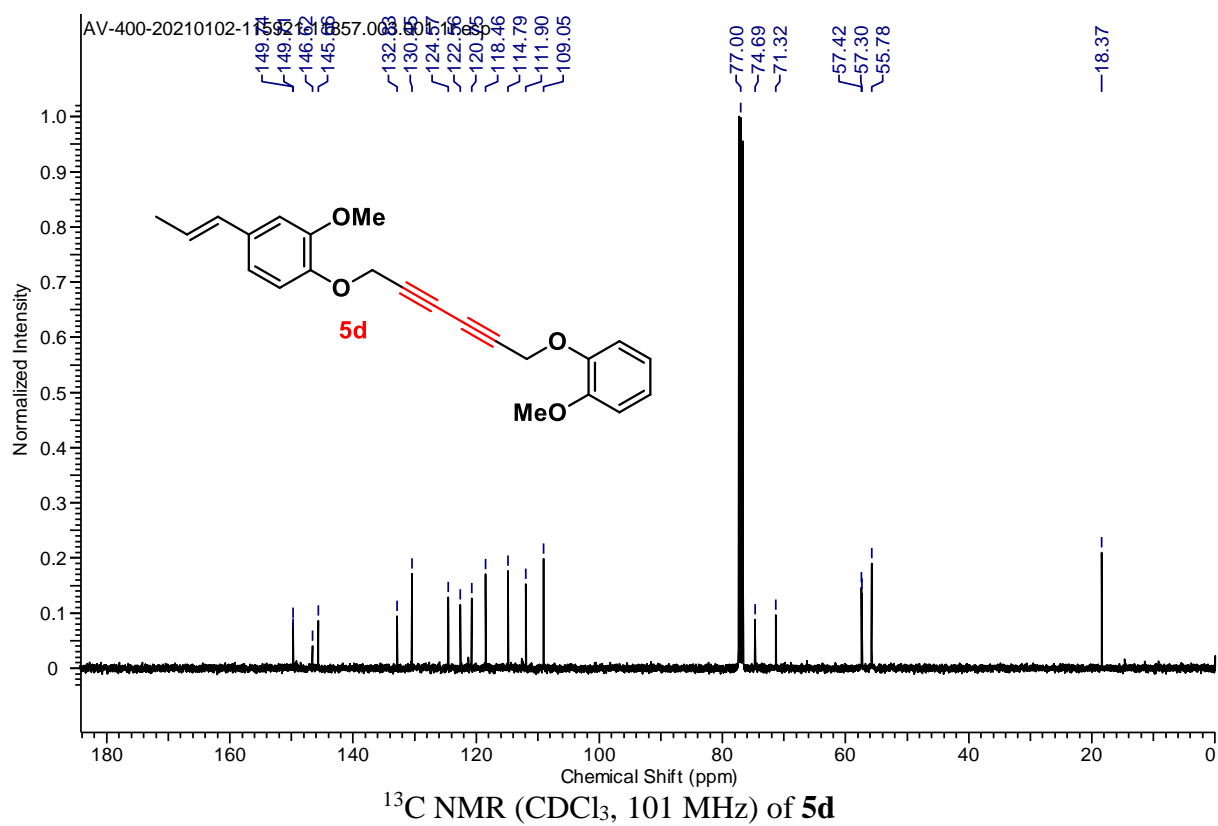
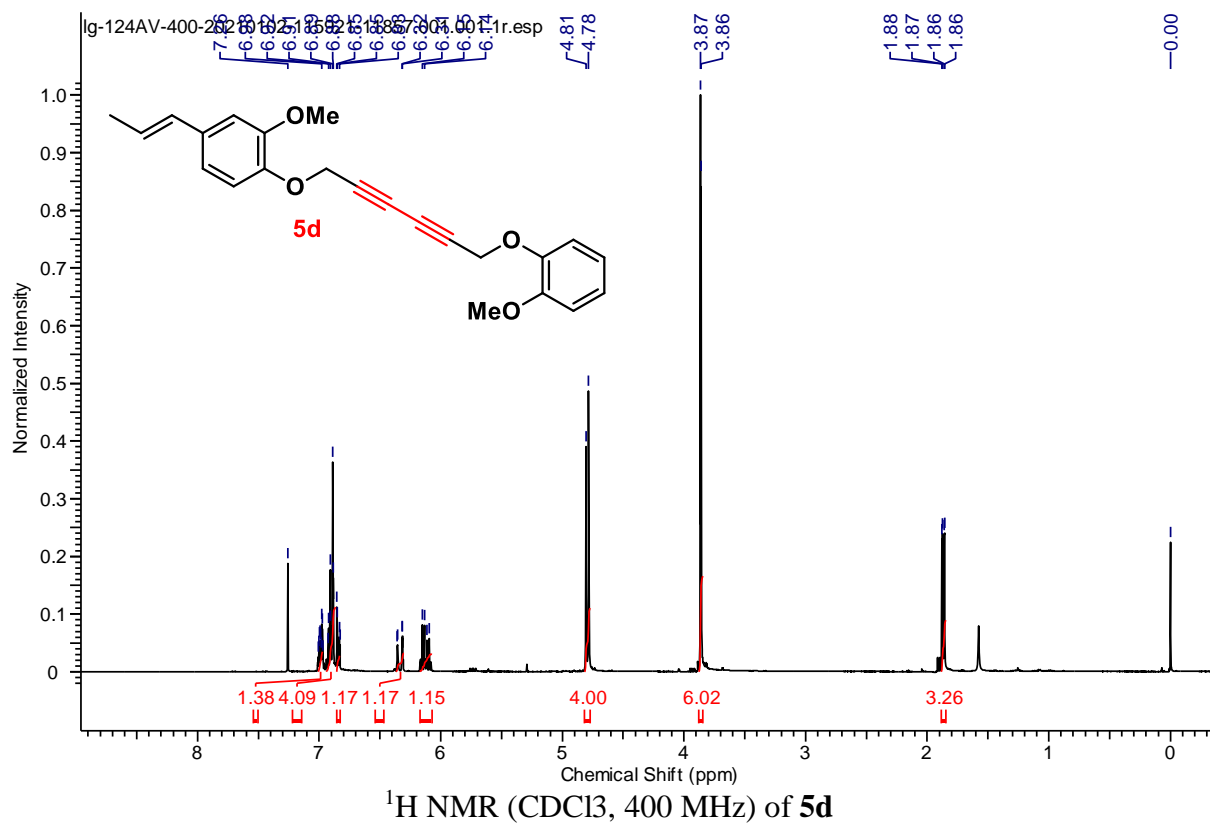
 ^1H NMR (CDCl_3 , 500 MHz) of **3d** ^{13}C NMR (CDCl_3 , 126 MHz) of **3d**

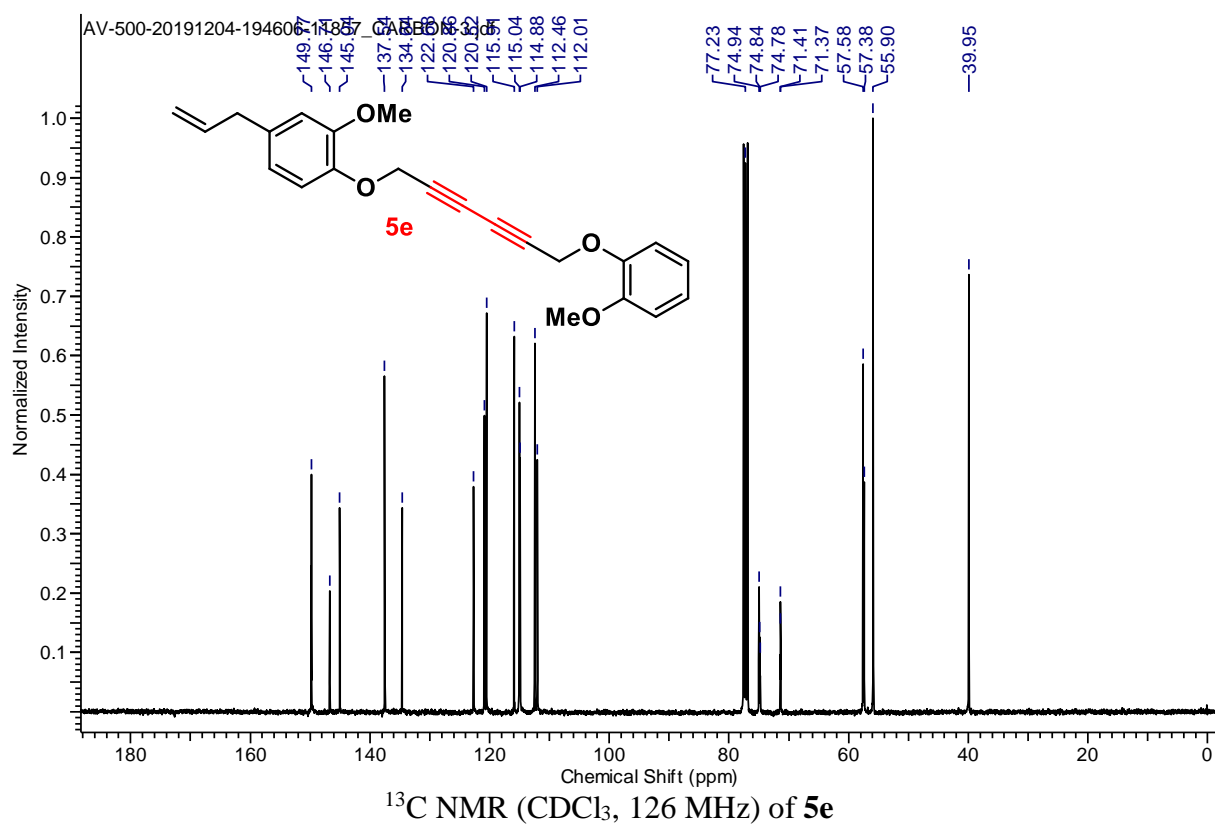
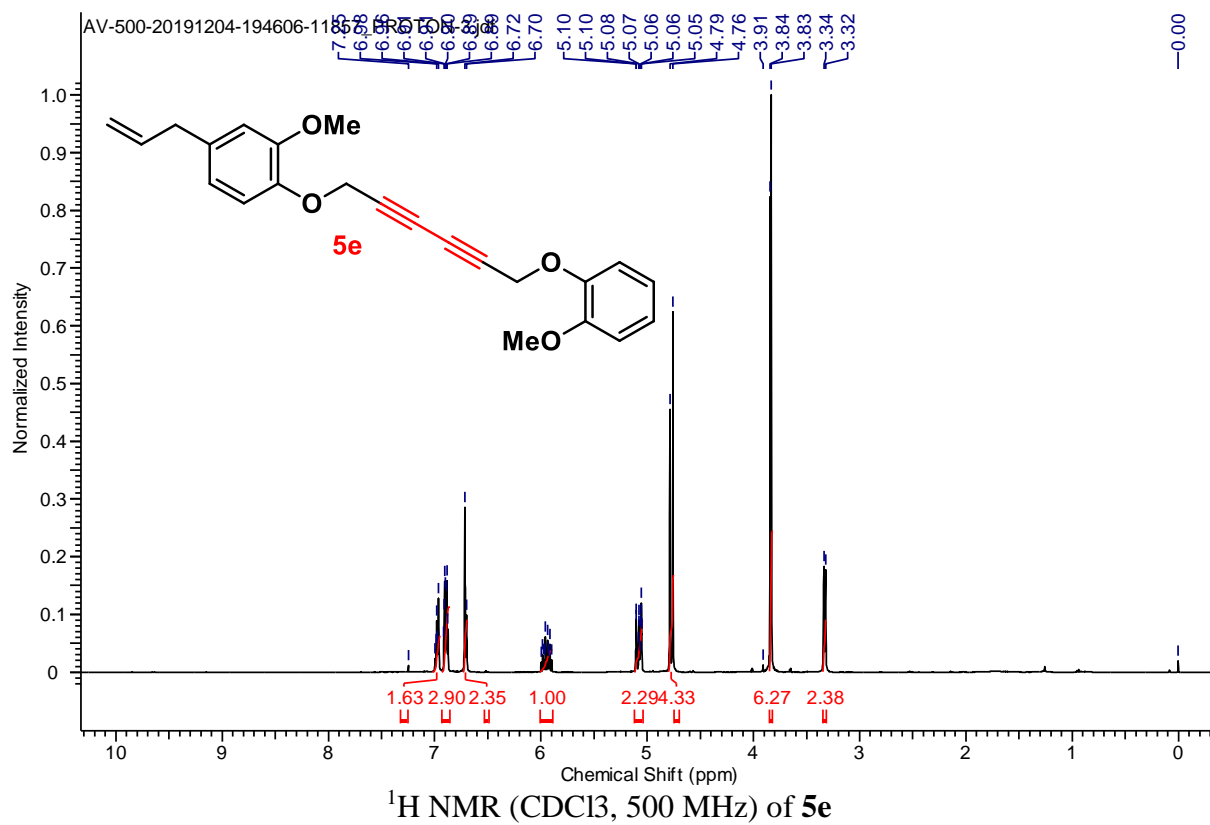


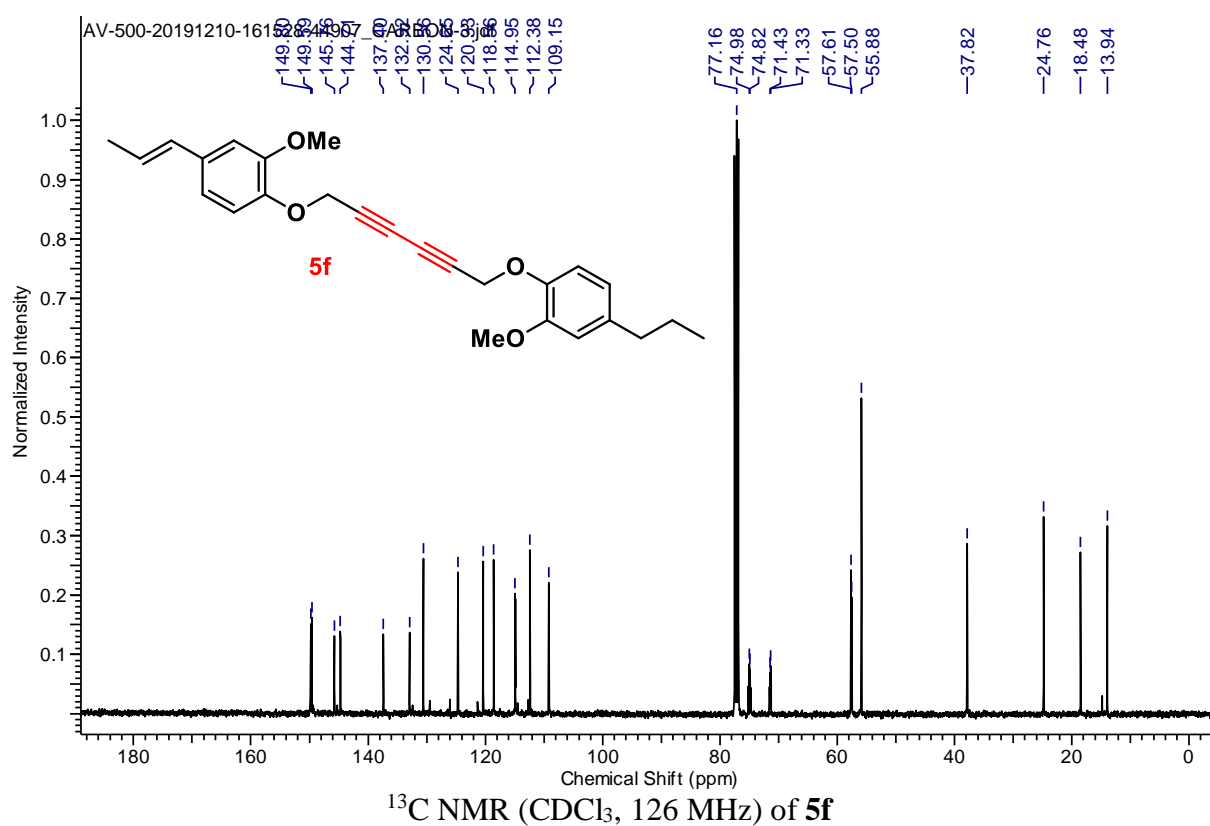
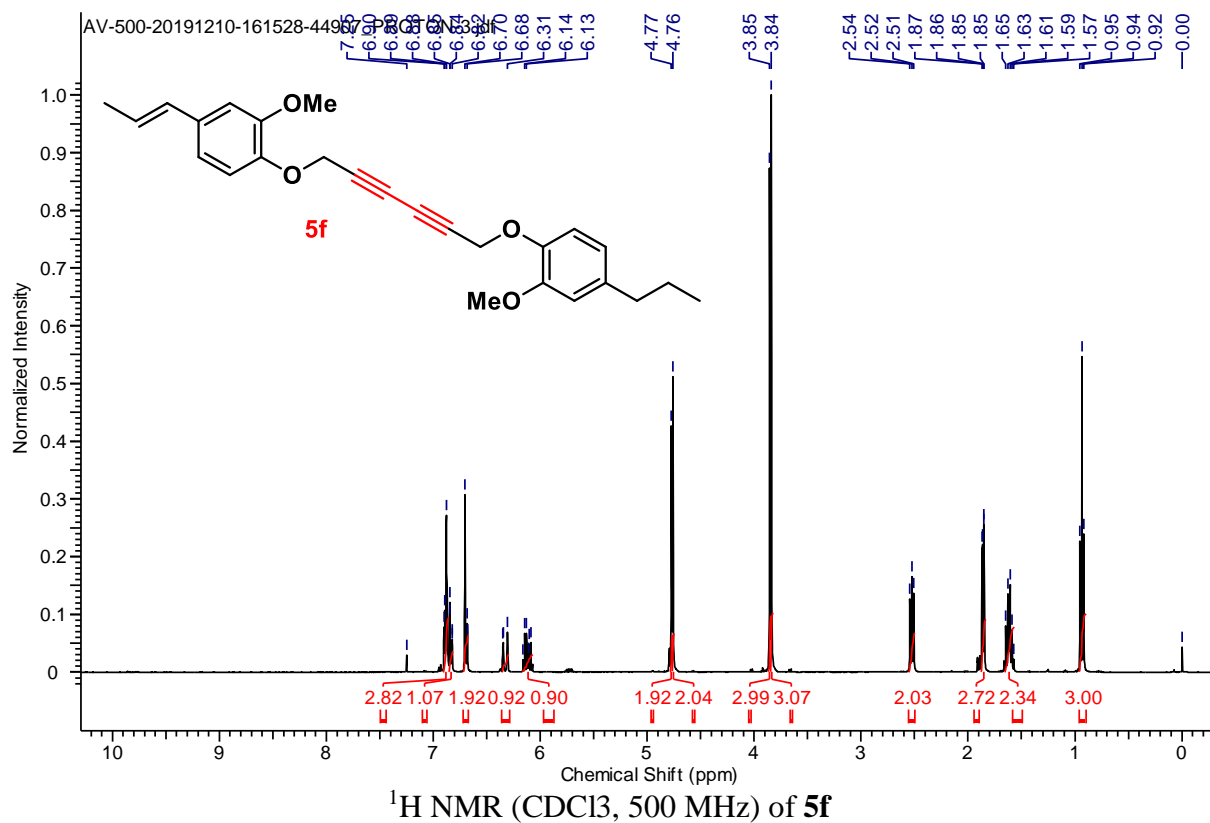


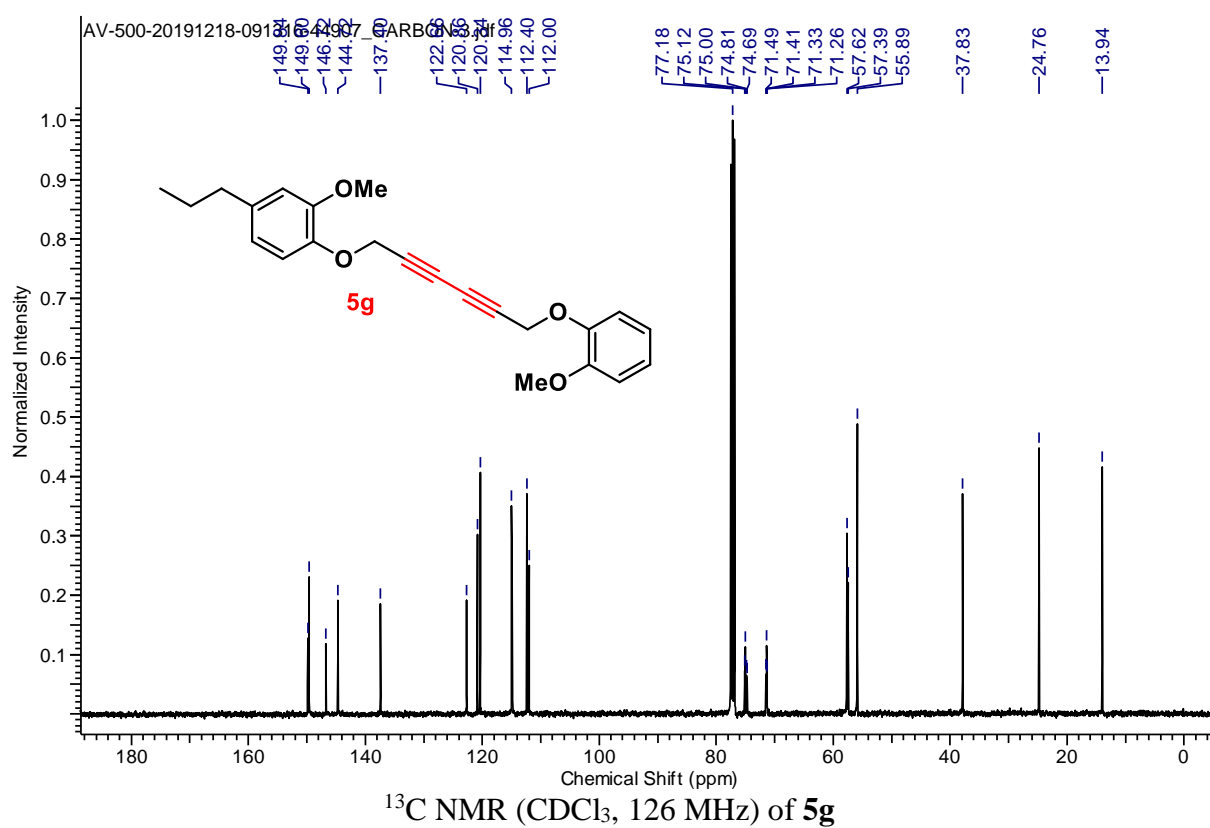
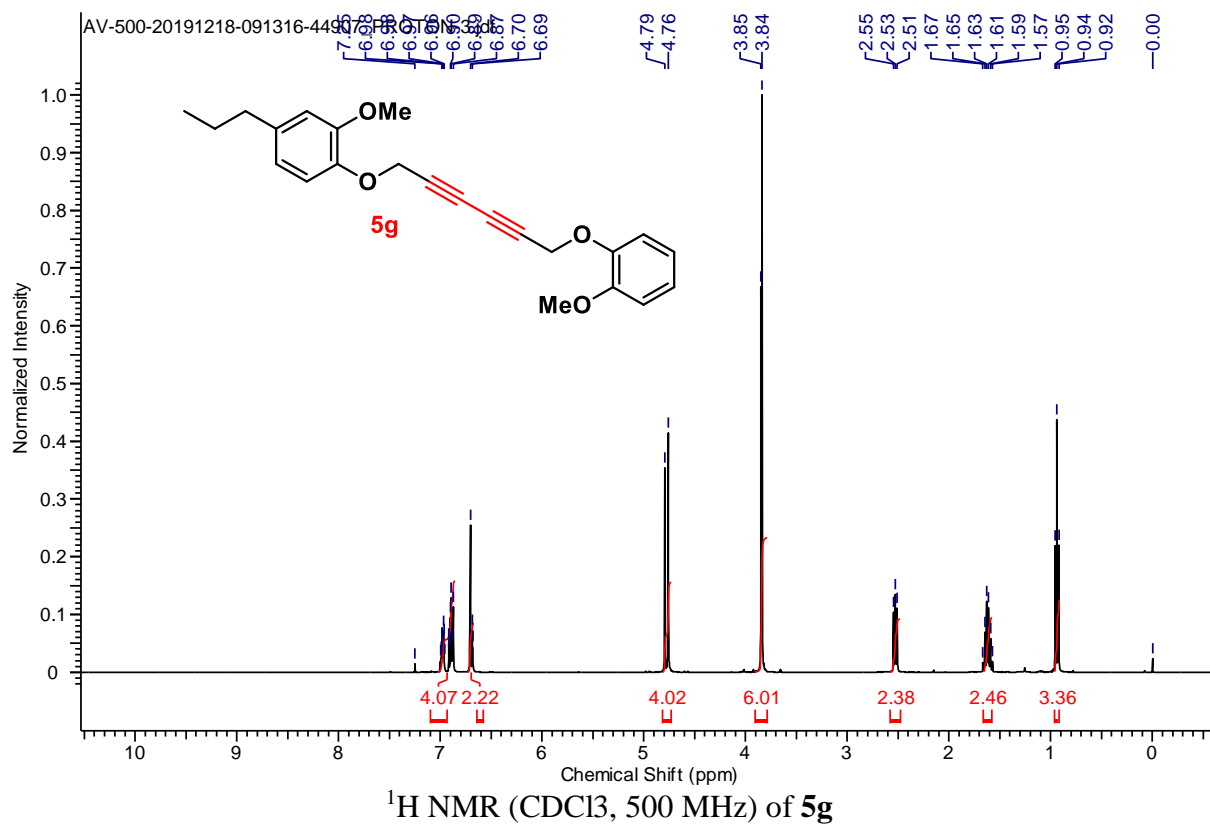


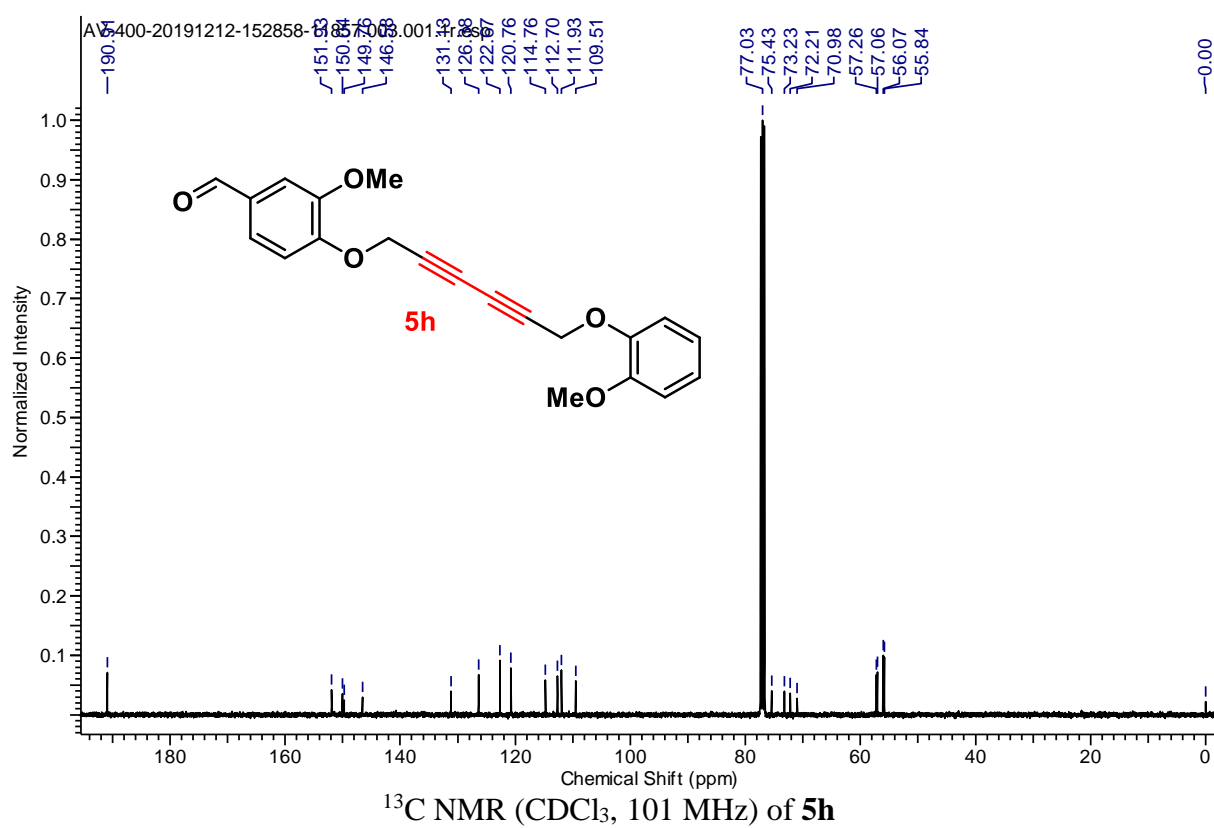
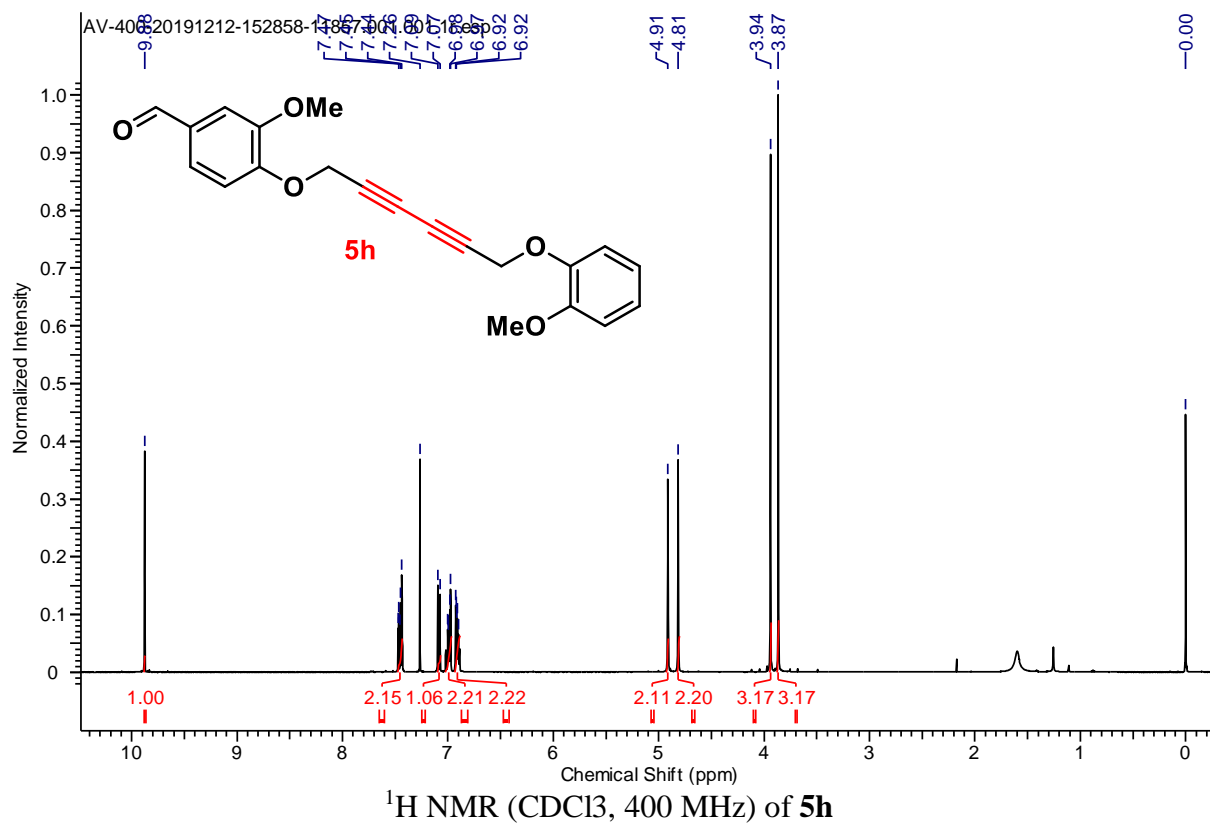


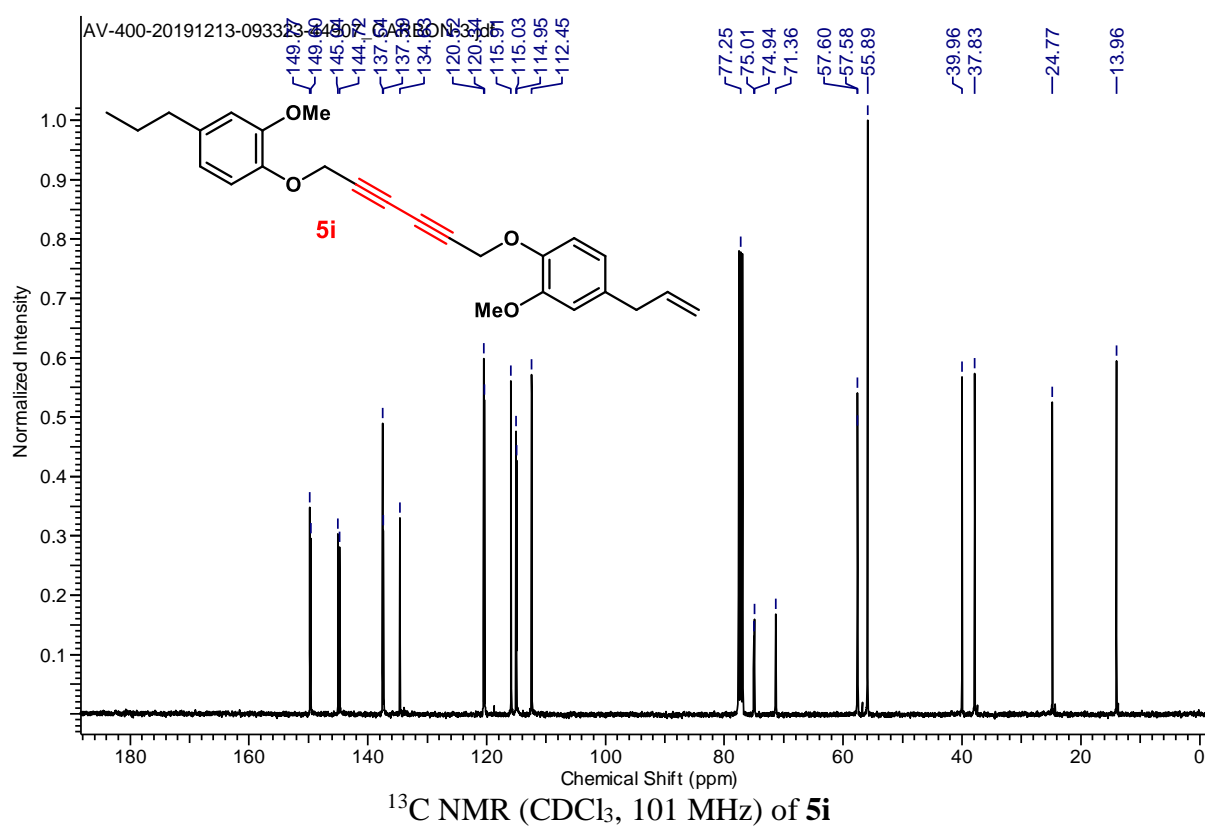
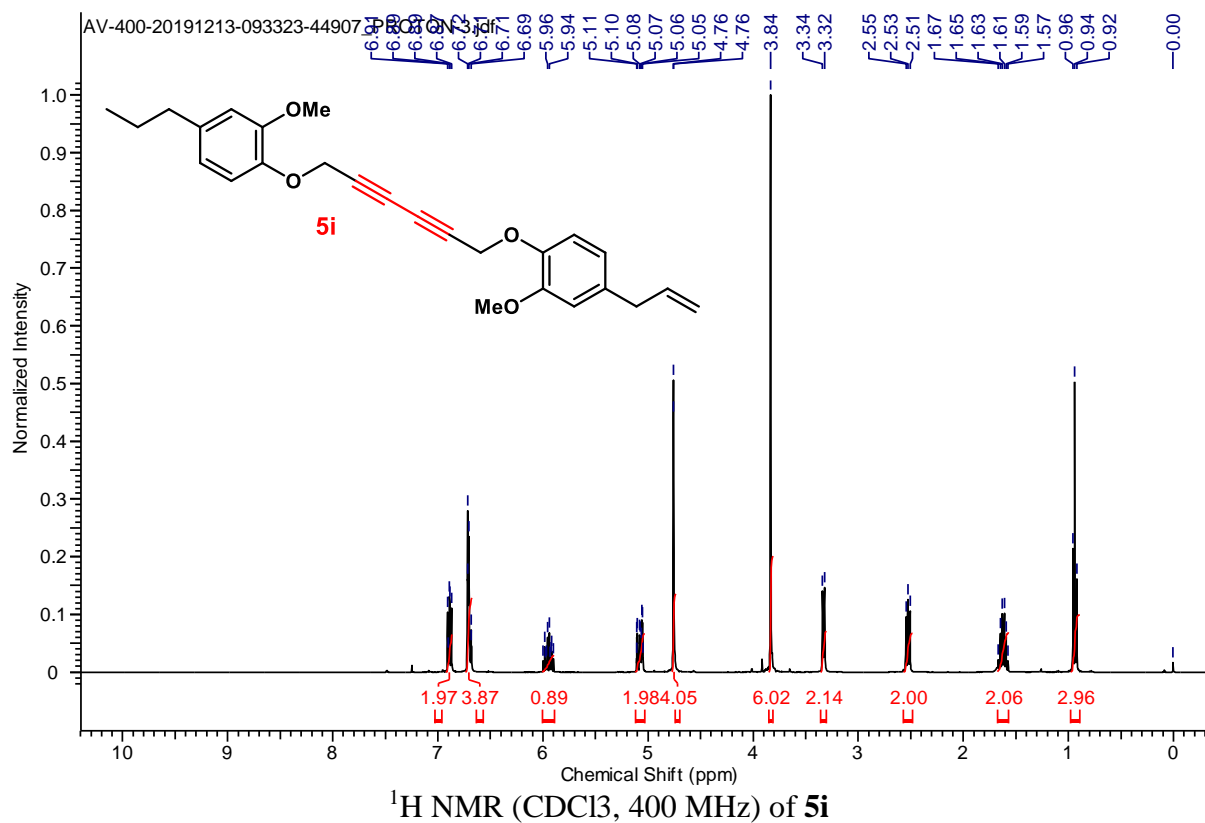


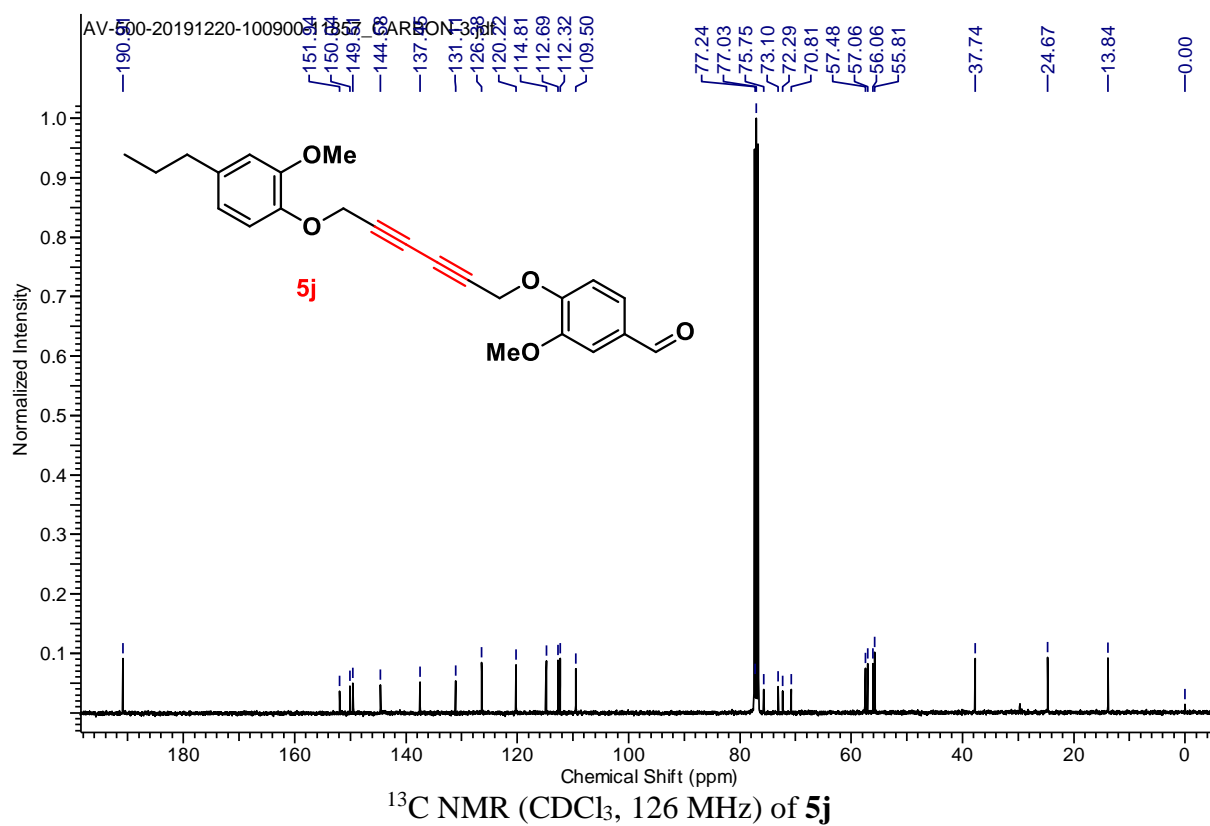
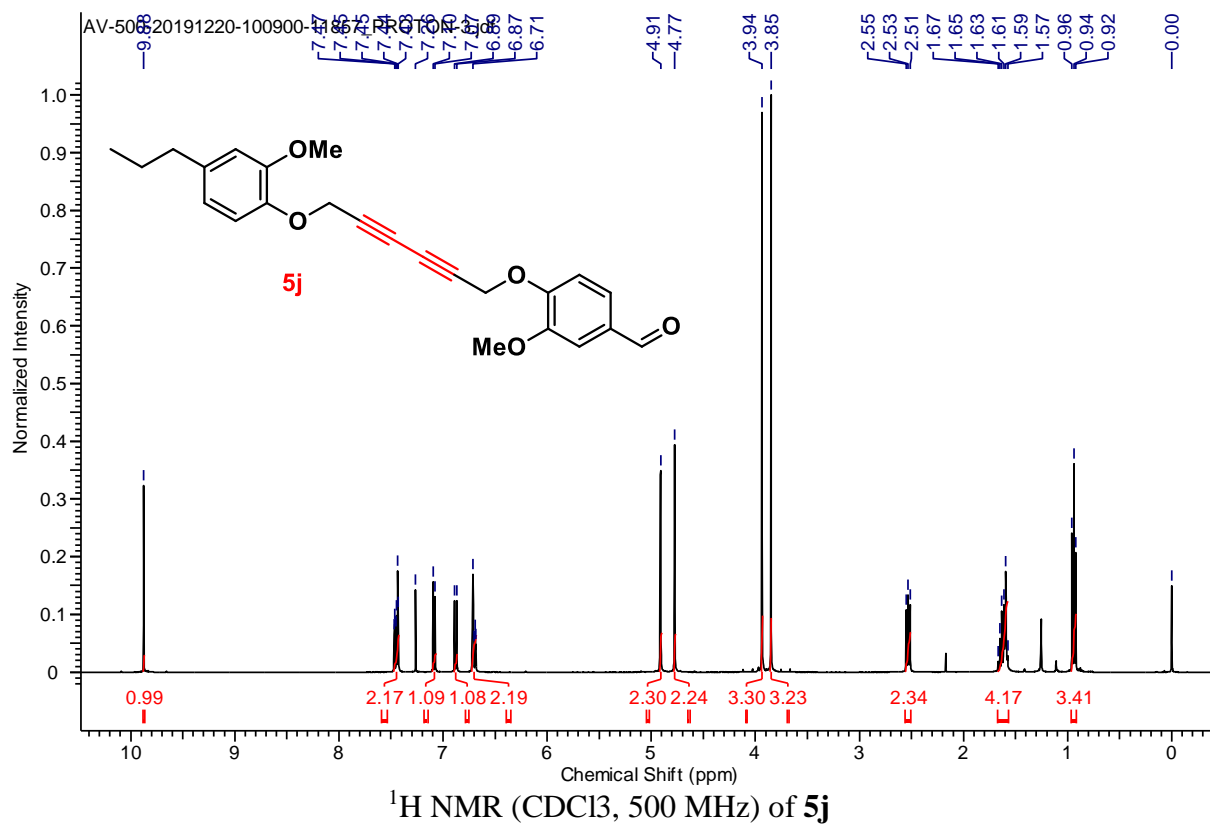












Chapter 11

*Cu-catalyzed C-C bond-
forming reactions
employing donor-accepter
cyclopropanes*

2. Cu-catalyzed C–C bond-forming reactions employing donor-accepter cyclopropanes

2.1 Introduction

Functionalized 1,4-diphenyl butan-1-one or 1,3-diphenyl propane-1-one derivatives hold a basic framework of many biologically important plant-based chalcones and synthetically available compounds.¹ This scaffolding is ambiguous to many naturally occurring flavonoids, chalcones, heterocyclic flavonoids, coumarins etc. with one atom shortage whereas, this substructure is present as it is in many synthetically available compounds.¹ Each class of naturally occurring skeletons mentioned herein comprises numerous biologically active molecules and other applications.²⁻¹¹ Some of the bioactive molecules have been portrayed in (Figure 1).

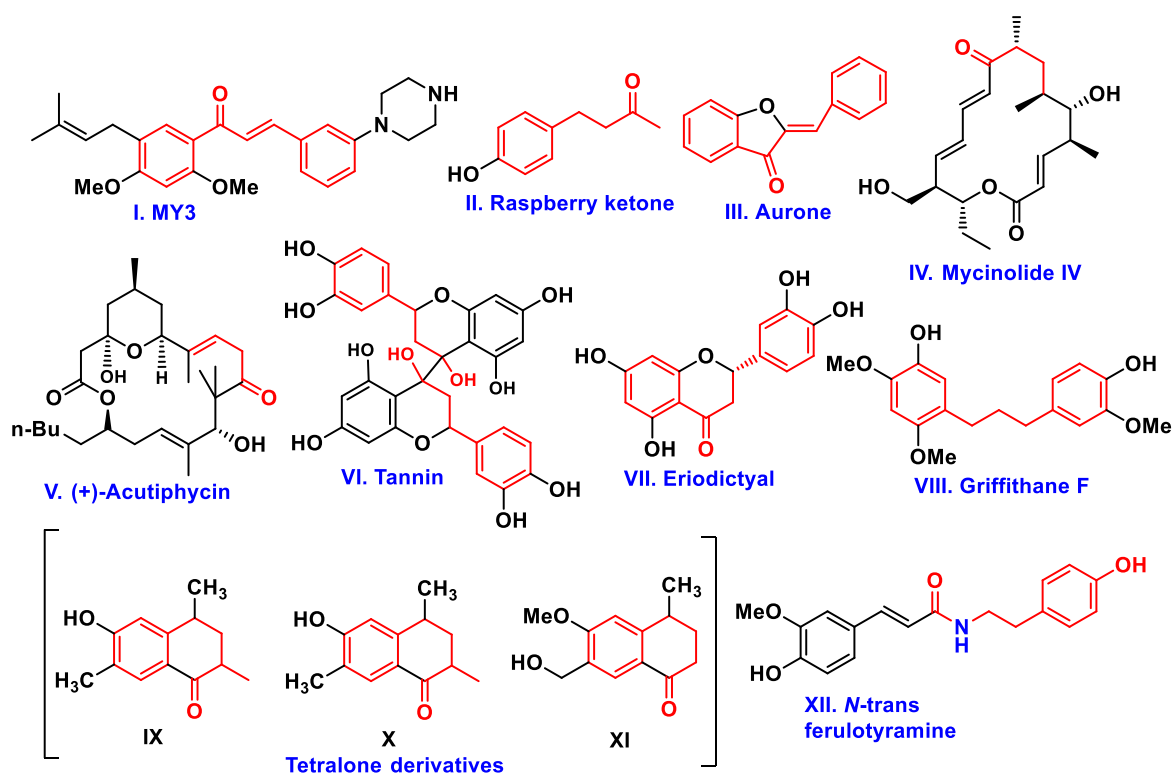


Figure 1: Natural products containing 1,3-diphenyl propane-1-one or 1,4-diphenyl butane core

Compound (I) reported by Ma *et al*² displayed cytotoxicity (IC₅₀: 1.02 μM) along with sternforemost DOX resistance in MCF-7/DOX cells by suppressing P-glycoprotein 1. Remarkably, MY3 also improves the capability of DOX treatment in MCF-7 tumor xenografts.² Compound (II) commonly known as raspberry ketone is a natural phenolic compound extracted primarily from red raspberries, cranberries, and blackberries and used in perfumes, cosmetics and as food additive.³ Aurones (III) are type of flavonoids which exists as diastereomers [(E)- and (Z)-configurations] and some of the derivatives of aurones are reported to be antifungals.⁴ Compound (IV) (Mycinolide IV), a macrocyclic molecule reported from *Micromonospora griseorubida* sp displayed antibiotic properties.⁵ Another macrolide (V) (+)-acutiphyacin, extracted from the alga *Oscillatoria acutissima* exhibited an antineoplastic effect against murine cancer cells.⁶ Hemlock bark has high proportion of tannin (VI) (10-12%) used in collagen proteins binding in leather industries for water resistance and is less prone to decaying.⁷ A flavone eriodictyol (VII) isolated from *Eriodictyon californicum*, *Millettia duchesnei*, *Eupatorium arnotianum* comprises bitter taste masking features.⁸ Ethyl acetate extract of *Combretum griffithii* stems resulted in the isolation of griffithanes F (VIII) which showed weak anticancer activity against KB, MCF-7 and NCI-H187 cancer cell lines.⁹ Isolation of tetralones (IX-XI) has been reported in literature¹⁰ by various groups from *Aristolochia* spp.¹⁰ *N*-feruloyltyramine (XII), belongs to alkaloid class of natural products which is reported from *Piper nigrum* possesses antioxidant and anti-inflammatory properties as it is an inhibitor of COX-1 and COX-2.¹¹

2.1.1 Donor–Acceptor cyclopropane reactivity

Donor–Acceptor (DA) cyclopropanes have been widely employed in the recent past for the synthesis of new molecular entities as well as for the synthesis of complex organic molecules. D–A cyclopropanes are easily cleaved due to their constrained three membered cyclic ring into dipolar ion or 1, 3-zwitterion intermediate in presence of Lewis/Brønsted acids. Afterward, these dipolar ions are attacked by electrophiles, nucleophiles and dipolarophiles to furnish functionalized products (**Figure 2**).¹ The reactivity of these D–A cyclopropanes is attributed to the bond angle strain of their saturated three membered ring. Hence, D–A cyclopropane has been immensely reported to be utilized in inter and intramolecular annulation with substituted alkenes, alkynes and allenes in one of the synthetic steps for the synthesis of natural or unnatural products.^{1, 12}

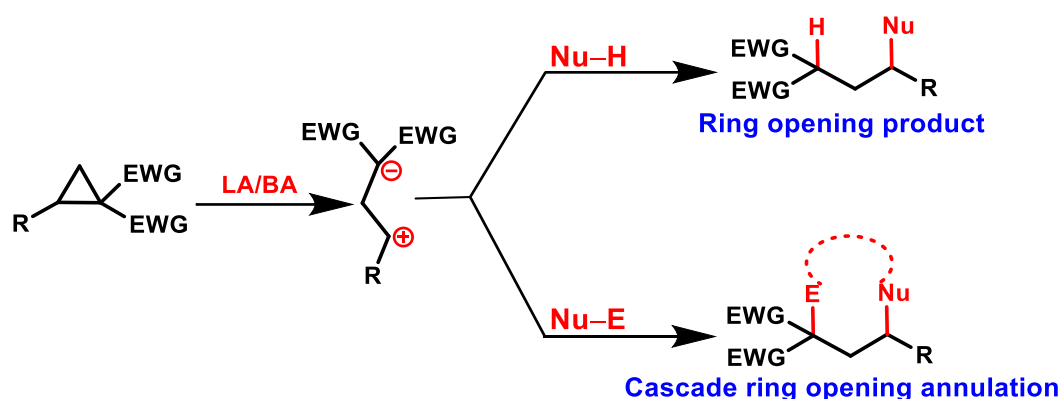
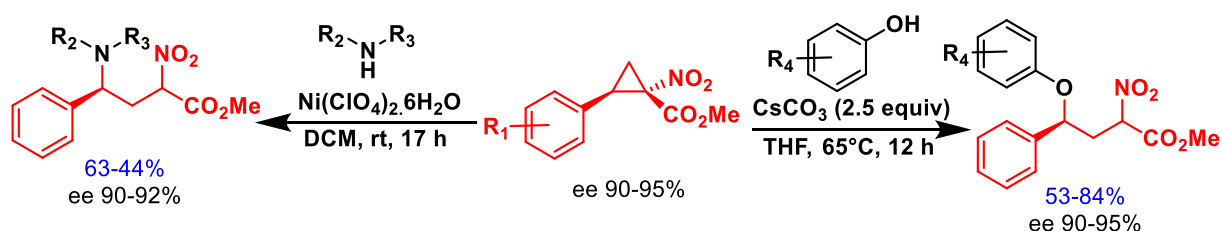


Figure 2: Generalized reactivity pattern of D–A cyclopropane

2.1.2 Donor–Acceptor cyclopropane ring opening *via* heteroatom-centered nucleophiles

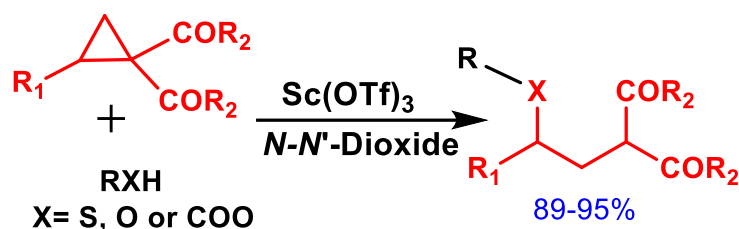
Donor–Acceptor cyclopropane cascade ring opening annulations has emerged in organic chemistry for the development of new chemical motifs for the construction of complex chemical architectures. However, there are limited reports in the literature on the Donor–Acceptor cyclopropane ring opening reactions. The very first report of nucleophilic ring opening of D–A cyclopropane was by André B. Charette and co-workers¹³ in presence of cesium carbonate at 65 °C using tetrahydrofuran as solvent (**Scheme 1**). Nevertheless, the ring-opening reaction was promoted *via* oxygen-centered nucleophiles thus furnishing heteroalkylated products in 90–95% enantiomeric excess.^{13a} They further extended their work on amine nucleophiles using $\text{Ni}(\text{ClO}_4)_2 \cdot 6\text{H}_2\text{O}$ as a Lewis acid catalyst.^{13b}



Scheme 1: Ring-opening reaction *via* oxygen-centered nucleophile by André B. Charette and co-workers¹³

This work was further elaborated by Feng *et al*¹⁴ on phenols, carboxylic acids and thiols by using scandium (III) complex as a catalyst for asymmetric ring-opening reaction of D–A cyclopropyl ketones. In this reaction, catalytic asymmetric ring-opening of D–A

cyclopropanes with thiols, alcohols, or carboxylic acids have been reported (**Scheme 2**). In all the cases, heteroatom-containing nucleophiles are trapped by cleaved dipolar ions from D–A cyclopropanes to furnish *O*– or *S*–alkylated product.¹⁴



Scheme 2: Asymmetric ring-opening reaction *via* heteroatom-centered nucleophile by Feng *et al*¹⁴

2.1.3 Donor–Acceptor cyclopropane ring opening *via* carbon-centered nucleophiles

Donor–Acceptor cyclopropanes have been used as a source of alkylating agent for alkylation reactions and have been used to alkylate various types of substrates involving heteroatom so far.^{1,13,14} Earlier reports have generally shown heteroatom-centered alkylation (*O*, *S* or *N*–alkylation) using Donor–Acceptor cyclopropanes as alkylating agents.^{13,14} There are fewer reports of *C*–alkylation *via* Donor–Acceptor cyclopropanes so far (**Figure 3**). D–A cyclopropanes assisted alkylation reaction catalyzed by Lewis acid follows a dearomatization/rearomatization pathway.¹

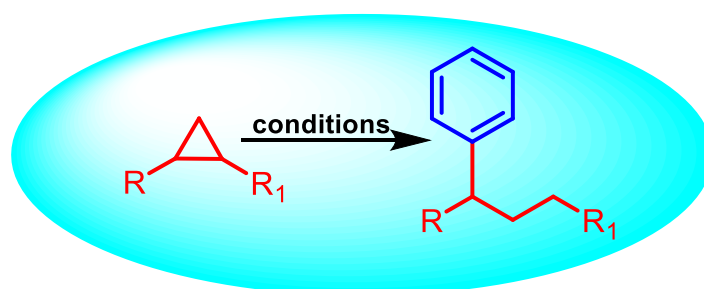
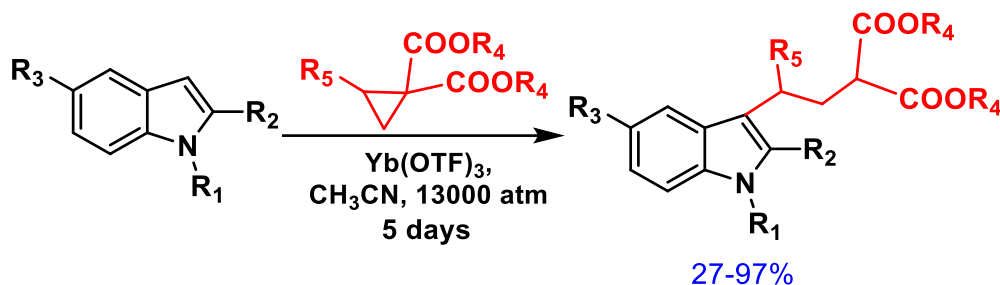


Figure 3: A general approach for *C*–alkylation *via* Donor–Acceptor cyclopropanes

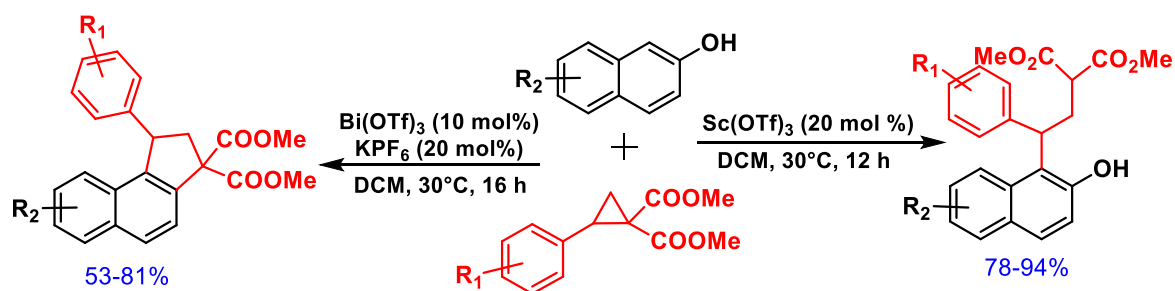
The carbon nucleophilic ring opening of cyclopropanes was primarily reported by Michael A. Kerr and co-workers¹⁵ using catalytic amount of ytterbium triflate under high pressure to afford Friedel-Craft adduct in 27-97% of yields (**Scheme 3**). Use of metal catalyst, high

pressure, longer reaction time and low yields of the C-alkylated products were the major limitations of the procedure.¹⁵



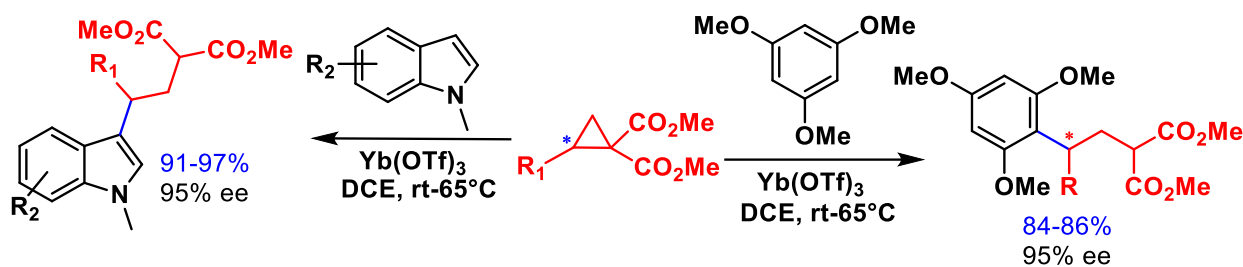
Scheme 3: C-alkylation of indoles employing ytterbium triflate as Lewis acid by Michael A. Kerr and co-workers¹⁵

Biju *et al*¹⁶ reported Friedel–Crafts-type addition of 2-naphthols to 2-substituted cyclopropane 1,1-dicarboxylates employing Sc(OTf)_3 as Lewis acid along with the synthesis of naphthalene-fused cyclopentane in presence of Bi(OTf)_3 as the Lewis acid (**Scheme 4**). Though the yields of both the reactions were good to moderate however use of transition-metal catalyst, longer reaction time and substrate scope limited to naphthol only curtails its synthetic utility.¹⁶



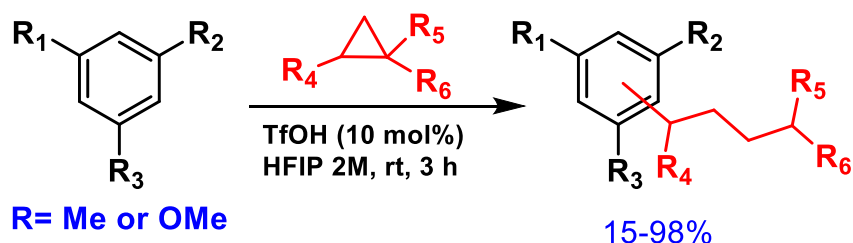
Scheme 4: C-alkylation of 2-naphthols employing scandium triflate as Lewis acid by Biju *et al*¹⁶

A much reliable approach was shown by Ghorai and co-workers¹⁷ by reacting 1,3,5-trimethoxybenzene or *N*-methyl indoles employing Yb(OTf)_3 as Lewis acid catalyst to afford ring opening of substituted D–A cyclopropane with good yields (**Scheme 5**). This advancement also furnished product in 95% of enantiomeric excess on reaction with enantiopure D–A cyclopropane and the reaction proceeds through the $\text{S}_{\text{N}}2$ -type reaction pathway.¹⁷



Scheme 5: C-alkylation of indoles and trimethoxybenzene employing ytterbium triflate as Lewis acid by Ghorai and co-workers¹⁷

Moran *et al*¹⁸ proposed carbon-centered nucleophilic ring-opening reactions of D–A cyclopropanes with substituted arenes using 10 mol% of trifluoromethanesulfonic acid (TfOH) in 2M HFIP at moderately elevated temperature (40–50°C) to generate Friedel-Craft adducts in moderate to excellent yields (**Scheme 6**). In case of reaction with 2,6-dimethyl phenol, product was obtained in low to moderate yields.¹⁸ Moran and co-workers¹⁸ generally utilized substituted arenes with blocked *meta* and *para* positions to produce *ortho* adducts hence restricting the substrate scope.



Scheme 6: C-alkylation of trisubstituted or disubstituted arenes employing Brønsted acid catalyst by Moran *et al*¹⁸

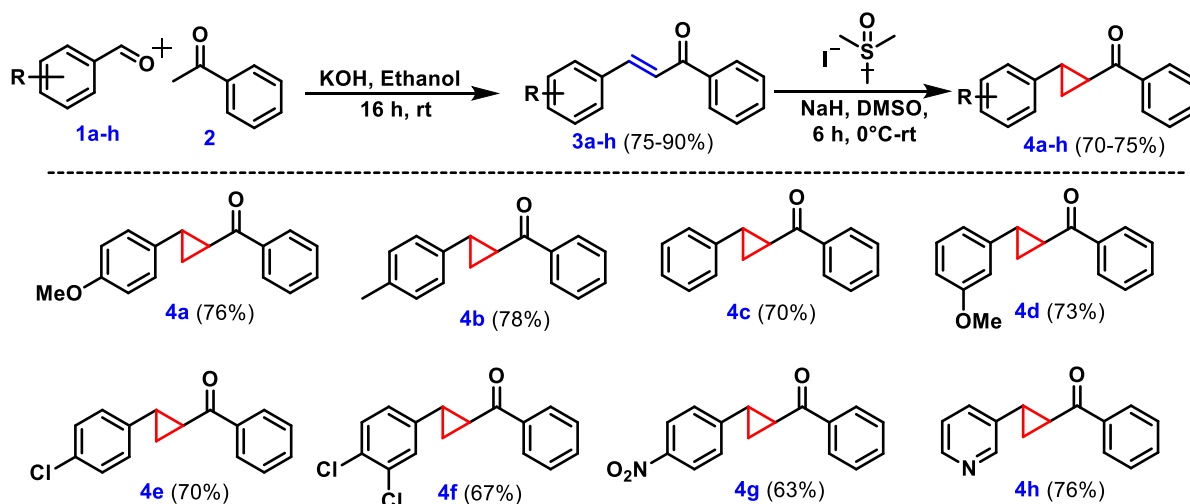
2.1.4 Conclusions

Ring-opening reactions of D–A cyclopropanes have garnered attention of organic chemists for synthesizing Friedel-Craft alkylated adducts. D–A cyclopropanes actively take part in Friedel-Craft alkylation due to their reactivity pattern with nucleophiles in presence of Lewis or Brønsted acids which makes them easy competitors for alkylation. A wide range of D–A cyclopropanes have been studied with *N,N*-dimethylanilines, benzofuran, 2-naphthol, indoles etc for *O*–, *N*–, *S*– or *C*–alkylation.^{1,12-18} In the present decade, remarkable advancements in

C-alkylation *via* ring opening of D–A cyclopropanes have been made.^{1,12-18} However, there is still a lot of scope in terms of arenes scaffolds that can be alkylated using Donor–Acceptor cyclopropanes as alkylating partners. Apart from this, TM-free alkylation are yet to be fully explored using cheaper, safer, biodegradable materials and milder reaction conditions employing Donor–Acceptor cyclopropanes.

2.2 Present work

Herein we report Brønsted catalysed Friedel-Craft alkylation of phenols employing D–A cyclopropanes. Due to the presence of 1,4-diphenyl butan-1-one and 1,3-diphenyl propane-1-one cores in various natural products and their biological significances prompted us to carry out synthesis of these kind of scaffolds using cheaper catalyst in higher yields. First, we synthesized chalcones by reacting various substituted benzaldehydes (**1a-h**) with acetophenone (**2**) using KOH as a base and MeOH as solvent in good yields following the literature methods¹⁹ (**Scheme 7**). Afterward, these chalcones (**3a-h**) were treated with TMSI in presence of NaH as a base and DMSO as a solvent in accordance with the literature reports¹⁹ to furnish cyclopropyl ketones (**4a-h**). We have achieved synthesis of cyclopropyl ketones containing EDGs, weak EWGs and strong EWGs.

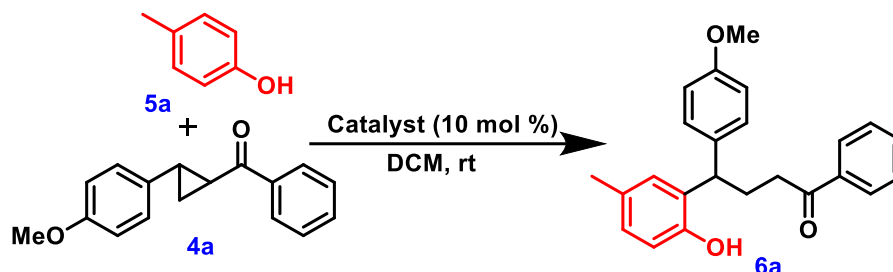


Scheme 7: Synthesis of various D–A cyclopropanes (**4a-h**)

Initially, we treated *p*-cresol (**5a**) with cyclopropyl ketone (**4a**) in DCM using Cu(OAc)₂ as a Lewis acid catalyst (**Table 1**) at room temperature in an open round bottom flask for 24 h. Even after 24 hours of stirring, no product formation was observed on TLC. Then we

performed the reaction with $\text{Bi}(\text{NO}_3)_3 \cdot 5\text{H}_2\text{O}$ as Lewis acid in DCM at room temperature, we observed product formation after 12 hours (TLC). The reaction mixture was dried *in vacuo*.

Table 1: Optimization of the reaction conditions



Entry	Lewis/Brønsted acid (10 mol%)	Time (h)	Solvent	Temperature (°C)	Yield (%)
1	$\text{Cu}(\text{OAc})_2$	24	DCM	rt	No reaction
2	$\text{Bi}(\text{NO}_3)_3 \cdot 5\text{H}_2\text{O}$	12	DCM	rt	70
3	ZrCl_4	24	DCM	rt	No reaction
4	$\text{Mn}(\text{OAc})_3$	24	DCM	rt	No reaction
5	$\text{Cu}(\text{OTf})_2$	4	DCM	rt	84
6	$\text{Cu}(\text{OTf})_2$	4	DCE	60	84
7	$\text{Bi}(\text{OTf})_3$	10	DCM	rt	79
8	H_2SO_4	5	DCM	rt	Inseparable mix.
9	TfOH	2	DCM	rt	Inseparable mix.
10	MeSO_3H	3	DCM	rt	86
11	MeSO_3H	3	DCE	60	86
12	MeSO_3H	6	Acetone	rt	75
13	MeSO_3H	4	Methanol	rt	70
14	AcOH	5	DCM	rt	Inseparable mix.
15	No Catalyst	24	DCM	rt	No reaction

The product formed was isolated by flash chromatography using RediSep® pre-packed column (SiO_2 , 12g) and EtOAc-petroleum ether mixture as eluents to afford a pure

compound, which was found to be the desired product (**6a**) by NMR and mass spectrum. In case of reaction with metal salts *i.e.* $\text{Cu}(\text{OAc})_2$, ZrCl_4 and $\text{Mn}(\text{OAc})_3$ as catalyst did not result in any product formation even after 24 hours of stirring while organic acids such as AcOH , TfOH and H_2SO_4 afforded an inseparable reaction mixture which could not be purified using available chromatographic techniques. When reactions were performed using $\text{Cu}(\text{OTf})_2$ and MeSO_3H as acid catalysts at room temperature, the formation of desired alkylated product (**6a**) was observed in 84 and 86% in 4 and 3 hours, respectively. Increases in reaction temperature did not enhance product yield. However, in the case of $\text{Bi}(\text{OTf})_3$ and $\text{Bi}(\text{NO}_3)_3$, reactions proceeded at a slower rate and product yields were also comparatively lower than the reaction with MeSO_3H and $\text{Cu}(\text{OTf})_2$ (**Table 1**). No trace amount of product formation was observed when the reaction was carried out in the absence of any acid catalyst. Cost effectiveness and biodegradable nature²¹ of Brønsted acid, MeSO_3H over $\text{Cu}(\text{OTf})_2$ prompted us to use this as acid catalyst for further exploration of substrate scope.

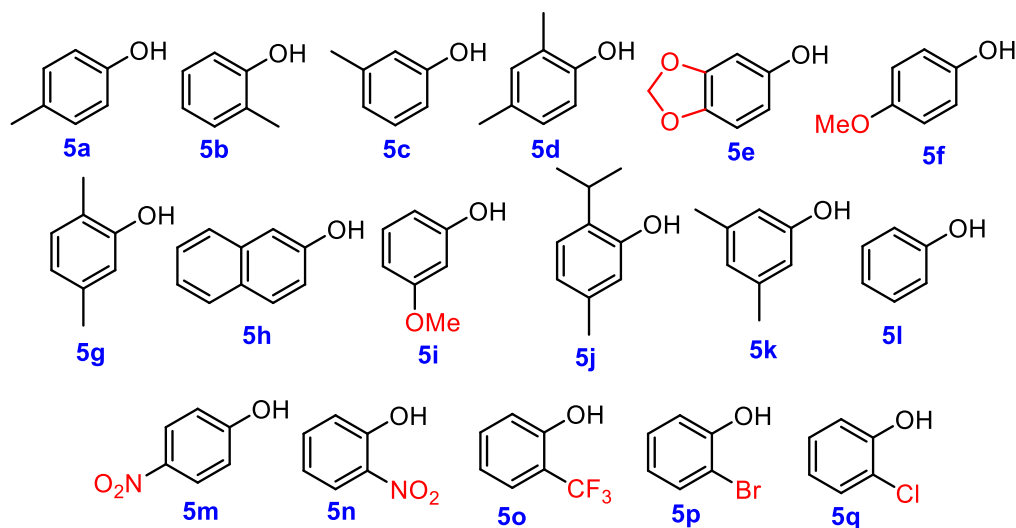
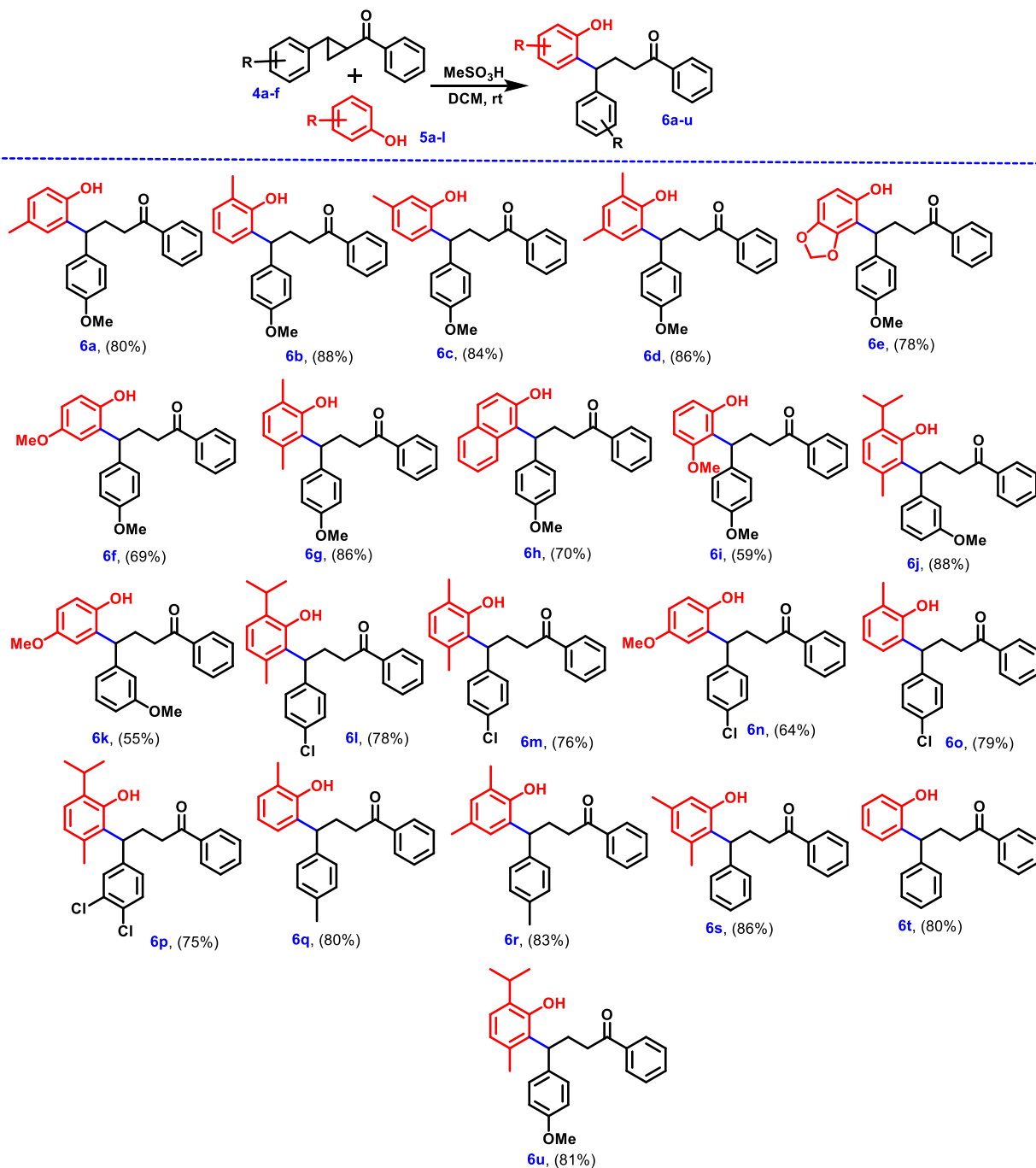


Figure 4: Various phenols studied for D–A cyclopropanes ring opening reactions

With the optimized reaction condition in hand, we elaborated the substrate scope with various phenols (**5a–q**) (**Figure 4**) and D–A cyclopropanes (**4a–h**) (**Scheme 7**). A wide variety of phenols (**5a–l**) on reaction with various D–A cyclopropanes (**4a–f**) in presence of MeSO_3H as Brønsted acid catalyst resulted in the formation of the product in moderate to very good yields (**Table 2**).

Table 2: Substrate scope with phenols **5a-l**^{a,b}

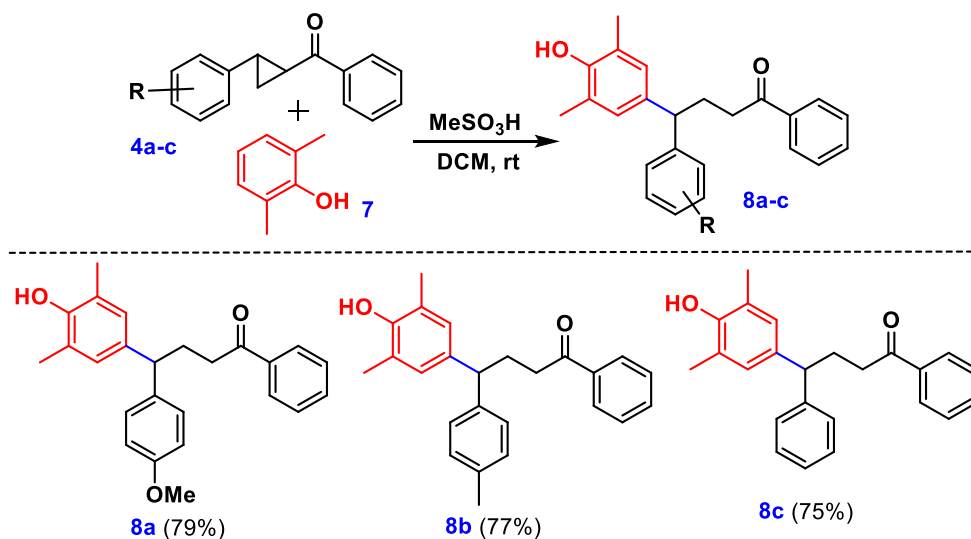
Reaction conditions: ^aPhenols (**5a-l**) (1 equiv.), **4a-f** (1.5 equiv.) and MeSO_3H (10 mol%) in DCM (5 mL) at rt under open air, ^bYields are expressed in percentage with respect to phenols.

It is pertinent to mention here that D–A cyclopropanes (**4a-c**) did not yield any product on reaction with phenols (**5m-q**). Also, no product formation even in trace amount was

observed in case of reaction of D–A cyclopropanes (**4g** and **4h**) with phenols (**5a–q**), respectively and the unreacted reactants were obtained as such.

It was observed that alkylation of phenols took place at *ortho*-position in all the cases by the attack of ring-opened D–A cyclopropane adduct. It is pertinent to mention here that published literature reports^{15–18} also supports the formation of *ortho*-functionalized phenols. We opined it would be interesting to study the same reaction with *ortho*-position blocked phenols. Thus, we investigated this reaction with 2,6-dimethylphenol (**7**) as a substrate where both the *ortho*-positions are blocked with D–A cyclopropanes (**4a–c**). Interestingly exclusively *para*-functionalized products (**8a–c**) were obtained in good yields (**Table 3**).

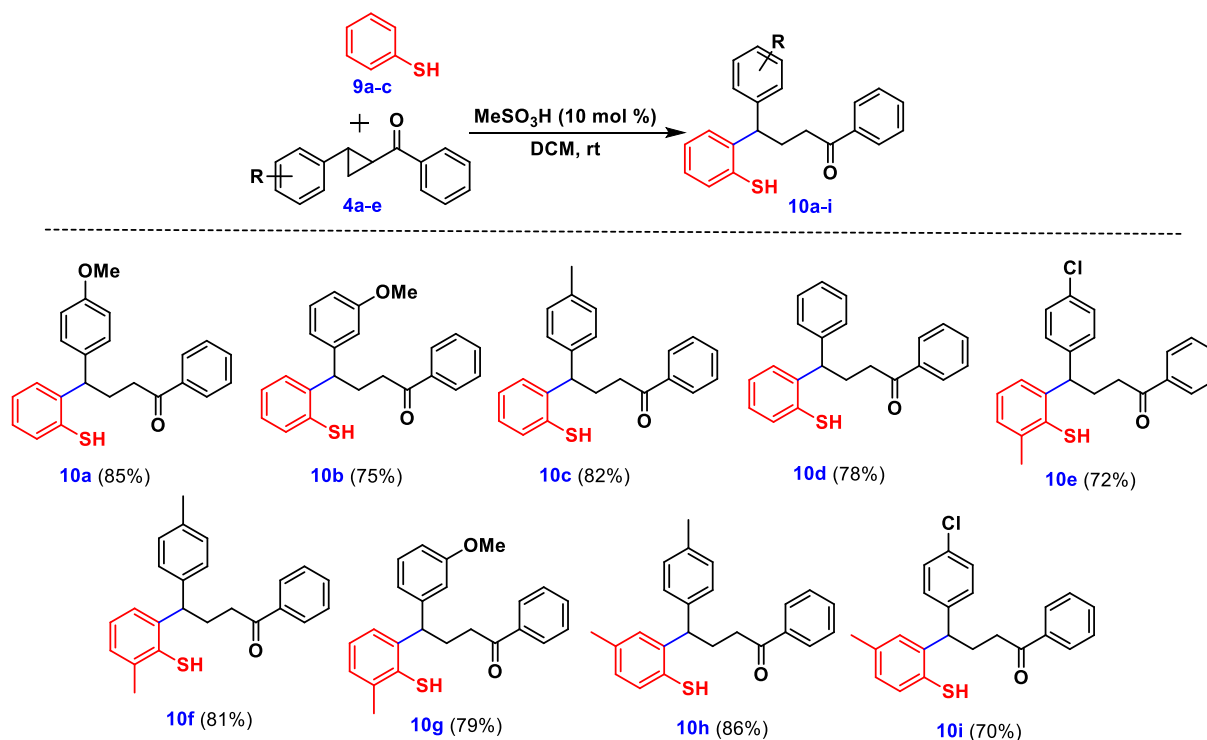
Table 3: Reaction with *ortho*-position blocked phenol **7**^{a,b}



Reaction conditions: ^aPhenol (**7**) (1 equiv.), **4a–c** (1.5 equiv.) and MeSO₃H (10 mol%) in DCM (5 mL) at rt under open air, ^bYields are expressed in percentage with respect to phenol **7**

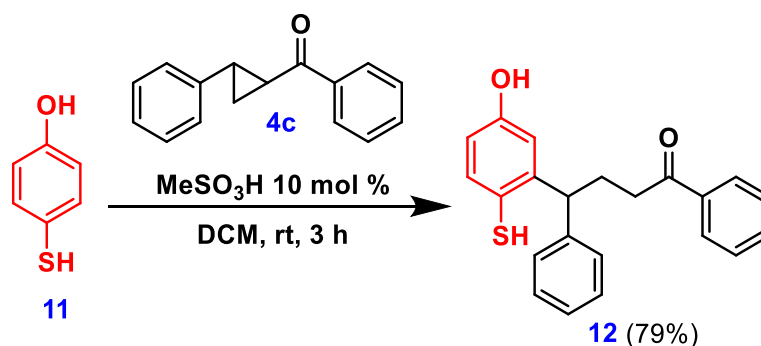
Further, the developed synthetic protocol was applied to various thiophenols (**9a–c**) and as expected reaction proceeded smoothly and *ortho*-substituted Friedel–Crafts adducts (**10a–i**) were formed in good yields (**Table 4**).

Table 4: Reaction with thiophenols **9a–c**^{a,b}



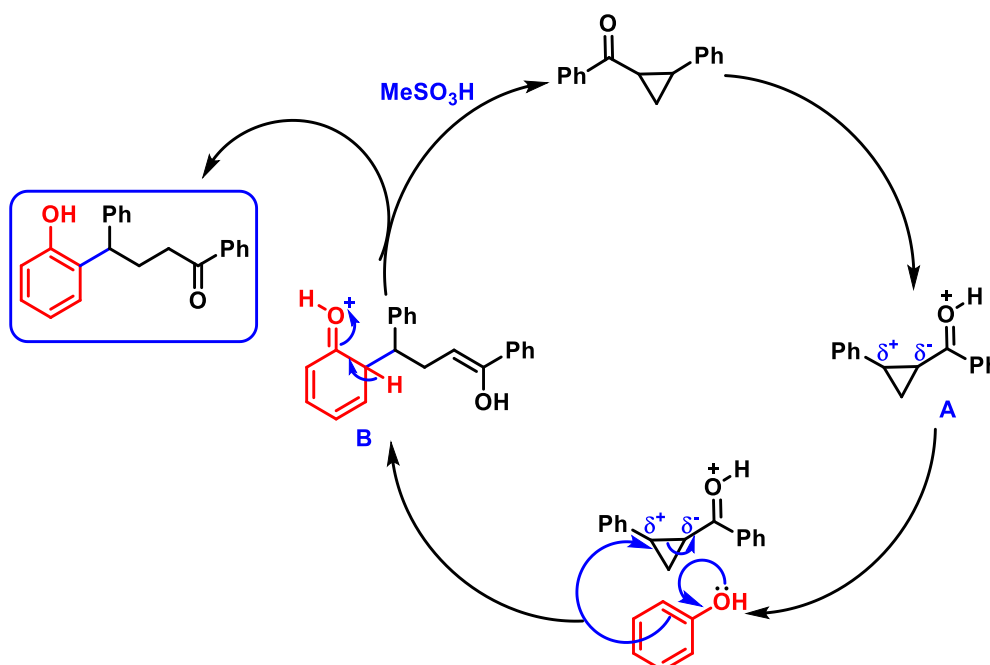
Reaction conditions: ^aThiophenols (**9a-c**) (1 equiv.), **4a-e** (1.5 equiv.) and MeSO_3H (10 mol%) in DCM (5 mL) at rt under open air, ^bYields are expressed in percentage with respect to thiophenol

In order to examine the regioselectivity of $-\text{OH}$ and $-\text{SH}$ group, we applied optimized reaction condition to 4-hydroxy thiophenol (**11**). On reaction of D-A cyclopropane (**4c**) with 4-hydroxy thiophenol (**11**) using MeSO_3H as an acid catalyst, we obtained a product (**12**) in 79% yield. Nucleophilicity of thiol group is more than that of hydroxyl group, which resulted in the alkylation taking place *ortho*- to $-\text{SH}$ group (**Scheme 8**).



Scheme 8: Examination of the regioselectivity of $-\text{OH}$ and $-\text{SH}$ groups

It is presumed that the reaction leads through a dearomatization and rearomatization pathway in presence of methanesulfonic acid (MeSO_3H) affording highly regioselective product in moderate to good yield. Based on previous literature reports,²⁰ a plausible mechanism for this Brønsted acid catalysed reaction is depicted in **Scheme 9**. Methane sulphonic acid (MeSO_3H) acts as an activating agent for cyclopropanes to produce intermediate **A** by protonation of the carbonyl group attached to the cyclopropane ring in preliminary stage. Protonation of carbonyl group leads to the polarization of C–C bond in D–A cyclopropane. Further ring opening of cyclopropane took place by Friedel Craft mechanism by phenols offering intermediate **B** which results in final alkylation product by subsequent proton transfer (**Figure 4**).²⁰



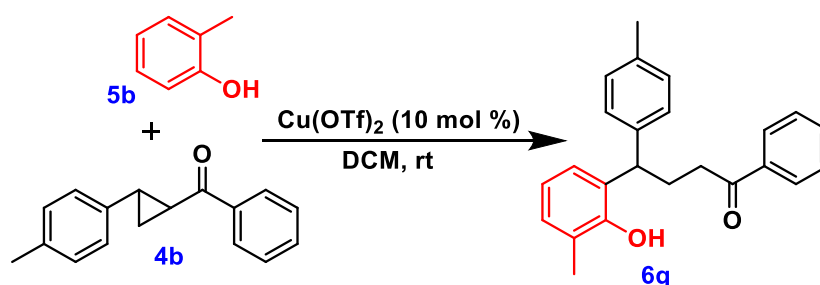
Scheme 9: Plausible mechanism

2.2.1 Preliminary studies towards the enantioselective Friedel-Crafts adducts

Since we obtained racemic product on reaction of D-A cyclopropanes with phenol catalysed by MeSO_3H , we opined that it would of interest to study this reaction for the enantioselective product formation by carrying out this presence of Lewis acid using chiral ligands. We used *R*-(-)-mandelic acid, (-)-quinine, *L*-(+)-tartaric acid, *R*-BINOL and *R*-BINAP as chiral ligands and $\text{Cu}(\text{OTf})_2$ as Lewis acid (**Table 5**). In case of reaction with *R*-(-)-mandelic acid, *L*-(+)-

tartaric acid and *R*-BINAP furnished the alkylated products (**6q1-3**). Each alkylated products (**6q1-3**) were subjected to chiral HPLC for the estimation of enantiomeric excess (*ee*). Chiral HPLC (using CHIRALART AMYLOSE SA and 10% isopropanol in hexane as eluent system) of product (**6q-3**) showed only 2.6% *ee* whereas products (**6q1-2**) did not show any *ee*.

Table 5: Optimization of the enantioselective reaction conditions



Entry	Ligand (10 mol%)	Time (hours)	Product (Yields%)	<i>ee</i> (%)
1	<i>R</i> -(-)-Mandelic acid	3 h	6q-1 (80)	No
2	(-)-Quinine	24 h	No reaction	-
3	L-(+) Tartaric acid	3 h	6q-2 (80)	No
4	<i>R</i> -BINOL	24 h	No reaction	-
5	<i>R</i> -BINAP	3 h	6q-3 (80)	2.6

2.3 Conclusions

In conclusion, regioselective Brønsted acid catalyzed ring-opening reactions of D–A cyclopropanes with various phenols have been studied. The Friedel–Crafts-type adducts were synthesized by utilizing biodegradable²¹ MeSO₃H as the Brønsted acid which lead to the functionalized phenylbutan–1–one motifs in moderate to good yields. Also, reaction of D–A cyclopropanes with *ortho*-position blocked phenols resulted in the formation of exclusive *para*-functionalized products. We have extended our developed synthetic protocol for reaction with thiophenols and obtained alkylated products in good yields. Our developed

synthetic protocol is cost effective, transition-metal and additives free, uses biodegradable acid catalyst, and is a versatile method for synthesis of these chemical frameworks.

1.4 Experimental procedures

General Procedure for the synthesis of Chalcones (3a-3h):

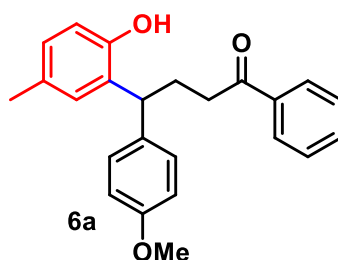
A dry round-bottom flask was charged with a mixture of acetophenone (**2**) (1.94 mL, 16.66 mmol, 1.0 equiv.) and 4-methoxy benzaldehyde (**1a**) (2.492 mL, 18.326 mmol, 1.1 equiv.) dissolved in methanol (20 mL) at 0 °C and was vigorously stirred for 10 mins at same temperature. To this solution KOH (2.798 g, 49.98 mmol, 3 equiv.) was added while maintaining the temperature at 0°C and then the reaction mixture was stirred at rt for 5 h. After completion of the reaction (monitored by TLC) aqueous HCL (2M) was added to the pH at 7 and was this reaction mixture was further diluted with DCM (30 mL). The resulting solution was extracted twice with DCM (30 mL) and washed with water. The organic layer obtained was dried over anhydrous sodium sulphate (Na₂SO₄), concentrated *in vacuo* to furnish a residue which was purified by flash chromatography using a RediSep column (SiO₂, 12g) with EtOAc-petroleum ether mixture as eluent. The spectral data (¹H and ¹³C) and yields of all the synthesized chalcones (**3a-3h**) were in agreement with the reported literature data.¹⁹

General Procedure for the synthesis of D–A cyclopropyl ketones (4a-4h):

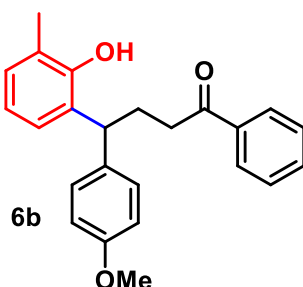
To a stirred solution of trimethyl sulfoxonium iodide (1.02 g, 4.6218 mmol, 1.1 equiv.) and NaH (184.872 mg, 4.618 mmol, 1.1 equiv.) in DMSO (10 mL) chalcone (**3a**) (1 g, 4.201 mmol, 1 equiv.) dissolved in DMSO (10 mL) was added slowly at 0°C and were stirred at rt for 4 hours. After completion of the reaction (monitored by TLC) the reaction mixture was quenched with cold water and then extracted twice with diethyl ether (30-40 mL). The organic layer was dried over anhydrous sodium sulphate (Na₂SO₄) and concentrated *in vacuo* to furnish a crude mixture which was further purified *via* flash chromatography using a RediSep column (SiO₂, 12g) with EtOAc-petroleum ether mixture as eluent to afford desired compound (**4a-4h**). The physical and spectral data (¹H and ¹³C) of all the synthesized cyclopropyl ketones (**4a-4h**) were consistent with those previously reported data.¹⁹

General Procedure for the functionalization of phenol with D–A cyclopropyl ketones (6a–6u):

To a dry round bottom flask *p*-cresol (**3**) (29 mL, 0.277 mmol, 1 equiv.) and D–A cyclopropyl ketones (**4a**) (104.7 mg, 0.415 mmol, 1.5 equiv.) were dissolved in DCM (5 mL) at rt with a catalytic amount of MeSO₃H (20 mol %) and the reaction mixture was stirred at rt for 3 h. After the completion of the reaction (monitored by TLC) the reaction mixture was reduced *in vacuo* to furnish crude compound mixture which was further purified by using flash chromatography using a RediSep column (SiO₂, 12g) with EtOAc-petroleum ether mixture as eluent to afford desired compound.

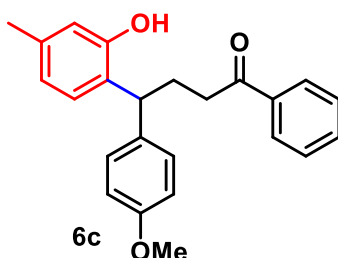
4-(2-hydroxy-5-methylphenyl)-4-(4-methoxyphenyl)-1-phenylbutan-1-one (6a):

Yellowish solid (80 mg, 80%); m.p.: 122–124 °C; *R*_f 0.15 (20% ethyl acetate in petroleum ether); ¹H NMR (400 MHz, CDCl₃) δ _H 7.89 (dd, *J* = 8.4, 1.4 Hz, 2H), 7.54–7.48 (m, 1H), 7.40 (dd, *J* = 8.3, 7.0 Hz, 2H), 7.24–7.20 (m, 2H), 7.18–7.13 (m, 1H), 6.85 (d, *J* = 8.7 Hz, 2H), 6.77 (d, *J* = 8.1 Hz, 2H), 6.64 (s, 1H), 4.30–4.22 (m, 1H), 3.76 (s, 3H), 3.03–2.95 (m, 2H), 2.41 (td, *J* = 15.2, 14.7, 7.9 Hz, 2H), 2.18 (s, 3H); ¹³C NMR (101 MHz, CDCl₃) δ _C 201.43, 158.14, 151.65, 136.52, 134.35, 133.29, 130.75, 129.42, 129.33, 128.97, 128.50, 128.25, 128.16, 128.13, 127.83, 116.06, 113.94, 55.14, 42.50, 36.29, 28.84, 20.65; *m/z* for C₂₄H₂₄O₃Na (M + Na)⁺, calcd: 383.1622, found: 383.1615.

4-(2-hydroxy-3-methylphenyl)-4-(4-methoxyphenyl)-1-phenylbutan-1-one (6b):

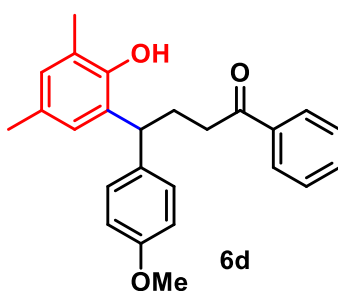
Yellowish solid (78 mg, 78%); m.p.: 82-84 °C; R_f 0.30 (20% ethyl acetate in petroleum ether); $^1\text{H NMR}$ (400 MHz, CDCl_3) δ_{H} 7.90 (d, $J = 7.6$ Hz, 2H), 7.55 (t, $J = 7.2$ Hz, 1H), 7.44 (t, $J = 7.6$ Hz, 2H), 7.21 (d, $J = 8.5$ Hz, 2H), 7.03 (s, 1H), 6.97 (d, $J = 8.1$ Hz, 1H), 6.87 (d, $J = 8.5$ Hz, 2H), 6.76 (d, $J = 8.1$ Hz, 1H), 5.92 (s, 1H), 3.90 (t, $J = 7.8$ Hz, 1H), 3.80 (s, 3H), 2.97 (t, $J = 7.4$ Hz, 2H), 2.47 (dd, $J = 14.9, 7.6$ Hz, 2H), 2.25 (s, 3H); $^{13}\text{C NMR}$ (101 MHz, CDCl_3) δ_{C} 200.91, 157.78, 152.47, 137.10, 136.74, 136.48, 133.00, 130.30, 128.59, 128.44, 128.00, 125.90, 123.98, 114.89, 113.83, 55.14, 48.83, 37.03, 30.22, 15.91; HRMS: m/z for $\text{C}_{24}\text{H}_{24}\text{O}_3$ ($\text{M} + \text{H}$) $^+$, calcd: 361.1803, found: 361.1797.

4-(2-hydroxy-4-methylphenyl)-4-(4-methoxyphenyl)-1-phenylbutan-1-one (6c):



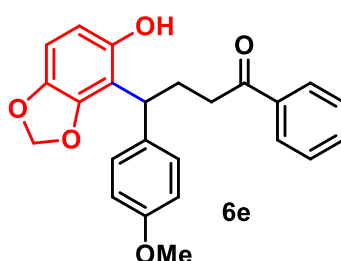
white solid (84 mg, 84%); m.p.: 149-152 °C; R_f 0.18 (20% ethyl acetate in petroleum ether); $^1\text{H NMR}$ (500 MHz, CDCl_3) δ_{H} 7.87 (d, $J = 8.0$ Hz, 2H), 7.54 (t, $J = 6.8$ Hz, 1H), 7.42 (t, $J = 7.4$ Hz, 2H), 7.19 (d, $J = 8.3$ Hz, 1H), 7.12 (d, $J = 8.2$ Hz, 2H), 6.82 (d, $J = 8.3$ Hz, 2H), 6.71 (d, $J = 8.3$ Hz, 1H), 6.65 (s, 1H), 5.67 (s, 1H), 4.08 (t, $J = 7.8$ Hz, 1H), 3.77 (s, 3H), 3.03–2.90 (m, 2H), 2.41 (dd, $J = 14.9, 7.4$ Hz, 2H), 2.19 (s, 3H); $^{13}\text{C NMR}$ (126 MHz, CDCl_3) δ_{C} 200.69, 157.76, 153.88, 137.92, 136.84, 136.53, 134.44, 133.02, 128.97, 128.51, 128.02, 127.47, 117.47, 113.77, 112.80, 55.19, 44.57, 36.92, 30.61, 19.84; m/z for $\text{C}_{24}\text{H}_{24}\text{O}_3\text{Na}$ ($\text{M} + \text{Na}$) $^+$, calcd: 383.1622, found: 383.1623.

4-(2-hydroxy-3,5-dimethylphenyl)-4-(4-methoxyphenyl)-1-phenylbutan-1-one (6d):



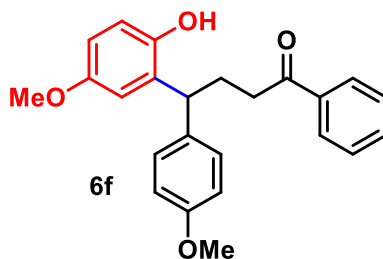
Yellowish viscous liquid (80 mg, 80%); R_f 0.32 (20% ethyl acetate in petroleum ether); ^1H NMR (400 MHz, CDCl_3) δ_{H} 7.98–7.92 (m, 2H), 7.57 (t, $J = 7.4$ Hz, 1H), 7.45 (t, $J = 7.7$ Hz, 2H), 7.25 (d, $J = 8.6$ Hz, 2H), 6.92–6.88 (m, 2H), 6.84 (s, 1H), 6.73 (s, 1H), 6.60 (s, 1H), 4.24 (dd, $J = 9.9, 5.0$ Hz, 1H), 3.82 (s, 3H), 3.08–2.99 (m, 2H), 2.46 (ddt, $J = 11.0, 8.2, 5.6$ Hz, 1H), 2.36 (ddd, $J = 15.2, 10.9, 5.6$ Hz, 1H), 2.28 (s, 3H), 2.19 (s, 3H); ^{13}C NMR (101 MHz, CDCl_3) δ_{C} 201.52, 158.29, 149.95, 136.52, 133.97, 133.40, 130.23, 129.58, 129.54, 128.65, 128.56, 128.18, 125.79, 124.56, 114.03, 55.18, 42.89, 36.08, 28.73, 20.64, 16.19; HRMS: m/z for $\text{C}_{25}\text{H}_{26}\text{O}_3\text{Na}$ ($\text{M} + \text{Na}$) $^+$, calcd: 397.1779, found: 397.1768.

4-(4-hydroxybenzo[d][1,3]dioxol-5-yl)-4-(4-methoxyphenyl)-1-phenylbutan-1-one (6e):



Brown liquid (78 mg, 78%); R_f 0.12 (20% ethyl acetate in petroleum ether); ^1H NMR (400 MHz, CDCl_3) δ_{H} 7.98–7.91 (m, 2H), 7.59–7.53 (m, 1H), 7.44 (dd, $J = 8.3, 7.1$ Hz, 2H), 7.20 (d, $J = 8.6$ Hz, 2H), 6.87 (d, $J = 8.7$ Hz, 2H), 6.51 (s, 1H), 6.36 (s, 1H), 5.83 (dd, $J = 8.7, 1.5$ Hz, 2H), 4.17 (dd, $J = 9.1, 5.8$ Hz, 1H), 3.80 (s, 3H), 3.02 (dd, $J = 6.8, 5.6$ Hz, 2H), 2.40–2.28 (m, 2H); ^{13}C NMR (101 MHz, CDCl_3) δ_{C} 201.70, 136.43, 133.56, 129.47, 128.62, 128.26, 114.14, 107.24, 100.86, 99.00, 77.00, 55.26, 42.31, 35.86, 28.80; HRMS: m/z for $\text{C}_{24}\text{H}_{22}\text{O}_5\text{Na}$ ($\text{M} + \text{Na}$) $^+$, calcd: 413.1364, found: 413.1354.

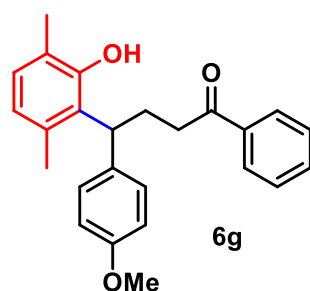
4-(2-hydroxy-5-methoxyphenyl)-4-(4-methoxyphenyl)-1-phenylbutan-1-one (6f):



Brown liquid (63 mg, 69%); R_f 0.32 (20% ethyl acetate in petroleum ether); ^1H NMR (400 MHz, CDCl_3) δ_{H} 7.96–7.90 (m, 2H), 7.59–7.51 (m, 1H), 7.47–7.40 (m, 2H), 7.24–7.20 (m,

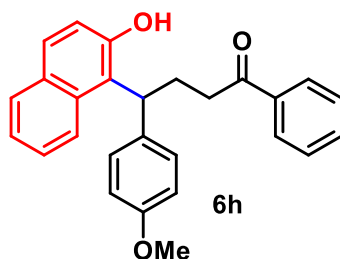
2H), 6.89–6.80 (m, 3H), 6.65 (dd, $J = 8.7, 3.0$ Hz, 1H), 6.52 (d, $J = 3.0$ Hz, 1H), 6.41 (s, 1H), 4.23 (dd, $J = 9.5, 5.5$ Hz, 1H), 3.79 (s, 3H), 3.68 (s, 3H), 3.02 (t, $J = 6.4$ Hz, 2H), 2.38 – 2.30 (m, 2H); ^{13}C NMR (101 MHz, CDCl_3) δ_{C} 201.34, 158.38, 153.37, 148.00, 136.53, 133.71, 133.42, 132.26, 129.51, 128.59, 128.20, 116.90, 114.16 (d, $J = 11.9$ Hz), 111.72, 66.80, 55.61, 55.24, 42.85, 36.09; HRMS: m/z for $\text{C}_{24}\text{H}_{24}\text{O}_4$ ($\text{M} + \text{H}$) $^+$, calcd: 377.1747, found: 377.1739.

4-(2-hydroxy-3,6-dimethylphenyl)-4-(4-methoxyphenyl)-1-phenylbutan-1-one (6g):



white semisolid (79 mg, 86%); R_f 0.24 (20% ethyl acetate in petroleum ether); ^1H NMR (400 MHz, CDCl_3) δ_{H} 7.91–7.87 (m, 2H), 7.58–7.53 (m, 1H), 7.44 (t, $J = 7.7$ Hz, 2H), 7.17–7.12 (m, 2H), 7.08 (s, 1H), 6.86–6.80 (m, 2H), 6.58 (s, 1H), 4.70 (s, 1H), 4.07 (t, $J = 7.8$ Hz, 1H), 3.79 (s, 3H), 2.97 (dt, $J = 8.0, 6.3$ Hz, 2H), 2.46–2.38 (m, 2H), 2.25 (s, 3H), 2.19 (s, 3H); ^{13}C NMR (101 MHz, CDCl_3) δ_{C} 200.35, 157.77, 151.78, 136.94, 136.63, 135.17, 134.59, 132.94, 129.01, 128.96, 128.50, 128.02, 120.87, 117.04, 113.76, 55.20, 44.53, 36.98, 30.61, 19.38, 15.57; HRMS: m/z for $\text{C}_{25}\text{H}_{26}\text{O}_3\text{Na}$ ($\text{M} + \text{Na}$) $^+$, calcd: 397.1774, found: 397.1767.

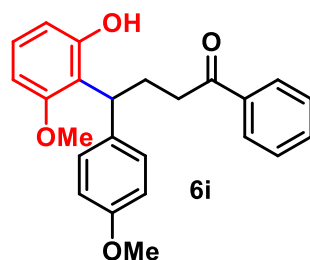
4-(2-hydroxynaphthalen-1-yl)-4-(4-methoxyphenyl)-1-phenylbutan-1-one (6h):



Brown liquid (58 mg, 70%); R_f 0.21 (20% ethyl acetate in petroleum ether); ^1H NMR (400 MHz, CDCl_3) δ_{H} 7.95 (d, $J = 7.0$ Hz, 1H), 7.76 (d, $J = 7.6$ Hz, 3H), 7.68 (d, $J = 8.8$ Hz, 1H), 7.49 (t, $J = 7.4$ Hz, 1H), 7.33 (dt, $J = 12.1, 5.6$ Hz, 6H), 7.09 (d, $J = 8.7$ Hz, 1H), 6.83 (d, $J = 8.6$ Hz, 2H), 5.17–5.05 (m, 1H), 3.77 (s, 3H), 2.98–2.84 (m, 3H), 2.78–2.66 (m, 1H); ^{13}C

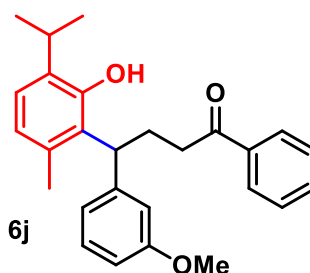
NMR (126 MHz, CDCl_3) δ_{C} 201.04, 158.08, 152.21, 136.68, 134.95, 133.01, 129.78, 128.97, 128.81, 128.46, 128.43, 128.05, 126.39, 123.01, 121.78, 119.28, 114.13, 55.20, 38.91, 36.54, 26.17; m/z for $\text{C}_{27}\text{H}_{24}\text{O}_3\text{Na}$ ($\text{M} + \text{Na}$)⁺, calcd: 419.1622, found: 419.1609.

4-(2-hydroxy-6-methoxyphenyl)-4-(4-methoxyphenyl)-1-phenylbutan-1-one (6i):



white solid (53 mg, 59%); m.p.: 144-147 °C; R_f 0.08 (20% ethyl acetate in petroleum ether); ^1H NMR (400 MHz, CDCl_3) δ_{H} 7.97–7.90 (m, 2H), 7.60–7.53 (m, 1H), 7.44 (dd, $J = 8.3, 7.1$ Hz, 2H), 7.21 (d, $J = 8.6$ Hz, 2H), 7.05 (s, 1H), 6.91–6.85 (m, 2H), 6.77 (d, $J = 8.5$ Hz, 1H), 6.50 (d, $J = 2.6$ Hz, 1H), 6.37 (dd, $J = 8.5, 2.6$ Hz, 1H), 4.15 (dd, $J = 9.7, 5.1$ Hz, 1H), 3.80 (s, 3H), 3.75 (s, 3H), 3.07–2.99 (m, 2H), 2.48–2.25 (m, 2H); ^{13}C NMR (101 MHz, CDCl_3) δ_{C} 201.72, 159.27, 155.09, 136.49, 133.90, 133.52, 129.58, 128.61, 128.39, 128.24, 114.06, 105.81, 102.29, 55.25, 42.27, 36.00, 28.77; HRMS: m/z for $\text{C}_{24}\text{H}_{24}\text{O}_4\text{Na}$ ($\text{M} + \text{Na}$)⁺, calcd: 399.1572, found: 399.1572.

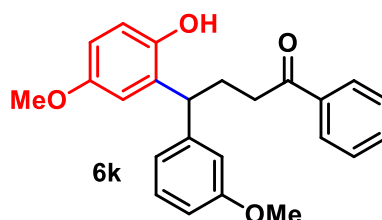
4-(2-hydroxy-3-isopropyl-6-methylphenyl)-4-(3-methoxyphenyl)-1-phenylbutan-1-one (6j):



white solid (71 mg, 88%); m.p.: 88-90 °C; R_f 0.08 (20% ethyl acetate in petroleum ether); ^1H NMR (500 MHz, CDCl_3) δ_{H} 7.90–7.86 (m, 2H), 7.55 (t, $J = 7.4$ Hz, 1H), 7.43 (t, $J = 7.7$ Hz, 2H), 7.20 (s, 1H), 7.12–7.07 (m, 4H), 6.54 (s, 1H), 4.92 (d, $J = 5.7$ Hz, 1H), 4.09 (t, $J = 7.9$ Hz, 1H), 3.21 (dt, $J = 13.8, 6.9$ Hz, 1H), 3.04–2.89 (m, 2H), 2.45 (q, $J = 7.6$ Hz, 2H), 2.31 (s, 3H), 2.16 (s, 3H), 1.28 (t, $J = 7.2$ Hz, 6H); ^{13}C NMR (126 MHz, CDCl_3) δ_{C} 200.55, 150.81,

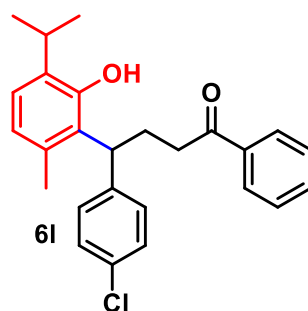
141.48, 135.41, 134.79, 134.28, 132.94, 131.67, 129.04, 128.49, 128.03, 127.91, 124.49, 117.48, 45.42, 37.06, 30.73, 27.09, 22.80, 22.66, 20.92, 19.25; HRMS: m/z for $C_{27}H_{30}O_3$ ($M - H$)⁺, calcd: 401.2111, found: 401.2106.

4-(2-Hydroxy-5-methoxyphenyl)-4-(3-methoxyphenyl)-1-phenylbutan-1-one (6k):



Viscous liquid (50 mg, 55%); R_f 0.33 (20% ethyl acetate in petroleum ether); 1H NMR (400 MHz, $CDCl_3$) δ_H 7.93 (d, $J = 7.6$ Hz, 2H), 7.56 (t, $J = 7.1$ Hz, 1H), 7.44 (t, $J = 7.3$ Hz, 2H), 7.21 (d, $J = 7.8$ Hz, 1H), 7.06 (s, 1H), 6.88 (d, $J = 7.9$ Hz, 2H), 6.79 (d, $J = 8.4$ Hz, 1H), 6.50 (s, 1H), 6.38 (d, $J = 8.5$ Hz, 1H), 4.17 (dd, $J = 8.7, 4.9$ Hz, 1H), 3.86–3.70 (m, 6H), 3.03 (s, 2H), 2.37 (ddd, $J = 14.6, 11.3, 6.3$ Hz, 2H); ^{13}C NMR (101 MHz, $CDCl_3$) δ_C 201.69, 159.24, 158.31, 155.06, 134.04, 133.47, 129.54, 128.59, 128.40, 128.22, 123.45, 114.05, 105.80, 102.28, 55.22, 42.25, 36.06, 28.81; HRMS: m/z for $C_{24}H_{24}O_4$ ($M + H$)⁺, calcd: 377.1747, found: 377.1739.

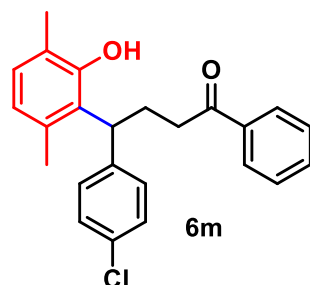
4-(4-chlorophenyl)-4-(2-hydroxy-3-isopropyl-6-methylphenyl)-1-phenylbutan-1-one (6l):



Viscous liquid (63 mg, 78%); R_f 0.28 (20% ethyl acetate in petroleum ether); 1H NMR (400 MHz, $CDCl_3$) δ_H 7.85 (d, $J = 7.6$ Hz, 2H), 7.52 (t, $J = 7.1$ Hz, 1H), 7.40 (t, $J = 7.5$ Hz, 2H), 7.21 (d, $J = 8.2$ Hz, 2H), 7.11 (d, $J = 8.8$ Hz, 3H), 6.54 (s, 1H), 5.21 (s, 1H), 4.09 (t, $J = 7.7$ Hz, 1H), 3.27–3.13 (m, 1H), 3.01–2.85 (m, 2H), 2.42 (dd, $J = 14.8, 7.4$ Hz, 2H), 2.09 (s, 3H), 1.24 (t, $J = 6.4$ Hz, 6H); ^{13}C NMR (101 MHz, $CDCl_3$) δ_C 200.33, 151.15, 143.18, 136.78, 134.77, 133.32, 133.11, 133.07, 131.97, 129.35, 128.64, 128.57, 128.53, 128.45, 127.98,

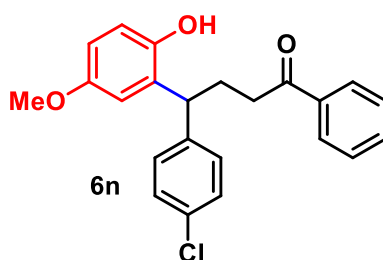
124.44, 117.60, 45.13, 36.75, 30.43, 27.06, 22.76, 22.64, 19.20; HRMS: m/z for $C_{26}H_{27}O_2Cl$ ($M + H$)⁺, calcd: 407.1778, found: 407.1785.

4-(4-chlorophenyl)-4-(2-hydroxy-3,6-dimethylphenyl)-1-phenylbutan-1-one (6m):

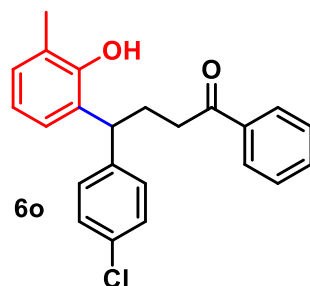


white solid (70 mg, 76%); m.p.: 128-130 °C; R_f 0.15 (20% ethyl acetate in petroleum ether); 1H NMR (400 MHz, $CDCl_3$) δ_H 7.85 (dd, $J = 8.4, 1.4$ Hz, 2H), 7.57–7.51 (m, 1H), 7.42 (ddd, $J = 8.1, 6.7, 1.3$ Hz, 2H), 7.25–7.20 (m, 2H), 7.16–7.11 (m, 2H), 7.03 (s, 1H), 6.56 (s, 1H), 4.60 (s, 1H), 4.08 (t, $J = 7.8$ Hz, 1H), 2.94 (d, $J = 5.5$ Hz, 2H), 2.40 (d, $J = 7.6$ Hz, 2H), 2.22 (s, 3H), 2.14 (s, 3H); ^{13}C NMR (101 MHz, $CDCl_3$) δ_C 152.00, 143.16, 135.28, 133.65, 133.05, 131.72, 129.39, 129.04, 128.55, 128.50, 127.98, 121.07, 117.15, 44.71, 36.72, 19.38, 15.56; HRMS: m/z for $C_{24}H_{23}O_2ClNa$ ($M + Na$)⁺, calcd: 401.1284, found: 401.1276.

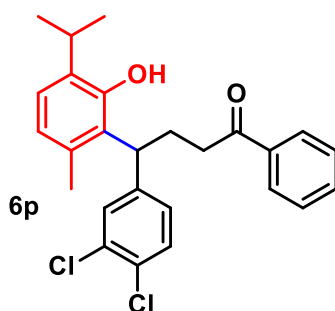
4-(4-chlorophenyl)-4-(2-hydroxy-5-methoxyphenyl)-1-phenylbutan-1-one (6n):



Viscous liquid (59 mg, 64%); R_f 0.24 (20% ethyl acetate in petroleum ether); 1H NMR (400 MHz, $CDCl_3$) δ_H 7.93–7.88 (m, 2H), 7.57–7.52 (m, 1H), 7.44–7.40 (m, 2H), 7.26–7.24 (m, 3H), 7.20–7.16 (m, 1H), 6.80 (d, $J = 8.7$ Hz, 1H), 6.64 (dd, $J = 8.7, 3.1$ Hz, 1H), 6.53 (d, $J = 3.0$ Hz, 1H), 6.37 (s, 1H), 4.31 (dd, $J = 9.0, 6.2$ Hz, 1H), 3.68 (s, 3H), 2.99 (t, $J = 6.7$ Hz, 2H), 2.45–2.35 (m, 2H); ^{13}C NMR (101 MHz, $CDCl_3$) δ_C 201.07, 153.48, 147.81, 140.93, 136.46, 133.44, 132.31, 131.50, 129.78, 128.68, 128.60, 128.15, 116.82, 114.16, 111.86, 55.61, 42.77, 36.09, 28.55; HRMS: m/z for $C_{23}H_{21}ClO_3$ ($M + H$)⁺, calcd: 381.1252, found: 381.1245.

4-(4-chlorophenyl)-4-(2-hydroxy-3-methylphenyl)-1-phenylbutan-1-one (6o):

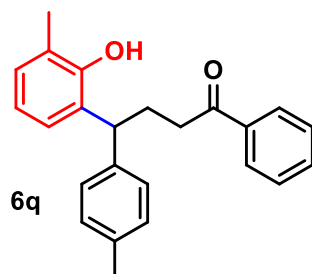
semisolid (80 mg, 79%); R_f 0.35 (20% ethyl acetate in petroleum ether); ^1H NMR (400 MHz, CDCl_3) δ_{H} 7.87–7.82 (m, 2H), 7.56–7.51 (m, 1H), 7.45–7.39 (m, 3H), 7.23 (d, $J = 2.2$ Hz, 1H), 7.17 (d, $J = 8.5$ Hz, 2H), 6.97–6.91 (m, 2H), 6.70 (d, $J = 8.1$ Hz, 1H), 3.89 (t, $J = 7.9$ Hz, 1H), 2.91 (dd, $J = 8.0, 6.8$ Hz, 2H), 2.42 (td, $J = 7.9, 6.9$ Hz, 2H), 2.20 (s, 3H); ^{13}C NMR (101 MHz, CDCl_3) δ_{C} 152.48, 143.50, 136.83, 135.88, 133.06, 131.88, 130.40, 129.87, 129.08, 128.68, 128.60, 128.54, 128.50, 128.38, 128.17, 127.98, 127.95, 126.16, 123.98, 115.00, 49.03, 36.78, 29.85, 15.87; HRMS: m/z for $\text{C}_{23}\text{H}_{21}\text{O}_2\text{Cl}$ ($\text{M} + \text{H}$) $^+$, calcd: 365.1308, found: 365.1300.

4-(3,4-dichlorophenyl)-4-(2-hydroxy-3-isopropyl-6-methylphenyl)-1-phenylbutan-1-one (6p):

Viscous liquid (66 mg, 75%); R_f 0.43 (20% ethyl acetate in petroleum ether); ^1H NMR (400 MHz, CDCl_3) δ_{H} 7.88–7.83 (m, 2H), 7.57–7.52 (m, 1H), 7.43 (dd, $J = 8.3, 7.0$ Hz, 2H), 7.32 (d, $J = 8.3$ Hz, 1H), 7.26 (s, 1H), 7.10 (s, 1H), 7.03 (dd, $J = 8.4, 2.1$ Hz, 1H), 6.54 (d, $J = 0.8$ Hz, 1H), 4.75 (s, 1H), 4.10 (t, $J = 7.8$ Hz, 1H), 3.17 (p, $J = 6.9$ Hz, 1H), 3.02–2.84 (m, 2H), 2.41 (q, $J = 7.4$ Hz, 2H), 2.12 (s, 3H), 1.28–1.24 (m, 6H); ^{13}C NMR (101 MHz, CDCl_3) δ_{C} 145.16, 134.92, 133.12, 132.72, 130.28, 129.99, 128.59, 127.97, 127.41, 124.51, 117.71,

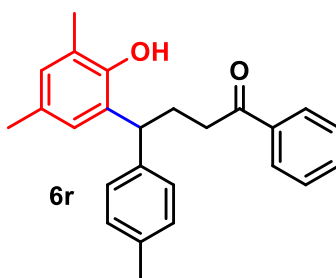
44.90, 36.53, 30.24, 27.13, 22.75, 22.64, 19.26; HRMS: m/z for $C_{26}H_{26}O_2Cl_2$ ($M + H$)⁺, calcd: 441.1383, found: 441.1370.

4-(2-hydroxy-3-methylphenyl)-1-phenyl-4-(*p*-tolyl) butan-1-one (6q):



semisolid (76 mg, 80%); R_f 0.33 (20% ethyl acetate in petroleum ether); 1H NMR (400 MHz, $CDCl_3$) δ_H 7.83 (dd, $J = 8.4, 1.4$ Hz, 2H), 7.52–7.47 (m, 1H), 7.37 (dd, $J = 8.4, 7.0$ Hz, 2H), 7.15–7.11 (m, 2H), 7.07 (d, $J = 7.9$ Hz, 2H), 6.98 (d, $J = 2.2$ Hz, 1H), 6.92 (dd, $J = 8.2, 2.3$ Hz, 1H), 6.69 (d, $J = 8.1$ Hz, 1H), 3.85 (t, $J = 7.9$ Hz, 1H), 2.91 (dd, $J = 8.3, 6.7$ Hz, 2H), 2.47–2.38 (m, 2H), 2.28 (s, 3H), 2.18 (s, 3H); ^{13}C NMR (101 MHz, $CDCl_3$) δ_C 152.42, 141.88, 136.77, 136.47, 135.57, 132.98, 130.35, 129.14, 128.45, 128.42, 128.01, 127.55, 125.99, 114.89, 77.00, 49.31, 37.08, 30.08, 20.90, 15.91; HRMS: m/z for $C_{24}H_{24}O_2Na$ ($M + Na$)⁺, calcd: 367.1673, found: 367.1684.

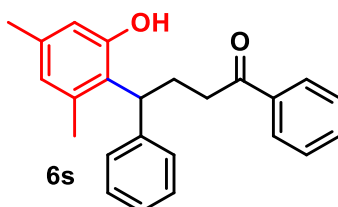
4-(2-hydroxy-3,5-dimethylphenyl)-1-phenyl-4-(*p*-tolyl)butan-1-one (6r):



white solid (73 mg, 83%); m.p.: 122–124 °C; R_f 0.29 (20% ethyl acetate in petroleum ether); 1H NMR (400 MHz, $CDCl_3$) δ_H 7.89–7.82 (m, 2H), 7.55–7.50 (m, 1H), 7.45–7.37 (m, 2H), 7.12–7.04 (m, 5H), 6.54 (s, 1H), 4.06 (t, $J = 7.8$ Hz, 1H), 2.94 (ddd, $J = 8.2, 6.3, 4.1$ Hz, 2H), 2.45–2.35 (m, 2H), 2.29 (s, 3H), 2.21 (s, 3H), 2.16 (s, 3H); ^{13}C NMR (101 MHz, $CDCl_3$) δ_C 200.37, 151.78, 141.47, 135.46, 135.17, 134.49, 132.92, 129.07, 128.49, 128.02, 127.91,

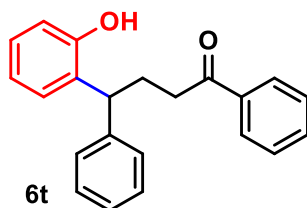
120.87, 117.01, 44.95, 37.01, 30.52, 20.94, 19.41, 15.57; HRMS: m/z for $C_{25}H_{26}O_2Na$ ($M + Na$)⁺, calcd: 381.1830, found: 381.1831.

4-(2-hydroxy-4,6-dimethylphenyl)-1,4-diphenylbutan-1-one (6s):

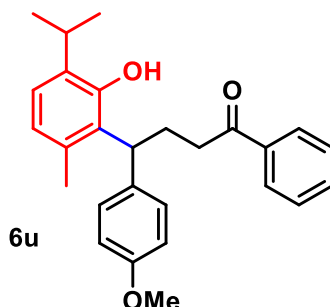


white solid (73 mg, 86%); m.p.: 127-129 °C; R_f 0.5 (20% ethyl acetate in petroleum ether); 1H NMR (400 MHz, $CDCl_3$) δ_H 7.86 (dd, $J = 8.4, 1.3$ Hz, 2H), 7.55–7.50 (m, 1H), 7.41 (dd, $J = 8.3, 7.0$ Hz, 2H), 7.34 (dt, $J = 8.2, 1.1$ Hz, 2H), 7.28 (dd, $J = 8.5, 6.8$ Hz, 2H), 7.21–7.16 (m, 1H), 6.59–6.56 (m, 1H), 6.46 (d, $J = 1.8$ Hz, 1H), 4.94 (s, 1H), 4.54 (dd, $J = 9.9, 6.1$ Hz, 1H), 3.00–2.94 (m, 2H), 2.78–2.68 (m, 1H), 2.66–2.55 (m, 1H), 2.22 (s, 6H); ^{13}C NMR (101 MHz, $CDCl_3$) δ_C 200.69, 154.34, 143.31, 138.02, 137.33, 136.86, 132.97, 128.52, 128.48, 128.07, 127.49, 126.20, 125.62, 124.41, 115.75, 36.67, 25.90, 20.90, 20.81; HRMS: m/z for $C_{24}H_{24}O_2Na$ ($M + Na$)⁺, calcd: 367.1673, found: 367.1667.

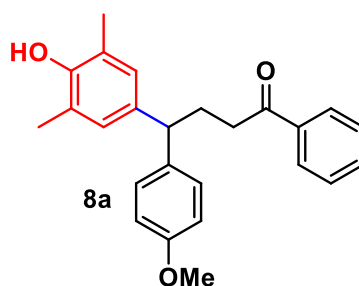
4-(2-hydroxyphenyl)-1,4-diphenylbutan-1-one (6t):



white solid (80 mg, 80%); m.p.: 102-104 °C; R_f 0.5 (20% ethyl acetate in petroleum ether); 1H NMR (400 MHz, $CDCl_3$) δ_H 7.88–7.81 (m, 2H), 7.55–7.49 (m, 1H), 7.43–7.37 (m, 2H), 7.30–7.22 (m, 4H), 7.11 (d, $J = 8.5$ Hz, 2H), 6.76 (d, $J = 8.5$ Hz, 2H), 5.43 (s, 1H), 3.94 (t, $J = 8.0$ Hz, 1H), 2.92 (dd, $J = 8.2, 6.8$ Hz, 2H), 2.46 (td, $J = 8.0, 6.8$ Hz, 2H); ^{13}C NMR (101 MHz, $CDCl_3$) δ_C 200.61, 154.14, 144.72, 136.80, 136.47, 133.07, 128.93, 128.52, 128.03, 127.76, 126.24, 115.39, 49.66, 36.96, 30.03; HRMS: m/z for $C_{22}H_{21}O_2$ ($M + H$)⁺, calcd: 317.1536, found: 317.1532.

4-(2-hydroxy-3-isopropyl-6-methylphenyl)-4-(4-methoxyphenyl)-1-phenylbutan-1-one (6u):

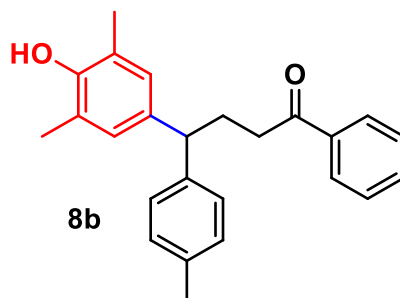
Viscous liquid (65 mg, 81%); R_f 0.34 (20% ethyl acetate in petroleum ether); $^1\text{H NMR}$ (500 MHz, CDCl_3) δ_{H} 7.90 (dd, $J = 8.4, 1.3$ Hz, 2H), 7.59 – 7.53 (m, 1H), 7.45 (dd, $J = 8.3, 7.2$ Hz, 2H), 7.20 (s, 1H), 7.15 (d, $J = 8.7$ Hz, 2H), 6.84 (d, $J = 8.7$ Hz, 2H), 6.59 – 6.55 (m, 1H), 5.18 (s, 1H), 4.10 (t, $J = 7.8$ Hz, 1H), 3.80 (s, 3H), 3.24 (p, $J = 6.9$ Hz, 1H), 3.07 – 2.91 (m, 2H), 2.45 (q, $J = 7.6$ Hz, 2H), 2.16 (s, 3H), 1.32 – 1.27 (m, 6H); $^{13}\text{C NMR}$ (126 MHz, CDCl_3) δ_{C} 200.67, 157.78, 150.95, 136.95, 136.75, 134.79, 134.36, 133.03, 131.80, 129.02, 128.56, 128.09, 124.46, 117.57, 113.81, 55.26, 45.06, 37.10, 30.89, 27.14, 22.88, 22.75, 19.29. HRMS: m/z for $\text{C}_{27}\text{H}_{30}\text{O}_3$ ($\text{M} - \text{H}$) $^+$, calcd: 401.2111, found: 401.2105.

4-(3-hydroxy-2,4-dimethylphenyl)-4-(4-methoxyphenyl)-1-phenylbutan-1-one (8a):

Viscous liquid (72 mg, 79%); R_f 0.32 (20% ethyl acetate in petroleum ether); $^1\text{H NMR}$ (400 MHz, CDCl_3) δ_{H} 7.89 (ddt, $J = 6.7, 2.5, 1.3$ Hz, 2H), 7.57 – 7.50 (m, 1H), 7.42 (td, $J = 7.6, 1.2$ Hz, 2H), 7.26 – 7.20 (m, 2H), 6.93 – 6.84 (m, 4H), 5.07 (s, 1H), 3.87 (td, $J = 7.8, 3.0$ Hz, 1H), 3.78 (d, $J = 1.7$ Hz, 3H), 2.95 (ddt, $J = 7.7, 6.1, 3.0$ Hz, 2H), 2.51 – 2.42 (m, 2H), 2.23 (t, $J = 3.1$ Hz, 6H); $^{13}\text{C NMR}$ (101 MHz, CDCl_3) δ_{C} 158.05, 137.44, 137.07, 136.43, 133.16, 133.14, 133.13, 128.81, 128.80, 128.66, 128.24, 128.22, 128.22, 127.97, 114.07, 114.05,

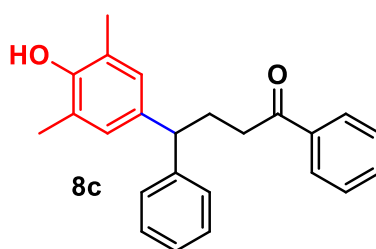
55.36, 49.15, 37.31, 30.47, 16.31, 16.29; HRMS: m/z for $C_{25}H_{26}O_3Na$ ($M + Na$)⁺, calcd: 397.1779, found: 397.1788.

4-(4-hydroxy-3,5-dimethylphenyl)-1-phenyl-4-(p-tolyl)butan-1-one (8b):

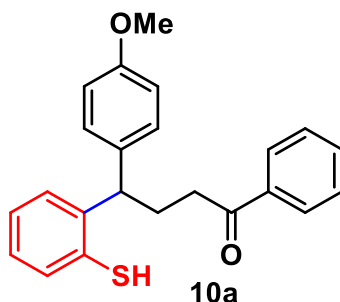


Viscous liquid (67 mg, 77%); R_f 0.48 (20% ethyl acetate in petroleum ether); 1H NMR (400 MHz, $CDCl_3$) δ_H 7.84 (dd, $J = 8.0, 2.0$ Hz, 2H), 7.52 – 7.46 (m, 1H), 7.41 – 7.35 (m, 2H), 7.15 (dd, $J = 8.3, 2.4$ Hz, 2H), 7.07 (dd, $J = 8.2, 2.0$ Hz, 2H), 6.85 (d, $J = 2.6$ Hz, 2H), 4.76 (s, 1H), 3.82 (td, $J = 8.0, 2.4$ Hz, 1H), 2.95 – 2.86 (m, 2H), 2.42 (qd, $J = 7.7, 2.5$ Hz, 2H), 2.28 (d, $J = 2.0$ Hz, 3H), 2.20 – 2.15 (m, 6H); ^{13}C NMR (101 MHz,) δ_C 200.58, 150.74, 142.15, 137.02, 136.27, 135.67, 133.02, 129.28, 128.56, 128.14, 127.94, 127.66, 123.18, 49.54, 37.25, 30.23, 21.05, 16.16; HRMS: m/z for $C_{25}H_{26}O_2$ ($M + H$)⁺, calcd: 359.2011, found: 359.2003.

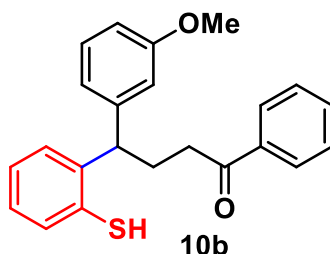
4-(4-hydroxy-3,5-dimethylphenyl)-1,4-diphenylbutan-1-one (8c):



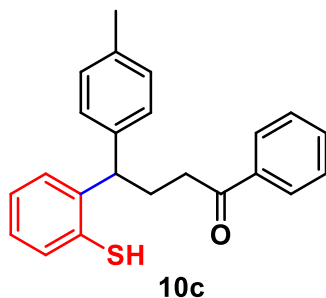
white solid (63 mg, 75%); m.p.: 102-104 °C; R_f 0.4 (20% ethyl acetate in petroleum ether); 1H NMR (400 MHz, $CDCl_3$) δ_H 7.88 – 7.78 (m, 2H), 7.46 (td, $J = 7.5, 1.7$ Hz, 1H), 7.34 (td, $J = 7.7, 7.1, 1.6$ Hz, 2H), 7.25 (dt, $J = 5.2, 3.0$ Hz, 4H), 7.18 – 7.10 (m, 1H), 6.90 – 6.82 (m, 2H), 3.91 – 3.81 (m, 1H), 2.96 – 2.84 (m, 2H), 2.50 – 2.39 (m, 2H), 2.21 – 2.12 (m, 6H); ^{13}C NMR (101 MHz, $CDCl_3$) δ_C 200.48, 145.00, 136.75, 135.73, 132.88, 128.39, 127.94, 127.79, 127.61, 126.04, 123.15, 49.72, 37.00, 29.99, 16.03, 16.00; HRMS: m/z for $C_{24}H_{24}O_2$ ($M + H$)⁺, calcd: 345.1854, found: 345.1855.

4-(2-mercaptophenyl)-4-(4-methoxyphenyl)-1-phenylbutan-1-one (10a):

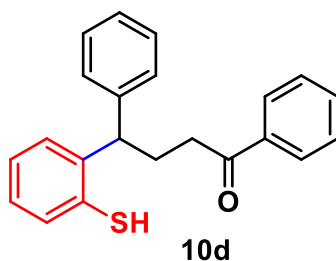
Viscous liquid (92 mg, 85%); R_f 0.68 (20% ethyl acetate in petroleum ether); ^1H NMR (400 MHz, CDCl_3) δ_{H} 7.87 (d, $J = 7.7$ Hz, 2H), 7.54 (t, $J = 6.8$ Hz, 1H), 7.43 (t, $J = 7.0$ Hz, 2H), 7.30 (d, $J = 7.6$ Hz, 2H), 7.24–7.19 (m, 4H), 6.82 (d, $J = 7.3$ Hz, 2H), 4.28 (t, $J = 7.2$ Hz, 1H), 3.79 (s, 3H), 3.02 (t, $J = 6.9$ Hz, 2H), 2.43 (dd, $J = 14.0, 7.0$ Hz, 1H), 2.33 (dt, $J = 14.1, 7.1$ Hz, 1H); ^{13}C NMR (101 MHz, CDCl_3) δ_{C} 199.36, 158.75, 136.80, 134.81, 133.36, 133.01, 132.28, 128.84, 128.69, 128.52, 127.96, 127.01, 113.87, 55.21, 52.02, 36.25, 30.63; HRMS: m/z for $\text{C}_{23}\text{H}_{22}\text{O}_2\text{SNa}$ ($\text{M} + \text{Na}$) $^+$, calcd: 385.1238, found: 385.1231.

4-(2-mercaptophenyl)-4-(3-methoxyphenyl)-1-phenylbutan-1-one (10b):

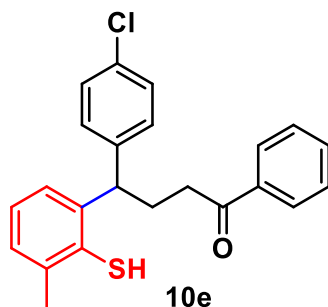
Viscous liquid (81 mg, 75%); R_f 0.71 (20% ethyl acetate in petroleum ether); ^1H NMR (400 MHz, CDCl_3) δ_{H} 7.87–7.81 (m, 2H), 7.54–7.47 (m, 1H), 7.39 (dd, $J = 8.4, 7.0$ Hz, 2H), 7.32–7.27 (m, 2H), 7.20–7.14 (m, 4H), 7.07 (d, $J = 7.8$ Hz, 2H), 4.28 (ddd, $J = 8.4, 6.6, 1.7$ Hz, 1H), 3.00 (t, $J = 7.2$ Hz, 2H), 2.47–2.37 (m, 1H), 2.30 (s, 4H); ^{13}C NMR (101 MHz, CDCl_3) δ_{C} ^{13}C NMR (101 MHz,) δ 199.30, 138.27, 136.91, 136.73, 134.90, 132.96, 132.01, 129.17, 128.66, 128.46, 127.91, 127.60, 126.90, 52.22, 36.20, 30.55, 21.03; HRMS: m/z for $\text{C}_{23}\text{H}_{22}\text{O}_2\text{SNa}$ ($\text{M} + \text{Na}$) $^+$, calcd: 385.1211, found: 385.1230.

4-(2-mercaptophenyl)-1-phenyl-4-(*p*-tolyl) butan-1-one (10c):

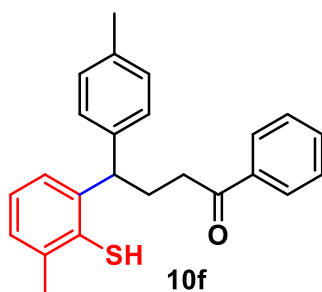
Viscous liquid (77 mg, 82%); R_f 0.75 (20% ethyl acetate in petroleum ether); ^1H NMR (400 MHz, CDCl_3) δ_{H} 7.85 (dd, $J = 7.9, 2.4$ Hz, 2H), 7.51 (t, $J = 7.4$ Hz, 1H), 7.40 (t, $J = 7.6$ Hz, 2H), 7.33–7.27 (m, 2H), 7.21–7.15 (m, 4H), 7.08 (dd, $J = 8.3, 2.7$ Hz, 2H), 4.28 (dd, $J = 6.0, 2.7$ Hz, 1H), 3.00 (td, $J = 7.2, 2.5$ Hz, 2H), 2.42 (dt, $J = 14.2, 7.1$ Hz, 1H), 2.37–2.28 (m, 4H); ^{13}C NMR (101 MHz, CDCl_3) δ_{C} 138.29, 136.94, 136.76, 132.99, 132.04, 129.20, 128.69, 128.49, 127.95, 127.62, 126.93, 52.25, 36.23, 30.58, 21.06; HRMS: m/z for $\text{C}_{23}\text{H}_{22}\text{OSNa}$ ($\text{M} + \text{Na}$) $^+$, calcd: 369.1288, found: 369.1299.

4-(2-mercaptophenyl)-1,4-diphenylbutan-1-one (10d):

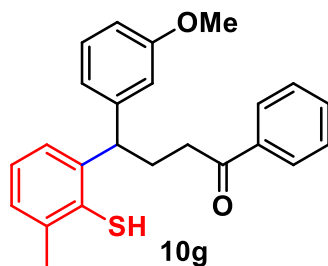
Viscous liquid (70 mg, 78%); R_f 0.6 (20% ethyl acetate in petroleum ether); ^1H NMR (400 MHz, CDCl_3) δ_{H} 7.93 (dd, $J = 7.3, 1.8$ Hz, 2H), 7.59 – 7.53 (m, 1H), 7.45 (dd, $J = 8.5, 7.0$ Hz, 3H), 7.37 (ddd, $J = 11.0, 7.3, 5.4$ Hz, 6H), 7.30 – 7.22 (m, 4H), 4.41 (ddt, $J = 8.1, 6.5, 2.6$ Hz, 1H), 3.09 (t, $J = 7.2$ Hz, 2H), 2.59 – 2.38 (m, 2H); ^{13}C NMR (101 MHz, CDCl_3) δ_{C} 199.31, 141.66, 136.88, 136.88, 133.17, 132.37, 128.88, 128.73, 128.67, 128.17, 128.09, 127.94, 127.49, 127.22, 52.76, 36.34, 30.67; HRMS: m/z for $\text{C}_{22}\text{H}_{20}\text{OS}$ ($\text{M} + \text{H}$) $^+$, calcd: 333.1313, found: 333.1311.

4-(4-chlorophenyl)-4-(2-mercapto-3-methylphenyl)-1-phenylbutan-1-one (10e):

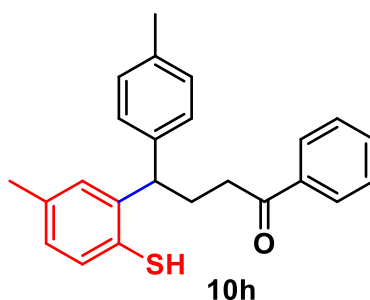
white solid (66 mg, 75%); m.p.: 71-73 °C; R_f 0.6 (20% ethyl acetate in petroleum ether); ^1H NMR (400 MHz, CDCl_3) δ_{H} 7.94 – 7.87 (m, 2H), 7.61 – 7.54 (m, 1H), 7.50 – 7.43 (m, 2H), 7.30 – 7.26 (m, 1H), 7.26 – 7.21 (m, 3H), 7.18 – 7.04 (m, 3H), 4.25 (dd, $J = 8.3, 6.9$ Hz, 1H), 3.12 – 3.05 (m, 2H), 2.53 – 2.34 (m, 2H), 2.33 (s, 3H); ^{13}C NMR (101 MHz, CDCl_3) δ_{C} 199.14, 140.37, 133.55, 133.20, 132.96, 132.82, 130.31, 129.09, 129.09, 128.68, 128.65, 128.00, 127.43, 126.38, 51.57, 36.20, 30.49, 20.70; HRMS: m/z for $\text{C}_{23}\text{H}_{20}\text{OCIS}$ ($\text{M} - \text{H}$) $^+$, calcd: 379.0918, found: 379.0920.

4-(2-mercapto-3-methylphenyl)-1-phenyl-4-(p-tolyl) butan-1-one (10f):

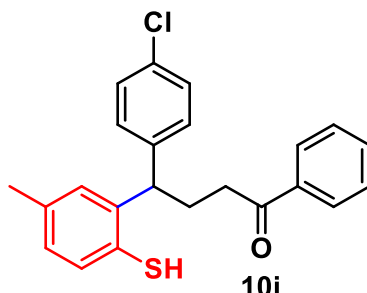
Viscous liquid (71 mg, 81%); R_f 0.28 (20% ethyl acetate in petroleum ether); ^1H NMR (400 MHz, CDCl_3) δ_{H} 7.88 – 7.83 (m, 2H), 7.55 – 7.49 (m, 1H), 7.44 – 7.38 (m, 2H), 7.31 (dd, $J = 7.3, 1.8$ Hz, 1H), 7.18 (d, $J = 8.1$ Hz, 2H), 7.14 – 7.11 (m, 1H), 7.08 (dt, $J = 6.2, 1.1$ Hz, 3H), 4.24 (dd, $J = 8.7, 6.4$ Hz, 1H), 3.01 (dd, $J = 7.7, 6.8$ Hz, 2H), 2.49 – 2.33 (m, 2H), 2.31 (d, $J = 3.7$ Hz, 6H); ^{13}C NMR (101 MHz, CDCl_3) δ_{C} 199.50, 139.73, 138.44, 136.91, 134.45, 133.14, 132.20, 130.24, 129.35, 128.64, 128.09, 127.71, 127.00, 126.37, 51.73, 36.44, 30.78, 21.21, 20.77; HRMS: m/z for $\text{C}_{24}\text{H}_{23}\text{OS}$ ($\text{M} - \text{H}$) $^+$, calcd: 359.1464, found: 359.1463.

4-(2-mercapto-3-methylphenyl)-4-(4-methoxyphenyl)-1-phenylbutan-1-one (10g):

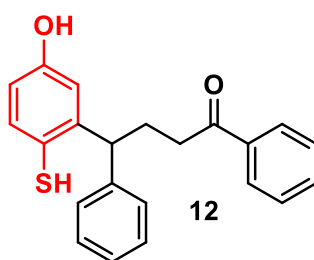
Viscous liquid (71 mg, 79%); R_f 0.42 (20% ethyl acetate in petroleum ether); ^1H NMR (400 MHz, CDCl_3) δ_{H} 7.89 – 7.83 (m, 2H), 7.56 – 7.49 (m, 1H), 7.45 – 7.38 (m, 2H), 7.30 (dd, $J = 7.3, 1.8$ Hz, 1H), 7.18 (t, $J = 7.9$ Hz, 1H), 7.14 – 7.03 (m, 3H), 6.87 (dt, $J = 7.8, 1.2$ Hz, 1H), 6.80 – 6.74 (m, 2H), 4.21 (dd, $J = 8.6, 6.6$ Hz, 1H), 3.73 (d, $J = 0.6$ Hz, 3H), 3.03 (t, $J = 7.2$ Hz, 2H), 2.50 – 2.33 (m, 2H), 2.31 (s, 3H); ^{13}C NMR (101 MHz, CDCl_3) δ_{C} 199.45, 139.96, 136.89, 134.19, 133.17, 132.50, 130.26, 129.62, 128.66, 128.09, 127.19, 126.39, 120.22, 113.23, 113.07, 52.15, 36.40, 30.65, 20.77; HRMS: m/z for $\text{C}_{24}\text{H}_{23}\text{O}_2\text{S}$ ($\text{M} - \text{H}$) $^+$, calcd: 375.1413, found: 375.1411.

4-(2-mercapto-5-methylphenyl)-1-phenyl-4-(p-tolyl)butan-1-one (10h):

Viscous liquid (75 mg, 86%); R_f 0.47 (20% ethyl acetate in petroleum ether); ^1H NMR (400 MHz, CDCl_3) δ_{H} 7.89 – 7.84 (m, 2H), 7.55 – 7.50 (m, 1H), 7.44 – 7.39 (m, 2H), 7.23 – 7.16 (m, 4H), 7.10 (d, $J = 8.0$ Hz, 2H), 7.05 – 7.00 (m, 2H), 4.22 (dd, $J = 8.6, 6.5$ Hz, 1H), 3.01 (t, $J = 7.3$ Hz, 2H), 2.47 – 2.31 (m, 5H), 2.29 (s, 3H); ^{13}C NMR (101 MHz, CDCl_3) δ_{C} 199.54, 138.62, 137.35, 137.01, 133.13, 133.00, 129.66, 129.33, 128.64, 128.12, 127.82, 52.90, 36.46, 30.61, 21.25; HRMS: m/z for $\text{C}_{24}\text{H}_{23}\text{OS}$ ($\text{M} - \text{H}$) $^+$, calcd: 359.1464, found: 359.1462.

4-(4-chlorophenyl)-4-(2-mercapto-5-methylphenyl)-1-phenylbutan-1-one (10i):

Viscous liquid (64 mg, 70%); R_f 0.44 (20% ethyl acetate in petroleum ether); ^1H NMR (400 MHz, CDCl_3) δ_{H} 7.89 – 7.84 (m, 2H), 7.57 – 7.50 (m, 1H), 7.46 – 7.39 (m, 2H), 7.24 – 7.20 (m, 2H), 7.16 – 7.12 (m, 3H), 7.00 (dt, $J = 7.8, 0.7$ Hz, 2H), 4.17 (dd, $J = 8.2, 7.1$ Hz, 1H), 3.03 (t, $J = 7.2$ Hz, 2H), 2.44 – 2.22 (m, 5H); ^{13}C NMR (101 MHz, CDCl_3) δ_{C} 199.26, 140.53, 137.82, 136.83, 133.43, 133.25, 132.93, 130.25, 129.72, 129.25, 128.69, 128.08, 52.67, 36.27, 30.26, 21.21; HRMS: m/z for $\text{C}_{23}\text{H}_{20}\text{OCIS}$ ($\text{M} - \text{H}$) $^+$, calcd: 379.0918, found: 379.0914.

4-(5-hydroxy-2-mercaptophenyl)-1,4-diphenylbutan-1-one (12):

Viscous liquid (66 mg, 79%); R_f 0.28 (20% ethyl acetate in petroleum ether); ^1H NMR (400 MHz, CDCl_3) δ_{H} 7.89 – 7.83 (m, 2H), 7.56 – 7.49 (m, 1H), 7.44 – 7.38 (m, 2H), 7.24 (d, $J = 2.2$ Hz, 1H), 7.23 – 7.20 (m, 1H), 7.17 (dd, $J = 8.1, 1.6$ Hz, 2H), 7.15 – 7.11 (m, 2H), 6.69 – 6.63 (m, 2H), 5.36 – 5.27 (m, 1H), 4.08 (dd, $J = 8.5, 6.8$ Hz, 1H), 3.06 – 2.98 (m, 2H), 2.44 – 2.24 (m, 2H); ^{13}C NMR (101 MHz, CDCl_3) δ_{C} 155.98, 141.64, 136.83, 136.38, 133.25, 128.67, 128.52, 128.13, 127.95, 124.53, 115.89, 54.09, 36.50, 30.00; HRMS: m/z for $\text{C}_{22}\text{H}_{20}\text{O}_2\text{S}$ ($\text{M} + \text{H}$) $^+$, calcd: 349.1262, found: 349.1256.

HPLC Methods:

In our method pure racemic compound was analyzed to get retention time using Agilent 1260 Infinity normal phase HPLC unit (with 254 nm wavelength and 1 mL/min flow rate), HPLC Chemstation software with CHIRALART AMYLOSE SA columns (250 x 4.6 mm, 5 μ m) and 10% isopropanol in hexane as mobile phase. Then all the compounds synthesised *via* using chiral ligands were injected using same conditions to match the retention times and integrating the peaks elucidated the *ee* of synthesised compounds.

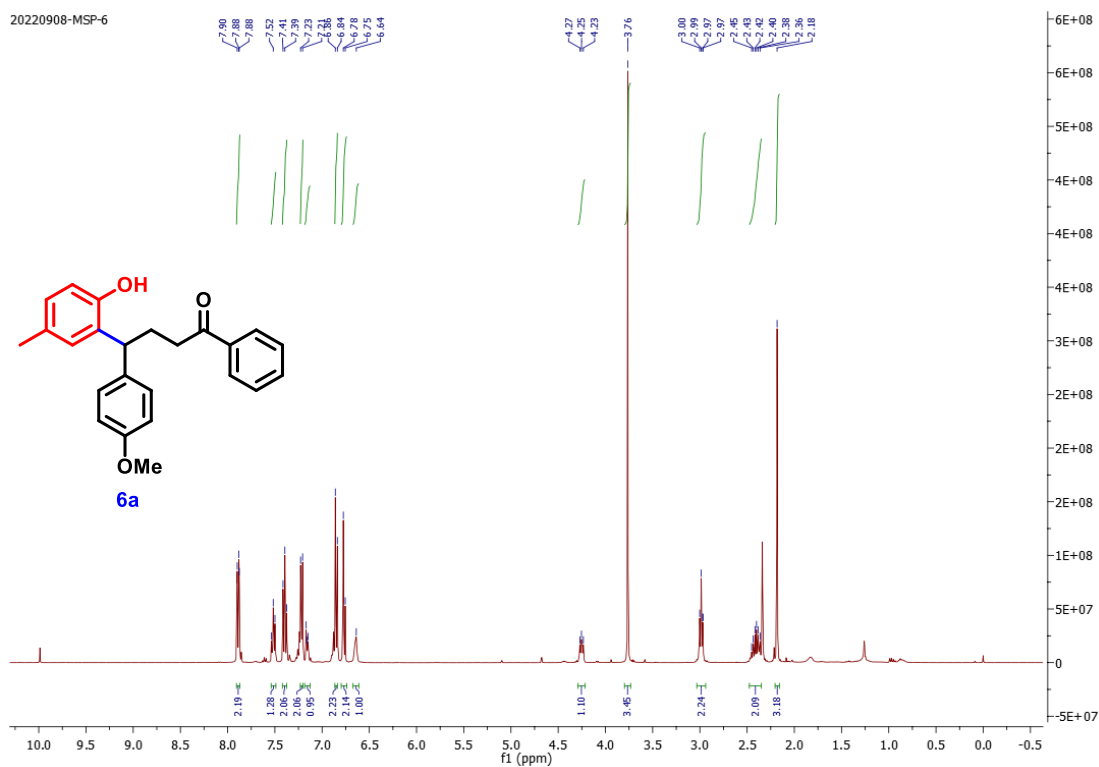
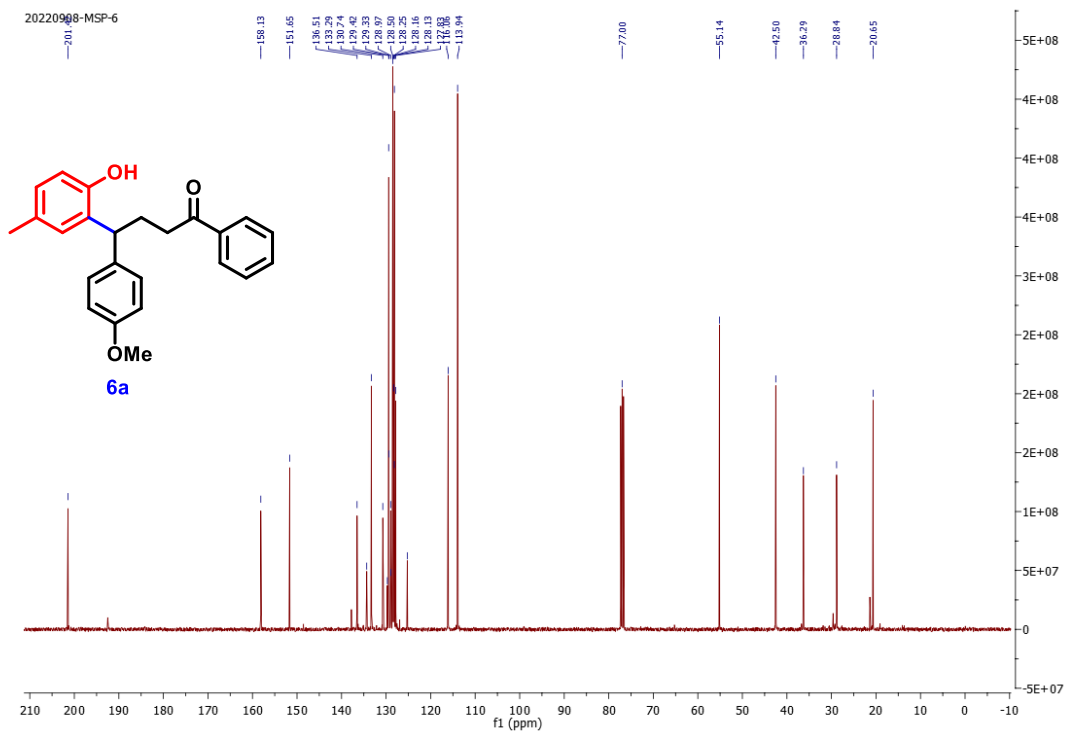
Entry	Ligands	column	Mobile phase (Isopropanol:Hexane)
1	R(-) Mandelic acid	CHIRALART AMYLOSE SA	10:90
2	L (+) Tartaric acid	CHIRALART AMYLOSE SA	10:90
3	R-Binap	CHIRALART AMYLOSE SA	10:90
4	No catalyst	CHIRALART AMYLOSE SA	10:90

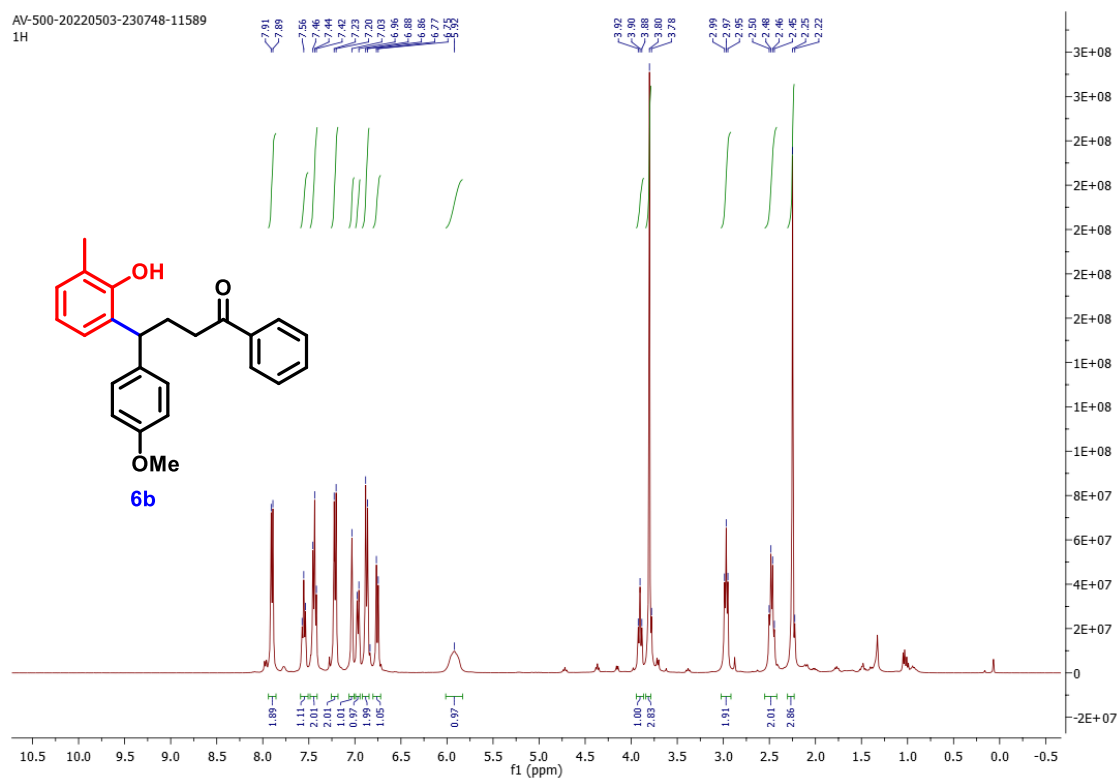
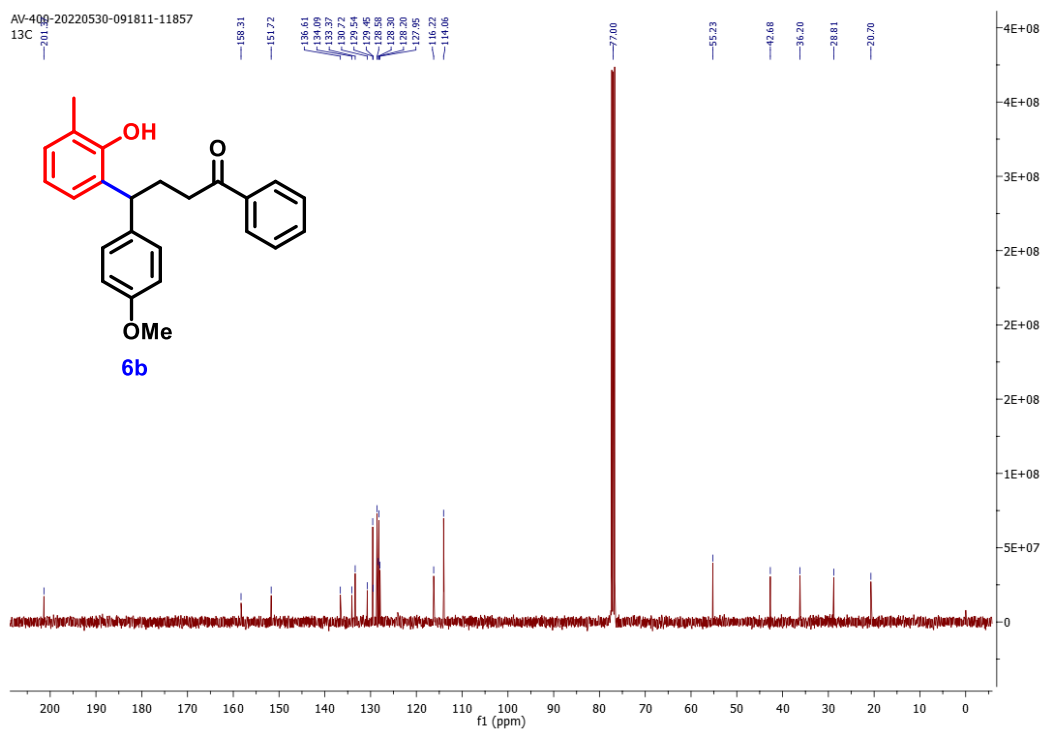
2.5 References

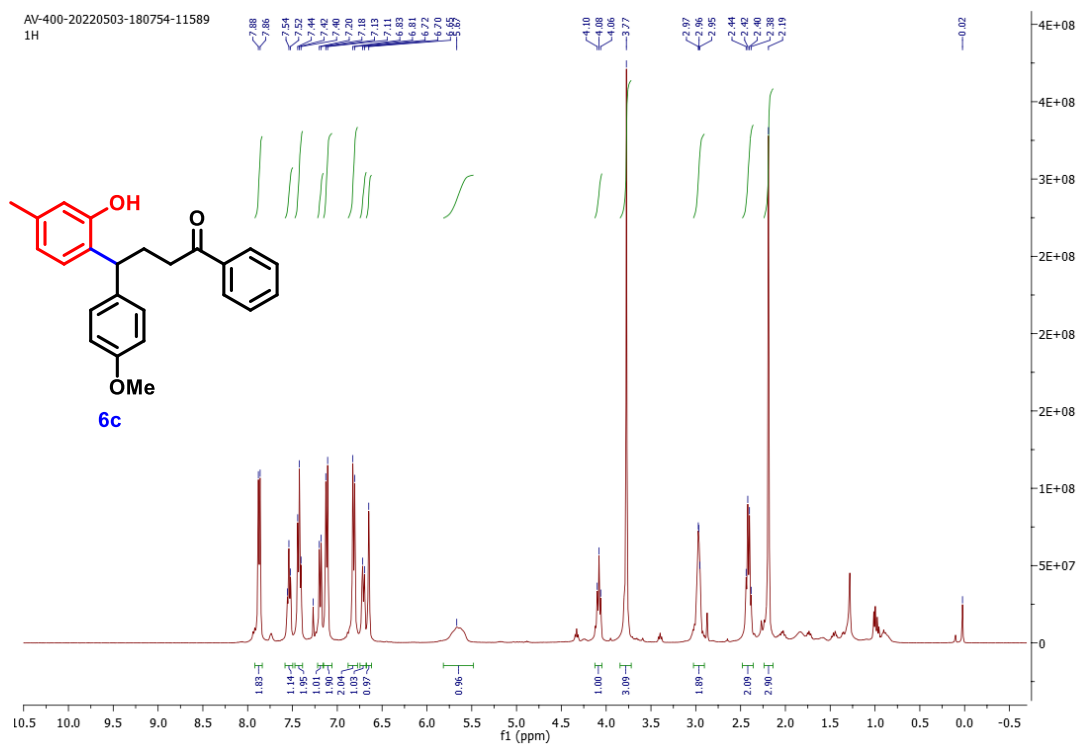
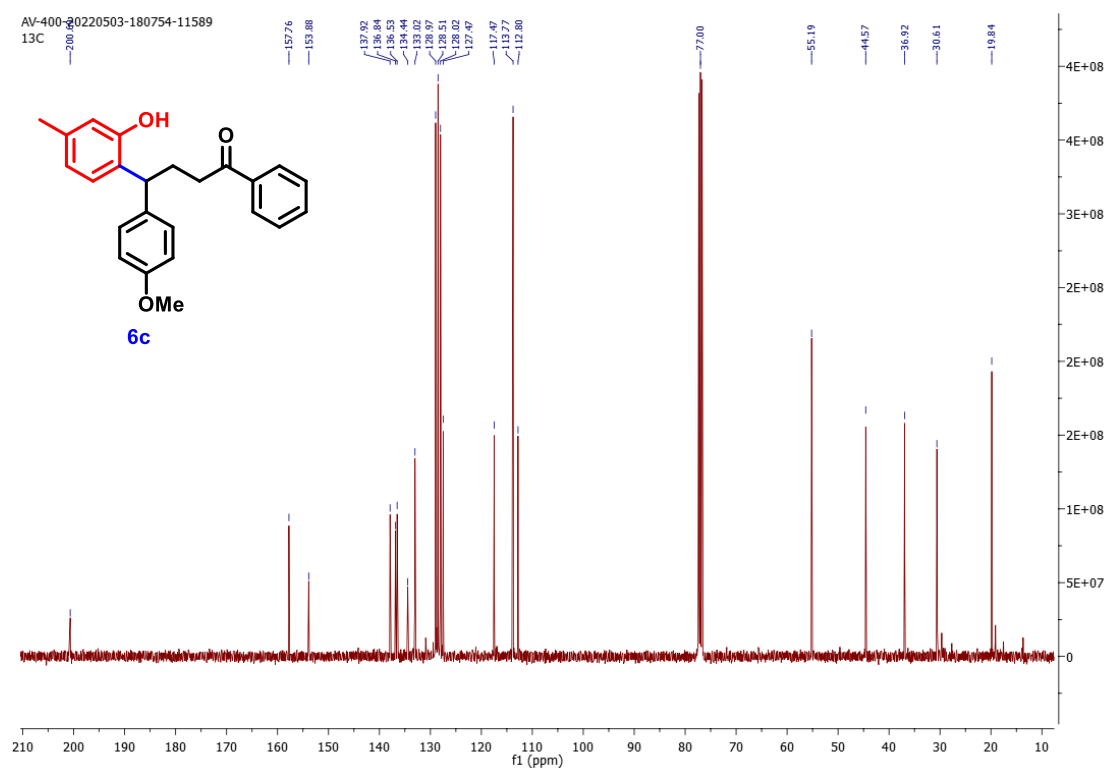
1. (a) K. Ghosh and S. Das, *Org. Biomol. Chem.*, **2021**, *19*, 965–982; (b) H. K. Grover, M. E. Emmett and M. A. Kerr, *Org. Biomol. Chem.*, **2015**, *13*, 655–671; (c) R. Talukdar, A. Saha and M. K. Ghorai, *Isr. J. Chem.*, **2016**, *56*, 445–453.
2. (a) H. Yin, J. Dong, Y. Cai, X. Shi, H. Wang, G. Liu, Y. Tang, J. Liu, L. Ma, *Eur. J. Med. Chem.*, **2019**, *180*, 350–366. (b) Y. Ouyang, J. Li, X. Chen, X. Fu, S. Sun, and Q. Wu, *Biomolecules*, **2021**, *11*, 894.
3. (a) Y. Fukuda, M. Nagano, K. Tsukamoto and M. Futatsuka, *J. Occup. Health*, **1998**, *40*, 137–142; (b) R. Nishida, O. Iwahashi and K. H. Tan, *J. Chem. Ecol.*, **1993**, *4*, 713–722.
4. T. Nakayama, *J. Biosci. Bioeng.*, **2002**, *6*, 487–491.
5. B. Herl, G. Späth, L. Schreyer and A. Fgrstner, *Angew. Chem.* **2021**, *133*, 7972–7978.
6. M. M. Heravi and A. Nazari, *RSC Adv.*, **2022**, *12*, 9944–9994.
7. A. Pizzi, *Monomers, Polymers and Composites from Renewable Resources*, **2008**, 179–199.
8. (a) E. Hvattum, *Rapid Commun. Mass Spectrom.*, **2002**, *16*, 655–662; (b) J. P. Ley, G. Krammer, G. Reinders, I. L. Gatfield and H-J. Bertram, *J. Agric. Food Chem.* **2005**, *53*, 6061–6066.
9. (a) P. Moosophon, S. Kanokmedhakul, K. Kanomedhakul, M. Buayairaksa, J. Noichan and K. Poopasit, *J. Nat. Prod.* **2013**, *76*, 1298–1302.
10. P-C. Kuo¹, Y-C. Li and T-S. Wu, *Journal of Traditional and Complementary Medicine*, **2012**, *2*, 249–266.
11. C. A. B. Amaro, M. González-Cortazar, M. Herrera-Ruiz, R. Román-Ramos, L. Aguilar-Santamaría, J. Tortoriello and E. Jiménez-Ferrer, *Molecules*, **2014**, *19*, 11366–11384.
12. (a) M. S. Gordon, *J. Am. Chem. Soc.* **1980**, *102*, 7419–7422; (b) Xu, H.; Qu, J-P.; Liao, S.; H. Xiong, and Y. Tang, *Angew. Chem. Int. Ed.*, **2013**, *52*, 4004–4007.
13. (a) O. Lifchits, D. Alberico, I. Zakharian and A. B. Charette, *J. Org. Chem.*, **2008**, *73*, 6838–6840. (b) O. Lifchits and A. B. Charette, *Org. Lett.*, **2008**, *10*, 2809–2812.
14. Y. Xia, L. Lin, F. Chang, X. Fu, X. Liu and X. Feng, *Angew. Chem. Int. Ed.*, **2015**, *54*, 13748–13752.
15. P. Harrington and M. K. Kerr, *Tetrahedron Lett.*, **1997**, *38*, 5949–5952.

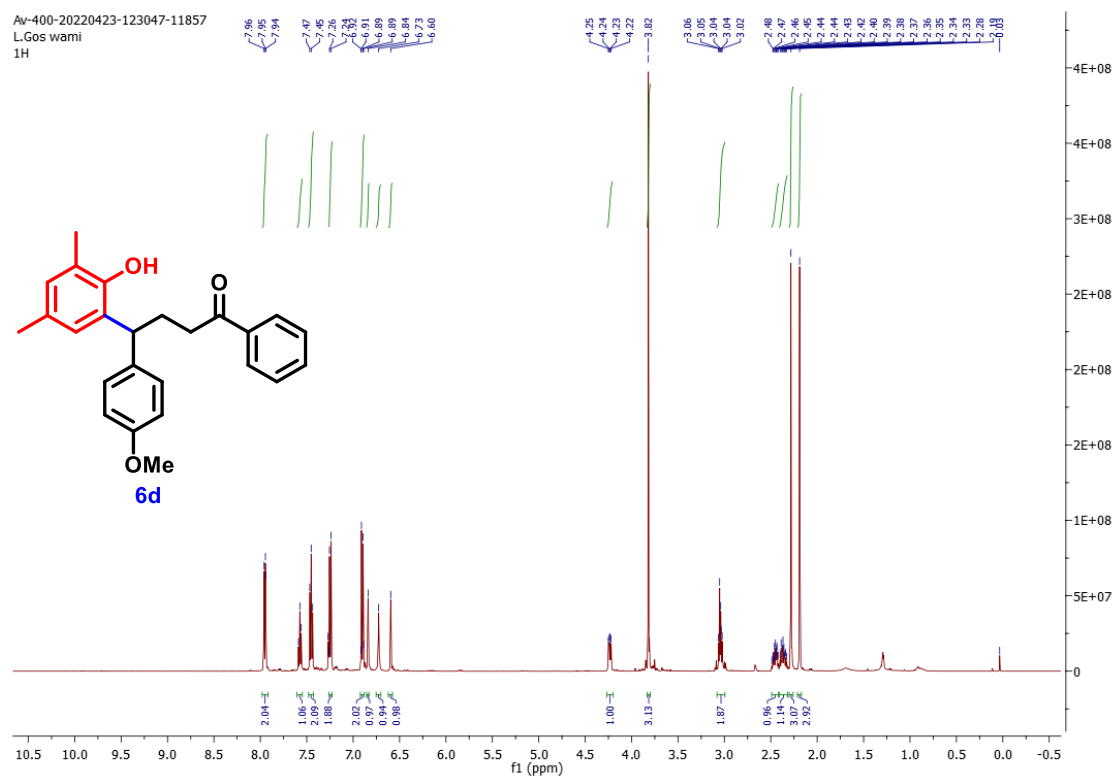
16. T. Kaicharla, T. Roy, M. Thangaraj, R. G. Gonnade and A. T. Biju, *Angew. Chem. Int. Ed.*, **2016**, *55*, 10061–10064.
17. R. Talukdar, A. Saha, D. P. Tiwari and M. K. Ghorai, *Tetrahedron*, **2016**, *72*, 613-624.
18. (a) E. Richmond, V. D. Vuković, and J. Moran, *Org. Lett.*, **2018**, *20*, 574–577. (b) E. Richmond, J. Yi, V. D. Vuković, F. Sajadi, C. N. Rowley and J. Moran, *Chem. Sci.*, **2018**, *9*, 6411–6416.
19. (a) S. Gupta, J. A. Melanson, L. Vaillancourt, W. A. Nugent, G. J. Tanoury, G. Schatte and V. Snieckus, *Org. Lett.*, **2018**, *20*, 3745–3748. (b) N. A. A. Elkanzi, H. Hrichi, R. A. Alolayan, W. Derafa, M. Fatin, F. M. Zahou and R. B. Bakr, *ACS Omega*, **2022**, *7*, 27769–27786.
20. H. Zhao, P. Shen, D. Sun, H. Zhai and Y. Zhao, *Front. Chem.*, **2021**, Vol-9. (doi.org/10.3389/fchem.2021.711257)
21. S. C. Baker, *Nature*, **1991**, *350*, 627.

2.6 Copies of NMR and spectra spectrum HPLC chromatogram:

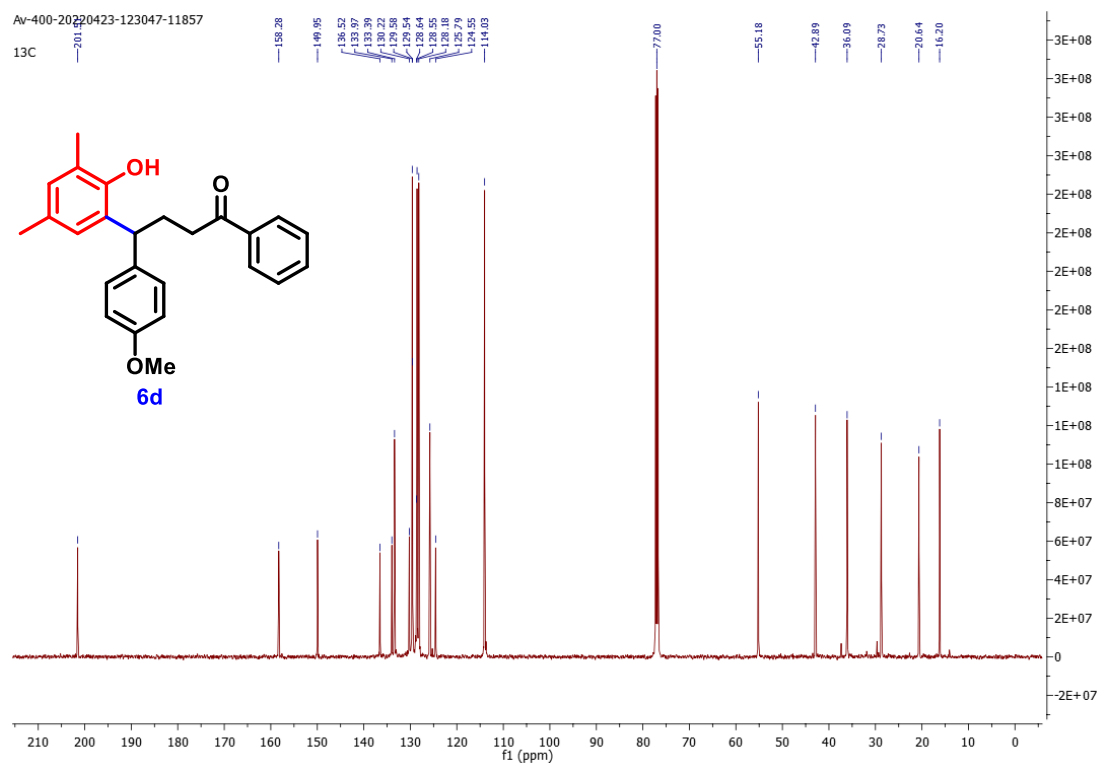
 ^1H NMR (CDCl_3 , 400 MHz) of **6a** ^{13}C NMR (CDCl_3 , 101 MHz) of **6a**

 ^1H NMR (CDCl_3 , 500 MHz) of **6b** ^{13}C NMR (CDCl_3 , 101 MHz) of **6b**

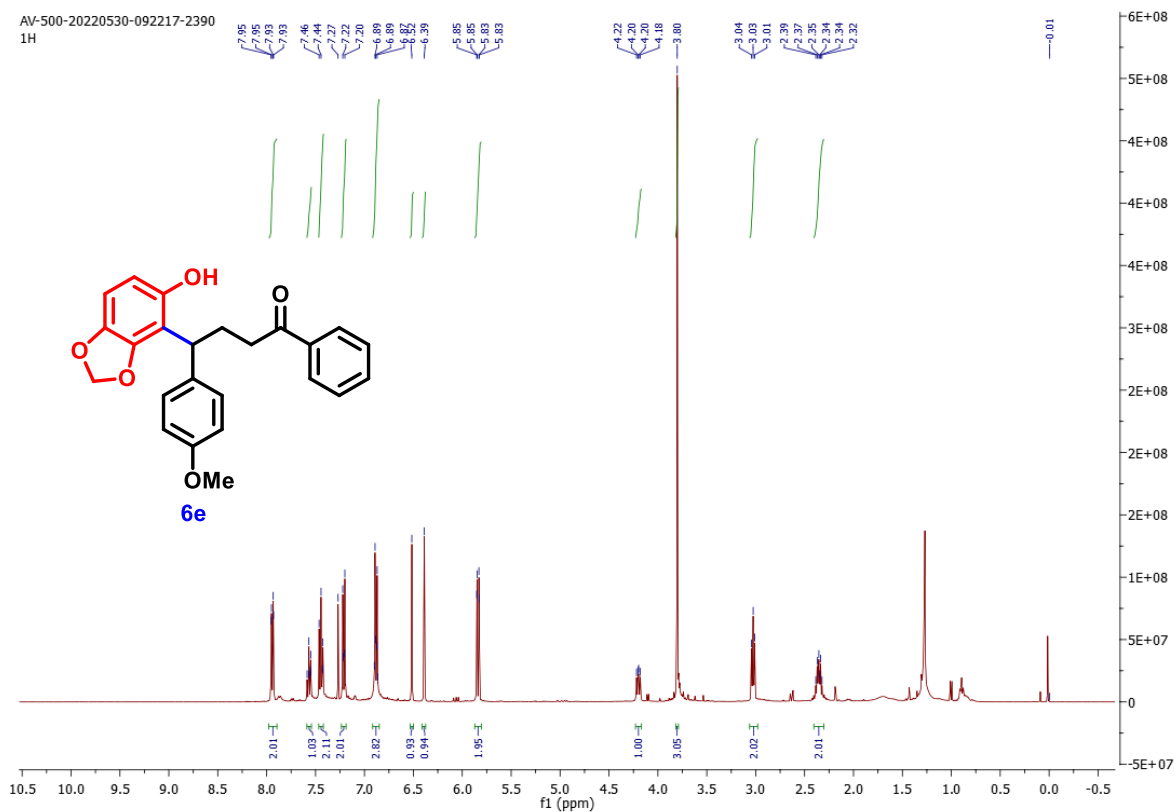
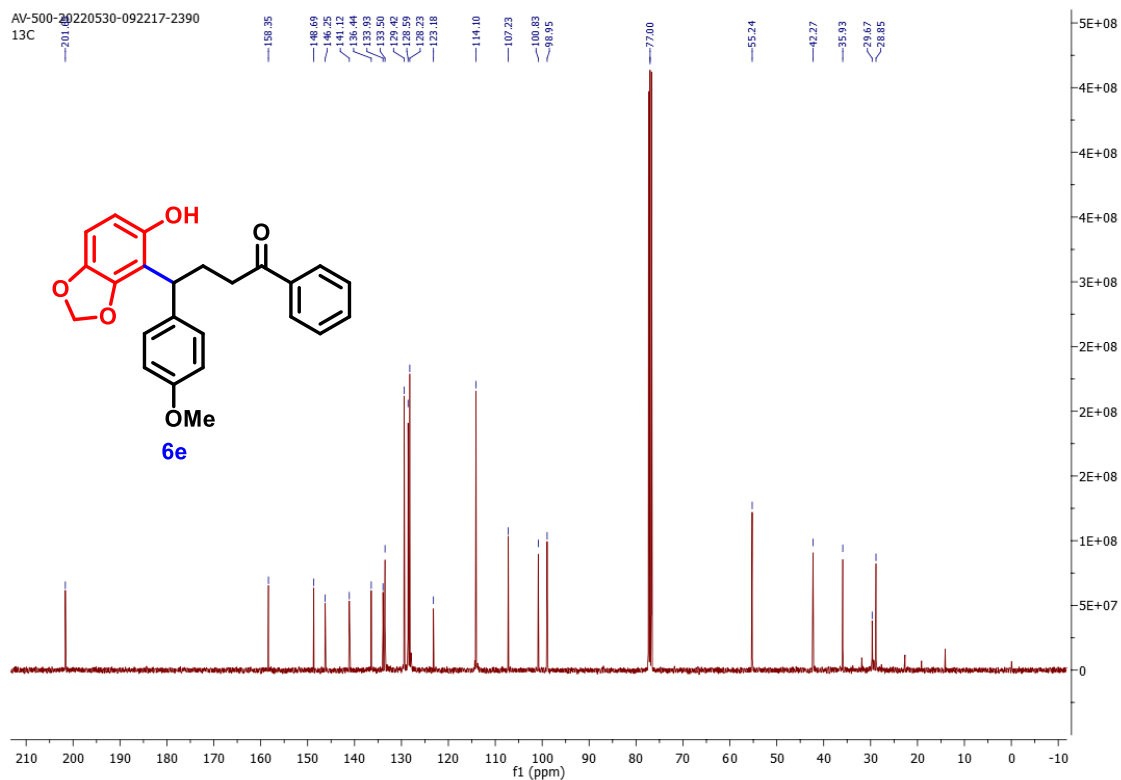
 ^1H NMR (CDCl_3 , 400 MHz) of **6c** ^{13}C NMR (CDCl_3 , 101 MHz) of **6c**

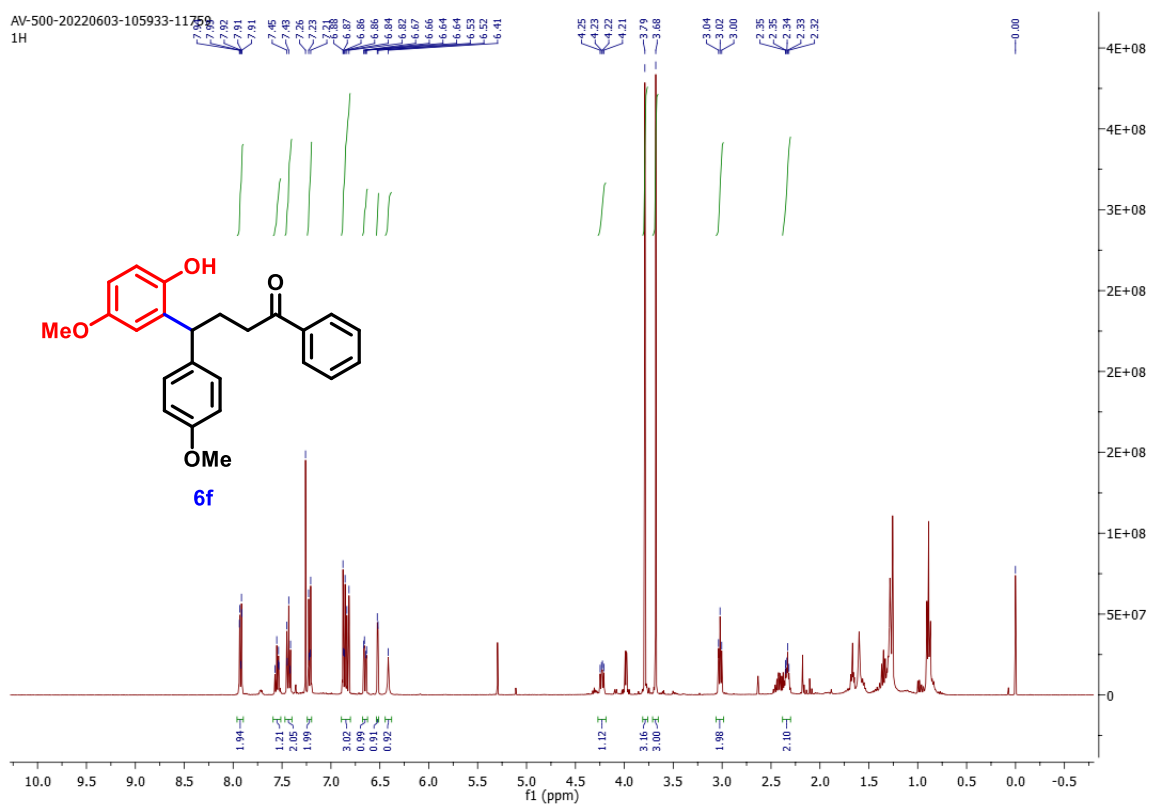


^1H NMR (CDCl_3 , 400 MHz) of **6d**

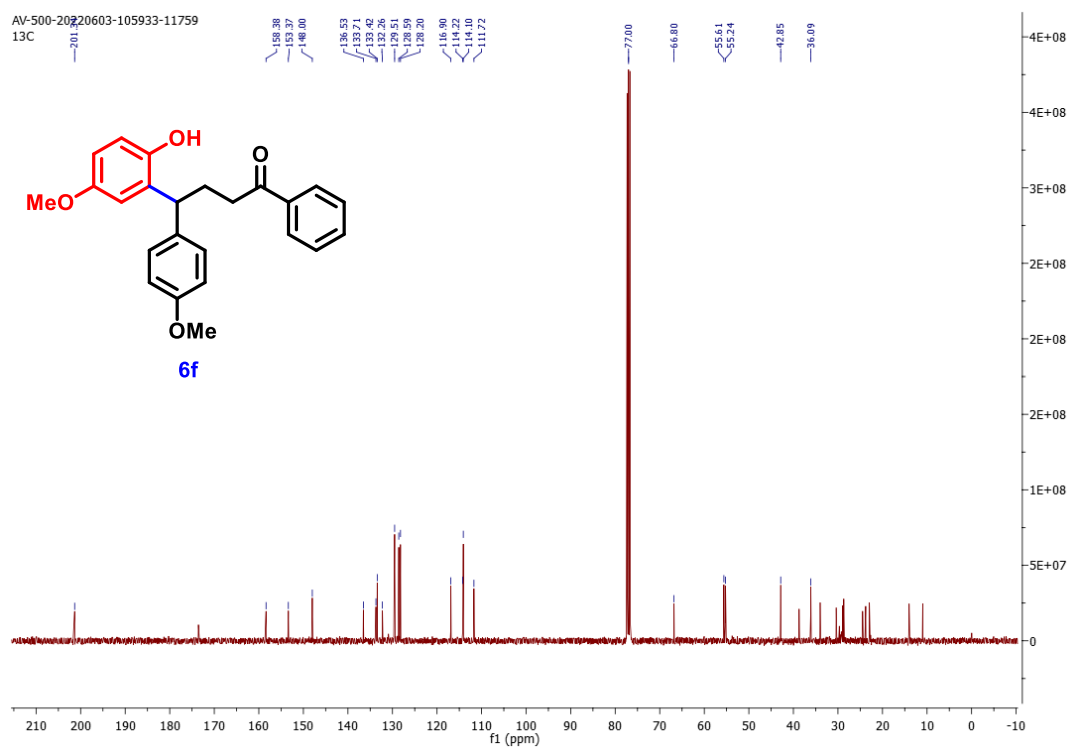


^{13}C NMR (CDCl_3 , 101 MHz) of **6d**

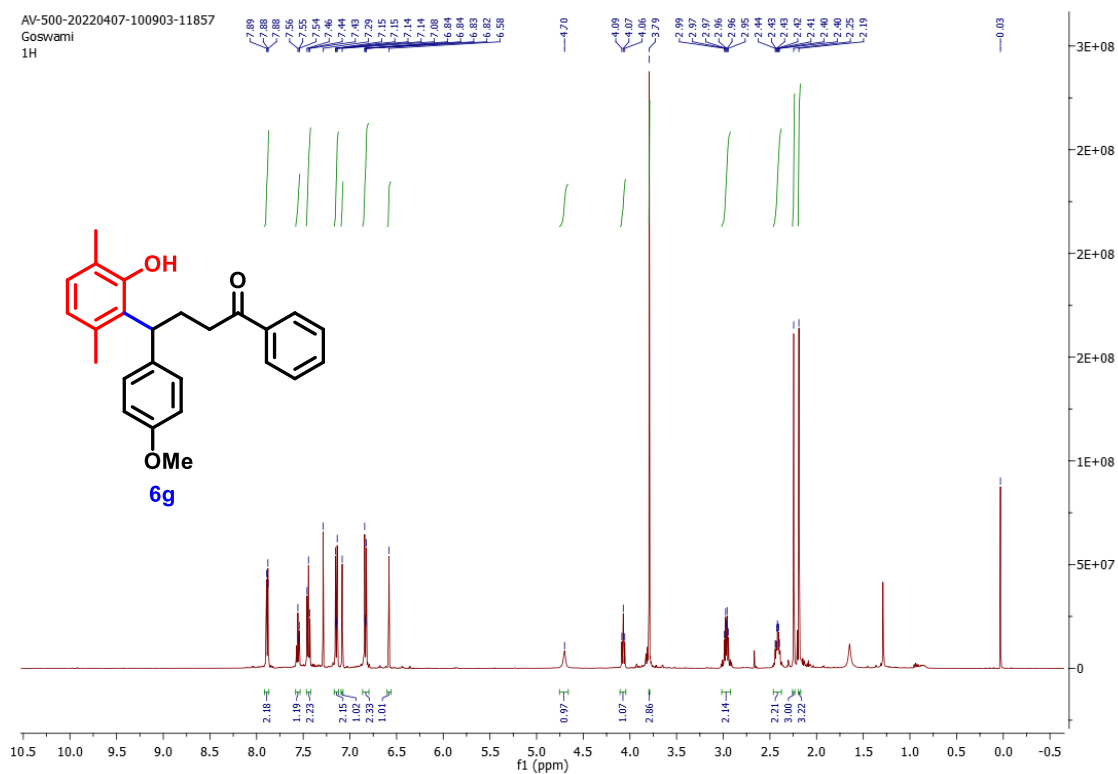
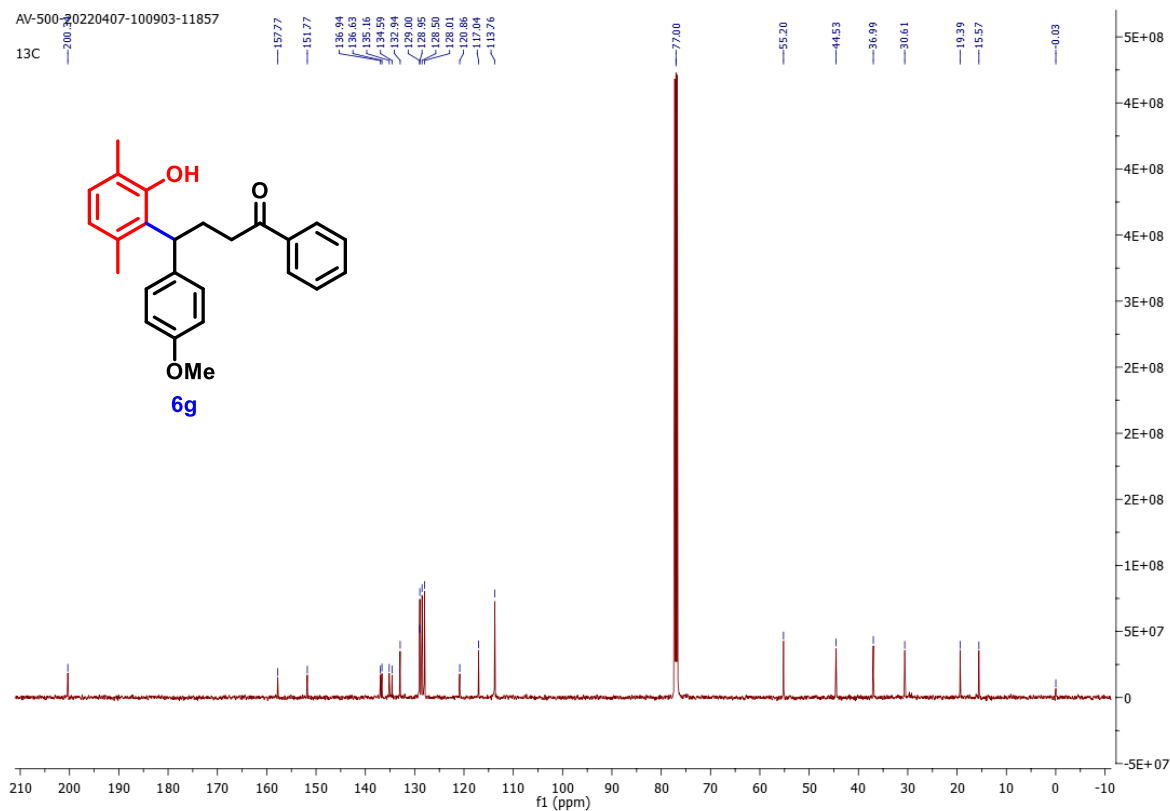
 ^1H NMR (CDCl_3 , 500 MHz) of **6e** ^{13}C NMR (CDCl_3 , 126 MHz) of **6e**

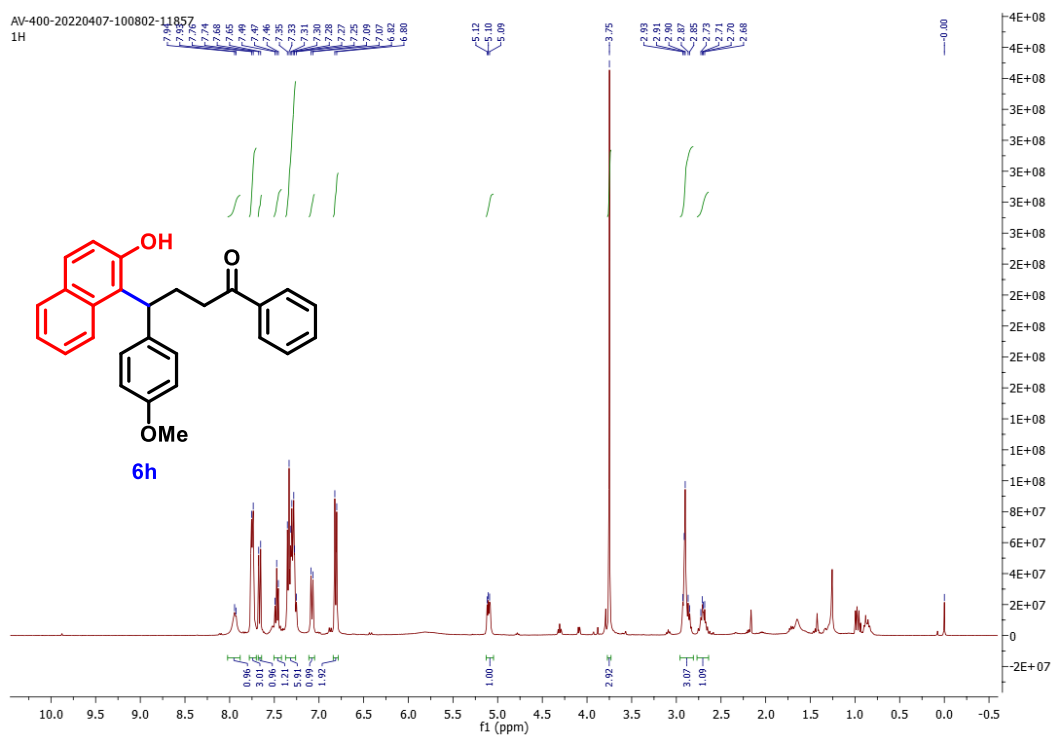
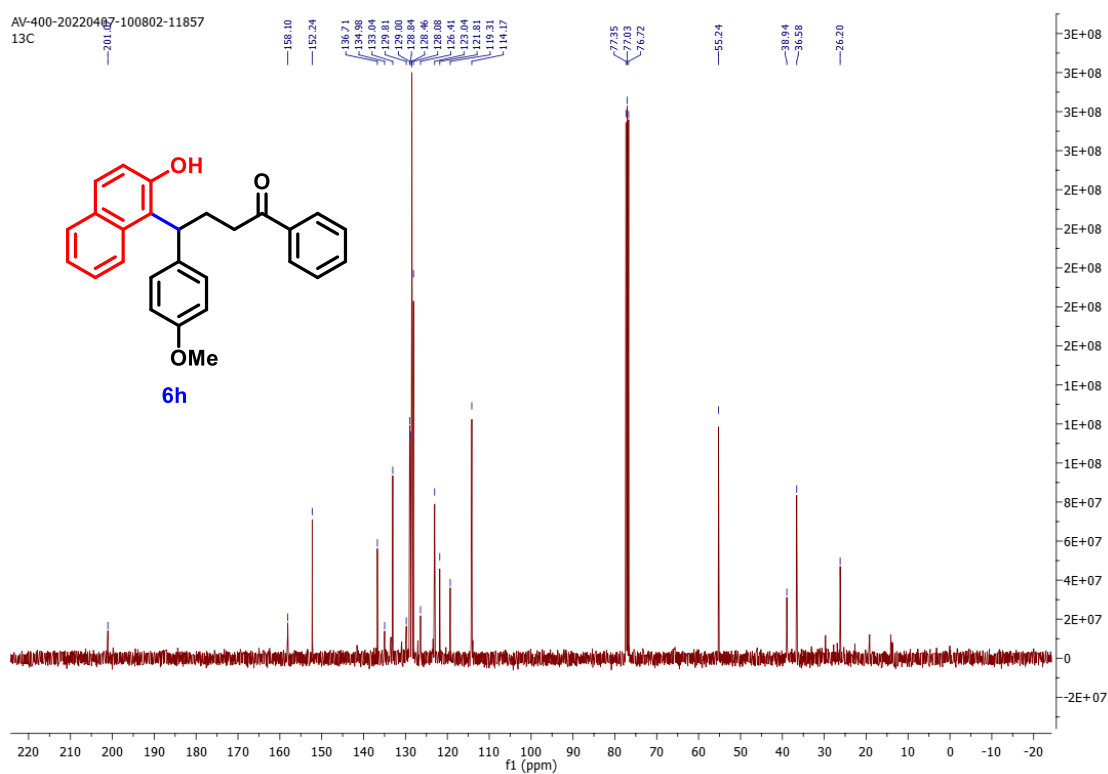


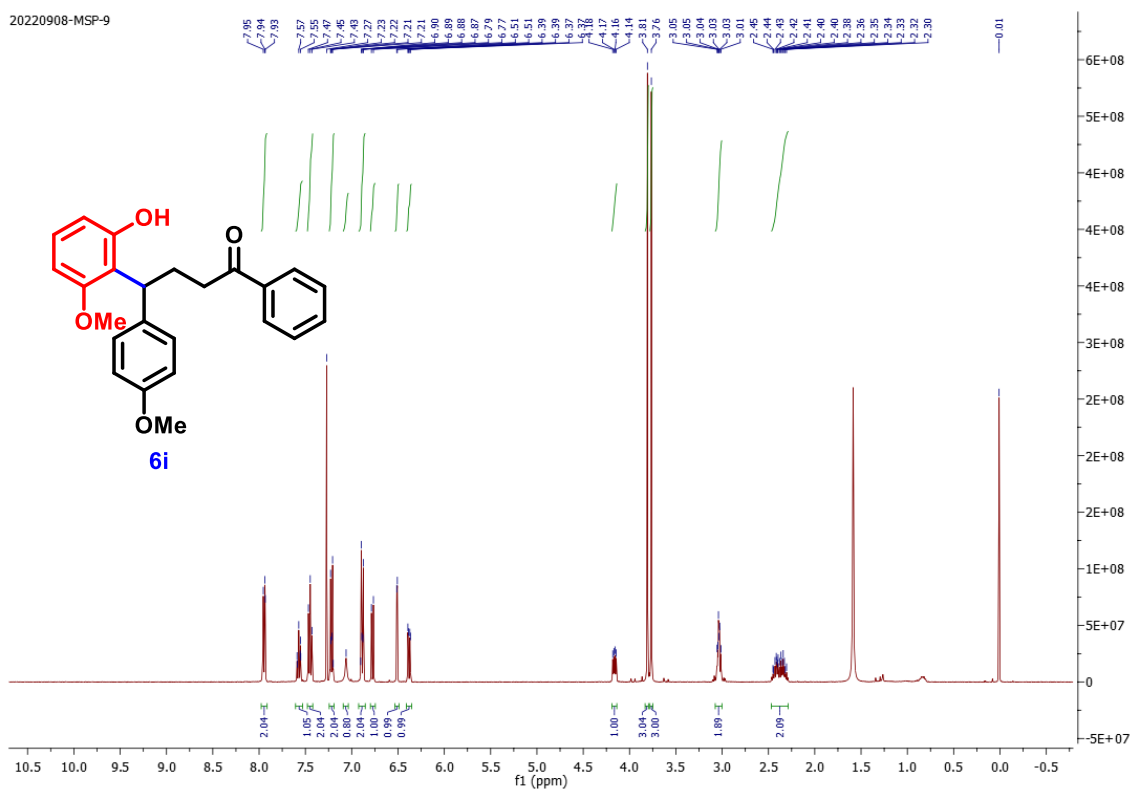
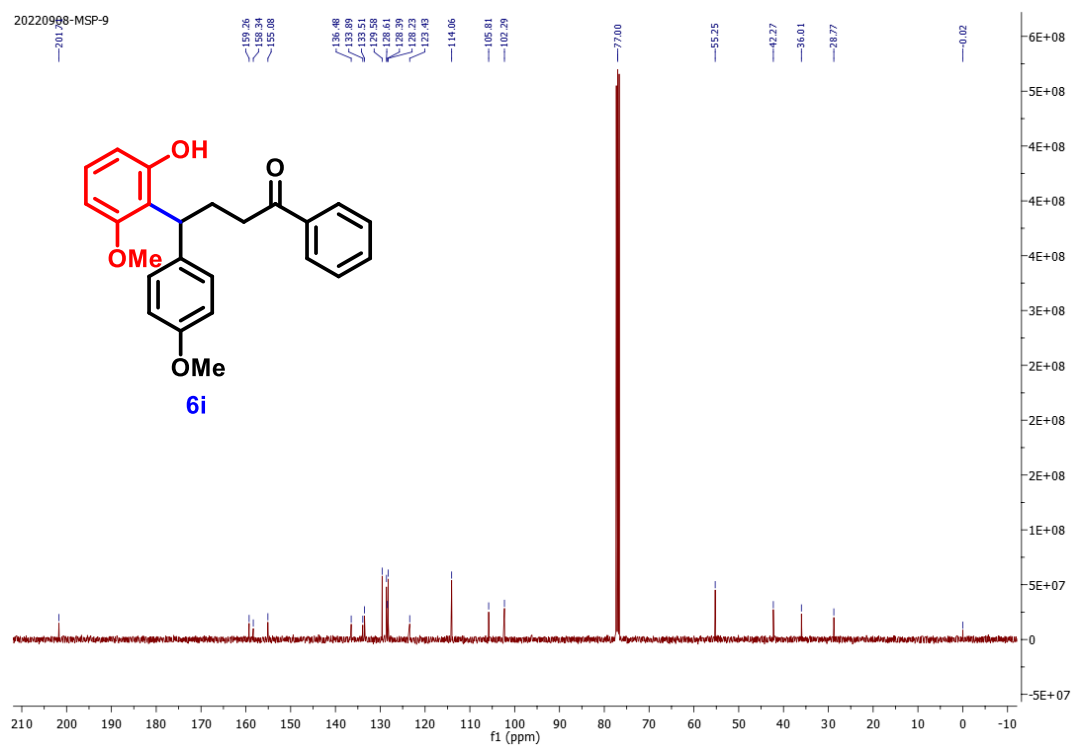
^1H NMR (CDCl_3 , 500 MHz) of **6f**

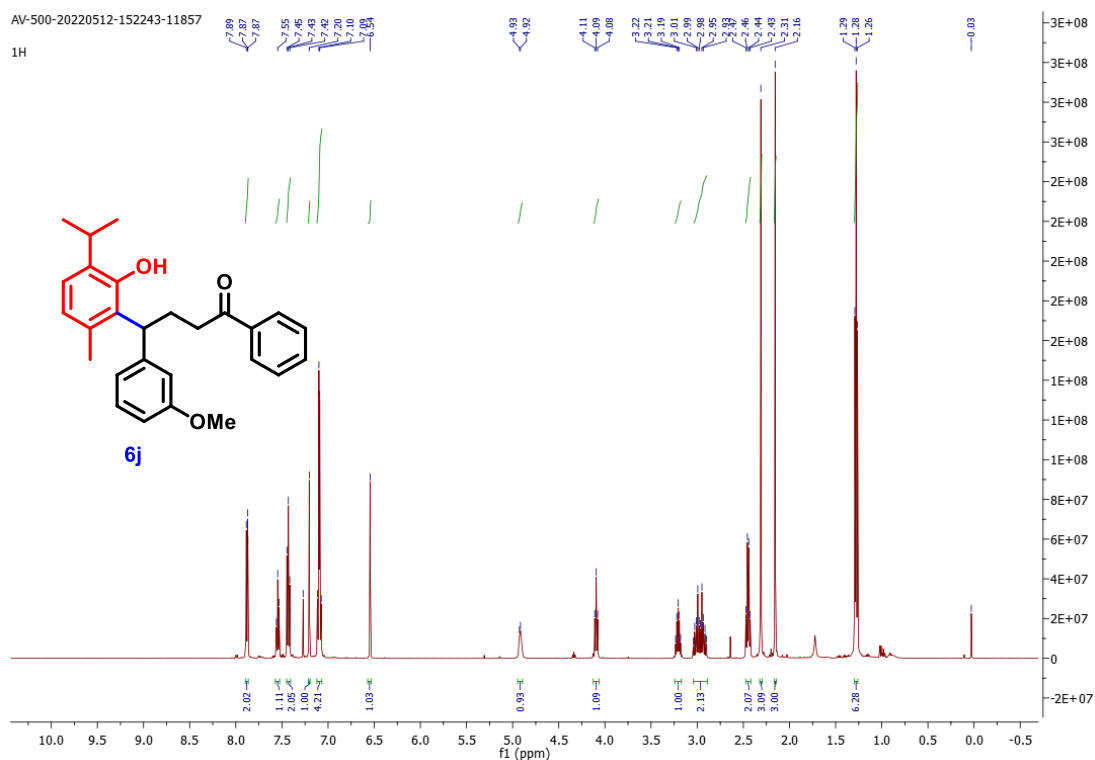


^{13}C NMR (CDCl_3 , 126 MHz) of **6f**

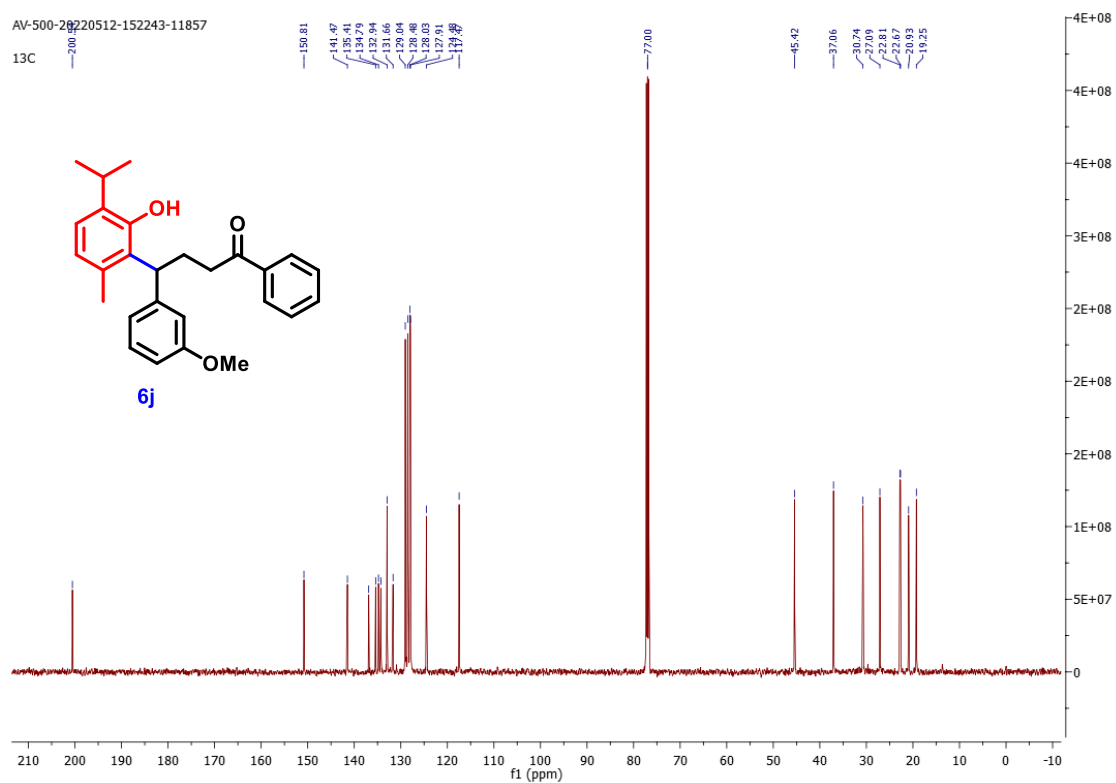
 ^1H NMR (CDCl_3 , 500 MHz) of **6g** ^{13}C NMR (CDCl_3 , 126 MHz) of **6g**

 ^1H NMR (CDCl_3 , 400 MHz) of **6h** ^{13}C NMR (CDCl_3 , 101 MHz) of **6h**

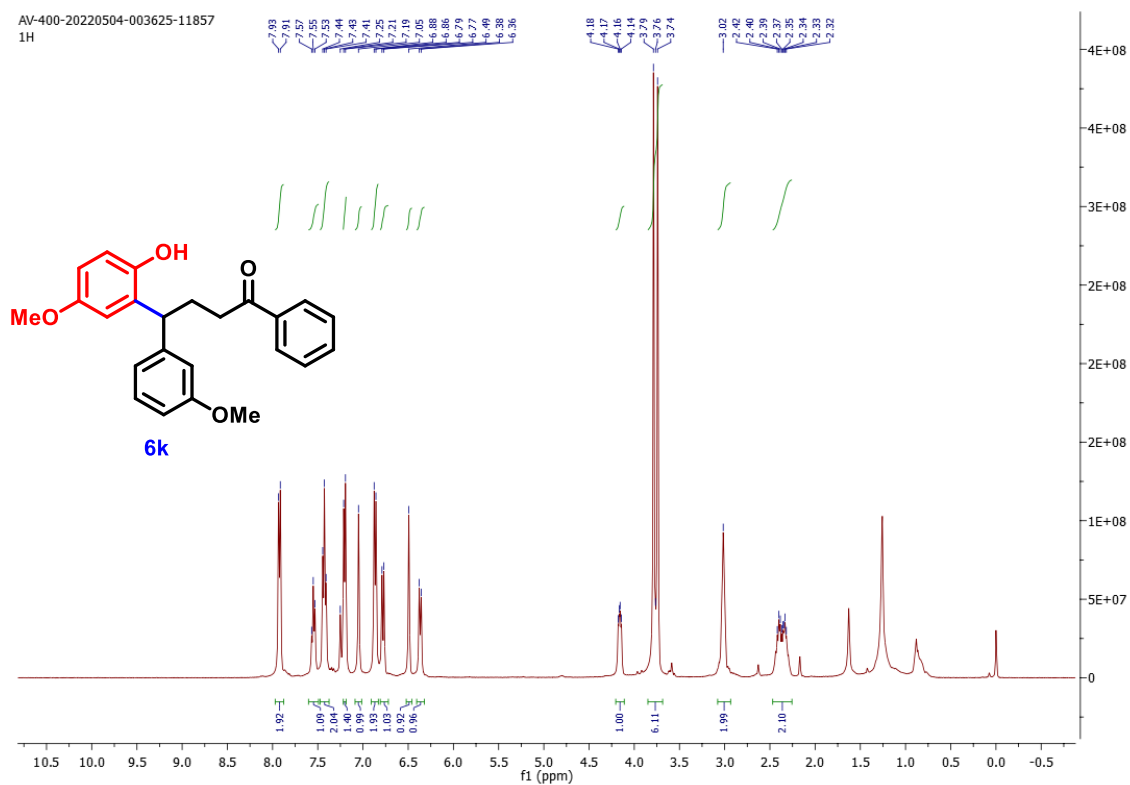
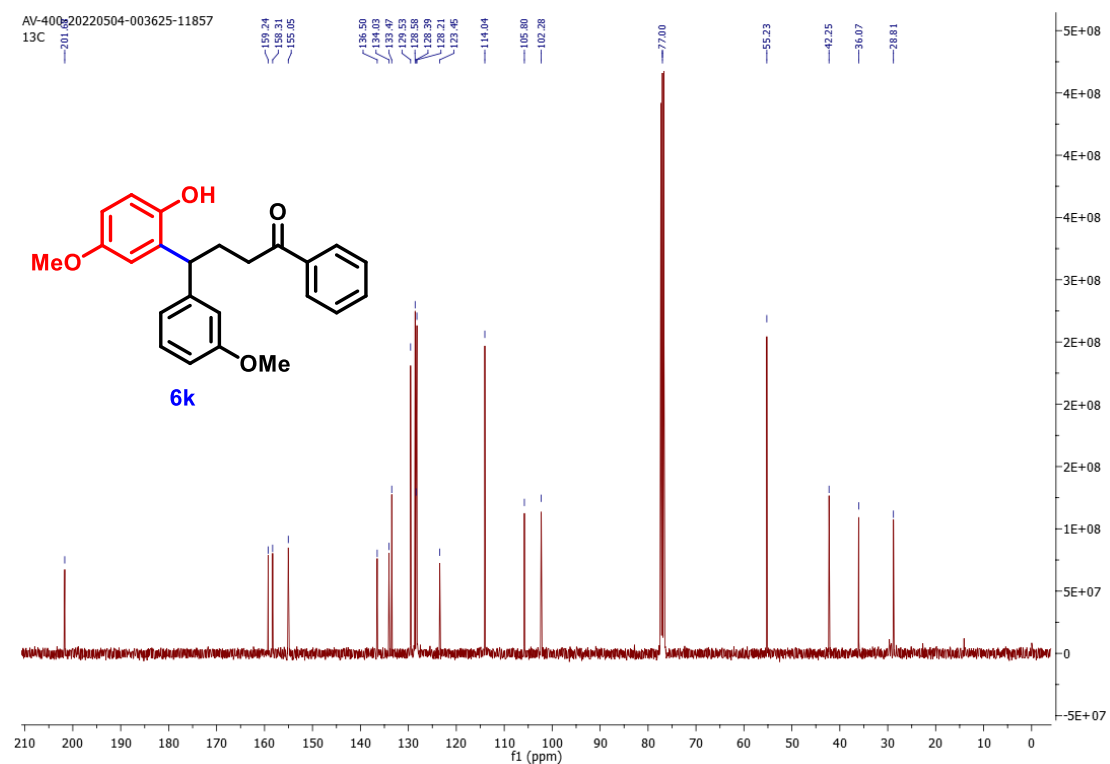
 $^1\text{H NMR}$ (CDCl_3 , 400 MHz) of **6i** $^{13}\text{C NMR}$ (CDCl_3 , 101 MHz) of **6i**

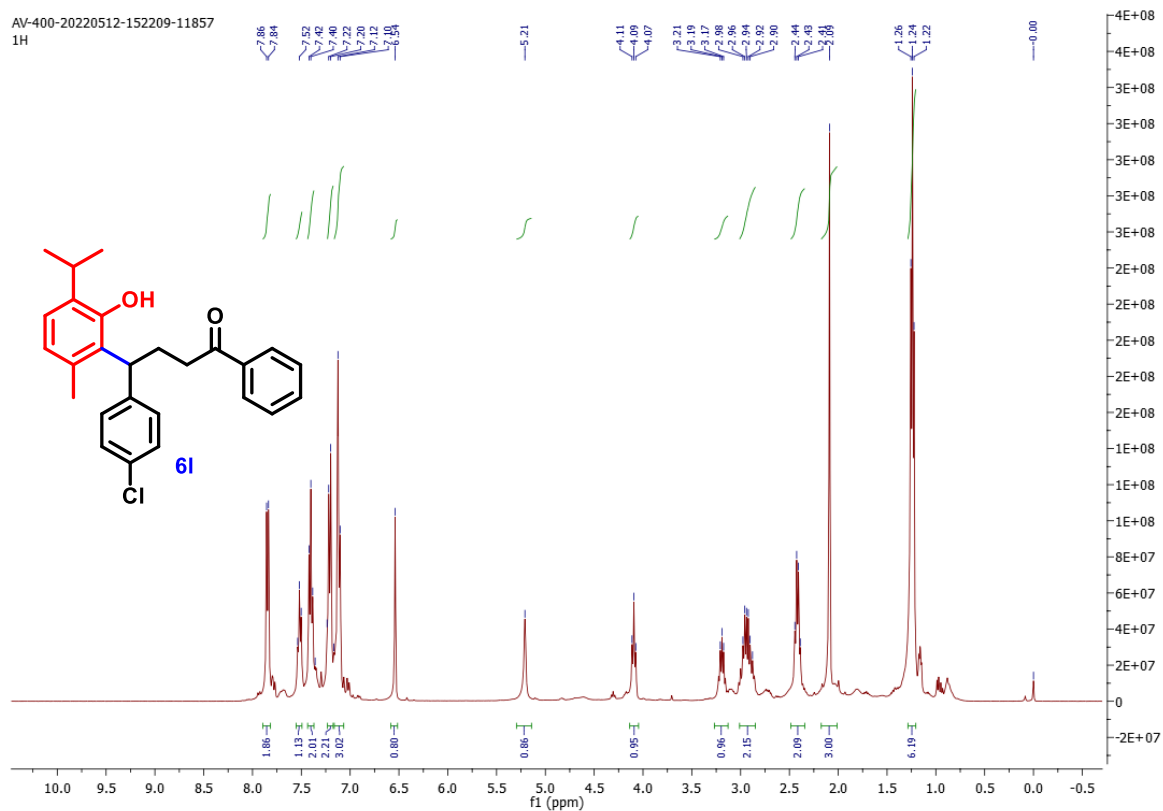
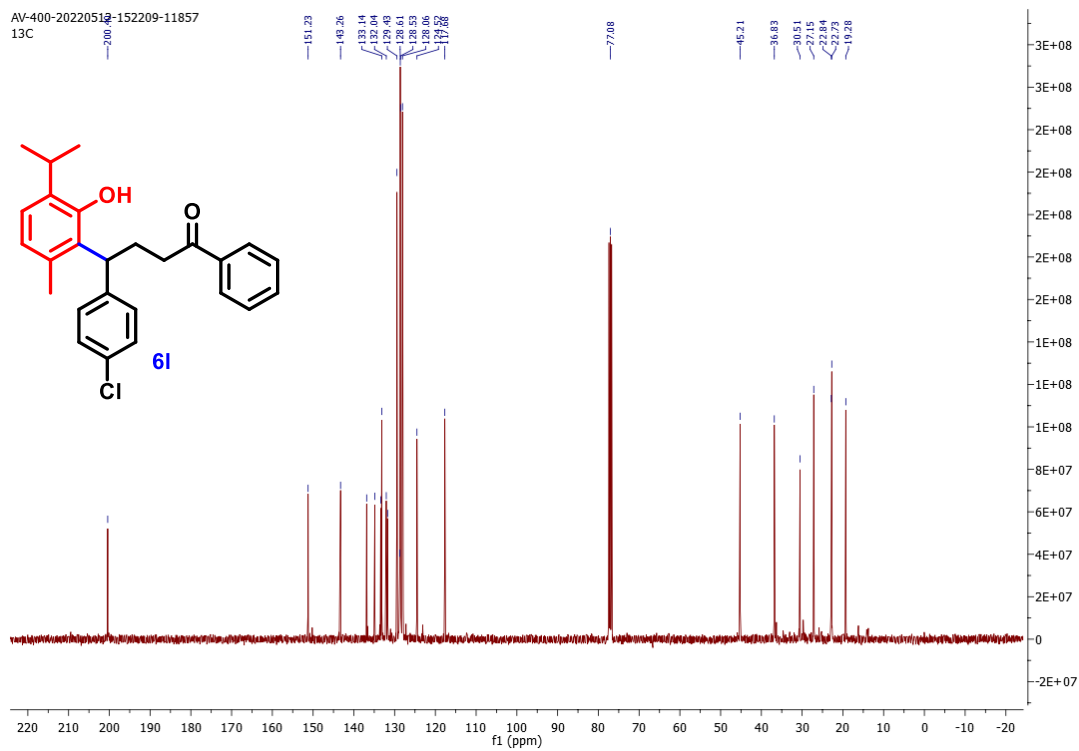


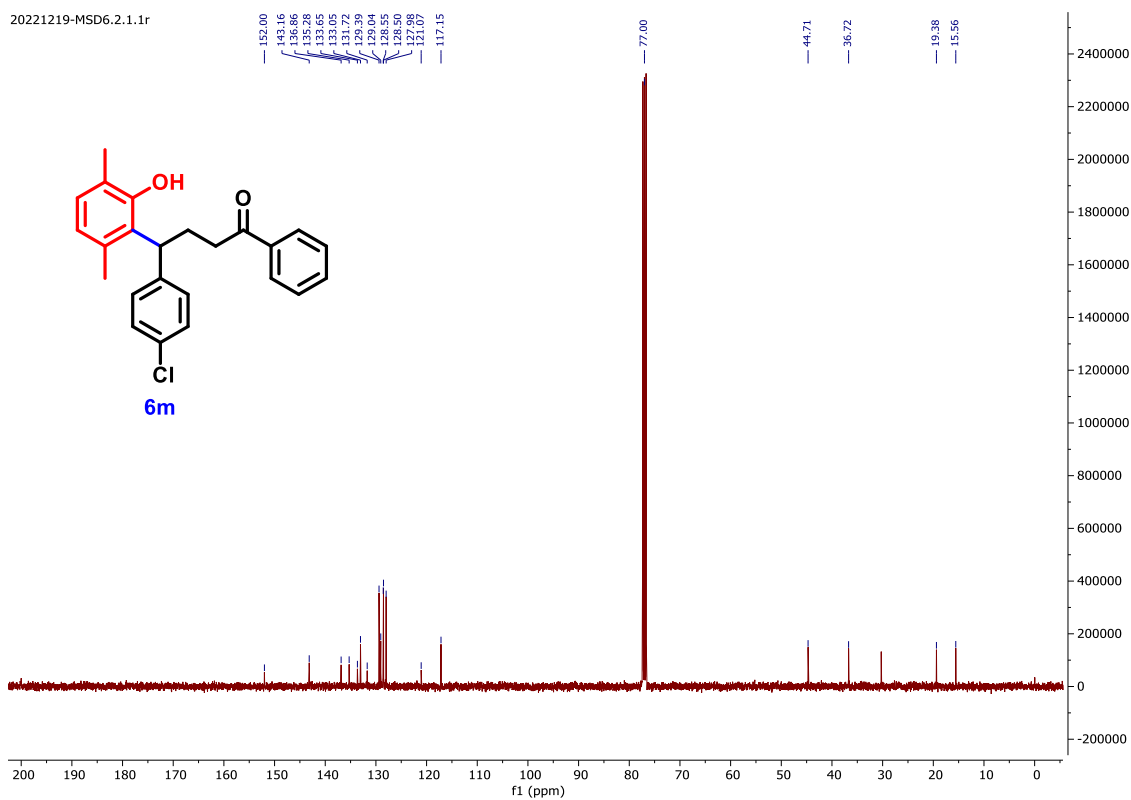
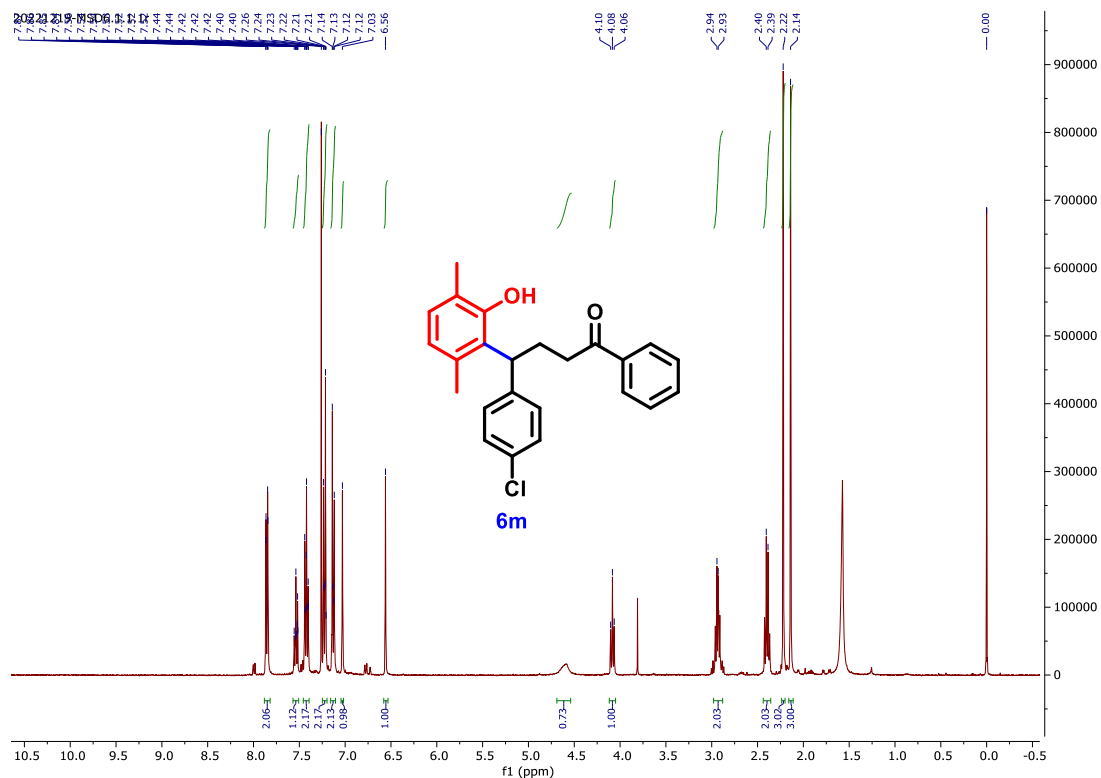
¹H NMR (CDCl₃, 500 MHz) of **6j**

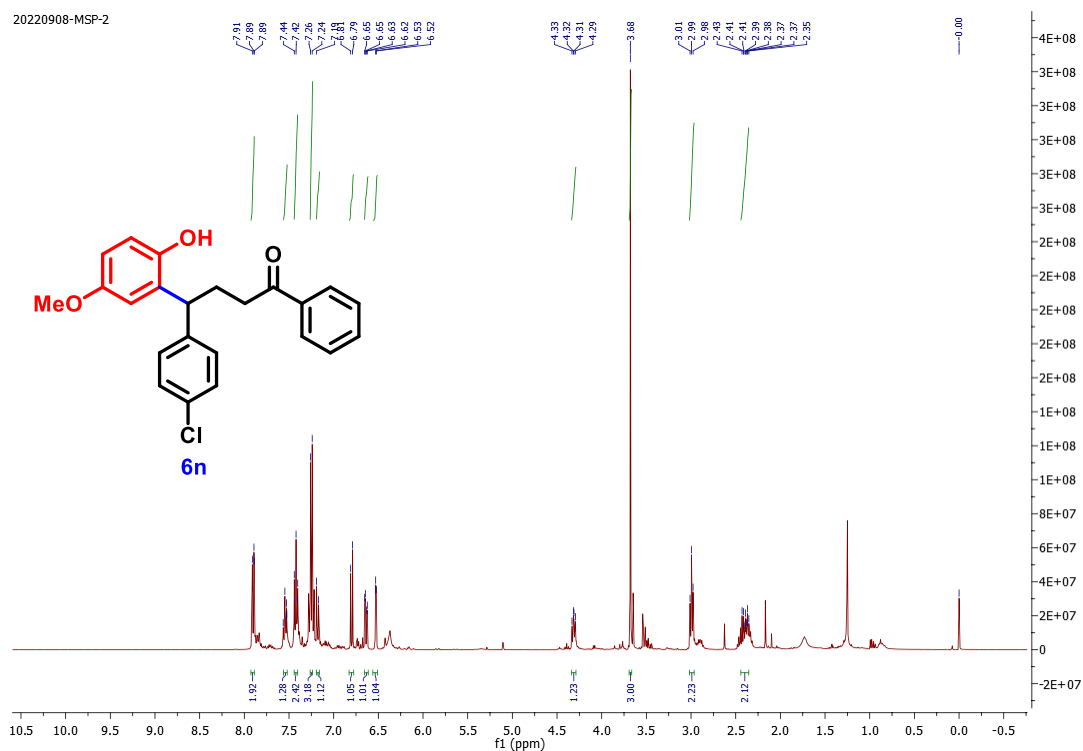
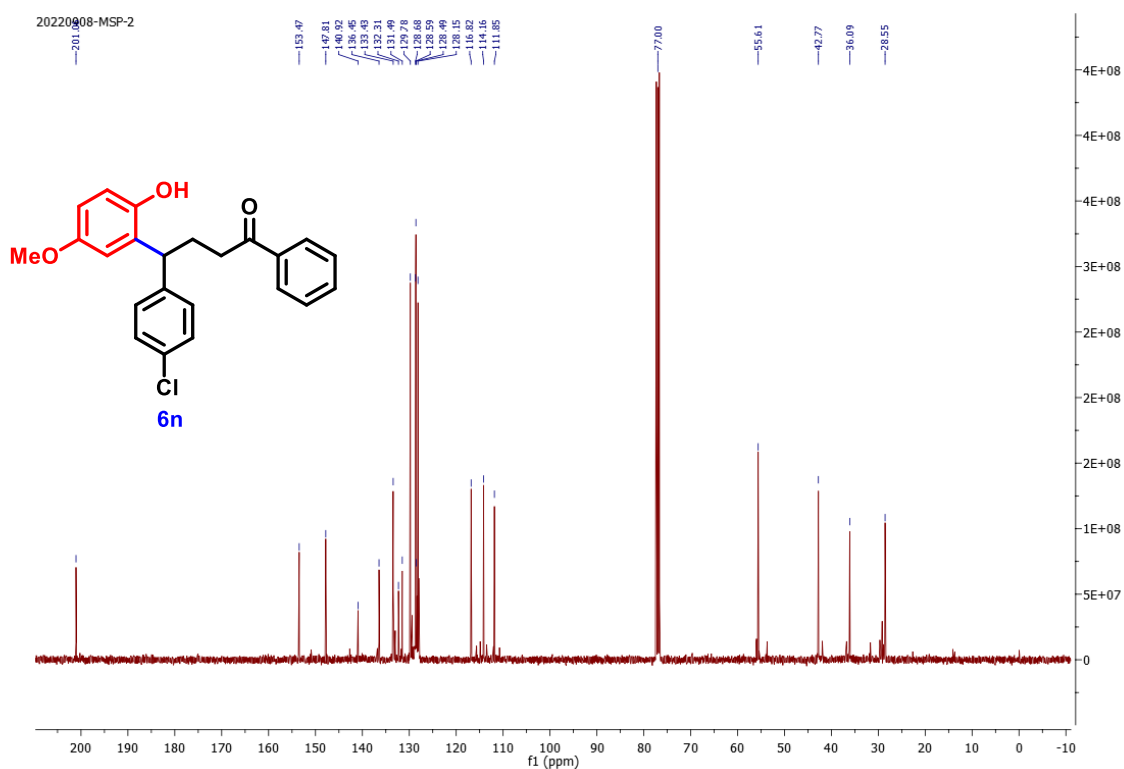


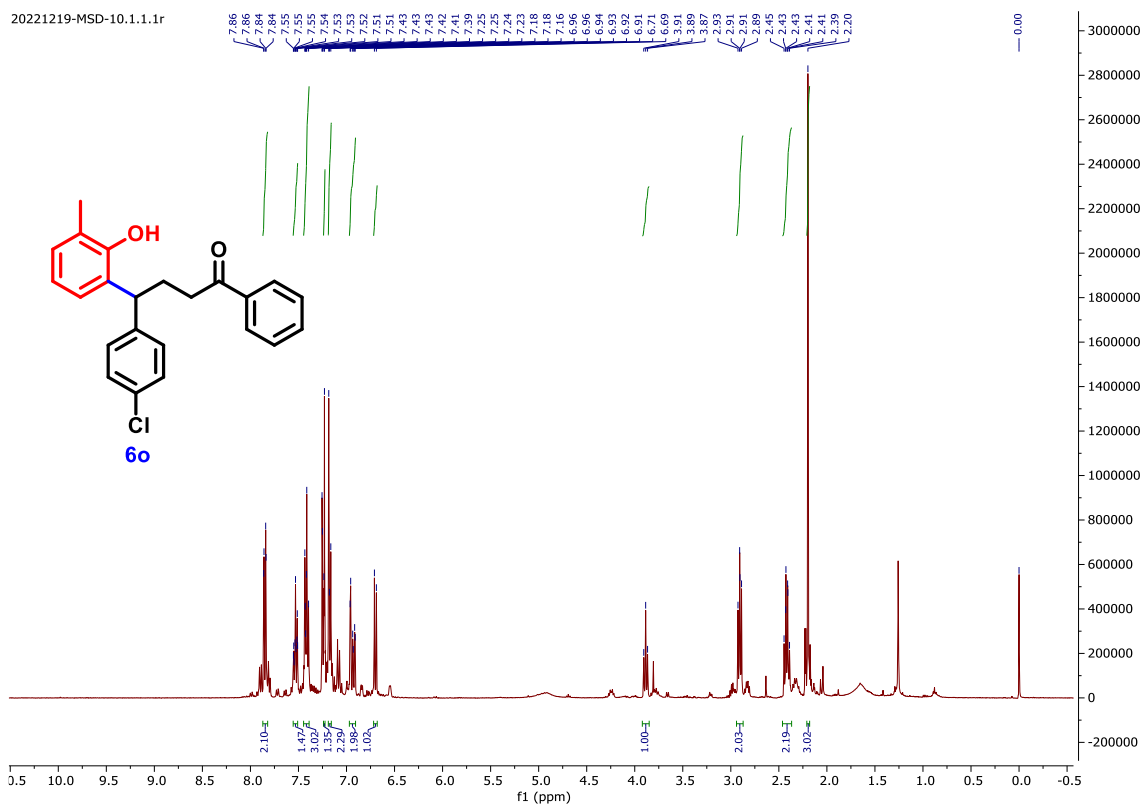
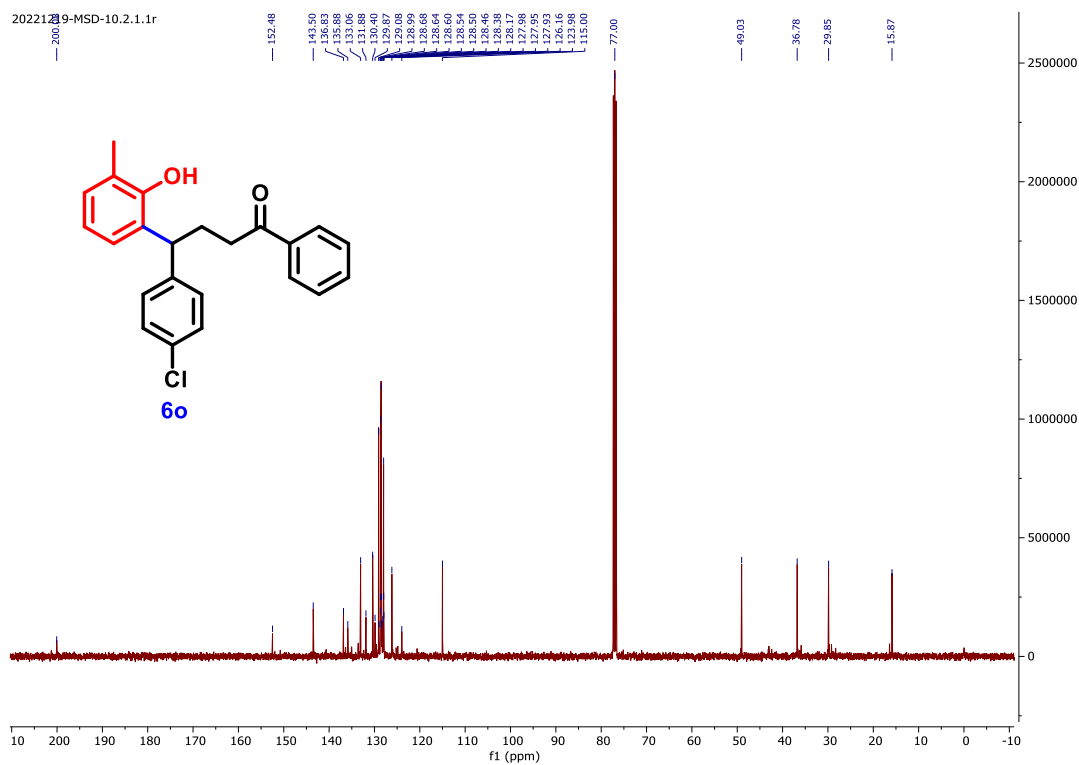
¹³C NMR (CDCl₃, 126 MHz) of **6j**

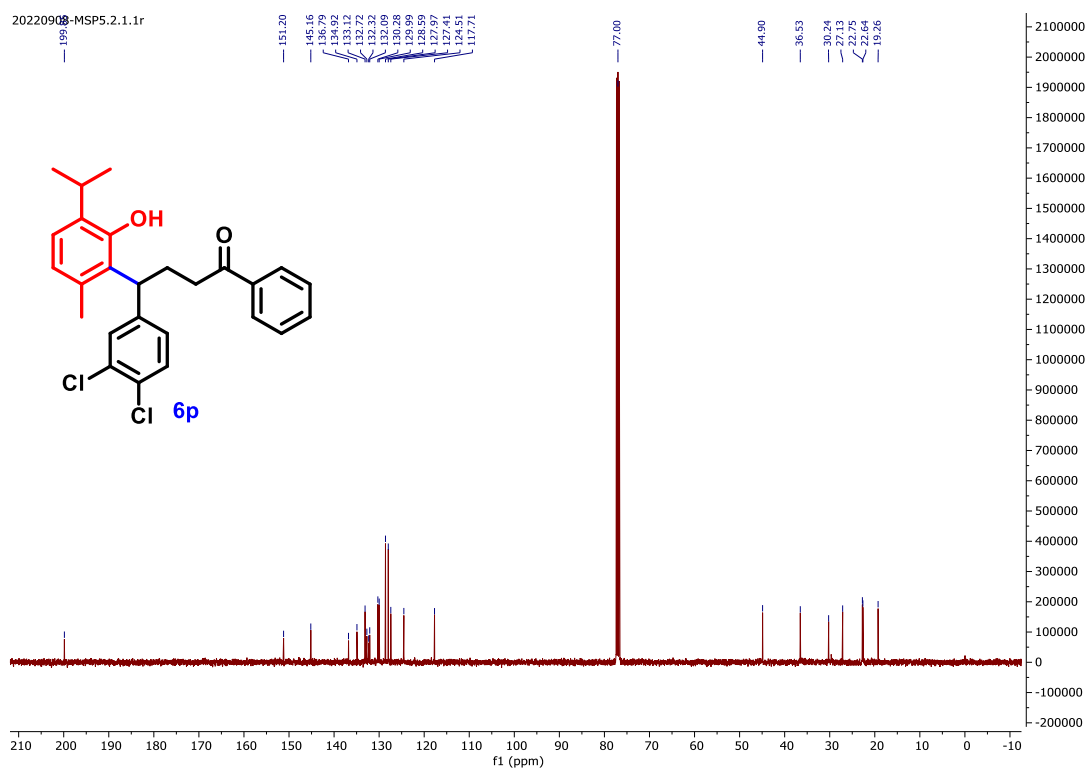
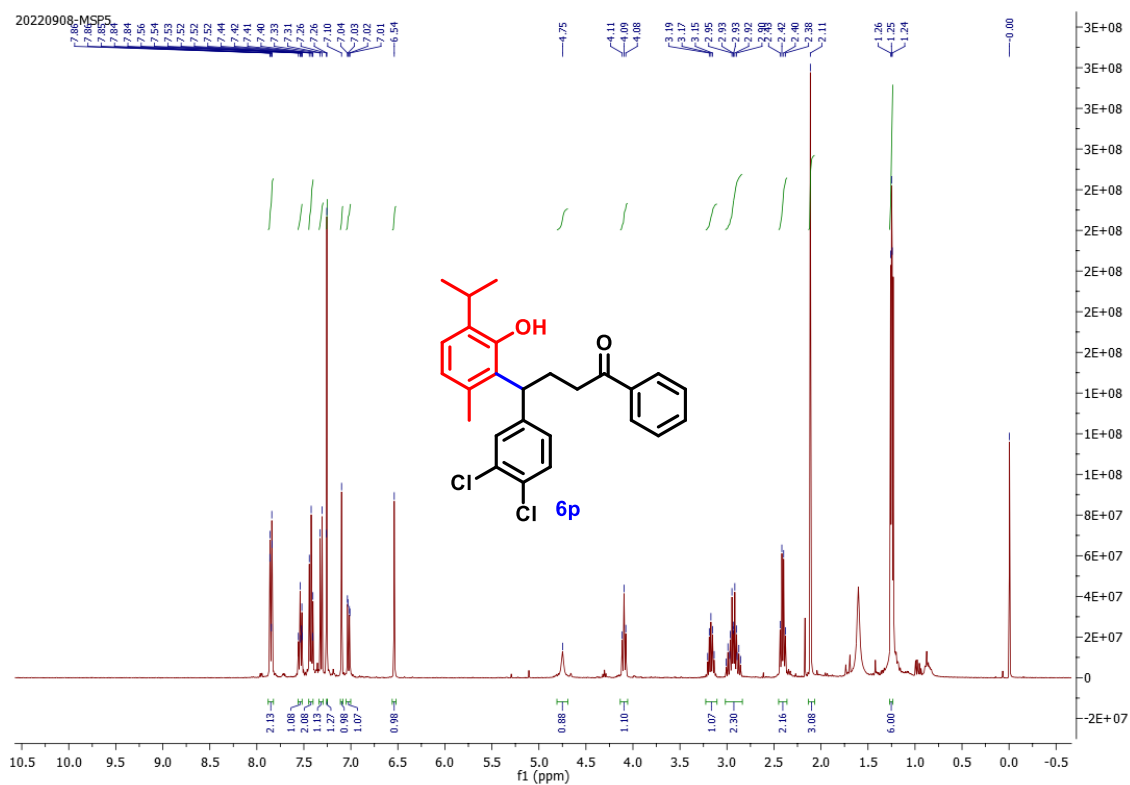
 ^1H NMR (CDCl_3 , 400 MHz) of **6k** ^{13}C NMR (CDCl_3 , 101 MHz) of **6k**

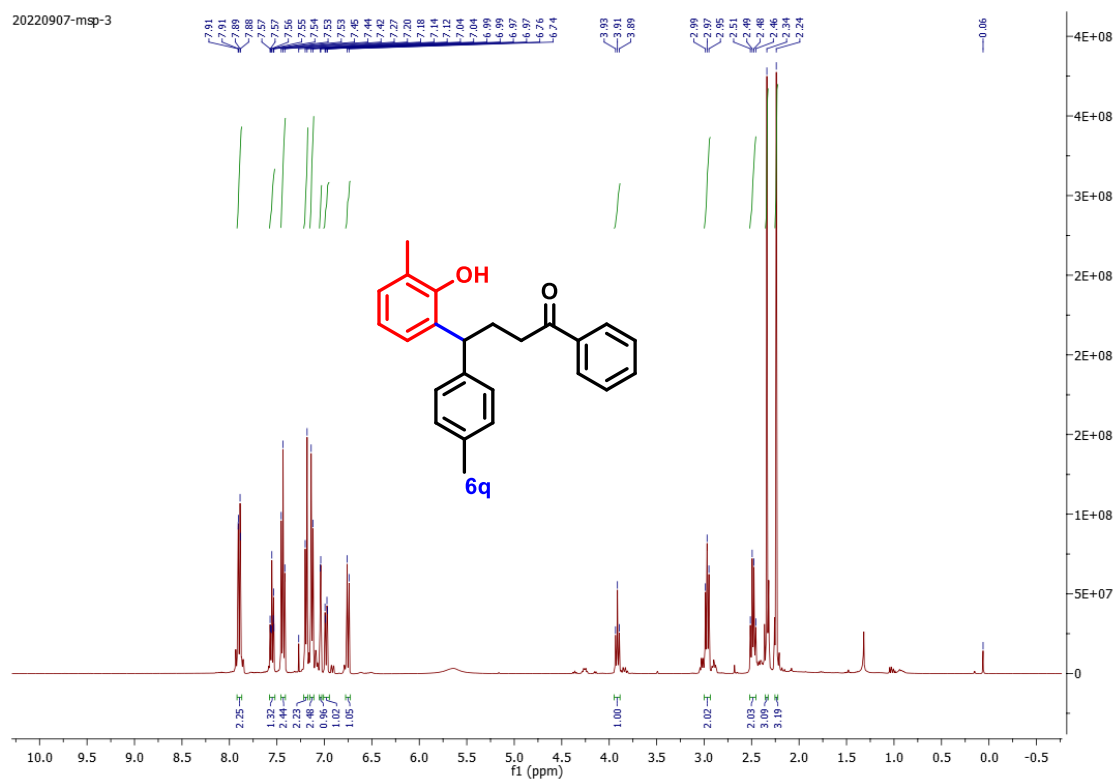
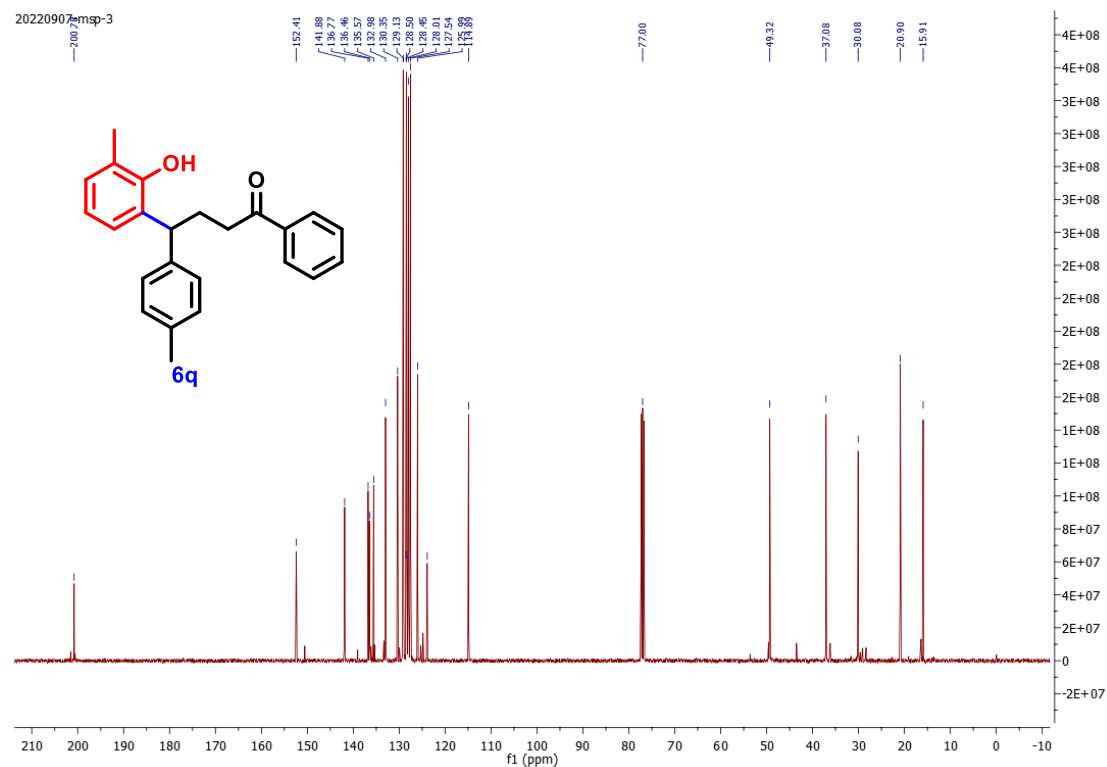
 ^1H NMR (CDCl_3 , 400 MHz) of **6I** ^{13}C NMR (CDCl_3 , 101 MHz) of **6I**

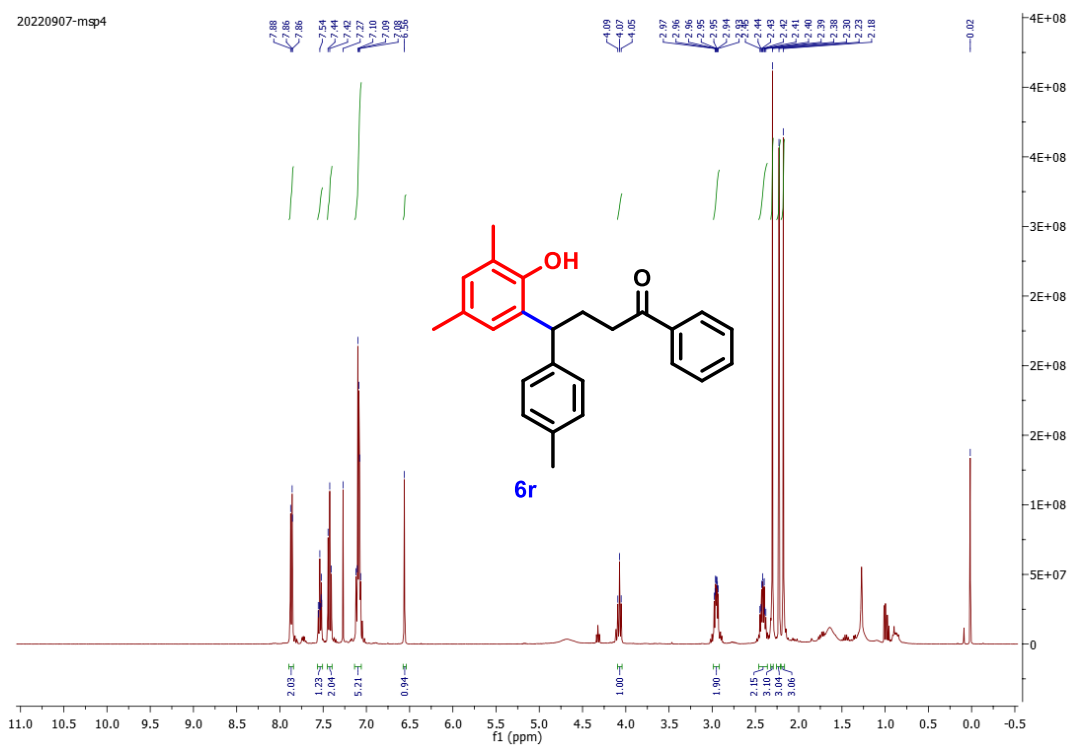
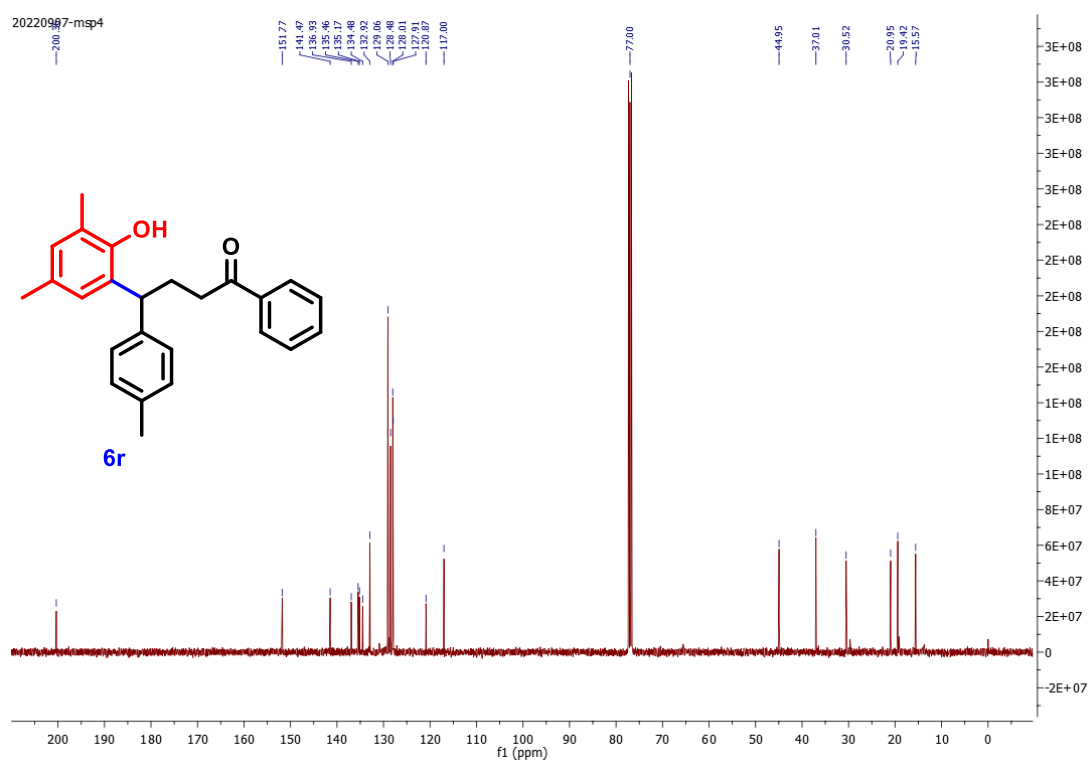


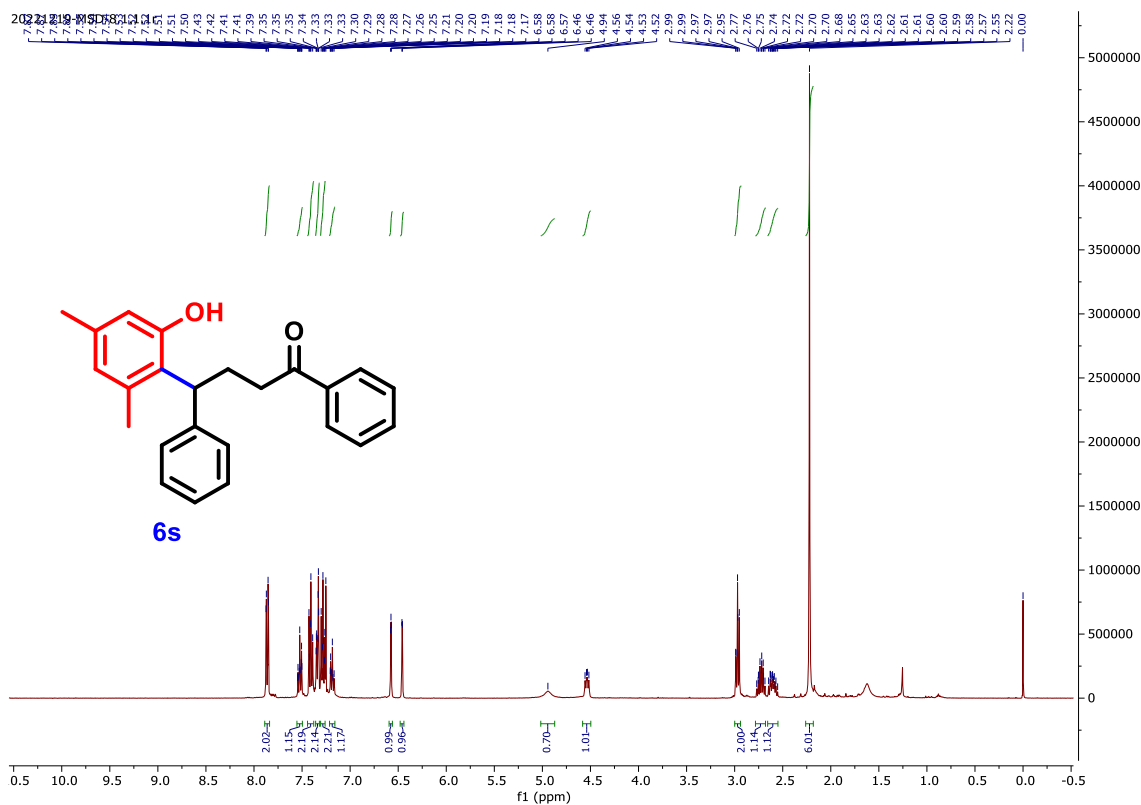
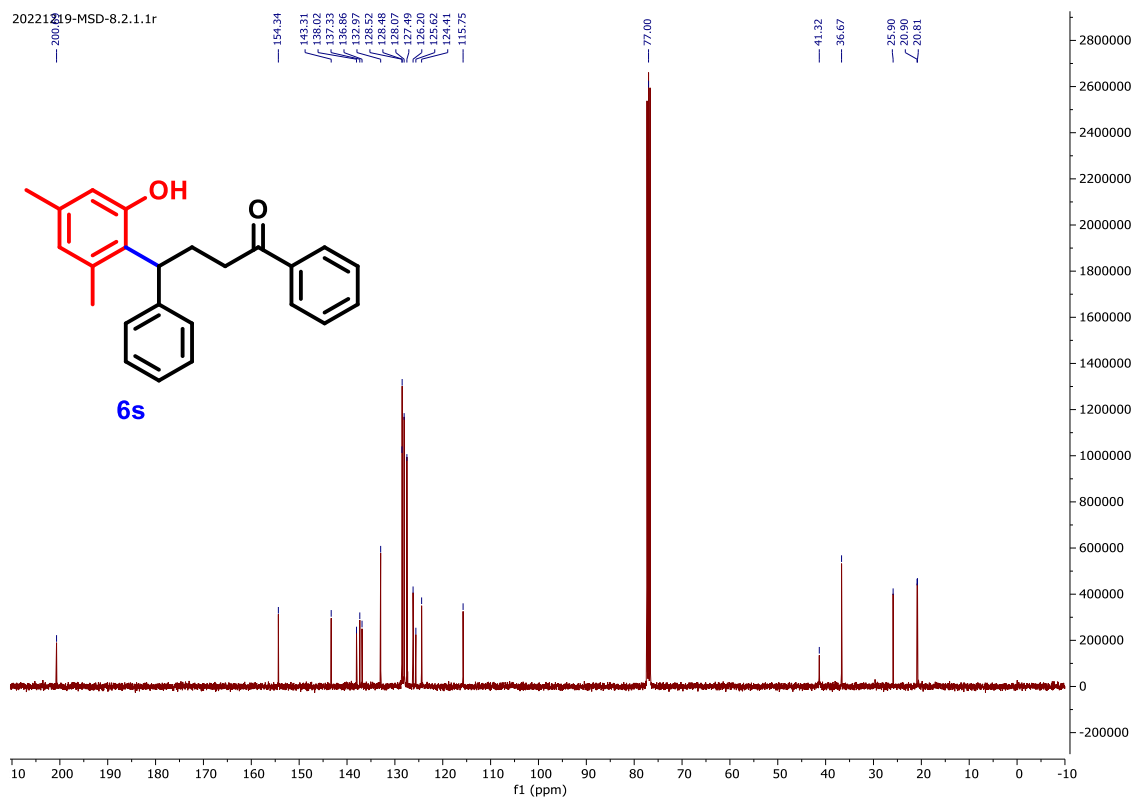
 ^1H NMR (CDCl_3 , 400 MHz) of **6n** ^{13}C NMR (CDCl_3 , 101 MHz) of **6n**

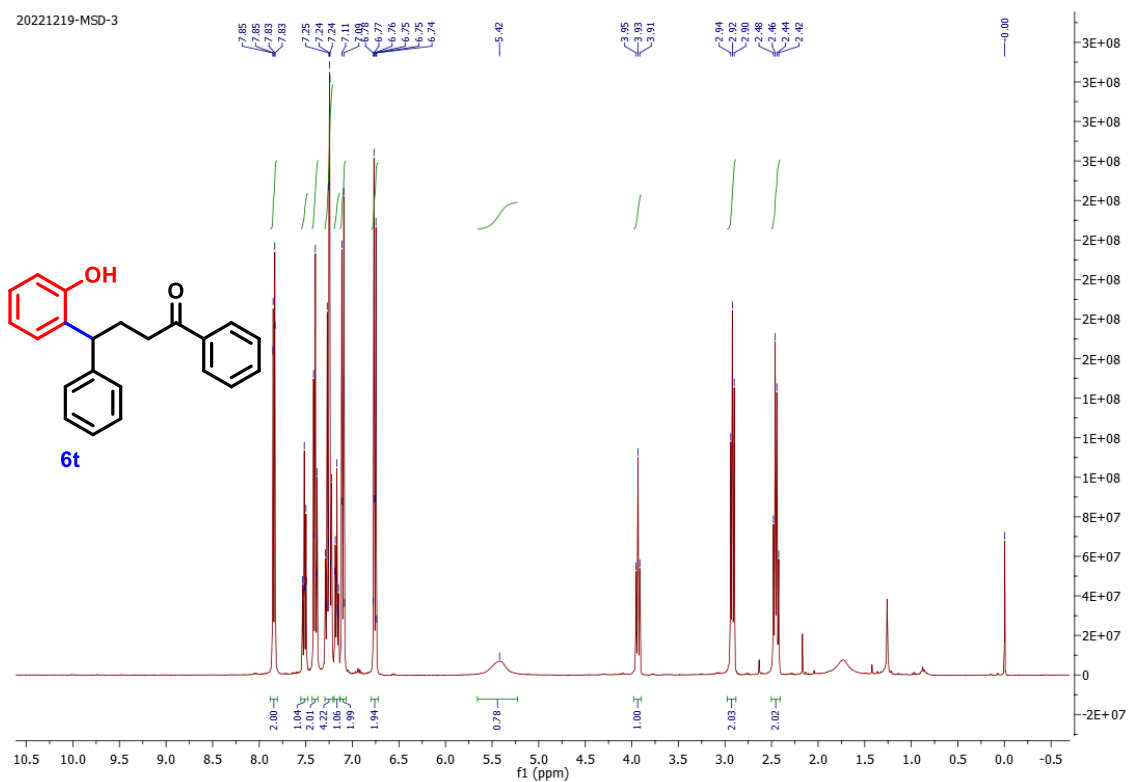
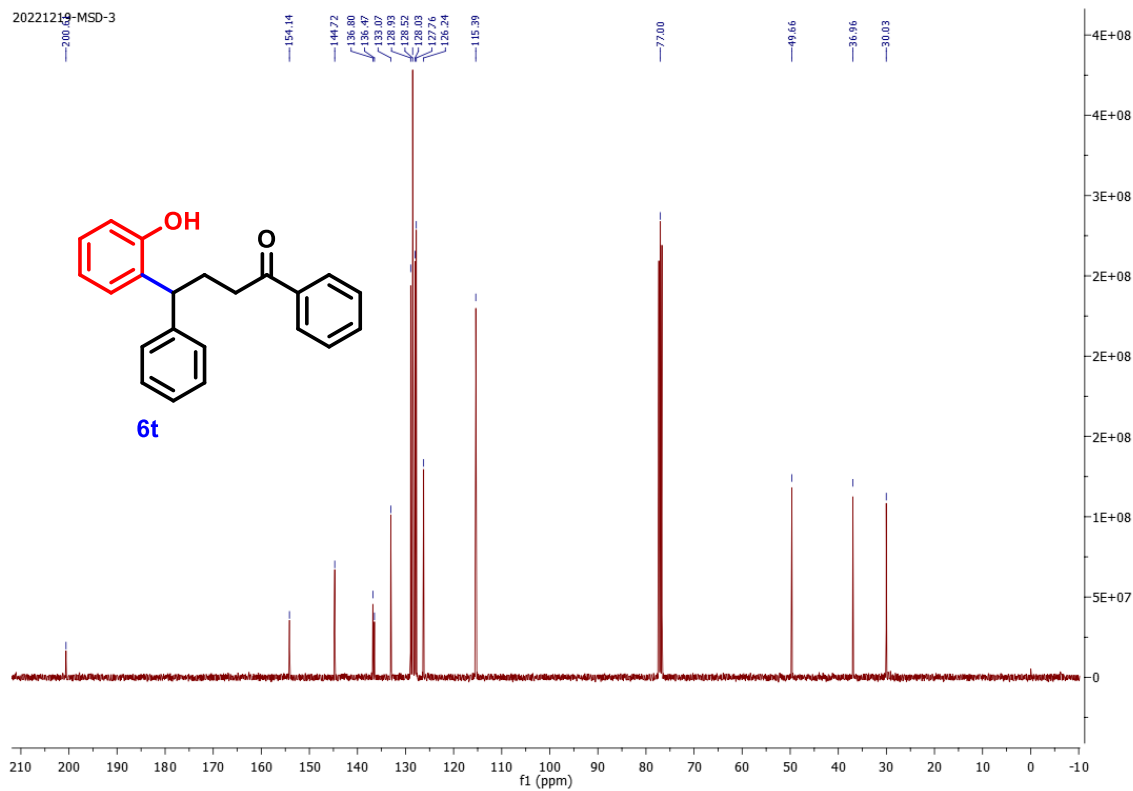
 ^1H NMR (CDCl_3 , 400 MHz) of **6o** ^{13}C NMR (CDCl_3 , 101 MHz) of **6o**

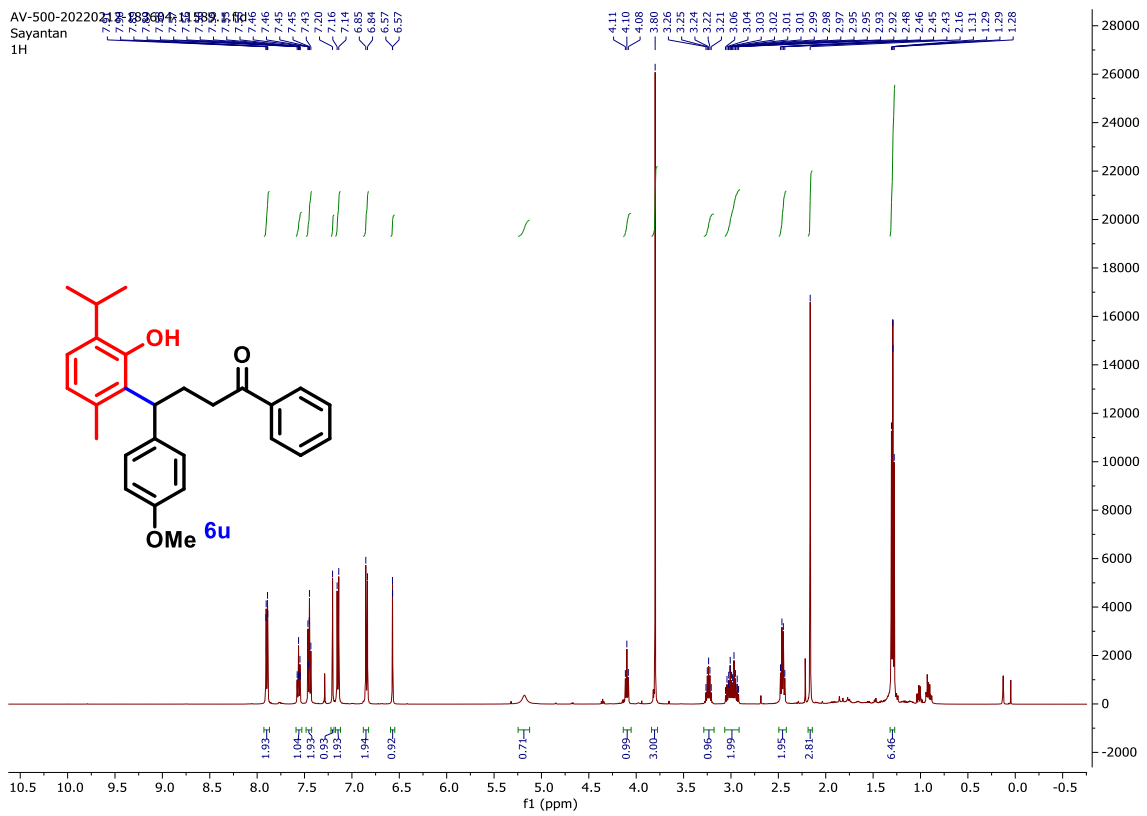


 $^1\text{H NMR}$ (CDCl_3 , 400 MHz) of **6q** $^{13}\text{C NMR}$ (CDCl_3 , 101 MHz) of **6q**

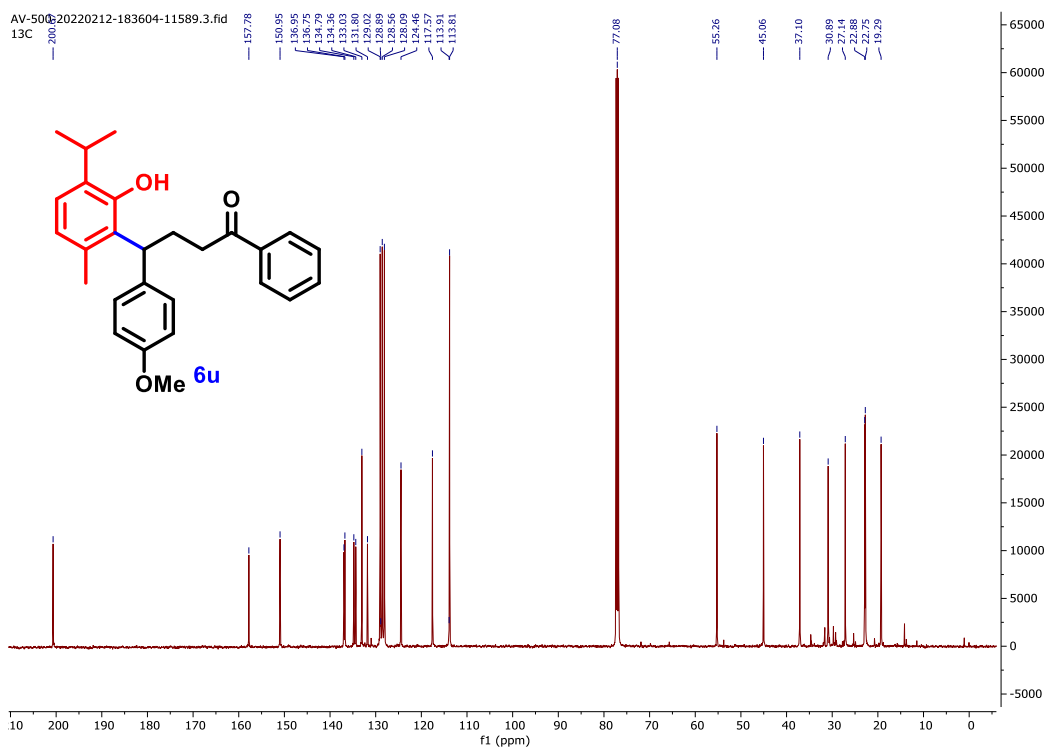
 $^1\text{H NMR}$ (CDCl₃, 400 MHz) of **6r** $^{13}\text{C NMR}$ (CDCl₃, 101 MHz) of **6r**

 ^1H NMR (CDCl_3 , 400 MHz) of **6s** ^{13}C NMR (CDCl_3 , 101 MHz) of **6s**

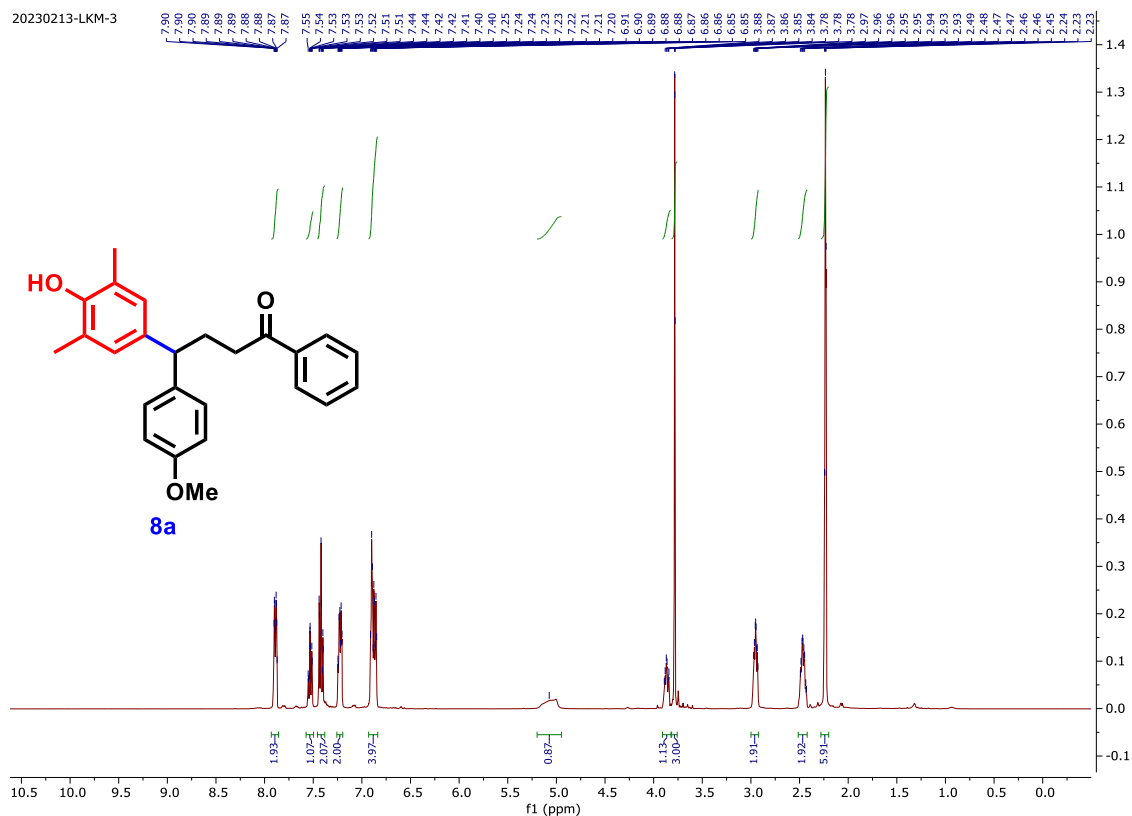
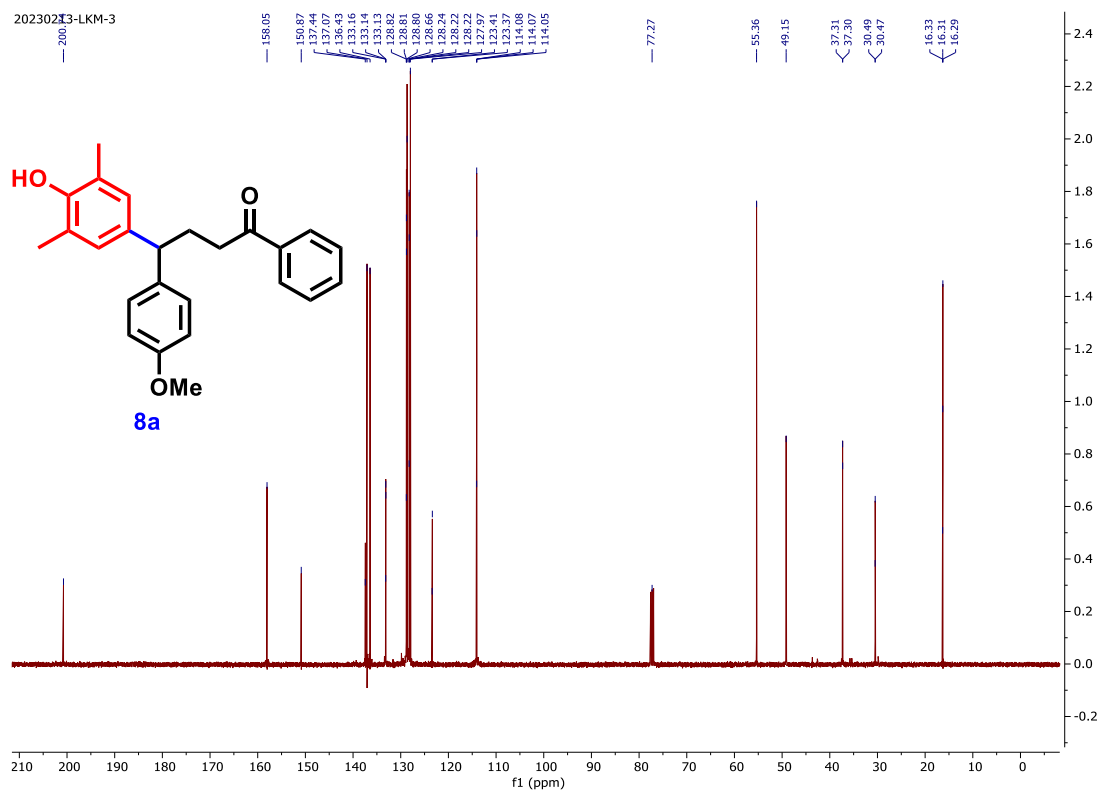
 ^1H NMR (CDCl_3 , 400 MHz) of **6t** ^{13}C NMR (CDCl_3 , 101 MHz) of **6t**

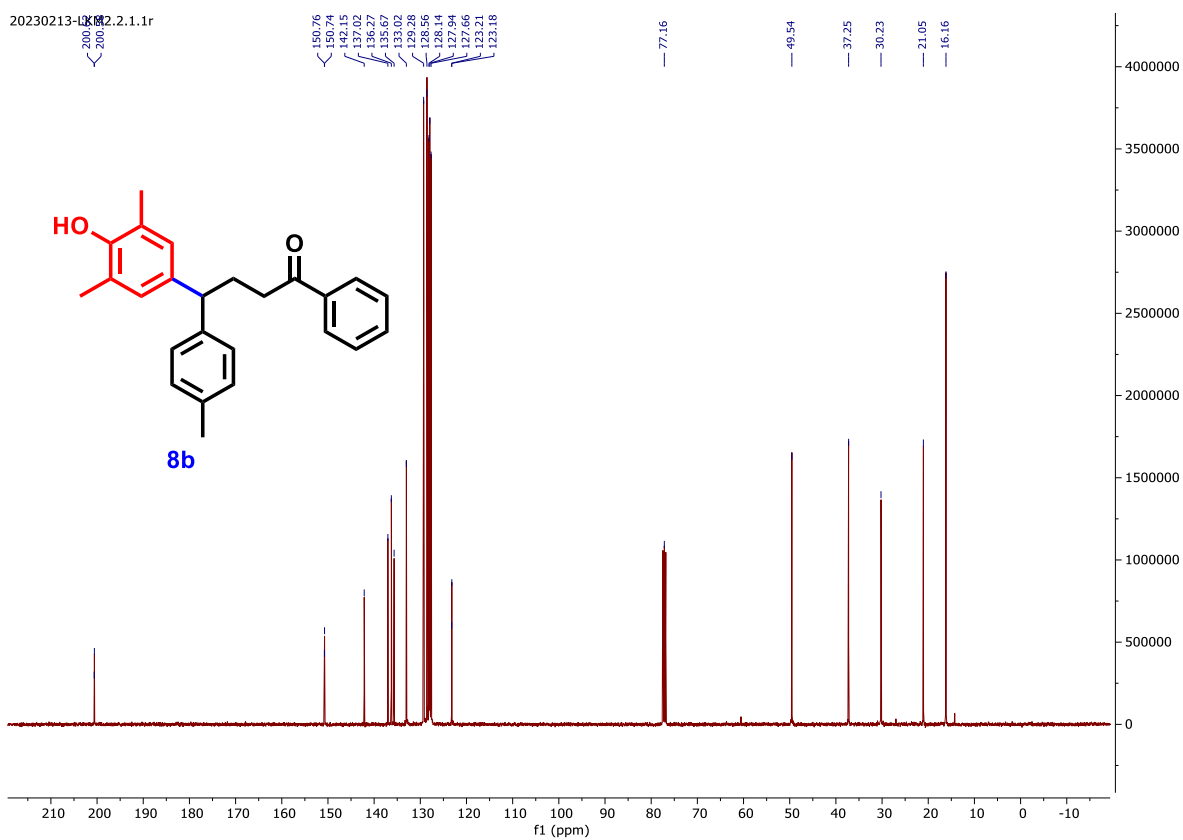
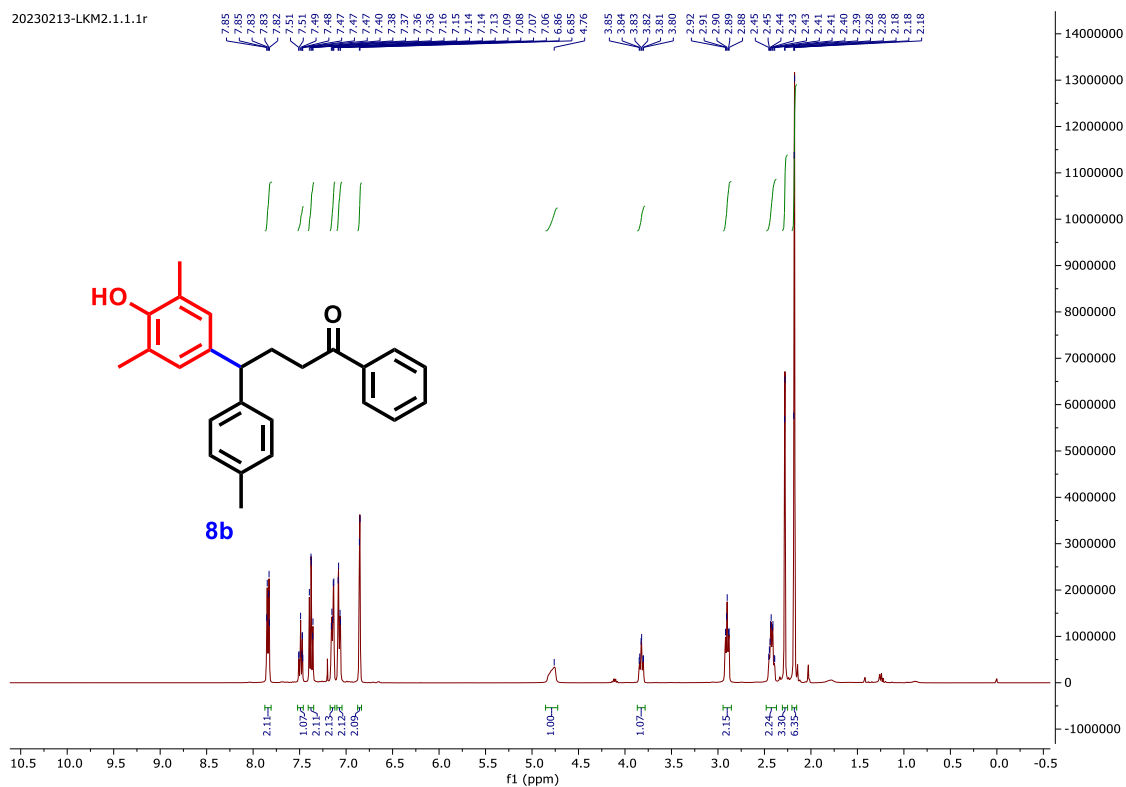


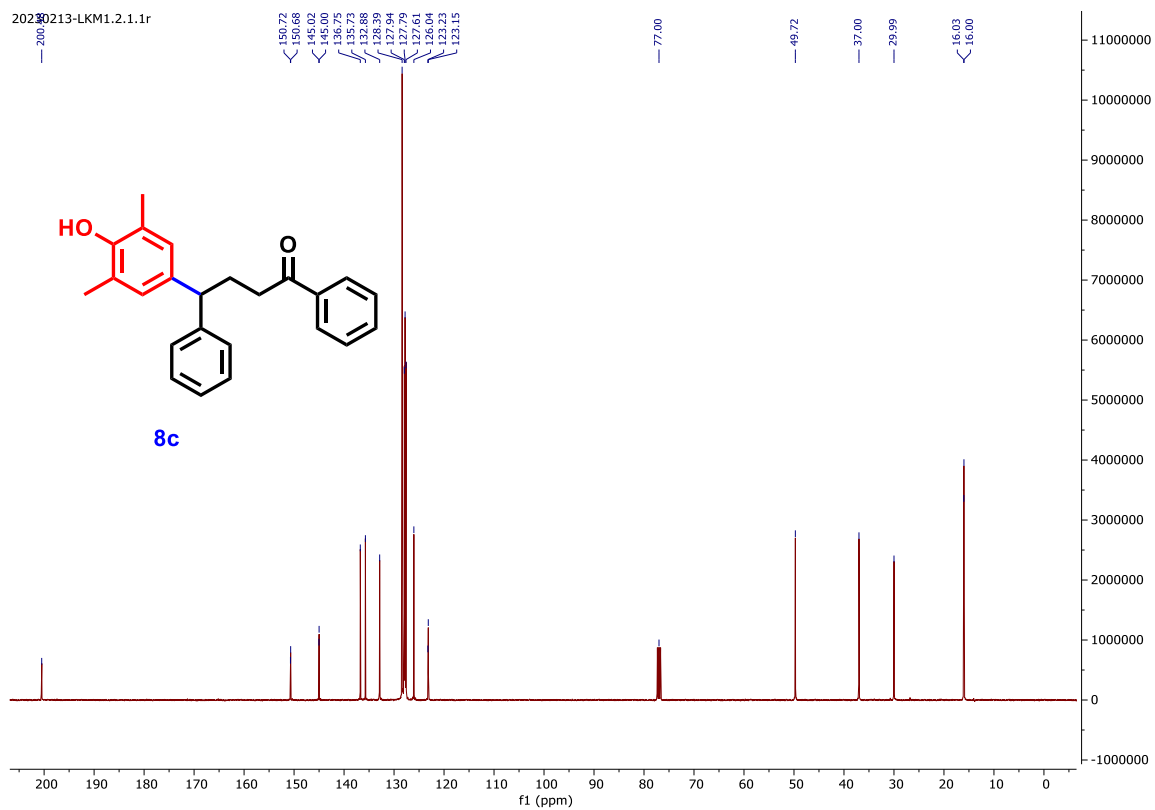
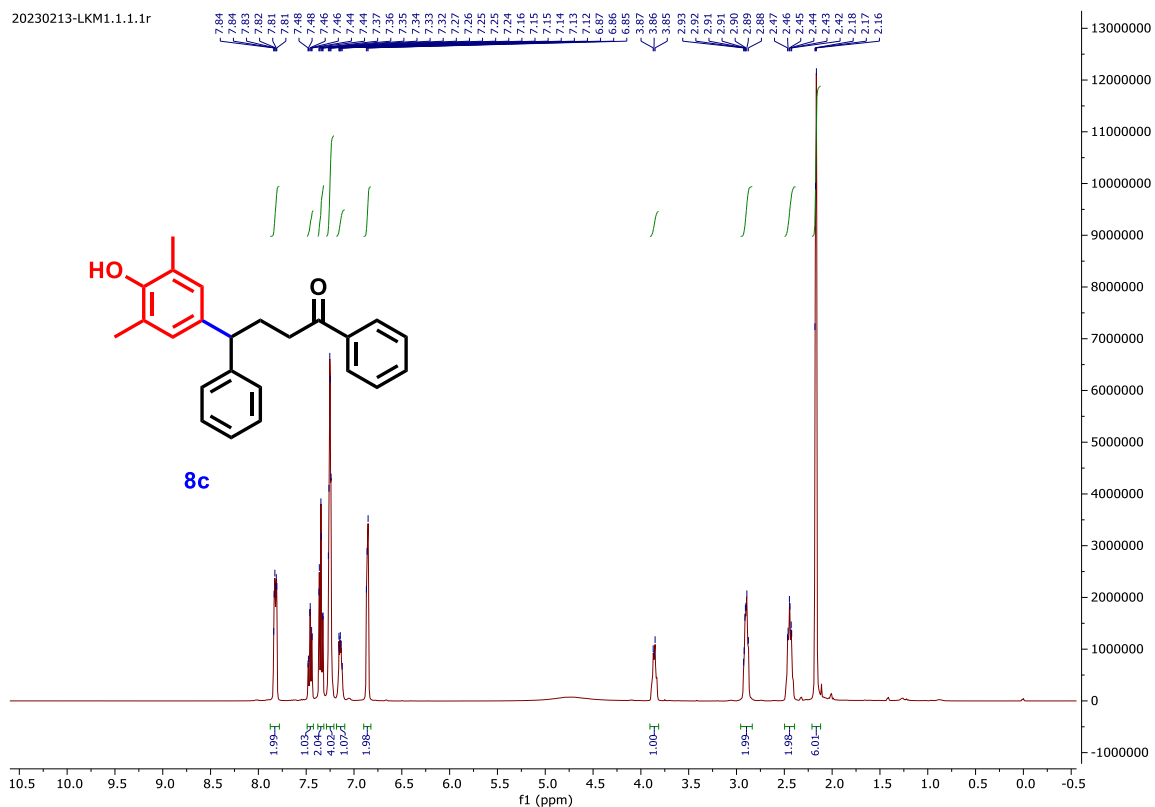
¹H NMR (CDCl₃, 500 MHz) of **6u**

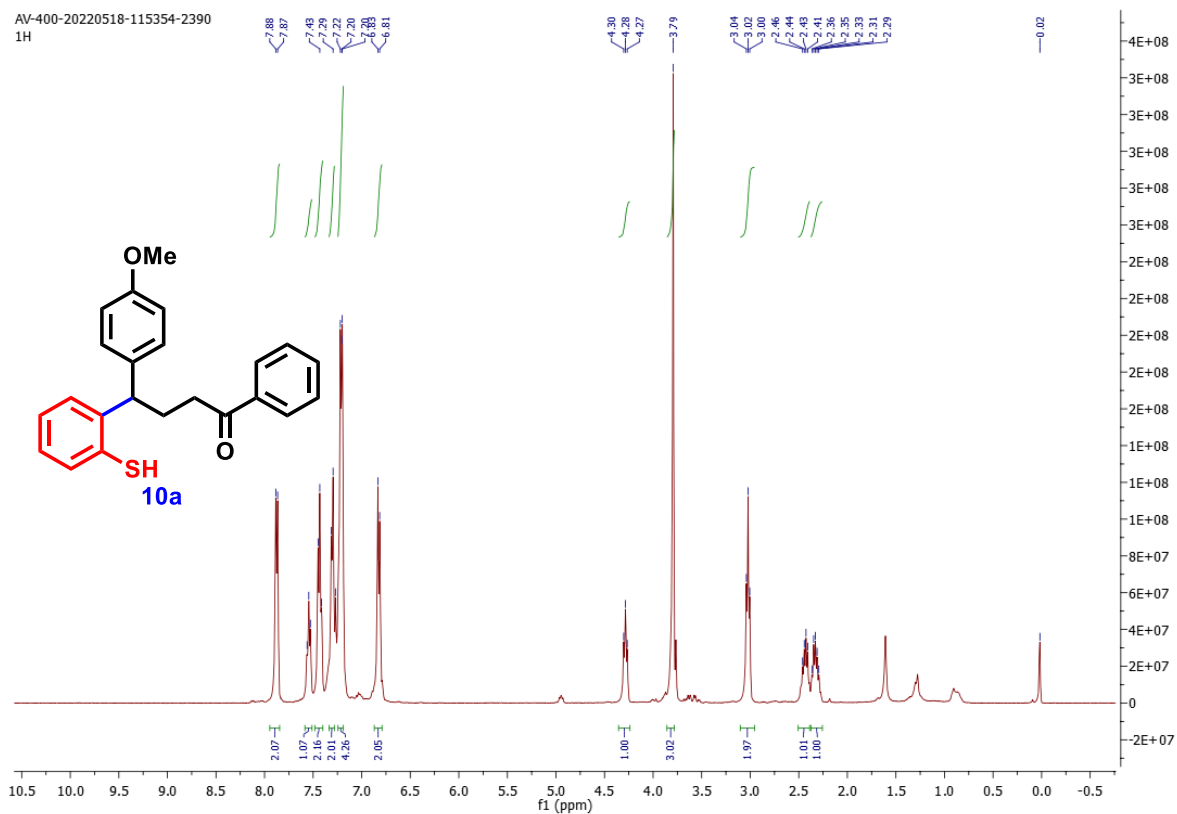
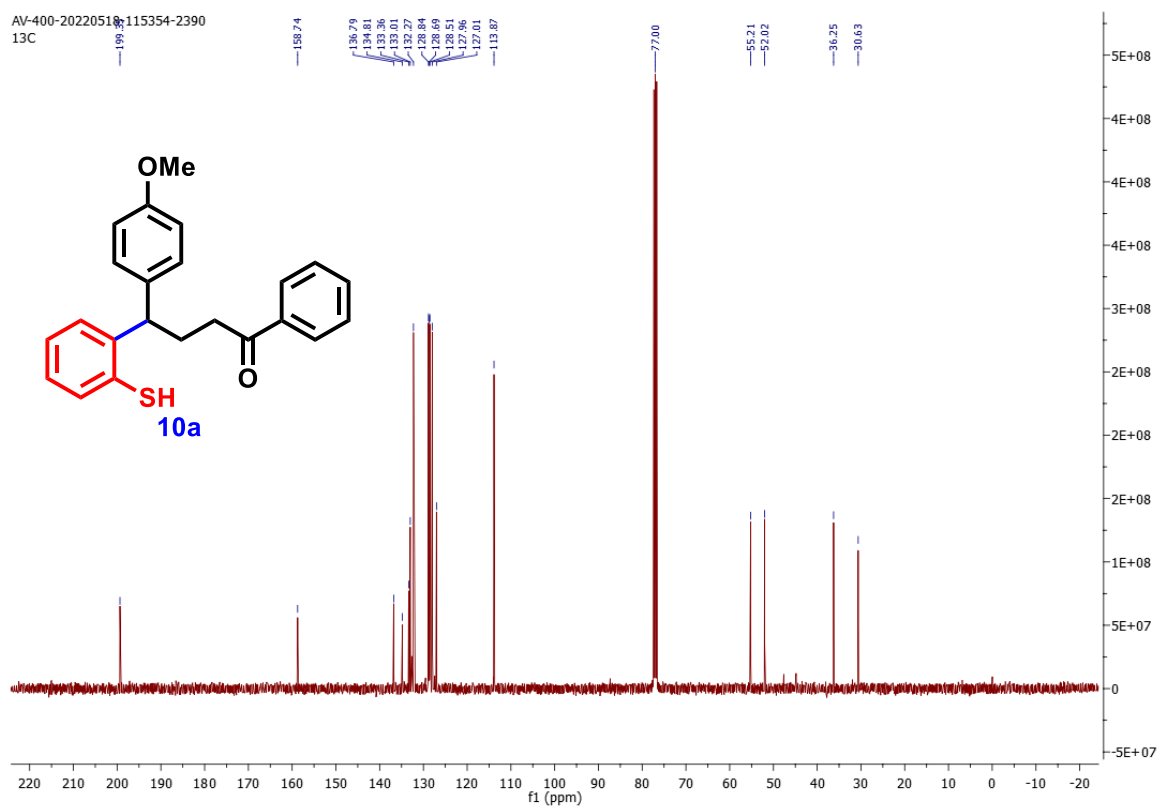


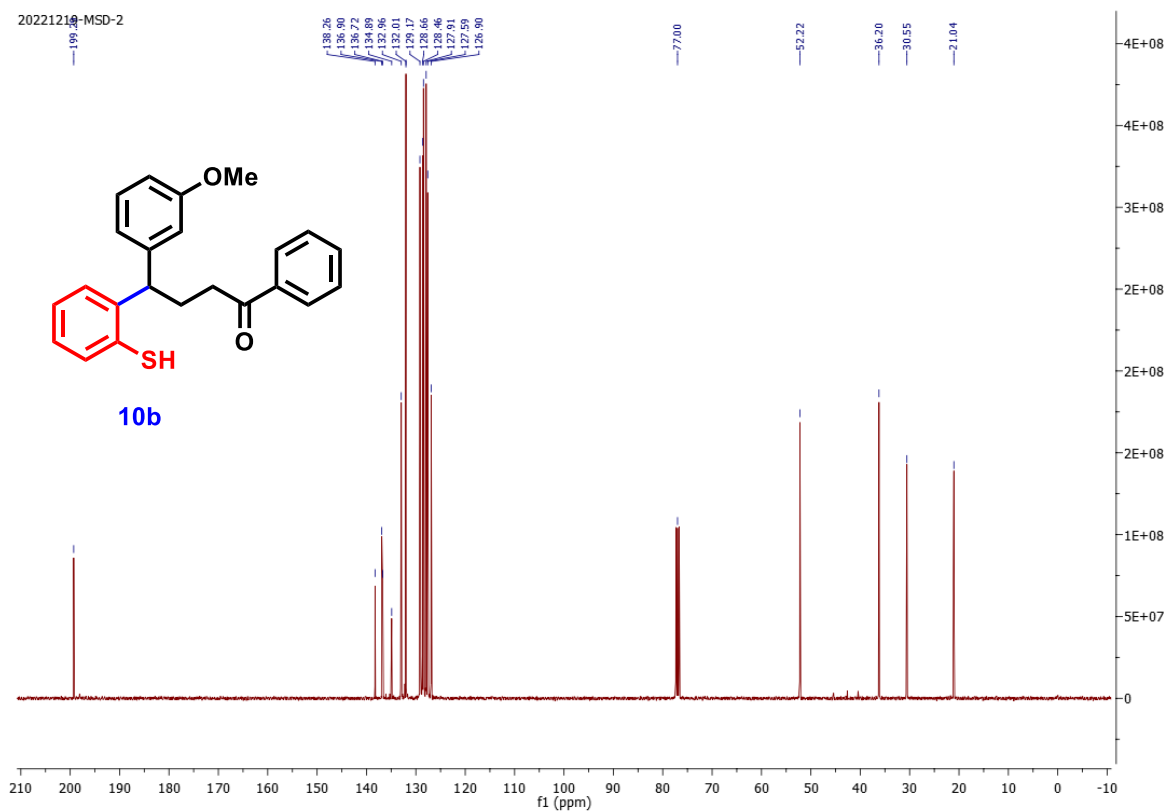
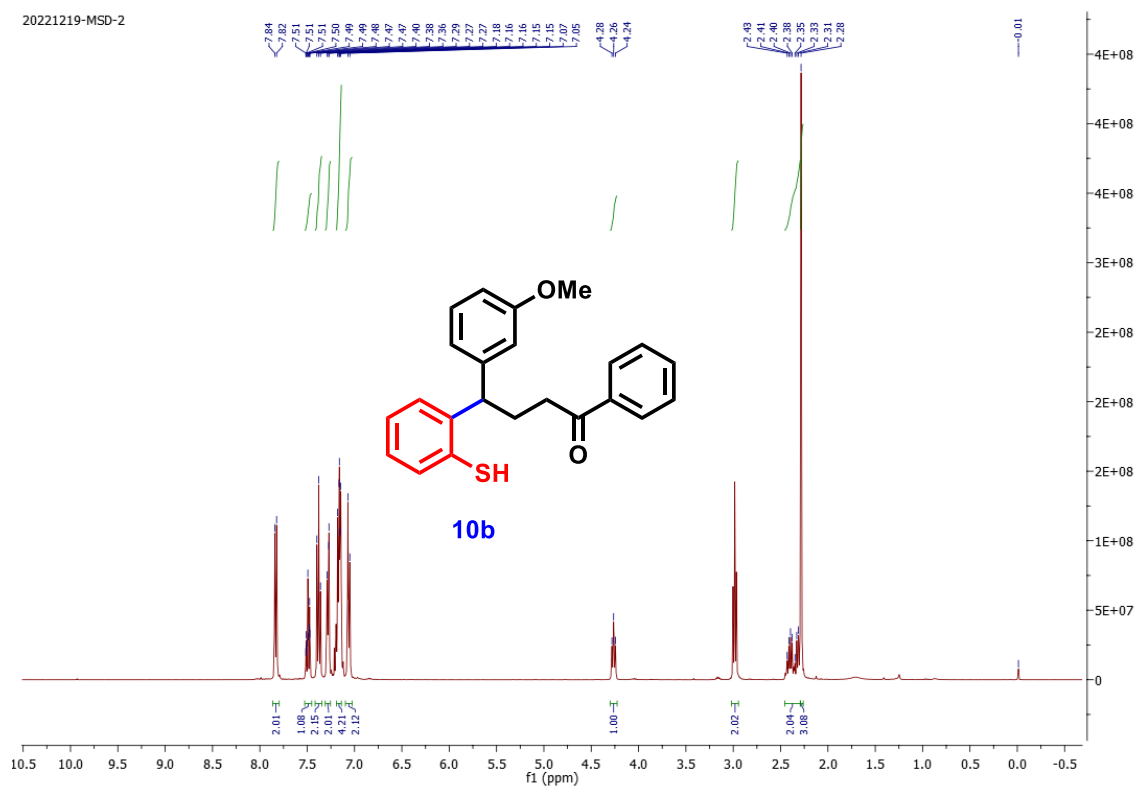
¹³C NMR (CDCl₃, 126 MHz) of **6u**

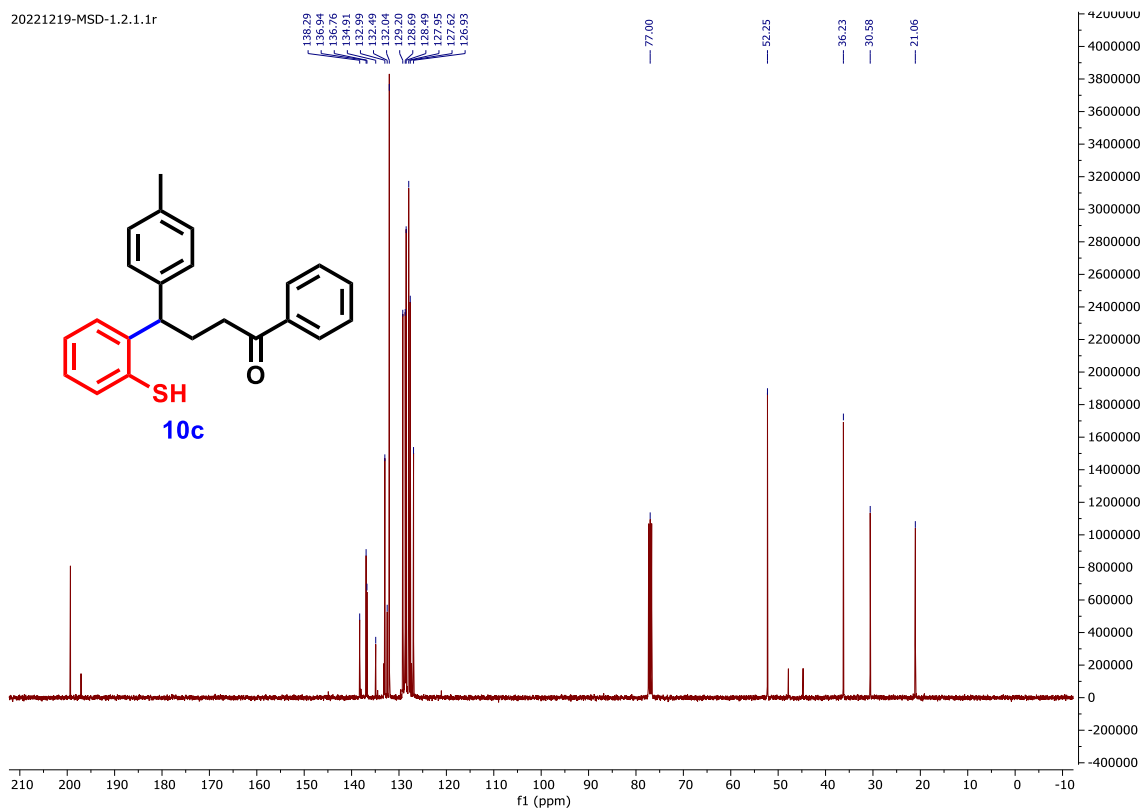
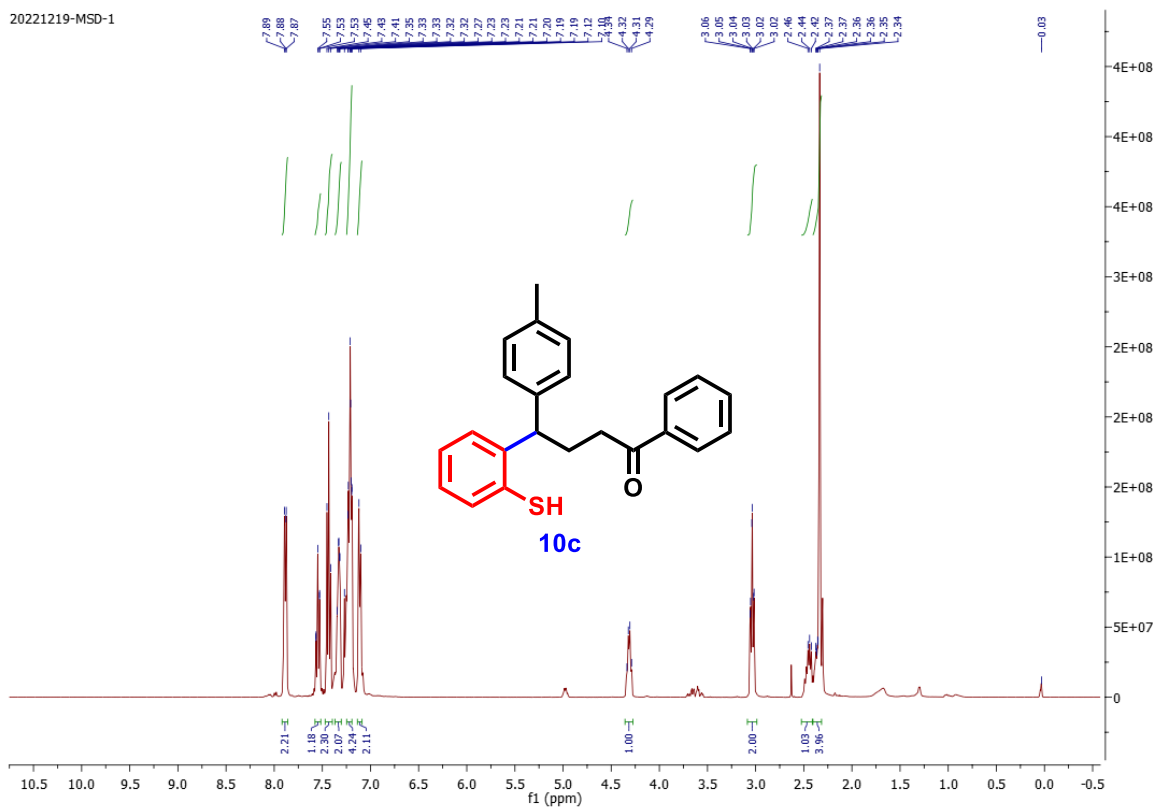
 ^1H NMR (CDCl_3 , 500 MHz) of **8a** ^{13}C NMR (CDCl_3 , 126 MHz) of **8a**

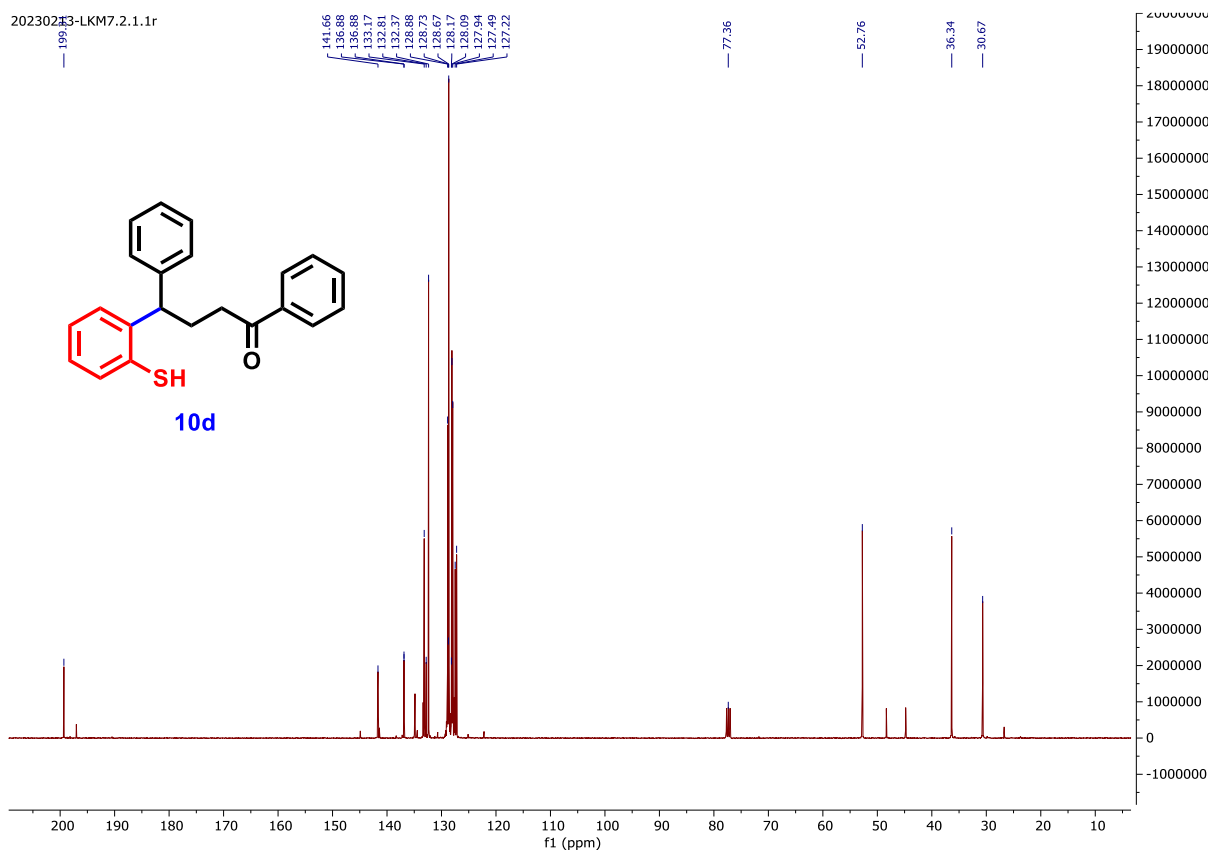
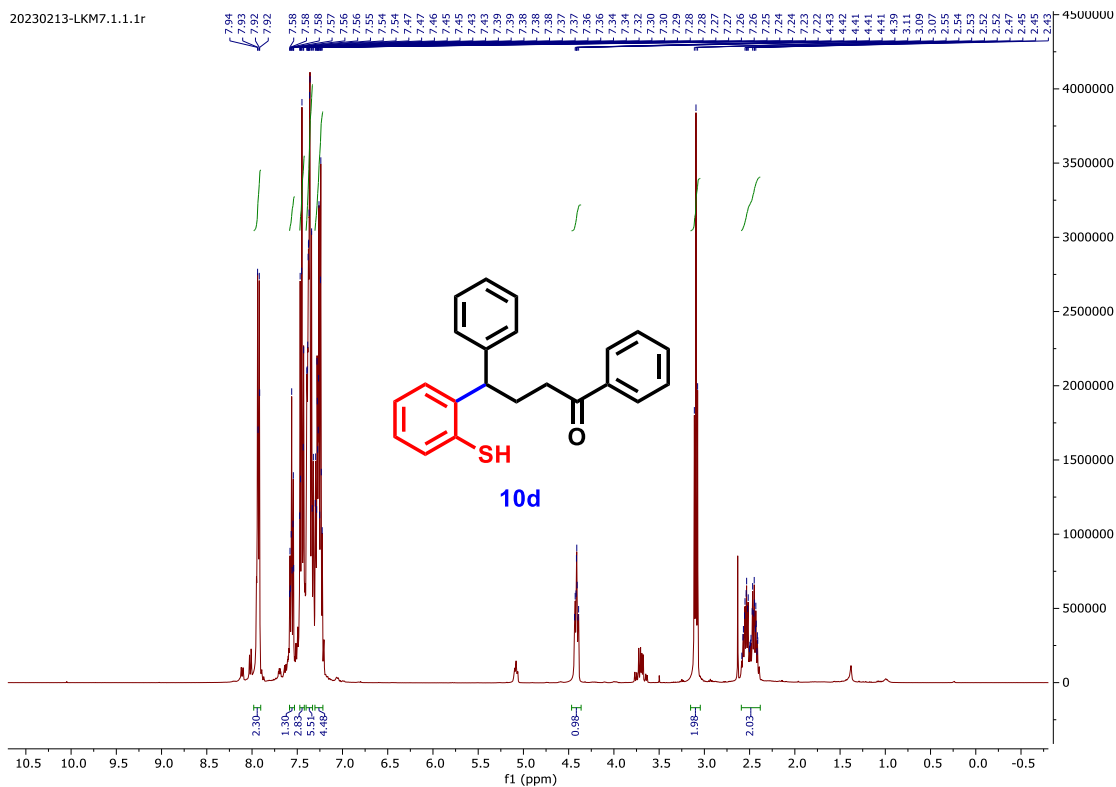


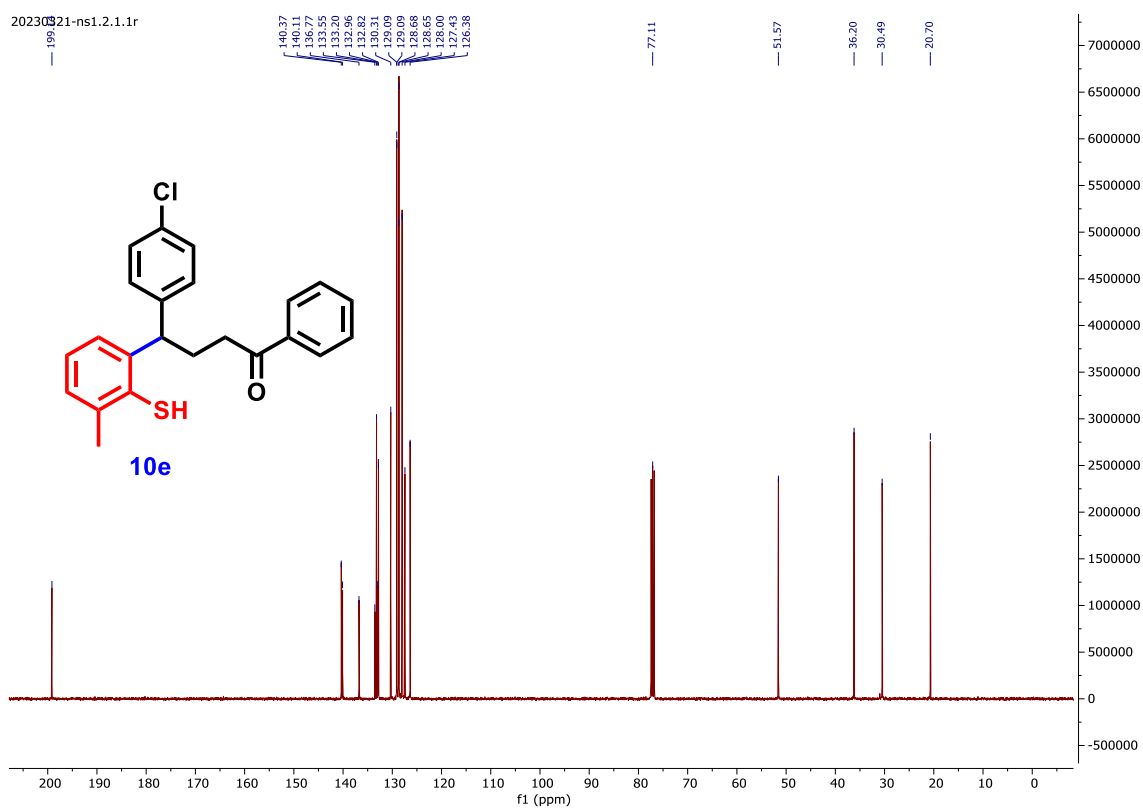
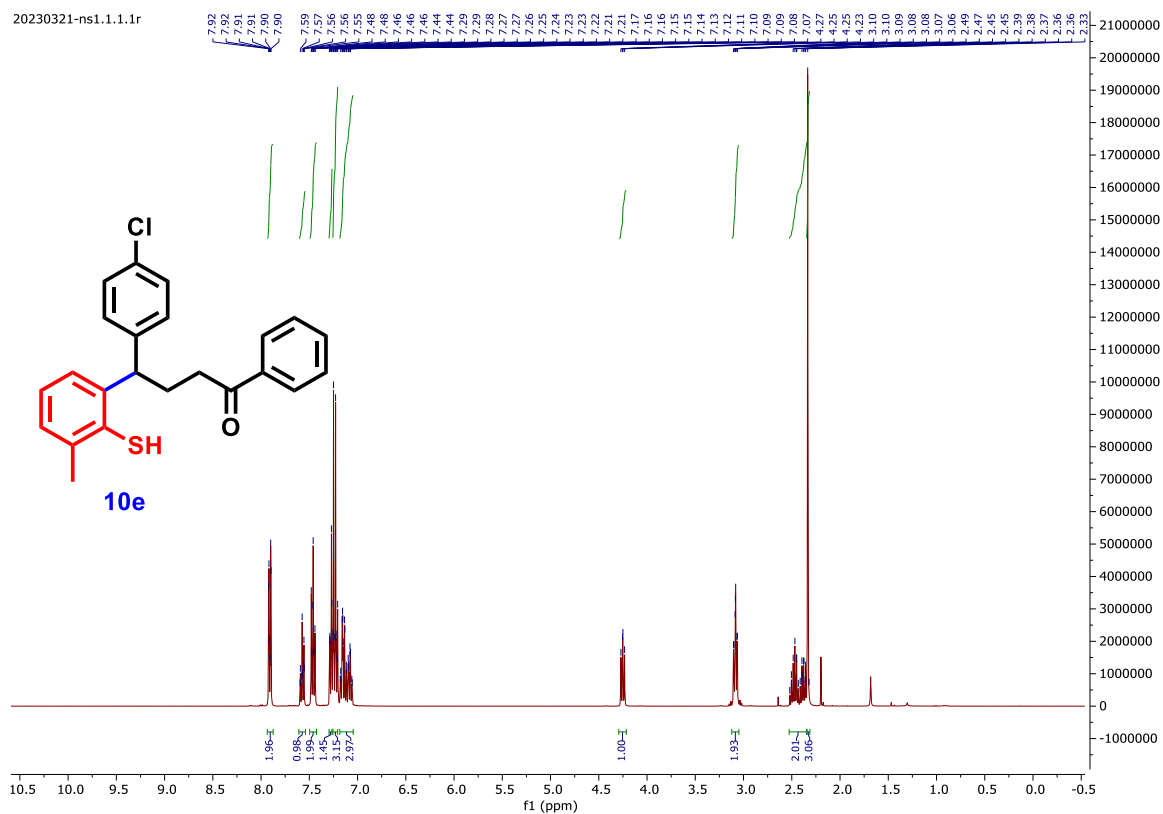


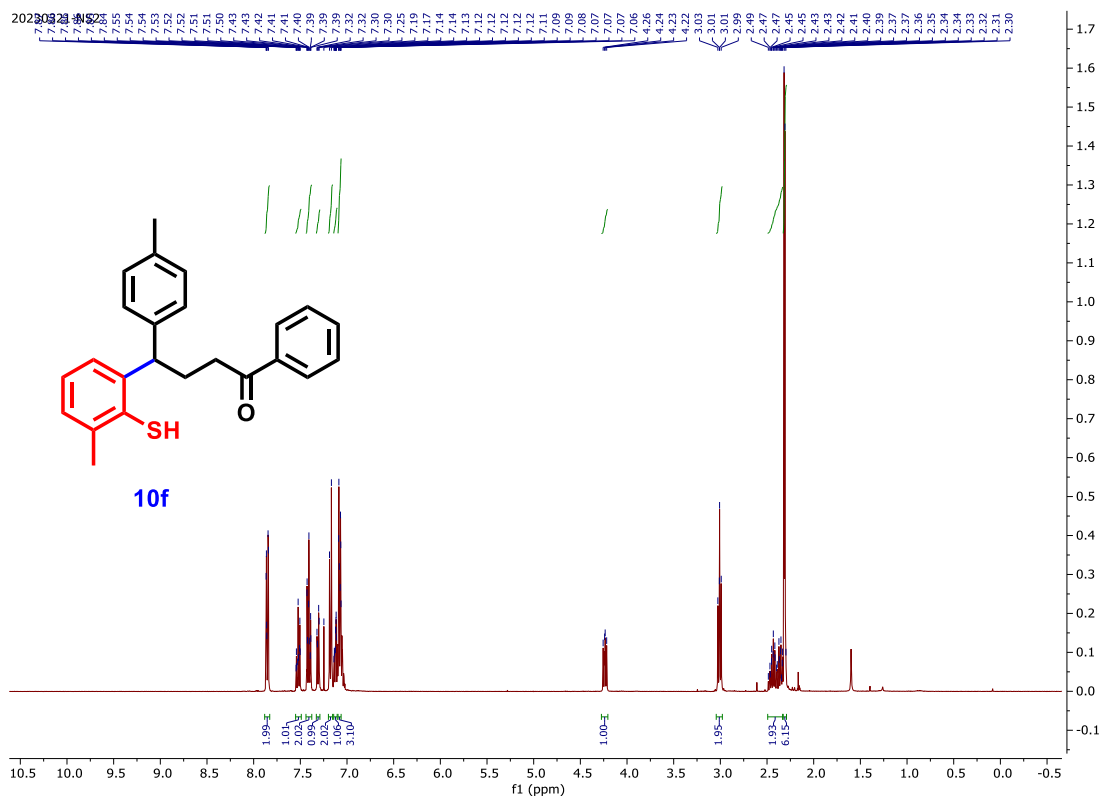
 ^1H NMR (CDCl_3 , 400 MHz) of **10a** ^{13}C NMR (CDCl_3 , 101 MHz) of **10a**



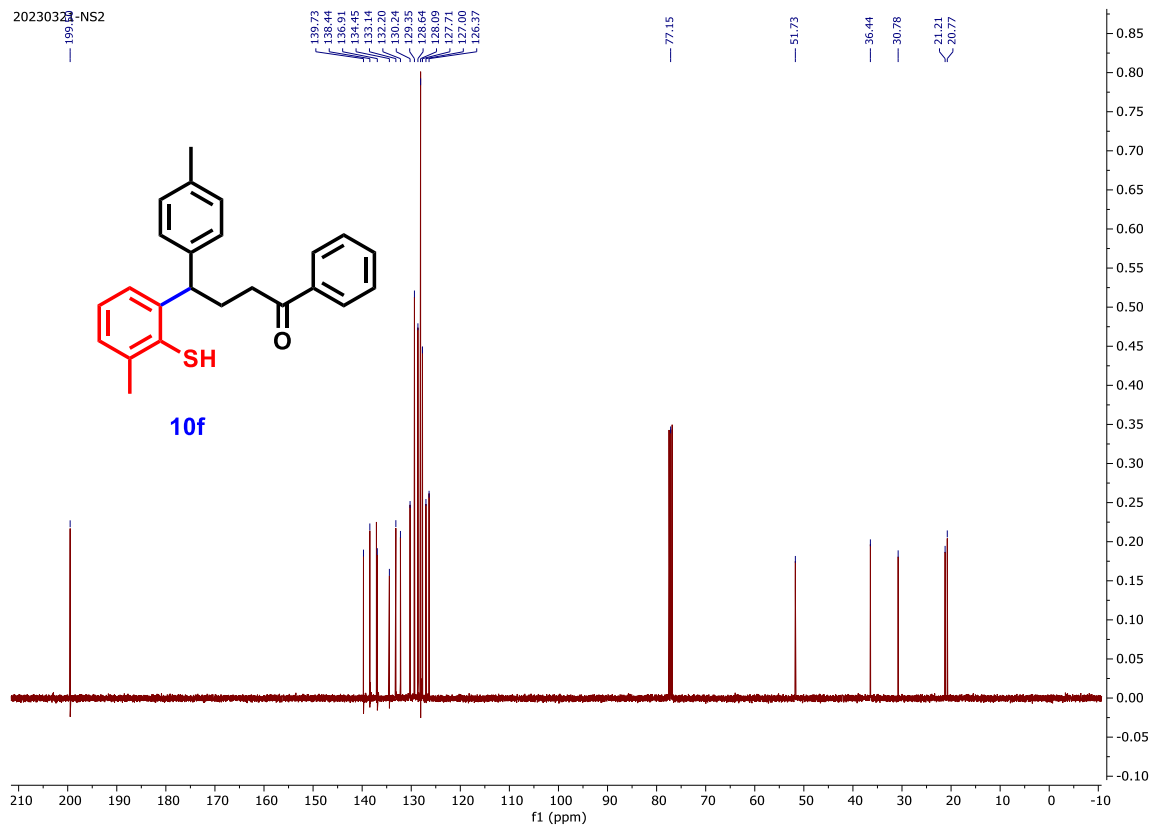




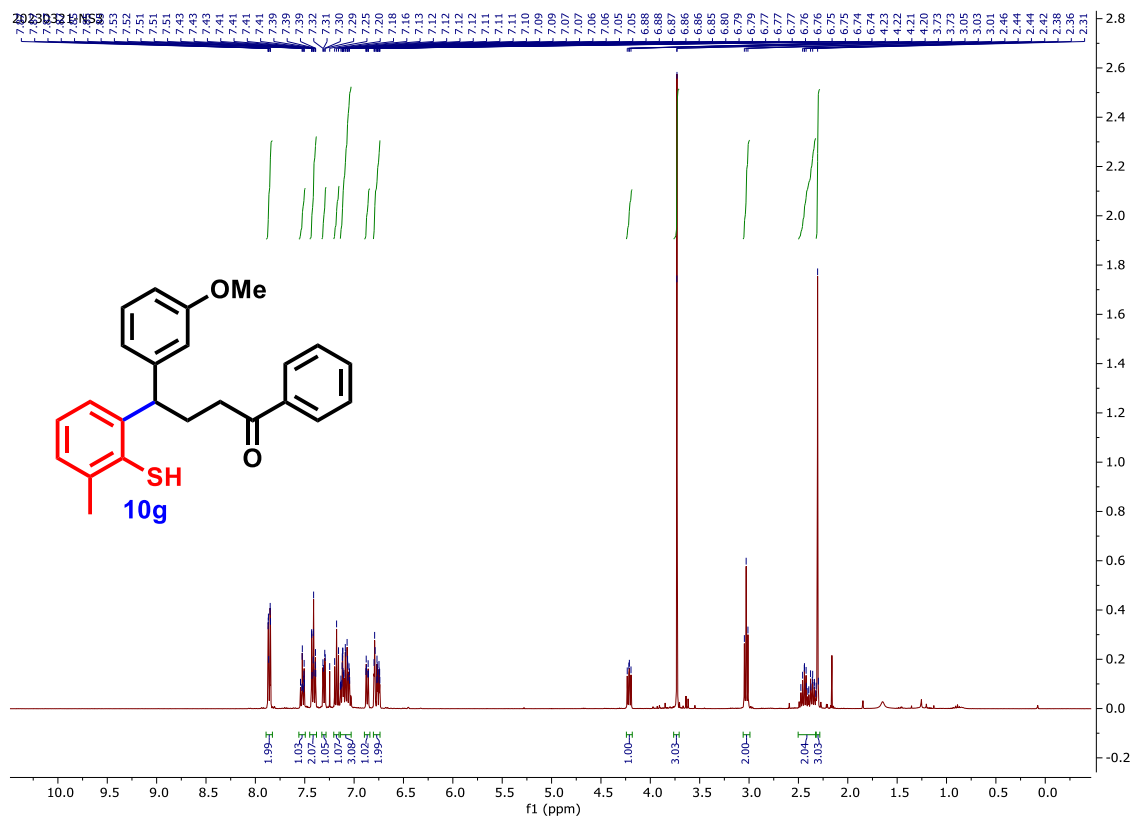
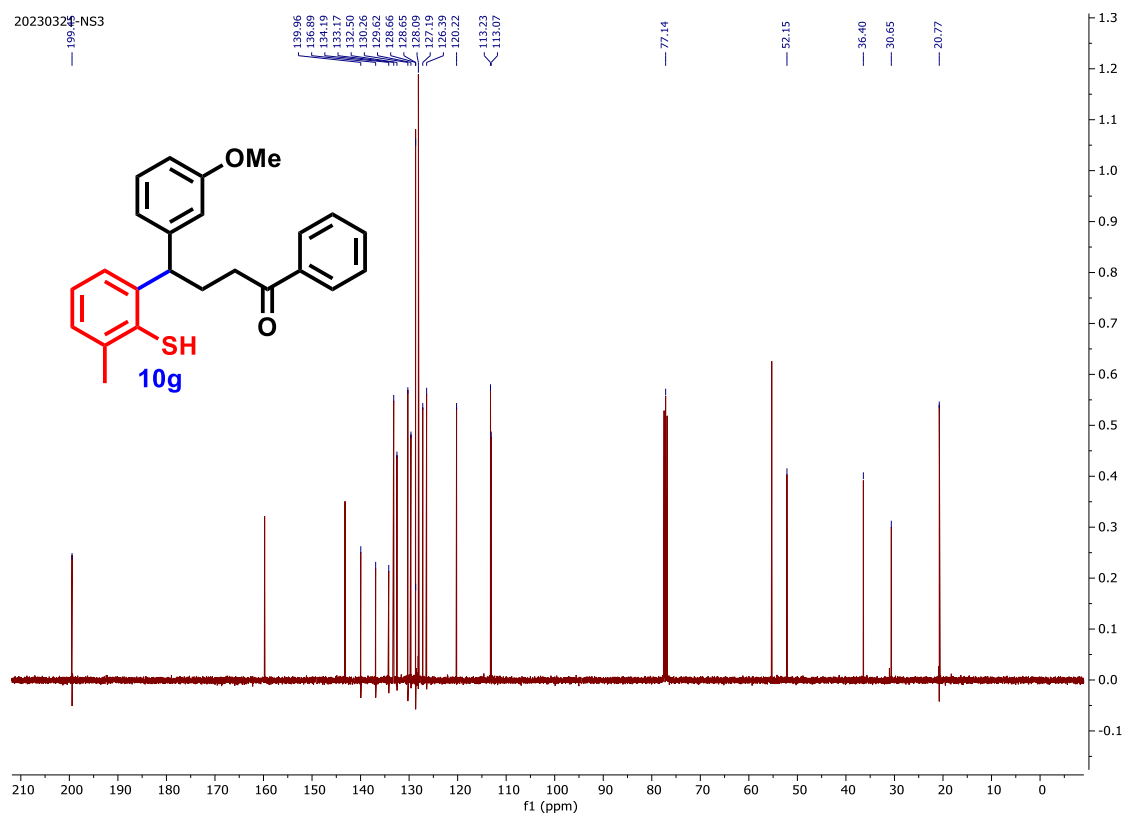


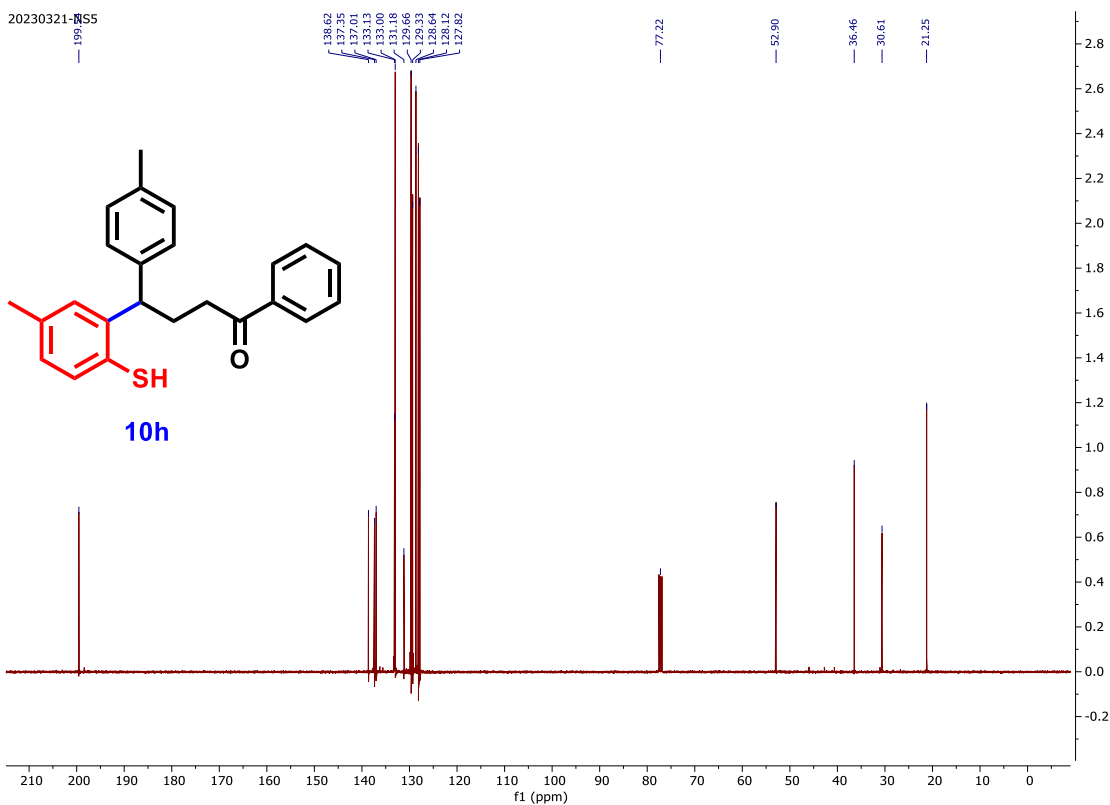
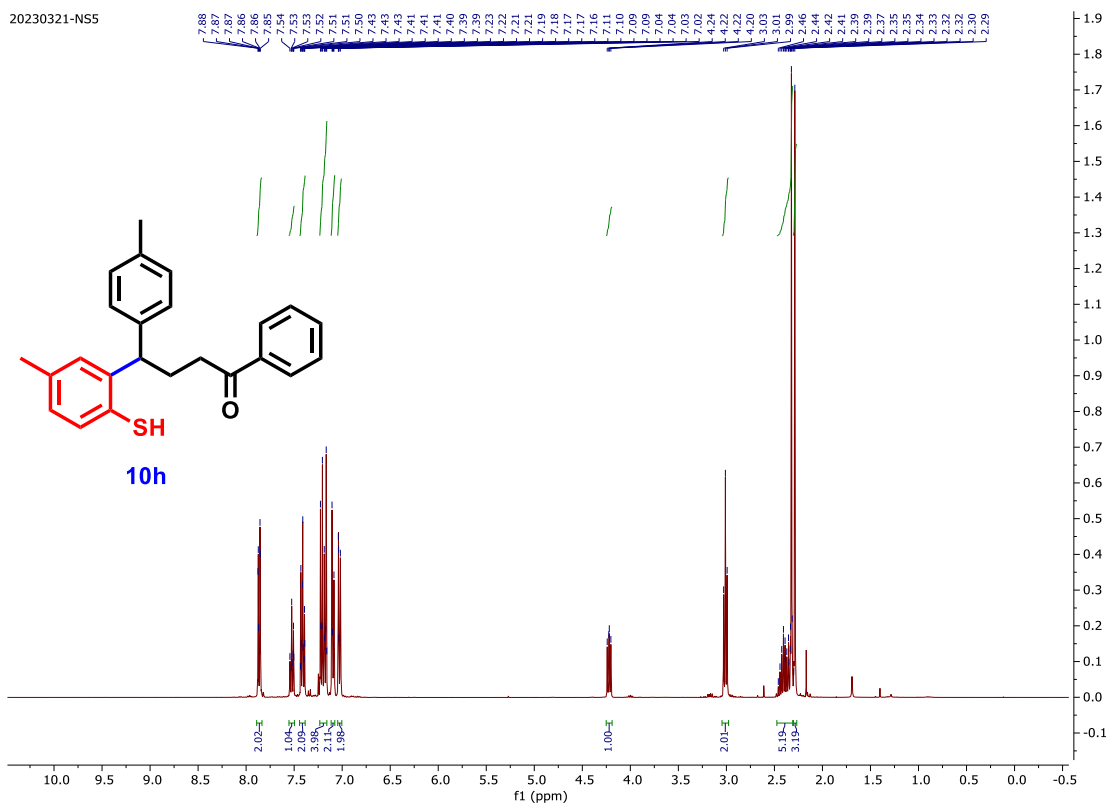


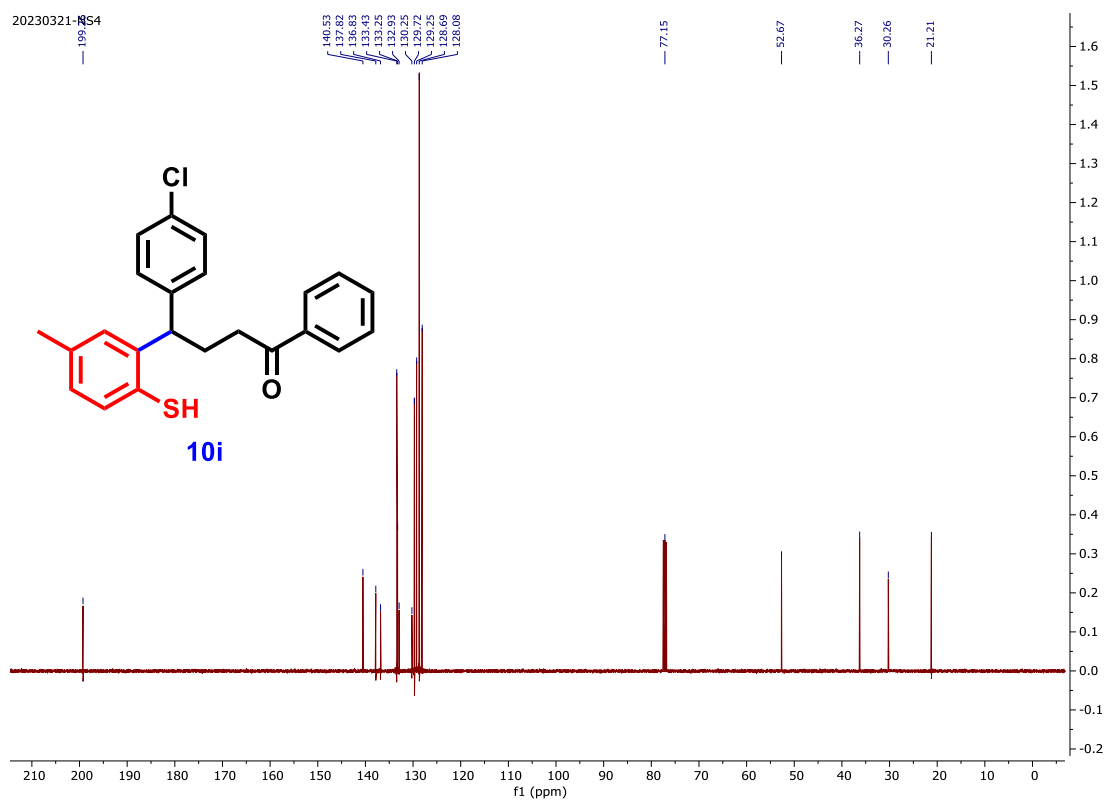
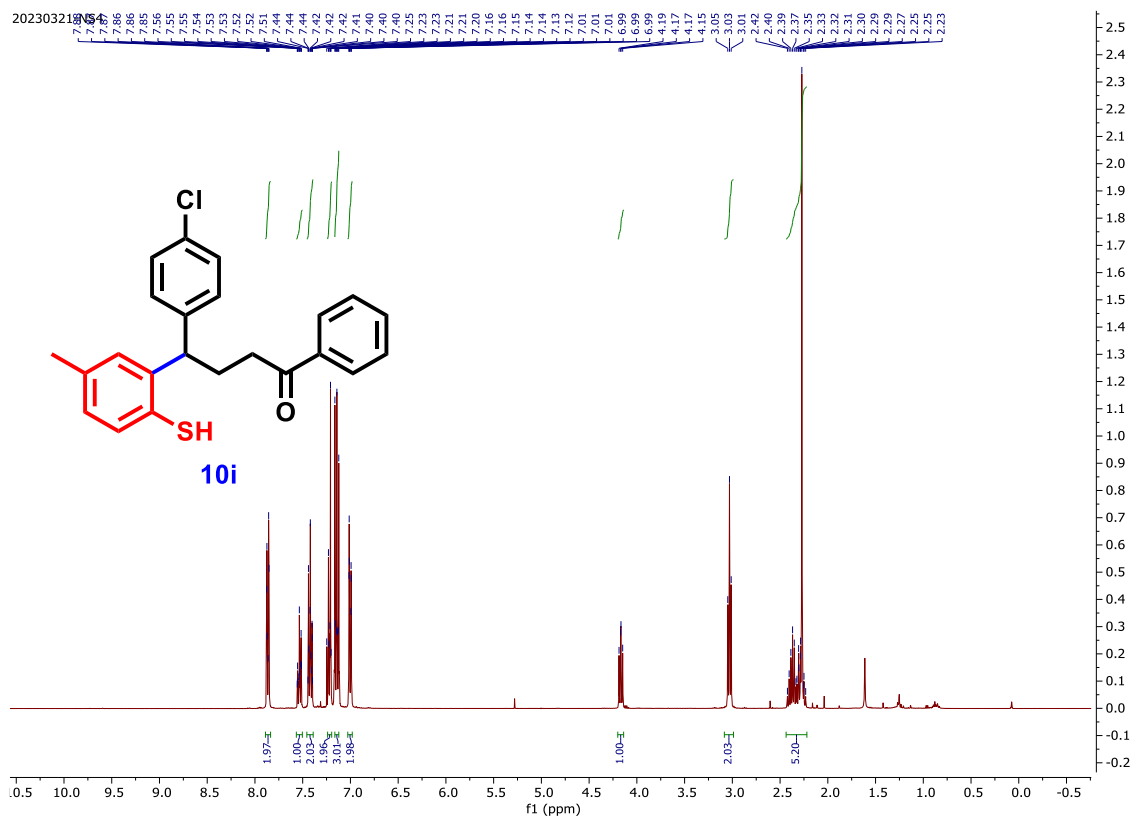
¹H NMR (CDCl₃, 400 MHz) of 10f

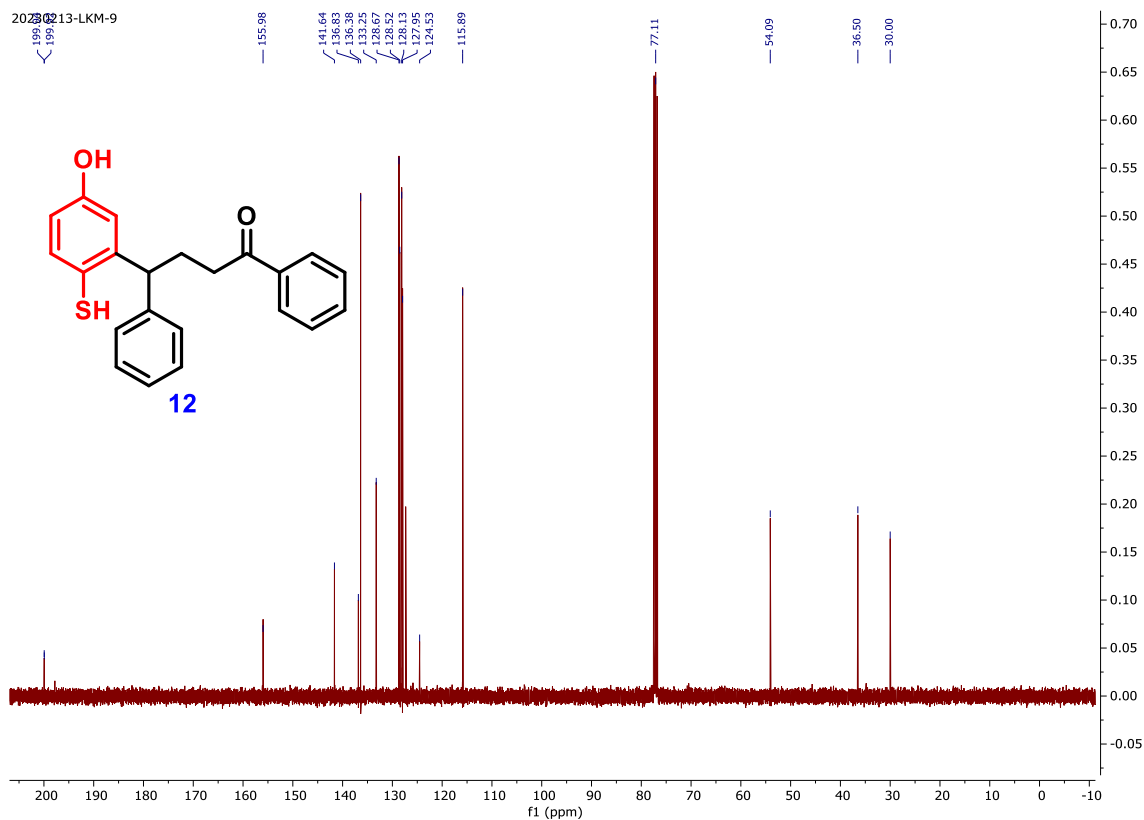
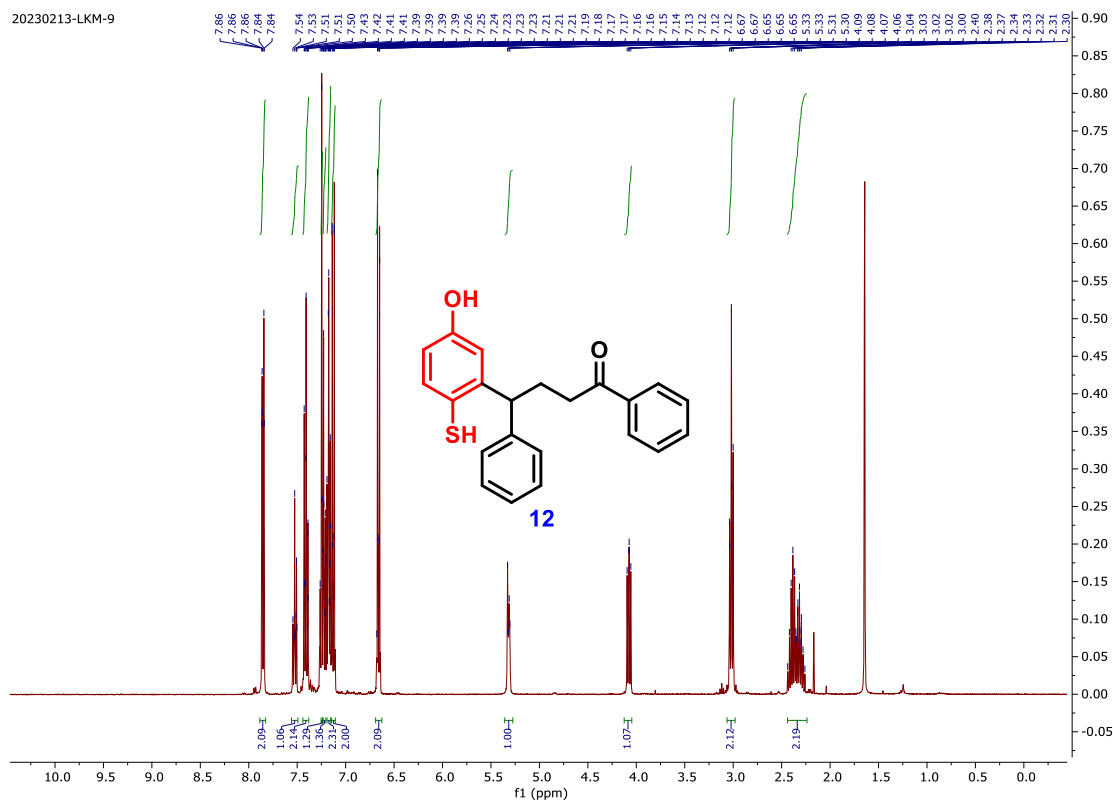


¹³C NMR (CDCl₃, 101 MHz) of 10f

¹H NMR (CDCl₃, 400 MHz) of **10g**¹³C NMR (CDCl₃, 101 MHz) of **10g**

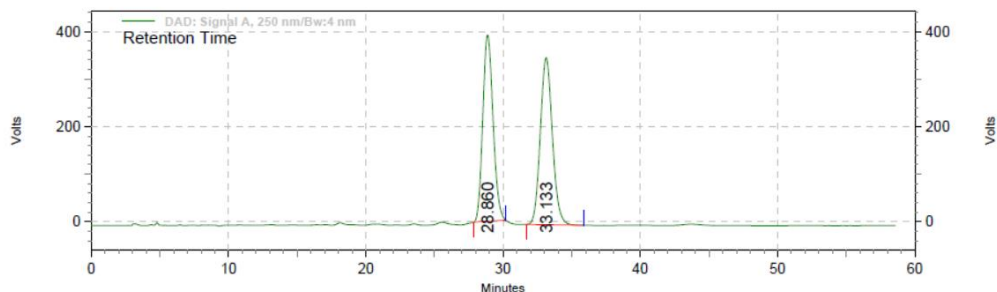
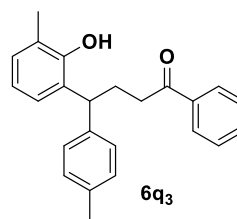






Area % Report

Data File: E:\Dr. AKB\Laxmi\lg-1 95hex 10ipa 1ml-min.dat
Method: E:\Dr. AKB\Laxmi\25_05_2022_10%IPA_Hex.met
Acquired: 5/25/2022 11:54:03 AM
Printed: 5/25/2022 12:53:50 PM



DAD: Signal A,
250 nm/Bw:4 nm
Results

Retention Time	Area	Area %	Height	Height %
28.860	42750987	48.70	821696	52.73
33.133	45026329	51.30	736558	47.27
Totals	87777316	100.00	1558254	100.00

HPLC chromatogram of 6q3

Chapter III

*Bioactives from
Aspergillus terreus*

3. Bioactives from *Aspergillus terreus*

2.1 Introduction

The discovery of penicillin by Alexander Fleming and streptomycin by Selman Waksman has evolved the extraction of microbial natural products.¹ Microorganisms are rich source of natural products with unique structural framework and medicinally important properties.¹ Apart from this microbes are source of many commercial enzymes used for fermentation in food industries, water treatment, energy production, soil fertilization etc.²

The genus *Aspergillus* comprises over 800 mould species and can habitat in acute to normal range of climatic conditions. *Aspergillus* is a genus of saprophytic fungus which was first discovered by Pier Antonio Micheli in 1920.³ These moulds are generally pathogenic in nature as they take nourishment from organic matter like animals/humans/plants. This peculiar genus belongs to kingdom fungi and division Ascomycota and majority of them reproduces asexually *via* producing conidium.³ Despite of their morbific nature many of these spp are of medicinal importance and a relevant source of natural products with new chemical entities.³ More than 3000 compounds have been isolated from the genus *Aspergillus* so far.⁴ Recent reports³ showed isolation of natural products with unusual core motifs from this particular genus. Most of the compounds isolated from this genus were reported to be biologically active, with some of them displaying promising cytotoxicity against various human cancer cell lines (U937, K562, BGC-823, MOLT-4, Mcf7, and A549 etc. cell lines) as well as significant antimicrobial (against *Escherichia coli*, *Bacillus subtilis*, *Micrococcus lysolei* and Gram-positive bacteria), antifungal (against *Aspergillus niger*) and antiviral (H1N1 and H3N2 influenza virus) activities.^{4,10,12,17} These new molecules with unique scaffolds provide vast variety of pharmacologically potent molecules.⁴

Frequently extraction has been carried out on species like *Aspergillus niger*, *A. flavipes*, *A. fumigatus*, *A. ochraceus* and *A. terreus* etc. *A. niger* is reported⁵ to yield motifs like campyrones, naphthopyrones, quinones and coumarins etc. The fungus *A. niger* (CAFT160) obtained from the leaves of *Z. lemairei* and fermented in rice culture furnished six compounds, campyrones A-C (1-3) (**Figure 1**) together with citric acid, ergosterol, and

ergosterol peroxide, which were further bioassayed. The new compounds exhibited weak toxicity on brine shrimp larvae (*Artemia salina*).⁵

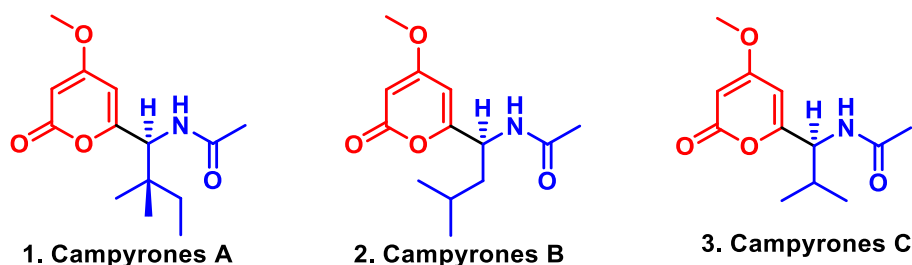


Figure 1: Structures of campyrones A-C (1-3) isolated from *A. niger* (CAFT160)

In 2007, Bouras and *et al* reported⁶ aurasperone G (4), from the culture extracts of *A. niger* (C-433) along with known compound aurasperone F (5) (Figure 2).

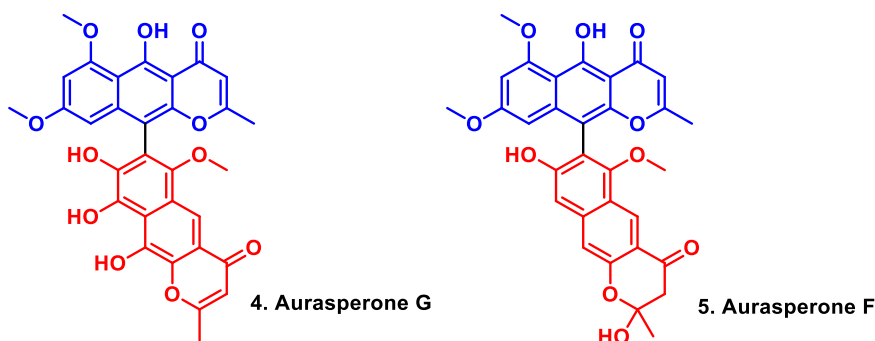


Figure 2: Structures of aurasperone G and F (4 and 5) isolated from *A. niger* (C-433)

Akiyama *et al* in 2003⁷ reported dimeric naphthopyrones, asperpyrones A (6), B (7), and C (8), along with known compounds, fonsecinone A (9) and aurasperone A (10), from *A. niger* (JV-33-48) (Figure 3). Compounds 6, 9, and 10 showed inhibitory activity on Taq DNA polymerase. Naphthopyrones 6, 9 and 10 displayed low inhibition activity in the TRAP assay, while 7 and 8 did not exhibit promising activity at 100 µg/mL. The inhibition percentages of compounds 6, 9, and 10 were at 41%, 40%, and 52% respectively.

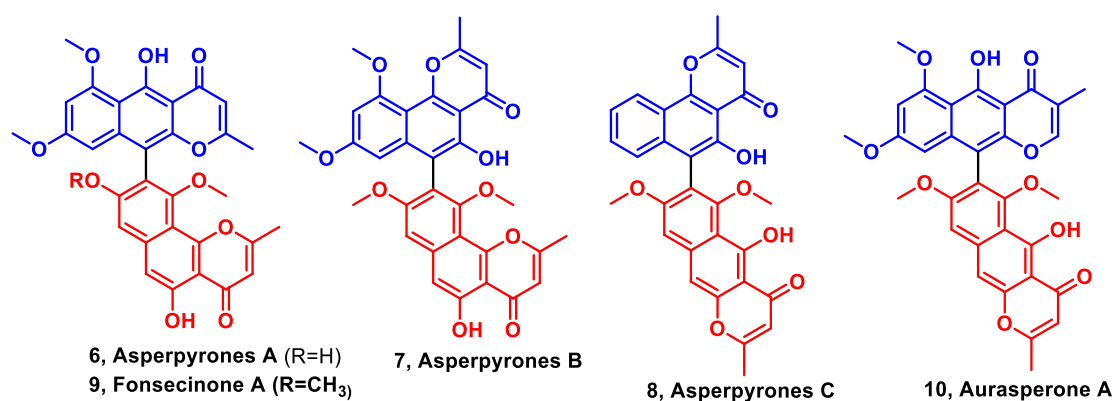


Figure 3: Structures of compounds **6-10** isolated from *A. niger* (JV-33-48)

A. niger isolated from the Mediterranean sponge *Axinella damicornis* furnished eight secondary metabolites, out of which seven compounds (**12-18**) were new natural products (**Figure 4**).⁸ None of the isolated compound was able to inhibit the growth of brine shrimp or other assayed microorganisms cultured in the agar plate. However compound **15** inhibited the growth of neonate larvae of the plant pest insect *Spodoptera littoralis* when given an artificial diet. The given highest concentration of compound **15** *i.e.* 100 ppm, the average weight increase of the larvae over 7 days was reduced to 29% while the survival rate was 85% at 100 ppm of compound **15**. Bicoumanigrin A (**12**) displayed mediocre inhibition of cell growth of various leukemia and carcinoma cell lines. Bicoumanigrin A (**12**) (1-20 $\mu\text{g/mL}$) showed an average growth inhibition of up to 50% depending on the type of cell line taken for assay within a time period of 48 hours. However **15** was inactive at all concentrations tested, both **13** and **14** have shown average value of cytotoxicity *i.e.* 50 $\mu\text{g/mL}$.⁸

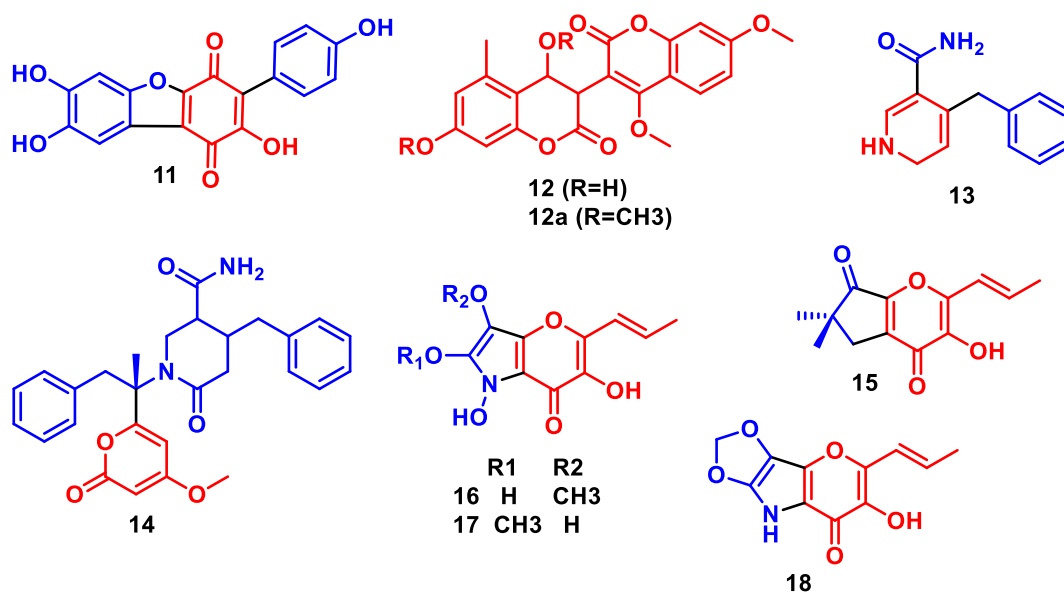


Figure 4: Structures of compounds **11–18** isolated from *A. niger* isolated from the Mediterranean sponge *Axinella damicornis*

A new category of merocytochalasan, cytochathiazines A–C (**19–21**) were found from coculture of *Chaetomium globosum* and *A. flavipes* by Zhang *et al*^{9a} in 2018 (**Figure 5**). Compounds **19–20** are the new motifs of 2*H*-1,4-thiazine core from natural sources formed by the fusion of a dipeptide and a cytochalasan. Cytochalasans are commonly known fungi metabolites.^{9b} Cytochalasans have a wide variety of biological activities^{9b} as a consequence of alter in amino acid residues and polyketides involved in PKS-NRPS hybrid biosynthesis pathways.

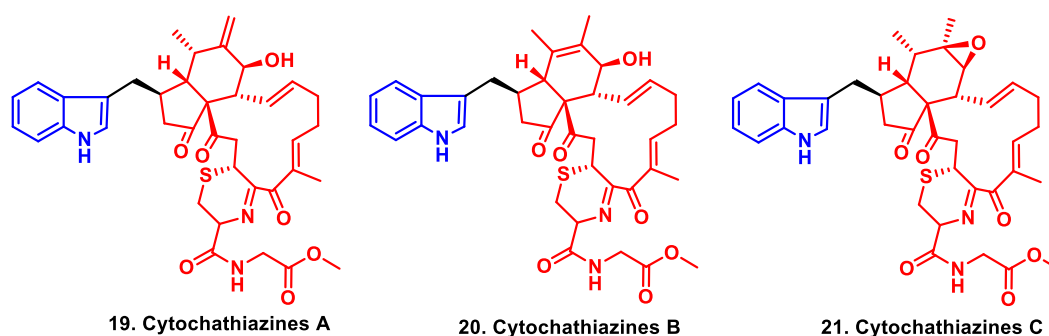


Figure 5: Structures of cytochathiazines A–C (**19–21**) isolated from coculture of *Chaetomium globosum* and *A. flavipes*

Flavimycins A (**22**) and B (**23**), (**Figure 6**) featuring dimeric 1, 3- dihydroisobenzofurans, were reported from *A. flavipes* with its inhibitory effects on peptide deformylase. Compounds **22** and **23** are epimer and display tautomerism. Compounds **22** and **23** have inhibitory effects on *Staphylococcus aureus* peptide deformylase with IC₅₀ values of 35.8 and 100.1 μM, respectively.¹⁰

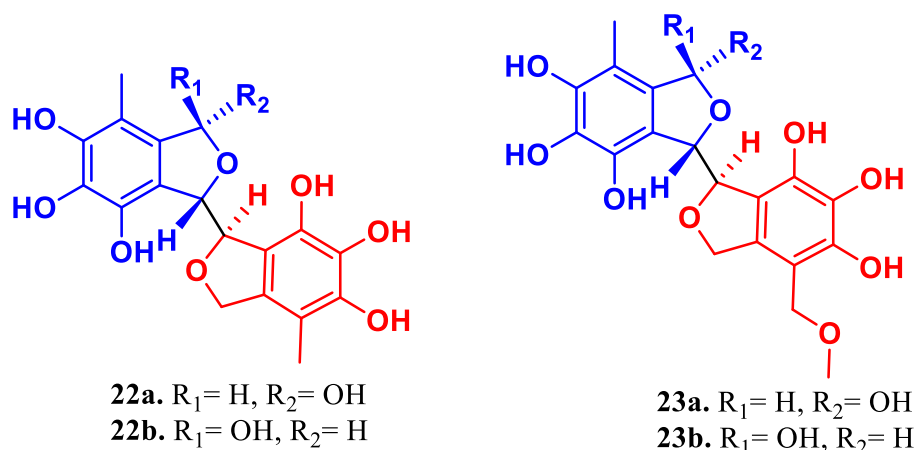


Figure 6: Structures of flavimycins A and B (**22-23**) isolated from *A. flavipes*

A. flavipes originally obtained from soil yielded spiroquinazoline (**24**) and was found to be a substance P inhibitor. This isolated compound (**24**) contains a new spiro-carbon center (**Figure 7**). This culture also reported¹¹ to give new natural product, benzodiazepinedione (**25**), (**Figure 7**) and known compounds containing acyl aszonalenin (**27**), *N*-benzoyl-L-phenylalaninol, and seven diketopiperazines. Spiroquinazoline shows skeletal similarities to fumiquinazoline C (**26**) obtained from the marine fungus *A. fumigatus*, and also to the fiscalins, from the fungus *Neosartorya fischeri* which is also known to display substance P inhibitors activity.¹¹

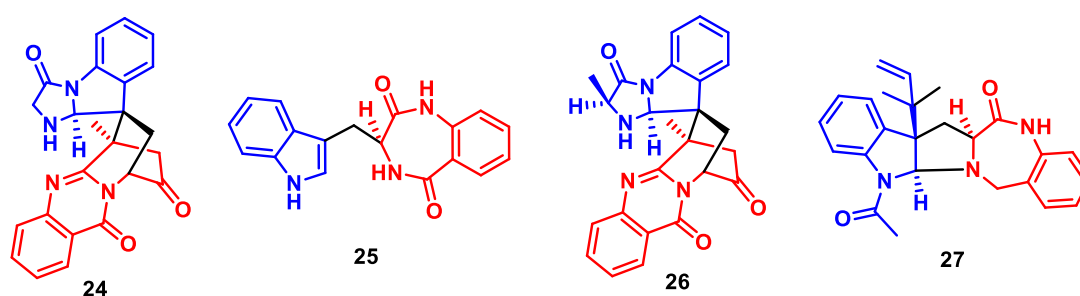


Figure 7: Structures of compound **24-27** isolated from *A. flavipes*

An endophytic fungus *A. ochraceus* (EN-31) obtained from the marine brown alga *Sargassum kjellmanianum* was a source of 7-Nor-ergosterolide (**28**), and two new steroid derivatives (**29** and **30**) along with, nine already discovered steroids (**Figure 8**).¹² Compound **28** displayed cytotoxicity against NCI-H460, SMMC-7721 and SW1990 cell lines displaying IC₅₀ values of 5.0, 7.0, and 28.0 $\mu\text{g/mL}$ respectively. None of the newly isolated compounds **28-30** have displayed antibacterial activities against *Staphylococcus aureus* and *Escherichia coli* and antifungal activity against *A. niger*.¹²

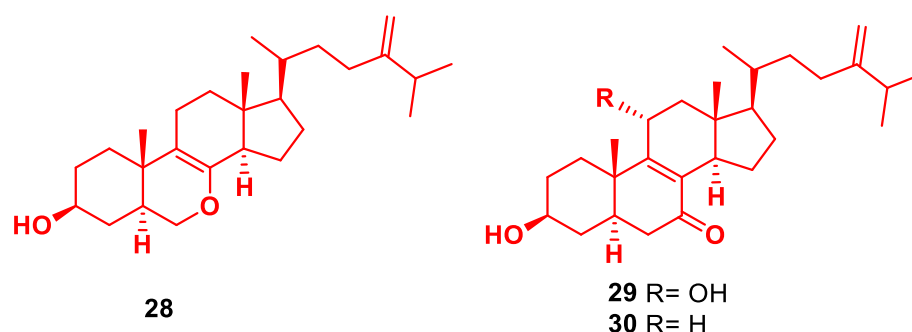


Figure 8: Structures of compound **28-30** isolated from *A. ochraceus* (EN-31)

Tan *et al* in 2018 reported¹³ isolation of new nitrobenzoyl sesquiterpenoids, insulicolide B (**31**), insulicolide C (**33**) and a new natural compound 14-*O*-acetylinsulicolide A (**32**) from the *A. ochraceus* (Jcm1F17) which is a marine-derived fungus (**Figure 9**). They also reported isolation of three known nitrobenzoyl sesquiterpenoids (**34-36**) and a sesquiterpenoid derivative (**37**) (**Figure 9**).

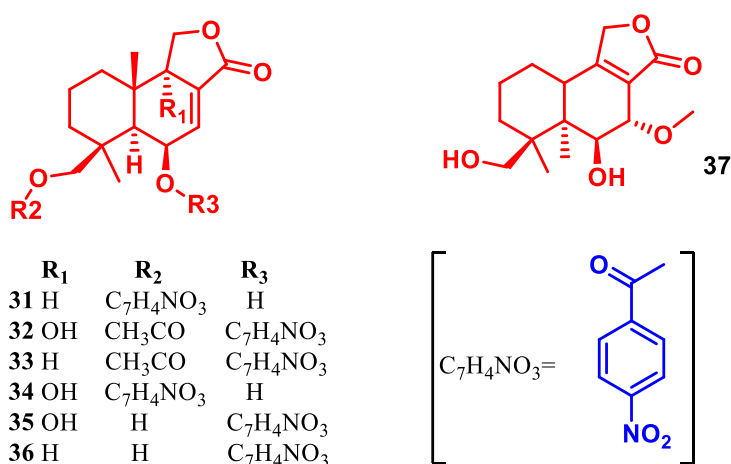


Figure 9: Structures of compounds (**31-37**) isolated from *A. ochraceus* (Jcm1F17)

All of the nitrobenzoyl sesquiterpenoids (**31–36**) were evaluated for their cytotoxicities against carcinoma cell lines, ACHN, OS-RC-2, and 786-O cells (**Table-1**). Insulicolide A (**35**) displayed the most promising activities, with IC_{50} values of 1.5, 1.5, and 0.89 μM against these cell lines respectively.¹³

Table- 1: Cytotoxicities of compounds (**31–36**) against ACHN, OS-RC-2, and 786-O cell lines

Compound	ACHN	OS-RC-2	786-O
	IC_{50} (μM)	IC_{50} (μM)	IC_{50} (μM)
31	30	23	24
32	4.1	5.3	2.3
33	13	11	14
34	11	8.2	4.3
35	1.5	1.5	0.89
36	25	30	20
Sorafenib	3.4	7.0	4.9

Glowr *et al* reported¹⁴ isolation of three new metabolites with diketopiperazine framework **38–40** from the extract of *A. ochraceus* (NRRL 3519) (**Figure 10**).¹⁴ When assayed against lepidopteran crop pest *Helicoverpa zea*, these isolated compounds (**38–40**) exhibited weak reduction in weight gain.^{14,15}

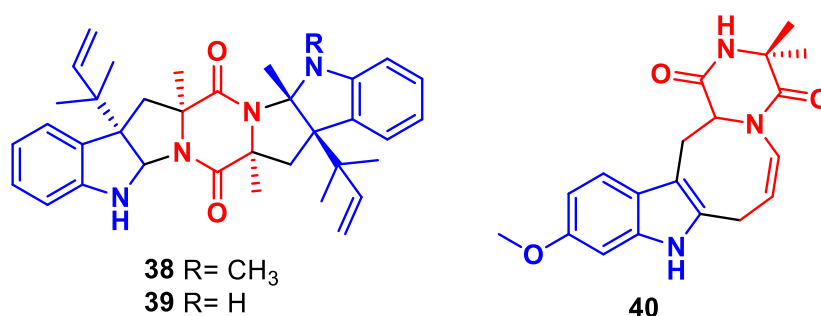


Figure 10: Structures of compounds (**38-40**) isolated from *A. ochraceus* (NRRL 3519)

Terretonin (**47**), a toxic compound from *A. terreus* was reported¹⁵ along with already known toxins citrinin (**41**) and patulin (**42**) and other metabolites including terreic acid (**43**), quadrone (**44**), asperterric acid (**45**), and aspergillide B (**46**) (**Figure 11**).¹⁶

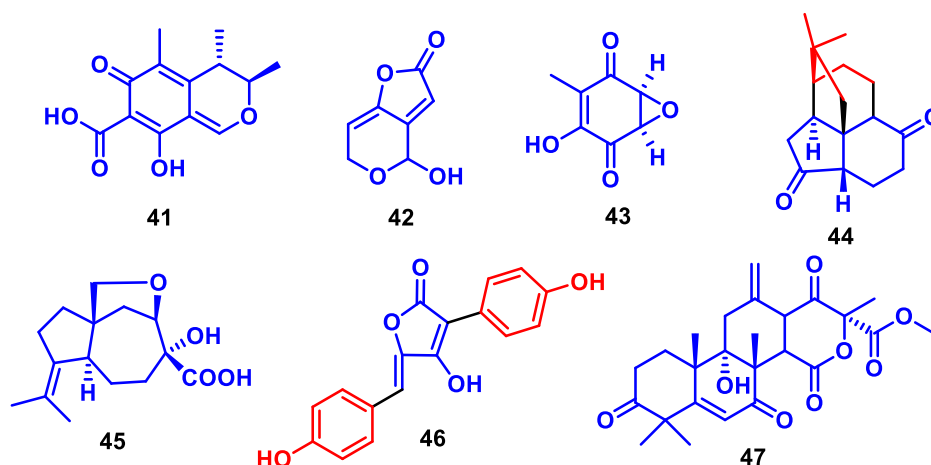


Figure 11: Structures of compound (**41-47**) isolated from *A. terreus*

Butyrolactone I 3-sulfate (**48**) and butyrolactone I 4''-sulfate (**49**) (**Figure 12**) were reported¹⁶ from *A. terreus* containing an unexplored sulfate moiety along with known butyrolactone I (**50**) (**Figure 12**). These reported compounds were examined on CDK1/cyclin B, CDK5/p25, DYRK1A, CK1 and GSK-3 α/β kinases. Compounds **49** and **50** were also assayed for their cytotoxic and antiproliferative activities. Butyrolactone I 3-sulfate (**48**) displayed inhibitory activity against CDK1/cyclin B and CDK5/p25, however it was found to be 15–30 fold less active than butyrolactone I (**50**). Likewise, butyrolactone I 3-sulfate (**48**) exhibited moderate cytotoxicity only against HeLa cells (CC₅₀ 80.7 μ M).¹⁷

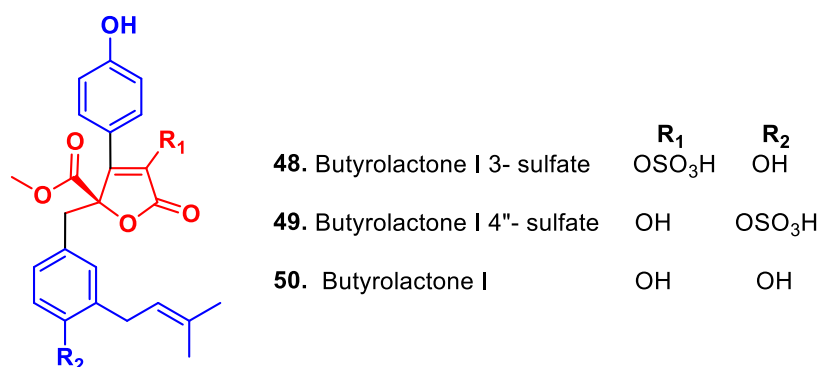


Figure 12: Structures of butyrolactones (**48-50**) isolated from *A. terreus*

He et al reported¹⁸ isolation of a cyclic tetrapeptide, asperterrestide A (**51**) from the marine-derived fungus *A. terreus* (SCSGAF0162) which was found to be cytotoxic and antiviral (**Figure 13**). They also reported isolation of a new alkaloid, terreimide C (**52**), and a new aromatic butenolide, aspernolide E (**53**), along with previously reported compounds. Compound **51** (**Figure 13**) was assayed for cytotoxicity against human leukemic monocyte lymphoma U937, erythroid leukemic K562, gastric carcinoma BGC- 823, acute lymphoblastic leukemia MOLT-4, breast adenocarcinoma MCF-7, and lung carcinoma A549 cell lines and showed IC_{50} values of 1.9, 4.9, 3.5, 1.8, 5.0, and 3.6 nM, respectively. Only compound **51** was tested for its antiviral activity. Compound **51** was tested against influenza virus strain A/WSN/33 (H1N1) (an M2-resistant strain) and strain A/Hong Kong/8/68(H3N2) (an M2-sensitive strain) and it showed IC_{50} values of 20.2 and 0.41 μ M, respectively against H1N1 and H3N2.¹⁸

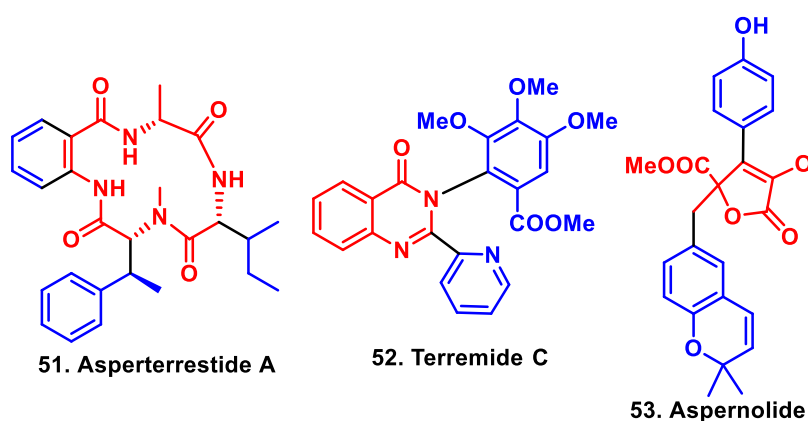


Figure 13: Structures of compounds (**51-53**) isolated from *A. terreus* (SCSGAF0162)

A new nor-neolignan, asperjinone (**54**) along with terrein (**55**) and twelve other known compounds (**Figure 14**) were isolated from *A. terreus* by Liao *et al.*¹⁹ Terrein (**55**) displayed dominant cytotoxicity against breast cancer MCF-7 cells and it also inhibited growth of ABCG2-expressing breast cancer cells. The IC_{50} value of terrein (**55**) was more effective than that of paclitaxel (0.1 μ M) against breast cancer MCF-7 cells *i.e.* 1.1 nM. Other compound isolated was almost inactive, showing values at 100 μ M. Terrein (**55**) also exhibited good cytotoxicity against PANC-1 cells (IC_{50} value, 9.8 μ M) and HepG2 cells (IC_{50} value, 66.8 nM).

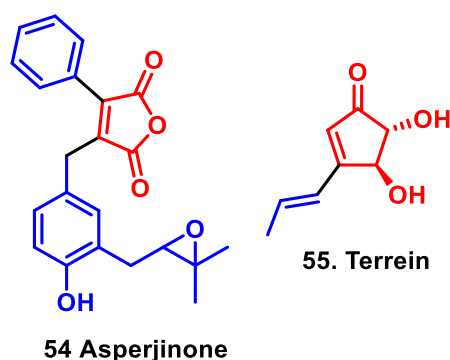


Figure 14: Structures of asperjinone (**54**) and terrein (**55**) isolated from *A. terreus*

Extraction of *A. terreus* (No.GX7-3B), an *endosymbiont fungus of mangrove furnished* thiophene compound (**56**) along with anhydrojavanicin (**57**), 8-*O*-methylbostrycoidin (**58**), 8-*O*-methyljavanicin (**59**), botryosphaerone D (**60**), 6-ethyl-5-hydroxy-3,7-dimethoxy-naphthoquinone (**61**), 3 β ,5 α -dihydroxy-(22*E*,24*R*)-ergosta-7,22-dien-6-one (**62**), 3 β ,5 α ,14 α -trihydroxy-(22*E*,24*R*)-ergosta-7, 22-dien-6-one (**63**), NGA0187 (**64**) and beauvericin (**65**) (**Figure 15**). Compounds **57**, **58**, **64** and **65** exhibited IC₅₀ values 2.01, 6.71, 1.89, and 3.09 μ M, respectively when assayed against α -acetylcholinesterase (AChE) and compounds **62** and **65** were strong to moderately cytotoxic against various cancer cell lines as shown with IC₅₀ values respectively, MCF-7 (4.98 and 2.02 μ M), A549 (1.95 and 0.82 μ M), Hela (0.68 and 1.14 μ M), and KB (1.50 and 1.10 μ M).²⁰

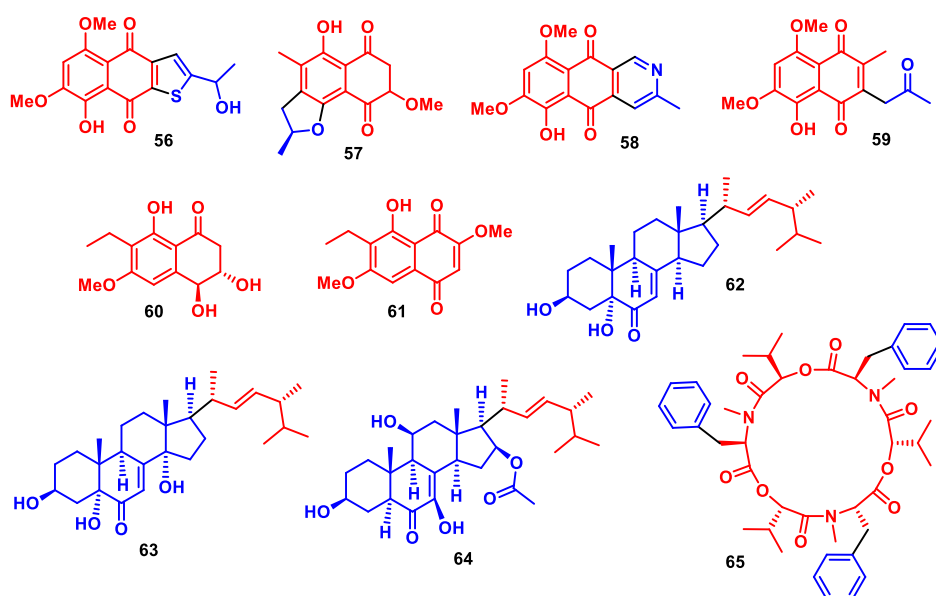


Figure 15: Structures of compounds (**56-65**) isolated from *A. terreus* (GX7-3B)

3.2 Present work

On perceiving the significance of natural product isolation from microbial culture, we initiated isolation of secondary metabolites from *Aspergillus terreus*. We obtained the crude EtOAc extract of *A. terreus* from Biochemical Sciences Division, CSIR-National Chemical Laboratory (CSIR-NCL), Pune. Initially, the strain was grown on potato dextrose agar medium (PDA) in petri dish which was then inoculated into a 500 mL of Erlenmeyer flasks each containing 100 mL of the seed medium (agar-agar, dextrose). The crude lyophilized material obtained was extracted with EtOAc which on evaporation yielded 1.3 g of crude extract. This extract was further fractionized into three fractions *via* flash chromatography using ethyl acetate-pet ether as eluents. The individual fractions were further purified by using flash chromatography (CombiFlash Rf 200i equipped with UV/VIS and ELSD (Isco Teledyne Inc., USA) using RediSep® pre-packed column (SiO₂) using ethyl acetate-pet ether as mobile phase. We have isolated three major compounds **66-68**. On rigorous examination of the spectral data (1D, 2D NMR and FTIR) and their mass spectrum, the isolated compounds were identified as 2,5,6-trihydroxy-3-methylcyclohex-2-ene-1,4-dione (**66**; 10 mg), phenyl acetic acid (**67**; 38 mg) and 4-(1,2-dihydroxyethyl)-5-methylfuran-2(3*H*)-one (**68**; 15 mg) (**Figure 16**).

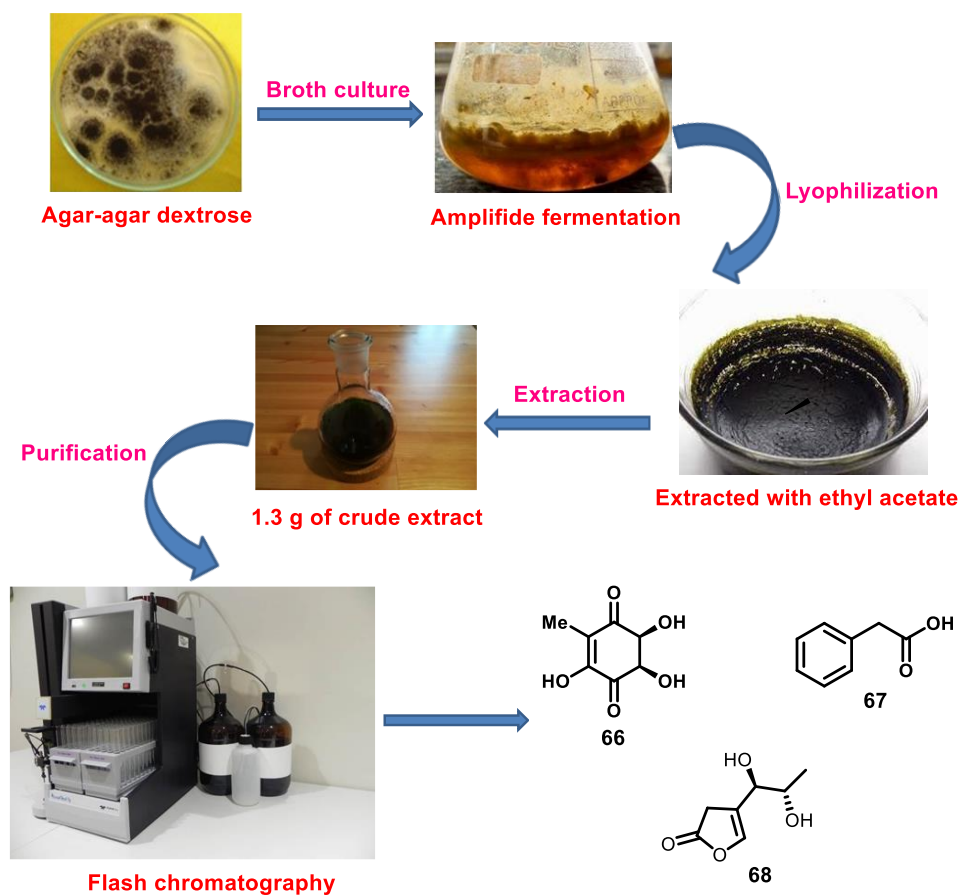


Figure 16: pictorial depiction of isolation processes and structure isolated compounds

Compound **66** possess a quinone core motif as previously isolated compounds (**56-61**) from *A. terreus* GX7-3B. Quinones are common oxidizing agents in biological system hence play an important role in living system for example vitamin K, a naphthoquinone takes part in coagulation of blood (**Figure 17**), ubiquinone-10, a benzoquinone is used in respiratory devices and plastoquinone takes part in redox reaction of photosynthesis process (**Figure 17**).²¹

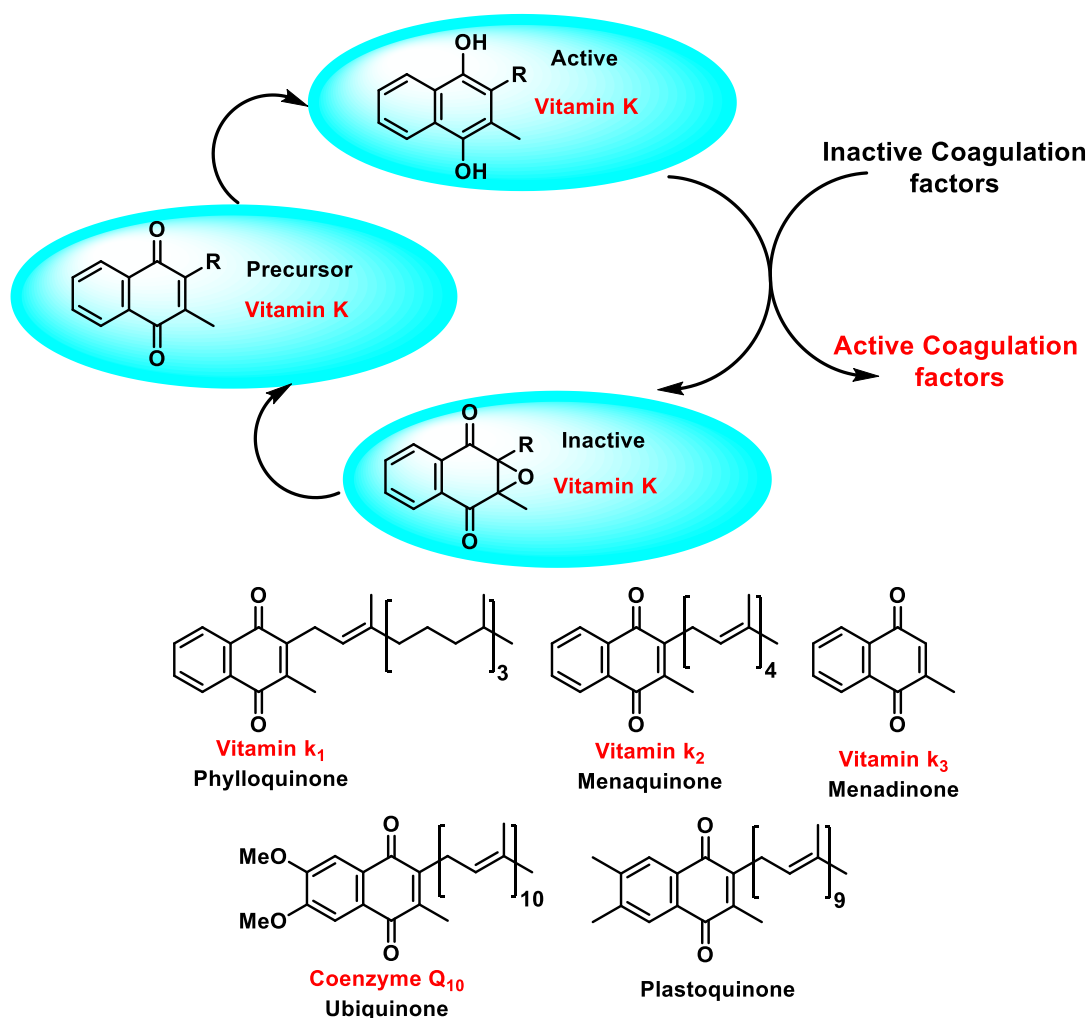


Figure 17: Acton mechanism cycle of vitamin K and structure of vitamin K₁, K₂, and K₃.

The Heteronuclear Multiple Bond Correlation (HMBC), NOESY and coupling constants of H-2/H-3 via 1D and 2D NMR for the compound **66** is depicted in **Figure 18**. The coupling constants between protons H-2/H-3 ($J = 3.56$ Hz) designates that diol are *cis* to each other as shown in 3D model (drawn using Chem 3D 15.1) of compound **66** (**Figure 18**). Although stereo of both the –OH groups is still unclear but we propose that both the –OH groups are above the plane as we compared compound **66** with the reported¹⁵ compound **43**. In the FTIR spectrum of compound **66**, we have observed O–H stretching of hydroxyl groups at 3443 cm^{-1} , 3391 cm^{-1} and the C=O stretching of carbonyl groups at 1698 cm^{-1} and 1649 cm^{-1} .

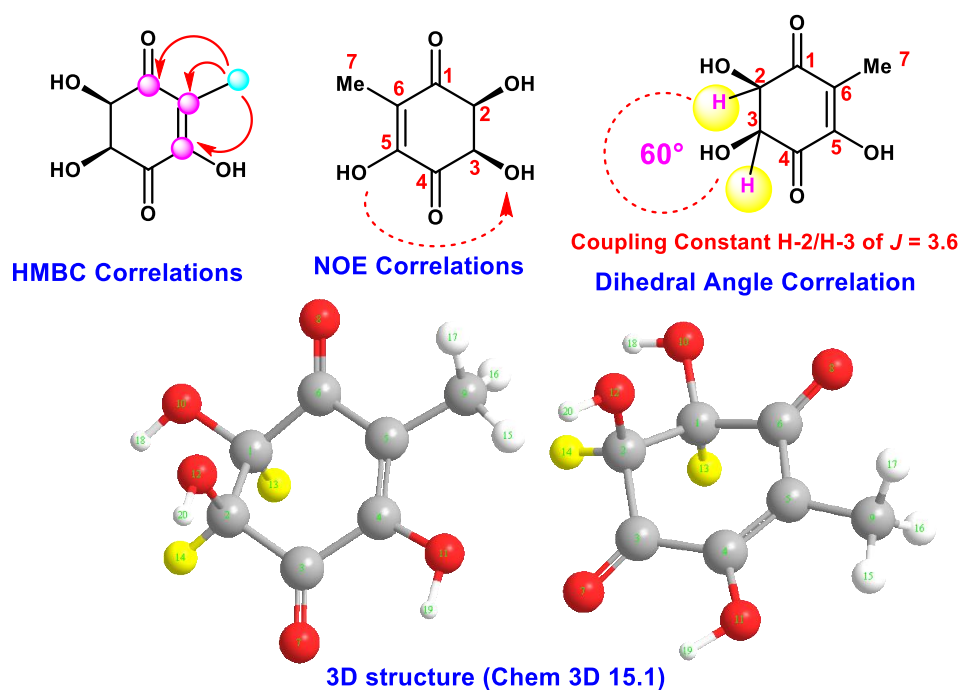


Figure 18: HMBC (arrows), NOE and dihedral angle correlations (dotted lines) and 3D structure (drawn using Chem 3D 15.1) of the compound **66**.

Compound **67** was identified as phenyl acetic acid. Compound **68** also showed resemblances to patulin¹⁵ (**42**) and other butyrolactone type of secondary metabolites isolated from *A. terreus*. The HMBC and NOESY correlation for the compound **68** is depicted in **Figure 19**. Values from In the FTIR spectrum of compound **68**, we observed O–H stretching of hydroxyl group at 3225 cm^{-1} and the C=O stretching of carbonyl group at 1648 cm^{-1} .

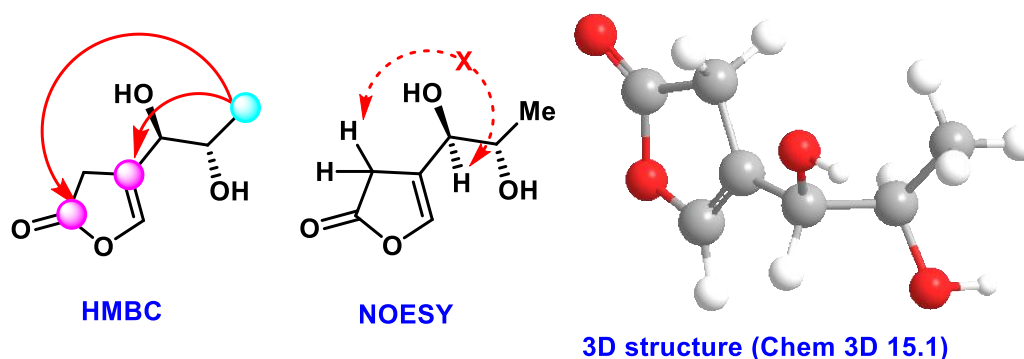


Figure 19. HMBC correlations (arrow), NOESY (dotted lines) and 3D structure (drawn using Chem 3D 15.1) of the compound **68**.

3.3 Conclusion:

In summary we have undertaken isolation of secondary metabolites from *A. terreus* and we have isolated three secondary metabolites. All the three compounds isolated have shown structural resemblance to previously isolated natural products from *A. terreus*. The structure of these compounds were elucidated using 1D, 2D NMR, FTIR, mass spectroscopy. In future we will isolate the compounds in large quantities to synthesize some of the analogues, which will be assayed for their biological activities.

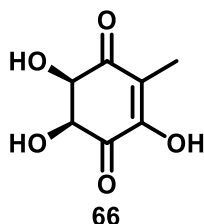
3.4 Experimental procedures

General Information; Flash chromatography was performed with CombiFlash Rf 200i equipped with UV/VIS and ELSD (Isco Teledyne Inc., USA) using RediSep®pre-packed column (SiO₂). ¹H NMR spectra were recorded on a Bruker 400 or 500 MHz spectrometer and ¹³C NMR spectra were recorded at 100 or 125 MHz, respectively. Chemical shifts are reported as δ values (ppm) relative to residual solvent peak of CDCl₃ and methanol-D₄. HRMS (ESI) were recorded on an Orbitrap (quadrupole plus ion trap) and TOF mass analyzer. Petroleum ether and ethyl acetate were distilled by usual methods. FTIR was recorded in Bruker ALPHA-E FT-IR spectrometer. The catalytic hydrogenation was performed in stainless steel Amar pressure reactor using glass vial inside the reactor.

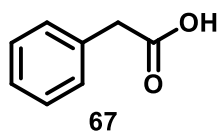
General procedure for isolation of natural products (66-68):

At CSIR-National Chemical Laboratory (NCL), Pune initially this strain was grown on potato dextrose agar medium (PDA) medium in a Petri dish for 7 days then directly inoculated into 500 mL of in Erlenmeyer flasks each containing 100 mL of the seed medium (agar-agar, dextrose). Subsequently amplified fermentation was carried out in 1L Erlenmeyer flasks and the crude lyophilized material obtained was extracted with EtOAc which yielded 1.3 g of crude extract We obtained this crud ethyl acetate extract (1.3 g) from biochemical sciences division, CSIR-National Chemical Laboratory (CSIR-NCL), Pune. The crude material was further purified *via* CombiFlash Rf 200i equipped with UV/VIS and ELSD (Isco Teledyne Inc., USA) using RediSep®pre-packed column (SiO₂) using EtOAc-Pet ether as eluent to isolate compound **66** (10 mg, 0.76%), **67** (38 mg, 2.9%) and **68** (15 mg; 1.15%).

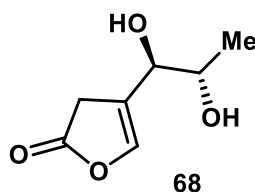
Compound 66



Yellow solid; $R_f = 0.53$ (40% ethyl acetate in petroleum ether); IR (CHCl_3) (cm^{-1}) 3443, 3391, 2965, 2924, 1698, 1649; ^1H NMR (400 MHz, CDCl_3) δ_{H} 6.83 (s, 1H), 3.92 – 3.87 (m, 2H), 1.95 (s, 3H), 1.62 (s, 2H); ^{13}C NMR (101 MHz, CDCl_3) δ_{C} 190.72, 187.52, 151.87, 120.41, 77.03, 53.82, 51.59, 8.80; HRMS: m/z for $\text{C}_7\text{H}_7\text{O}_5$ ($\text{M} - \text{H}$) $^+$, calcd: 173.0450, found: 173.0457.

Compound 67:

White solid; $R_f = 0.46$ (40% ethyl acetate in petroleum ether); IR (CHCl_3) (cm^{-1}) 3028, 1694; ^1H NMR (500 MHz, Methanol- d_4) δ_{H} 6.78 (s, 5H), 2.59 (s, 2H); ^{13}C NMR (126 MHz, Methanol- d_4) δ_{C} 166.68, 133.80, 28.41. HRMS: m/z for $\text{C}_8\text{H}_7\text{O}_2$ ($\text{M} - \text{H}$) $^+$, calcd: 137.0602, found: 137.0599.

Compound 68

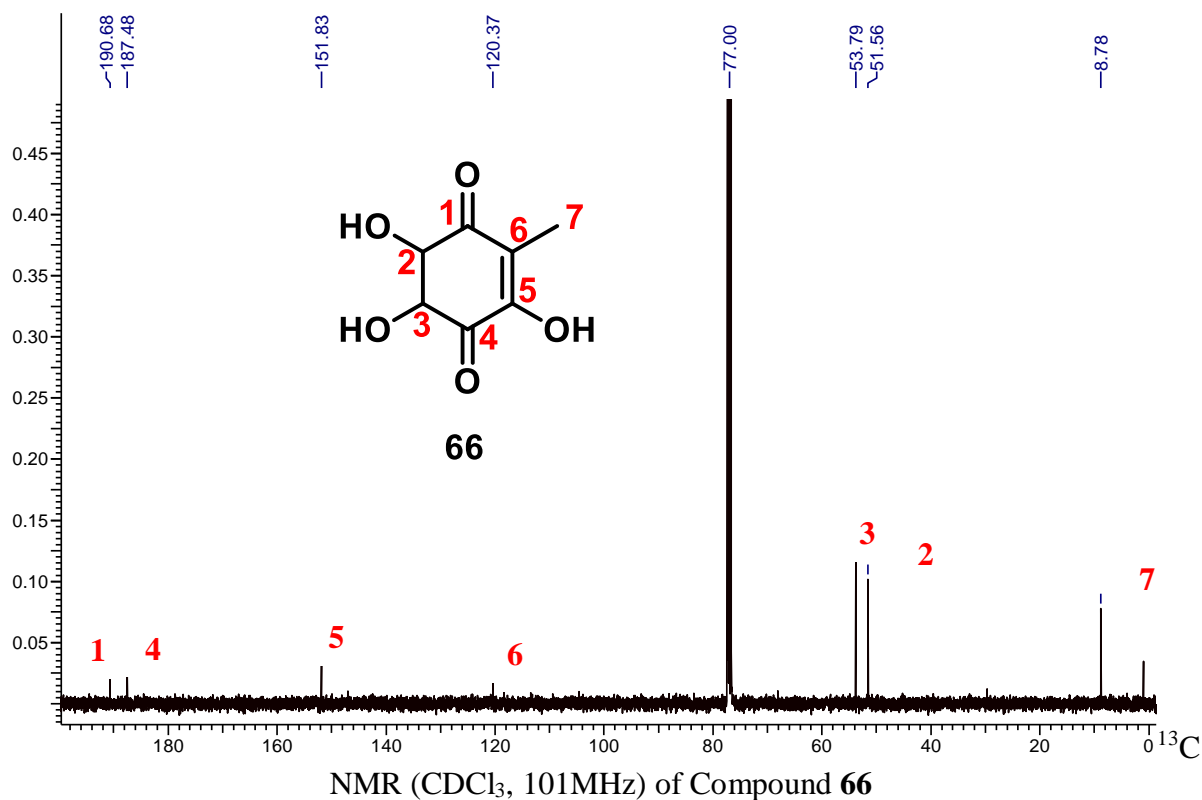
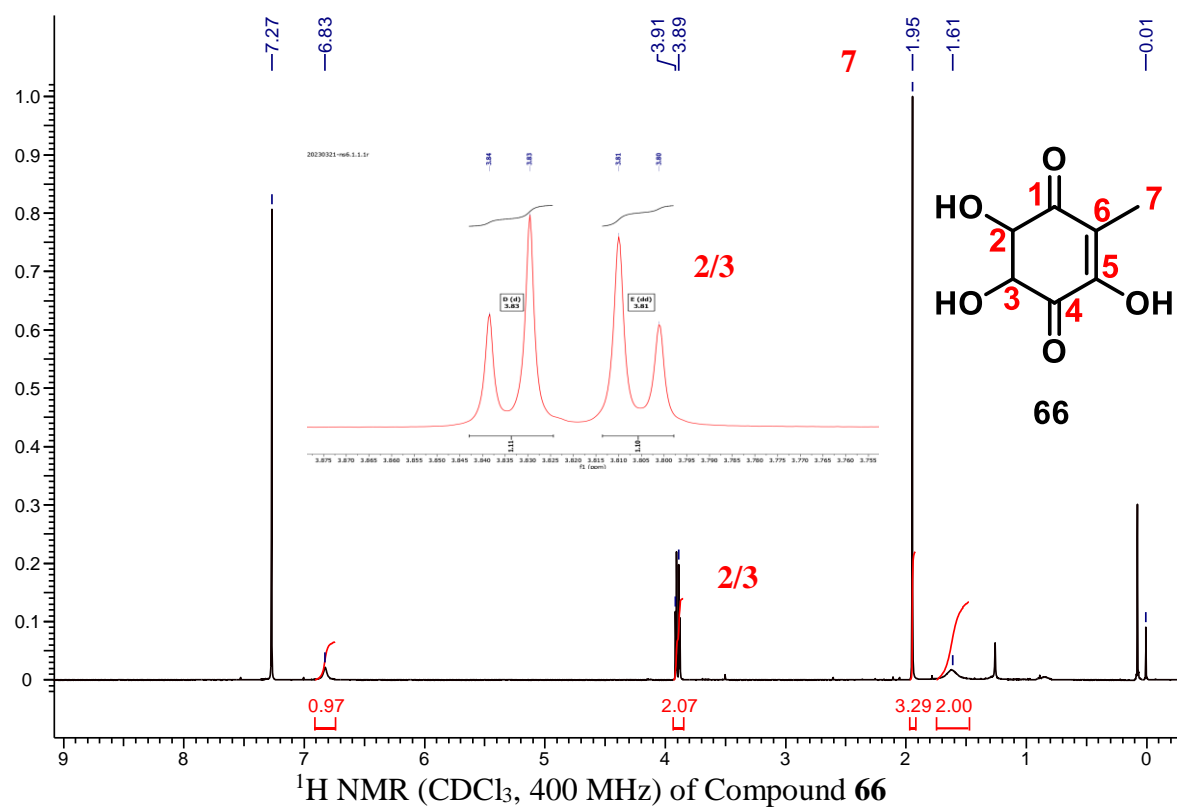
Yellow solid; $R_f = 0.15$ (40% ethyl acetate in petroleum ether); IR (CHCl_3) (cm^{-1}) 3225, 2924, 1648; ^1H NMR (500 MHz, Methanol- d_4) δ_{H} 4.50 (s, 1H), 3.64 (dd, $J = 3.8$, 1.3 Hz, 1H), 3.40 (dd, $J = 3.7$, 1.2 Hz, 1H), 2.59 (s, 2H), 1.69 (s, 3H); ^{13}C NMR (126 MHz, Methanol- d_4) δ_{C} 174.80, 107.78, 64.99, 28.44, 6.00; HRMS: m/z for $\text{C}_7\text{H}_9\text{O}_4$ ($\text{M} - \text{H}$) $^+$, calcd: 157.0495, found: 157.0495.

3.5 References:

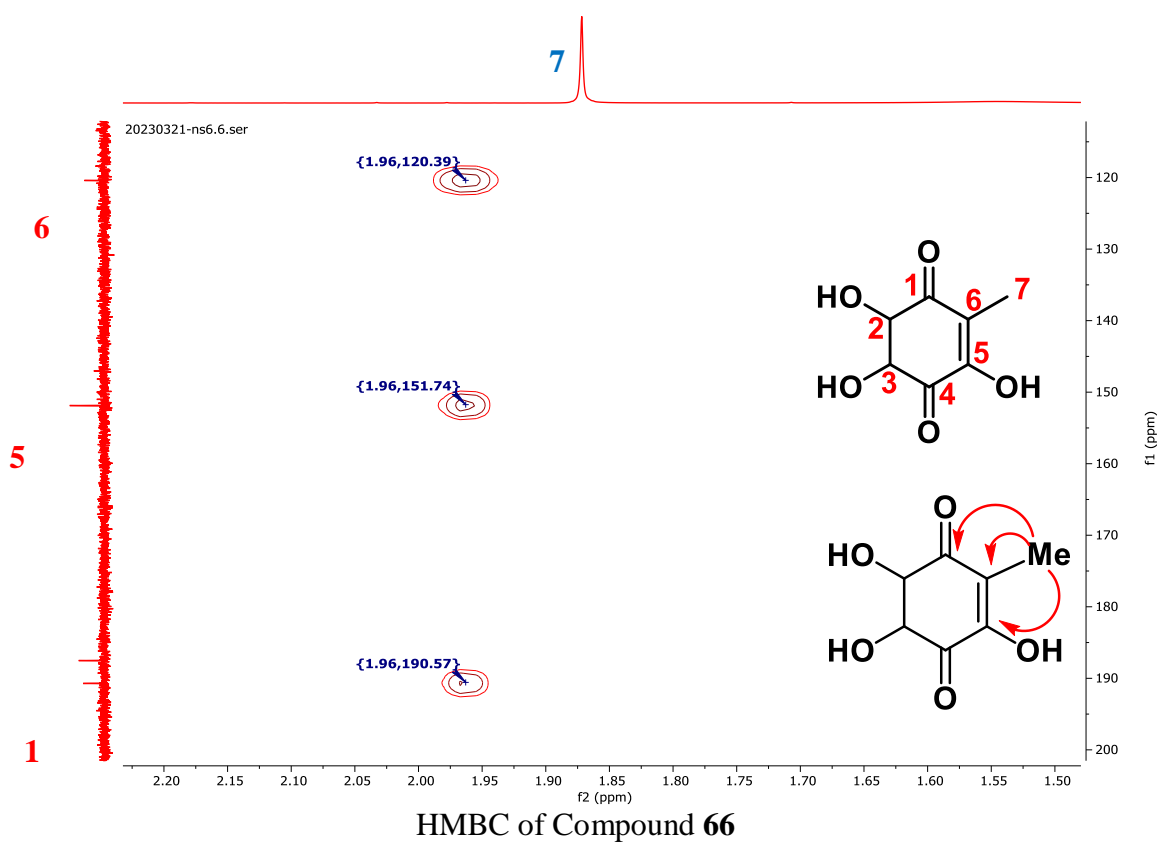
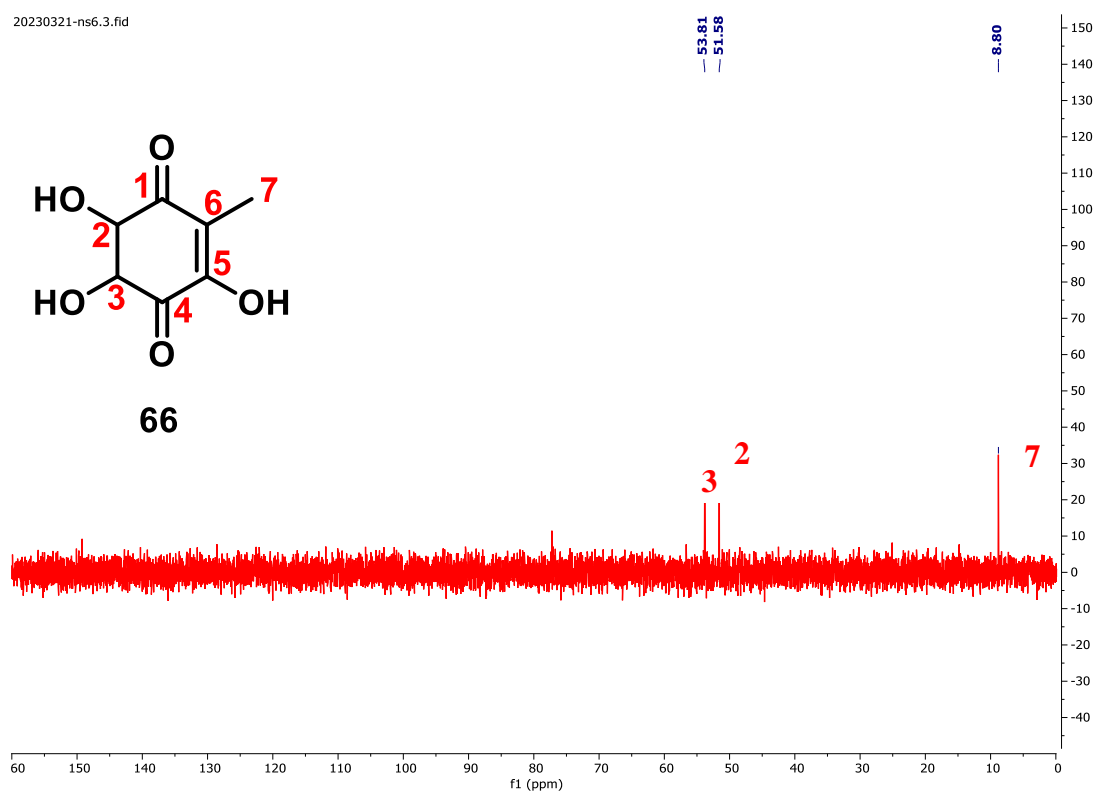
1. (a) L. Colebrook, "Alexander Fleming 1881–1955" *Biographical Memoirs of Fellows of the Royal Society*. **1956**, **2**, 117–126. (doi:10.1098/rsbm.1956.0008). (b) S. Waksman and H. B. Woodruff, *J. Bacteriol.* **1941**, **42**, 231-249.
2. L.A. Underkofler, R.R. Barton and S.S. Rennert, *Microbiological Process Report*, **1958**, **6**, 212-2021.
3. J. Bennett, "An Overview of the Genus *Aspergillus*". *Aspergillus: Molecular Biology and Genomics*. Caister Academic Press. **2010**, ISBN 978-1-904455-53-0. (a) X. Bai, Y. Sheng, Z. Tang, J. Pan, S. Wang, B. Tang, T. Zhou, L. Shi and H. Zhang, *J. Fungi*, **2023**, **9**, 261. (b) Y. Jiang, J. Wu, H. Kawagishi, C. Jiang, Q. Zhou, Z. Tong, Y. Tong and P. Wang, *Int. J. Anal. Chem.* **2022**, 1-11.
4. (a) D. J. Newman and G. M. Cragg, *J. Nat. Prod.* 2007, **70**, 461. (b) A. L. Harvey, *Drug Discovery Today* **2008**, **13**, 894; (c) D. J. Newman, G. M. Cragg, *J. Nat. Prod.* **2012**, **75**, 311; (d) E. C. Barnes, R. Kumar, R. A. Davis, *Nat. Prod. Rep.* **2016**, **33**, 372.
5. (a) D. L. Hawksworth, *Medical Mycology*, **2011**, **49** (Suppl. 1), S70–S76. (b) S-S. Zhang, Z-H. Meng, G-Z. Zhao, H-T. Wu and F. Cao, *Studies in Natural Products Chemistry*, Chapter 7-*Aspergillus versicolor* as a source of diversified metabolic products with pharmacological activities, 2022, **74**, 225-277. (c) Lima, M. A. S.; de Oliveira, M. C. F.; Pimentaa, A. T. A.; Uchôab, P. K. S. *J. Braz. Chem. Soc.* **2019**, **30** (10), 2029-2059. (d) F. S. Youssef and A. N. B. Singab, *Evidence-Based Complementary and Alternative Medicine*. **2021**, 2021, 1-11.
6. F. M. Talontsi, M. D. K. Tatong, B. Dittrich, C Douanla-Meli, and H. Laatsch, *Tetrahedron*. **2013**, **69**,7147-7151.
7. N. Bouras, F. Mathieu, Y. Coppel, S. E. Strelkov and A. Lebrihi, *J. Agric. Food Chem.* **2007**, **55**, 8920–8927.
8. K. Akiyama, S. Teraguchi, Y. Hamasaki, M. Mori, K. Tatsumi, K. Ohnishi and H. Hayashi, *J. Nat. Prod.* **2003**, **66**,136-139.
9. J. Hiort, K. Maksimenka, M. Reichert, S. Perovic´-Ottstadt, W. H. Lin, V. Wray, K. Steube, K. Schaumann, H. Weber, P. Proksch, S. R. Ebel, W. E. G. Muller and G. Bringmann, *J. Nat. Prod.* **2004**, **67**, 1532-1543.

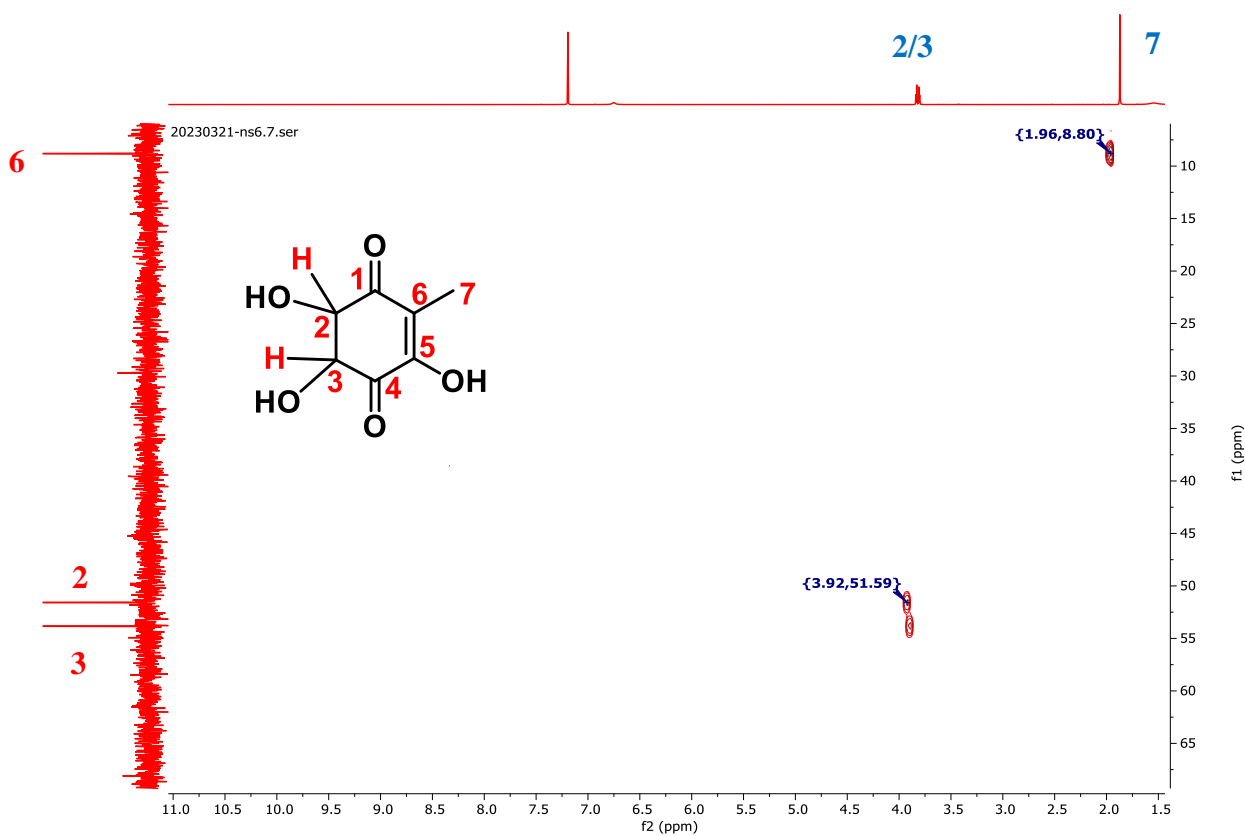
10. (a) W. Wang, F. Zeng, Q. Bie, C. Dai, C. Chen, Q. Tong, J. Liu, J. Wang, Y. Zhou, H. Zhu and Y. Zhang, *Org. Lett.* **2018**, *20*, 6817–6821. (b) (a) K. Scherlach, D. Boettger, N. Remme, C. Hertweck, *Nat. Prod. Rep.*, **2010**, *27*, 869–886. (b) E. Skellam, *Nat. Prod. Rep.* **2017**, *34*, 1252–1263.
11. Y. Kwon, M. Sohn, C. Kim, H. Koshino and W. Kim. *J. Nat. Prod.* **2012**, *75*, 271–274.
12. Barrow, C. J.; Sun. H. H. *J. Nat. Prod.* **1994**, *57*, 471-476.
13. C. Cui, X. Li, L. Meng, C. Li, C. Huang and B. Wang, *J. Nat. Prod.* **2010**, *73*, 1780–1784.
14. Y. Tan, B. Yang, X. Lin, X. Luo, X. Pang, L. Tang, Y. Liu, X. Li, X. Zhou, *J. Nat. Prod.* **2018**, *81*, 92–97.
15. F. S. de Guzman, J. B. Gloer, D. T. Wicklow and P. F. Dowd, *J. Nat. Prod.* **1992**, *55*, 931-939.
16. J. P. Springer, J. W. Dorner, R. J. Cole and R. H. Cox, *J. Org. Chem.* **1979**, *44*, 4852-4854.
17. X. Niu, H. Dahse, K. Menzel, O. Lozach, G. Walther, L. Meijer, S. Grabley and I. Sattler, *J. Nat. Prod.* **2008**, *71*, 689–692.
18. F. He, J. Bao, X. Zhang, Z. Tu, Y. Shi and S. Qi. *J. Nat. Prod.* **2013**, *76*, 1182–1186.
19. W. Liao, C. Shen, L. Lin, Y. Yang, H. Han, J. Chen, S. Kuo, S. Wu and C. Lia, *J. Nat. Prod.* **2012**, *75*, 630–635.
20. C-M. Deng, S-X. Liu, C-H. Huang, J-Y. Pang and Y-C Lin, *Mar. Drugs*, **2013**, *11*, 2616-2624
21. (a) G. G. Dumancas, L. Viswanath, R. Wang, E. Gondek, S. K. Lageshetty, B. Solivio, A. A. Lubguban and R. M. Malaluan, *Reference Module in Biomedical Sciences*, Elsevier, **2022**, ISBN 9780128012383, doi.org/10.1016/B978-0-12-824315-2.00255-4. (b) P. Dowd, S-W. Ham, S. Naganathan and R. Hershline, *Annu. Rev. Nutr.*, **1995**, *15*, 419-40. (c) N. El-Najjar, H. Gali-Muhtasib, R. A. Ketola, P. Vuorela, A. Urtti and H. Vuorela, *Phytochem Rev.*, **2011**, *10*, 353–370. (d) J. L. Bolton and T. Dunlap, *Chem.Res.Toxicol.* **2017**, *30*, 13–37.

3.6 Copies of NMR spectra

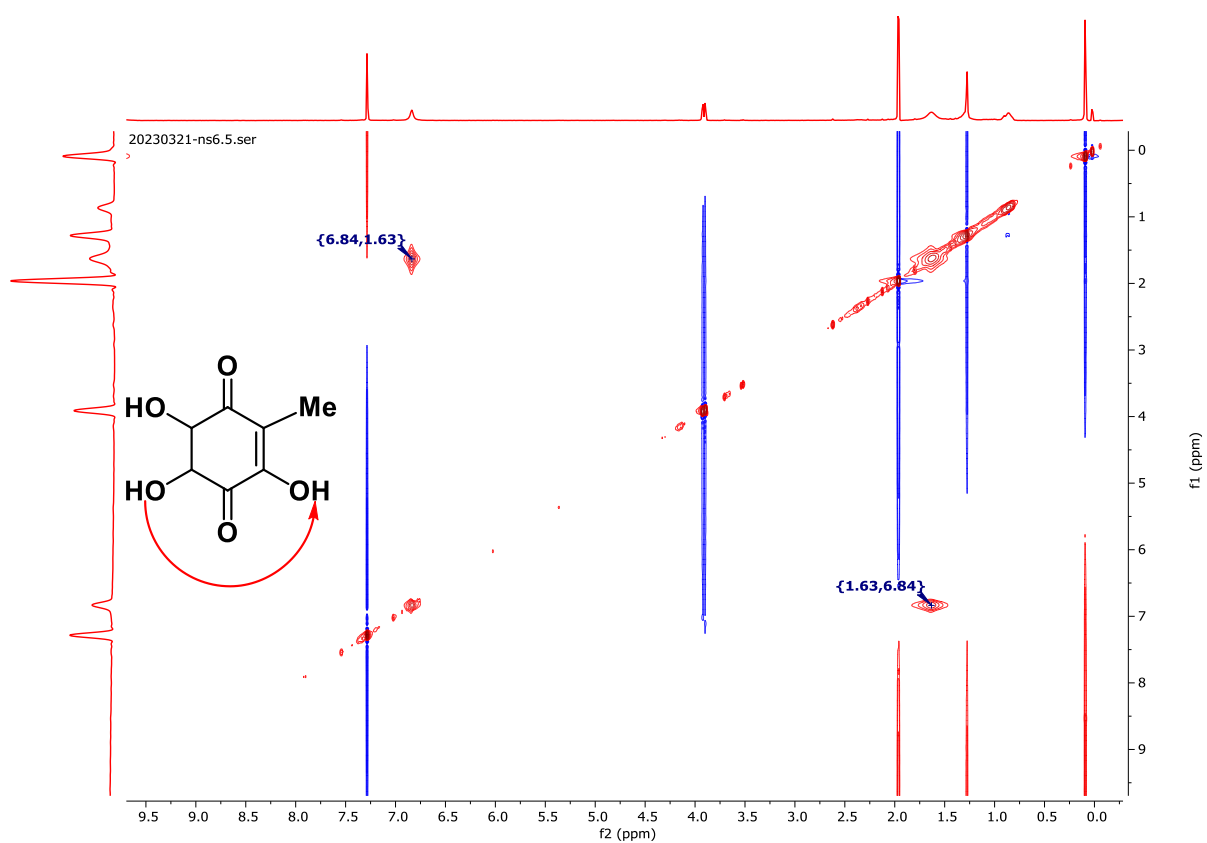


20230321-ns6.3.fid

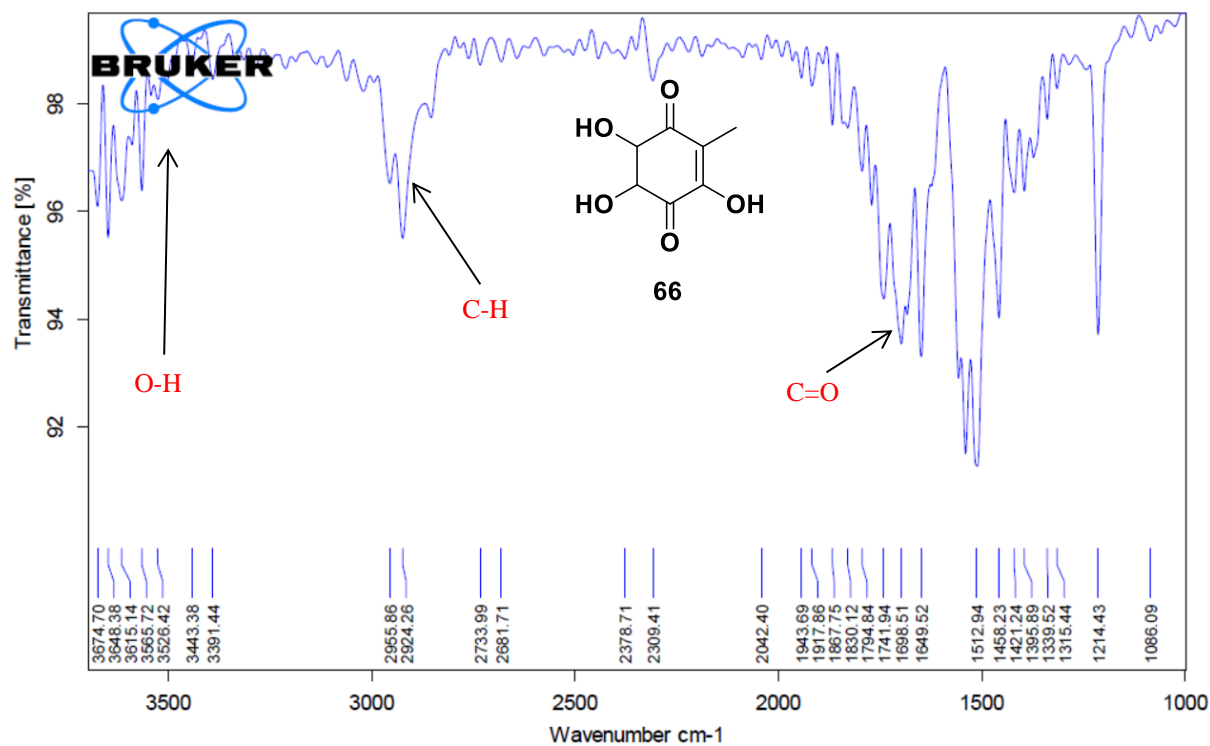
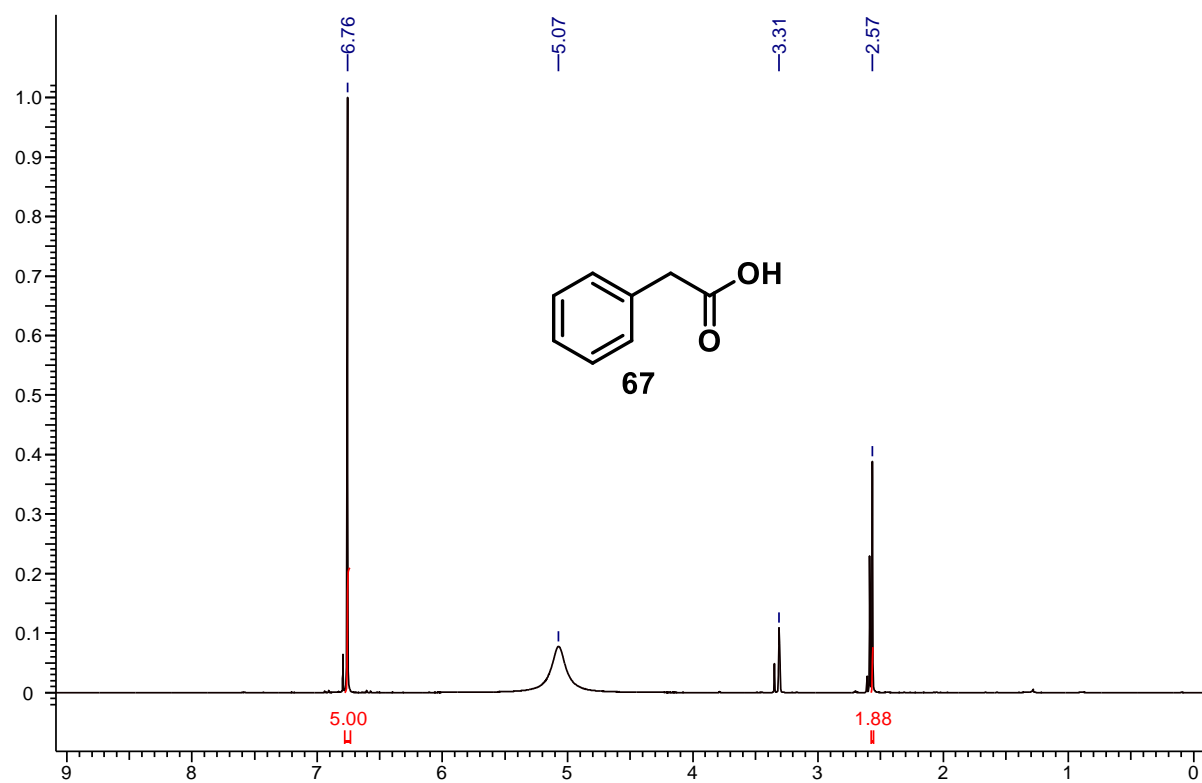


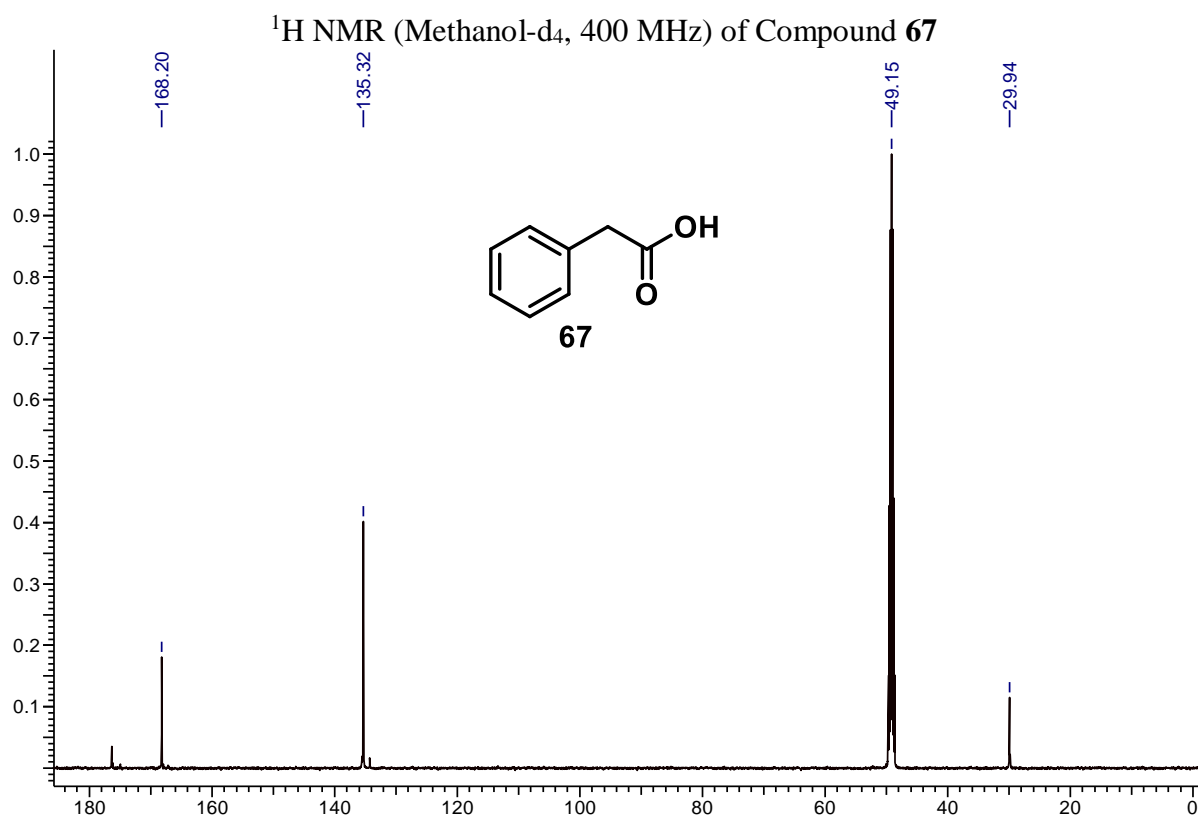


HSQC of Compound 66

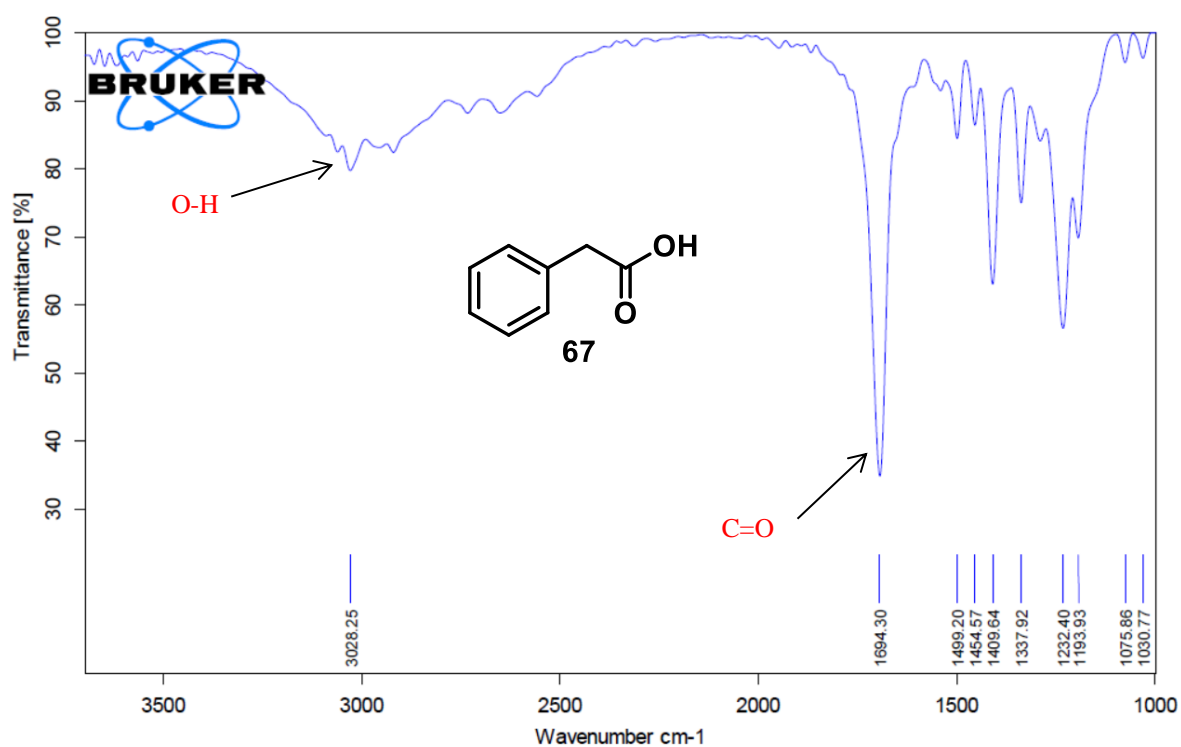


NOSY of Compound 66

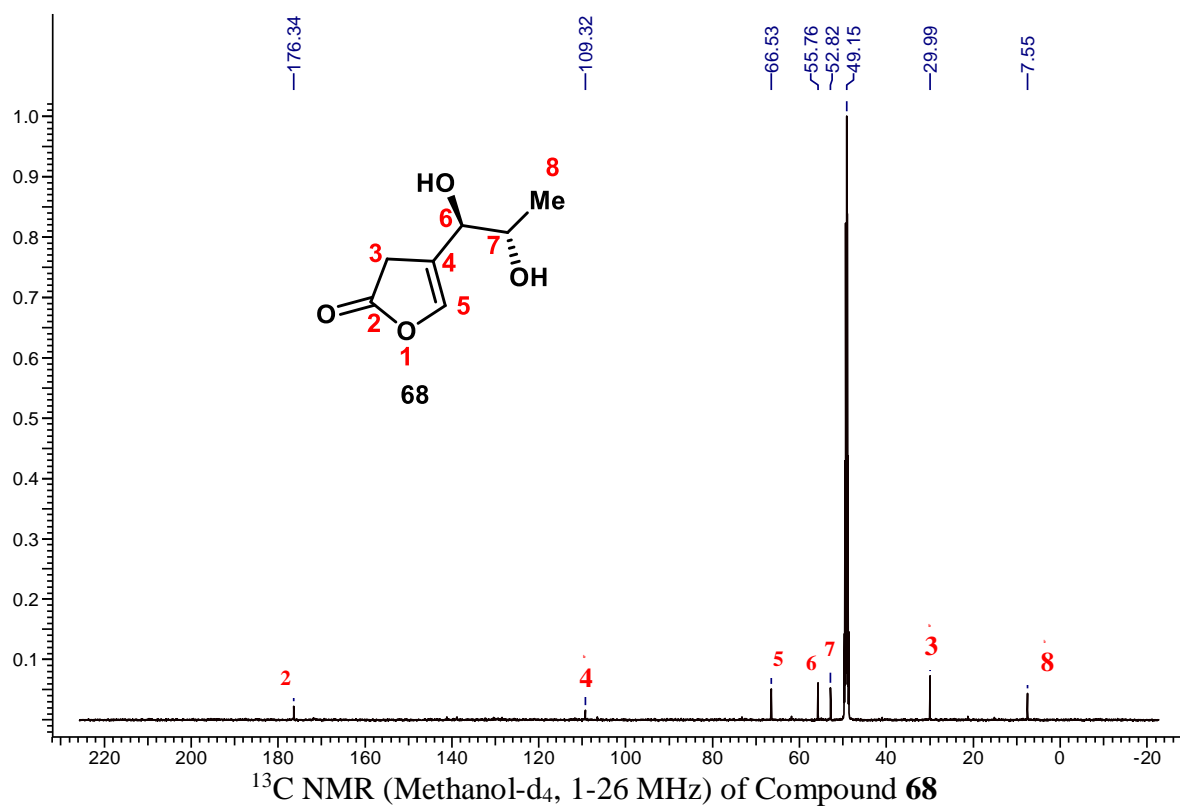
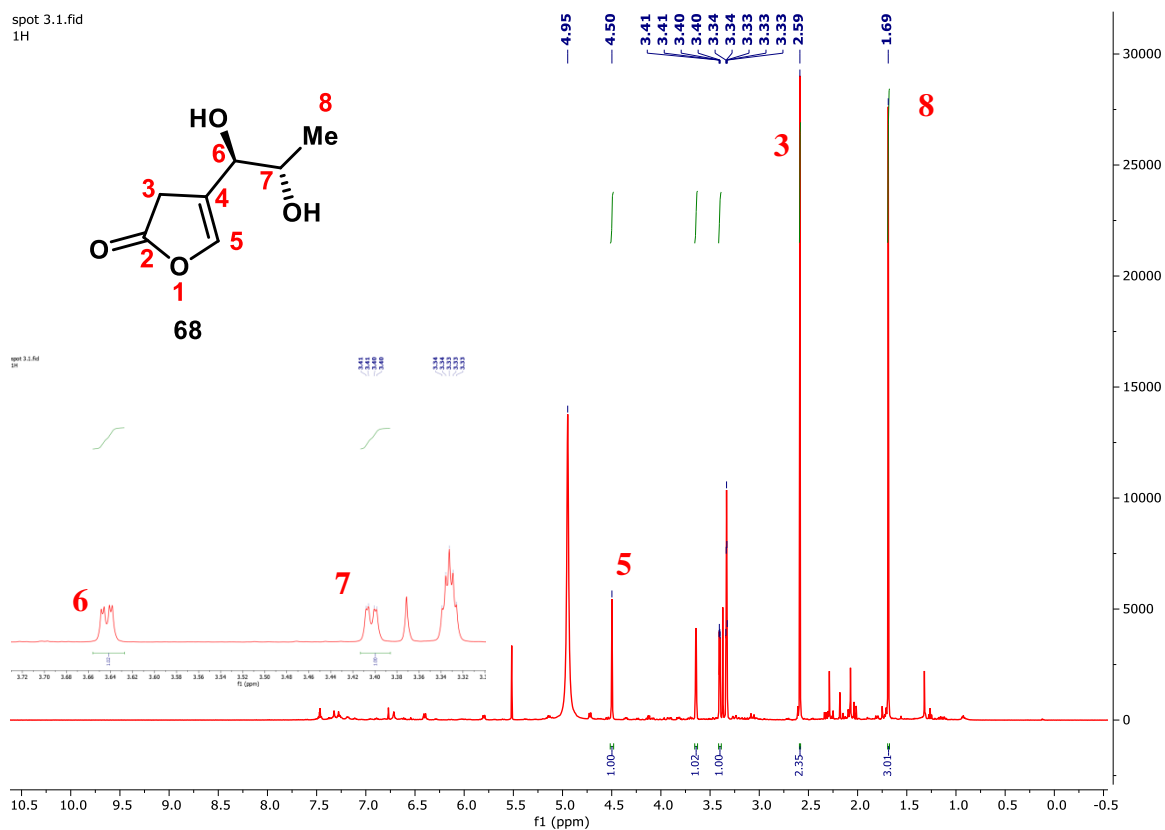
FT-IR spectra of compound **66**

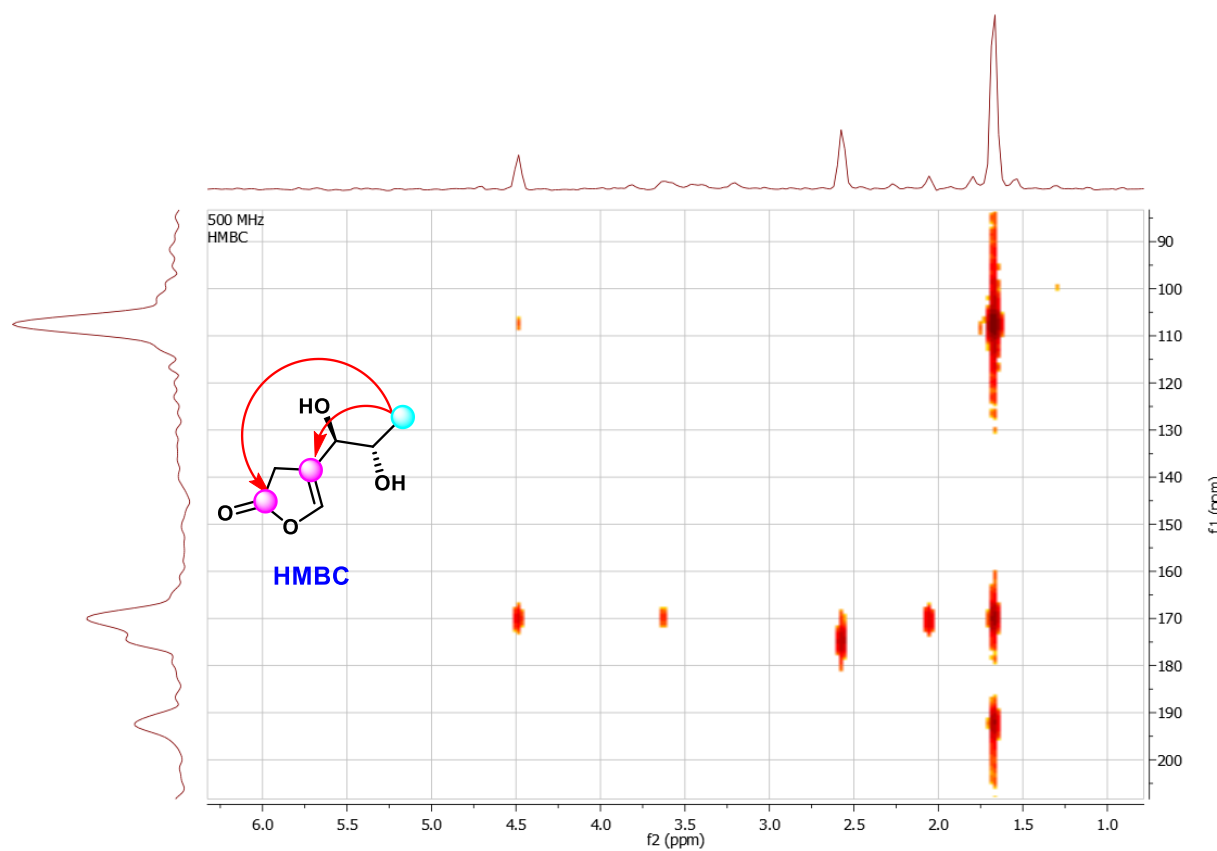
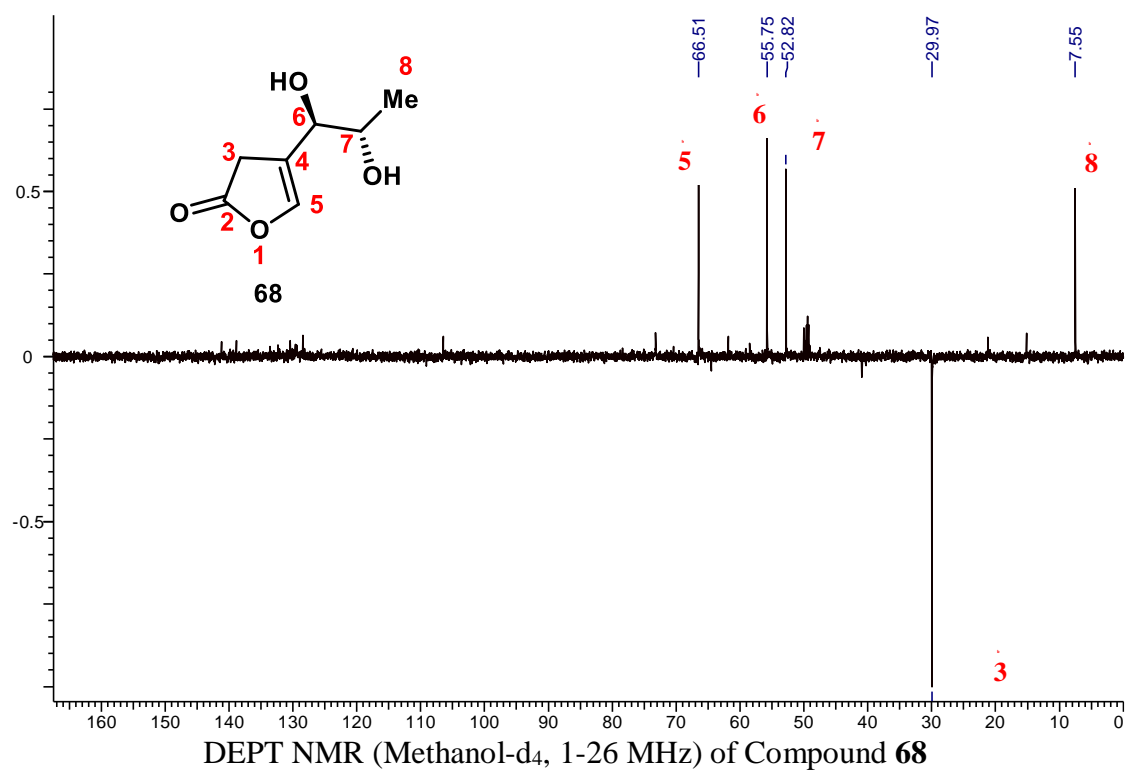


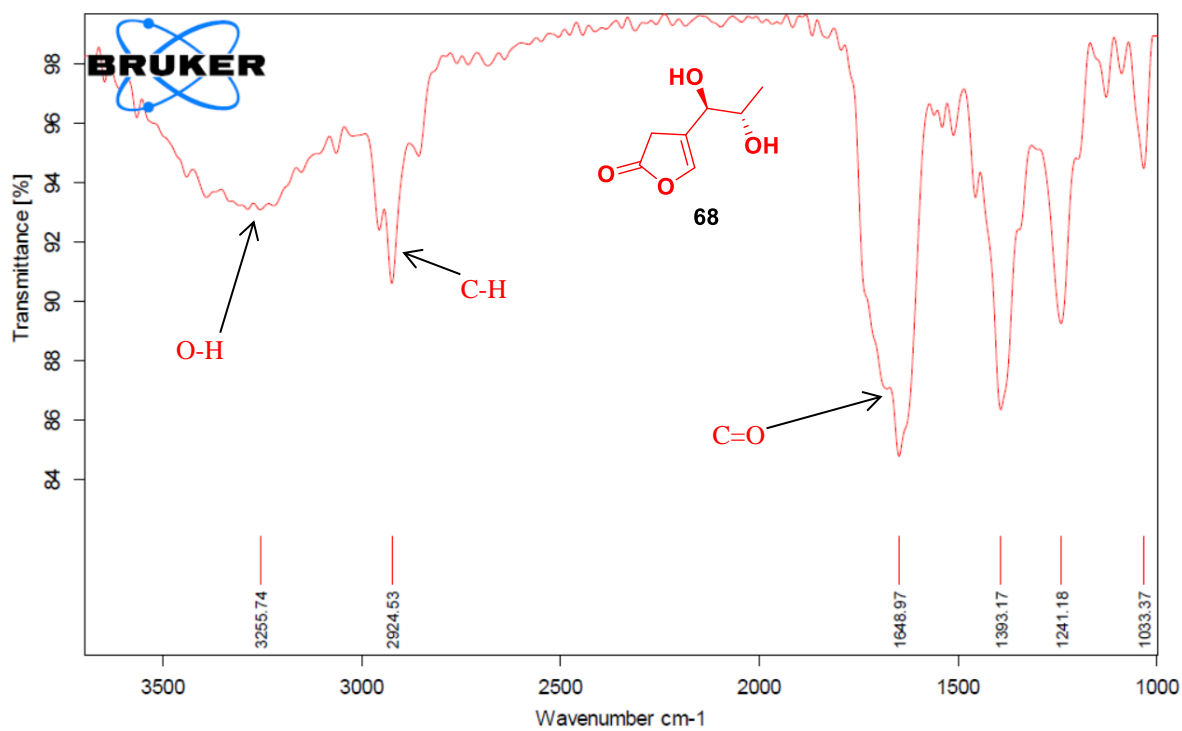
^{13}C NMR (Methanol- d_4 , 101MHz) of Compound **67**



FT-IR spectra of compound **67**





FT-IR spectra of compound **68**

Name of the Student: Lakshmi Goswami

Registration No. : 10CC17A26013

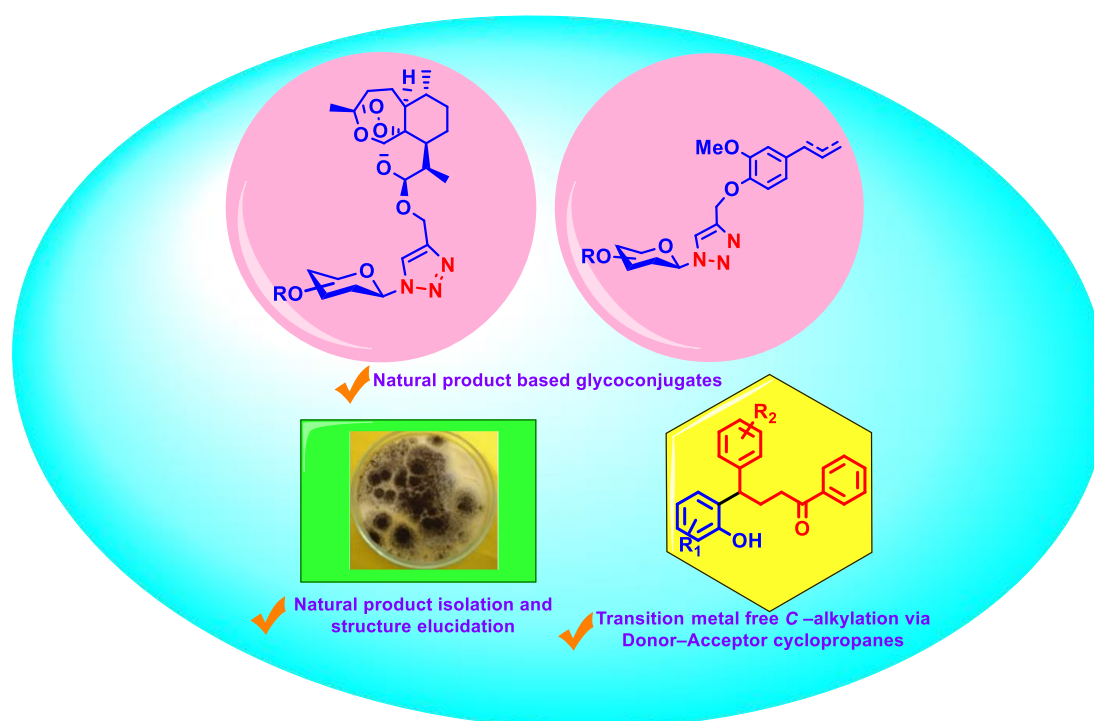
Faculty of Study: Chemical Science

Year of Submission: 2023

AcSIR academic centre/CSIR Lab: CSIR–National Chemical Laboratory

Name of the Supervisor: Dr. Asish K. Bhattacharya

Title of the thesis: Design and synthesis of potent bioactive scaffolds *via* [3+2] cycloaddition, Glaser and Cadiot-Chodkiewicz coupling reactions; Cu catalyzed C–C bond forming reactions employing donor-accepter cyclopropanes and bioactives from *Aspergillus terreus*



This present thesis is divided into three chapters. Chapter 1 deals with the synthesis of glycoconjugates incorporating natural products *via* [3+2] Click reaction and other synthetic analogues to furnish potent bioactive compounds. Artemisinin based glycoconjugates are at present being assayed for their anti-cancer studies meanwhile eugenol and isoeugenol based glycoconjugates and other synthetic derivatives were tested against *Aspergillus fumigatus* for their antifungal activities. Eugenol and isoeugenol derivatives were found to be much potent than their parent molecules as perceived from their improved antifungal activities data. Chapter 2 deals with the transition-metal free C-alkylation of phenols employing donor-acceptor cyclopropanes. Alkylation of phenols led us to the formation of functionalized 1, 4-diphenylbutan-1-one derivatives, an important core ubiquitous in many plant based chalcones as well as synthetic compounds. Chapter 3 describes the isolation of secondary metabolites from the microbial culture. *Aspergillus terreus* is a rich source of authentic butenolide derived natural products. We herein report isolation and structure elucidation of secondary metabolites from *Aspergillus terreus*.

List of Publications Emanating from the Thesis Work

1. Design and synthesis of eugenol/isoegenol glycoconjugates and other analogues as antifungal agents against *Aspergillus fumigatus*.
L. Goswami[†], L. Gupta[†], S. Paul, M. Vermani, P. Vijayaraghavan, A. K. Bhattacharya, *RSC Med. Chem.*, **2022**, *13*, 955-965. (†*Equal contribution*)
2. Design and Synthesis of 1,3-Diynes as Potent Antifungal Agents against *Aspergillus fumigatus*.
L. Goswami[†], L. Gupta[†], S. Paul, P. Vijayaraghavan and A. K. Bhattacharya, *ChemMedChem*, **2023**, e202300013. (doi.org/10.1002/cmdc.202300013) (†*Equal contribution*)

List of Publications not Emanating from the Thesis Work

1. Synthesis of artemisinin derived glycoconjugates inspired by click chemistry.
L. Goswami[†], S. Paul[†], T. K. Kotammagari and A. K. Bhattacharya, *New J. Chem.*, **2019**, *43*, 4017-4021. (†*Equal contribution*)

List of Poster, oral presentations and Conferences attended

1. Presented poster on “*Artemisinin Based Glycoconjugates as Potent Anti-Cancer Agents*” during **National Science Day 2018** at CSIR-National Chemical Laboratory Pune, India in February 2018.

Abstract: Artemisinin is isolated from the plant *Artemisia annua*, a herb which has been traditionally used in Chinese medicines to cure fever. We report herein design and synthesis of an interesting class of molecules which could prove to be potent anticancer agents. Included here, is synthesis of exclusive β -propargylated dihydroartemisinin along with the synthesis of artemisinin based glycoconjugates by employing Cu(I) catalysed click reaction between β -propargylated artemisinin and azido sugars, in moderate to very good yields.


2. Presented poster on “*Design and Synthesis of Glycoconjugates and Other Analogues of Eugenol and Isoeugenol Isolated from Myristica fragrance as Novel Antifungal Agents*” during **XIV J-NOST Conference 2018** at CSIR-Indian Institute of Chemical Technology Hyderabad, India in December 2018.

Abstract: Several secondary metabolites isolated from various natural sources have shown potent antifungal activities. As part of our ongoing project on the isolation of novel antifungals from medicinal plants, eugenol and isoeugenol isolated from the plant *Myristica fragrance* have shown promising antifungal activities. In order to enhance the bioactivities, we have undertaken design and synthesis of glycoconjugates of eugenol and isoeugenol utilizing click chemistry. The Cu(I) catalysed click reaction between propargylated eugenol/isoegenol and several azido-sugars furnished the glycoconjugates in good yields. All the synthesized molecules were assayed for their antifungal activities.

Erratum

Cite this: *RSC Med. Chem.*, 2022, 13, 955

Design and synthesis of eugenol/isoegenol glycoconjugates and other analogues as antifungal agents against *Aspergillus fumigatus*[†]

Lakshmi Goswami,^{‡,ab} Lovely Gupta,^{‡,c} Sayantan Paul,^{ab} Maansi Vermani,^c Pooja Vijayaraghavan^{*c} and Asish K. Bhattacharya ^{*ab}

Glycoconjugates are biologically significant molecules as they tend to serve a wide range of intra- and extra-cellular processes depending on their size and complexity. The secondary metabolites of the plant *Myristica fragrans*, eugenol and isoegenol, have shown antifungal activities (IC₅₀ 1900 μM). Therefore, we envisioned that glycoconjugates based on these two scaffolds could prove to be potent antifungal agents. Triazole-containing compounds have shown prominent activities as antifungal agents. Based on this, we opined that a Cu(I) catalyzed click reaction could serve as the bridging tool between a eugenol/isoegenol moiety and sugars to synthesize eugenol/isoegenol based glycoconjugates. In our present work, we have coupled propargylated eugenol/isoegenol and azido sugar to furnish eugenol/isoegenol based glycoconjugates. In another approach, we have carried out hydroxylation of the double bond of eugenol and subsequent azidation of a primary alcohol followed by intramolecular coupling reactions leading to various other analogues. All the synthesized compounds were assayed against an opportunistic pathogenic fungus, *Aspergillus fumigatus*. Among the synthesized compounds, two analogues have exhibited significant antifungal activities with IC₅₀ values of 5.42 and 9.39 μM, respectively. The study suggested that these two analogues inhibit cell wall-associated melanin hydrophobicity along with the number of conidia. The synthesized compounds were found to be non-cytotoxic to an untransformed cell line.

Received 6th May 2022,
Accepted 1st June 2022

DOI: 10.1039/d2md00138a

rsc.li/medchem

Introduction

Aspergillus infections pose a significant threat to immune-compromised, organ transplant, neutropenic, and cancer patients and especially in patients having underlying lung diseases including asthma, tuberculosis, and chronic obstructive pulmonary disease. Multiple forms of aspergillosis have been estimated to affect about 1–4 million people worldwide, with more than 90 percent mortality rate.¹ Recent studies have reported the incidence of invasive pulmonary aspergillosis in 19.6–33.3% of COVID-19 patients.^{2,3} The higher mortality rate of *Aspergillus* infections has been attributed to the virulence of the pathogen, delay in specific diagnosis, variable drug bioavailability, toxicity, and

development of resistance towards drugs.⁴ *Aspergillus fumigatus* is the most common *Aspergillus* species implicated in respiratory infections.⁴ It exhibits polygenic factors contributing to its virulence which include its small conidial size, biofilm formation, melanin layer, cell surface adhesion molecules, nutrient uptake that contributes towards protection during oxidative stress, and immunological inertness against the host killing mechanism.⁵ As the majority of virulence factors are associated with the fungal cell surface, it is a favourable target for the development of antifungal drugs. Subsequently, the increased incidence of fungal infections is also attributed to the availability of less toxic and efficient antifungal drugs. In the same regard, the matter of concern is the limited spectrum of efficacious antifungal drugs, which are not completely effective for the eradication of fungi. Amphotericin B (Amp B), itraconazole, fluconazole, voriconazole, ketoconazole, terbinafine, miconazole, etc. are available for the treatment of a wide array of fungal infections (Fig. 1). The majority of these antifungal drugs target cell membrane biosynthesis either at the final stage or by binding to the intermediary compound of its biosynthesis.⁶ There are a few other antifungal drugs targeting fungal cell wall components, nucleic acids, and microtubule biosynthesis. The toxicity associated with current

^a Division of Organic Chemistry, CSIR-National Chemical Laboratory (CSIR-NCL), Dr. Homi Bhabha Road, Pune, 411 008, India. E-mail: ak.bhattacharya@ncl.res.in

^b Academy of Scientific and Innovative Research (AcSIR), Ghaziabad, 201 002, India

^c Antimycotic and Drug Susceptibility Laboratory, J3 Block, Amity Institute of Biotechnology, Amity University Uttar Pradesh, Sector-125, Noida, India.

E-mail: vrpooja@amity.edu

[†] Electronic supplementary information (ESI) available. See DOI: <https://doi.org/10.1039/d2md00138a>

[‡] These authors contributed equally to this work.

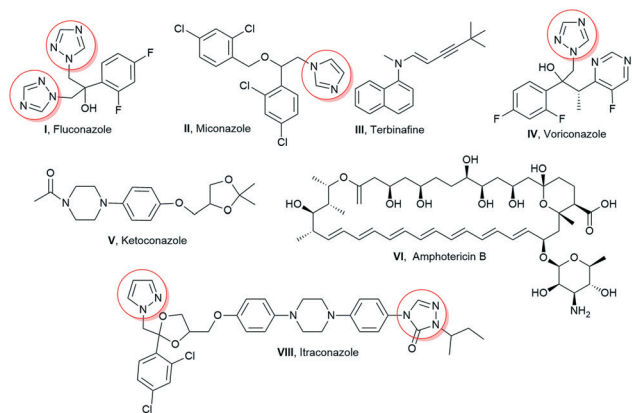


Fig. 1 Clinically used antifungal drugs.

antifungal drugs and the emergence of resistance have enthused an urgent need to improve existing antimicrobial scaffolds to develop novel antifungals. Hence, these antifungals have also been structurally modified to enhance their therapeutic index. Eugenol **1** and isoeugenol **2** are naturally occurring phenolic monoterpenes belonging to the phenylpropanoid group and have been traditionally isolated from *Eugenia caryophyllata*, *Myristica fragrans*, and *Syzygium aromaticum* (Fig. 2).⁷

Isoeugenol **2** is produced by a range of plants such as the *Petunia* flower, *Clarkia breweri*, and *Ocimum basilicum*.⁷ Eugenol and isoeugenol have demonstrated analgesic, antioxidant, anti-inflammatory, anti-carcinogenic, anti-mutagenic, and even insect repellent properties.⁸ Besides, both of these compounds have been reported to exhibit antimicrobial activity.⁹ Eugenol **1** and isoeugenol **2** interfere with microbial membrane functions (membrane binding and permeability alteration) or suppress virulence factors including toxins, enzymes, the melanin biosynthesis pathway, hydrophobins, and formation of biofilms.^{10–12} They also induce the generation of H₂O₂ and increase the free Ca²⁺ concentration in the cytoplasm. Structural modifications in available drugs as well as naturally active lead moieties are conducted to enhance the drug efficacy and reduce their side effects. Alkylation of drug scaffolds has resulted in derivatives with promising antifungal activity. For example, 2,4-difluoro-2-(1*H*-1,2,4-triazol-1-yl) acetophenone compounds with linear C5–C8 alkyl chains¹³ and *n*-alkylated ebsulfur derivatives with a linear C5 alkyl chain displayed enhanced antifungal activity against *Aspergillus* species.¹⁴ In addition, aminoglycosides (kanamycin B and tobramycin) with linear C12 and C14 alkyl chains displayed significant antifungal activities. It has also been reported that the conjugation of a carbohydrate scaffold

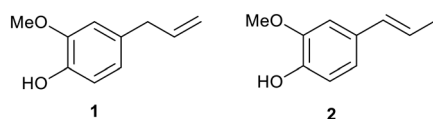


Fig. 2 Chemical structures of eugenol **1** and isoeugenol **2**.

to naturally occurring bioactive molecules has led to enhanced bioactivity and manifestation of superior biological properties such as solubility, stability, and bioactivity compared to the parent molecule.^{15–17} Therefore, glycoconjugates of bioactive natural products can be ideal candidates for efficacious therapeutic agents. The hypervalent nature of sugar assists the drug molecule to reach target cells, thus playing a major role in the drug delivery system. In addition, the incorporation of the 1,2,4-triazole ring with therapeutically active compounds aids in the development of new antifungal agents.^{18,19}

Results and discussion

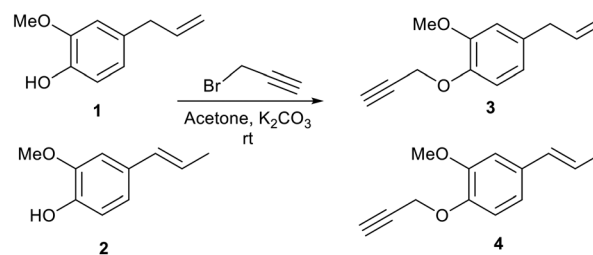
We report herein the design and synthesis of novel glycoconjugates of eugenol **1** and isoeugenol **2** incorporating the 1,2,4-triazole ring and other derivatives and evaluated the antifungal activities of all the synthesised derivatives against *A. fumigatus* specifically targeting various cell wall associated virulence factors.

Synthesis and characterization of the synthesized compounds

When we treated eugenol **1** and isoeugenol **2** with propargyl bromide in acetone in the presence of potassium carbonate (K₂CO₃) as base at room temperature, we obtained propargylated products **3** and **4**, respectively (Scheme 1).

Azido sugars **5a–f** (Fig. 3) were synthesized as per reported literature methods and their spectral data were found to be consistent with the reported literature data.^{15,20,21} The stereochemistries of the anomeric configurations of the azido sugars **5a–f** were assigned as the β-configurations on the basis of comparison with reported data²⁰ as well as their coupling constants in the ¹H NMR (nuclear magnetic resonance) spectra. In general, the anomeric proton of the azido sugars appeared as a doublet integrated to one proton at 4.61–4.98 ppm in the ¹H NMR spectra with a coupling constant in the range of 8.5–8.8 Hz, which unequivocally proves that the azide groups are β-oriented.^{15,20}

After synthesizing propargylated eugenol **3**, isoeugenol **4**, and azido sugars **5a–f**, synthesis of eugenol and isoeugenol derived glycoconjugates was initiated utilizing click chemistry (Table 1).^{21–24} Propargylated eugenol **3**, isoeugenol **4**, and azido sugars **5a–f** on reaction in the presence of catalytic amounts of copper iodide (CuI) and *N,N*-diisopropylethylamine (DIPEA) as



Scheme 1 Synthesis of propargylated derivatives of eugenol **1** and isoeugenol **2**.

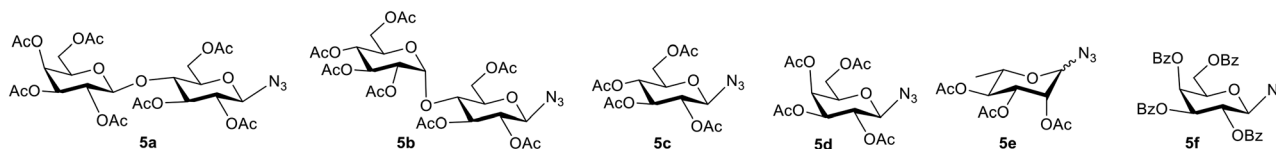
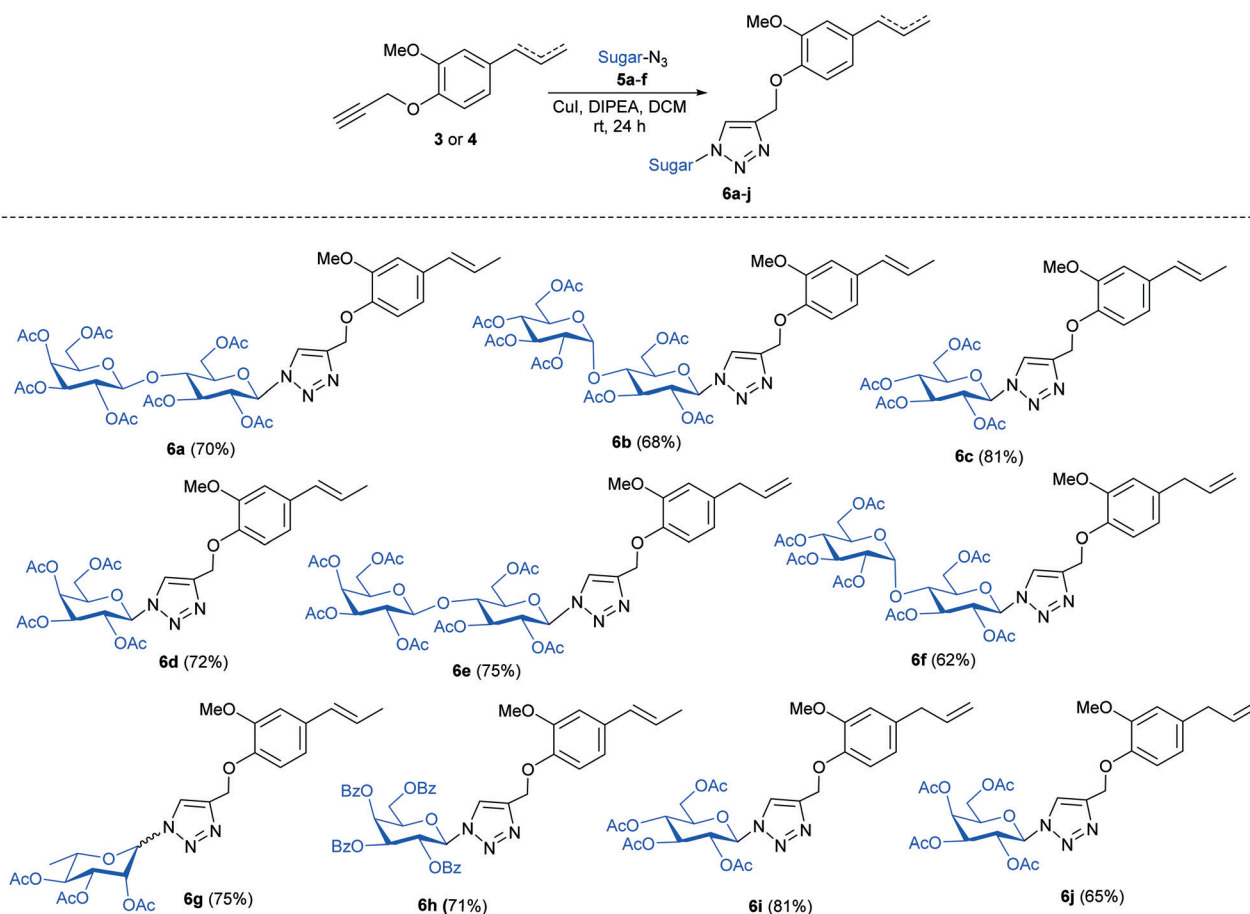


Fig. 3 Structures of the azido sugars (5a–f) used for the synthesis of glycoconjugates.

Table 1 Substrate scope^{a,b}



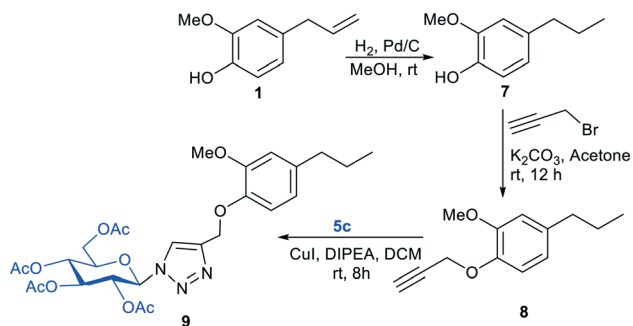
^a Reaction conditions: propargylated eugenol/isoeugenol 3 or 4 (30 mg, 0.1485 mmol, 1 equiv.), azido sugars 5a–f (0.1782 mmol, 1.2 equiv.), DCM (3 ml), CuI (15.55 mg, 0.0816 mmol, 0.55 equiv.), and DIPEA (26 μ l, 0.1485 mmol, 1.0 equiv.). ^b Isolated yield.

base in dichloromethane (DCM) afforded glycoconjugates (6a–j) in good to very good yields. Slightly better yields of glycoconjugates were obtained in the case of reactions with lactose azide (6a and 6e) than those with maltose azide (6b and 6f). Azides of monosaccharides also furnished glycoconjugates (6c, d, and g–j) in good yields (Table 1). Azido glucose 5c furnished glycoconjugates (6c and 6i) in higher yields (81%, respectively) than glycoconjugates (6d and 6j) furnished by azido galactose 5d. Benzoate protected azido galactose (5f) also furnished glycoconjugate 6h in good yield. Compound 6i returned an IC_{50} value of 5.42 μ M against *A. fumigatus*.

Furthermore, to explore the role of the *exo*-methylene double bond present in eugenol 1 in the antifungal activity,

we reduced the *exo*-methylene double bond by using Pd–C/H₂ to yield the reduced product, eugenol 7 (ref. 25) (Scheme 2). The free –OH group of compound 7 was propargylated with propargyl bromide to afford compound 8. We then coupled compound 8 with 5c to provide compound 9. Among compounds 7, 8, and 9, compound 7 gave an IC_{50} value of 9.39 μ M against *A. fumigatus*.

We further deprotected the acetyl groups present in compounds 6i and 9 in order to find out the role of the protecting group of sugar (Scheme 3).²⁶ Compounds 10 and 11 were obtained after deprotection of acetyl groups present in compounds 6i and 9. However, the IC_{50} values of compounds 10 and 11 were found to be greater than 25 μ M.



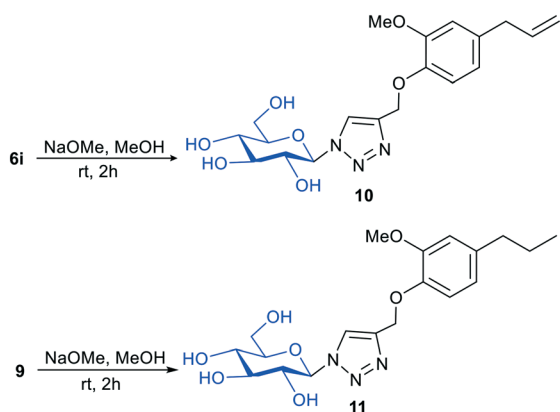
Scheme 2 Reduction of the double bond present in eugenol **1** and subsequent glycoconjugation.

In order to synthesize more analogues other than glycoconjugates, the free -OH group of eugenol **1** was protected as OTBS by treating **1** with *tert*-butyldimethylsilyl chloride (TBDMS-Cl) in the presence of a combination of imidazole and 4-dimethyl-aminopyridine (DMAP) as bases in DCM to furnish compound **12**. Compound **12** was subjected to dihydroxylation²⁷ using AD-mix- β in a water-*tert* butanol solvent system to obtain compound **13** in which the primary hydroxyl group was treated with tosyl chloride only to facilitate azidation upon treatment with sodium azide (NaN_3) in dimethylformamide (DMF) in the presence of a catalytic amount of tetrabutylammonium iodide (TBAI) to furnish compound **14** (Scheme 4).

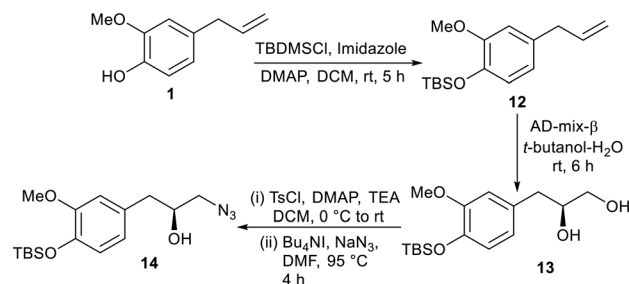
It is well established that often dimers of biologically active molecules exhibit higher activity than the monomeric unit.^{28,29} With compound **14** at hand, we envisaged to synthesize dimeric compounds. In this regard, we treated compound **14** with compounds **8**, **3**, and **4** *via* a click reaction to afford compounds **15**, **16**, and **17**, respectively (Scheme 5).

Biological evaluation of all the synthesized compounds

Eugenol **1**, isoeugenol **2**, and all the synthesized molecules (**3**, **4**, **6a-j**, and **7-17**) were assayed for their anti-fungal activities against *A. fumigatus*. Preliminary data are furnished in Table 2.



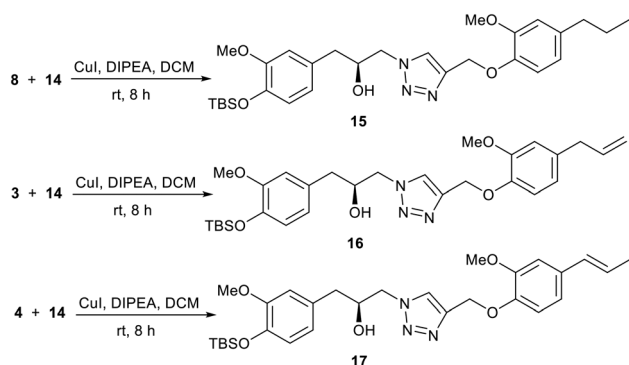
Scheme 3 Deacetylation of compounds **6i** and **9**.



Scheme 4 Dihydroxylation followed by azidation of eugenol **1**.

As shown in Table 2, eugenol **1** demonstrated an IC_{50} value of 1900 μM against *A. fumigatus*. Conjugation of the glucose moiety with eugenol along with the azole group (compound **6i**) increases the activity, as exhibited by the IC_{50} value of 5.42 μM . It is pertinent to mention here that the other sugars did not yield any notable activities. Galactose, which is the epimer of glucose having a different stereochemistry at C-4 than glucose, was also found to be less effective when linked to eugenol **1** which led us to believe that glucose, having all the OH bonds in equatorial positions, could be playing a pivotal role in terms of cellular interaction; however, when we coupled glucose with isoeugenol (compound **6c**) we did not observe any significant activity. These observations envisaged us to look for the SAR associated with the position of the double bond as well and its presence. The non-activity of the isoeugenol-glucose conjugate **6c** can be explained on the basis of non-terminal positioning of the double bond, whereas the eugenol-glucose conjugate **6i** was found to be active with the terminal double bond. When we reduced the double bond of eugenol **1**, the reduced eugenol **7** was found to exhibit an IC_{50} value of 9.39 μM . Inspired by this revelation we coupled compound **7** with glucose azide **5c**. However, we did not observe any activity. We also assayed the dimeric compounds (**15-17**) with each of them returning an IC_{50} value greater than 25 μM .

The antifungal potency of the synthesized compounds of eugenol and isoeugenol (compounds **3**, **4**, **6a-j**, and **7-17**) against *A. fumigatus* was calculated using the micro-broth dilution assay as per the Clinical and Laboratory Standards



Scheme 5 Synthesis of dimeric compounds.

Table 2 IC₅₀ values of compounds **3**, **4**, **6a–j**, and **7–17** against *A. fumigatus*

Compound codes	IC ₅₀ values	Compound codes	IC ₅₀ values
1	1900 μM	6j	10.86 μM
2	1900 μM	7	9.39 μM
3	>25 μM	8	>25 μM
4	>25 μM	9	>25 μM
6a	14.47 μM	10	>25 μM
6b	14.47 μM	11	>25 μM
6c	21.73 μM	12	>25 μM
6d	10.86 μM	13	>25 μM
6e	14.47 μM	14	>25 μM
6f	14.47 μM	15	>25 μM
6g	12.08 μM	16	>25 μM
6h	15.18 μM	17	>25 μM
6i	5.42 μM	Amp B	1.08 μM

Institute (CLSI) protocol.³⁰ Amongst the synthesised compounds, only **6i** and **7** inhibited the conidial as well as mycelial growth of *A. fumigatus* at significantly low MIC values *i.e.* 10.86 μM and 15.54 μM, respectively. The remaining compounds showed MIC >20 μM and, therefore, they were not considered for further experiments. The MIC and IC₅₀ of both parent molecules (eugenol **1** and isoeugenol **2**) were 3800 μM and 1900 μM, respectively. The MIC values of the drug control Amp B and itraconazole were 0.216 μM and 0.552 μM, respectively. The positive control showed *A. fumigatus* conidia with a characteristic greenish-grey color, whereas in compound-treated colonies white pigment-less conidia were visualized at IC₅₀. The compounds exhibited MIC values ranging from 10–20 μM compared with the MIC value of 3800 μM of the parent molecules, indicating the higher antifungal potency of the compounds (more than 100-fold).

The crucial parameter for developing any antifungal molecule is its selective toxicity for fungal cells over mammalian cells. L-132 was referred to as an excellent cell line for cytotoxicity analysis.³¹ It consists of normal epithelial cells derived from human embryonic lungs. Hence, the compounds (**6i** and **7**) were tested against the normal lung epithelial cell line L-132 along with the FDA-approved antifungal agent Amp B as a positive control. Cytotoxicity screening revealed that compounds were non-toxic on the

untransformed cell line (compound **6i** up to 43.46 μM and compound **7** up to 152.32 μM).

The concentration range selected for cytotoxicity covered the antifungal activity against *A. fumigatus*. The CC₅₀ (cytotoxic concentration-50) values for compounds **6i** and **7** were calculated as 43.46 μM and 150.5 μM. The reported sub-lethal cytotoxicity of the antifungal drug Amp B was in the range of 5.4–10.82 μM.³² The selectivity index (SI) values for **6i** and **7** were calculated as 8.01 and 16.02, respectively. The compounds with a higher SI are considered to be promising drug candidates as the concentration of the compounds required to induce antimicrobial activity is lower than that which induces cytotoxicity in host cells. The SI of eugenol was reported to be 0.2 against non-filamentous fungi.³³ By comparison, the SI values of the compounds tested were higher than the reported value for eugenol. Therefore, our results indicate that the compounds are safe and can be further investigated as promising antifungal molecules. The magnitude of the biological activity of an active molecule, in terms of specific interactions with the molecular target, along with drug-related side effects is strongly influenced by its pharmacokinetics properties. The compounds (**6i** and **7**) were screened through Lipinski's rule of five for oral bioavailability, health effects, maximum passive adsorption, and central nervous system (CNS) activity.

In silico prediction of the physico-chemical and pharmacokinetic properties of the two synthesised compounds (**6i** and **7**) is summarized in Table 3. Compound **7** had a lower molecular weight of 164.12 g mol⁻¹ possibly enhancing its absorption. Log⁻¹*P* values of the two compounds (**6i** and **7**) were less than 5. The *in silico* analysis of the compounds revealed that compound **7** conformed with all the listed parameters whereas compound **6i** violated four physico-chemical properties. It is worth mentioning here that compound **7** complied with all the parameters of Lipinski's rule for oral bioavailability (30–70%). Compound **6i**, on the other hand, violated three parameters according to Lipinski's rule, which might suggest poor oral bioavailability (<30%). Further, we studied the topological polar surface area (TPSA) of the active compounds **6i** and **7**. The TPSA value was less than 150 for **7**, but **6i** has a little higher value of TPSA. As can be seen in

Table 3 *In silico* prediction of the physico-chemical and pharmacokinetic properties of compounds **6i** and **7**

S. no.	Property	Criterion	<i>In silico</i> analysis	
			Compound 6i	Compound 7
1.	Molecular weight (g mol ⁻¹)	<500	575.21	164.12
2.	Hydrogen donor	<5	0	0
3.	Hydrogen acceptor	<10	13	1
4.	Log <i>P</i> (lipophilicity)	<5	4.17	4.32
5.	Rotational bonds	<10.0	15	3
6.	Topological polar surface area (TPSA)	<140 Å ²	163.6 Å ²	9.23 Å ²
7.	Log <i>S</i> (solubility)	—	-4.54	-3.58
8.	Oral bioavailability	—	<30%	30–70%
9.	Drug likeness score	—	-0.55	-0.81
	Lipinski violations		2	0

Table 3, compound 7 has TPSA values under the threshold of 140 Å, which might suggest good intestinal absorption and better CNS penetration, but not compound 6i. The synthesized compounds (6i and 7) meet the criteria of drug likeness with scores of -0.81 and -0.55 for 7 and 6i, respectively.

In order to determine the conidia formation in the presence of compound treatment, *A. fumigatus* was cultured at IC₅₀. Consequently, the reduction in absorbance at 530 nm was significant which corresponds to the decrease in conidia formation on treatment with compounds 6i and 7; whereas in the case of eugenol and Amp B, there was an increase in conidia production compared to the positive control (Fig. 4; $p < 0.005$). No effect on hyphae formation was observed in any of the samples except the Amp B treated sample. The key regulator of the conidiation pathway, which has been well studied in *Aspergillus nidulans* as well as in *A. fumigatus*, is the transcription factor *BrlA*. It was observed that the $\Delta brlA$ mutant was unable to form conidia, and it depicted increased hyphal growth³⁴ and exhibited widespread transcriptional dysregulation of genes linked to conidiation, growth, and virulence. Molecular analysis is further warranted to gain insight into the target exposure of compounds.

Further, we carried out studies directed at the formation of DHN-melanin, a cell wall-associated parameter in *A. fumigatus*, which imparts a greenish-grey colour to the conidia. The formation of DHN-melanin is a fungal protective mechanism against diverse environmental factors such as UV radiation, oxidising agents, and extremes of temperatures. Since the compound-treated *A. fumigatus* conidia were pigment-less (albino), the melanin was extracted from the compound-treated as well as untreated control *A. fumigatus* conidia. Similar results were reported in our previously published paper showing a significant decrease in DHN-melanin in *A. fumigatus* in the presence of isoeugenol.¹²

A significant reduction in the melanin content of 6i and 7 treated conidia with reference to eugenol and the positive control was observed. According to Kumar *et al.*,³⁵ the absorption spectra showed characteristic absorption peaks in the UV region ranging from 265–290 nm, but not in the visible

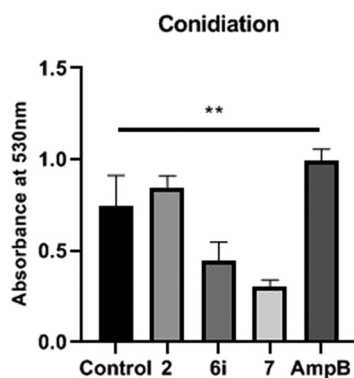


Fig. 4 Effect of isoeugenol and the compounds (6i and 7) on the production of *A. fumigatus* conidia. Control – untreated *A. fumigatus*; $p < 0.005$ statistically.

region. The overall characteristic absorption peak was observed at 275 nm (see ESI† Fig. S1). The optical densities at 275 nm were 1.126, 0.399, 0.295, and 0.176 in the positive control and compound 2, 6i, and 7 treated conidia, respectively. Targeting the melanin biosynthesis process in *A. fumigatus* could be a potential strategy for antimicrobial drug development. The white colour of *A. fumigatus* conidia appears due to mutations in the *pksP/alb1* gene, encoding a polyketide synthase required for conidial pigmentation. Pigment-less conidia were found to be less virulent than wild type strains of *A. fumigatus* in murine models of disseminated aspergillosis, possibly due to an increased susceptibility to phagocytosis and reactive oxygen species (ROS).³⁶ In addition, the defect in the melanin biosynthesis pathway could contribute to the marked loss of adherence properties of the conidia.

The cell wall of *A. fumigatus* conidia consists of a hydrophobin layer, a dense melanin layer, and a plasma membrane.³⁷ According to Amanianda *et al.*,³⁸ conidia are normally round, but oval shapes were observed in rodlet mutants, which is responsible for hydrophobicity. Consequently, the conidial cell surface morphology was analysed and compared at IC₅₀ via scanning electron microscopy (SEM). Compound-treated conidia revealed a smooth conidial surface with the absence of protrusions and a decrease in the number of conidia (Fig. 5a), whereas untreated conidia possess a dense number of conidia with an echinulate surface (Fig. 5b). Correspondingly, transmission electron

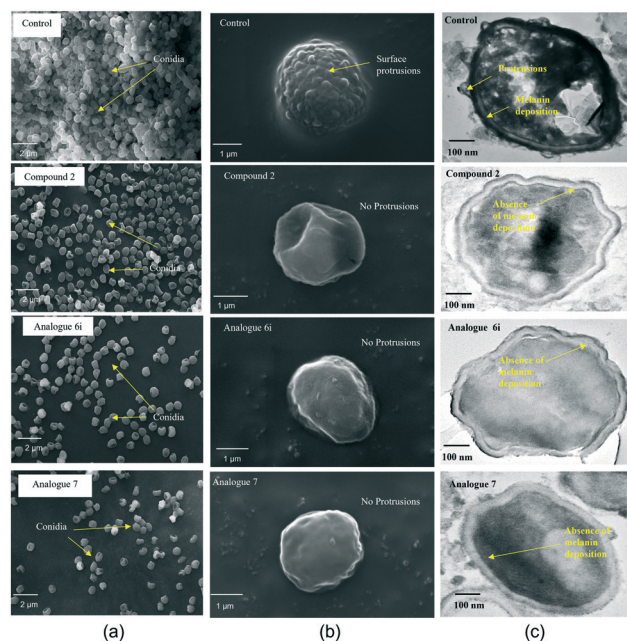


Fig. 5 SEM and TEM visualisations of the conidial surface of *A. fumigatus*: (a) reduction in the number of conidia in the compound-treated sample compared to the control; (b) compound-treated single conidium revealed loss of protrusions and a smooth surface compared to the echinulate conidial surface in the untreated control; (c) compound-treated single conidium showing loss of protrusions as well as the electron dense melanin layer of the conidial cell wall compared to control conidia showing protrusions and melanin deposition.

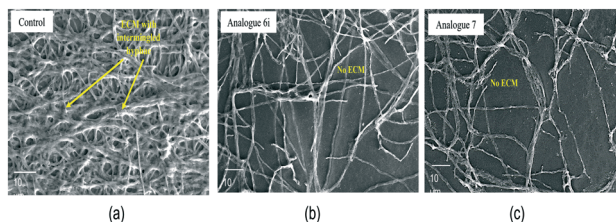


Fig. 6 SEM of the *A. fumigatus* biofilm surface. (a) *A. fumigatus* biofilm; the yellow arrow indicates ECM embedded in the hyphal network. (b) at IC₅₀ of compound **6i** *A. fumigatus* without ECM. (c) at IC₅₀ of compound **7** *A. fumigatus* without ECM. Magnification at 1000 \times ; scale – 10 μ m.

microscopy (TEM) analysis supported the presence of protrusions in untreated conidia as observed in SEM, whereas compound-treated conidial sections revealed a protrusionless outer surface with a visible clear inner surface indicating the absence of a melanin layer (Fig. 5c). Besides, there was accumulation of cytoplasmic content in wild type conidia, which was reduced in compound-treated conidia probably due to the alteration in the membrane, leading to leakage of cellular contents.

Fungal biofilms are very intricate structures, which provide a protective environment for a pathogen to thrive in hostile surroundings.³⁹ This complex structure helps in developing resistance to antimicrobial agents. The signature proof of biofilm formation of a pathogen is the extracellular matrix (ECM) that is produced by the biofilm within 24 h of its colonisation *in vitro* as well as *in vivo*, in the case of *A. fumigatus*. In the *A. fumigatus* biofilm, ECM is a key component for colonisation by gluing together mycelial threads and is composed of polysaccharides (glucans and galactomannan), some hydrophobic proteins, and melanin.⁴⁰ In contrast to other species, it lacks β -(1,3) glucan and chitin.

In the present study, the eradication of *A. fumigatus* biofilms was assessed under exposure to the synthesised compounds of eugenol. Compounds **6i** and **7** eradicated preformed fungal biofilms effectively at concentration ranges of 69.53–86.92 μ M and 243.60–304.5 μ M, respectively. At the same concentrations, the surface morphology of fungal biofilms showed the complete absence of ECM on the hyphae. Meanwhile, in the present study, the biofilm eradication concentration was higher than that of the planktonic culture and greater than the CC₅₀ of the compounds. Despite that, the compounds effectively worked to eliminate the formed ECM, which linked the hyphae to cause infection and were responsible for its stability as well. Under SEM analysis, the positive control of the *A. fumigatus* biofilm surface displayed a highly coordinated network of hyphal structures with dense ECM accumulation (Fig. 6a), whereas in compound-treated ones only hyphae were observed (Fig. 6b and c).

Conclusions

In summary, we have accomplished the design and synthesis of eugenol and isoeugenol derived glycoconjugates and

investigated their antifungal activity against *A. fumigatus*. A small library of diverse molecules have been synthesised with various sugar moieties attached to the eugenol and isoeugenol core *via* click chemistry. Other analogues were also synthesized by functionalization of the olefinic group present in eugenol. It is pertinent to mention here that the glycoconjugates of eugenol were found to exhibit significant antifungal activities amongst all the synthesised compounds. It is presumed that these studies regarding the antifungal activity of eugenol and isoeugenol and related compounds could lead the way for designing future drug-like candidates.

Author contributions

L. Goswami and SP performed the synthesis of compounds and the click chemistry part; L. Gupta performed all experiments on antifungal activities of the synthesised compounds; MV critically reviewed the manuscript and corrected it; AKB and PV conceptualised the idea and critically analysed all the experiments as well as corrected the manuscript. All the authors searched the literature, recreated the figures, and drafted the manuscript.

Conflicts of interest

There are no conflicts to declare.

Acknowledgements

The authors would like to thank the Department of Science and Technology-Science and Engineering Research Board (DST-SERB) (EMR/2016/005752) New Delhi, Govt. of India for the financial support. LG and SP are grateful to UGC, New Delhi, India and CSIR, New Delhi, India for financial support in the form of UGC-SRF and CSIR-SRF, respectively. PV would like to thank Amity University Uttar Pradesh for providing the infrastructure and facilities for extensive research work.

Notes and references

- C. Kosmidis and D. W. Denning, *Thorax*, 2015, **70**, 270–277.
- C.-C. Lai and W.-L. Yu, *J. Microbiol., Immunol. Infect.*, 2021, **54**, 46–53.
- A. M. Borman, M. D. Palmer, M. Fraser, Z. Patterson, C. Mann, D. Oliver, C. J. Linton, M. Gough, P. Brown, A. Dziejczyk, M. Hedley, S. McLachlan, J. King and E. M. Johnson, *J. Clin. Microbiol.*, 2020, **59**, e02136-20.
- M. Richardson, P. Bowyer and R. Sabino, *Med. Mycol.*, 2019, **57**(Supplement_2), S145–S154.
- C. A. Croft, L. Culibrk, M. M. Moore and S. J. Tebbutt, *Front. Microbiol.*, 2016, **7**, 472.
- L. Scorzoni, A. C. A. de Paula, E. Silva, C. M. Marcos, P. A. Assato, W. C. M. A. de Melo, H. C. de Oliveira, C. B. Costa-Orlandi, M. J. S. Mendes-Giannini and A. M. Fusco-Almeida, *Front. Microbiol.*, 2017, **8**, 36.
- T. Koeduka, E. Fridman, D. R. Gang, D. G. Vassão, B. L. Jackson, C. M. Kish, I. Orlova, S. M. Spassova, N. G. Lewis,

- J. P. Noel, T. J. Baiga, N. Dudareva and E. Pichersky, *Proc. Natl. Acad. Sci. U. S. A.*, 2006, **103**, 10128–10133.
- 8 G. Chung, S. T. Im, Y. H. Kim, S. J. Jung, M.-R. Rhyu and S. B. Oh, *Neuroscience*, 2014, **261**, 153–160.
- 9 E. Pinto, L. Vale-Silva, C. Cavaleiro and L. Salgueiro, *J. Med. Microbiol.*, 2009, **58**, 1454–1462.
- 10 A. Marchese, R. Barbieri, E. Coppo, I. E. Orhan, M. Daglia, S. F. Nabavi, M. Izadi, M. Abdollahi, S. M. Nabavi and M. Ajami, *Microbiology*, 2017, **43**, 668–689.
- 11 S. Hoda, M. Vermani, R. K. Joshi, J. Shankar and P. Vijayaraghavan, *BMC Complementary Med. Ther.*, 2020, **20**, 67, DOI: [10.1186/s12906-020-2859-z](https://doi.org/10.1186/s12906-020-2859-z).
- 12 L. Gupta, P. Sen, A. K. Bhattacharya and P. Vijayaraghavan, *Arch. Microbiol.*, 2022, **204**, 214, DOI: [10.1007/s00203-022-02817-w](https://doi.org/10.1007/s00203-022-02817-w).
- 13 S. K. Shrestha, A. Garzan and S. G. Tsodikova, *Eur. J. Med. Chem.*, 2017, **133**, 309–318.
- 14 H. X. Ngo, S. K. Shrestha and S. G. Tsodikova, *ChemMedChem*, 2016, **11**, 1507–1516.
- 15 T. K. Kotamagari, S. Paul, G. K. Barik, M. K. Santra and A. K. Bhattacharya, *Org. Biomol. Chem.*, 2020, **18**, 2252–2263, and references cited therein.
- 16 in *Essentials of Glycobiology*, ed. A. Varki, R. D. Cummings, J. D. Esko, H. H. Freeze, P. Stanley, C. R. Bertozzi, G. W. Hart and M. E. Etzler, Cold Spring Harbor Laboratory Press, 2nd edn, 2009.
- 17 W. Szeja, G. Gryniewicz and A. Rusin, *Curr. Org. Chem.*, 2017, **21**, 218–235.
- 18 D. Gupta and D. K. Jain, *J. Adv. Pharm. Technol. Res.*, 2015, **6**, 141–146.
- 19 B. S. Holla, M. Mahalinga, M. S. Karthikeyan, B. Poojary, P. M. Akberali and N. S. Kumari, *Eur. J. Med. Chem.*, 2005, **40**, 1173–1178.
- 20 L. Goswami, S. Paul, T. K. Kotamagari and A. K. Bhattacharya, *New J. Chem.*, 2019, **43**, 4017–4021.
- 21 B. H. M. Kuijpers, S. Groothuys, A. R. Keereweer, P. J. L. M. Quaedflieg, R. H. Blaauw, F. L. van Delft and F. P. J. T. Rutjes, *Org. Lett.*, 2004, **6**, 3123–3126.
- 22 R. Huisgen, *Angew. Chem., Int. Ed. Engl.*, 1963, **2**, 565–632.
- 23 R. Huisgen, *Angew. Chem., Int. Ed. Engl.*, 1963, **2**, 633–696.
- 24 V. V. Rostovtsev, L. G. Green, V. V. Fokin and K. B. Sharpless, *Angew. Chem., Int. Ed.*, 2002, **41**, 2596–2599.
- 25 J. Bomon, M. Bal, T. K. Achar, S. Sergeev, X. Wu, B. Wambacq, F. Lemièrre, B. F. Sels and B. U. W. Maes, *Green Chem.*, 2021, **23**, 1995–2009.
- 26 M. Bednarski and S. Danishefsky, *J. Am. Chem. Soc.*, 1986, **108**, 7060–7067.
- 27 E. K. Aratikatla, T. R. Valkute, S. K. Puri, K. Srivastava and A. K. Bhattacharya, *Eur. J. Med. Chem.*, 2017, **138**, 1089–1105.
- 28 A. Paquin, C. R. Moreno and G. Bérubé, *Molecules*, 2021, **26**, 2340.
- 29 A. Çapcı, L. Herrmann, H. M. Sampath Kumar, T. Fröhlich and S. B. Tsogoeva, *Med. Res. Rev.*, 2021, **41**, 2927–2970.
- 30 Clinical and Laboratory Standards Institute [CLSI], *Reference Method for Broth Dilution Antifungal Susceptibility Testing of Filamentous Fungi*, Clinical and Laboratory Standard Institute, Wayne, PA, 2nd edn, 2008.
- 31 M. Kasper, C. Roehlecke, M. Witt, H. Fehrenbach, A. Hofer, T. Miyata, C. Weigert, R. H. W. Funk and E. D. Schleicher, *Am. J. Respir. Cell Mol. Biol.*, 2000, **23**, 485–491.
- 32 S. Harmsen, A. C. McLaren, C. Pauken and R. McLemore, *Clin. Orthop. Relat. Res.*, 2011, **469**, 3016–3021.
- 33 L. I. S. de Carvalho, D. J. Alvarenga, L. C. F. do Carmo, L. G. de Oliveira, N. C. Silva, A. L. T. Dias, L. F. L. Coelho, T. B. de Souza, D. F. Dias and D. T. Carvalho, *J. Chem.*, 2017, e5207439.
- 34 J. I. P. Stewart, V. M. Fava, J. D. Kerkaert, A. S. Subramanian, F. N. Gravelat, M. Lehoux, P. L. Howell, R. A. Cramer and D. C. Sheppard, *MBio*, 2020, **11**, e03202–e03219.
- 35 C. G. Kumar, P. Mongolla, S. Pombala, A. Kamle and J. Joseph, *Lett. Appl. Microbiol.*, 2011, **53**, 350–358.
- 36 V. Sugareva, A. Härtl, M. Brock, K. Hübner, M. Rohde, T. Heinekamp and A. A. Brakhage, *Arch. Microbiol.*, 2006, **186**, 345–355.
- 37 J. P. Latgé, A. Beauvais and G. Chamilos, *Annu. Rev. Microbiol.*, 2017, **71**, 99–116.
- 38 V. Aïmanianda, J. Bayry, S. Bozza, O. Kniemeyer, K. Perruccio, S. R. Elluru, C. Clavaud, S. Paris, A. A. Brakhage, S. V. Kaveri, L. Romani and J.-P. Latgé, *Nature*, 2009, **460**, 1117–1121.
- 39 E. Melloul, S. Luiggi, L. Anaïs, P. Arné, J.-M. Costa, V. Fihman, B. Briard, E. Dannaoui, J. Guillot, J.-W. Decousser, A. Beauvais and F. Botterel, *PLoS One*, 2016, **11**, e0166325.
- 40 N. A. R. Gow, J.-P. Latge and C. A. Munro, *Microbiol. Spectrum*, 2017, **5**, DOI: [10.1128/microbiolspec.FUNK-0035-2016](https://doi.org/10.1128/microbiolspec.FUNK-0035-2016).

Design and Synthesis of 1,3-Diynes as Potent Antifungal Agents against *Aspergillus fumigatus*

Lakshmi Goswami[†],^[a, b] Lovely Gupta[†],^[c] Sayantan Paul,^[a, b] Pooja Vijayaraghavan,^{*[c]} and Asish K. Bhattacharya^{*[a, b]}

Eugenol and isoeugenol, secondary metabolites isolated from the plant *Myristica fragrans* have displayed antifungal activities against *Aspergillus fumigatus* (IC₅₀ 1900 μM). Compounds having conjugated unsaturation have been of great use as antifungals *i.e.* amphotericin B, nystatin and terbinafine etc. Hence, in the present study, we have designed and synthesised 1,3-diynes by utilizing Glaser-Hay and Cadiot-Chodkiewicz coupling reactions to furnish possible antifungal agents. Synthesis of 1,6-diphenoxyhexa-2,4-diyne derivatives was achieved by Cu(I) catalysed coupling of propargylated eugenol, isoeugenol, guaiacol, vanillin and dihydrogenated eugenol or eugenol in good to excellent yields. All the synthesized compounds were evaluated against pathogenic fungus *A. fumigatus*. Among all the

synthesized compounds, one of the compounds was found to be exhibiting promising antifungal activity with IC₅₀ value of 7.75 μM thereby suggesting that this type of scaffold could pave the way for developing new antifungal agents. The most active compound was found to be low cytotoxic when assayed against L-132 cancer cell line. Effect of the most active compound on ergosterol biosynthesis has also been studied. Also, the most active compound exhibited significant anti-biofilm activity although the concentration was found to be higher than its anti-fungal activity. Morphological changes in the biofilm were remarkable under confocal laser scanning microscopy.

Introduction

Aspergillus fumigatus is an airborne opportunistic fungus which is adapted to survive in a wide range of climatic conditions and poses a serious health threat to humans.^[1] Breathing spores of *Aspergillus* is common in day-to-day life for us, but it could be life-threatening for individuals with incapacitated immunology or pulmonary diseases like tuberculosis, lung cancer, asthma, pneumonia, and other respiratory complications. Its favourable conidial size makes it efficient to invade deep inside the respiratory system reaching to the alveoli resulting in lethal infection in patients with underlying lung diseases and susceptible immune system.^[2] The efficient and unique adhesion of conidia to host cell also assist in its binding, nutrition uptake and proliferation on the surface of host cell.^[3] Its conidia possess surface proteins which masks its recognition by host immune response.^[4]

Over the time, this pathogen has developed resistance against cellular self-defence mechanism of humans and specially to known antifungal drugs. Nowadays readily available antifungals in market are amphotericin B (Amp B), nystatin, miconazole, ketoconazole, fluconazole, voriconazole, terbinafine, itraconazole, etc. (Figure 1). These drugs have been widely categorized into four major classes *i.e.* polyenes, azoles, allylamines, echinocandins depending on their mode of action and chemical framework.^[5] Polyenes and allylamines work either making fungal cell wall more porous or inhibit the enzyme secretion by the fungal cell wall needed for normal functioning. Extensive use of these drugs renders *A. fumigatus* immune to certain classes of antifungals. Hence, it is of utmost importance to develop new potent antifungal drugs with better efficacy, least toxicity and enhanced bioavailability.^[6] We opined 1,3-diyne scaffolds could affect the functioning of the cell wall of *A. fumigatus*. Symmetrical or unsymmetrical 1,3-diynes could be synthesized by utilizing Cu(I)-catalysed Glaser-Hay or Cadiot-Chodkiewicz coupling reactions, respectively.

[a] L. Goswami,[†] Dr. S. Paul, Prof. A. K. Bhattacharya
Division of Organic Chemistry
CSIR-National Chemical Laboratory (CSIR-NCL)
Dr. Homi Bhabha Road
Pune 411 008 (India)
E-mail: ak.bhattacharya@ncl.res.in

[b] L. Goswami,[†] Dr. S. Paul, Prof. A. K. Bhattacharya
Academy of Scientific and Innovative Research (AcSIR)
Ghaziabad 201 002 (India)

[c] L. Gupta,[†] Prof. P. Vijayaraghavan
Amity Institute of Biotechnology
Amity University Uttar Pradesh
Sector-125, Noida (India)
E-mail: vrpooja@amity.edu

[[†]] These authors contributed equally to this work.

Supporting information for this article is available on the WWW under <https://doi.org/10.1002/cmdc.202300013>

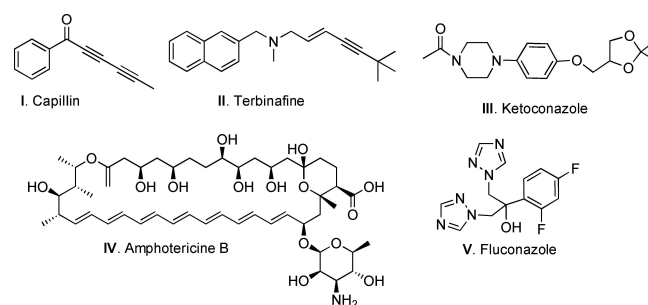


Figure 1. Examples of some of the well-known antifungal agents.

Eugenol **1a** and isoeugenol **1b** are the naturally occurring phenylpropanoids and has been traditionally isolated from the plants *Syzygium aromaticum* and *Eugenia caryophyllata*, *Myristica fragrans* (Figure 2).^[7] Eugenol and isoeugenol have shown antifungal activities against *A. fumigatus* with IC₅₀ value of 1900 μM.^[7b] Both compounds exhibited antifungal activity against filamentous as well as non-filamentous fungi.^[7c] The antifungal activity of these compounds may cause severe damage to the fungal membrane and cell walls, leading to morphological deformations and collapse and deterioration of conidia and/or hyphae.^[7d] The antifungal activity can be attributed due to the presence of an aromatic nucleus and a phenolic OH group which is known to be reactive and to form hydrogen bonds with active sites of target enzymes. Hence, we utilized propargylated derivatives of eugenol, isoeugenol and other phenolics for the synthesis of 1,3-diyne.

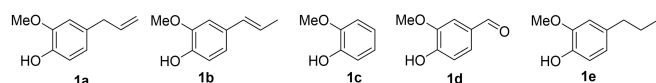
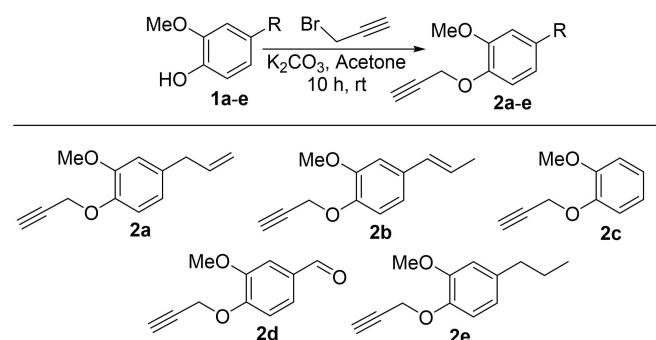
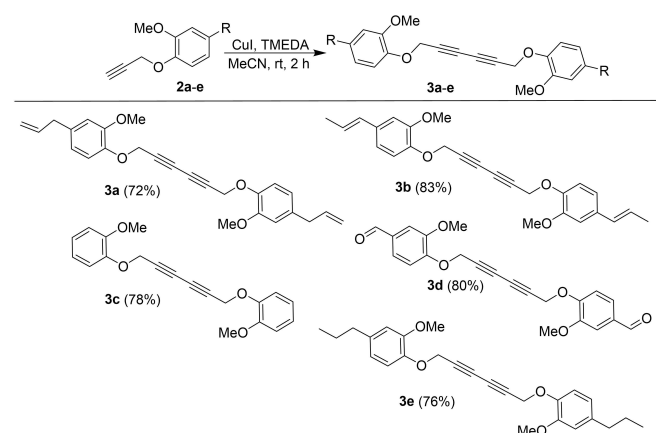


Figure 2. Eugenol (**1a**), isoeugenol (**1b**) and other phenolics (**1c-e**) utilized for the synthesis of 1,3-diyne.



Scheme 1. Synthesis of propargylated phenols **2a-e**.



Scheme 2. Synthesis of homo coupled products **3a-e**.

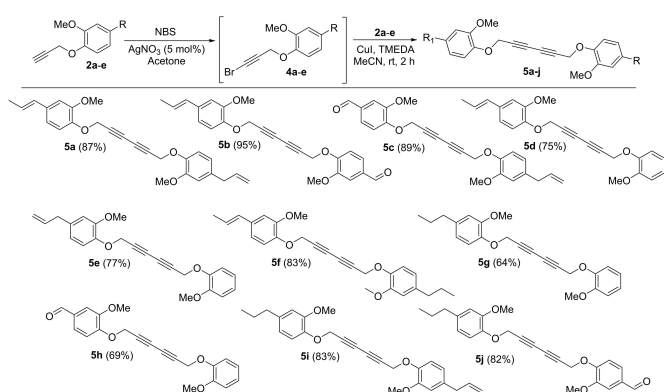
Results and Discussion

In order to synthesize homo or symmetric diynes, we opined to employ Glaser-Hay coupling reaction conditions.^[8] To begin with; we treated eugenol **1a**, isoeugenol **1b**, guaiacol **1c**, vanillin **1d** and dihydrogenated eugenol or eugenol **1e** with propargyl bromide in presence of base, potassium carbonate (K₂CO₃) in acetone as solvent to furnish propargylated compounds **2a-e** (Scheme 1).

These propargylated compounds **2a-e** were treated in presence with catalytic amount of copper iodide (CuI) and tetramethylethylenediamine (TMEDA) in acetonitrile to furnish homo coupled products **3a-e** via Glaser-Hay coupling in good to excellent yield (Scheme 2). The homo coupled 1,3-diyne were characterized from their corresponding NMR spectra. In ¹H NMR spectrum of **3a**, the absence of acetylenic proton of **2a** (δ_H 2.48 ppm)^[7b] indicates the coupling of two units of propargylated eugenol **2a**. All the synthesized products were identified by their ¹H, ¹³C NMR spectra and HRMS.

However, to avoid the formation of homo or symmetric dienyne during the synthesis of hetero or unsymmetric dienyne, we opined to employ Cadiot-Chodkiewicz coupling reaction.^[9] At first the propargylated compounds **2a-e** were brominated using *N*-bromosuccinamide (NBS) in presence of 5 mol% of silver nitrate (AgNO₃) in acetone at room temperature to furnish compound **4a-e** which were used as such without further purification in the next step. These brominated compounds **4a-e** were treated with propargylated eugenol, isoeugenol, guaiacol, vanillin and eugenol (**2a-e**) individually in presence of catalytic amount of CuI, TMEDA as base in acetonitrile as solvent to obtain hetero or unsymmetric diynes **5a-j** in good to excellent yields (Scheme 3). All the hetero coupled products were identified by their ¹H, ¹³C NMR spectra and HRMS.

All the synthesized intermediates (**2a-e**) and 1,3-diyne (**3a-e** and **5a-j**) were subjected to antifungal activities against *A. fumigatus*. The antifungal potency of the synthesized compounds (**2a-e**, **3a-e** and **5a-j**) was calculated using the micro-broth dilution assay as per the Clinical and Laboratory Standards Institute (CLSI) protocol.^[10] The IC₅₀ value of all the synthesised compounds and drug control amphotericin B (Amp



Scheme 3. Synthesis of hetero coupled products **5a-j**.

B) are summarised in the Table 1. Among all the synthesized compounds assayed, only compound **3a** showed lowest IC₅₀ value, *i. e.* 7.75 μM, respectively whereas calculated IC₅₀ value of all other compounds were found to be at twice the values of compound **3a** against *A. fumigatus*.

Structure-activity-relationship analysis

It is evident from antifungal activity of all the synthesized compounds summarized in Table 1, in general diynes (**3a-e** and **5a-j**) have shown greater activity than their corresponding monomers (**2a-e**). Homo-coupled diyne **3a** exhibited several times greater activity as (IC₅₀ 7.75 μM) as compared to the parent compound, eugenol **1a** (IC₅₀ 1900 μM).^[7b] The antifungal activity data of homo- and hetero-coupled diynes (**3a-e** and **5a-j**) suggests that conjugation has profound effect against *A. fumigatus* as evident from Table 1 barring two compounds (**3b** and **3c**). Other synthesized diynes also proved to be moderately active against *A. fumigatus*. In general, the activity ranges from 7.75 μM to 17.85 μM except compounds **3b** and **3c** with phenol containing an olefinic side chain furnished better activities than the rest.

Cell cytotoxicity of compound **3a** was analysed against normal lung epithelial cell line L-132 along with FDA-approved antifungal drug Amp B as a drug control. The CC₅₀ (cytotoxic concentration-50) value for compound **3a** was calculated as 62.16 μM indicating that the fraction is low cytotoxic. The concentration range selected for cytotoxicity comprised antifungal activity against *A. fumigatus*. The CC₅₀ of **3a** on L-132 cell line was determined four times higher than the MIC value of it against *A. fumigatus*. The sub-lethal cytotoxicity of Amp B reported was in the range of 5.4-10.82 μM.^[11]

The selectivity index (SI) was calculated to evaluate the toxicity of the compounds studied against normal cells and to predict their therapeutic potential.^[12] The SI for compound **3a** was determined as 8.01, which indicates that it could be a potential antifungal agent. According to literature,^[13] reported SI of eugenol (**1a**) was 0.2 against non-filamentous fungi. It should be emphasised that compound **3a** has greater selectivity than that of unmodified eugenol **1a**.

Table 1. IC₅₀ values of compounds **2a-e**, **3a-e**, and **5a-j** against *A. fumigatus*.

Compd	IC ₅₀ [μM]	Compd	IC ₅₀ [μM]
1a	1900	3d	16.52
1b	1900	3e	15.38
1c	≥25	5a	15.54
1d	≥25	5b	16.01
1e	9.39	5c	16.01
2a	≥25	5d	17.25
2b	≥25	5e	17.25
2c	≥25	5f	15.46
2d	≥25	5g	17.16
2e	≥25	5h	17.85
3a	7.75	5i	15.46
3b	31.08	5j	15.93
3c	38.81	Amp B	1.08

In-silico ADMET prediction studies are a central component of pharmaceutical research and drug discovery, as it provides helpful guidance in the early evaluation of the *in-vivo* efficiency and safety of a drug.^[14] The magnitude of the biological activity of an active molecule, in terms of specific interactions with the molecular target, along with the drug-related side effects, are strongly influenced by its pharmacokinetics properties.^[15] The active compound **3a** was screened through Lipinski's rule of five for oral bioavailability by predicting its physico-chemical and pharmacokinetic properties *via in-silico* approach. In result, compound **3a** was found to follow Lipinski's rule of five with no violation; molecular weight is 402.18 g/mol, 4 hydrogen bond acceptors, no hydrogen bond donor, LogP value 4.17 which is less than 5, Topological Polar Surface Area (TPSA) is 36.92 Å².

The oral bioavailability radar of compound **3a** was generated *via* Swiss ADME predictor (Figure 3) demonstrating six physiochemical properties, flexibility, lipophilicity, saturation, size, polarity and solubility and compound **3a** follows drug-like properties.

Conidiation is an effective proliferation approach that helps the fungus to escape from unfavourable conditions. To determine the conidiation process in the presence of compound **3a**, fungal strain was cultured at IC₅₀ of it. Consequently, the reduction in absorbance at 530 nm was significant which corresponds to the decrease in conidia formation on treatment with compounds **3a**. Simultaneously, there was an increase in conidia production when *A. fumigatus* treated with eugenol **1a** and Amp B in comparison to control (Figure 4A; p < 0.05).

Ergosterol is major fungal sterol, which is present in the cell membrane and therefore involved in cell membrane integrity, fluidity and fungal survival and development.^[17] The key enzymes involved in ergosterol biosynthesis have been potential targets for antifungal drugs. Amp B target site is ergosterol in fungal cell membrane,^[18] hence ergosterol content was analysed on treating with the compound **3a** and eugenol **1a** in comparison with control and Amp B (drug control). Ergosterol content quantification indicated that there is no such difference in the percentage of ergosterol at IC₅₀ of eugenol **1a** and compound **3a** in comparison to control, whereas Amp B showed marked decrease in ergosterol content (Figure 4B). But

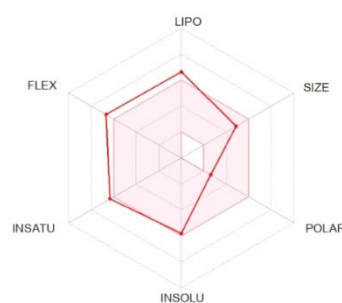


Figure 3. The oral bioavailability radar of compound **3a** using Swiss ADME predictor. The six physiochemical properties taken into account to consider a molecule as drug-like are flexibility (FLEX), lipophilicity (LIPO), saturation (INSATU), size (SIZE), polarity (POLAR) and solubility (INSOLU).

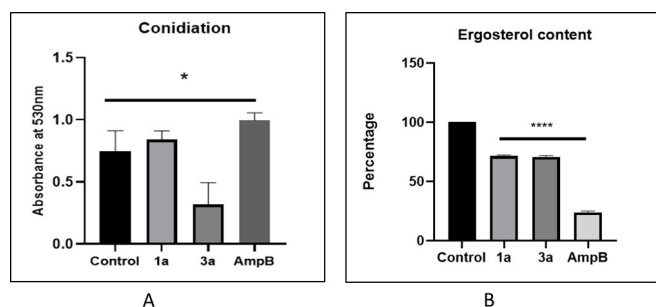


Figure 4. Effect of eugenol **1a**, compound **3a** on the (A) production of *A. fumigatus* conidia and (B) ergosterol content in comparison to control, where control-untreated *A. fumigatus*; $p < 0.05$.

still reduction in the ergosterol level was observed in presence of compound **3a**.

The conidial surface of *A. fumigatus* consists of hydrophobin layer, dense melanin layer, polysaccharides and proteins then plasma membrane.^[19] According to Aïmanianda *et al.*^[4] conidia are generally round, but oval shapes were observed in rodlet mutants which is responsible for hydrophobicity. The effect of compound **3a** on conidial cell surface morphology was visualised *via* SEM. Results revealed that cell surface morphology of compound **3a** treated conidia was completely different to that of resting conidia. Compound **3a** treated conidia appeared smooth with absence of protrusions (Figure 5B) whereas untreated conidia possess echinulate surface (Figure 5A), suggesting that compound **3a** significantly interacted with the conidial surface proteins and altered its surface characteristics.

Fungal biofilms are complex, highly coordinated network of hyphal structures, coated with extracellular matrix (ECM). For treatment of *A. fumigatus* biofilms, higher dosage of antifungal and in combinations were given as therapy for better penetration into the fungal cells.^[20]

The 24 h grown biofilms were more rigid, complex structure, where high level of antifungal drug resistance was observed. Under such conditions, compound **3a** showed significant anti-biofilm activity at IC_{50} of 62.16 μ M, which was found to be higher than its anti-fungal activity. Notable morphological changes in the biofilm were observed under confocal laser scanning microscopy (CLSM). Component of biofilm was stained

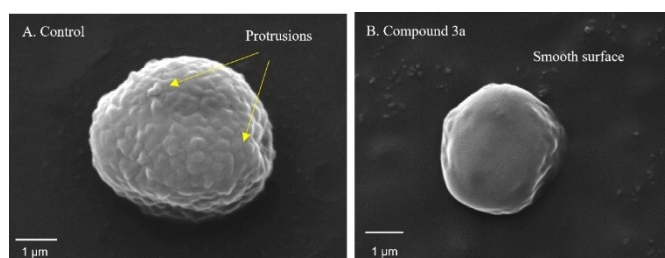


Figure 5. Scanning electron microscope images of resting conidia of *A. fumigatus* (A) control (B) compound **3a** treated. Scale bar- 1 μ m.

with fluorochrome dye (calcofluor white), in result there was disintegrated hyphae observed in presence of compound **3a** (Figure 6D–F). Figure 6A indicated compact hyphal growth of *A. fumigatus* biofilm, which was grown on glass coverslip for 48 h, whereas compound **3a** effectively eradicated the biofilm within 24 h of its treatment. It has been reported^[21] that isoeugenol also exhibits similar results when visualised under CLSM but at high concentration which is 156 μ g/mL.

Conclusion

Herein, we report design and synthesis of dienynes based potent antifungal agent employing Glaser as well as Cadiot-Chodkiewicz coupling reactions. Glaser reactions was utilised for synthesizing homo coupled product while Cadiot-Chodkiewicz coupling furnished hetero coupled product. The eugenol dimeric 1,3-diyne product **3a** have shown the best activity among all the synthesized compound. Apart for carrying out the antifungal activities of synthesized compounds, we performed the cytotoxicity, conidia formation, ergosterol biosynthesis and fungal biofilm formation studies of compound **3a**. It was observed that compound **3a** considerably reduce the conidia formation. It effectively interacted with the conidial surface proteins and altered the surface characteristics, also significantly eradicated the biofilm upon treatment. Moreover, compound **3a** was found to be decreasing the ergosterol level when acted upon.

Experimental Section

General information

All melting points were recorded on a Büchi melting point apparatus in open capillaries and are uncorrected. Flash chromatography was performed with CombiFlash Rf 200i equipped with UV/VIS and ELSD (Isco Teledyne Inc., USA) using RediSep[®] pre-packed column (SiO_2). 1H NMR spectra were recorded on a Bruker

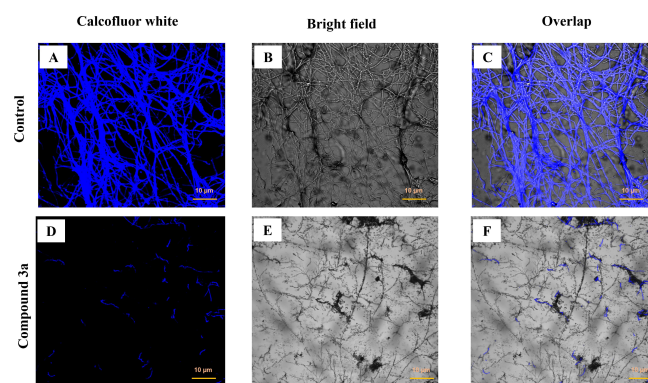


Figure 6. *Aspergillus fumigatus* biofilm eradication. Confocal laser scanning microscopy (CLSM) images of 48 h *A. fumigatus* biofilm on glass coverslips (A–C) control were stained with Calcofluor white dye depicting intense hyphal growth with ECM; (D–F) compound **3a** treated biofilm possess disintegrated hyphae at 40 \times magnification. Scale Bar- 10 μ m

200, 400 or 500 MHz spectrometer and ^{13}C NMR spectra were recorded at 50, 100 or 125 MHz, respectively. Chemical shifts are reported as δ values (ppm) relative to residual solvent peak of CDCl_3 . HRMS (ESI) were recorded on an Orbitrap (quadrupole plus ion trap) and TOF mass analyzer. Petroleum ether and ethyl acetate were distilled by usual methods. All the starting materials and dried solvent were purchased and used without further drying.

General procedure for the propargylation of phenols

Appropriate phenol (1 equiv.) was dissolved in acetone (20 mL) at 25°C under inert atmosphere. After that, potassium carbonate K_2CO_3 (1.5 equiv.) and propargyl bromide (2.5 equiv.) were added to the above-mentioned solution at 25°C . After completion of the reaction (TLC), the reaction mixture was evaporated *in vacuo* to obtain residue which was purified by flash chromatography using a RediSep column (SiO_2 , 12 g) with EtOAc-petroleum ether mixture as eluent to furnish compound **2a-e**. Spectral data of all the synthesized propargylated phenol were found to be consistent with the previous literature reports.^[7b,22]

General procedure for the Glaser coupling of propargylated phenols

Compounds **2a-e** (1 equiv.) were dissolved in acetonitrile (5 mL) and treated with catalytic amount (5 mol%) of copper iodide (CuI) and *N,N,N,N*-tetramethylethylenediamine (TMEDA) (1.2 equiv.). After completion of the reaction (TLC), the reaction mixture was evaporated to dryness to furnish a crude which was further purified *via* flash chromatography using a RediSep column (SiO_2 , 12 g) with EtOAc-petroleum ether mixture as eluents to yield purified compounds **3a-e**.

1,6-Bis(4-allyl-2-methoxyphenoxy)hexa-2,4-diyne (3a)

Brown liquid (722 mg, 72%); ^1H NMR (200 MHz, CDCl_3) δ_{H} 6.96–6.84 (m, 2H), 6.79–6.66 (m, 4H), 6.07–5.85 (m, 2H), 5.17–5.07 (m, 2H), 5.04 (s, 2H), 4.83–4.71 (m, 4H), 3.85 (s, 6H), 3.34 (d, $J=6.6$ Hz, 4H); ^{13}C NMR (50 MHz, CDCl_3) δ_{C} 149.7, 145.0, 137.5, 134.6, 134.0, 120.4, 115.9, 114.9, 112.4, 75.7, 74.8, 71.3, 57.5, 56.9, 55.8, 39.9, 29.7; HRMS: m/z for $\text{C}_{26}\text{H}_{27}\text{O}_4$ ($\text{M}+\text{H}$) $^+$: calcd 403.1904, found 403.1899, m/z for $\text{C}_{26}\text{H}_{26}\text{O}_4\text{Na}$ ($\text{M}+\text{Na}$) $^+$: calcd 425.1723, found 425.1719.

1,6-Bis(2-methoxy-4-((*E*)-prop-1-en-1-yl)phenoxy)hexa-2,4-diyne (3b)

Yellowish solid (830 mg, 83%); m.p.: $110\text{--}112^\circ\text{C}$; R_f 0.3 (10% EtOAc in petroleum ether); ^1H NMR (400 MHz, CDCl_3): δ_{H} 6.92–6.86 (m, 4H), 6.86–6.81 (m, 2H), 6.31 (d, $J=1.5$ Hz, 1H), 6.35 (d, $J=1.6$ Hz, 1H), 6.18–6.06 (m, 2H), 4.82–4.73 (m, 4H), 3.86 (s, 6H), 1.86 (dd, $J=1.6$, 6.6 Hz, 6H); ^{13}C NMR (101 MHz, CDCl_3): δ_{C} 164.8, 161.9, 148.4, 147.1, 133.4, 130.2, 128.5, 127.2, 126.8, 124.0, 116.4, 114.5, 113.8, 77.1, 55.5; HRMS: m/z for $\text{C}_{26}\text{H}_{27}\text{O}_4$ ($\text{M}+\text{H}$) $^+$: calcd 403.1904, found 403.1902.

1,6-Bis(2-methoxyphenoxy)hexa-2,4-diyne (3c)

Brown solid (780 mg, 78%); m.p.: $64\text{--}66^\circ\text{C}$; R_f 0.65 (40% EtOAc in petroleum ether); ^1H NMR (400 MHz, CDCl_3): δ_{H} 7.04–6.95 (m, 4H), 6.95–6.86 (m, 4H), 4.81 (s, 4H), 3.86 (s, 6H); ^{13}C NMR (101 MHz, CDCl_3): δ_{C} 149.7, 146.6, 122.6, 120.8, 114.7, 111.8, 77.1, 74.7, 71.3, 57.3, 55.8; HRMS: m/z for $\text{C}_{20}\text{H}_{19}\text{O}_4$ ($\text{M}+\text{H}$) $^+$: calcd 323.1278, found 323.1277.

4,4'-(Hexa-2,4-diyne-1,6-diylbis(oxy))bis(3-methoxybenzaldehyde) (3d)

Off-white solid (800 mg, 80%); m.p.: $158\text{--}160^\circ\text{C}$; R_f 0.31 (40% EtOAc in petroleum ether); ^1H NMR (400 MHz, CDCl_3): δ_{H} 9.88 (s, 2H), 7.50–7.39 (m, 4H), 7.07 (d, $J=8.0$ Hz, 2H), 4.91 (s, 4H), 3.94 (s, 6H); ^{13}C NMR (101 MHz, CDCl_3): δ_{C} 190.9, 151.9, 150.0, 131.2, 126.2, 112.7, 109.6, 77.3, 77.0, 76.7, 74.0, 71.8, 57.0, 56.1; HRMS: m/z for $\text{C}_{22}\text{H}_{19}\text{O}_6$ ($\text{M}+\text{H}$) $^+$: calcd 379.1176, found 379.1170.

1,6-Bis(2-methoxy-4-propylphenoxy)hexa-2,4-diyne (3e)

Brown solid (760 mg, 76%); m.p.: $60\text{--}62^\circ\text{C}$; R_f 0.2 (10% EtOAc in petroleum ether); ^1H NMR (400 MHz, CDCl_3): δ_{H} 6.89 (d, $J=8.0$ Hz, 2H), 6.77–6.67 (m, 4H), 4.77 (s, 4H), 3.85 (s, 6H), 2.59–2.49 (m, 4H), 1.66–1.60 (m, 4H), 0.94 (t, $J=7.3$ Hz, 6H); ^{13}C NMR (101 MHz, CDCl_3): δ_{C} 149.5, 144.6, 137.3, 120.3, 114.9, 112.3, 74.9, 71.3, 57.6, 55.8, 37.7, 24.7, 13.8; HRMS: m/z for $\text{C}_{26}\text{H}_{31}\text{O}_4$ ($\text{M}+\text{H}$) $^+$: calcd 407.2217, found 407.2216.

General procedure for the bromination of propargylated phenols

Terminal alkynes **2a-e** (1 equiv.) were dissolved in acetone (10–15 mL) and to this silver nitrate (5 mol%) and *N*-bromosuccinimide (1.2 equiv.) were added subsequently and stirred at room temperature for 3 h. After completion of the reaction, reaction mixture was diluted with dichloromethane (20 mL) and filtered through celite; the filtrate was concentrated to furnish compounds **4a-e** which were used without further purification in the next step.

General procedure for the Cadiot-Chodkiewicz coupling of propargylated phenols 2a-e with brominated derivatives 4a-e

Terminal alkynes **2a-e** (1 equiv.) and brominated propargyl **4a-e** (1.1 equiv.) in acetonitrile (10 mL) and afterwards TMEDA (1.5 equiv.) and copper iodide (5 mol%) were added in an inert atmosphere. The reaction mixture was stirred at room temperature for 3 h. After completion of the reaction (TLC), reaction mixture was evaporated *in vacuo* and further purified *via* flash chromatography using a RediSep column (SiO_2 , 12 g) with EtOAc-petroleum ether mixture as eluent to yield purified compounds **5a-j**.

(*E*)-4-allyl-2-methoxy-1-((6-(2-methoxy-4-(prop-1-en-1-yl)phenoxy)hexa-2,4-diyne-1-yl)oxy)benzene (5a)

Brown solid (250 mg, 87%); m.p.: $103\text{--}105^\circ\text{C}$; R_f 0.28 (10% EtOAc in petroleum ether); ^1H NMR (400 MHz, CDCl_3): δ_{H} 6.93–6.87 (m, 3H), 6.86–6.82 (m, 1H), 6.76–6.65 (m, 2H), 6.33 (dd, $J=1.4$, 15.7 Hz, 1H), 6.12 (qd, $J=6.6$, 15.7 Hz, 1H), 6.02–5.89 (m, 1H), 5.13–5.03 (m, 2H), 4.78 (d, $J=3.4$ Hz, 4H), 3.84 (s, 3H), 3.86 (s, 3H), 3.34 (d, $J=6.8$ Hz, 2H), 1.86 (dd, $J=1.5$, 6.6 Hz, 3H); ^{13}C NMR (101 MHz, CDCl_3): δ_{C} 149.8, 149.7, 145.7, 145.0, 137.5, 134.6, 132.9, 130.5, 129.4, 126.0, 124.6, 121.3, 120.4, 118.5, 115.8, 115.0, 114.9, 114.4, 112.7, 112.4, 109.1, 77.3, 77.1, 74.9, 74.8, 74.7, 74.7, 71.4, 71.4, 71.3, 71.3, 59.5, 58.9, 57.5, 57.5, 57.4, 56.1, 55.8, 55.8, 39.9, 29.0, 18.4, 17.8, 14.7; HRMS: m/z for $\text{C}_{26}\text{H}_{27}\text{O}_4$ ($\text{M}+\text{H}$) $^+$: calcd 403.1904, found 403.1898.

(*E*)-3-methoxy-4-((6-(2-methoxy-4-(prop-1-en-1-yl)phenoxy)hexa-2,4-diyne-1-yl)oxy)benzaldehyde (5b)

Brown solid (138 mg, 95%); m.p.: $110\text{--}112^\circ\text{C}$; R_f 0.37 (10% EtOAc in petroleum ether); ^1H NMR (400 MHz, CDCl_3): δ_{H} 9.87 (d, $J=1.1$ Hz,

1H), 7.48-7.41 (m, 2H), 7.08 (d, $J=8.1$ Hz, 1H), 6.91-6.81 (m, 3H), 6.33 (d, $J=15.6$ Hz, 1H), 6.18-6.07 (m, 1H), 4.91 (s, 2H), 4.79 (s, 2H), 3.93 (s, 3H), 3.86 (s, 3H), 1.87 (d, $J=6.6$ Hz, 3H); ^{13}C NMR (101 MHz, CDCl_3): δ_{C} 190.9, 151.9, 150.1, 149.8, 145.6, 133.0, 131.1, 130.4, 126.4, 124.7, 118.4, 114.8, 112.7, 109.5, 109.1, 77.0, 75.5, 73.3, 72.2, 71.0, 57.4, 57.1, 56.1, 55.8, 18.4; HRMS: m/z for $\text{C}_{24}\text{H}_{22}\text{O}_3\text{Na}$ ($\text{M}+\text{Na}$) $^+$: calcd 413.1364, found 413.1358.

4-((6-(4-Allyl-2-methoxyphenoxy) hexa-2,4-diyne-1-yl) oxy)-3-methoxybenzaldehyde (5c)

Yellowish solid (130 mg, 89%); m.p.: 106–108 °C; R_f 0.34 (10% EtOAc in petroleum ether); ^1H NMR (400 MHz, CDCl_3): δ_{H} 9.88 (s, 1H), 7.48-7.42 (m, 2H), 7.08 (d, $J=8.4$ Hz, 1H), 6.90 (d, $J=8.4$ Hz, 1H), 6.74-6.69 (m, 2H), 6.01-5.89 (m, 1H), 5.12-5.05 (m, 2H), 4.91 (s, 2H), 4.78 (s, 2H), 3.94 (s, 3H), 3.85 (s, 3H), 3.34 (d, $J=6.1$ Hz, 2H); ^{13}C NMR (101 MHz, CDCl_3): δ_{C} 190.9, 151.9, 150.0, 149.7, 144.9, 137.4, 134.7, 131.1, 126.4, 120.4, 115.9, 114.9, 112.7, 112.4, 109.5, 77.2, 77.0, 75.6, 73.2, 72.2, 70.9, 57.5, 57.1, 56.1, 55.8, 39.9; HRMS: m/z for $\text{C}_{24}\text{H}_{23}\text{O}_5$ (M^+): calcd 391.1540, found 391.1537.

(E)-2-methoxy-1-((6-(2-methoxyphenoxy) hexa-2,4-diyne-1-yl) oxy)-4-(prop-1-en-1-yl) benzene (5d)

Brown solid (60 mg, 75%); m.p.: 68–70 °C; R_f 0.33 (10% EtOAc in petroleum ether); ^1H NMR (400 MHz, CDCl_3): δ_{H} 7.01-6.97 (m, 1H), 6.94-6.86 (m, 4H), 6.86-6.83 (m, 1H), 6.34 (dd, $J=1.6$, 15.6 Hz, 1H), 6.12 (dd, $J=6.6$, 15.7 Hz, 1H), 4.80 (d, $J=9.3$ Hz, 4H), 3.86 (d, $J=1.9$ Hz, 6H), 1.87 (dd, $J=1.6$, 6.5 Hz, 3H); ^{13}C NMR (101 MHz, CDCl_3): δ_{C} 149.7, 149.7, 146.6, 145.7, 132.8, 130.5, 124.6, 122.6, 120.8, 118.5, 114.8, 111.9, 109.1, 74.7, 71.3, 57.4, 57.3, 55.8, 55.8, 18.4; HRMS: m/z for $\text{C}_{23}\text{H}_{23}\text{O}_4$ (M^+): calcd 363.1591, found 363.1584.

4-Allyl-2-methoxy-1-((6-(2-methoxyphenoxy) hexa-2,4-diyne-1-yl) oxy) benzene (5e)

Brown semisolid (200 mg, 77%); R_f 0.33 (10% EtOAc in petroleum ether); ^1H NMR (400 MHz, CDCl_3): δ_{H} 7.02-6.95 (m, 2H), 6.93-6.86 (m, 3H), 6.73-6.69 (m, 2H), 5.95 (tdd, $J=6.6$, 10.3, 17.0 Hz, 1H), 5.12-5.04 (m, 2H), 4.77 (d, $J=11.4$ Hz, 4H), 3.83 (s, 3H), 3.84 (s, 3H), 3.33 (d, $J=6.9$ Hz, 2H); ^{13}C NMR (101 MHz, CDCl_3): δ_{C} 149.8, 149.8, 146.7, 145.0, 137.5, 134.6, 122.7, 120.9, 120.5, 115.9, 115.0, 114.9, 112.5, 112.0, 77.2, 75.0, 74.9, 74.8, 71.4, 71.4, 71.4, 71.3, 57.6, 57.4, 55.9, 39.9; HRMS: m/z for $\text{C}_{23}\text{H}_{23}\text{O}_4\text{Na}$ ($\text{M}+\text{Na}$) $^+$: calcd 385.1415, found 385.1415.

(E)-2-methoxy-1-((6-(2-methoxy-4-(prop-1-en-1-yl) phenoxy) hexa-2,4-diyne-1-yl) oxy)-4-propylbenzene (5f)

Yellowish solid (120 mg, 83%); m.p.: 60–62 °C; R_f 0.28 (10% EtOAc in petroleum ether); ^1H NMR (400 MHz, CDCl_3): δ_{H} 6.91-6.85 (m, 3H), 6.85-6.82 (m, 1H), 6.72-6.67 (m, 2H), 6.33 (dd, $J=1.5$, 16.0 Hz, 1H), 6.12 (dd, $J=6.5$, 15.6 Hz, 1H), 4.77 (d, $J=5.3$ Hz, 4H), 3.85 (s, 3H), 3.84 (s, 3H), 2.55-2.47 (m, 2H), 1.86 (dd, $J=1.5$, 6.1 Hz, 3H), 1.67-1.55 (m, 2H), 0.93 (t, $J=7.2$ Hz, 3H); ^{13}C NMR (101 MHz, CDCl_3): δ_{C} 149.8, 149.6, 145.8, 144.7, 137.4, 132.9, 130.6, 124.7, 120.3, 118.6, 114.9, 114.9, 112.4, 109.1, 77.2, 75.1, 75.0, 74.8, 74.7, 71.5, 71.4, 71.3, 71.3, 57.6, 57.5, 55.9, 37.8, 24.8, 18.5, 13.9; HRMS: m/z for $\text{C}_{26}\text{H}_{29}\text{O}_4$ (M^+): calcd 405.2060, found 405.2053.

2-Methoxy-1-((6-(2-methoxyphenoxy) hexa-2,4-diyne-1-yl) oxy)-4-propylbenzene (5g)

Brown semisolid (50 mg, 64%); R_f 0.4 (10% EtOAc in petroleum ether); ^1H NMR (400 MHz, CDCl_3): δ_{H} 7.02-6.85 (m, 4H), 6.73-6.67 (m, 2H), 4.78 (d, $J=13.7$ Hz, 4H), 3.84 (s, 4H), 3.85 (s, 2H), 2.58-2.48 (m, 2H), 1.66-1.58 (m, 3H), 0.94 (t, $J=7.2$ Hz, 3H); ^{13}C NMR (101 MHz, CDCl_3): δ_{C} 149.8, 149.6, 146.7, 144.7, 137.4, 122.7, 120.9, 120.3, 115.0, 114.9, 112.4, 112.0, 77.2, 75.1, 75.0, 74.8, 74.7, 71.5, 71.4, 71.3, 71.3, 57.6, 57.4, 55.9, 55.9, 37.8, 24.8, 13.9; HRMS: m/z for $\text{C}_{23}\text{H}_{25}\text{O}_4$ (M^+): calcd 365.1747, found 365.1746.

3-Methoxy-4-((6-(2-methoxyphenoxy) hexa-2,4-diyne-1-yl) oxy) benzaldehyde (5h)

Yellowish solid (90 mg, 69%); m.p.: 85–87 °C; R_f 0.27 (10% EtOAc in petroleum ether); ^1H NMR (400 MHz, CDCl_3): δ_{H} 9.88 (s, 1H), 7.48-7.43 (m, 2H), 7.08 (d, $J=8.1$ Hz, 1H), 7.02-6.96 (m, 2H), 6.94-6.88 (m, 2H), 4.91 (s, 2H), 4.81 (s, 2H), 3.94 (s, 3H), 3.87 (s, 3H); ^{13}C NMR (101 MHz, CDCl_3): δ_{C} 190.9, 151.9, 150.0, 149.8, 146.6, 131.1, 126.4, 122.7, 120.8, 114.8, 112.7, 111.9, 109.5, 77.0, 75.4, 73.2, 72.2, 71.0, 57.3, 57.1, 56.1, 55.8; HRMS: m/z for $\text{C}_{21}\text{H}_{18}\text{O}_5$ (M^+): calcd 351.1227, found 351.1222, m/z for $\text{C}_{21}\text{H}_{18}\text{O}_5\text{Na}$ ($\text{M}+\text{Na}$) $^+$: calcd 373.1046, found 373.1035.

4-Allyl-2-methoxy-1-((6-(2-methoxy-4-propylphenoxy) hexa-2,4-diyne-1-yl) oxy) benzene (5i)

Yellowish semisolid (120 mg, 83%); R_f 0.34 (10% EtOAc in petroleum ether); ^1H NMR (400 MHz, CDCl_3): δ_{H} 6.92-6.86 (m, 2H), 6.74-6.67 (m, 4H), 6.00-5.89 (m, 1H), 5.12-5.03 (m, 2H), 4.77-4.73 (m, 4H), 3.84 (s, 6H), 3.33 (d, $J=6.9$ Hz, 2H), 2.57-2.48 (m, 2H), 1.62 (qd, $J=7.5$, 14.9 Hz, 2H), 0.98-0.89 (m, 3H); ^{13}C NMR (101 MHz, CDCl_3): δ_{C} 149.8, 149.6, 145.0, 144.7, 137.5, 137.4, 134.6, 120.5, 120.3, 115.9, 115.0, 115.0, 112.4, 112.4, 77.2, 75.0, 74.9, 71.4, 71.3, 57.6, 57.6, 55.9, 40.0, 37.8, 24.8, 14.0; HRMS: m/z for $\text{C}_{26}\text{H}_{28}\text{O}_4\text{Na}$ ($\text{M}+\text{Na}$) $^+$: calcd 427.2020, found 427.2012.

3-Methoxy-4-((6-(2-methoxy-4-propylphenoxy) hexa-2,4-diyne-1-yl) oxy) benzaldehyde (5j)

Yellowish solid (120 mg, 82%); m.p.: 58–60 °C; R_f 0.27 (10% EtOAc in petroleum ether); ^1H NMR (400 MHz, CDCl_3): δ_{H} 9.88 (s, 1H), 7.48-7.42 (m, 2H), 7.08 (d, $J=8.4$ Hz, 1H), 6.88 (d, $J=8.4$ Hz, 1H), 6.73-6.68 (m, 2H), 4.91 (s, 2H), 4.77 (s, 2H), 3.94 (s, 3H), 3.85 (s, 3H), 2.56-2.50 (m, 2H), 1.67-1.57 (m, 4H), 0.94 (t, $J=7.2$ Hz, 3H); ^{13}C NMR (101 MHz, CDCl_3): δ_{C} 190.9, 151.9, 150.0, 149.5, 144.6, 137.5, 131.1, 126.4, 120.2, 114.8, 112.7, 112.3, 109.5, 77.2, 77.0, 75.8, 73.1, 72.3, 70.8, 57.5, 57.1, 56.1, 55.8, 37.7, 24.7, 13.8; HRMS: m/z for $\text{C}_{24}\text{H}_{24}\text{O}_5\text{Na}$ ($\text{M}+\text{Na}$) $^+$: calcd 415.1516, found 415.1497.

Biological evaluation

In-vitro antifungal activity of synthesized compounds of 1a and 1b. Antifungal activity of synthesized compounds **3a-e** and **5a-j** against *A. fumigatus* was performed according to the CLSI M38-A2 microbroth dilution method for filamentous fungi (CLSI, 2016). Briefly, *A. fumigatus* ATCC-46645 strain was cultured on Czapek Dox broth/agar (CzB/CzA) and incubated at $28 \pm 2^\circ\text{C}$ for 5 days for conidiation. The conidia were harvested, and conidia/ml concentration was adjusted as per our previous published paper.^[7b] Two-fold dilutions of synthesized compounds (**3a-e** and **5a-j**) and eugenol **1a** were carried out in triplicate using a 96-well polystyrene plate (Tarsons, India), having growth media CzB. 100 μL

of conidial suspension was added to each well except negative control. The wells which contain only inoculated broth, was kept as positive control and amphotericin B (Amp B) was used as drug control. The plates were incubated statically for 5 days at $28 \pm 2^\circ\text{C}$. The MIC and IC_{50} values were calculated and expressed in micro molar.

Cytotoxicity of compound 3a in normal lung epithelial cell line L-132 as well as *in-silico* screening for its therapeutic activity. Cytotoxicity analysis of compound 3a, which showed antifungal activity at lowest concentration among all tested compounds against *A. fumigatus*, was performed. The selected compound 3a was taken forward for all experiments. The lung epithelial normal cell line L-132 were grown, cultured as reported in the supplier's guide which was provided by National Centre for Cell Science (NCCS), Pune, India. The MTT assay was applied as described in our previous studies.^[7b] The CC_{50} and IC_{50} value of compound 3a was calculated from the graph of percentage viability against concentrations by applying regression analysis on GraphPad prism software 8.0.2.263 version. All experiments were performed in triplicates.

The percentage relative cell viability (Venkatraman et al. 2005) was calculated as:

$$\frac{([A570 \text{ of treated sample}])}{([A570 \text{ of untreated sample}])} \times 100$$

where A570 = absorbance at wavelength 570 nm.

The selectivity index (SI) was determined by $\text{CC}_{50}/\text{IC}_{50}$ ratio against *A. fumigatus*. The SI is an indirect measure of the therapeutic window and it can serve as a predictor of safety during *in vivo* trials for a given pathogen infection.^[23] (CC_{50} - cytotoxic concentration 50 where 50% cells were found to be dead)

In-silico study was conducted to determine drug-likeness and quantitative parameters of absorption, distribution, metabolism, excretion, and toxicity of compound 3a which was predicted by Swiss ADME program (<http://www.swissadme.ch/index.php>). The parameters deployed to predict the physicochemical properties of the compound (Molecular weight, hydrogen donor, hydrogen acceptor, LogP value, TPSA).^[24]

Effect of compound 3a on conidia production- One cubic centimeter of agar block containing treated and untreated fungal culture was excised from CzA media plate supplemented with IC_{50} of compound 1a, 3a and AmpB using a sterile surgical blade and transferred to a sterile test tube. 5 ml of phosphate buffered saline with 0.05% Tween 20 ($1 \times \text{PBST}$) was added to each tube, shaken vigorously to remove conidia. The absorbance of treated and untreated *A. fumigatus* conidia was measured at 530 nm using UV-vis spectrophotometer (CLSI 2008).

Biochemical estimation of ergosterol content- Fungal ergosterol content was isolated from compound 1a, 3a, Amp B treated *A. fumigatus* culture and compared with the control as described by.^[25] Briefly, fungal mycelia were harvested, washed with autoclaved distilled water, dried, and weighed. Alcoholic potassium hydroxide solution (25%, 3 mL) was added to each pellet in a test tube and vortexed it for 1 min. Test tubes were incubated at 85°C for 1 h in boiling water bath. After cooling to room temperature, sterols were extracted in the 1:3 ratio of water: n-octane mixture by a vigorous vortex for 3 min and then allowed to get separate in two phases. The octane layer was collected in screw capped test tube and stored at -20°C . For analysis, 200 μL of extracted sterol was mixed with 800 μL absolute ethanol and was spectrophotometrically measured at 281.5 nm and 230 nm. The conversion from optical density to ergosterol was calculated as follows:

$$\text{Ergosterol \%} = \frac{[(A281.5/290 \times F) \div \text{weight of pellet}] - [(A230/518 \times F) \div \text{weight of pellet}]$$

in which *F* is the ethanol dilution factor.

Scanning electron microscopy (SEM) of *A. fumigatus* conidial surface - Synthesized compound 3a treated and untreated conidia of *A. fumigatus* were harvested, washed, and fixed in 4% glutaraldehyde in 1x PBS under vacuum for 24 hours. After washing, the cells were post-fixed with 1% osmium tetroxide for 60 min and dehydrated by passage through ethanol solutions of increasing concentration. The prepared sample were then mounted on aluminium sheet and coated with gold-palladium alloy. The observations were made using a Zeiss SEM, MA EVO -18 Special Edition.^[21,26]

Effect of compound 3a on *A. fumigatus* biofilm. The IC_{50} of biofilm eradication concentration of compound 3a on pre-formed *A. fumigatus* biofilm was calculated by performing MTT assay in a 96-well flat bottom microtiter plate. The MTT assay was applied according to our previous studies.^[7b] Biofilm eradication property of compound 3a was analysed on fully grown *A. fumigatus* biofilm on 12-well polystyrene plate for 48 h. The biofilm was treated with IC_{50} of compound 3a for another 24 h.^[21,27] To visualise the effect of compound 3a in comparison to positive control (untreated), confocal laser scanning microscopy (CLSM) was performed, and samples were processed as described by Gupta et al^[21] and viewed under Nikon Instruments A1 Confocal Laser Microscope Series with NIS elements C software, Japan.

Statistical analyses

For the statistical analyses, one-way ANOVA was used, comparing the results of conidiation, ergosterol for compound 3a with wild type untreated and Amp B treated strain. All experiments were conducted in biological triplicates. GraphPad Prism software 8.0.2.263 version was used for all the statistics analysis and Microsoft Excel. $p < 0.05$ was considered statistically significant.

Acknowledgements

The authors would like to thank the Department of Science and Technology-Science and Engineering Research Board (DST-SERB) (EMR/2016/005752) New Delhi, Government of India for the financial support and AIRF-JNU, New Delhi, AIARS-Amity University Uttar Pradesh and AIMT-Amity University Uttar Pradesh, India for transmission electron microscopy, scanning electron microscopy and confocal microscopy facilities, respectively. LG and SP are grateful to UGC, New Delhi, India and CSIR, New Delhi, India for financial support in the form of UGC-SRF and CSIR-SRF, respectively. PV would like to thank Amity University Uttar Pradesh for providing the infrastructure and facilities for extensive research work.

Conflict of Interest

The authors declare no conflict of interest.

Data Availability Statement

The data that support the findings of this study are available in the supplementary material of this article.

Keywords: 1,3-Diynes · Glaser-Hay · Cadiot-Chodkiewicz · Antifungal Agents · *Aspergillus fumigatus*

- [1] a) A. Arastehfar, A. Carvalho, J. Houbraken, L. Lombardi, R. G. -Rubio, J. D. Jenks, O. R. -Menendez, R. Aljohani, I. D. Jacobsen, J. Berman, N. Osherov, M. T. Hedayati, M. Ilkit, D. A. -James, T. Gabaldón, J. Meletiadis, M. Kostrzewa, W. Pan, C. L. -Flörl, D. S. Perlin, M. Hoenigl, *Stud. Mycol.* **2021**, *100*, 100115; b) J.-P. Latgé, *Clin. Microbiol. Rev.* **1999**, *12*, 310–350.
- [2] a) D. W. Denning, *Clin. Infect. Dis.* **1998**, *26*, 781–803; b) K. A. Marr, R. A. Carter, M. Boeckh, P. Martin, L. Corey, *Blood* **2002**, *100*, 4358–4366; c) L. Pagano, C. Girmenia, L. Mele, P. Ricci, M. E. Tosti, A. Nosari, M. Buelli, M. Picardi, B. Allione, L. Corvatta, D. D'Antonio, M. Montillo, L. Melillo, A. Chierichini, A. Cenacchi, A. Tonso, L. Cudillo, A. Candoni, C. Savignano, A. Bonini, P. Martino, A. D. Favero, *Haematologica* **2001**, *86*, 862–870; d) M. J. Post, C. Lass-Floerl, G. Gastl, D. Nachbaur, *Transpl. Infect. Dis.* **2007**, *9*, 189–195; e) N. P. Wiederhold, R. E. Lewis, D. P. Kontoyiannis, *Pharmacother.* **2003**, *23*, 1592–1610.
- [3] C. A. Croft, L. Culibrk, M. M. Moore, S. J. Tebbutt, *Front. Microbiol.* **2016**, *7*, 472.
- [4] V. Amanianda, J. Bayry, S. Bozza, O. Kniemeyer, K. Perruccio, S. R. Elluru, C. Clavaud, S. Paris, A. A. Brakhage, S. V. Kaveri, L. Romani, J.-P. Latgé, *Nature* **2009**, *460*, 1117–1121.
- [5] a) S. C. A. Chen, T. C. Sorrell, *Med. J. Aust.* **2007**, *187*, 404–409; b) M. A. Ghannoum, L. B. Rice, *Clin. Microbiol. Rev.* **1999**, *12*, 501–517.
- [6] a) V. S. Brauer, C. P. Rezende, A. M. Pessoni, R. G. De Paula, K. S. Rangappa, S. C. Nayaka, V. K. Gupta, F. Almeida, *Biomol. Eng.* **2019**, *9*, 521; b) G. Wall, J. L. L. -Ribot, *Antibiotics* **2020**, *9*, 445; c) Q. Lin, Y. Li, M. Sheng, J. Xu, X. Xu, J. Lee, Y. Tan, *LWT* **2023**, *173*, 114237; d) J. Prajapati, P. Rao, L. Poojara, D. Acharya, S. K. Patel, D. Goswami, R. M. Rawal, *Curr. Microbiol.* **2023**, *80*, 47.
- [7] a) T. Koeduka, E. Fridman, D. R. Gang, D. G. Vassão, B. L. Jackson, C. M. Kish, I. Orlova, S. M. Spassova, N. G. Lewis, J. P. Noel, T. J. Baiga, N. Dudareva, E. Pichersky, *Proc. Nat. Acad. Sci.* **2006**, *103*, 10128–10133; b) L. Goswami, L. Gupta, S. Paul, M. Vermani, P. Vijayaraghavan, A. K. Bhattacharya, *RSC Med. Chem.* **2022**, *13*, 955–965; c) H. A. Hassan, M. M. Geniady, S. F. Abdelwahab, M. I. Abd-Elghany, H. A. Sarhan, A. A. Abdelghany, M. S. Kamel, A. E. Rodriguez, J. L. Alio, *Ophthalmic Res.* **2018**, *60*, 69–79; d) D. Campaniello, M. R. Corbo, M. Sinigaglia, *J. Food Prot.* **2010**, *73*, 1124–1128.
- [8] a) C. Glaser, *Liebigs Ann.* **1870**, *154*, 137–171; b) C. Glaser, *Chem. Ber.* **1869**, *2*, 422–424; c) A. S. Hay, *J. Org. Chem.* **1962**, *27*, 3320–3321; d) K. S. Sindhu, G. Anilkumar, *RSC Adv.* **2014**, *4*, 27867–27887.
- [9] a) P. Cadiot, W. Chodkiewicz, in *Chemistry of Acetylenes*, (Eds: Marcel Dekker), V. H. G., New York, **1969**, 597–647; b) W. Chodkiewicz, P. Cadiot, A. Willemart, *Compt. Rend.* **1957**, *245*, 2061; c) W. Chodkiewicz, *Ann. Chim. Paris* **1957**, *2*, 819; d) K. S. Sindhu, A. P. Thankachan, P. S. Sajitha, G. Anilkumar, *Org. Biomol. Chem.* **2015**, *13*, 6891–6905.
- [10] Clinical and Laboratory Standards Institute. (2016). Performance standards for antimicrobial susceptibility testing, 26th ed CLSI document M100-S. Clinical and Laboratory Standards Institute, Wayne, PA.
- [11] S. Harmsen, A. C. McLaren, C. Pauken, R. McLemore, *Clin. Orthop. Relat. Res.* **2011**, *469*, 3016–3021.
- [12] J. Krzywik, W. Mozga, M. Aminpour, J. Janczak, E. Maj, J. Wietrzyk, J. A. Tuszyński, A. Huczynski, *Molecules* **2020**, *25*, 1789.
- [13] L. I. S. de Carvalho, D. J. Alvarenga, L. C. F. do Carmo, L. G. de Oliveira, N. C. Silva, A. L. T. Dias, L. F. L. Coelho, T. B. de Souza, D. F. Dias, D. T. Carvalho, *J. Chem.* **2017**, e5207439.
- [14] F. Wu, Y. Zhou, L. Li, X. Shen, G. Chen, X. Wang, X. Liang, M. Tan, Z. Huang, *Front. Chem.* **2020**, *8*, 726.
- [15] A.-I. Pricopie, I. Ionuț, G. Marc, A.-M. Arseniu, L. Vlase, A. Grozav, L. I. Găină, D. C. Vodnar, A. Pîrnău, B. Tîperciuc, O. Oniga, *Molecules* **2019**, *24*, 3435.
- [16] L. Z. Benet, C. M. Hosey, O. Ursu, T. I. Oprea, *Adv. Drug Delivery Rev.* **2016**, *101*, 89–98.
- [17] L. Scorzoni, A. C. A. de Paula e Silva, C. M. Marcos, P. A. Assato, W. C. M. A. de Melo, H. C. de Oliveira, C. B. Costa-Orlandi, M. J. S. M. -Giannini, A. M. F. -Almeida, *Front. Microbiol.* **2017**, *8*, 36.
- [18] P. Sen, M. Vijay, S. Singh, S. Hameed, P. Vijayaraghavan, *Drug Target Insights* **2022**, *16*, 25–35.
- [19] a) V. Voltersen, M. G. Blango, S. Herrmann, F. Schmidt, T. Heinekamp, M. Strassburger, T. Krüger, P. Bacher, J. Lother, E. Weiss, K. Hünninger, H. Liu, P. Hortschansky, A. Scheffold, J. Löffler, S. Krappmann, S. Nietzsche, O. Kurzai, H. Einsele, O. Kniemeyer, S. G. Filler, U. Reichard, A. A. Brakhage, *mBio* **2018**, *9*, e01557–18; b) L. Gupta, S. Hoda, M. Vermani, P. Vijayaraghavan, *Mycol. Progress* **2021**, *20*, 365–380.
- [20] F.-M. C. Müller, M. Seidler, A. Beauvais, *Med. Mycol.* **2011**, *49*, S96–S100.
- [21] L. Gupta, P. Sen, A. K. Bhattacharya, P. Vijayaraghavan, *Archiv. Microbiol.* **2022**, *204*, 214–227.
- [22] P. S. Hellwig, A. M. Barcellos, R. Cargnelutti, T. Barcellos, G. Perin, *J. Org. Chem.* **2022**, *87*, 15050–15060.
- [23] D. Insuasty, O. Vidal, A. Bernal, E. Marquez, J. Guzman, B. Insuasty, J. Quiroga, L. Svetaz, S. Zacchino, G. Puerto, R. Abonia, *Antibiotics* **2019**, *8*, 239.
- [24] C. A. Lipinski, F. Lombardo, B. W. Dominy, P. J. Feeney, *Adv. Drug Delivery Rev.* **2001**, *46*, 3–26.
- [25] S. Hoda, M. Vermani, R. K. Joshi, J. Shankar, P. Vijayaraghavan, *BMC Complementary Med. Ther.* **2020**, *20*, 67.
- [26] M. Pihet, P. Vandeputte, G. Tronchin, G. Renier, P. Saulnier, S. Georgeault, R. Mallet, D. Chabasse, F. Symoens, J.-P. Bouchara, *BMC Microbiol.* **2009**, *9*, 177.
- [27] a) S. Hoda, L. Gupta, H. Agarwal, G. Raj, M. Vermani, P. Vijayaraghavan, *J. Pure Appl. Microbiol.* **2019**, *13*, 1207–1216; b) H. Sav, H. Rafati, Y. Öz, B. D. -Cilo, B. Ener, F. Mohammadi, M. Ilkit, A. D. V. Diepeningen, S. Seyedmousavi, *J. Fungi.* **2018**, *4*, 16.

Manuscript received: January 12, 2023
Revised manuscript received: February 23, 2023
Accepted manuscript online: February 28, 2023
Version of record online: March 20, 2023